

Hugh Summers, Martin O'Mullane, Alessandra Giunta

Dissemination report 4

16 December 2013

Workpackages : 29-1, 29-2, 29-3
Category : DRAFT

This document has been prepared as part of the ADAS-EU Project. It is subject to change without notice. Please contact the authors before referencing it in peer-reviewed literature.
© Copyright, The ADAS Project.

Dissemination report 4

Hugh Summers, Martin O'Mullane, Alessandra Giunta

Department of Physics, University of Strathclyde, Glasgow, UK

Abstract: *The report reviews the supplementary dissemination work package, WP29, task completion for project months 49-57. It spans the ADAS-EU Workshop and Advanced Training Courses (WATC) specified in Annex I: amendment 2 of the ADAS-EU: Adas for fusion in Europe agreement. The WATC presentations were designed to guide participants over the full range of ADAS capabilities and up to the leading edge of the physics themes of the ADAS-EU Project.*

Contents

| | |
|---|------------|
| 1 ADAS-EU WATC overview | 3 |
| 1.1 The visits | 3 |
| 1.1.1 ASIPP, Hefei, Anhui Province, China: 29 - 31 May 2013 | 3 |
| 1.1.2 NIFS, Tajimi Japan: 18 - 22 June 2013 | 14 |
| 1.1.3 KSTAR, Daejeon, South Korea: 22-15 July 2013 | 20 |
| 1.1.4 ASDEX, IPP Garching, Germany | 24 |
| 1.1.5 ITER/CEA Cadarache, France | 28 |
| 1.1.6 EFDA-JET Facility Culham Laboratory, Abingdon, UK | 32 |
| 1.2 Work package 29-1, 29-2, 29-3, deliverable DISSEM4 and milestone DSM4 | 39 |
| A ADAS-EU WATC: Introductory presentations | 40 |
| A.1 Welcome on behalf of EFDA-JET - Dr. Lorne Horton | 40 |
| A.2 Welcome on behalf of EU Commission - Dr. Lars-Goran Eriksson | 52 |
| A.3 The ITER perspective - Dr. Mike Walsh | 80 |
| A.4 The ADAS and ADAS-EU Projects - Prof. Hugh Summers | 115 |
| B ADAS-EU WATC: lecture viewgraphs | 139 |
| B.1 module_1 | 139 |
| B.2 module_2 | 162 |
| B.3 module_3 | 185 |
| B.4 module_4 | 205 |
| B.5 module_5 | 226 |
| B.6 module_6 | 249 |
| B.7 module_7 | 271 |
| B.8 module_8 | 294 |
| C ADAS-EU WATC: demonstration scripts | 319 |

| | | |
|----------|--|------------|
| C.1 | module_1 | 319 |
| C.2 | module_2 | 356 |
| C.3 | module_3 | 385 |
| C.4 | module_4 | 401 |
| C.5 | module_5 | 413 |
| C.6 | module_6 | 464 |
| C.7 | module_7 | 498 |
| C.8 | module_8 | 525 |
| D | ADAS-EU WATC: Other talks | 586 |
| D.1 | Modelling Lyman and Fulcher band spectra - Prof. Kurt Behringer | 586 |
| D.2 | H ₂ collisional-radiative modelling - Dr. Francisco Guzman | 598 |
| D.3 | The JET-ILW and plasma edge spectroscopy in metallic fusion devices - Dr. Sebasjan Brezinsek | 609 |
| D.4 | ADAS forward discussion - Dr. William Morris | 633 |
| E | ADAS-EU WATC: ADAS codes and data formats | 643 |
| E.1 | ADAS manual: version 4.0: contents pages | 643 |

Chapter 1

ADAS-EU WATC overview

The extended dissemination programme authorised under the ADAS-EU Amendment 2 envisaged up to eight visits to fusion laboratories - four in Europe and four outwith Europe. Each was intended to be of approximately three days duration and follow a similar format. The first day should be devoted to presentation by researchers at the visited laboratory and interested parties in the country visited at the discretion of the local organisers. The second and third days would be devoted to an intensive detailed description of the ADAS atomic physics for fusion scope and capabilities, especially the new capabilities enabled by the ADAS-EU Support Action, incorporating up to eight lectures and linked active demonstrations. The concluding part of the last day should be devoted to review and discussion of opportunities and interests for future collaboration.

In practice, three visits were made outwith Europe (ASIPP China, NFRI Korea and NIFS Japan) and three within Europe (IPP Garching Germany, ITER/CEA France and EFDA-JET/CCFE Culham UK). A visit originally scheduled for FZ-Juelich Germany had to be cancelled by FZ-Juelich because of timing clashes with mobility travel of some of its key staff. A possible visit to IPR India could not be scheduled in 2013. It is intended that visits to the USA and India will take place during 2014, outwith the ADAS-EU grant period, funded by ADAS and local monies. This will mean that nearly all the countries with ITER Domestic Agencies will have been visited - and objective aspired to in Amendment 2. The programme content of the visits were adjusted to suit local special interests. Thus the visits to China, Korea and Japan followed most closely the original programme designs, while the visits to Germany and France, where there was more familiarity with ADAS-EU and ADAS, varied more strongly from the pattern. The final visit to the UK was the summative meeting and most complete with special presentations from EU Commission , EFDA-JET and CCFE Culham senior staff and a special final planning session. The latter meeting also included some specialists from European Universities who had contributed to ADAS-EU sub-contracts.

1.1 The visits

1.1.1 ASIPP, Hefei, Anhui Province, China: 29 - 31 May 2013

The first ADAS-EU visit took place at the Chinese Academy of Sciences Institute for Plasma Physics, Hefei, China - the site of the EAST tokamak. The WATC meeting took place over two and a half days 29 May - 31 May (morning). The initial agenda and list of participants is attached as appendix A. There were 65 participants from 9 institutions.

On the first day, after introductory welcome and remarks by Professor Boanian Wan for ASIPP and Dr. Manfred von Hellermann for the EU Commission (a presentation for Dr. Rosa Antidormi), eight presentations were made by representatives of participating institutions in China. The day was completed by an overview talk on ADAS and ADAS- EU by Prof. Summers. The second day was devoted to four 45min. lectures (by Prof. Summers) and linked 45 min. demonstrations of ADAS (by Dr. O'Mullane and Dr. Giunta). Modules presented were 1, 5, 2 and a final composite of module 8 with some of module 4. This enabled coverage of material a little more closely linked to the spheres of activity described on the first day than that of the initial agenda. Printed copies of lectures 1 and 5

were available. On day 3, Prof. Summers firstly presented module 3 on molecules to meet a local request. This was followed by the review of atomic studies for the conceptual design of ITER diagnostics by Dr. O'Mullane. Professor Summers led the concluding discussions. Contributions and queries from the participants were varied, very relevant and well reasoned. They spanned special spectral diagnostics (including series limit features of hydrogen and satellite line features of Ar+15 /Ar+16), lithium and the LiH molecule, beam stopping and emission by multiple impurity plasmas, utilisation of effective data in MHD and Monte Carlo codes (the dressed reaction concept was introduced by Prof. Summers in response).

Agenda



中国科学院等离子体物理研究所
国际 ADAS 研讨暨培训会

会议手册

中国科学院等离子体物理研究所
2013 年 5 月 25 日

ADAS/ADAS-EU Workshop/Training Course Agenda

| Wednesday 29 th May (4# 601) | | | |
|--|-------------------|---|---|
| 08:30 | 08:50 | Registration | |
| Opening session | | | |
| 08:50 | 09:00 | Prof. Baonian Wan | Welcome |
| 09:00 | 09:30 | Prof. Liqun Hu | Introduction of ASIPP |
| 09:30 | 10:00 | Dr. Manfred von Hellermann | General introduction on behalf of the EU and Euartom. |
| 10:00 | 10:30 | | photo, coffee break |
| session 1: ADAS in experimental programme (Chairman: Dr. Manfred Von Hellermann) | | | |
| 10:30 | 11:00 (25'+5') | Dr. Deliang Yu (SWIPP) | Development of neutral-beam-aided diagnostics on HL-2A. |
| 11:00 | 11:30 (25'+5') | Dr. Zhifeng Cheng (HUST) | Introduction of the visible spectra study on J-TEXT. |
| 11:30 | 12:00 (25'+5') | Dr. Juan Huang (ASIPP) | Role of ADAS in Spectroscopy diagnostics and analysis on EAST. |
| 12:00 | 13:30 | lunch (2 nd floor of Kexi Restaurant) | |
| session 2: ADAS in modeling programme (Chairman: Pro. Sizheng Zhu) | | | |
| 13:30 | 14:00 (25'+5') | Dr. Yiping Chen (ASIPP) | Application of ADAS in the simulation of edge plasma on tokamak. |
| 14:00 | 14:30 (25'+5') | Dr. Chaofeng Sang (DLUT) | Simulation of divertor plasma and hydrogen isotope retention processes. |
| 14:30 | 15:00 (25'+5') | Dr. Lu Sun (BUAA) | Modeling and Simulation of Hydrogen/Helium Behaviors in Tungsten at Different Scales. |
| session 3: molecular and atomic data study (Chairman: Dr. Martin O' Mullan) | | | |
| 15:00 | 15:35 (30'+5') | Pro. Roger Hutton (Fudan University) | The applications of EBIT in plasma dis-entanglement and atomic data studies. |
| 15:35 | 16:00 (20'+5') | Dr. Xincheng Wang (Fudan University) | Recoil ion momentum spectroscopy for electron-molecule and electron- atom collisions. |
| 16:00 | 16:15 | Coffee break | |
| 16:15 | 17:00 | Prof. H.P. Summers | Overview of ADAS and ADAS-EU principal scientific themes, objectives and relationships. |
| 17:15 | | reception at ZHESHANG International Holiday Hotel | |
| Thursday 30 th May Training courses (4# 601) | | | |

| | | | |
|--------------------------------------|-------|---|---|
| 09:00 | 10:30 | course 1: Impurity atomic species in fusion plasma, their ionisation state and radiating characteristics the ADAS approach | |
| 10:30 | 11:00 | coffee break | |
| 11:00 | 12:30 | course 2: Charge exchange and beam emission spectroscopy. Modeling emitter populations and analyzing spectra | |
| 12:30 | 14:00 | lunch (2 nd floor of Kexi Restaurant) | |
| 14:00 | 15:30 | course 3: Spectral diagnostics and methods for special environments - the interface between fusion and astrophysics | |
| 15:30 | 16:00 | coffee break | |
| 16:00 | 17:30 | course 4: A survey of molecular modeling, fundamental atomic calculations and advanced modeling in ADAS | |
| Friday 31 st May (4# 601) | | | |
| 08:30 | 08:45 | Prof. H.P Summers | Collaborating, developing and knowledge pooling in atomic physics for the ITER era. |
| 08:45 | 09:30 | Dr. Martin O' Mullane | Atomic studies for the conceptual design of ITER Diagnostics |
| 09:30 | 11:00 | Round-table discussion: Experimental spectroscopy/ analysis - a forward look. Individual contributions including needs from ADAS and useful avenues for ADAS-EU input. | |
| 11:00 | 11:30 | coffee break | |
| 11:30 | 12:30 | Prof. H.P Summers | Summary for Workshop/Training course |
| 12:30 | 13:40 | lunch (2 nd floor of Kexi Restaurant) | |
| 13:40 | 14:20 | EAST tour | |
| 14:20 | 16:30 | Hefei Museum tour | |

CONTACT:

Zheshang International Holiday Hotel:

No. 65, Xuancheng Road, Hefei, Anhui Province; +8613645694957

Grand Park Hotel:

No. 258, Fan Hua Road, Hefei, Anhui Province, +8615855170891

Institute of Plasma Physics, Chinese Academy of Sciences:

No. 350 Shushanhu Rd., Hefei, Anhui, China, +8613865940928

Participants

Contacts for ADAS/ADAS-EU Workshop and Training Course

| 序号 | 姓名 | 性别 | 单位 | 专业方向 | 电话 | 邮箱 |
|----|------------------------|----|------------------------------------|--|--------------|------------------------------|
| 1 | Hugh Summers | 男 | University of Strathclyde | 聚变原子分子分析 theoretical atomic collision physics | | summers@phys.strath.ac.uk |
| 2 | Alessandra Giunta | 女 | CCFE(英国卡拉姆聚变中心) | 聚变原子分子分析 theoretical atomic collision physics | | martin.omullane@jet.uk |
| 3 | Martin O'Mullane | 男 | University of Strathclyde, CCFE | 聚变原子分子分析 theoretical atomic collision physics, and impurity transport code | | alessandra.giunta@stfc.ac.uk |
| 4 | Manfred von Hellermann | 男 | CCFE, ITER | 光谱诊断 spectroscopic diagnostic and spectral analysis code | | m.g.vonhellermann@diffen.nl |
| 5 | 万宝年 | 男 | 等离子体所 ASIPP | 等离子体物理 tokamak plasma | 055165591352 | bnwan@ipp.ac.cn |
| 6 | 胡立群 | 男 | 等离子体所 ASIPP | 等离子体物理 plasma diagnostics | 055165591604 | lqhu@ipp.ac.cn |
| 7 | 毛红敏 | 男 | 等离子体所 ASIPP | 等离子体物理-边界重杂质光谱诊断 high z spectroscopic diagnostics | 18255169430 | hmmao@ipp.ac.cn |
| 8 | 曹斌 | 男 | 等离子体所 ASIPP | 等离子体物理 wall recycling and retention | 18655199057 | caobin@ipp.ac.cn |
| 9 | 丁芳 | 男 | 等离子体所 ASIPP | 等离子体物理-边界重杂质光谱诊断 | 13225833926 | fding@ipp.ac.cn |

| | | | | | |
|----|-----|---|-------------|--|------------------------------------|
| 10 | 张鹏飞 | 男 | 等离子体所 ASIPP | high z spectroscopic diagnostics 等离子体物理 | 15665415181 pfzhang@ipp.ac.cn |
| 11 | 段艳敏 | 女 | 等离子体所 ASIPP | tokamak plasma experiments 等离子体物理诊断和实验 | 18019950839 ynduan@ipp.ac.cn |
| 12 | 刘晓菊 | 女 | 等离子体所 ASIPP | bolometer diagnostic 聚变堆诊断 | 13966725740 julie1982@ipp.ac.cn |
| 13 | 李小椿 | 男 | 等离子体所 ASIPP | computational material science 计算材料学 | 13696511985 xcli@ipp.ac.cn |
| 14 | 张洪明 | 男 | 等离子体所 ASIPP | plasma and surface interaction 等离子体光谱诊断 | 18756094521 Hmzhang@ipp.ac.cn |
| 15 | 谢海 | 男 | 等离子体所 ASIPP | spectroscopic diagnostics 等离子体与材料相互作用 | 18256900168 xiehai@ipp.ac.cn |
| 16 | 李永春 | 男 | 等离子体所 ASIPP | low-frequency driven plasma LHCD | 18355107203 ycunli@ipp.ac.cn |
| 17 | 王文章 | 男 | 等离子体所 ASIPP | 等离子体物理实验 plasma experimental study | 15665415138 www.qq@qq.com |
| 18 | 刘祥 | 男 | 等离子体所 ASIPP | 等离子体物理 plasma physics | 18756090730 jentle@hotmail.com |
| 19 | 姚方伟 | 男 | 等离子体所 ASIPP | ion cyclotron heating ICRH | 13083085626 fwyzao2008@163.com |
| 20 | 向玲燕 | 女 | 等离子体所 ASIPP | tokamak等离子体物理实验 divertor plasma | 18255111319 lyxiang@ipp.ac.cn |
| 21 | 梁立振 | 男 | 等离子体所 ASIPP | 中性束注入 neutral beam injection | 15905602477 lizhang@ipp.ac.cn |
| 22 | 许棕 | 男 | 等离子体所 ASIPP | 光谱诊断 | 18355111209 song1989214@126.com |

| | | | | | | |
|----|-----|---|-------------|---|--------------|---------------------|
| 23 | 陈一平 | 男 | 等离子体所 ASIPP | spectroscopic diagnostic 等离子体物理 | 13637088331 | ypetlen@ipp.ac.cn |
| 24 | 胡广海 | 男 | 等离子体所 ASIPP | edge plasma simulation 边界等离子体诊断 | 15955129630 | ghhu@ipp.ac.cn |
| 25 | 胡庆生 | 男 | 等离子体所 ASIPP | 等离子体偏滤器物理 diverter plasma | 18956086631 | qshu@ipp.ac.cn |
| 26 | 朱思铮 | 男 | 等离子体所 ASIPP | 边界等离子体模拟 edge plasma simulation | 13866156205 | szzhu@ipp.ac.cn |
| 27 | 刘烨露 | 男 | 等离子体所 ASIPP | 托卡马克等离子体光谱诊断 spectroscopic diagnostic | 18326045207 | yelulu@gmail.com |
| 28 | 司机 | 男 | 等离子体所 ASIPP | 偏滤器及边界等离子体数值模拟 edge plasma simulation | 13721061769 | hsj@ipp.ac.cn |
| 29 | 牛国鉴 | 男 | 等离子体所 ASIPP | 等离子体物理 plasma and surface interaction | 15956914928 | niugi@ipp.ac.cn |
| 30 | 陈玉庆 | 男 | 等离子体所 ASIPP | 中性束注入 neutral beam injection | 18005695252 | chenyq205@ipp.ac.cn |
| 31 | 吕波 | 男 | 等离子体所 ASIPP | 中性束注入 spectroscopic diagnostic (XCS, XEUV) | 055165591309 | blu@ipp.ac.cn |
| 32 | 李颖颖 | 女 | 等离子体所 ASIPP | 中性束注入 spectroscopic diagnostic (CXRS, BES) | 055165591309 | liyy@ipp.ac.cn |
| 33 | 符佳 | 男 | 等离子体所 ASIPP | 中性束注入 spectroscopic diagnostic (CXRS, BES) | 055165592369 | fujia@ipp.ac.cn |
| 34 | 沈永才 | 男 | 等离子体所 ASIPP | 中性束注入 spectroscopic diagnostic (XCS, XEUV) | 055165595663 | syc@ipp.ac.cn |
| 35 | 迟源 | 男 | 等离子体所 ASIPP | 中性束注入 | 055165595663 | ychi@ipp.ac.cn |

| | | | | | | |
|----|-----|---|-----------------|---|-------------|----------------------|
| 36 | 陈颖杰 | 男 | 等离子体所 ASIPP | spectroscopic diagnostic (XCS, XEUV) 等离子体诊断 spectroscopic (bremsstrahlung) | 13866187900 | bestfaye@gmail.com |
| 37 | 高伟 | 男 | 等离子体所 ASIPP | 等离子体光谱诊断 spectroscopic diagnostic (UV/VIS) | 13075587249 | gaowei@ipp.ac.cn |
| 38 | 张凌 | 女 | 等离子体所 ASIPP | 等离子体物理 spectroscopic diagnostic(UV/VIS,XEUV) | 13866196771 | zhangling@ipp.ac.cn |
| 39 | 黄娟 | 女 | 等离子体所 ASIPP | 光谱诊断及模拟 UV/VIS, FIDA, edge simulation | 13855105273 | juan.huang@ipp.ac.cn |
| 40 | 张伟 | 男 | 等离子体所 ASIPP | 等离子体物理 Li-BES, He-BES | 18955196211 | zhangwei@ipp.ac.cn |
| 41 | 王福琼 | 女 | 等离子体所 ASIPP | 偏振器及边界等离子体数值模拟 edge plasma simulation | 18298026375 | wangfq@ipp.ac.cn |
| 42 | 徐海峰 | 男 | 吉林大学原子分子研究所 JLU | 原子与分子物理 atomic and molecular physics | 15843035135 | yanbing@jlu.edu.cn |
| 43 | 闫冰 | 男 | 吉林大学原子分子研究所 JLU | 原子与分子物理 atomic and molecular physics | 13504476975 | yanbing@jlu.edu.cn |
| 44 | 石英 | 男 | 吉林大学原子分子研究所 JLU | 原子与分子物理 atomic and molecular physics | 13943084815 | shi_ying@jlu.edu.cn |
| 45 | 孙平 | 男 | 核工业西南物理研究院 SWIP | 等离子体物理实验与诊断 tokamak plasma experiments | 02882850353 | sunping@swip.ac.cn |
| 46 | 魏彦玲 | 女 | 核工业西南物理研究院 SWIP | 等离子体物理实验与诊断 tokamak plasma experiments | 18728446364 | weiyi@swip.ac.cn |
| 47 | 王占辉 | 男 | 核工业西南物理研究院 SWIP | 超声分子束注入加料过程中的输运现象 | 15881151251 | zhwang@swip.ac.cn |

| | | | | | | |
|----|-----|---|---------------------------------------|---|-------------|----------------------------|
| | | | transport molecular beam injection | study during supersonic molecular beam injection | | |
| 48 | 余德良 | 男 | 核工业西南物理研究院 SWIP | 等离子体物理实验与诊断 active spectroscopic diagnostics | 13980493931 | yndl@swip.ac.cn |
| 49 | 孙璐 | 女 | 北京航空航天大学 BUAA | 凝聚态物理 simulation for plasma and surface interaction | 13811021408 | sunluicey@gmail.com |
| 50 | 孟超 | 男 | 北京航空航天大学 BUAA | 凝聚态物理 edge plasma simulation | 13401156896 | Mengchao915098@gmail.com |
| 51 | 侯氢 | 男 | 四川大学原子核科学技术研究 所 SCU | 原子物理和辐射物理 atomic and radiation physics | 13678106681 | qhou@scu.edu.cn |
| 52 | 丁愿 | 女 | 四川大学原子核科学技术研究 所 SCU | 辐射物理 atomic and radiation physics | 13541159570 | 1065843350@qq.com |
| 53 | 王晓双 | 女 | 四川大学原子核科学技术研究 所 SCU | 辐射物理 atomic and radiation physics | 15196634544 | 614107958@qq.com |
| 54 | 崔节超 | 男 | 四川大学原子核科学技术研究 所 SCU | 辐射物理 atomic and radiation physics | 13880149755 | 745149792@qq.com |
| 55 | 唐腾飞 | 男 | 大连理工大学 | 边界等离子体模拟 edge plasma simulation | 15140698546 | tang_tengfei.dut@gmail.com |
| 56 | 查学军 | 男 | 东华大学 DHU | 等离子体物理 plasma physics | 18930678636 | xizha@dhu.edu.cn |
| 57 | 钟德俊 | 男 | 东华大学 DHU | 等离子体物理 plasma physics | 18817962205 | 2121337@mail.dhu.edu.cn |
| 58 | 宗泽源 | 男 | 东华大学 DHU | 等离子体物理 plasma physics | 13764572961 | zongzeyuan@mail.dhu.edu.cn |
| 59 | 王新成 | 男 | 复旦大学 FUDAN | 原子物理、高电荷态物理 | 18321614135 | xinchengwang@fudan.edu.cn |

| | | | | | | |
|----|--------------|---|--------------------|--|-------------|-----------------------|
| 60 | 杨洋 | 男 | 复旦大学 FUDAN | 原子物理、高电荷态离子相关物理 atomic and highly charged ionic physics | 13816921906 | yangyang@fudan.edu.cn |
| 61 | 肖君 | 男 | 复旦大学 FUDAN | 原子物理、高电荷态离子相关物理 atomic and highly charged ionic physics | 13817291122 | xiao_jun@fudan.edu.cn |
| 62 | 姚科 | 男 | 复旦大学 FUDAN | 原子物理、高电荷态离子相关物理 atomic and highly charged ionic physics | 15201800530 | keyao@fudan.edu.cn |
| 63 | Roger Hutton | 男 | 复旦大学 FUDAN | 原子物理、高电荷态离子相关物理 atomic and highly charged ionic physics | | rhuutton@fudan.edu.cn |
| 64 | 程芝峰 | 男 | 华中科技大学 HUST | 原子物理、高电荷态离子相关物理 atomic and highly charged ionic physics | 15927617983 | chengfei@hust.edu.cn |
| 65 | 罗剑 | 男 | 华中科技大学 HUST | 边界等离子体物理、杂质行为 impurity transport | 18071748898 | 731074460@qq.com |
| | | | | 杂质行为 impurity transport | | |

BUAA: Beijing University of Aeronautics and Astronautics**DHU:** Donghua University**DLUT:** Dalian University of Technology**FUDAN:** Fudan University**HUST:** Huazhong University of Science and Technology**JLU:** Jilin University**SCU:** Sichuan University**SWIP:** Southwestern Institute of Physics**ASPP:** Institute of Plasma Physics, Chinese Academy of Sciences

1.1.2 NIFS, Tajimi Japan: 18 - 22 June 2013

The second ADAS-EU visit took place at the National Institute for Fusion Science, Tajimi, Japan over four days from 18 - 22 June. The ordering of the ADAS module presentations was arranged to suit the participants and was out of natural order. This was unavoidable but perhaps meant that some of the advanced modules were difficult for those less experienced in atomic physics. There were seventeen participants, including the ADAS staff, in total (see section 1.1.2). The agenda is given in section 1.1.2.

The introduction and all module lectures were delivered by Prof. Summers. There were many interesting presentations. Dr. Osakabe gave an update on fast ion diagnostic studies (FIDA) using charge exchange (called FICXS at LHD). Observation is of H α emission of fast ions originally sourced from the 180 keV neutral beam, detected by charge exchange with the 40keV beam. The measurement shows the fast ion orbit densities on flux surfaces. The fast ion feature is detected on the blue side to avoid contamination by BES. As is well known, the structured feature is sensitive to the CX cross-section shape and on the observational lines-of-sight. LHD can move the plasma radially. On moving outward, confinement is affected and there are changes in MHD stability, which affect the orbital densities. Osakabe uses a full Monte Carlo simulation of the orbits to predict the signals, which then are contrasted with the measurements. The methodology follows that of DIIID and the 2008 paper on which Allan Whiteford was a co-author. Comparisons seem rather good. He draws attention to the importance of the beam halo as a CX source which must be included in the models. Prof. Summers felt that there was little change in the ADAS cross-sections used for the modelling although he was a little unclear of how much of the hydrogen CR model of the excited halo donors was in the Monte Carlo simulations. Dr Ikeda gave an update on neutral beam attenuation measurement. This is achieved by BES measurements at two points along the 180 keV beam line on LHD. An important feature is the contribution of impurities to the beam stopping, which has been explored in the earlier ADAS collaborations with LHD (led again by Allan Whiteford). New results come from the use of pellets to provide transient impurity concentration enhancements in LHD. Results were shown of the influence of carbon stopping which seemed consistent with the carbon time decay. Carbon pellets are also used with a small inclusion of tungsten powder (a technique introduced by Goto). The amounts used seemed a small perturbation but results and conclusions at this stage seemed unclear. ADAS universal CX extensions to arbitrary ions, including tungsten would benefit these studies.

Prof. Murakami summarised the NIFS database activities and collections. These are very extensive, spanning many types of process - electron collisions with molecules, heavy particle collisions and so on. NIFS also has a number of satellite databases, usually created and maintained by a specific external person or group - differential cross-sections (collaboration with KAERI), proton impact with H₂, dissociative attachment to H₂ (v, J resolved) and also bibliographic contributions. Prof. Murakami also summarised some of the H₂ molecular CR modelling (Sawada) and molecular spectral emission (Hasuo & Fujii) and consequential analyses (Kubo) studies in Japan. Prof. Summers commented on the somewhat disconnected way in which Europe (Janev, Reiter, Fantz, Wunderlich, Guzman) and Japan operated in this area which seemed unfortunate. Prof. Watanbe (from the National Astronomical Observatories of Japan) spoke of time dependent CR models of Fe emission, contrasting Hinode/EIS measurements with LHD/Soxmos measurements. His focus was on the iron lines of FeVII - FEXXVI and also HeII, spanning a temperature range log Te = 5.5 - 7.5. He drew attention to the dynamic, magnetically active character of the sun and to the ionisation state relaxation timescales in the sun (from David Brooks thesis!) - 5-6 mins in the upper chromosphere, 3-20 mins in the transition region. His time dependent modelling was based on HULLAC data and some Chianti data. Studies included FeXIII density diagnostics, FeXVII branching ratios and blending. The link to LHD was with the iron transient studies from iron pellet injection. The primary thesis was the observability of ionisation stages in the non-equilibrium plasma and transient ionisation formed in a reconnecting outflow (see Imada 2011). From an ADAS perspective, issues raised include the variation of cross-sections between Autostructure/Rmatrix (ADAS preferred) and the other sources, the recurring truncation problem with Chianti work, and the GCR framework for transient evolution. A pathway for collaboration would be good, but would depend on the availability of time and commitment from Dr. Giunta.

Dr. Daijit Kato provided an illuminating account of high z behaviour (Z and αZ expansions) of complex ions (especially the Ti-like 3d4 system - see Doschek and Feldman) to identify visible M1 forbidden lines. This work was linked to measurements on the Tokyo Superbit. Dr. Kato reported observation of the W+26 M1 line at 389.37A with a possible identification of W+29 at 389.31A on LHD. Further line identification were expected from the recent

LHD campaign. Other interesting talks included Mr. Funaba (spectroscopy and impurity transport) which focussed on the impurity hole phenomenon (K. Ida). His investigations of the variation of inward and outward pinch velocity v used laser blow-off, EUV spectroscopy and the Dux version of Strahl for modelling. Mr Wang described the 2-D spectroscopy of impurities using a scanning EUV system (vertically and horizontally, the horizontal part exploiting the stellarator rotational transform to build the 2-d poloidal picture). Mr Wang examined a Te dependent line ratio near the last closed flux surface (calculated using ADAS and Chianti) and compared with Thomson scattering. ADAS values were within 10% with Chianti more discrepant. Prof. Summers commented on the truncation problem and noted the increasing divergence of the theoretical ratios at higher Te.

Dr. Kobayashi gave a powerful and insightful talk on impurity transport modelling in the stochastic layer of MHD. Background included the stellarator magnetic field structure, and the character of the divertor and strike zone following from the rotational transform of the field and the peripheral field distortions. A variant of B2-Eirene, EMC2-Eirene developed for Wendelstein X is used for LHD. The fluid part of the code (EMC2) is complex because of the 3-d grids required. These are handled in steps, remapping toroidally, creating a new grid periodically. A special Monte Carlo technique is used for the fluid equations, essentially Monte Carlo sampling the coefficients of the fluid equations. Dr. Kobayashi also discussed the various force terms in the equations - ion thermal gradient and friction, which are dominant, and so on. LHD has carbon divertor plates and a stainless steel first wall - but with carbon deposits. Simulations were shown and comparisons with experiment which reveal inner and outer regions with significant mismatches. It is speculated that these indicate variation of $\delta 3c722a5$. Density modelling seems good. Predictions of CIV emissivities, from 3-d modelling (using Chianti data) were shown at low and high density with increasing C+3 in/out concentration asymmetries and indications of carbon screening in the force balance. Dr. Kobayashi moved on to detached plasmas - showing how an RMP field can stabilise the detached plasma - as simulated by EMC3-Eirene. It shows a shift of peak radiation from inboard side to a new X-point. ADAS data is used. Attempts are made to match XUV multi-chord measurements - all this applies to carbon emission. Broad agreement (relative error factor 2) is obtained, with primary radiation localised on M1/1 magnetic islands and absolute errors factor 6 (probably due to uncertainty in sputtering sources). The pressing needs are estimations of screening efficiencies, power balance in detached plasmas and validation of the transport model. Atomic data and molecular data are used with more information needed for higher Z - Fe, W, Kr and Xe. This was a most interesting talk and subsequent discussion between Prof. Summers and Dr. Kobayashi suggested considerable interest in a tighter collaboration and flow of ADAS data into the modelling - which should be followed up.

Agenda

Appendix 2 : Agenda

ADAS/ADAS-EU Workshop and Advanced Training Course

Abstract: The ADAS-EU Euratom - Framework 7 Project of the European Community is sponsoring eight 3-day workshop/advanced training courses at fusion laboratories in Europe and in ITER participating countries outside Europe. The objectives are to examine atomic physics aspects of importance for participant laboratories, to inform by means of lectures and demonstrations about the principal advances made during the four years of ADAS-EU support, to explore the opportunities for new collaborative work on atomic physics with participants within the framework of the ADAS Project, cooperation with Europe and ITER.

| General Agenda | | |
|--|--|--|
| 18 June 2013: | | <i>Charge exchange and neutral beams</i> |
| 09.00 - 09.15: | Welcome & introduction | Prof. I. Murakami |
| 09.15 - 10.00: | Overview of ADAS and ADAS-EU | Prof. H. P. Summers |
| Coffee break | | |
| 10.30 - 11.00: | Charge exchange spectroscopy at NIFS | Dr. M. Osakabe |
| 11.00 - 11.30: | Neutral beam attenuation and emission on LHD | Dr. K. Ikeda |
| Lunch | | |
| 13.30 - 14.15: | <i>Module 5 Lecture:</i> Charge exchange and beam emission spectroscopy - modelling emitter populations, beam stopping and analysing spectra. | Prof. H. P. Summers |
| 14.15 - 15.00: | <i>Module 5 Demonstration:</i> | Dr. M. O'Mullane & Dr. A. Giunta |
| Coffee break | | |
| 15.30 - 16.15: | <i>Module 6 Lecture:</i> Advanced charge exchange plasma receiver and beam donor modelling - the current state. | Prof. H. P. Summers |
| 16.15 - 17.00: | <i>Module 6 Demonstration:</i> | Dr. M. O'Mullane & Dr. A. Giunta |
| 19 June 2013: | | |
| | | <i>Advanced thermal plasma modelling - atoms and molecules</i> |
| 9.00 - 9.30: | Molecules in the NIFS database | Prof. I. Murakami |
| 9.30 - 10.15: | <i>Module 3 Lecture:</i> H ₂ molecular emission and collisional-radiative modelling. | Prof. H.P. Summers |
| Coffee break | | |
| 10.45 - 11.30: | <i>Module 3 Demonstration:</i> | Dr. M. O'Mullane & Dr. A. Giunta |
| 11.30 - 12.00: | <i>Discussion</i> | |
| Lunch | | |
| <i>Spectral diagnostics at the fusion/astrophysics interface</i> | | |

| | | |
|----------------|--|----------------------------------|
| 13.30 - 14.15: | Spectral observations and analysis in the solar atmosphere. | Prof. T. Watanabe |
| 14:15 - 15.00: | <i>Module 8 Lecture:</i> Spectral diagnostics for special environments - the interface between fusion and astrophysics | Prof. H. P. Summers |
| Coffee break | | |
| 15.30 - 16.30: | <i>Module 8 Demonstration:</i> | Dr. M. O'Mullane & Dr. A. Giunta |
| 16.30 - 17.15: | <i>Discussion</i> | |

| | | |
|----------------|---|----------------------------------|
| 20 June 2013: | <i>Calculation of fundamental atomic data</i> | |
| 09.00 - 09.30: | The NIFS atomic database | Prof. I. Murakami |
| 09.30 - 10.00: | Atomic physics for highly charge ions | Dr. D. Kato |
| 10:00 – 10:45 | <i>Module 7 Lecture:</i> calculating fundamental atomic structure and electron impact cross-section data - Autostructure & R-matrix | Prof. H. P. Summers |
| Coffee break | | |
| 11:00 – 12:00 | <i>Module 7 Demonstration:</i> | Dr. M. O'Mullane & Dr. A. Giunta |

| | | |
|--|--|----------------------------------|
| 12:00 - 12.30: | <i>Discussion</i> | |
| Lunch | | |
| <i>Advanced thermal plasma modelling - atoms and molecules</i> | | |
| 14.00 - 14.30: | Spectroscopy of high Z elements | Dr. C. Suzuki |
| 14.30 – 15.00: | Collisional-radiative modelling for W ions | Dr. A. Sasaki |
| Coffee break | | |
| 15.30 - 16.15: | <i>Module 2 Lecture:</i> Complex species in the core and edge of the fusion plasma - the current state | Prof. H. P. Summers |
| 16.15 - 17.00: | <i>Module 2 Demonstration:</i> | Dr. M. O'Mullane & Dr. A. Giunta |
| 17.00 - 17.30: | <i>Discussion</i> | |

| | | |
|---------------|--|---------------|
| 21 June 2013: | <i>Impurity modelling and emission in the thermal plasma</i> | |
| 9.00 - 9.30: | Spectroscopy and impurity transport | Mr. H. Funaba |
| 9.30 - 10.00: | 2Dimensional spectroscopy for impurity study | Mr. E. Wang |
| Coffee break | | |

| | | |
|-----------------|---|----------------------------------|
| 10.30 - 11.00: | Impurity transport modeling in stochastic layer of LHD | Dr. M. Kobayashi |
| 11.00 -11.30: | CR modelling and spectra analysis | Dr. I. Murakami |
| Lunch | | |
| 13.30 - 14.15: | <i>Module 1 Lecture:</i> Impurity atomic species in fusion plasma, their ionisation state and radiating characteristics | Prof. H. P. Summers |
| 14.15 - 15.00.: | <i>Module 1 Demonstration:</i> | Dr. M. O'Mullane & Dr. A. Giunta |
| Coffee break | | |
| 15.30 - 16.00: | Diagnostic modelling for the ITER Conceptual design phase | Dr. M. O'Mullane |
| 16.00 - 17.00: | <i>Concluding discussion, future research collaboration and exchanges</i> | |

Participants

Appendix 1 : Meeting participant list

ADAS workshop (June. 17-21)

| Attendee | Affiliation | attending day | use of ADAS | research field |
|---------------------------|----------------------|-------------------|-------------|---|
| Masahiro Kobayashi | NIFS | | no | Impurity 2D/3D simulation |
| Chihiro Suzuki | NIFS | 20-21 | no | Spectroscopy for high Z elements |
| Hisamichi Funaba | NIFS | all | yes | spectroscopy & impurity transport |
| Yukio Nakamura | NIFS | partly | no | impurity transport study |
| Tomoaki Nogami | U. Tokyo | | yes | visible spectroscopy |
| Izumi Murakami | NIFS | all | yes | CR model / spectroscopy analysis |
| Daiji Kato | NIFS | all | no | atomic physics / spectroscopy analysis |
| Shigeru Morita or student | NIFS | (probably attend) | (yes) | spectroscopy (they use ADAS results for their analysis) |
| H. Wang | NIFS | all | | 2D spectroscopy for impurity study |
| Masaki Osakabe | NIFS | partly | yes | NBI (CXS) (Fast ion charge exchange spectroscopy) |
| Katsunori Ikeda | NIFS | partly | yes | NBI Optical meas. of neutral beam atten. in LHD |
| Shinji Kobayashi | Kyoto U. | except 20 | | NBI CXS |
| Takako Kato | NIFS(retired) | partly | yes | Helium-like Carbon studies after NBI |
| Tetsuya Watanabe | NAOJ | only 19 | no | solar spectroscopy (Hinode/EIS) |
| Hugh Summers | Univ. Of Strathclyde | | | |
| Martin O'Mullane | Univ. Of Strathclyde | | | |
| Alessandra Giunta | Univ. Of Strathclyde | | | |

1.1.3 KSTAR, Daejeon, South Korea: 22-15 July 2013

The third ADAS-EU visit took place at took place at KSTAR, National Institute for Fusion Science, Daejeon, Korea. The programme commenced with a welcome by Dr. Jong-Gu Kwak, Director of the KSTAR Research Centre.

Dr. Mi Young Song presented the work of the Data Centre for Plasma Properties (DCPP). The data Centre has moved from its location at NFRI Daejeon to a new Convergence Plasma Research Center in Gunsan City some 100 km to the West. Under the directorship of Dr. Jung-Sik Yoon, it has some 14 staff, divided between the Data, Simulation and Experimental groups. The Data Centre maintains good contacts with IAEA via the Data Centre Network and on IAEA CRPs , has many connections with Japan and participates in the EuropeanVAMDC project. Dr. Song is a regular participant in ADAS Workshops and courses.The Data Centre's activities have become very wide including heavy particle collisions, electron impact data reaction data with complex molecules (such as C4F8), complex chemical catabolic pathways for plasma technology and surface reactions. Measurements are made of total electron impact cross-sections with neutrals (using an electron beam into gas cell) and of dissociation cross-sections with a two electron beam experiment. The team also carries out data assessment such as electron impact excitation cross-sections and also of molecular reactions. Illustrations and discussions suggested a shifting periodic focus which meant that some assessed data (such as for He0) seemed outdated and derivative.The simulation group have implemented a 'Global Simulator' code, which is test calculation system with a simplified plasma model which can include chemical data. This model seemed more aimed at industrial processes than fusion plasmas.Later discussion with Dr. Song and Dr. Ko suggested that utilisation of Data Centre information was low and that access to ADAS (via a single IDL license on a DCPP workstation) was severely constraining for KSTAR. Prof. Summers felt that ADAS and the ADAS team could help in the focus and preparation of information for KSTAR analysis. However the impression was left of large management/administrative burdens which for the moment militates against this.

Dr. Won-Ha Ko, who leads the team exploiting charge exchange spectral emission measurements for plasma rotation and ion temperature. KSTAR is using a 100keV deuterium (heating) beam for diagnostic studies. the beam is modulated for passive emission subtraction and the 32 channel CXS system allows 5mm radial spatial resolution and 10msec temporal resolution. The system for toroidal rotation is operational and a system for poloidal rotation is in preparation. The studies were quite focussed on the link between rotation and temperature measurements and plasma behaviour, especially L-H transition and turbulence. The extraction of toroidal rotation speed and ion temperature from CXS signals was taken as 'read' without comment on error or precision. This seemed somewhat over-confident in so far as it was the sole (at present) heating beam which is used, which with chopping must give cause for concern that the background passive plasma is changing.The CXS measurements were on carbon ($n=8-7$) and deuterium was mentioned. Supplementary measurements included Ne fluctuations during ELM suppression using BES. Also CXS inferred rotation was contrasted with X-ray line measurement form the XICS system (measuring He-like argon).

Agenda

Appendix 1 : Meeting agenda and participant list



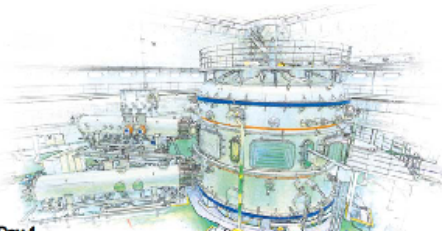
Mon 22 – Wed 24 July 2013
KSTAR Conference Room, National Fusion Research Institute, Daejeon, Korea

Mon 22 July 2013 – Workshop on ADAS and atomic physics for fusion

| Title | Time | Presenter | Affiliation |
|--|-------|----------------|---------------------------|
| Welcome | 09:20 | J.G. Kwak | NFRI |
| General introduction on behalf of the EU and EURATOM | 09:30 | M.G. O'Mullane | University of Strathclyde |
| Atomic physics research at NFRI | 10:00 | M.-Y. Song | NFRI |
| Observation of pedestal rotation and temperature from CVI impurity in H-mode KSTAR discharge | 10:30 | W.-H. Ko | NFRI |
| Coffee break | 11:00 | | |
| Plan for the carbon density profile measurement via charge exchange spectroscopy on KSTAR | 11:20 | H.H. Lee | NFRI |
| Lunch | 11:50 | | |
| Development of ITER VUV spectrometer and its application to impurity study in KSTAR plasmas | 13:20 | C. Seon | NFRI |
| Impurity transport research in KSTAR based on soft X-ray imaging and VUV spectroscopy | 13:50 | S. Lee | KAIST |
| Impurity transport analysis of 2012 KSTAR Ar transport experiment by UTC-SANCO code | 14:20 | J. Hong | KAIST |
| Coffee break | 14:50 | | |
| MSE spectrum simulations | 15:10 | G. Lange | TU/e |
| ADAS application for KSTAR MSE spectra | 15:40 | J. Ko | NFRI |
| Overview of ADAS and ADAS-EU principal scientific themes, objectives and relationships | 16:10 | H.P. Summers | University of Strathclyde |
| Adjourn | 16:55 | | |

(Continued to the next page)

ADAS-EU WATP – 20130722Mo

**Tue 23 July 2013 – Training courses on ADAS for fusion: Day 1**

| Title | Time | Lecturer | Demonstrators |
|--|-------|--------------|-----------------------------|
| Impurity atomic species in fusion plasmas, their ionization state and radiating characteristics – the ADAS approach | 09:00 | H.P. Summers | M.G. O'Mullane A. Giunta |
| Coffee Break | 10:30 | | |
| Complex species in the core and edge of the fusion plasma. Describing and calculating their characteristics – the state of the art | 10:50 | H.P. Summers | M.G. O'Mullane A. Giunta |
| Lunch | 12:20 | | |
| Spectral diagnostics for special environments – the interface between fusion and astrophysics | 13:20 | H.P. Summers | M.G. O'Mullane A. Giunta |
| Coffee Break | 14:50 | | |
| Charge exchange and beam emission spectroscopy. Modeling emitter populations and analyzing spectra | 15:10 | H.P. Summers | M.G. O'Mullane A. Giunta |
| Adjourn | 16:40 | | |

Wed 24 July 2013 – Training courses on ADAS for fusion: Day 2

| Title | Time | Lecturer | Demonstrators |
|--|-------|--------------|-----------------------------|
| CX with medium/heavy species. Advanced CX/beam models and data – the state of the art | 09:00 | H.P. Summers | M.G. O'Mullane A. Giunta |
| Coffee Break | 10:30 | | |
| Calculating fundamental atomic structure and electron impact cross-section data – Autostructure and R-Matrix | 10:50 | H.P. Summers | M.G. O'Mullane A. Giunta |
| Lunch | 12:20 | | |
| Collaborating, developing and knowledge pooling in atomic physics for the ITER era | 13:30 | | M.G. O'Mullane |
| Atomic studies for the conceptual design of ITER diagnostic | 13:45 | | M.G. O'Mullane |
| Coffee Break | 14:30 | | |
| Plasma modeling and atomic physics – a forward look. Individual contributions including needs from ADAS and useful avenues for ADAS-EU input | 14:50 | | M.-Y. Song J. Ko |
| Completion session | 15:50 | | H.P. Summers |
| Adjourn | 16:50 | | |

ADAS-EU WATP – 20130722Mo

Participants

Appendix 3: Email addresses of participants

| <u>Name</u> | <u>Institution</u> | <u>Email</u> |
|---|-----------------------------------|---|
| Dr. Won-Ha Ko | Nat. Fusion Res. Inst. | whko@nfri.re.kr jdfm@nfri.re.kr sseyoung@nfri.re.kr jamesjin@nfri.re.kr jmkwon74@nfri.re.kr jinseok@nfri.re.kr mysong@nfri.re.kr crseon@nfri.re.kr |
| Dr. Jae-Min Kwon | " | |
| Dr. Jinseok Ko | " | |
| Dr. Mi-Young Song | " | |
| Dr. Changrai Seon | " | |
| Mr. Joohwan Hong | Korean Adv. Inst. of Sci. & Tech. | leesh81@kaist.ac.kr joohwanhong@kaist.ac.kr ijwkim@kaist.ac.kr yunseong007@kaist.ac.kr zmal0103@kaist.ac.kr lee0816@kaist.ac.kr |
| Dr. Woochang Lee | Pohang Univ. of Sci. & Tech. | woochanglee@postech.ac.kr |
| Mr. Guido Lange | Tech. Univ. of Eindhoven | a.g.g.lange@student.tue.nl ong.henry@gmail.com |
| Prof. Hugh Summers Dr. Martin O'Mullane Dr. Alessandra Giunta | Univ. of Strathclyde | summers@phys.strath.ac.uk Martin.OMullane@ccfe.ac.uk alessandra.giunta@stfc.ac.uk |

1.1.4 ASDEX, IPP Garching, Germany

The fourth ADAS-EU visit took place at took place at Max-Planck-Institute for Plasma Physics, Garching, Germany. ADAS-EU presentations followed the sequence given in the agenda, however there was extended discussion both during the presentations, following the presentations and during coffee breaks. Some of these are highlighted in the following paragraph.

Lower energy extension of ion/atom collision date for halo contributions and so on. Pointed out exo/endo thermicity and threshold behaviour. Offer to follow up (Benedikt Geiger) .He0 populations in beams and as a source for fast particles. Harvey Anderson and my work for bmsii paper - draft passed over; issues of singlet and triplet systems, Stark effect and spin system breakdown. Questions of He+ populations structure as fast /slowing down species. Atomic data for this especially ion impact - use ion/ion collision capability of IP method - fetch out abd test from ADAS fortran subroutine libraries. (Athina Kappatou and Dr. McDermott). Questions of variation of nitrogen state selective charge exchange - Katharina, older unattributed ADAS nitrogen data set (Lorne Horton and my interpolation). Produced new nitrogen adf01 from universal formulation. Erratic behaviour in some of the datasets, strange alpha parameters, doubt of how alpha produced - including normalisation to total, extrapolation, discard of last n in close coupled calculations and consistency of alpha from nlast, nlast-1, nlast-2 and nlast-3. (Dr. Putterich, Dr McDermott). Issues of l-substate capture. Possibility of using the inverse matrix method for testing cross-sections but cast investigation onto the l-parametric form. Discussion of opacity/non-Maxwellians/DEM opportunities in tokamaks. Difficult task for spectroscopic systems (Dr. Dux, Dr. Putterich, Dr McDermott). Prof. Summers, Dr. Schweinzer and Dr McDermott examined the issues for continuation and further validation of the supercomputer-based CCAO model by Katharina Igenbergs. Katharina has left the field and, although a project student at TUW is working with the code, it appears that the long-term detailed extension, validation and development is Vienna is uncertain. The primary interest of the Vienna group is in experimental physics. Dr. Schweinzer felt that the code required more work and evaluation, since the nitrogen and argon results were generated quite close to the end of Katharina's thesis write-up. A useful task, which he wished to carry, out is rerunning of his original code on the nitrogen case for some cross-checking. Prof. Summers expressed his great interest in assuring and exploiting the code and pointed out that he had a new PhD student (Matthew Bluteau) beginning in October 2013. Prof. Summers intention is for this student to work in the advanced, zero-order Stark picture of beam emission and follow also the complementary advanced (heavier species) charge exchange emission modelling. Matthew comes with strong credentials and indications of high level computing ability. Prof. Summers speculated that, with the agreement of Dr. Schweinzer and Prof. Aumayr, he could assign Matthew to the CCAO continuation in close collaboration with and oversight from IPP and Vienna - including Matthew spending substantial time at IPP. Dr. Schweinzer was positive about such a step and agreed to raise the matter with his colleagues in Vienna. Prof. Summers pointed out that Matthew would spend an initial six months or so in Scotland at the Physics Department under the guidance of colleagues Prof. Badnell and Dr. Menchero - to bring him up to speed in atomic physics and computational collision physics. Then Matthew would be based at the JET Facility for the rest of his PhD, with Prof. Summers and Dr. O'Mullane. Depending on the reaction of Prof. Aumayr and the Vienna team, Prof. Summers will prepare a plan and time-line.

Agenda

Appendix 2 : Agenda

It was agreed, in the light of the longstanding connection between IPP participants and the ADAS/Univ. of Strathclyde/JET team, that the meeting should be quite informal with a relaxed schedule. In place of the full overview talk presented at other locations, Professor Summers gave a short summary of the ADAS-EU themes, special sub-contracts and the WATC presentations at other sites in-so-far as they bore upon IPP interests. Prior to the meeting, an initial list of expected topics for discussion was prepared included (a) Effect of W-lines on visible spectra; (b) What CXRS data is trustworthy, why and how to produce trustworthy data; (3) New features concerning molecules – how to proceed. In practice, discussion was largely focussed on (b), atomic data for fast ion modelling, the complexities of helium beams and fast ion products and added measures necessary to secure the quality of state selective charge transfer data. There was no discussion on molecules.

Mon. 9 Sep. 2013

| | | |
|---------------|--------------------|--|
| 8.45 - 9.00 | Brief introduction | Hugh Summers Highlights of ADAS-EU: principal theme and associated data developments; sub-contract results. |
| 9.15 - 10.00 | Module 1 | Hugh Summers Impurity atomic species in fusion plasma, their ionisation state and radiating characteristics |
| 10.00 - 10.45 | Demonstrations | Martin O'Mullane & Alessandra Giunta |

BREAK

| | | |
|---------------|----------|---|
| 11.15 - 12.15 | Module 2 | Hugh Summers Complex species in core and edge of the fusion plasma: Describing and calculating their characteristics - the current state |
|---------------|----------|---|

LUNCH BREAK

| | | |
|---------------|----------------|---|
| 13.30 - 14.15 | Demonstrations | Martin O'Mullane & Alessandra Giunta |
| 13.30 - 14.15 | Module 8 | H.P. Summers Spectral diagnostics for special environments – the interface between fusion and astrophysics |
| 14.15 - 15.00 | Demonstrations | Martin O'Mullane & Alessandra Giunta |

DISCUSSIONS

Tue. 10 Sep. 2013

| | | |
|--------------|----------------|--|
| 8.45 - 9.30 | Module 5 | Hugh Summers Charge exchange and beam emission spectroscopy. Modelling emitter populations, beam stopping and analysing spectra |
| 9.30 - 10.15 | Demonstrations | Martin O'Mullane & Alessandra Giunta |

BREAK

| | | |
|---------------|----------------|---|
| 10.30 - 11.15 | Module 6 | Hugh Summers Advanced charge exchange plasma receiver and beam donor modelling - the current state |
| 11.15 - 12.00 | Demonstrations | Martin O'Mullane & Alessandra Giunta |

LUNCH BREAK

| | | |
|---------------|---------------------|--------------|
| 13.30 - 14.15 | Module 7 (optional) | Hugh Summers |
|---------------|---------------------|--------------|

Calculating fundamental atomic structure and electron impact cross-section data -
Autostructure and R-matrix

14.15 - 15.00 Demonstrations Martin O'Mullane & Alessandra Giunta

rest of the day and Wednesday: DISCUSSIONS(in small working groups if desired)

Participants

Appendix 1 : Meeting participant list

| Participant | Affiliation | Email address | Special interests |
|-------------------|----------------|-----------------------------------|---|
| Ralph Dux | IPP | ralph.dux@ipp.mpg.de | Team leader |
| Thomas Pütterich | IPP | Thomas.Puetterich@ipp.mpg.de | Charge exchange and heavy species |
| Rachael McDermott | IPP | Rachael.McDermott@ipp.mpg.de | Impurity behaviour using charge exchange spectroscopy - CHEAP |
| Josef Schweinzer | IPP | josef.schweinzer@ipp.mpg.de | State selective charge transfer calculation for impurities |
| Benedikt Geiger | IPP | benedikt.geiger@ipp.mpg.de | FIDA |
| Eleonora Viezzer | IPP | elv@ipp.mpg.de | |
| Athina Kappatou | FOM Rijnhuizen | A.Kappatou@rijnhuizen.nl | Helium beams and FIDA |
| Livia Casali | IPP | livia.casali@ipp.mpg.de | |
| Marco Cavedon | IPP | mcavedon@ipp.mpg.de | |
| Tomas Odstrcil | IPP | tomas.odstrcil@ipp.mpg.de | |
| Felix Reimold | IPP | flr@ipp.mpg.de | |
| Alexander Lebschy | IPP | Alexander.Lebschy@ipp.mpg.de | |
| Markus Weiland | IPP | Markus.Weiland@ipp.mpg.de | |
| Gerd Meisl | IPP | gmeisl@ipp.mpg.de | |
| Hugh Summers | ADAS | summers@phys.strath.ac.uk | Nitrogen cooling in the divertor |
| Martin O'Mullane | ADAS | martin.omullane@phys.strath.ac.uk | |
| Alessandra Giunta | ADAS | alessandra.giunta@stfc.ac.uk | |

1.1.5 ITER/CEA Cadarache, France

The fifth ADAS-EU visit took place at Cadarache, France. There was a special request for an overview presentation at ITER itself as a forum where senior management staff from the Diagnostics (CODAC) and Plasma Operation (POP) teams could discuss future needs and intentions with the ADAS/ADAS-EU team. The introductory talk for ADAS-EU WATC was prepared in a special form, suited to the interests of ITER and included considerations of the long-term support of ADAS at ITER. The talk was presented at ITER in the afternoon of 18 Sep. The remainder of the ADAS-EU visit took place at CEA Cadarache. The participation at CEA meeting was the lowest of the whole set of ADAS-EU visits. The current shutdown of TORE-SUPRA for the WEST modification (W Environment in Steady-state Tokamak), means that at this time diagnostic activity with PhD and postdoctoral research staff is at a low point.

At ITER, there was varied discussion on the scientific content of the talk, especially on charge transfer and atomic data for transport models, raised by Dr. Von Hellermann and Dr Kukushkin respectively. Dr. von Hellermann, noted the very many tungsten CX lines in the visible spectral range. Although appearing as a below bremsstrahlung quasi-continuum feature, he pondered if in practice, because of the high resolution of visible spectrometry, the individual lines could be predicted with sufficient accuracy for direct modelling. Prof. Summers again noted the below bremsstrahlung level of signals, but did believe that precision wavelengths could be given by the ADAS codes. Dr Kukushkin commented that although superstages seemed to work well for radiated power when enabled in 2-d transport models (especially SOLPS), he understood that it was less good for the individual shell transport themselves, citing the explicit SOLPS calculation occupying very many months carried out by Dr. Coster. Prof. Summers had no detail on this, but believed that very gross superstaging had been used for tests at JET and probably for SOLPS. He stressed that considerably more sophistication was possible in the superstage concepts (such as accelerated and retarded solutions), but that the stability of extremely long SOLPS calculation for all tungsten ions would also need to be validated.

Attendance was principally by senior staff at ITER concerned with on-going support in atomic physics for ITER from ADAS. Subsequent discussion centred on this area. Dr. Barnsley noted the usefulness of ADAS in the conceptual design phase of spectrometers. The role of Dr. O'Mullane in providing expert support in ADAS use for the Domestic Agency design teams (especially Korea and India) was noted. He anticipated the need for even more of this in the full design stage. Dr. Pitts recognised the key role of ADAS at this stage in edge modelling and sought both extension of ADAS scope and reassurance on the long term continuation of ADAS. Prof. Summers drew attention to the molecular extension of ADAS in the series 9 codes and repeated the very large build up of strength in ADAS for very heavy species. Although ADAS would remain a system for modelling and diagnosing the radiating characteristics of species in the plasma phase (not on/in surfaces), Prof. Summers was confident of its capacity for full coverage of all ITER needs in the plasma phase and that ADAS extensions towards opacity, non-Maxwellians and double-differential DEM were already well ahead of current usages, but relevant to ITER. Dr. Walsh and Dr. Pitts addressed the issue of long-term staffing of ADAS, especially in the light of Prof. Summers age. Prof. Summers said that planning for the long term continuation of ADAS and its staffing was part of the ADAS-EU brief. He had already had discussion with the Principal, Dean of Science and Head of Physics at Strathclyde to assess their views. Also he had sought views from the Directors of CCFE and the EFDA-JET Facility, and from the scientific officers at the European Commission. All are supportive, although clearly a business plan, the setting up of suitable staff positions at the University and the availability of suitably experienced persons to fill them would all be essential for a long term future. Prof. Summers outlined his current thinking on these matters. He will prepare a final document for ADAS-EU on this after the concluding, summative ADAS-EU Workshop and Advanced Training Course at the JET Facility - 30 Sep. - 3 Oct. 2013. He hoped that useful discussion and ideas would be brought forward at that meeting and encouraged input from ITER to it. Prof. Summers indicated that he would be prepared to stay on part-time for up to two years to assist in preparing the plan and, if it is acceptable to all interested parties, to put it into action.

At CEA, the detailed ADAS-EU course modules were presented on 18 and 19 Sept at CEA Cadarache, hosted by Dr. Guirlet. Modules, excluding those on charge transfer and beams, were presented to a small set of interested persons. Dr. Guirlet said that the present long two-year shut down of Tore Supra, and hence low numbers of PhD and postdoctoral students at CES, accounted for the small numbers. The pedagogical aspects of the lecture presentations were considered helpful for the non-specialist and for PhD students. Prof. Summers pointed out that he had more extended lecture notes for the base modules 1, 5 and 8 which he would make available. There were detailed discussions on the H₂ molecular collisional-radiative modelling. Dr. Guzman presented a draft talk on further advances in the model, including additions to the ion impact database, photon efficiencies and the role of ion impact on vibrational

sub- structure populations. Prof. Summers was surprised by the magnitude of the effects of ion impact on ground state vibrational populations. It was felt such complicated models required further checking and consideration would be given to this in the run up to the final meeting at JET. Dr. Guzman and Prof. Summers would work on this together.

Agenda

Appendix 2 : Agenda

It was agreed, in the light of the longstanding connection between CEA participants and the ADAS/Univ. of Strathclyde/JET team, that the meeting should be quite informal with a relaxed schedule. In view of the full overview talk presented at ITER the previous day, it was agreed that Professor Summers would begin immediately on the core modules and that interjection and discussion during the presentations were encouraged.

Thu. 19 Sep. 2013

9.15 - 10.00 Module 1 Hugh Summers
Impurity atomic species in fusion plasma, their ionisation state and radiating characteristics

10.00 - 10.45 Demonstrations Martin O'Mullane & Alessandra Giunta

BREAK

11.15 - 12.15 Module 2 Hugh Summers
Complex species in core and edge of the fusion plasma: Describing and calculating
their characteristics - the current state

LUNCH BREAK

13.30 - 14.15 Demonstrations Martin O'Mullane & Alessandra Giunta

13.30 - 14.15 Module 8 H.P. Summers
Spectral diagnostics for special environments – the interface between fusion and
astrophysics

14.15 - 15.00 Demonstrations Martin O'Mullane & Alessandra Giunta

DISCUSSIONS

Fri. 20 Sep. 2013

9.30 - 10.15 Module 7 Hugh Summers
Calculating fundamental atomic structure and electron impact cross-section data -
Autostructure and R-matrix

BREAK

10.30 - 11.15 H₂ CR modelling extension Francisco Guzman
Ion impact, cross-section additions. The state of production of photon efficiencies .
Checks on vibrationally resolved (GCR) and unresolved (CR) populations and
coefficients.

11.15 - 12.00 Discussions

LUNCH BREAK

13.30- 14.30 Final discussion and ADAS support matters for attention

Participants

Appendix 1 : Meeting participant list

| Participant | Affiliation | Email address | Special interests |
|------------------------|--------------------|---------------------------------------|---|
| Michael Walsh | ITER | Michael.Walsh@iter.org | Head of Division, Diagnostics Division |
| Robin Barnsley | ITER | Robin.Barnsley@iter.org | Section Leader, Ex-Vessel Diagnostics Section |
| Richard Pitts | ITER | Richard.Pitts@iter.org | Section Leader, Divertor and Plasma-Wall Interactions Section |
| Andre Kukushkin | ITER | Andre.Kukushkin@iter.org | ITER consultant - theory |
| Manfred von Hellermann | ITER | M.G.V.vonHellermann@differ.nl | ITER consultant - charge exchange |
| * three others * | ITER | | |
| Remy Guirlet | CEA | remy.guirlet@cea.fr | Section Leader, spectroscopy |
| Francisco Guzman | Univ. of Marseille | francisco.guzmanfulgencio@univ-amu.fr | Research, CR-modelling of H ₂ |
| * three others * | CEA | | |
| Hugh Summers | ADAS | summers@phys.strath.ac.uk | |
| Martin O'Mullane | ADAS | martin.omullane@phys.strath.ac.uk | |
| Alessandra Giunta | ADAS | alessandra.giunta@stfc.ac.uk | |

1.1.6 EFDA-JET Facility Culham Laboratory, Abingdon, UK

The sixth ADAS-EU visit took place at The EFDA-JET Facility, Culham Laboratory, UK. The ADAS-EU workshop at EFDA-JET was just outside the funding period of the project. Also, the ADAS-EU staff, who stayed together to present this meeting, incurred no travel costs since they are local to Culham Laboratory. Nonetheless, the information on the workshop is presented here the form of a travel report paralleling the other five ADAS-EU visits. Participants at the meeting included University experts from Belgium, Rumania and Scotland who had contributed special fundamental atomic data to ADAS and ADAS-EU. External participants from Griefswald, Brussels and Cadarache connected via the broadcast system.

The introductory talk by Dr. Lorne Horton began by summarising the long ADAS engagement with JET. Dr. Horton then reviewed the EP2 upgrade to JET and its timeline. He placed particular emphasis on the beryllium and tungsten components of the ITER-like wall and impurity seeding as aspects which raised many questions for atomic modelling and ADAS. He looked to the continuation of ADAS and its atomic rigour with the new generation of young scientists. Dr. Lars-Goran Eriksson summarised the ADAS-EU project from the EU Commission's perspective with some details of the objectives, themes, work packages and deliverables. He then talked in more depth of ADAS integration into the Integrated Tokamak Modelling Task Force framework. He emphasised the modular and flexible simulation platform, the interlinks which connected atomic, molecular and nuclear data to it and then explored some of the workflows and how ADAS atomic data entered into them. Dr. Eriksson final slides discussed the evolution of the Commission's support mechanism for fusion in Europe fom FP7 to Horizon 2020. He drew attention to the need to ADAS to forge new links with the Consortium of National Fusion Institutional participants. Dr Mike Walsh began by bringing the audience up-to-date with the state of construction of ITER and it mission objectives. He then turned to the general diagnostic need and the circa forty-five systems intended to provide for these needs. He then focussed on spectral diagnostic measurement needs, the systems required to fulfill these needs and their locations around the ITER vessel. In one illustrative case, he explored the implementation of the diagnostic system in a port plug. He then turned to the atomic modelling being used by ITER for the conceptual design of some of the visible and UV spectroscopy with substantial engagement of ADAS and associated codes such as SANCO. Further illustrations included the edge charge exchange and MSE diagnostics. Presenting the time-line for ITER, he emphasised the part ADAS had played and the wish for ADAS to continue its role effectively in the future. Prof. Summers then presented an overview of ADAS and ADAS-EU as a prelude to the in- depth lectures and demonstrations to follow in the subsequent two days.

The module lectures were presented by Prof. Summers and the active demonstrations by Dr. O'Mullane and Dr. Giunta. There were supplementary talks in the molecular module by Porf. Behringer and Dr. Guzman. In the special feature module, Dr. Meigs gave an engrossing demonstration of how to make the AFS/FFS system work in spectral analysis which provoked and enthusiastic responses and queries from the audience.

The main wish list for ADAS at JET was presented on the last morning under the chairmanship of Dr. Zastrow, including an extended contribution from Dr. Brezinsek. Dr. Morris drew discussion together and worked to assemble a forward looking summary.

Agenda

ADAS-EU: Final meeting and special workshop

Location: HOW room, JET Facility, Culham Laboratory

Date: 30 Sep 2013 - 3 Oct 2013

Summary: The ADAS-EU Euratom - Framework 7 Support Action of the European Community commenced on 1 Jan 2009 and terminates on 30 Sep 2013. ADAS-EU in association with the ADAS Project has maintained atomic physics capabilities, developed new aspects and sought to anticipate future needs as required for fusion in Europe and for ITER. To disseminate and inform on these developments, ADAS-EU during the Spring and Summer of 2013 has sponsored special workshop/ advanced training courses at fusion laboratories across the world. This last meeting and workshop is the summative and concluding one.

The first half-day session is introductory, including an overview of the scope, principal themes and successes of ADAS-EU. The following four half-day sessions examine in detail the current state of the ADAS-EU scientific themes, reflected in and accessible through ADAS. There are eight modules of one and a half hours duration, each comprising a 45 minute lecture, presented by Prof. Hugh Summers and a 45 minute active ADAS demonstration, presented by Dr. Martin O'Mullane and Dr. Alessandra Giunta. For some of the modules, the demonstration session includes a short special update talk by an ADAS-EU associated expert. The final half-day session will seek to draw together opportunities and suggestions for on-going collaborative work on atomic physics within the framework of the ADAS Project, cooperation in Europe and engagement with ITER and ITER participant countries. It will also seek suggestions and opinion on the long-term profile of ADAS.

Arrangements: The meeting has fusion and astrophysics relevance and is open. All are welcome. The meeting will be broadcast with remote participation. Coffee will be available between sessions.

H.P. Summers
18 Sep 2013

General Agenda

30 Sep 2013:

| | | |
|----------------|---|-------------------------|
| 14.00 - 14.30: | Welcome | Dr. Lorne Horton |
| 14:30 - 15.00: | General introduction on behalf of the EU and Euratom. | Dr. Lars-Goran Eriksson |
| 15:00 - 15.30: | Atomic physics and the ITER perspective. | Dr. Mike Walsh |

Coffee break

| | | |
|----------------|--|---------------------|
| 16.00 - 16.45: | Overview of ADAS and ADAS-EU principal scientific themes, objectives and relationships | Prof. H. P. Summers |
|----------------|--|---------------------|

1 Oct 2013:

| | | |
|----------------|--|-----------------------------------|
| 08.45 - 09.30 | Module 1: Impurity atomic species in fusion plasma, their ionisation state and radiating characteristics. | Prof. H. P. Summers |
| 09.30 - 10:15: | <i>Demonstrations</i> | Dr. M. G. O'Mullane/Dr. A. Giunta |

Coffee break

| | | |
|----------------|--|-----------------------------------|
| 10.30 - 11.15: | Module 2: Complex species in core and edge of the fusion plasma: Describing and calculating their characteristics - the current state. | Prof. H. P. Summers |
| 11:15 - 12.00: | <i>Demonstrations</i> | Dr. M. G. O'Mullane/Dr. A. Giunta |

Lunch

| | | |
|----------------|---|-----------------------------------|
| 13.00 - 13.45: | Module 8: Spectral diagnostics for special environments - the interface between fusion and astrophysics. | Prof. H. P. Summers |
| 13.45 - 14.30: | <i>Demonstrations</i> | Dr. M. G. O'Mullane/Dr. A. Giunta |

Coffee break

| | | |
|----------------|---|---------------------|
| 14.45 - 15.30: | Module 7: Calculating fundamental atomic structure and electron impact cross-section data - Autostructure and R-matrix | Prof. H. P. Summers |
|----------------|---|---------------------|

| | | |
|---------------------|--|--|
| | | |
| 15.30 - 16.15: | <i>Demonstrations</i> <i>Special presentation (Update on R-matrix & Autostructure)</i> | Dr. M. G. O'Mullane/Dr. A. Giunta Prof. N. R. Badnell |
| 16:15 - 16.30: | Question and answer session | Prof. H. P. Summers/ Dr. M. G. O'Mullane/Dr. A. Giunta |
| 2 Oct 2013: | | |
| 08.45 - 09.30: | Module 5: Charge exchange and beam emission spectroscopy. Modelling emitter populations, beam stopping and analysing spectra. | Prof. H. P. Summers |
| 09.30 - 10.15: | <i>Demonstrations</i> | Dr. M. G. O'Mullane/Dr. A. Giunta |
| <i>Coffee break</i> | | |
| 10.30 - 11.15: | Module 6: Advanced charge exchange plasma receiver and beam donor modelling - the current state | Prof. H. P. Summers |
| 11:15 - 12:00: | <i>Demonstrations</i> | Dr. M. G. O'Mullane/Dr. A. Giunta |
| Lunch | | |
| 13.00 - 13.45: | Module 3: H ₂ molecular emission and collisional-radiative modelling. | Prof. H. P. Summers |
| 13.45 - 14.30: | <i>Demonstrations</i> <i>Special presentation (JET H₂ spectra)</i> <i>Special presentation (Update on H₂ vibronic modelling)</i> | Dr. M. G. O'Mullane/Dr. A. Giunta Prof. K. H. Behringer Dr. Francisco Guzman |
| <i>Coffee break</i> | | |
| 14.45 - 15.30: | Module 4: modelling and analysing spectral features - a unified approach. | Prof. H. P. Summers |
| 15.30 - 16.15: | <i>Demonstration</i> <i>Special presentation (JET spectral series)</i> | Dr. M. G. O'Mullane/Dr. A. Giunta Dr. A. Meigs |
| 16:15 - 16.30: | Question and answer session | Prof. H. P. Summers/ Dr. M. G. O'Mullane/Dr. A. Giunta |

| | | |
|-----------------|---|------------------------------------|
| 3 Oct 2013: | Shaping ADAS for the future | |
| 08.45 - 09.00: | Initial remarks and guidance for the discussions | Dr. K-D Zastrow (Session chairman) |
| 09.00 - 10.00: | Experimental spectroscopy/ modelling/analysis - what do we need from ADAS? What are the opportunities for collaboration? | Discussion led by Dr. S. Brezinsek |
| 010.00 - 11.00: | What should the ADAS profile be through to ITER and how should it staffed and resourced? | Discussion led by Dr. W. Morris |
| Coffee break | | |
| 11.15 - 12.00: | Completing remarks (Summary of the workshop/course opinions, thoughts and the next steps) | Prof. H. P. Summers |

THE END

Module contents

- Module 1: preliminaries and nomenclatures; basic population structure in plasmas; reaction processes and their description; ADAS population and ionisation state modelling; conclusions.
- Module 2: preliminaries; the whole atom, truncation, collisionality and top-up; ionisation state, partitions, condensations and superstages; supplementary modelling for dielectronic recombination, ionisation and impurity influx; conclusions.
- Module 3: preliminaries and nomenclatures; the molecular H₂ database; vibronic collisional-radiative modelling; rovibrational spectral simulation and comparison; conclusions.
- Module 4: preliminaries and nomenclatures; ADAS special features - application programming interface (API) and AFG; ADAS605; combination of functions for spectral fitting - FFS; conclusions.
- Module 5: preliminaries; modelling populations and emission following charge transfer; charge exchange spectroscopy, modelling beam stopping and emission; integrated analysis; conclusions.
- Module 6: charge exchange data for medium-weight and heavy receiver ions; extending population models for medium-weight receivers; exact Stark atom representations and field ionisation; collisions, directionality and orientation; conclusions.
- Module 7: preliminaries; atomic structure and collision cross-sections with the COWAN code; atomic structure and collision cross-sections with the AUTOSTRUCTURE code; mass production of data with scripts; collision cross-sections with the R-matrix code; conclusions.
- Module 8: introduction; emissivities, line-ratio studies and contribution functions; differential emission measure (DEM) analysis; escape probabilities and opacity; non-Maxwellian electron distributions; conclusions.

Participants

Participants: ADAS-EU concluding meeting 30 Sep - 3 Oct 2013

| Name | Email address | Affiliation |
|----------------------------|---------------------------------------|---|
| Dr. Lars-Goran Eriksson | Lars-Goran.ERIKSSON@ec.europa.eu | EURATOM, EU Commission, Brussels |
| Prof. Gerry Doyle | jgd@arm.ac.uk | Armagh Observatory, Northern Ireland |
| Dr. Patrick Palmeri | patrick.palmeri@umons.ac.be | Mons-Hainaut University, Belgium |
| Dr. Pascal Quinet | Pascal.QUINET@umons.ac.be | Mons-Hainaut University, Belgium |
| Dr. Viorica Stancalie | viorica.stancalie@inflpr.ro | INFLPR, Bucharest, Romania |
| Prof. Nigel Badnell | badnell@phys.strath.ac.uk | University of Strathclyde, Glasgow |
| Dr. Francisco Guzman | francisco.guzmanfulgencio@univ-amu.fr | CEA Cadarache, France |
| Mr. Matthew Bluteau | matthew.bluteau@gmail.com | University of Strathclyde, Glasgow |
| Dr. Jaime Suarez | jaime.suarez@uam.es | University Autonoma, Madrid, Spain |
| Prof. Kurt Behringer | behringer@ipp.mpg.de | IPP Garching, Germany |
| Dr. Michael Walsh | Michael.Walsh@iter.org | ITER, France |
| Dr. Lorne Horton | Daihong.Zhang@ipp.mpg.de | EFDA-JET, JET Facility, Culham Laboratory |
| Dr. William Morris | Lorne.Horton@jet.efda.org | CCFE Culham Laboratory |
| Dr. K-D. Zastrow | Klaus-Dieter.Zastrow@ccfe.ac.uk | CCFE Culham Laboratory |
| Dr. Andrew Meigs | Andrew.Meigs@ccfe.ac.uk | CCFE Culham Laboratory |
| Dr. Daihong Zhang | | IPP Griefswald, Germany |
| Dr. Knut Thomsen | Knud.THOMSEN@ec.europa.eu | EURATOM, EU Commission, Brussels |
| Dr. Robin Barnsley | Robin.Barnsley@iter.org | ITER, France |
| Dr. Nick Hawkes | Nick.Hawkes@ccfe.ac.uk | CCFE Culham Laboratory |
| Dr. Mike Stamp | Mike.Stamp@jet.uk | CCFE Culham Laboratory |
| Dr. James Harrison | James.Harrison@ccfe.ac.uk | CCFE Culham Laboratory |
| Dr. Sheena Menmuir | sheena@atom.kth.se | CCFE Culham Laboratory |
| Dr. Remy Guirlet | remy.guirlet@cea.fr | CEA Cadarache |
| Dr Oleksandr Marchuk | o.marchuk@fz-juelich.de | Fz-Juelich, Germany |
| Dr. Neil Conway | Neil.Conway@ccfe.ac.uk | CCFE Culham Laboratory |
| Dr. Ruth | | STFC Space Science Division |
| Dr. Manfred von Hellermann | M.G.V.vonHellermann@differ.nl | FOM Rijnhausen |
| - five others - | | CCFE Culham Laboratory/JET |
| - two others - | | IPP Griefswald, Germany |
| Prof. Hugh Summers | summers@phys.strath.ac.uk | University of Strathclyde, Glasgow |
| Dr. Martin O'Mullane | martin.omullane@phys.strath.ac.uk | University of Strathclyde, Glasgow |
| Dr. Alessandra Giunta | alessandra.giunta@stfc.ac.uk | University of Strathclyde, Glasgow |

The requirements of the work packages have been met.

1.2 Work package 29-1, 29-2, 29-3, deliverable DISSEM4 and milestone DSM4

The work package task comprises the preparation of this report.

Appendix A

ADAS-EU WATC: Introductory presentations

A.1 Welcome on behalf of EFDA-JET - Dr. Lorne Horton



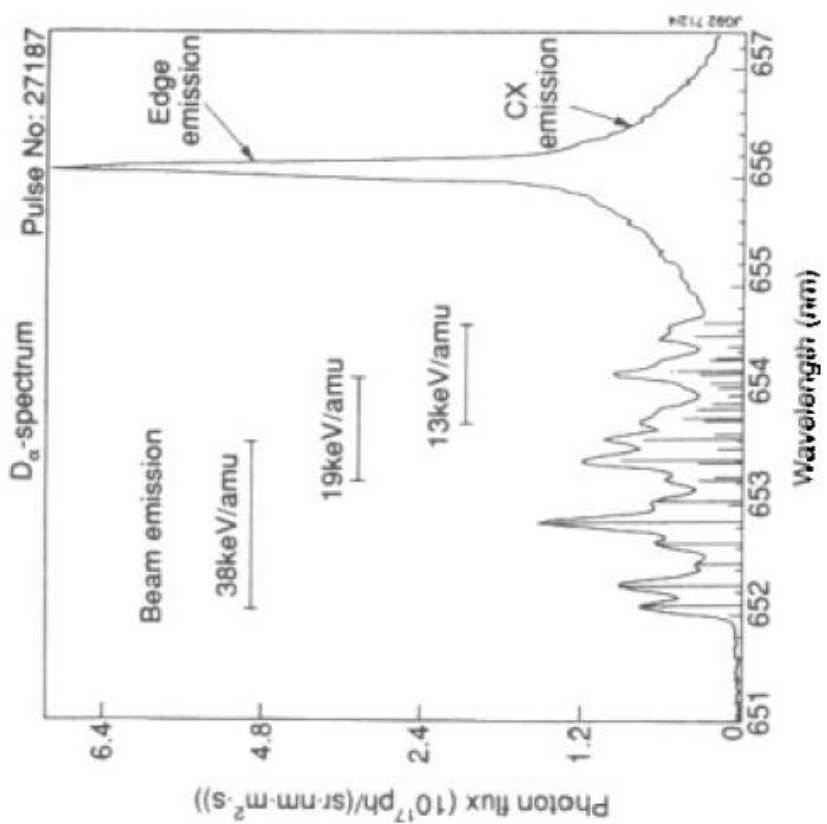
ADAS-EU: Final Meeting and Special Workshop

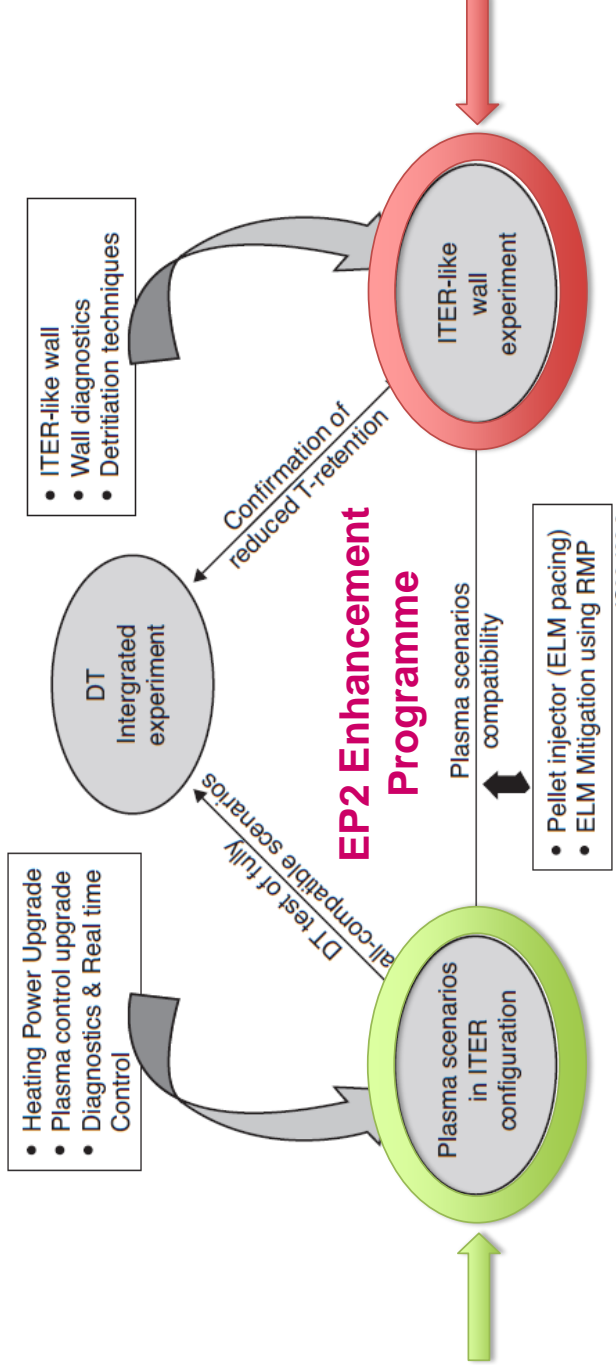
Welcome

*Lorne Horton
Head of EFDA JET Department*

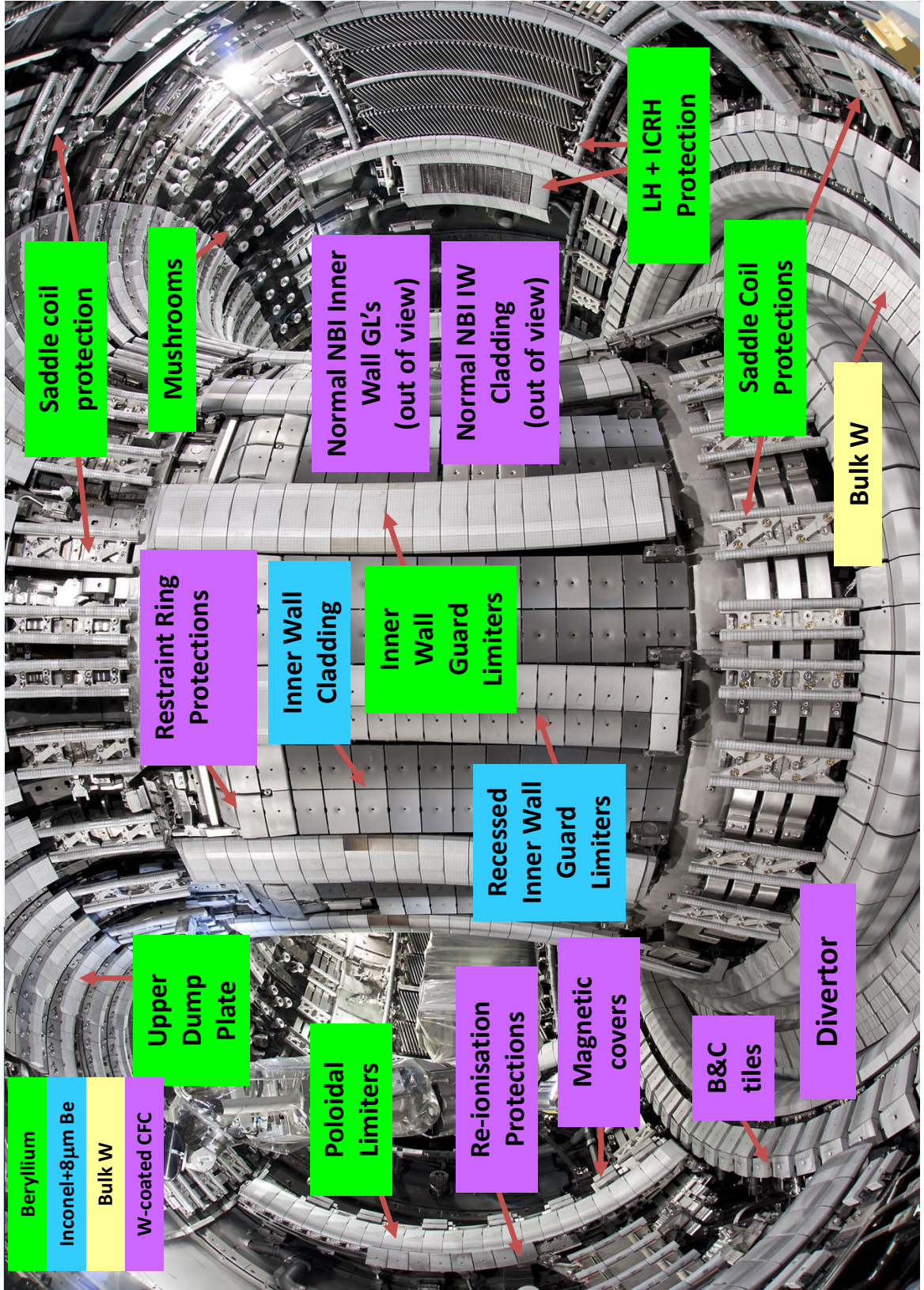


- ADAS has had a long and (very) successful association with JET
- The strength of the project, in my opinion, is its firm basis on experimental measurement and interpretation
- With this philosophy, it has been possible to focus scarce resources on important fusion problems and to bring to bear expertise in the atomic physics community that would otherwise not have been available





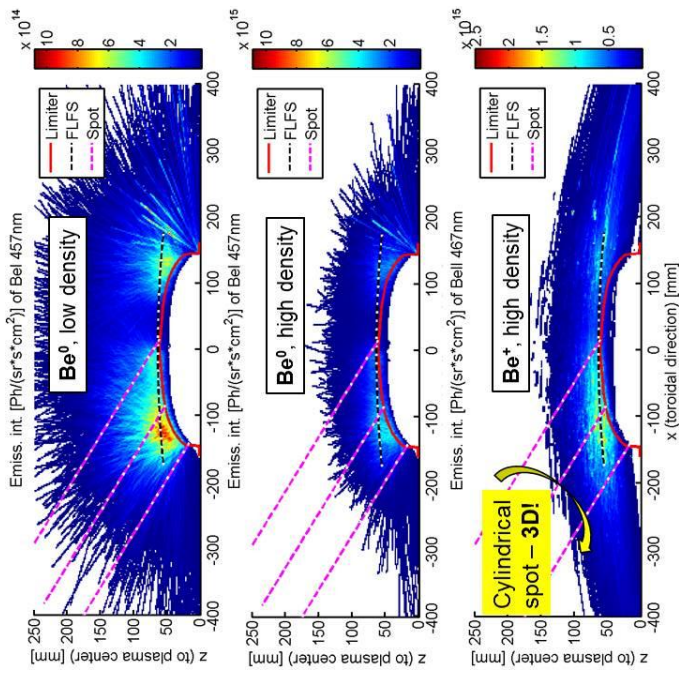
- **Phase 1: 2011-2012 (Deuterium Operation)**
“Full Characterisation of the *ITER-like Wall*”
- **Phase 2: 2013-2015 (Deuterium* Operation)**
“Expansion of *ITER Regimes of Operation*”
- **Phase 3: 2017**
“Deuterium-Tritium Campaigns”



ILW = 2880 installable items, 15828 tiles (~2 tonnes Be, ~2 tonnes W)

Be Erosion Studies

Be first wall material qualification: -
erosion and Be PFC life time
- power load capability

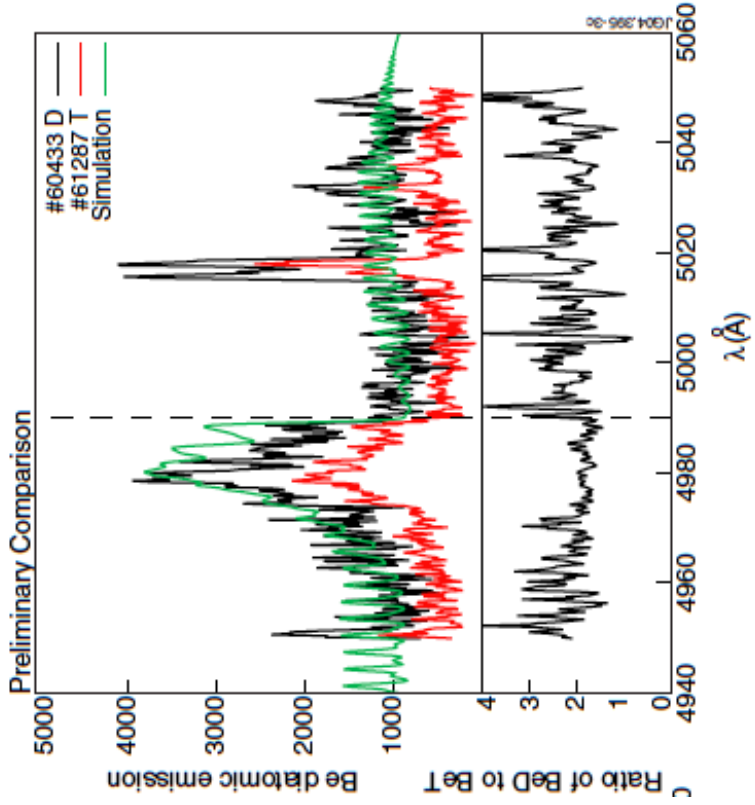


- Be erosion modelling and atomic data (steady-state) (**also molecular data (BeD / BeT)?**)
- Be erosion by transients (**kinetic effects? Do we need to go back to cross sections?**)
- Be re-erosion and transport to remote areas (**metastable states?**)



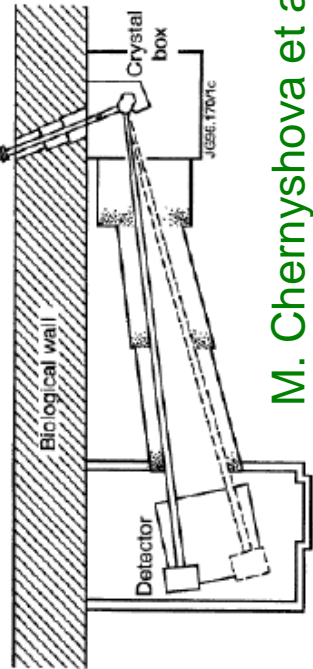
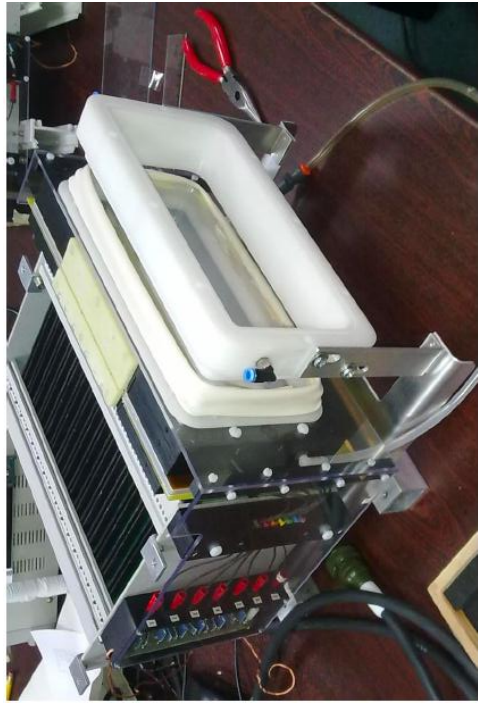
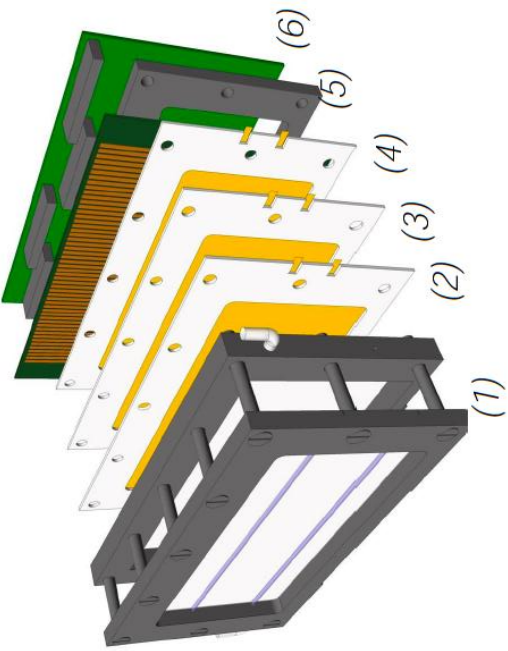
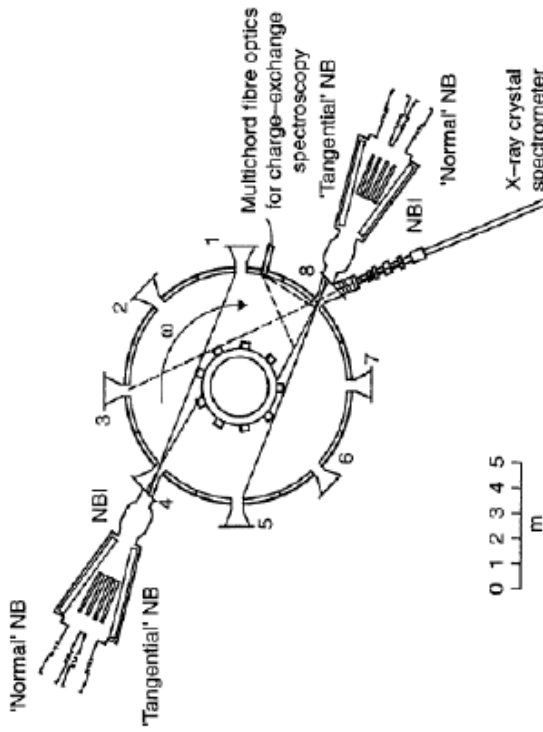
Be Erosion Studies

- Be first wall material qualification: -
erosion and Be PFC life time
- power load capability
- Be erosion modelling and atomic data
(steady-state) (**also molecular data**
(BeD / BeT))?
- Be erosion by transients (**kinetic**
effects? Do we need to go back to
cross sections?)
- Be re-erosion and transport to remote
areas (**metastable states?**)



Duxbury et al.

W Spectroscopy

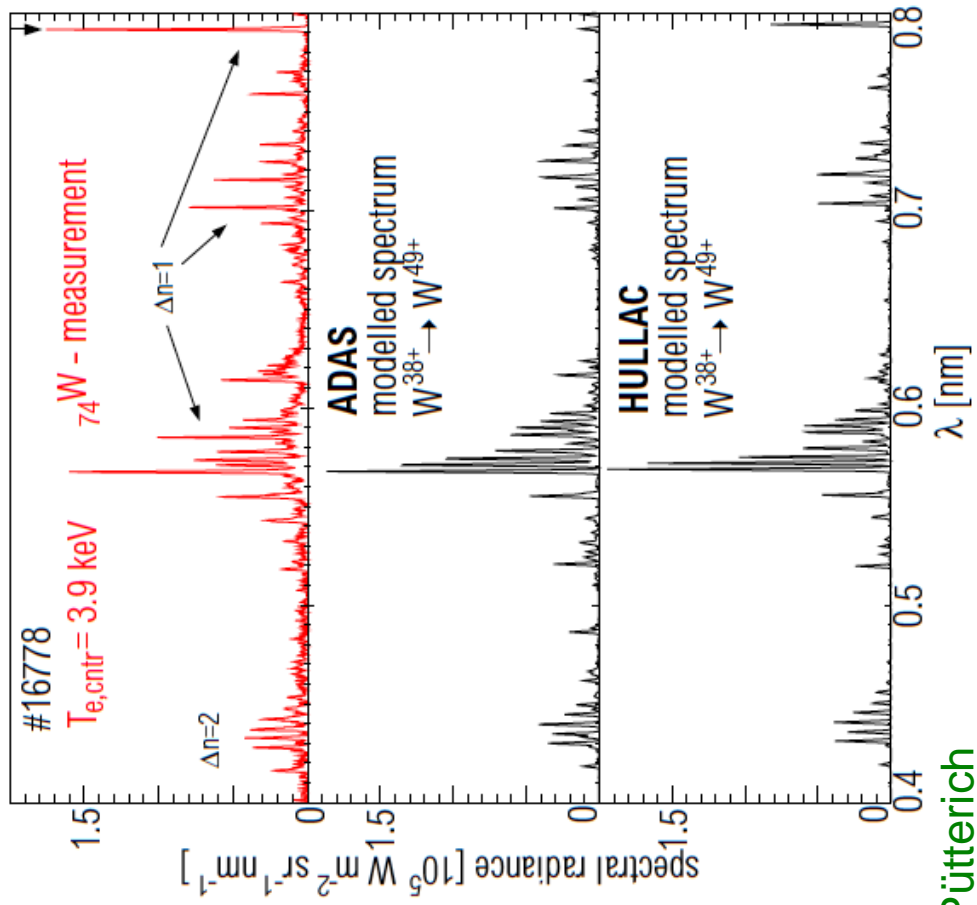


M. Chernyshova et al.



EEJET

W Spectroscopy



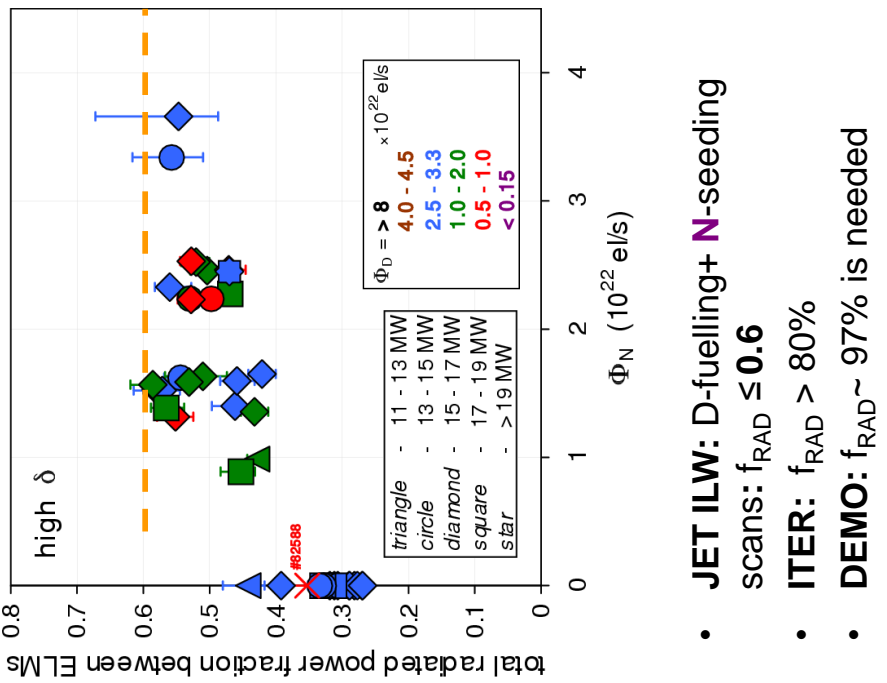
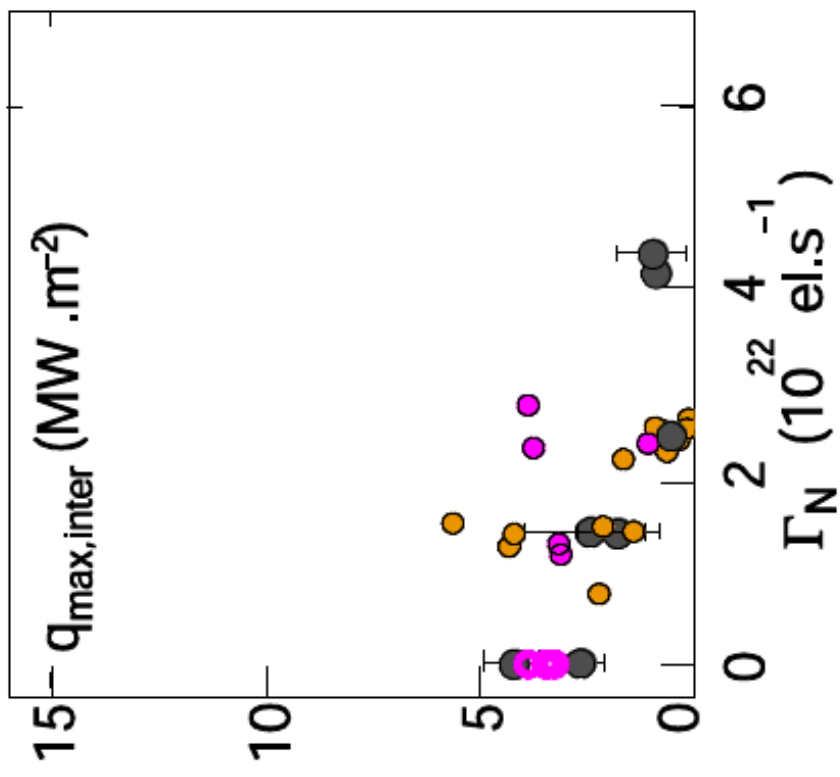
T. Pütterich

L.D. Horton 8

ADAS-EU

30 September 2013

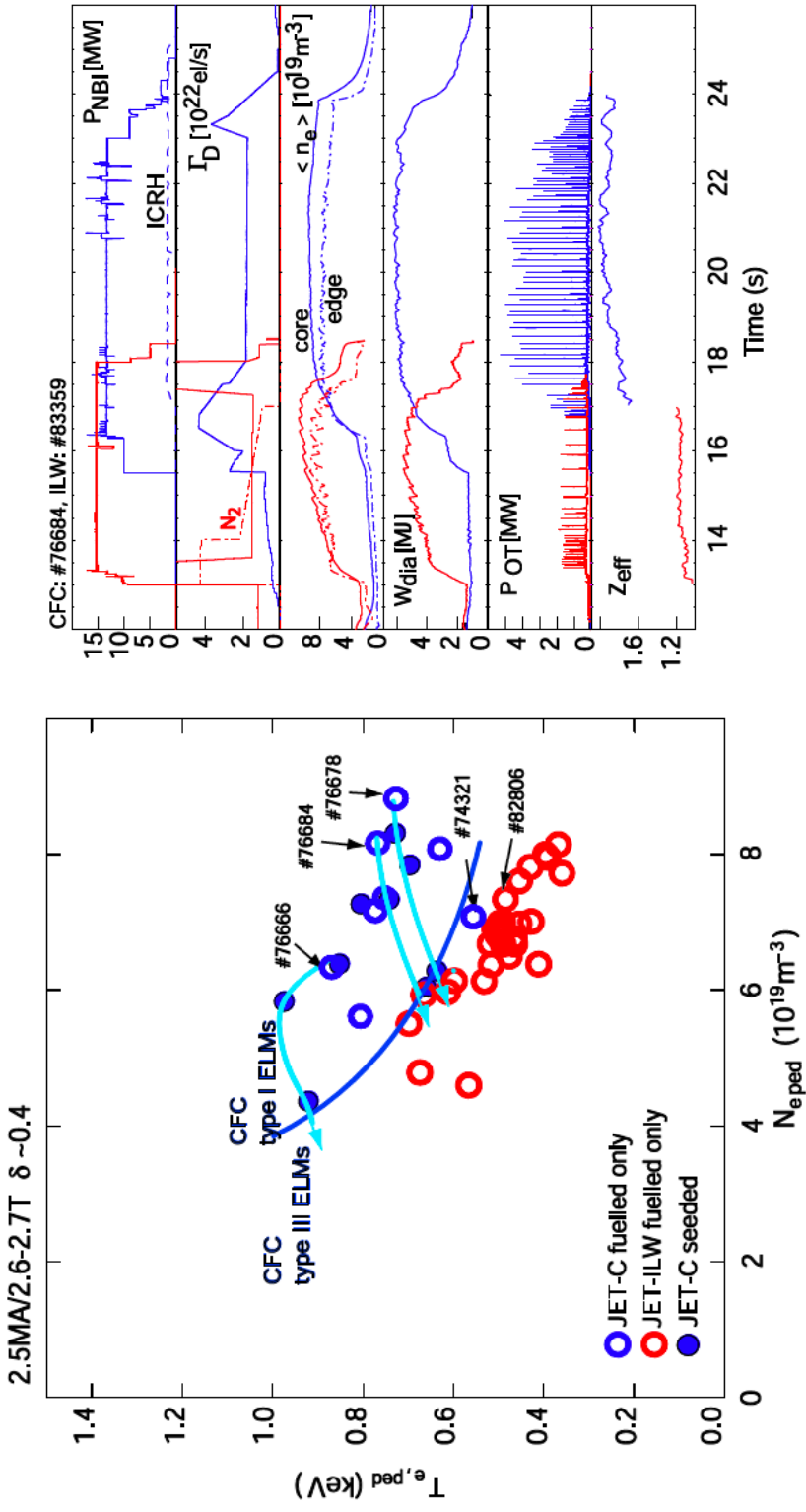
Impurity Seeding



- **JET ILW:** D-fuelling+ N-seeding
scans: $f_{RAD} \leq 0.6$
- **ITER:** $f_{RAD} > 80\%$
- **DEMO:** $f_{RAD} \sim 97\%$ is needed

C. Giroud et al.

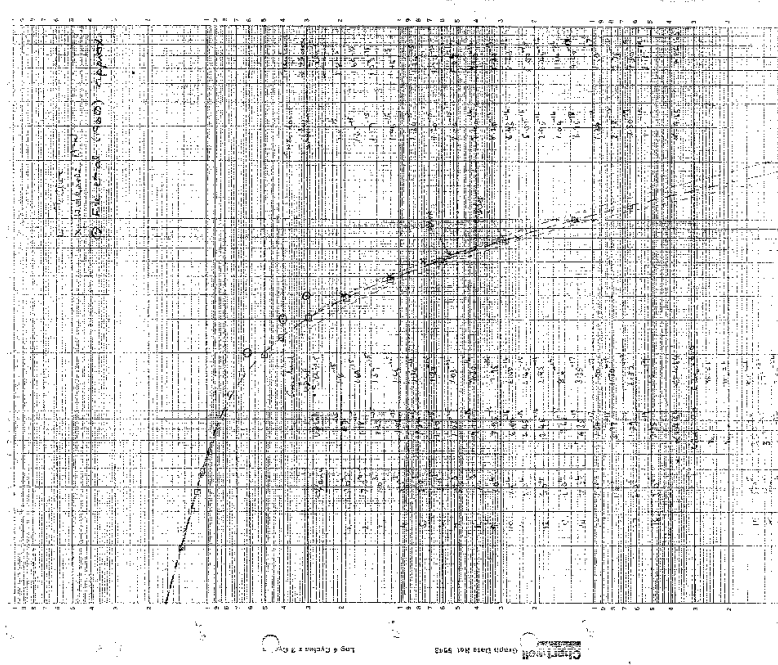
Impurity Seeding



C. Giroud et al.

HPS

- The technology in use in ADAS has changed over the years but the rigour applied has remained constant
- ADAS has profited from a series of very bright, very motivated students (it is a young man's game, if only to be able to read Hugh's miniature hand writing)
- It is a credit to Hugh that he been more than able to keep up with these students and I am personally very grateful for his contributions to ADAS and to JET



A.2 Welcome on behalf of EU Commission - Dr. Lars-Goran Eriksson



Final ADASS-EU Meeting; some introductory remarks

Lars-Göran Eriksson
Unit K6
Directorate General for Research & Innovation
European Commission



Outline

- *A few remarks on the ADAS-EU project*
- *ADAS-EU contribution to the Integrated Tokamak Modelling Task Force (ITM-TF)*
- *Organisation of the EU fusion programme (outside ITER) in Horizon 2020*
- *Conclusions*



A few words on the ADAS-EU project

- *The ADAS project, which has its origin at the JET Joint Undertaking and has grown to a project with global reach, was identified as an important support activity for the Fusion Programme in FP7.*
- *As a result, the Commission decided to contribute to the funding by awarding a "Coordination on and Support action" (an FP7 funding instrument) to the ADAS-EU project.*



- Originally the CSA covered the period 2009 to 2012, but the end date was extended to 30/09/2013 by an amendment in 2012.
- The CSA was awarded to the University of Strathclyde, with Prof Hugh Summers as the Coordinator of the project.
- There was also four lead Associated EU labs linked to ADAS-EU
 - **CCFE Culham**
 - **CEA Cadarache**
 - **IPP Garching/Greifswald**
 - **TEC Juelich**



- ***The objectives of the project included:***
 - support for efficient implementation of atomic data in:
 - diagnostics,
 - Modelling,
 - Transport,
 - Plasma wall interaction,
 - Heating and current drive,
- **Management of databases**
 - A number of science related objectives (see next slide)
- **Strong interaction with EFDA-JET and ITER was foreseen.**



European
Commission

There were five main science themes in the ADAS-EU plan:

- 1. Heavy element spectroscopy and models,**
- 2. Charge exchange spectroscopy,**
- 3. Beam stopping and emission,**
- 4. Special features,**
- 5. Diatomic spectra and collisional radiative models.**

The project objectives were largely to be achieved by:

- Placement of staff in selected EU fusion laboratories**
- Staff visits to EU fusion labs to interact with local programmes,**
- Training courses in ADAS data techniques and modelling,**
- A website (<http://www.adas-fusion.eu>).**



The CSA has allowed ADAS-EU to fund:

- Six part-time ADAS-EU personnel (corresponding to almost 3 fulltime professionals per year),
 - mission costs,
 - subcontracts to a number of EU universities,
 - IT equipment, software etc.,
 - administration and logistics.



- *The ADAS-EU project has involved 36 Work Packages,*
- *It has been monitored in terms of:*
 - **24 deliverables** (all have been received, but some updates expected)
 - **30 milestones** (2/3 reached 31/12/12).



- *The scientific achievements of ADAS-EU will not be discussed in this presentation.*
- *Nevertheless, it clear that ADAS-EU project has made substantial progress, not least for modelling of tungsten ions, which of course is very significant for JET with the I_LW and for ITER.*
- *On a personal note I would like to say that I had very positive interaction with ADAS-EU (especially Hugh Summers and Martin O'Mullane) during my time as deputy leader of the ITM task force.*



A few words on integration of ADAS data into the ITM-TF* framework

ITM-TF philosophy and approach

Comprehensive integrated tokamak modelling:

- ✓ infrastructure describing both **the tokamak physics and the machine within a unique framework**
- ✓ strategy: divide the global problem into Elementary Physics Problems (equilibrium, transport, MHD, sources, diagnostic response, ...)

*TF Leaders: G Falchetto, D. Coster and R. Coelho
<http://portal.efda-itm.eu/itm/portal/>



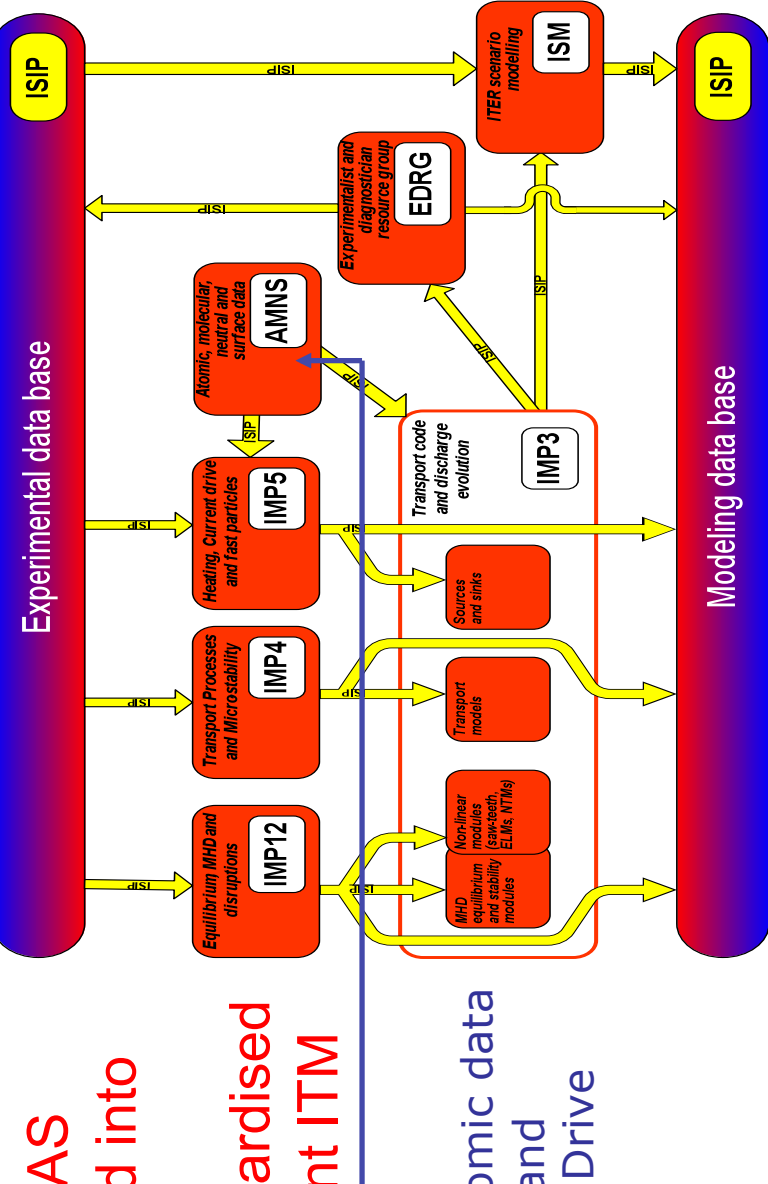
- ✓ fully modular and flexible simulation platform
 - ✓ standardized interfaces for physics and technology
 - Consistent Physical Objects (CPO)
 - **This includes to atomic data**
 - ✓ completely generic workflow
 - ✓ Verification and validation of codes and workflows should be an integral part of the process
- ✓ **Version control of all codes and data (including atomic) going into simulations is therefore essential**



European
Commission

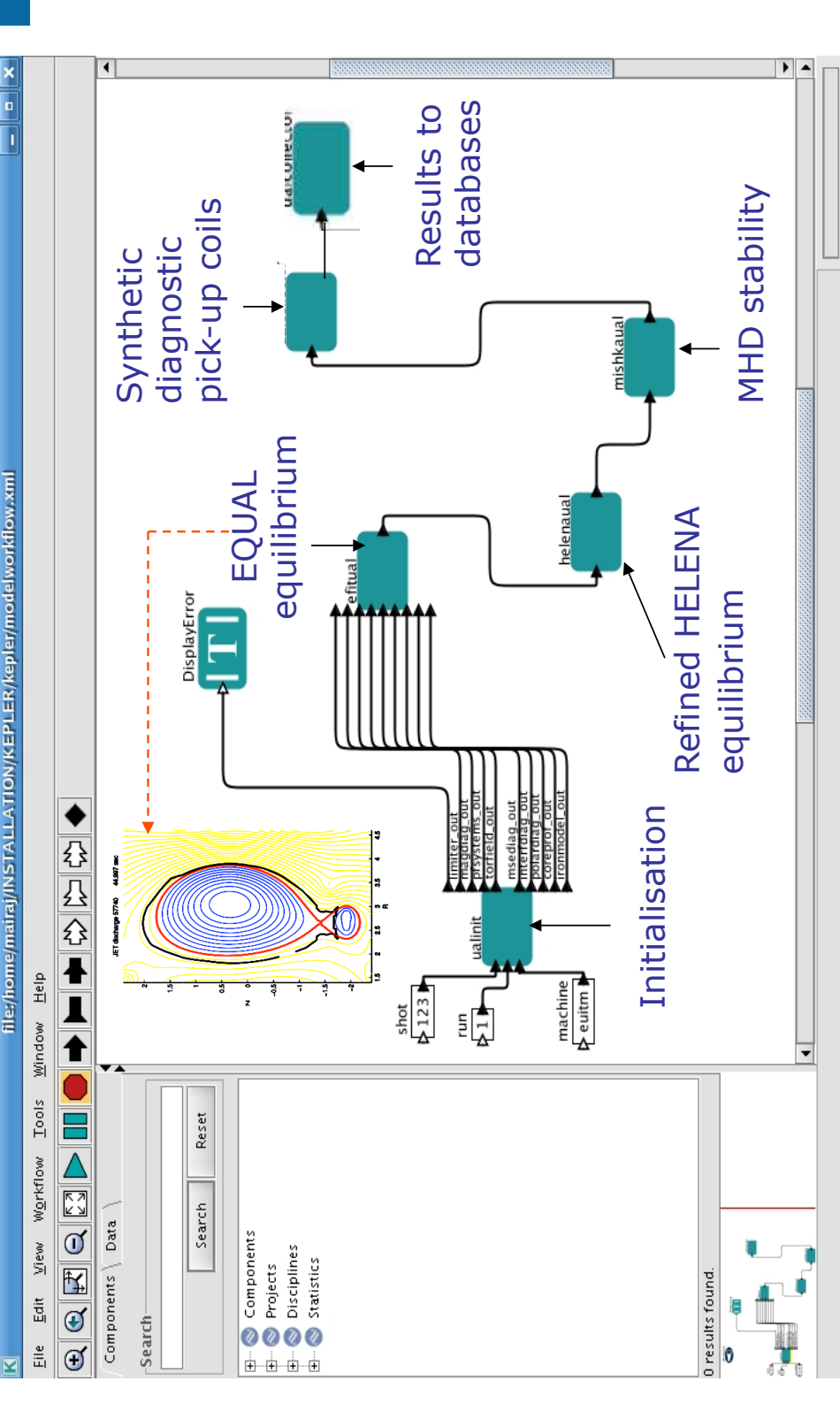
Schematic view of ITM-TF interlinking between models and AMNS (Atomic, Molecular, Nuclear Surface) data

Data from the ADAS database are read into an ITM database (AMNS) for standardised delivery to different ITM codes.



ITM-TF uses ADAS atomic data
e.g. for Transport and
Heating & Current Drive
modelling

Kepler platform (workflow) orchestrator

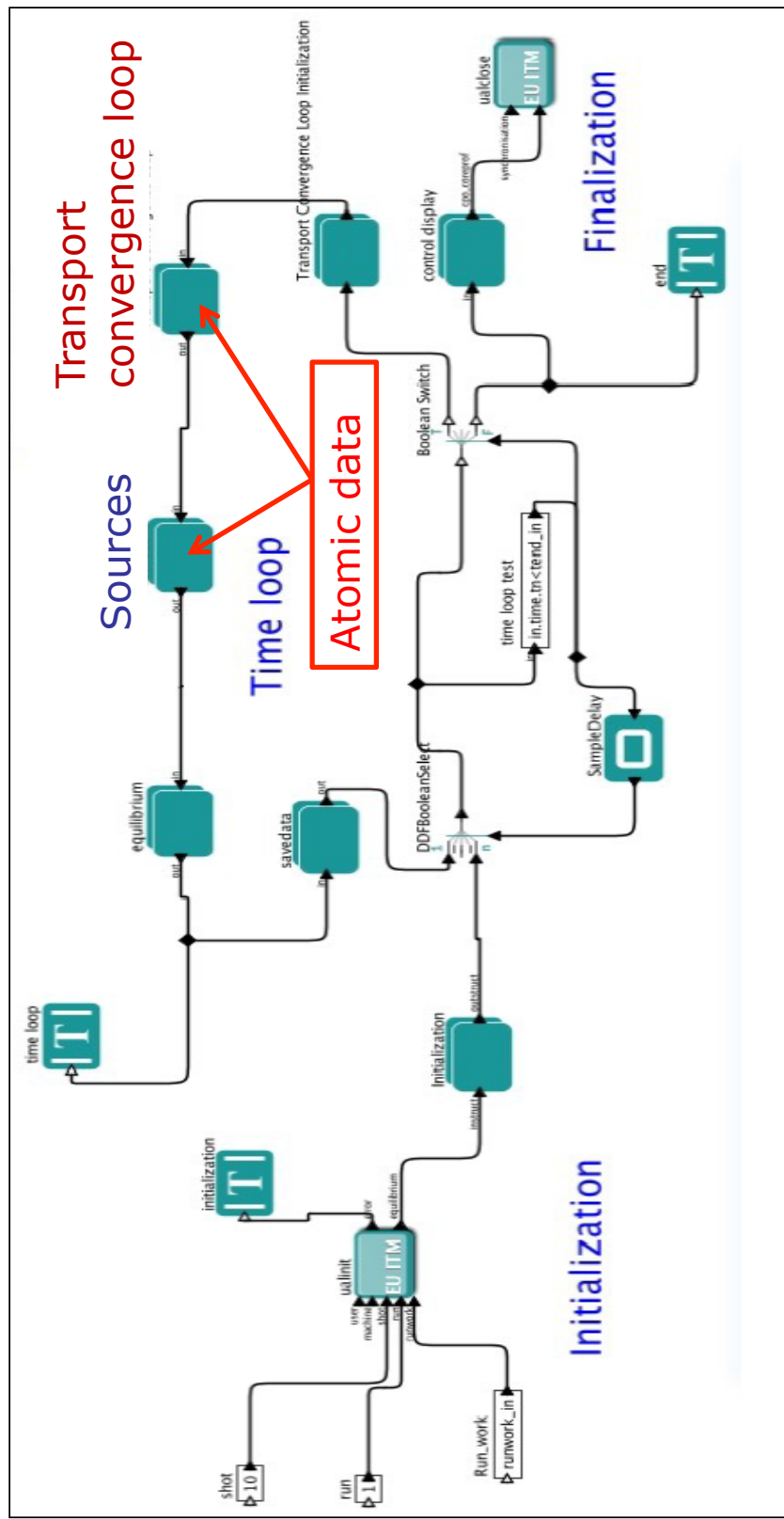


Data, in the form of CPOs, are transported between codes and finally stored by a dedicated software called the **Universal Access Layer (UAL)**



European
Commission

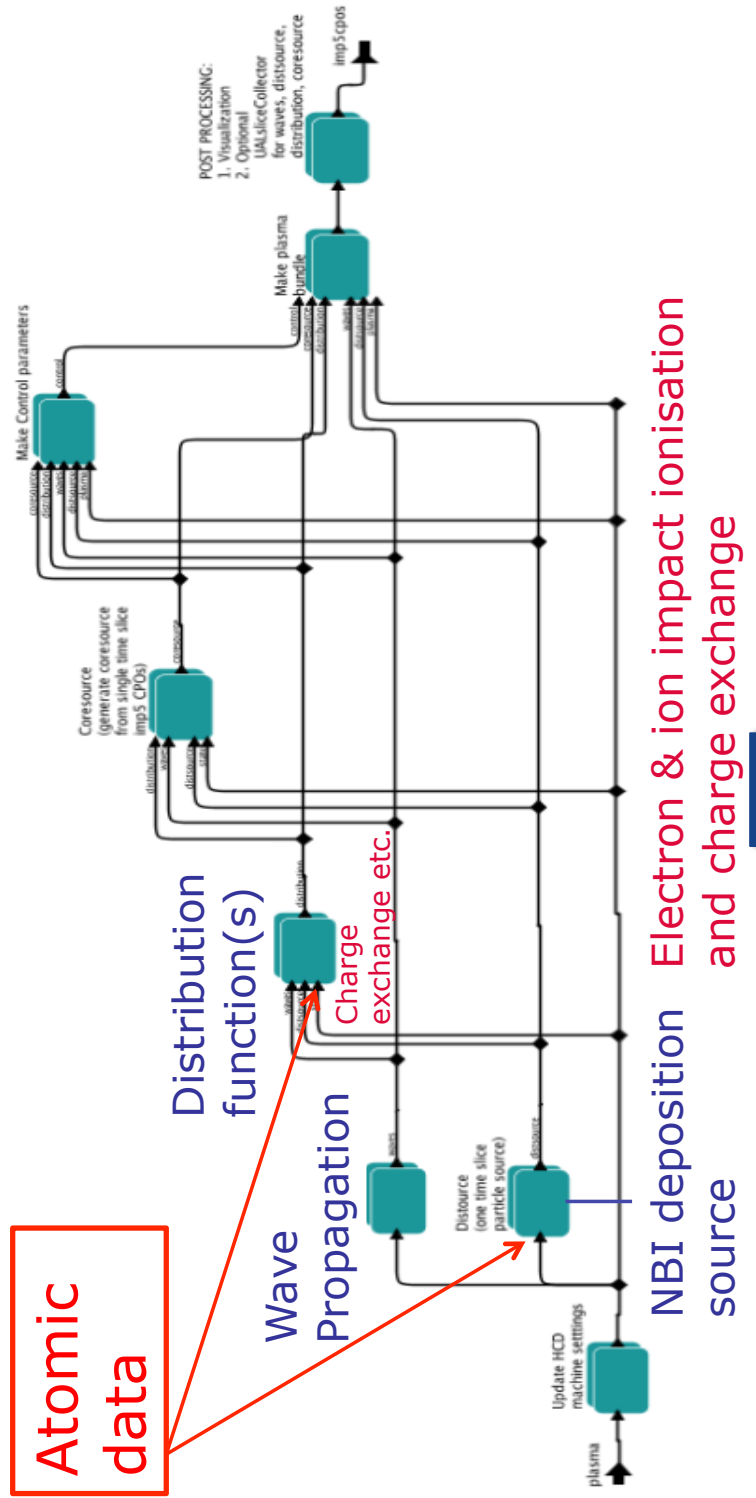
ETS (core transport) workflow





European
Commission

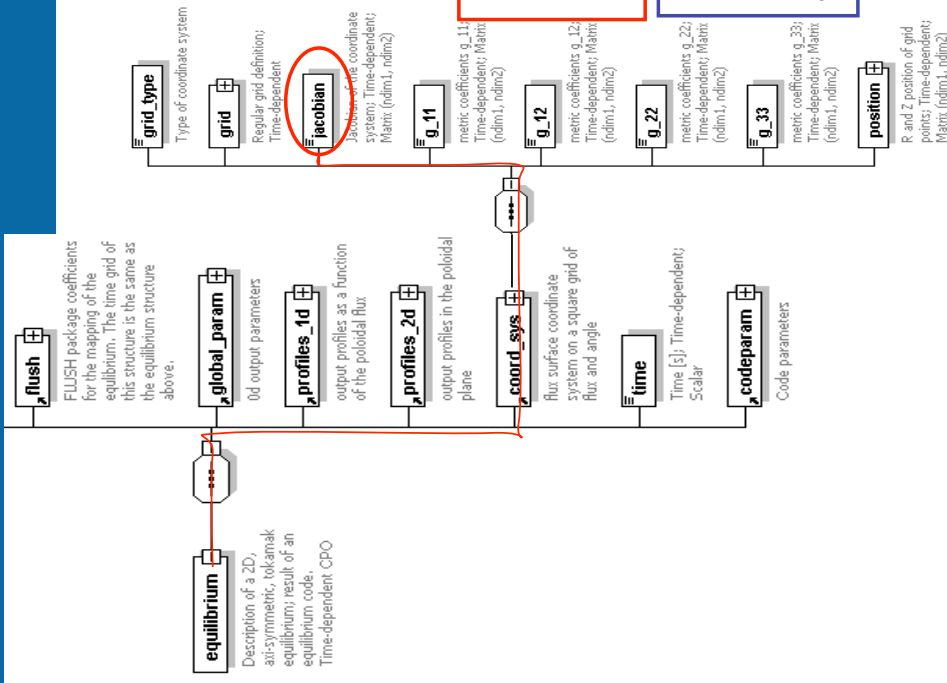
Auxiliary heating sources workflow





European
Commission

Equilibrium data structure



Jacobian at gridpoint (5,6). In Fortran 90, matlab and C++ we simply write:

Fortran 90:

```
jac = equilibrium(1)%coord_sys%jacobian(5,6)
```

Matlab

```
jac = equilibrium(1).coord_sys.jacobian(5,6)
```

C++:

```
jac = itm._equilibriumArray.array(1).coord_sys.jacobian(5,6)
```



Purpose and principles of the AMNS project* within the ITM-TF

- Provide the ITM-TF with Atomic, Molecular, Nuclear and Surface (AMNS) data from appropriate sources.
- Develop modules which deliver AMNS data in a standardised way to ITM-TF codes.
- The system must be such that the provenance of the data used for a particular simulation is recorded to ensure that a simulation can be exactly replicated at a later date.

*Leader D. Coster



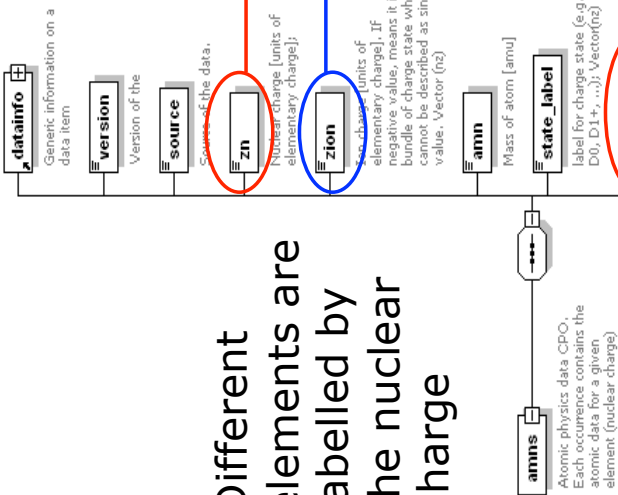
- A key feature of the ITM-TF is the use of special data structures to communicate data between codes in a consistent manner (these are called CPOS)
- The simulation platform is adapted to CPOS and there is special software to communicate CPOS to the ITM database: the UAL (Universal Access Layer)
- It was therefore natural to also store AMNS data in the form of ITM data structures

AMNS data structure released in the 4.08 version of the ITM

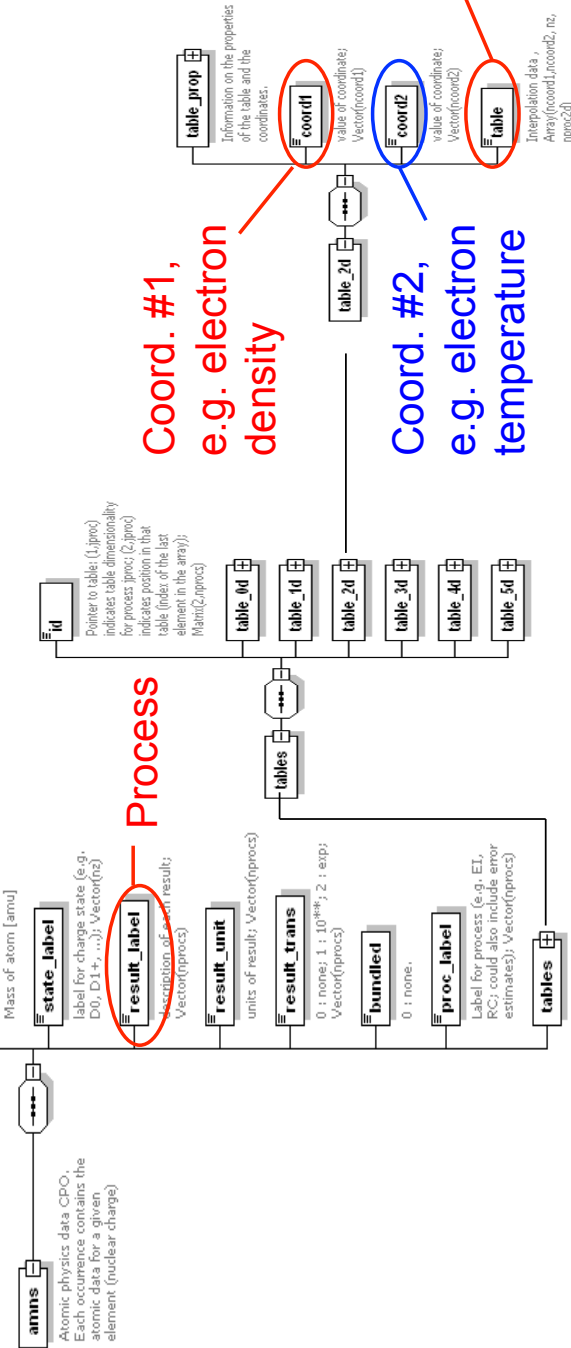
Different elements are labelled by the nuclear charge

Identification of the data structures element: nuclear charge.

Charge state



F90: amns%tables%table_2d%table



Result Table

19



ADAS involvement in ITM

- Supplying data (obviously)
- Contributed to the development software for transferring data from the ADAS data base to the ITM database and storage of atomic data in the amns data structure.
- Contributed to routines for retrieving AMNS data from the ITM data base in a standardised fashion



ADAS data currently used in ITM-TF

Release 11 [DEFAULT]

Data for H • Data for 2H • Data for 3He • Data for Li • Data for Be • Data for C •
Data for N • Data for O • Data for F • Data for Ne • Data for Al • Data for Si • Data for Cl • Data for Ar •
Data for Cr • Data for Fe • Data for Ni • Data for Cu • Data for Ge • Data for Kr • Data for Mo • Data for Xe • Data for W

For H: (i) Recombination; (ii) Electron Impact Ionisation; (iii) CX recombination coeffs; (iv) Recomb/brems power coeffs; (v) Line radiation; (vi) Effective Charge; (vii) Effective Square Charge; (viii) Effective Ionisation Potential; (ix) Total Elastic Cross-Section; (x) Differential Elastic Cross-Section

Conclusion ADAS data have been well integrated into the ITM-TF framework



EU fusion programme outside ITER

Current organisation (FP7)

- *The European Commission (Euratom)*

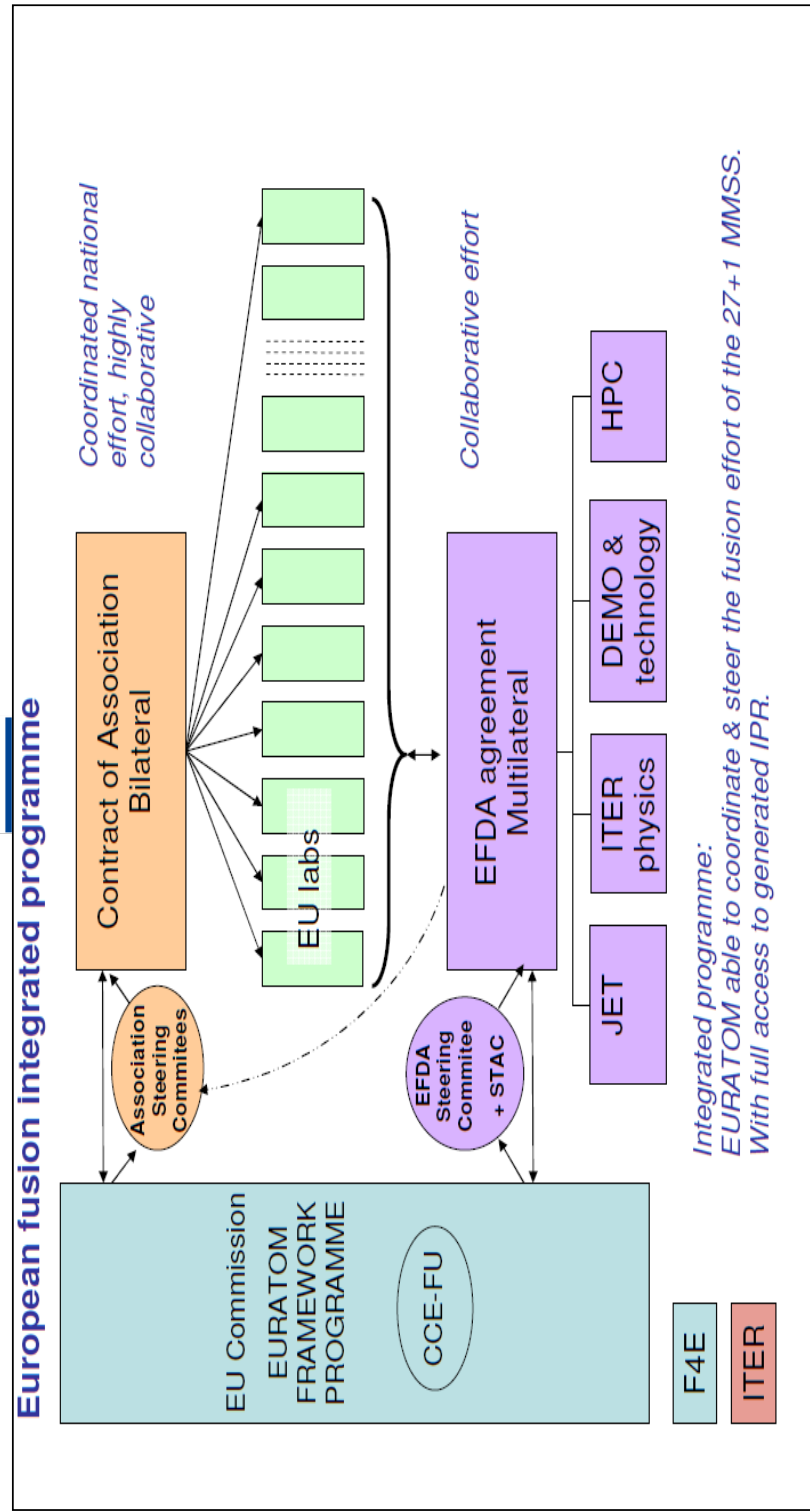
- Overall programme management (including funding, representation of the programme internationally (fusion co-operation Agreements))

- *Euratom Fusion Associations*

- 26 bilateral "Contracts of Association" between Euratom and EU member states' fusion institutions (plus Switzerland)

- *EFDA (The European Fusion Development Agreement)*

- An agreement between all the Associations and Euratom to support co-ordinated and collective activities



- *JET is linked to EFDA and operated under a bilateral contract, JOC, between the Commission and CCFE*



European
Commission

Structure of the Programme in Horizon 2020

- *The organisation of the EU fusion programme outside ITER will be radically restructured in Horizon 2020.*
- *The key aim is to make effective progress along the EFDA roadmap* while retaining the unity of the overall effort and the strengths of the current structure.*
- *The plan is to confer the implementation of the whole programme to a single Consortium made up of interested national fusion research institutions, with one national lab acting as a Consortium coordinator.*

* <http://www.efda.org/wpcms/wp-content/uploads/2013/01/JG12.356-web.pdf>



- *The Community funding of the Consortium should be via a so-called co-fund grant (a new Horizon 2020 funding instrument), i.e. the joint programming activities of the Consortium Members will be co-funded by the Community.*
- *JET is still planned to be operated under a bilateral contract between the Commission and CCFE in Horizon 2020.*
- *The scientific exploitation of JET will be entrusted to the consortium.*



- *As a result, the Commission will in Horizon 2020 have a much lesser role in the actual implementation of the fusion programme.*
- *It is in this context one must see how ADAS fits into the EU fusion programme in the future.*
- *The first port of call for discussions of how ADAS can continue to be well integrated to the EU fusion programme should be with the Consortium.*
- *The interim Programme Manager of the Consortium is Francesco Romanelli and meetings on the formation of the Consortium are chaired by Sibylle Günter.*



Conclusion

- *The ADAS-EU project has delivered on its objectives (scientifically, dispersal of knowledge, management of databases etc.).*
- *It is in the interest of fusion research that the built-up experience can be maintained.*
- *In the new structure of the EU fusion programme in Horizon 2020, the implementation of the fusion programme will be entrusted to a Consortium of EU fusion research institutions.*
- *It is principally this context one should consider the future of ADAS in the EU fusion programme.*

A.3 The ITER perspective - Dr. Mike Walsh

Atomic Physics and the ITER Perspective

ITER Team

Michael Walsh and Robin Barnsley
ITER Organisation

30/09/2013

Ack: Special thanks to all colleagues who provided support and information for this presentation

The views and opinions expressed herein do not necessarily reflect those of the ITER Organization



ADAS-EU Meeting– September - 2013

© 2013, ITER Organization

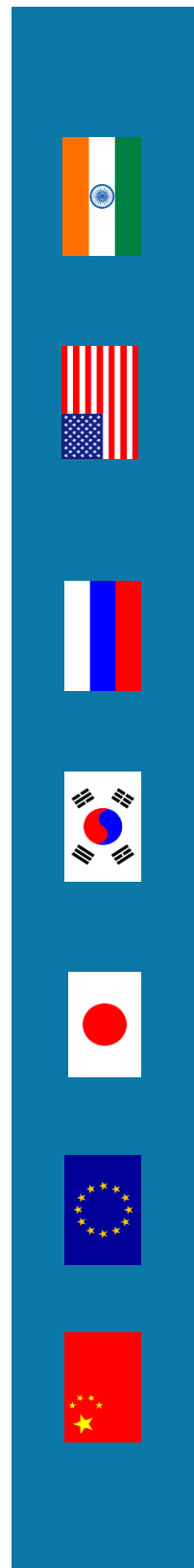
Outline

- Brief overview of ITER
- General Diagnostics
- Spectroscopic System examples
- Where are we going
- Summary



ADAS-EU Meeting– September - 2013
© 2013, ITER Organization

All ITER Parties and many Institutes and Industries Involved



ADAS-EU Meeting– September - 2013

© 2013, ITER Organization

ITER project



ADAS-EU Meeting– September - 2013

© 2013, ITER Organization

The Wider View



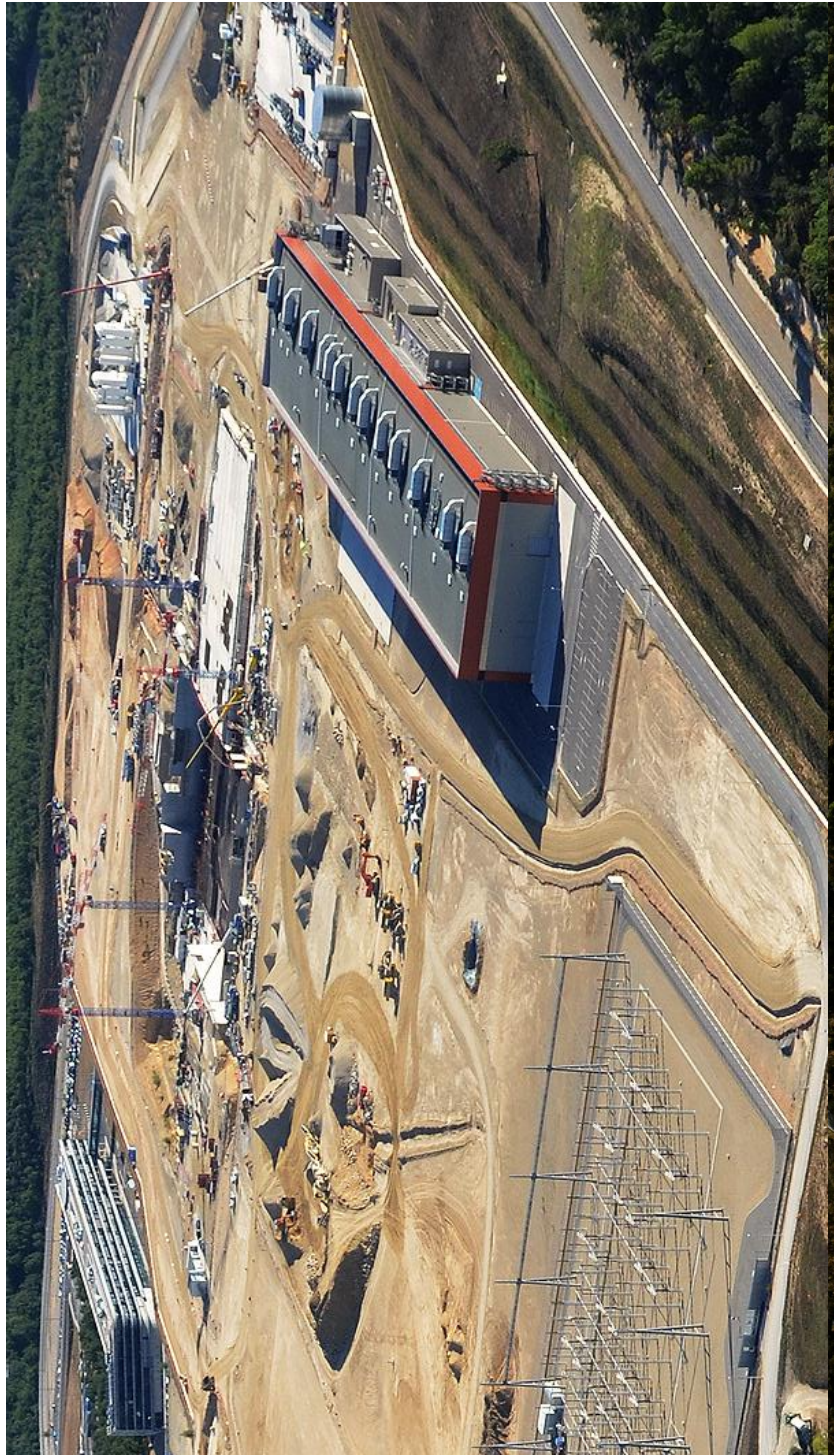
ITER Site consists of 37 buildings each dedicated to a supporting plant system



ADAS-EU Meeting– September - 2013

© 2013, ITER Organization

Site View now



ADAS-EU Meeting– September - 2013

© 2013, ITER Organization

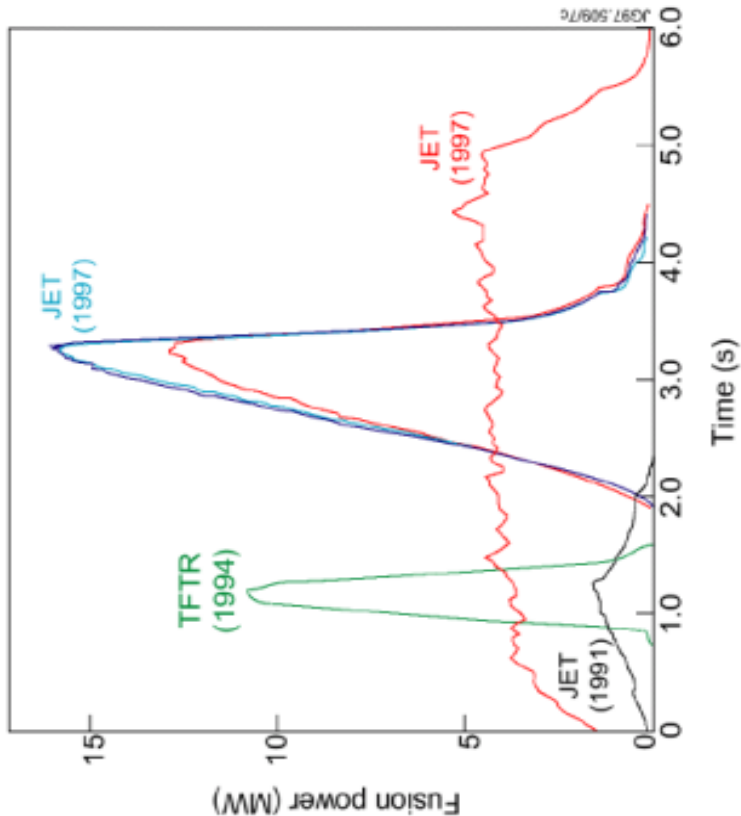
Fusion Progress and Records

Huge strides in physics, engineering and technology:

- Temperature (T_i): 10-20 keV
- Density (n_i): $\sim 10 \times 10^{19} \text{ m}^{-3}$
- Energy confinement time (t):
 $\sim 1 \text{ sec}$

• Experiments in JET and TFTR have initiated the study of plasmas with significant fusion power : record fusion power production of 16MW ($Q \sim 0.6$) at JET

• Use of superconductors : record pulse length 6 minutes
18 sec at Tore Supra



ITER Scope - Mission Goals

Physics:

- ITER is designed to produce a plasma dominated by α -particle heating

produce a significant fusion power amplification factor ($Q \geq 10$) in long-pulse operation (300 – 500 s)

- aim to achieve steady-state operation of a tokamak ($Q \geq 5 / \leq 3000$ s)
- retain the possibility of exploring ‘controlled ignition’ ($Q \geq 30$)

Technology:

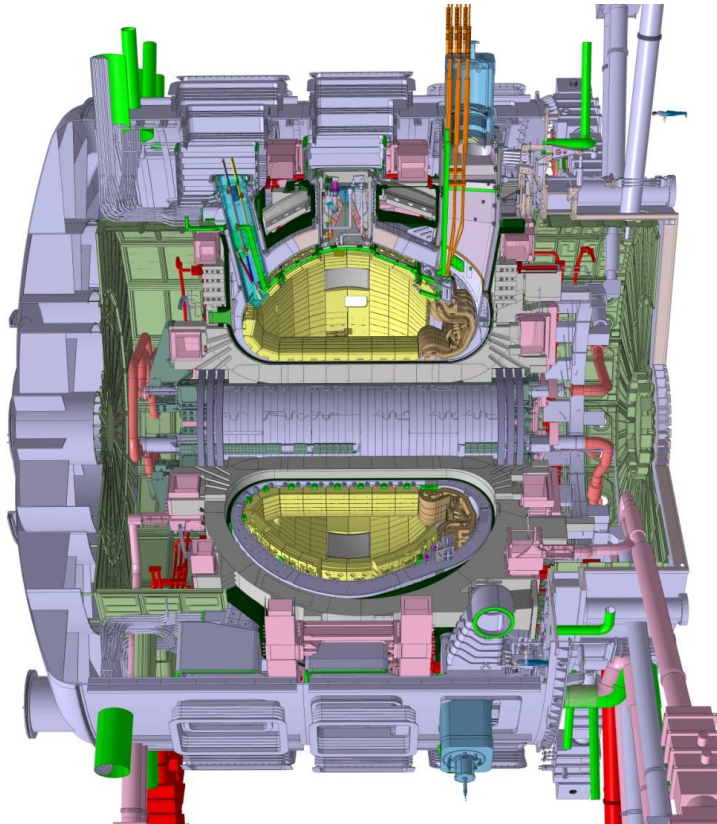
demonstrate integrated operation of technologies for a fusion power plant

- test components required for a fusion power plant
- test concepts for a tritium breeding module



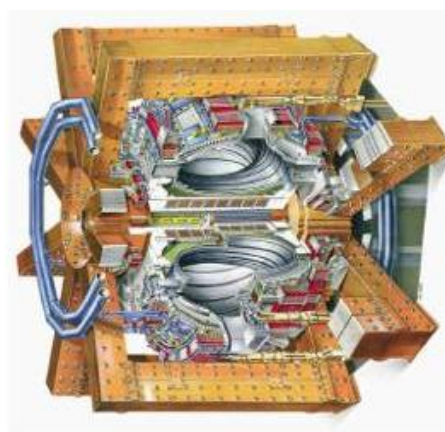
Is ITER different?

ITER is twice as large
as our largest existing
experiments



ITER

| | |
|--------------|----------------------|
| V_{plasma} | $830\ m^3$ |
| P_{fusion} | $\sim 500\ MW\ 500s$ |
| t_{plasma} | $\sim 400\ s$ |



JET

| | |
|--------------|-------------------|
| V_{plasma} | $80\ m^3$ |
| P_{fusion} | $\sim 16\ MW\ 2s$ |
| t_{plasma} | $\sim 30\ s$ |



ADAS-EU Meeting– September - 2013

© 2013, ITER Organization

What do we need to see and measure?

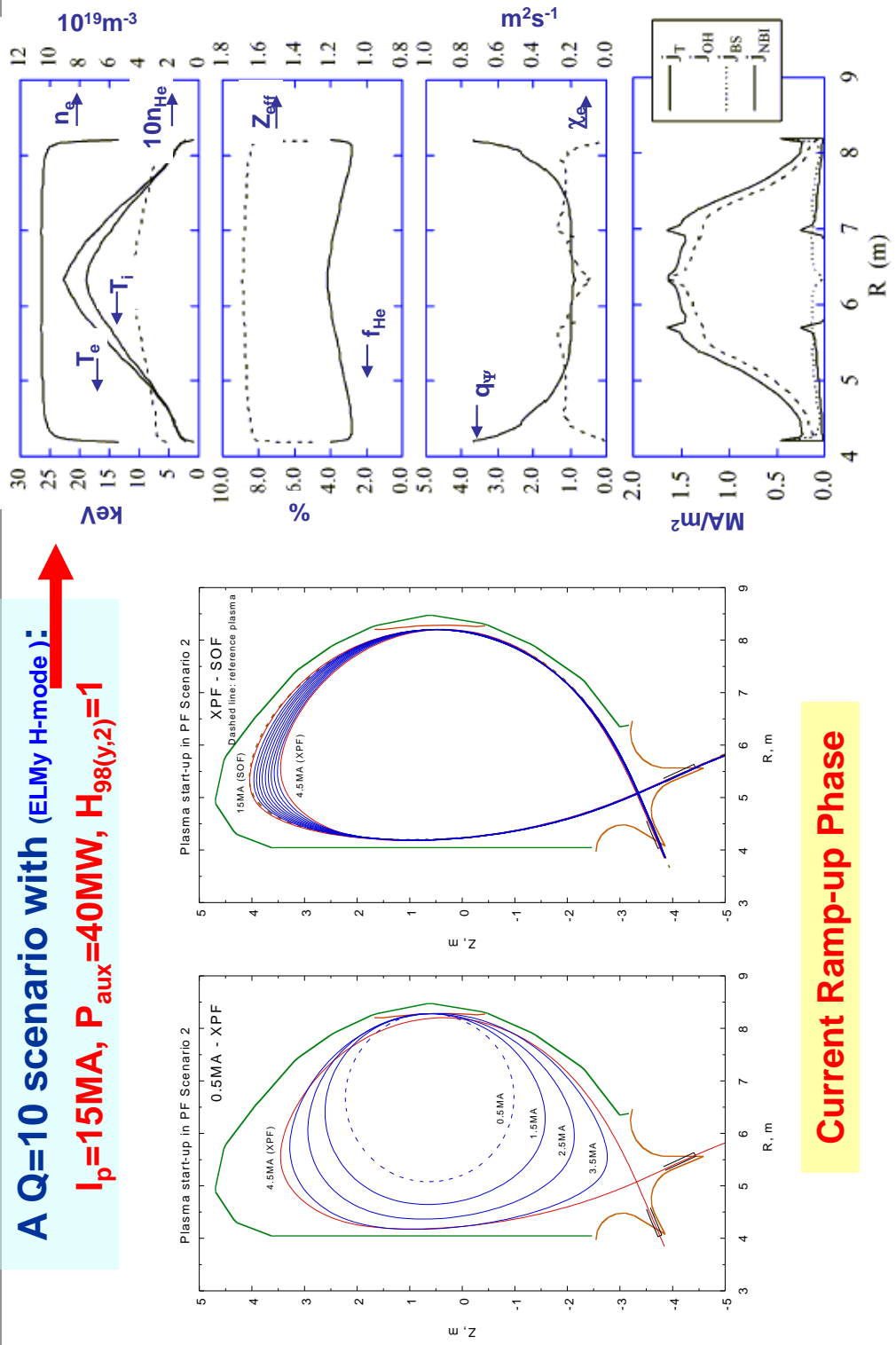


ADAS-EU Meeting– September - 2013

© 2013, ITER Organization

ITER Plasma Scenario - Example end result

A Q=10 scenario with (ELMy H-mode):
 $I_p = 15\text{MA}$, $P_{aux} = 40\text{MW}$, $H_{98(y,2)} = 1$



Types of Systems Used

About 45 different diagnostic identified for different measurement roles

- A- Magnetics systems
- B- Neutrons systems
- C- Optical systems
- D- Bolometry systems
- E- Spectroscopy systems
- F- Microwave systems
- G- Operational systems
- N- Electrical Services

All integrated directly in to machine or in the port plugs



ADAS-EU Meeting– September - 2013

© 2013, ITER Organization

How diagnostic functionality is grouped?

- 1) for machine protection or basic control
- 2) for advanced performance control, and
- 3) evaluating the plasma performance and understanding important physical phenomena



ADAS-EU Meeting– September - 2013

© 2013, ITER Organization

Measurement Requirements

Developed by International Teams based around ITPA

Now part of the ITER High Level Project Requirements

Next slide has some relating to Spectroscopy
Require good atomic data to predict physics phenomena and signal intensities



ADAS-EU Meeting– September - 2013

© 2013, ITER Organization

Spectroscopy Diagnostics Measurements Requirements

| MEASUREMENT | PARAMETER | CONDITION | RANGE or COVERAGE | RESOLUTION | ACCURACY |
|------------------------------|-----------------------------------|-----------|--|------------|-------------------------|
| 10. Plasma Rotation | V_{TOR} | | 1-200 km/s | 10 ms | a/30 |
| | V_{POL} | | 1-50 km/s | 10 ms | a/30 |
| | Be, C rel. conc. | | $1 \times 10^{-4} - 5 \times 10^{-2}$ | 10 ms | Integral 10 % (rel.) |
| | Be, C influx | | $4 \times 10^{16} - 2 \times 10^{19} / \text{s}$ | 10 ms | Integral 10 % (rel.) |
| | Cu rel. conc. | | $1 \times 10^{-5} - 5 \times 10^{-3}$ | 10 ms | Integral 10 % (rel.) |
| | Cu influx | | $4 \times 10^{15} - 2 \times 10^{18} / \text{s}$ | 10 ms | Integral 10 % (rel.) |
| | W rel. conc. | | $1 \times 10^{-6} - 5 \times 10^{-4}$ | 10 ms | Integral 10 % (rel.) |
| | W influx | | $4 \times 10^{14} - 2 \times 10^{17} / \text{s}$ | 10 ms | Integral 10 % (rel.) |
| | Extrinsic (Ne, Ar, Kr) rel. conc. | | $1 \times 10^{-4} - 2 \times 10^{-2}$ | 10 ms | Integral 10 % (rel.) |
| | Extrinsic (Ne, Ar, Kr) influx | | $4 \times 10^{16} - 8 \times 10^{18} / \text{s}$ | 10 ms | Integral 10 % (rel.) |
| 28. Ion Temperature Profile | Core Ti | r/a < 0.9 | 0.5 - 40 keV | 100 ms | a/10 10 % |
| | Edge Ti | r/a > 0.9 | 0.05 - 10 keV | 100 ms | 50 mm 10 % |
| 32. Impurity Density Profile | Fractional content, Z <= 10 | r/a < 0.9 | 0.5 - 20 % | 100 ms | a/10 20 % |
| | | r/a > 0.9 | 0.5 - 20 % | 100 ms | 50 mm 20 % |
| | Fractional content, Z > 10 | r/a < 0.9 | 0.01 - 0.3 % | 100 ms | a/10 20 % |
| | | r/a > 0.9 | 0.01 - 0.3 % | 100 ms | 50 mm 20 % |



ADAS-EU Meeting– September - 2013

© 2013 ITER Organization
china eu india japan korea russia usa

When these are expanded to systems



ADAS-EU Meeting– September - 2013

© 2013

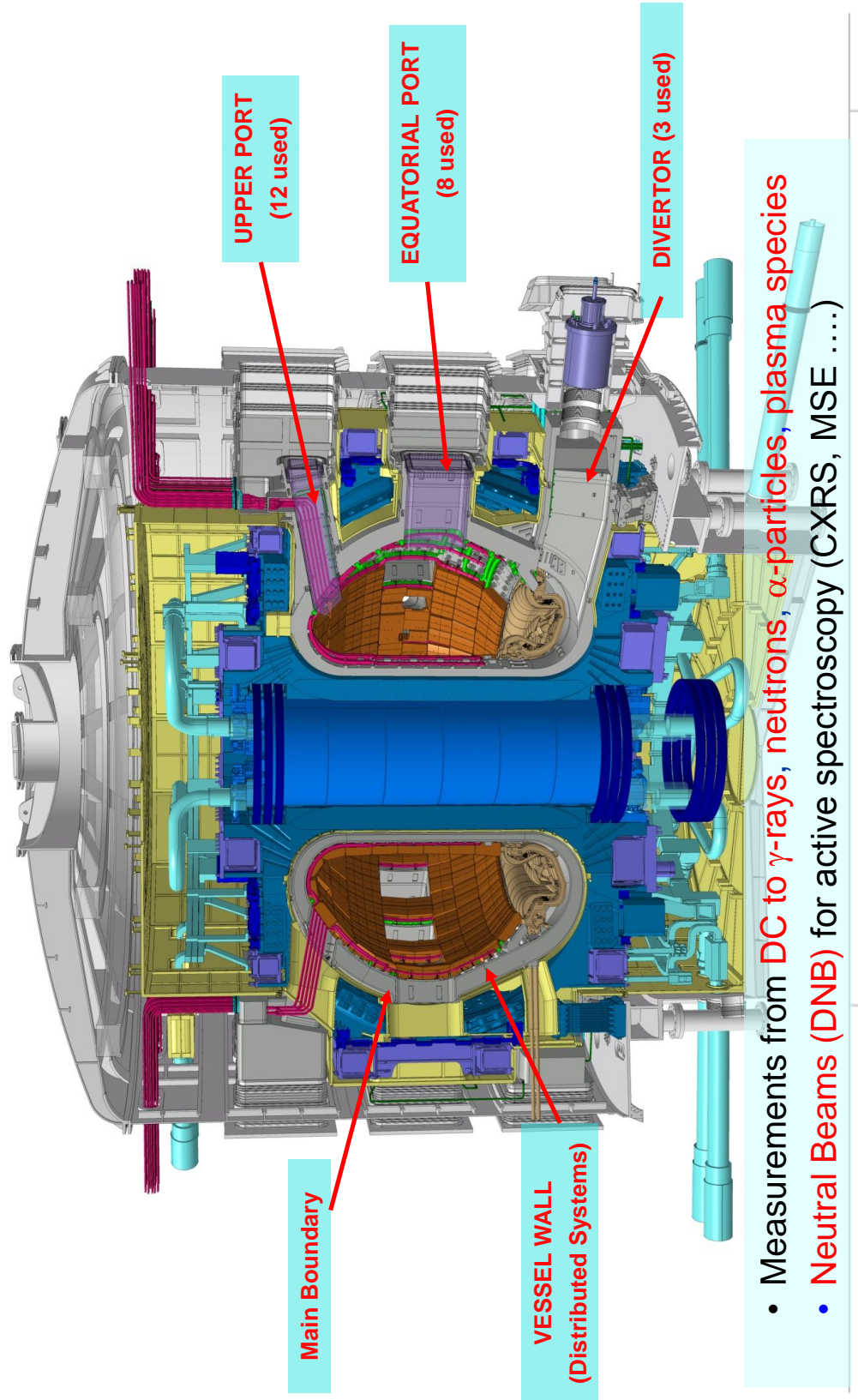
ITER Organization

Page 16

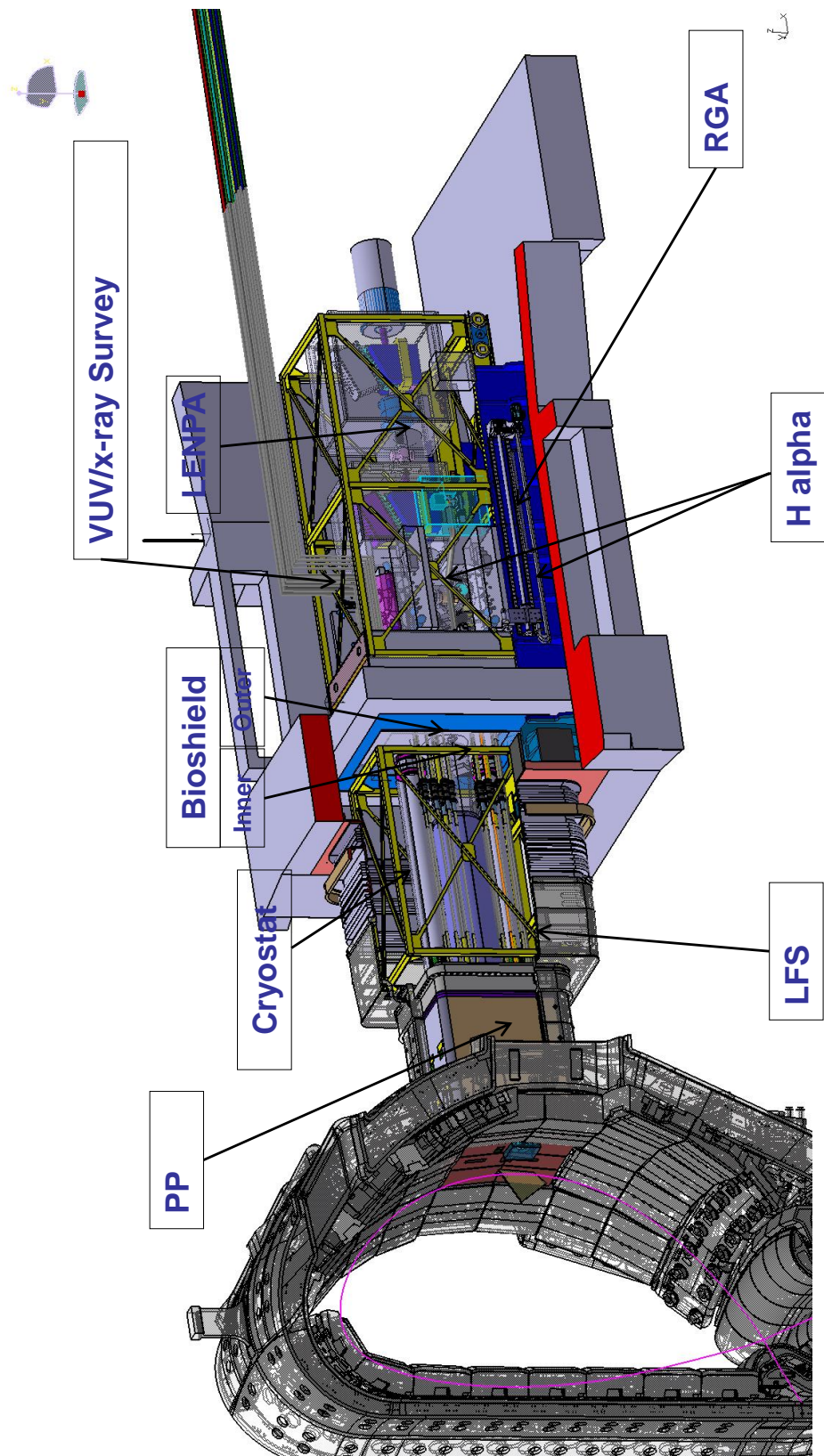
2013 + 2014 + 2015 + 2016

| PBS | System | Wavelength/ Energy range | Function | Status |
|------|---|---|--|---------------------------|
| 55E4 | Divertor impurity monitor | 200 – 1000 nm | Impurity species and influx, divertor He-density, ionisation front position, T_i . | PA signed |
| 55E2 | H α system | Visible region | ELMs, L/H mode indicator, n_r/n_D and n_H/n_D at edge and in divertor. | CDR closed |
| 55E3 | VUV spectroscopy - main | 2.3 – 160 nm | Impurity species identification. | PA signed |
| 55EG | VUV spectroscopy - divertor | 15 – 40 nm | Divertor impurity influxes, particularly Tungsten | PA signed |
| 55EH | VUV spectroscopy - edge | 15-40 nm | Edge impurity profiles | PA signed |
| 55ED | X-ray spectroscopy – survey | 0.1 – 10 nm | Impurity species identification | PA signed |
| 55EI | X-ray spectrometer - edge | 0.4 – 0.6 nm | Impurity species identification, plasma rotation, T_i . | PA signed |
| 55E5 | X-ray spectroscopy-core | 0.1 – 0.5 nm | Impurity species identification, plasma rotation, T_i . | CDR Jun 2013 |
| 55E7 | Radial x-ray camera | 1 – 200 keV | MHD, Impurity influxes, T_e | PA signed |
| 55EB | MSE | Visible region | $q(r)$, internal magnetic structure | CDR Jan 2013 |
| 55E1 | Core CXRS | Visible region | $T_i(r)$, He ash density, impurity density profile, plasma rotation, alphas. | CDR Mid 2014 |
| 55EC | Edge CXRS | Visible region | $T_i(r)$, He ash density, impurity density profile, plasma rotation, alphas. | CDR Oct 2012 |
| 55EF | BES | Visible region | Beam-attenuation and fluctuations. | CDR Oct 2012 |
| 55E8 | NPA | 10 keV,- 4 MeV) | n_r/n_D and n_H/n_D at edge and core. Fast alphas. | PA signed |
| 55EA | Laser-induced fluorescence | Visible | Divertor neutrals | Pre- CDR held |
| 55EB | china eu  Hard X-ray Monitor | Visible - September - 2013 © 2013, ITER  Asia Korea Monitor 20MeV | Runaway electron detection | Page 17 CDR Early 2014 |

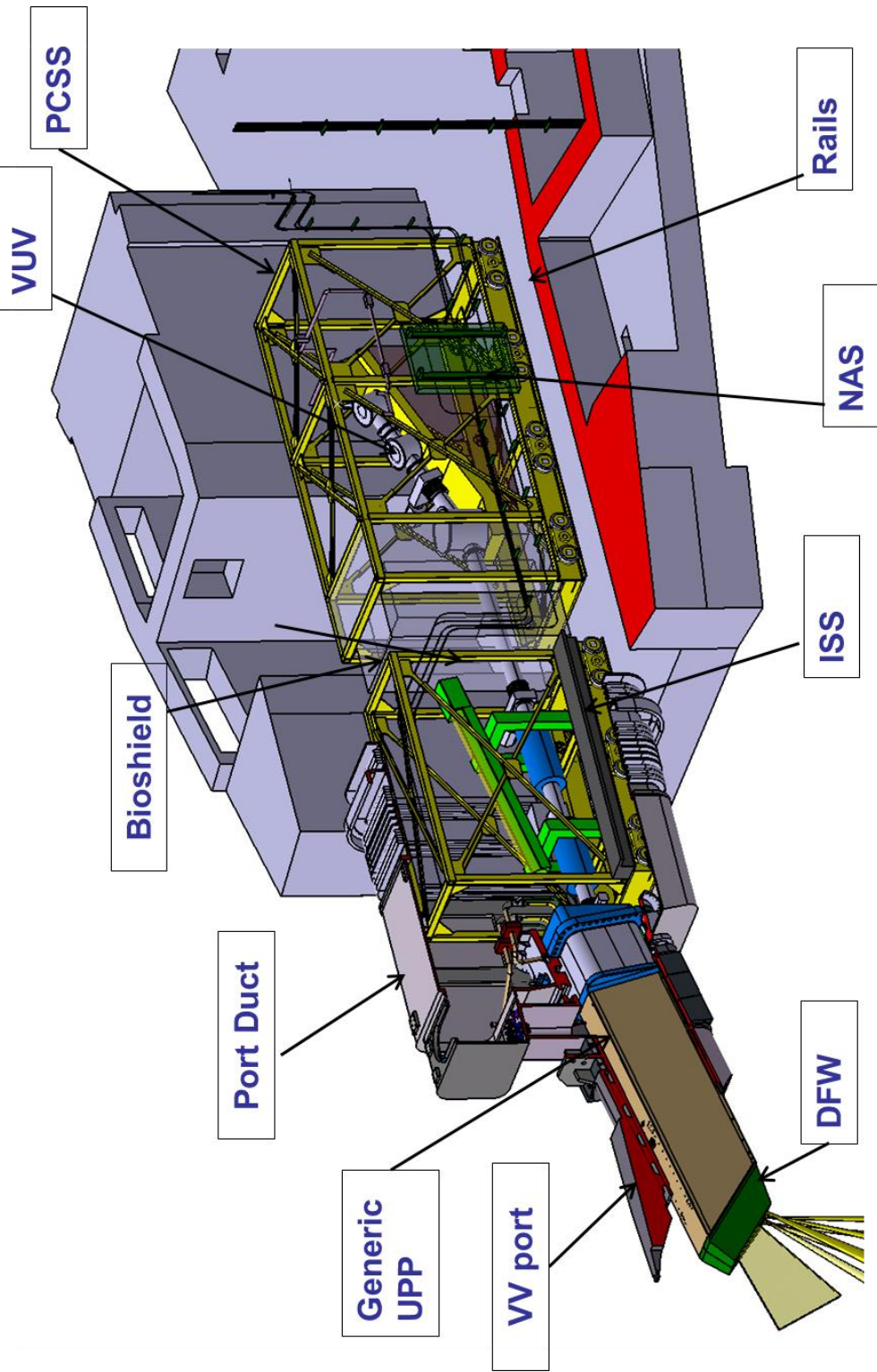
General Diagnostic Locations



General overview of a Hardware system on ITER



Integrated Upper Port #18

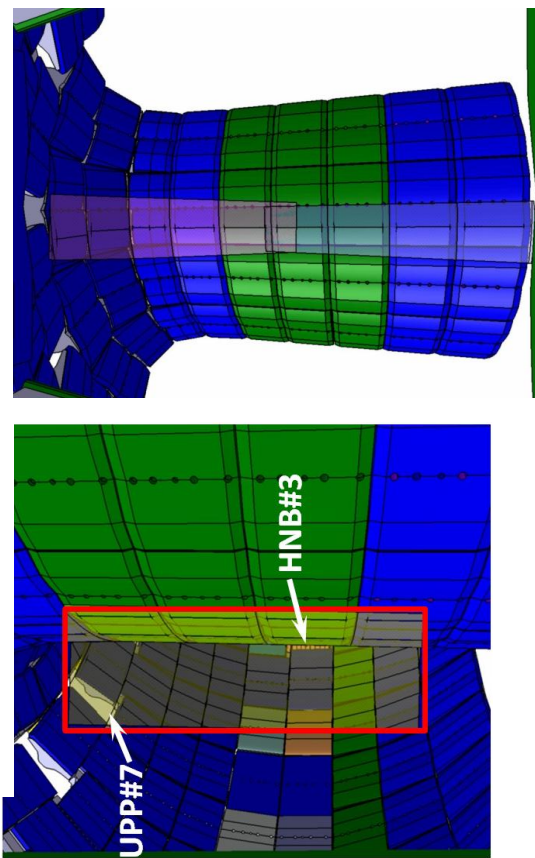


china eu india japan korea russia usa
© 2013, ITER Organization

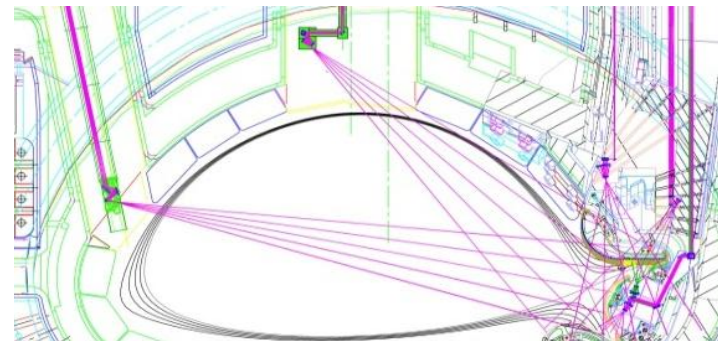
ADAS-EU Meeting – September - 2013

UV/Visible Spectroscopy

Ha and Vis has 4 views



DIM has 3 views



- Ha and Vis - Can see inner and outer wall
- Divertor can be bright
- Significant Reflection analysis carried out
- Various mitigation techniques – effort needed
- E.g. dumps and zeeman techniques etc



ADAS-EU Meeting– September - 2013

© 2013, ITER Organization

ITER Plasma emission modelling with ADAS-SANCO

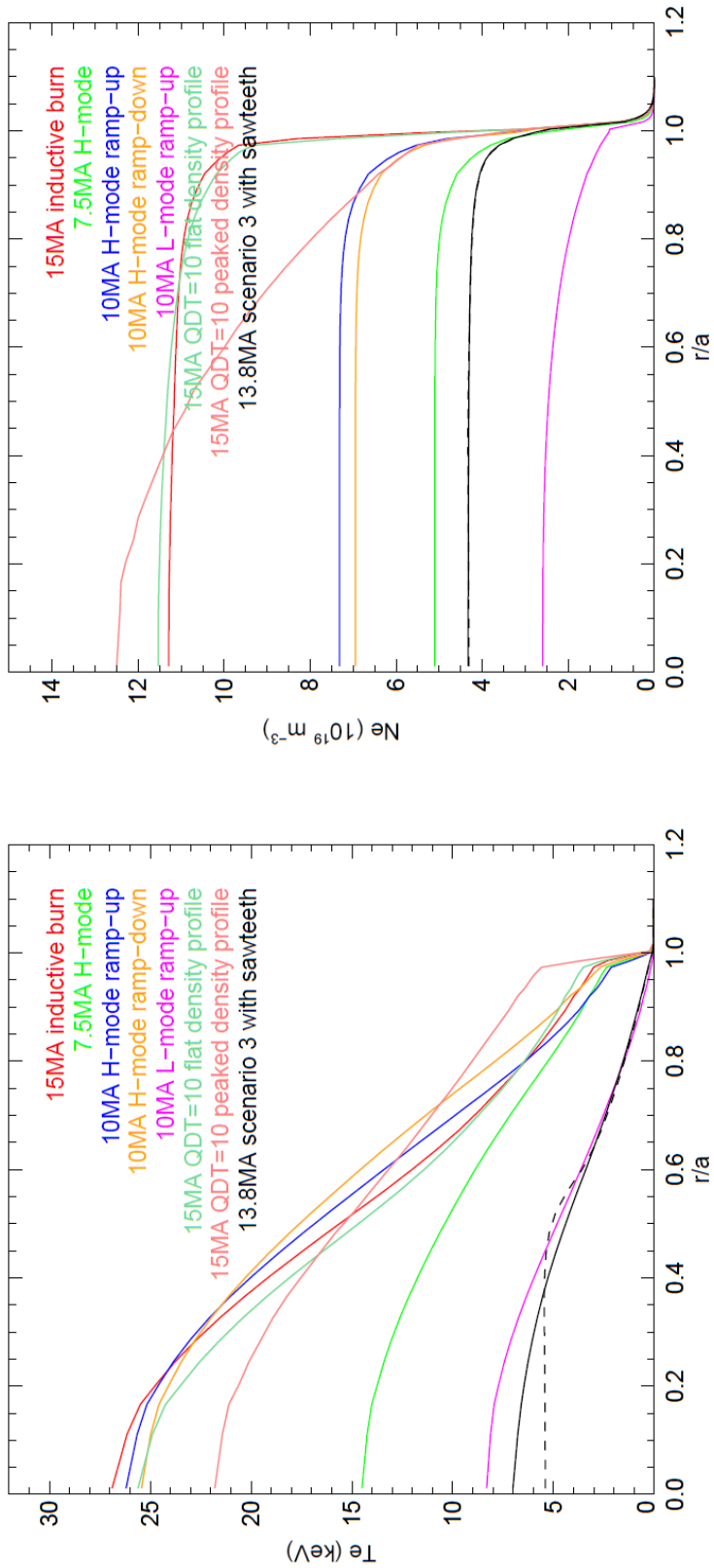
ADAS has been part of plasma emission modelling for ITER diagnostic design studies since 1995.

Increasingly developed during the recent round of Conceptual Design Studies 2010-2013

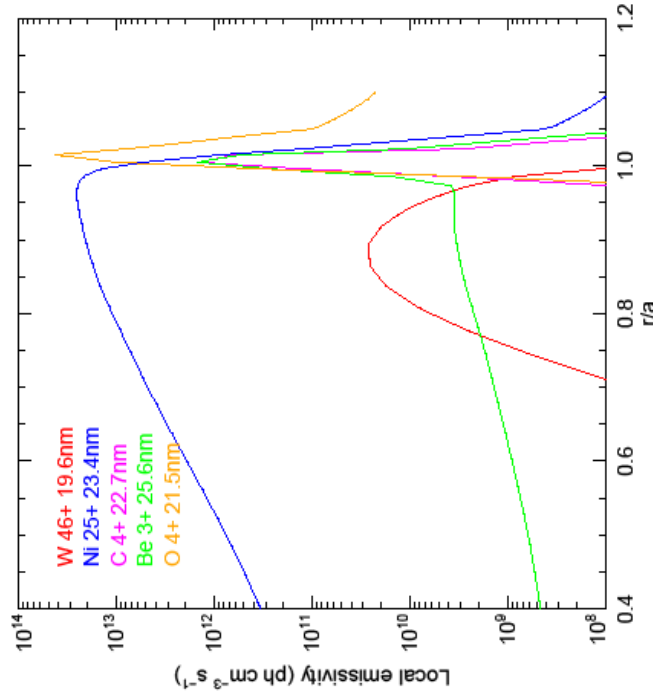
- Wide range of ITER plasma scenarios – start-up low current etc
- Wide spectrum now modelled – Visible > UV > VUV > X-ray
- Can include instrumental effects in modelled spectra
- Lines of sight and fan-views can be set up to suit actual diagnostic design
- Whole new area opening up with ITER



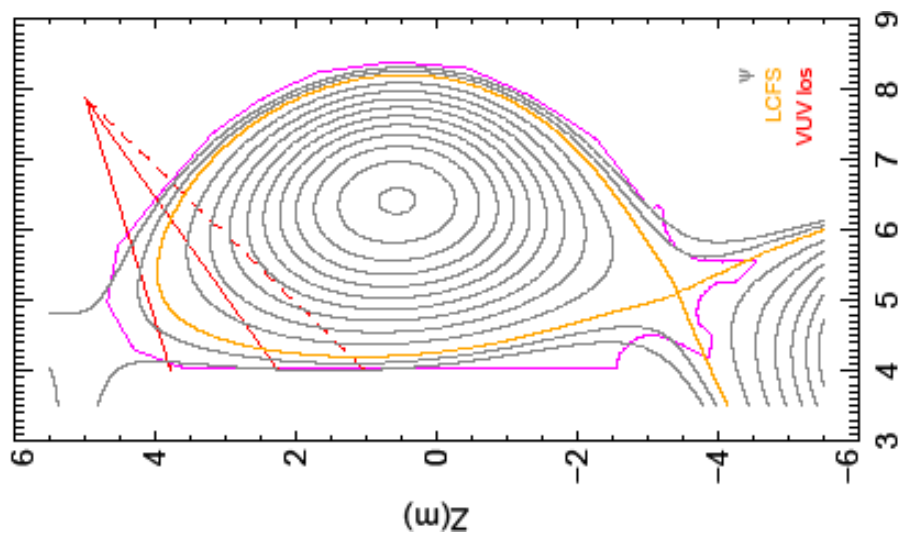
Wide range of plasma scenarios for ADAS-SANCO modelling



ADAS/SANCO Modelled emission of VUV spectral lines



VUV lines 10 – 100 nm
mostly in the outer plasma



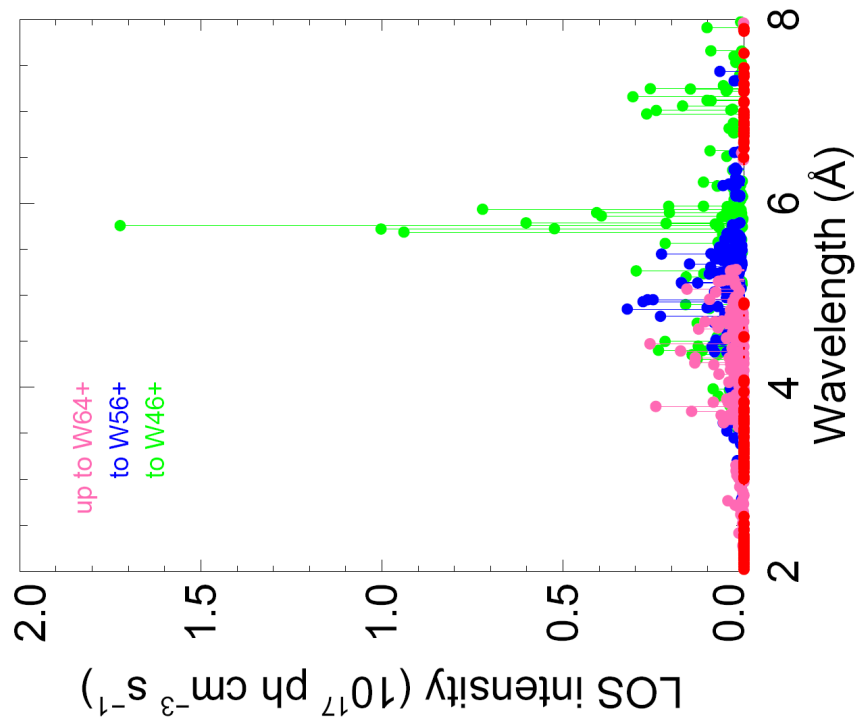
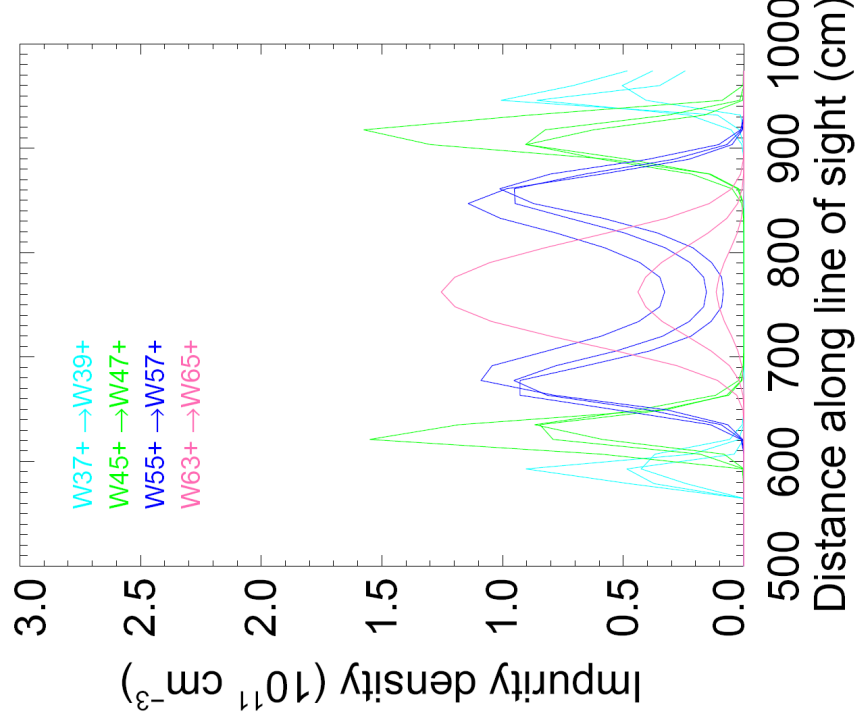
SANCO post-processing lines of sight
for imaging VUV spectrometer



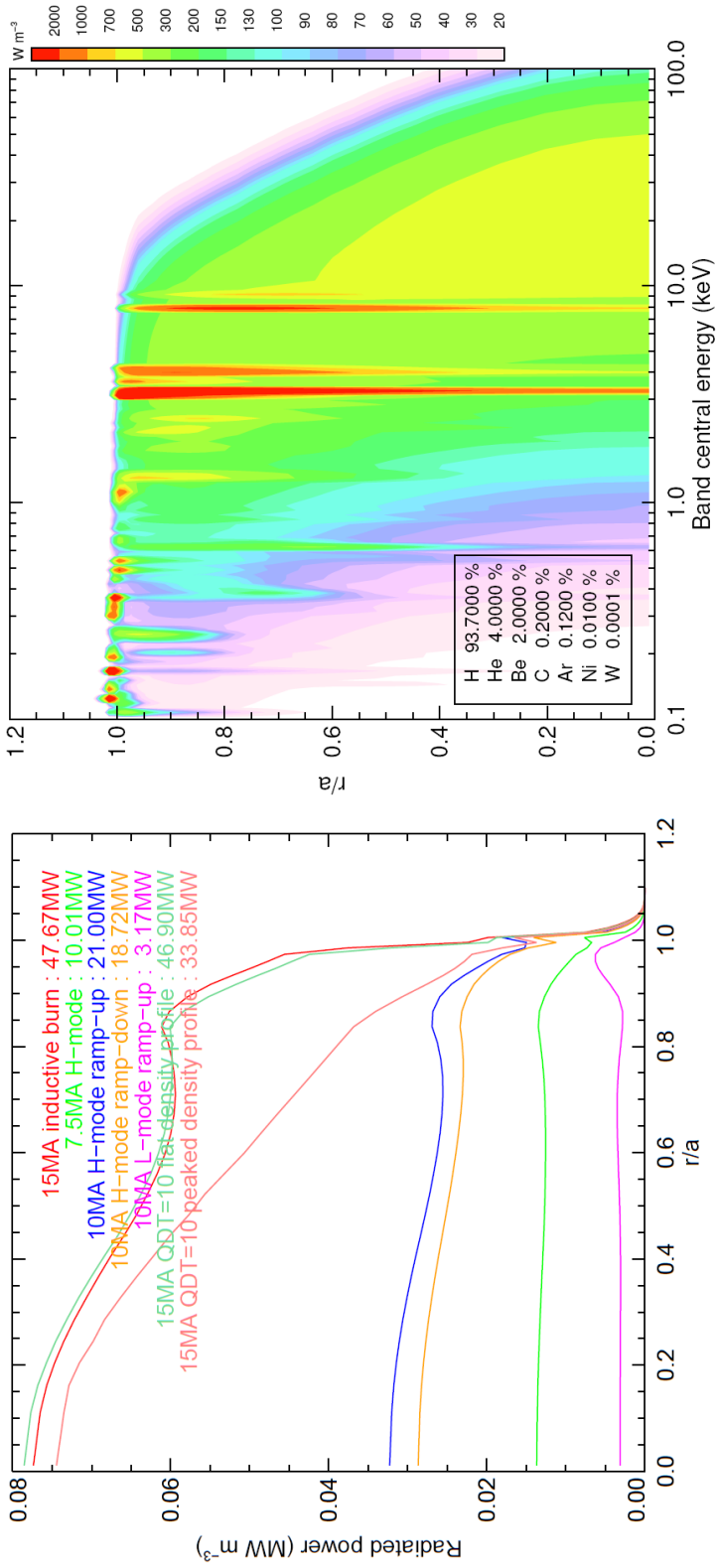
china eu india japan korea russia usa
© 2013, ITER Organization

ADAS-EU Meeting – September - 2013
ADAS Workshop, Armagh, 5 October 2010, R Barnsley

W chordal profiles for various ionization stages & synthetic soft x-ray spectrum



-
- Total core radiated power is around 50 MW – mostly x-rays**
- This is a strong test of atomic data and plasma modelling
- Requires all excitation phenomena to be handled
 - electron impact, recombination, continuum etc.



Total radiated power profiles for a range of plasma scenarios

X-ray profile resolved into 5% energy bands

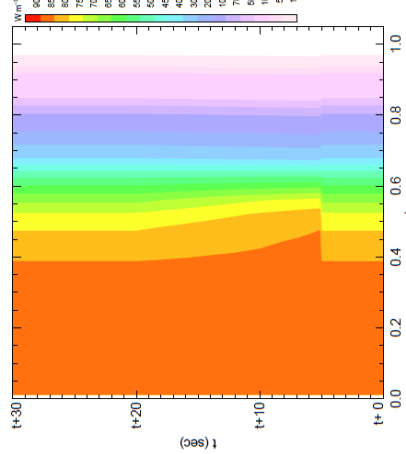


ADAS-EU Meeting– September - 2013

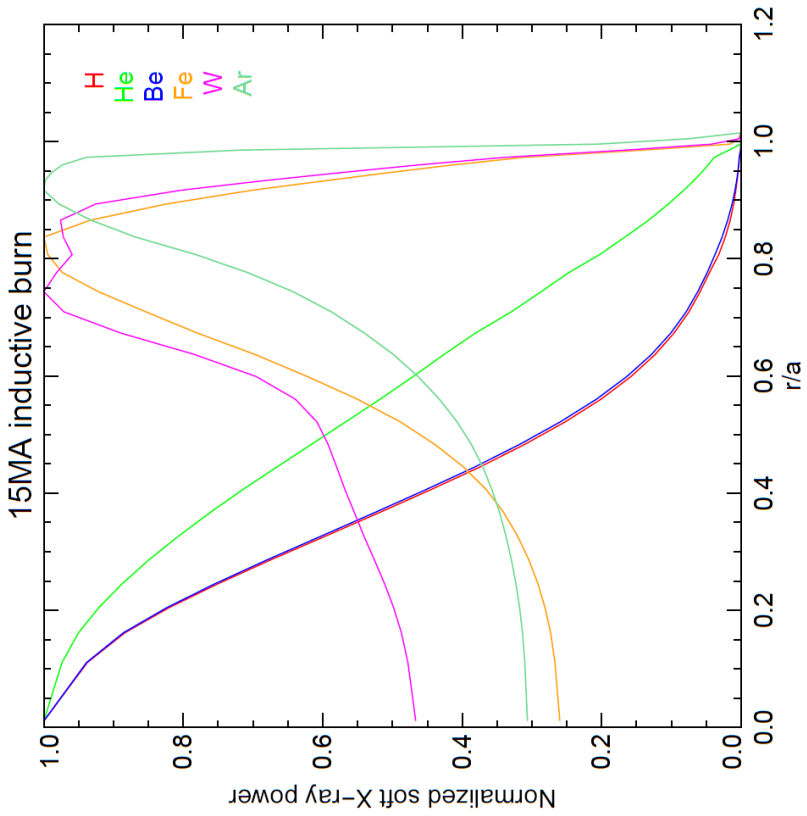
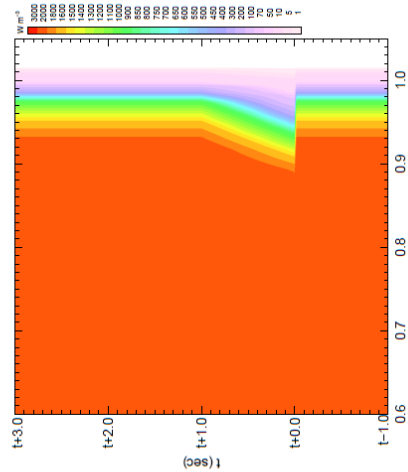
© 2013 ITER Organization

Characteristic impurity radiated power profiles

SXR emission during a sawtooth event



SXR response to uncontrolled ELMs



ADAS-EU Meeting– September - 2013

© 2013 ITER Organization

Active Spectroscopy



china eu india japan korea russia usa
© 2013, ITER Organization

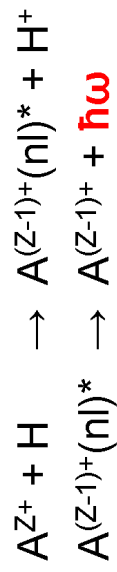
ADAS-EU Meeting– September - 2013

Page 28

ITER Active Beam Spectroscopy

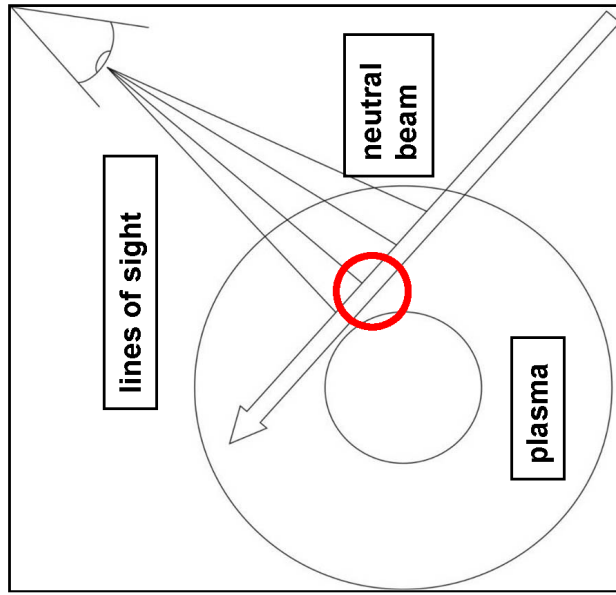
CXRS principle:

Emission of spectral lines $\hbar\omega$ excited by charge exchange collision:



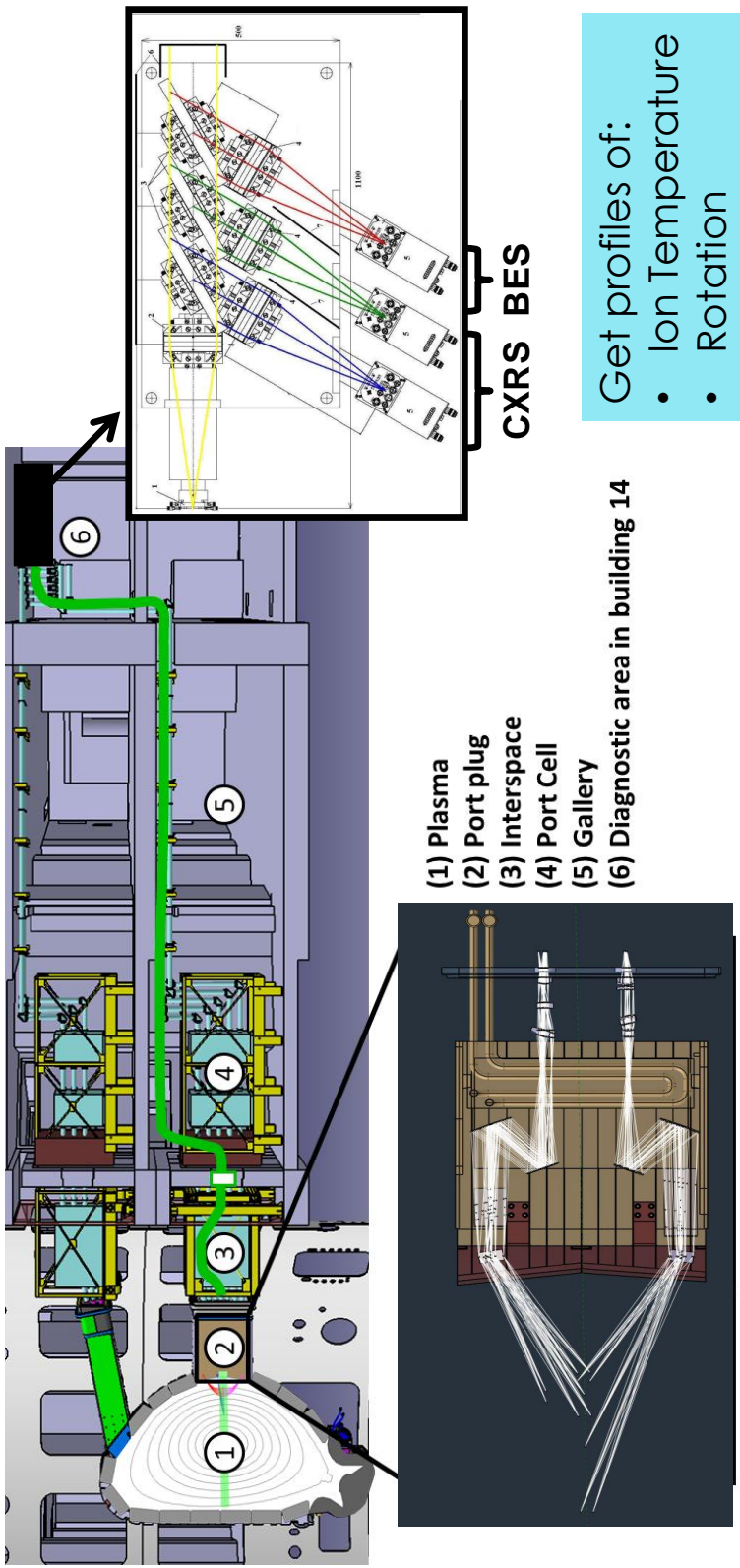
From spectrum analysis, ion density, temperature and velocity are obtained.

Also BES and MSE

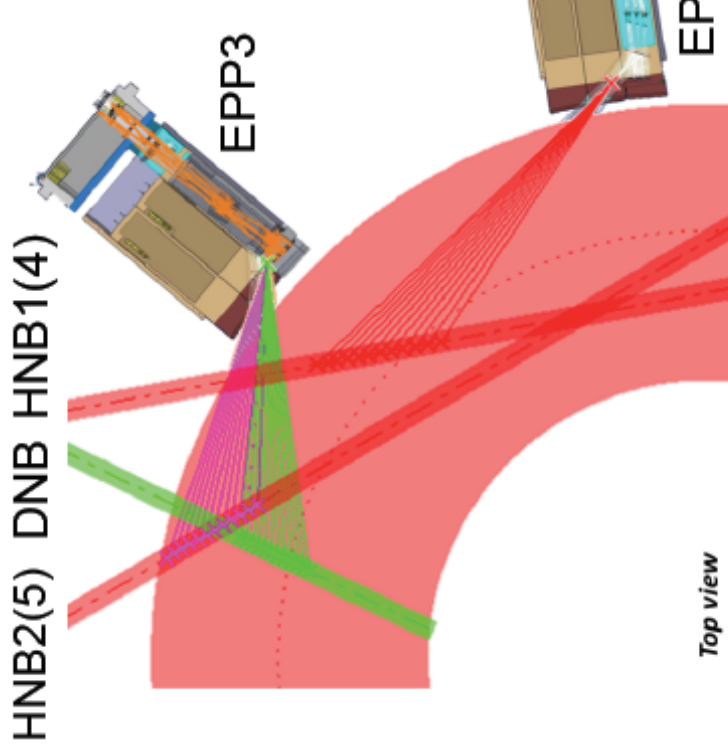


Outline Design for Edge CXRS in Eq3

- Measures the outer half of the plasma – key parameters

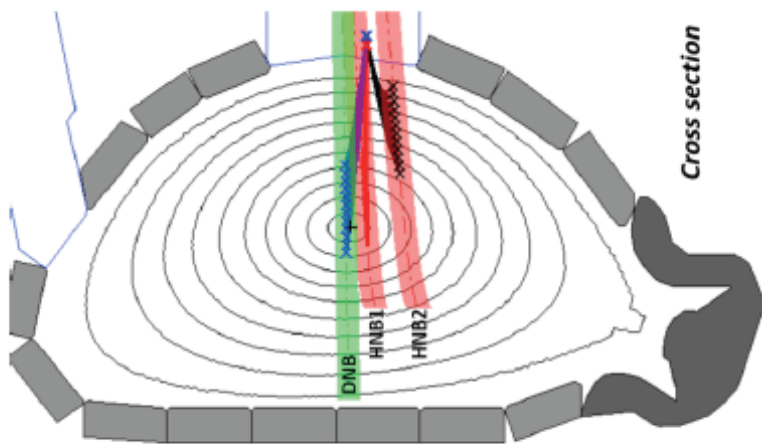


Overview of MSE



(from GLB7UC – MSE CDR- Lexington)

Heating beams may be on or off axis



Line Splitting versus Line Polarisation now an important discussion



© 2013, ITER Organization
china eu india japan korea russia usa

Where are we?



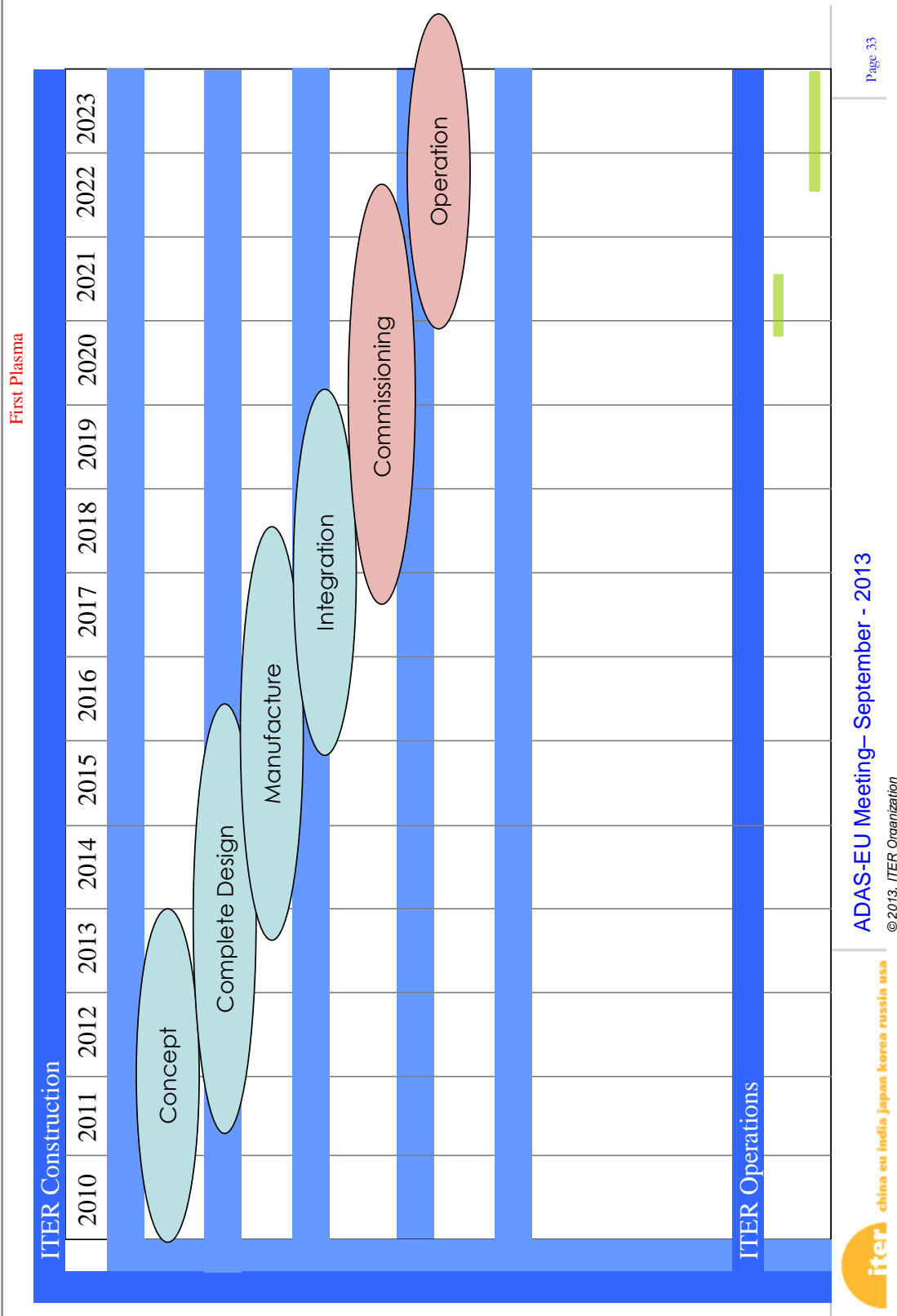
china eu india japan korea russia usa

© 2013, ITER Organization

ADAS-EU Meeting– September - 2013

Page 32

Present planning for ITER Diagnostics



Summary

- Conceptual design and integration of ITER spectroscopy is almost complete.
- Now entering Preliminary Design phase, in collaboration with international teams.
- ADAS has been essential input to diagnostic designs:
 - Management of huge atomic data archive
 - Availability of applications to retrieve and process atomic data
 - Availability of ADAS experts to model and interpret plasma emission
- Next Steps
 - More detailed analysis to support the advanced design stages
 - Validation of system designs
 - Update plasma emission modelling with new atomic data as available
 - Prepare for operation and data analysis phase
 - Please help us to tackle the new challenges



ADAS-EU Meeting– September - 2013

© 2013, ITER Organization

A.4 The ADAS and ADAS-EU Projects - Prof. Hugh Summers



Atomic data and modelling for fusion

The ADAS and ADAS-EU Project

Hugh Summers, Martin O'Mullane, Alessandra Giunta

University of Strathclyde

ADAS/ADAS-EU
29 May 2013
Hefei, China

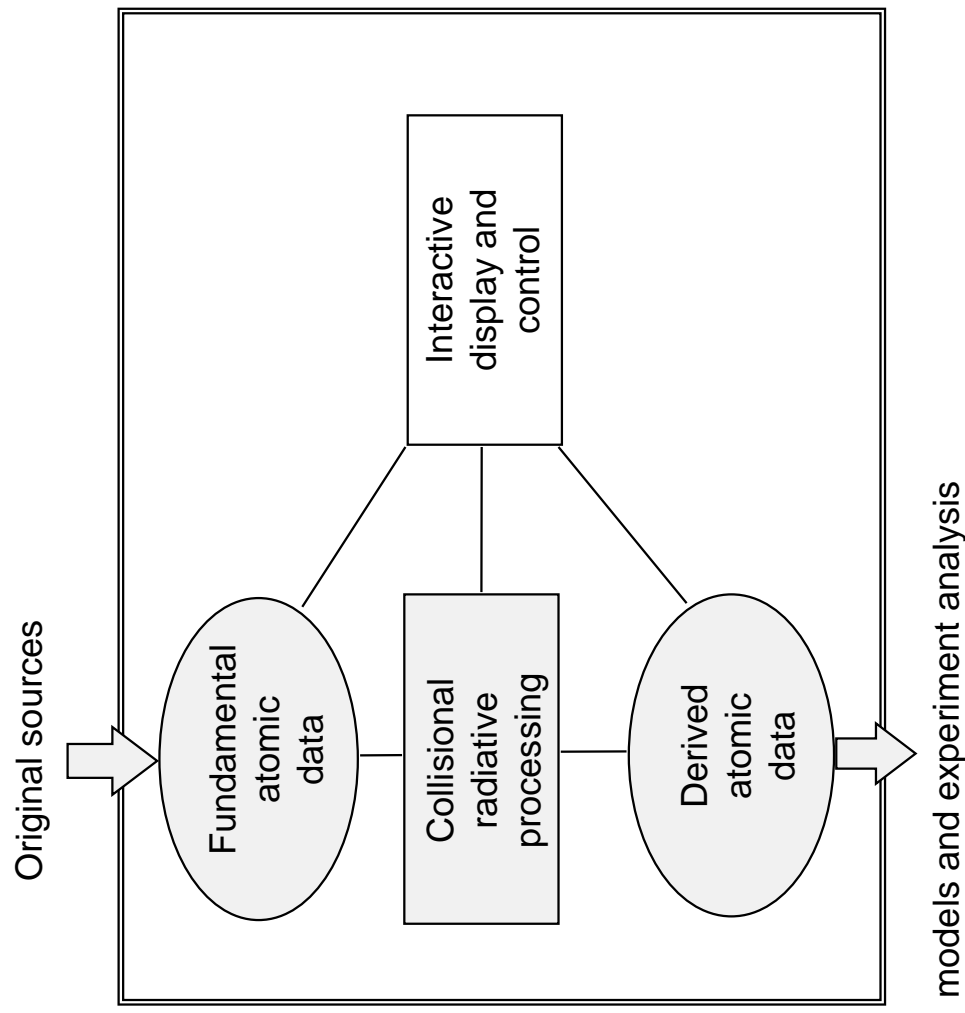
Contents

1. The Atomic Data and Analysis Structure, ADAS
2. ADAS-EU
3. Objectives of the workshop
4. Scope of ADAS modules

The establishment of the ADAS Project

- Theoretical atomic physics support commenced at JET - 1984
- Centralised atomic data and coding under EDII, JET - 1985
- First IBM/TSO interactive ADAS release - 1989
- UNIX conversion preparatory study - 1993
- Start of ADAS project managed by Strathclyde University - 1993
- ADAS UNIX/IDL conversion - 1993/95
- 1st ADAS annual Workshop - 1995
- Start of ADAS project on going maintenance - 1996
- First non-voting university members (TUV) - 1997

ADAS modelling schematic



Atomic Data and Analysis Structure

- **ADAS Project:** origin in JET-ADAS, self-funded by subscription of participating laboratories.

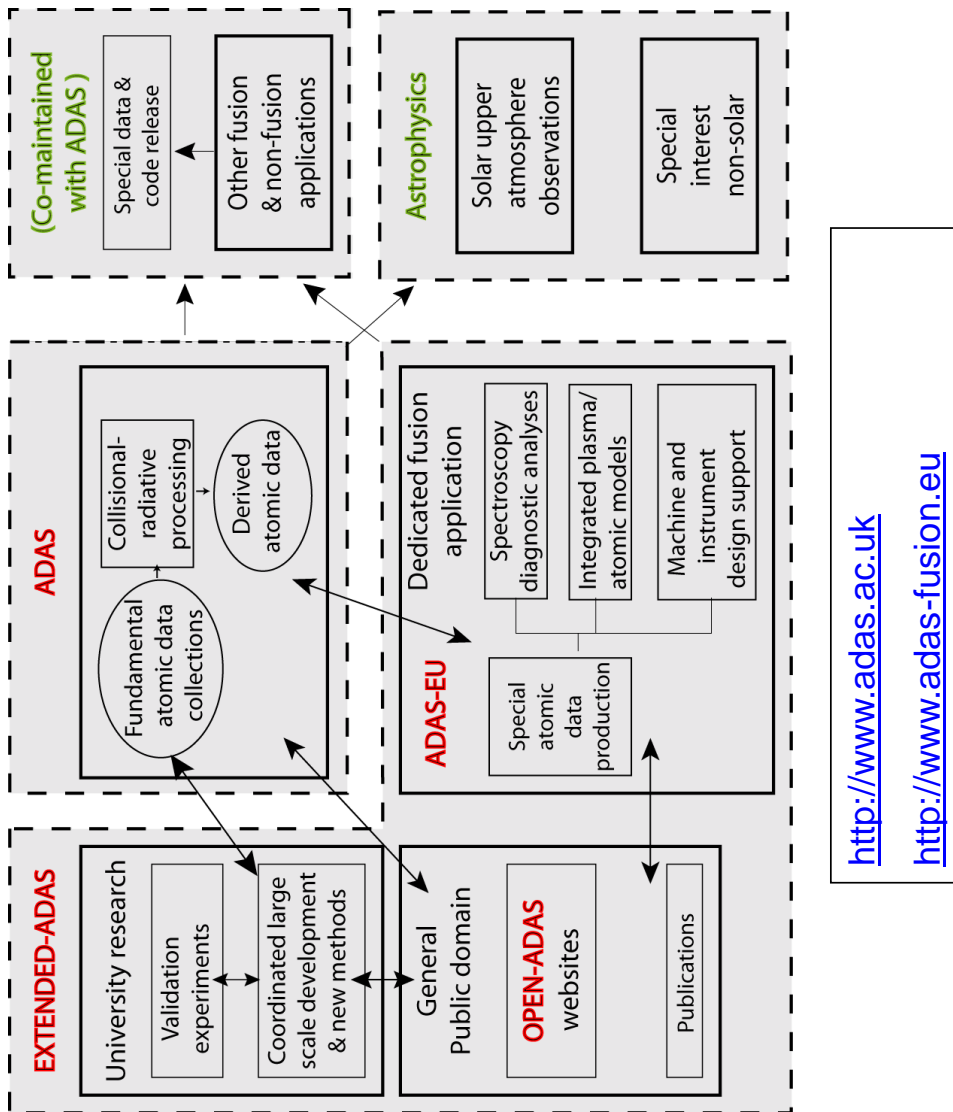
Membership:

EU Associated Labs.: JET, UKAEA Culham, IPP Garching/Greifswald, Fz-Juelich, CEA Cadarache, KTH Stockholm, CRPP Lausanne, CRFX Padua, TUW Vienna, FOM-Rijnhausen, NILPRP Bucharest, Romania.

International Fusion: NIFS Japan, JAEA Japan, IPR India, BIRLA Jaipur India, SWIP China, IPP-CAS China, GA USA, Madison USA, ORNL USA, Univ. of Texas, USA, Univ. of Toronto Canada, Auburn University USA, Triniti/Kurchatov Russia, Princeton Univ. USA, NFRI Korea, ITER. Other: Philips Research labs/JLT Aachen Germany, RAL Space Science UK, Catania Observatory/University Italy, Armagh Observatory Northern Ireland.

- **ADAS-EU:** European Union Framework 7 Support Action for fusion in Europe; Jan 2009 - Dec 2012; Univ. of Strathclyde research staff based full-time at fusion labs. in Europe - CCFE Culham/ JET Facility, IPP Garching, Fz-Juelich, CEA Cadarache/ITER. Extension to Sep 2013.
- **OPEN-ADAS:** open, web-based access to selected ADAS data, shared funding by IAEA A&M Data Unit and ADAS. A dissemination pathway for ADAS-EU. Upgrade 2013 by ADAS-EU.
- **EXTENDED-ADAS:** staff build and maintain shared analysis tools (eg CXSFIT, UTC) for fusion labs; support and prepare interfaces to primary fusion modelling codes; coordinate large scale developments for fundamental data generation.

ADAS overview and connections



<http://www.adas.ac.uk>

<http://www.adas-fusion.eu>

The character of ADAS

- ADAS is a reaction set database.
 - Comprises fundamental and derived data.
 - Associated with specific diagnostic or plasma model application purposes.
 - Reaction sets must be complete for a purpose, for example sufficient to support an excited population calculation for an ion.
 - ADAS implements its own *collisional-radiative* modelling to convert fundamental data to applied data.
 - The ADAS Project actively manages the procurement of fundamental data for its purposes.

<http://www.adas.ac.uk>

Fundamental and derived data

- Most spectroscopic diagnostic analysis of plasmas and most plasma models do not use fundamental reaction data directly.
- Derived data, combining the effects of perhaps many reactions through collisional-radiative models, are required, such as **effective emission coefficients** and **effective recombination coefficients**.
 - Plasma and atomic time constants determine the form of the derived coefficient data.
 - The derived data are, at minimum, functions of plasma Te and Ne.
- ADAS is quite prescriptive about the form and content of its fundamental and derived data – called ADAS data format numbers (**adf<nn>**).
- These formats are decided in advance with source producers and diagnosticians before substantive production.

Database

- Fundamental data, derived data, drivers etc. Currently ~ 18 Gbytes.
- There are ~ 55 different ADAS data formats.
- Some key ADFs and MDFs for general application
 - *ADF04* : specific ion data
 - *ADF11* : coll.-rad. ionis., recom. and related coefficients.
 - *ADF13* : ionisation per photon ratios
 - *ADF15* : emissivity coefficients
 - *ADF40* : envelope feature photon emiss. Coefficients
- MDFs:
 - *MDF00*: fundamental diatomic molecular constants
 - *MDF01*: rovibronic models
 - *MDF02*: fundamental cross-section data
 - *MDF04*: specific molecule data

Computational overview of ADAS

- The interactive user interface
 - ADAS series (9 series, ~85 programs)
- The fundamental and derived databases (~30,000 datasets)
 - ADAS data formats
- The application interface
 - ADAS Fortran subroutine (~1900) and IDL procedure (~1700) libraries
 - Data extraction procedures and subroutines by format: `xxdata_<nn>`,
`read_adf<nn>`, `xxdatm_<nn>`, `read_mdf<nn>`.
- Offline-ADAS for large scale production
 - 6 large scale production packages: `adas7#1`, `adas7#3`, `adas8#1`, `adas8#2`,
`adas8#3`, `adas8#4`.
- Documentation

OPEN-ADAS

- Path for release of ADAS data and support software into the public domain.
- Development cost shared with ADAS and IAEA Vienna. Implemented by Allan Whiteford.
- Operational for five years. Resides on Strathclyde servers, mirrored at IAEA Vienna, who maintain statistics on usage.
- Major upgrade, supported by an ADAS-EU sub-contract, implemented by Allan Whiteford. New version released in Feb 2013.

<http://open.adas.ac.uk>

OPEN-ADAS

OPEN-ADAS

Atomic Data and Analysis Structure

Re I (6145.8A)

Freeform Wavelength Ion

λ Z^{q+}

Select an element from the periodic table

| | | | | | | | | | | | | | | | | | |
|----|----|----|----|----|----|----|----|----|----|----|----|----|----|----|----|----|----|
| H | He | | | | | | | | | | | | | | | | |
| Li | Be | C | N | O | F | Ne | | | | | | | | | | | |
| Na | Mg | Al | Si | P | S | Cl | Ar | | | | | | | | | | |
| K | Ca | Sc | Ti | V | Cr | Mn | Fe | Co | Ni | Cu | Zn | Ga | Ge | As | Se | Br | Kr |
| Rb | Sr | Y | Zr | Nb | Mo | Tc | Ru | Rh | Pd | Ag | Cd | In | Sn | Sb | Te | I | Xe |
| Cs | Ba | La | Hf | Ta | W | Re | Os | Ir | Pt | Au | Hg | Tl | Pb | Bi | Po | At | Rn |
| Fr | Ra | Ac | Ce | Pr | Nd | Pm | Sm | Eu | Gd | Tb | Dy | Ho | Er | Tm | Yb | Lu | |
| Th | Pa | U | | | | | | | | | | | | | | | |

Or specify an element and/or charge

Element Charge +

Search

Freeform search Search by wavelength Search by ion

About OPEN-ADAS

OPEN-ADAS is a system to search and disseminate key data from the Atomic Data and Analysis Structure (ADAS).

ADAS is a computer program managed by the University of Strathclyde and made up of a consortium of over twenty members.

The OPEN-ADAS system enables non-members, with an interest in fusion and astrophysics, to download and use ADAS data.

[More about OPEN-ADAS](#)

26 Feb 2013 - Major update to the website

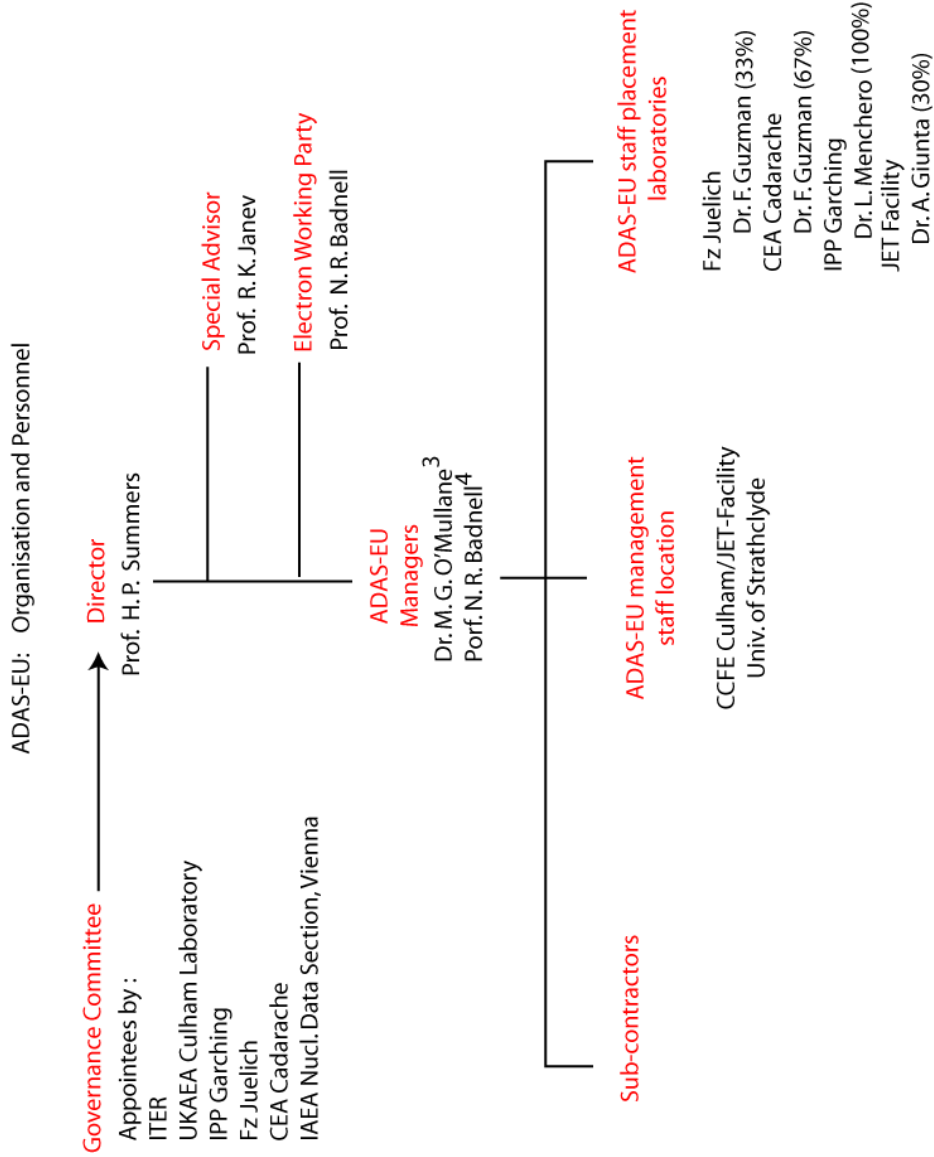
The OPEN-ADAS website has been updated with a new visual interface and the addition of three new data classes... [Read more](#)

The OPEN-ADAS data classes

The data contained within ADAS is strictly organised and precisely formatted. There are over fifty distinct types of data file. The scope of OPEN-ADAS is targeted on and limited to the release and organisation of general user relevant data from the ADAS databases and the provision of code, subroutines and procedures to enable such users of OPEN-ADAS to read the released data. These data classes are given below.

Done

ADAS-EU: organisation



The ADAS-EU team



Hugh Summers



Alessandra Giunta



Martin O'Mullane



Nigel Badnell



Luis Menchero



Francisco Guzman

ADAS-EU: physics theme support time chart

Figure 1

ADAS-EU: Physics theme and sub-theme support time chart

| Theme | Code | Actions | 2009 | 2010 | 2011 | 2012 |
|---|------|---|---|---|--|--|
| Heavy element spectroscopy and models | T1 | applic. fund. exploit. ³ | Baseline & emissivities ² Heavy species in ITER studies | Superstages & emissivities Tungsten spectral emission (ASDEX-U,JET) | Ionisation level 1 Atomic model support of ITM for ITER | Global scaling DR/GBPP level 1 Neutrals, level 2 |
| Charge exchange spectroscopy | T2 | applic. fund. exploit | CXSFIT shared analysis Bundle-n & I-mix models CXS line fitting extended to argon | Parametric CXS CTMC (improved) /CCAO/CCMC Multi-line CXS region observation | CXSFIT/transport link Bundle-nl models for partially stripped receivers Cross-linked CXS & passive diagnostic | |
| Beam stopping beam emission spectroscopy | T3 | applic. fund. exploit. | | Li/Na beam analysis and database Li/Na beam database | Beam emission/beam stopping consistency Bundle-n & Stark GCR | |
| Special features | T4 | applic. fund. exploit. | | | Integrated special feature fitting and display Zeeman, soft-X-ray, Balmer series special features | Beam emission exploitation for ITER |
| Diatomc spectra and coll-rad models | T5 | applic. fund. exploit. | | Fitting with spectral primitives H ₂ /H electr. & ion database | He-like soft X-ray line analysis H ₂ /H vibronic/GCR populations Composite continuum emission studies | Balmer series/limit observations H ₂ isotopomer spectral simul. Integrated edge modelling |

Notes: (1) Sets of 3 to 5 work packages make up the scientific support of each theme. Each work package is sub-divided into tasks.

(2) The completion of the sub-themes in the ‘applic.’ and ‘fund.’ categories mark science milestones. The sub-theme is an assembly of work package tasks.

(3) ‘exploit’ indicates the expected use by fusion plasma modellers and spectral diagnosticians on-site at European fusion laboratories, with which ADAS-EU staff will assist.

ADAS-EU: physics theme support time chart

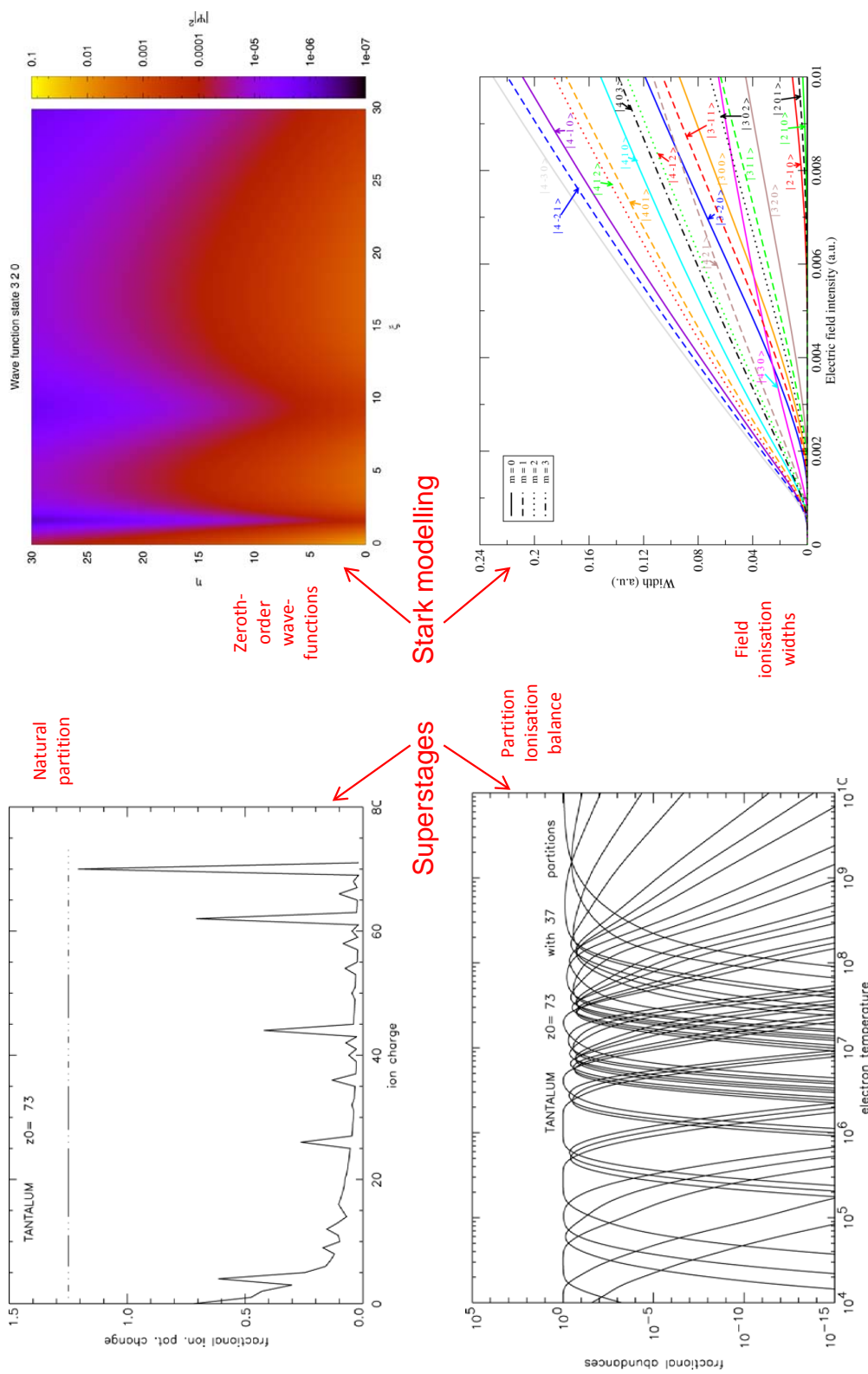
Figure 9a: Theme 6: Medium weight element Generalised-Collisional-Radiative modelling

| Work package | No. | Task | Task no. |
|---------------------------------------|-----|--|----------|
| AS/DW baseline lift to levels 1 and 2 | 27. | AUTOSTRUCTURE / Distorted Wave implementation in ls and ic coupling for ADAS adf04 production. | 27-1 |
| GCR ionisation and recombination | 28. | AUTOSTRUCTURE / Distorted Wave mass production for medium weight elements. | 27-2 |

ADAS-EU: sub-contract special studies

1. Univ. Autonoma, Madrid – Clara Illescas
Charge exchange and ion impact data for fusion plasma spectroscopy: State-selective charge transfer and excitation for low/medium charge projectiles and neutral hydrogen targets
2. Univ. Vilnius, Lithuania (x2) - Pavel Bogdanovich
Atomic structure and electron data for heavy element ions (1) configuration interaction and relativistic/quasi-relativistic structure. (2) auger/cascade, multiple ionisation and shake-off. (3) production of configuration interaction, quasi-relativistic atomic structure and cross-sections for the adas database. (4) atomic structure interchange.
3. Univ. Giessen, Germany – Alfred Mueller, Stefan Schippers
Electron impact cross-section data for fusion applications: Ionisation and recombination of heavy element ions
4. Tech. Univ. Vienna – Katherina Iggenbergs
Atomic data and models for neutral beam diagnostics. (1) lithium and sodium beam models and data.
(2) CCAO calculations for H (n=1,2) targets.
5. Queen's Univ. Belfast – Allan Hibbert, Kathy Ramsbottom
Electron collision cross-sections for heavy element ions : Pilot r-matrix calculations for tungsten – W⁺⁴⁴.
6. Univ. Mons-Hainaut (x2) - Pascal Quinet, Patrick Palmeri
Atomic structure and electron data for heavy element ions: (1) The tungsten ions W⁺⁰ to W⁺⁴ and adjacent element systems
(2) The ions w+3 to w+5 and adjacent element neutral/near-neutral ions. Atomic structure mapping between codes

ADAS/ADAS-EU: Important milestones and successes



ADAS-EU: dissemination and knowledge transfer

- **Courses:**
An intensive 1-2 week course on atomic modelling and using atomic data for fusion was presented annually.
8-16 Oct 2009: IPP Garching
7-15 Oct 2010: EFDA-JET Facility
26-30 Mar 2012: RFX Padua
26 Sep – 5 Oct 2012: CEA Cadarache
- **Spawnsed additional courses:** July 2010 Auburn USA, Dec 2010 ITER
- **Visits:**
Six support visits/year to fusion laboratories in Europe.
- **Collaborations:**
Small-scale sub-contracting to promote special studies for selective fundamental database improvement.

ADAS-EU: Modules

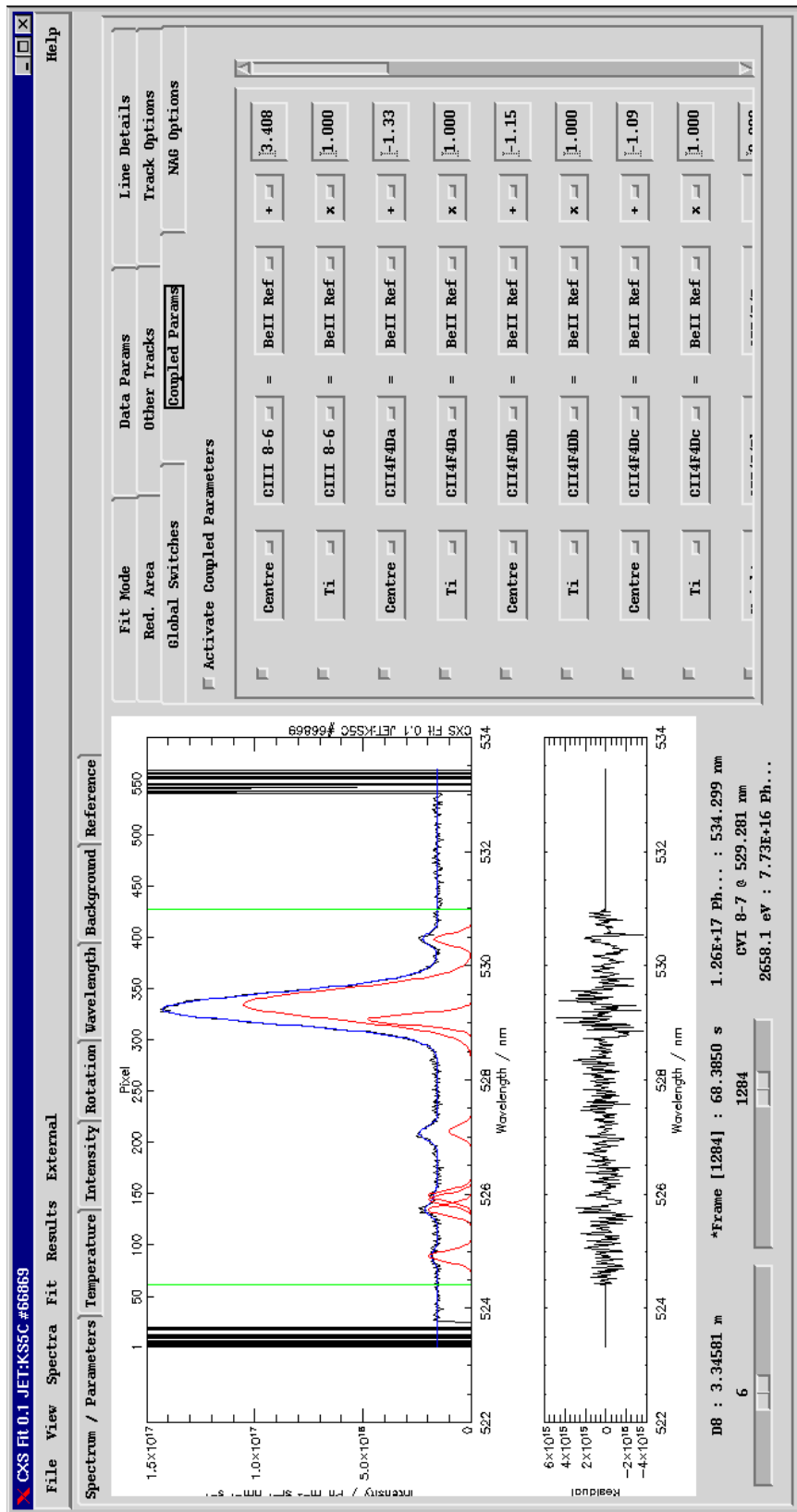
The **ADAS-EU Euratom - Framework 7 Project of the European Community** is sponsoring eight 3-day workshop/advanced training courses at fusion laboratories in Europe and in ITER participating countries outside Europe. The objectives are to examine atomic physics aspects of importance for participant laboratories, to inform by means of lectures and demonstrations about the principal advances made during the four years of ADAS-EU support, to explore the opportunities for new collaborative work on atomic physics with participants within the framework of the ADAS Project, cooperation with Europe and ITER.

There are eight modules available, each of duration 1.5 hours, comprising a lecture, demonstration and discussion.

1. Impurity atomic species in fusion plasma, their ionisation state and radiating characteristics - the ADAS approach.
2. Complex species in the core and edge of the fusion plasma. Describing and calculating their characteristics - the current state.
3. H₂ molecular emission and collisional-radiative modelling.
4. Modelling and analysing special spectral features. A unified approach.
5. Charge exchange and beam emission spectroscopy. Modelling emitter populations and analysing spectra.
6. Advanced charge exchange plasma receiver and beam donor modelling – the current state.
 1. Calculating fundamental atomic structure and electron impact cross-section data – Autostructure and R-Matrix .
 2. Spectral diagnostics for special environments – the interface between fusion and astrophysics.

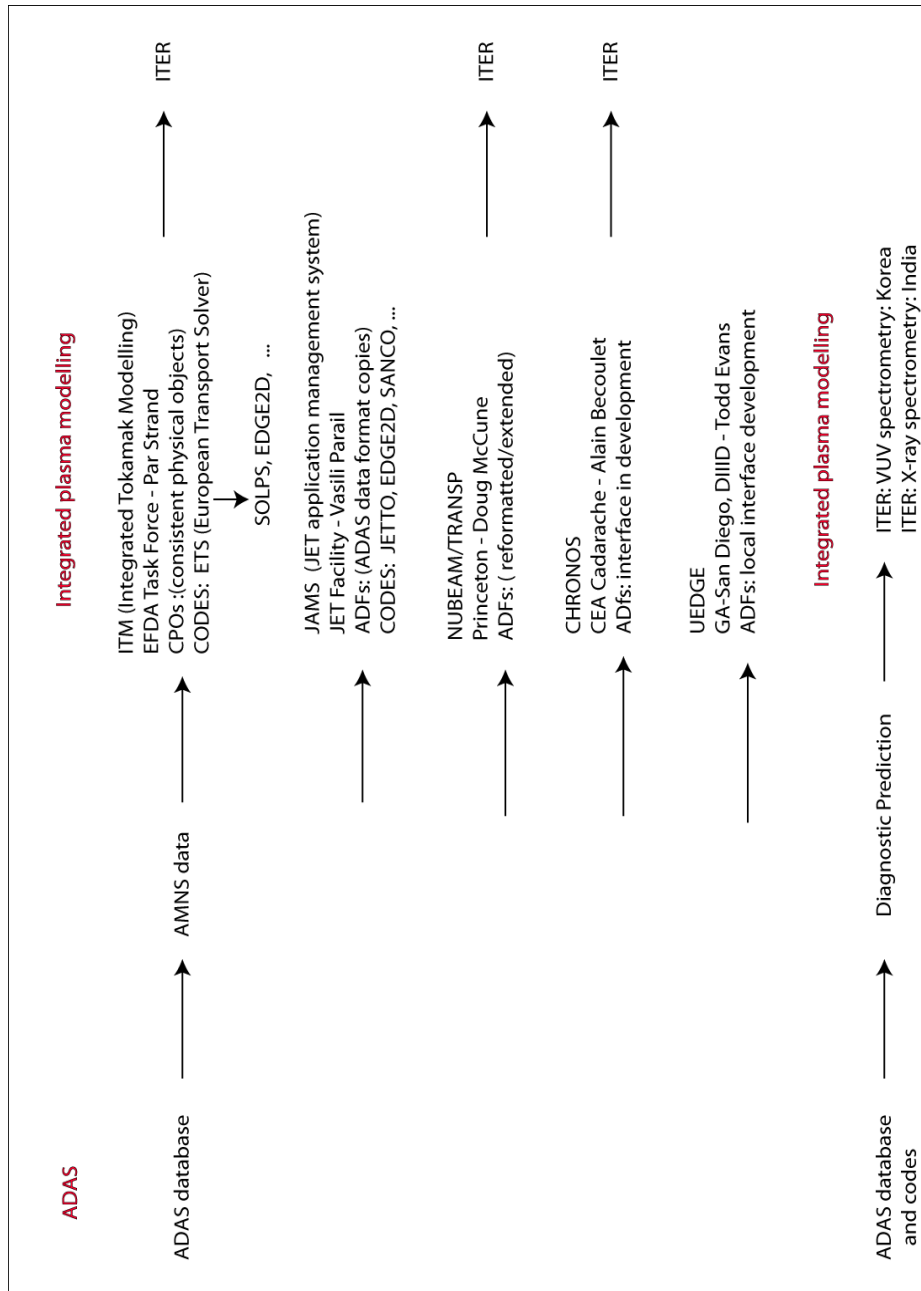
Extended ADAS: shared analysis tools

CXSFIT



Extended ADAS: Interfacing to integrated plasma modelling

Complexity develops as ADAS data is adopted and linked into large scale modelling and analysis efforts.



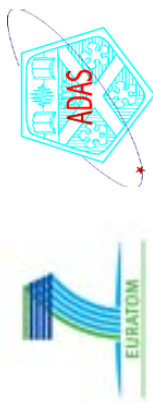
Conclusions

1. A brief history of the ADAS Project has been given.
2. The ADAS-EU Project has allowed strong growth in the capabilities of ADAS for fusion.
3. Tomorrow a full day is assigned to presenting and demonstrating some of these capabilities.
4. The time available is such that only four of the eight modules can be presented. However, ADAS/ADAS-EU staff will be here through until the end of the week so hopefully there will be opportunity for supplementary demonstrations, questions and discussions.
5. A primary wish is progress to the establishment of relevant collaborations in the support of ITER.
6. The third day is devoted to discussions in this regard.

Appendix B

ADAS-EU WATC: lecture viewgraphs

B.1 module_1



Module 1

Impurity atomic species in fusion plasmas, their ionisation state and radiating characteristics

Lecture viewgraphs

Hugh Summers, Martin O'Mullane and Alessandra Giunta

University of Strathclyde

Contents

1. Preliminaries and nomenclatures.
2. Basic population structure in plasmas.
3. Reaction processes and their description.
4. ADAS population and ionisation state modelling.
5. Conclusions

1.1 Preliminaries

In **thermodynamic equilibrium**, the radiation field and the distribution functions of particles at a specified temperature, T , are determined from statistical mechanics.

$$u(\tilde{v}) = \frac{8\pi h\tilde{v}^3}{c^3} / (e^{h\tilde{v}/kT} - 1)$$

$$\begin{aligned} u(\tilde{v}) &= \frac{8\pi h\tilde{v}^3}{c^3} / (e^{h\tilde{v}/kT} - 1) \\ &\quad \text{Planck radiation field energy density} \\ f(v) &= 4\pi \left(\frac{m}{2\pi kT} \right)^{3/2} e^{-\frac{1}{2}mv^2/kT} v^2 \\ &\quad \text{Maxwell speed distribution} \\ f(v) &= 4\pi \left(\frac{m}{2\pi kT} \right)^{3/2} e^{-\frac{1}{2}mv^2/kT} v^2 \\ &\quad \text{Boltzmann distribution} \\ \frac{N_i}{N_j} &= \frac{\omega_i}{\omega_j} e^{(I_i - I_j)/kT} \\ &\quad \text{Saha distribution} \\ \frac{N_i}{N_+ N_e} &= 8 \left(\frac{\pi a_0^2 I_H}{kT} \right)^{3/2} \frac{\omega_i}{2\omega_+} e^{I_i/kT} \end{aligned}$$

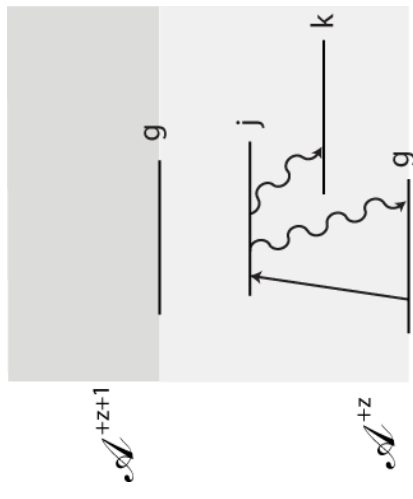
Radiation usually escapes freely from magnetic confinement fusion plasma, so the internal radiation field is zero and populations may be very different from those in thermo-dynamic equilibrium. This enables emission line spectroscopy, but adds complexity to modelling.

1.2 Nomenclature

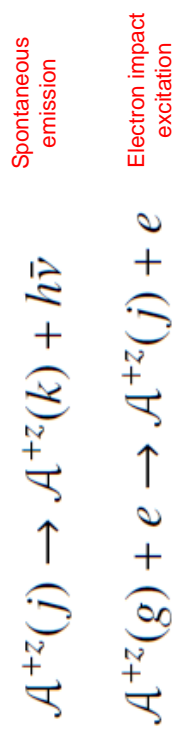
- For element \mathcal{A} , denote the ion charge by z , the nuclear charge by z_0 .
Introduce $z_1 = z+1$. The number of bound electrons $N = z_0 - z$.
- An **iso-electronic sequence** is the set of ions with the same number of electrons, such as the Be-like sequence:
 $\text{Be}^0, \text{B}^{+1}, \text{C}^{+2}, \text{N}^{+3}, \dots$
- An **iso-nuclear sequence**, is the set of ions with the same nuclear charge, such as the carbon iso-nuclear sequence:
 $\text{C}^0, \text{C}^{+1}, \text{C}^{+2}, \text{C}^{+3}, \text{C}^{+4}, \text{C}^{+5}, \text{C}^{+6}$
- A spectrum line is specified by giving initial and final states and the wavelength. $\text{CIII}(2s3p\ ^3P \rightarrow 2s3s\ ^3S) \ \lambda 464.7 \text{ nm}$
- A spectrum line is really a set of component lines between degenerate groups of initial and final states

| | | | | |
|----------------------|--------------------------|--------------------------|-------------------|------------------|
| <i>configuration</i> | $1s^2 2s 3p$ | n, l quantum numbers | \longrightarrow | transition array |
| <i>term</i> | $1s^2 2s 3p\ ^3P$ | $+ S, L$ quantum numbers | \longrightarrow | multiplet |
| <i>level</i> | $1s^2 2s 2p\ ^3P_1$ | $+ J$ quantum number | \longrightarrow | component |
| <i>state</i> | $1s^2 2s 2p\ ^3P_1^{-1}$ | $+ M$ quantum number | | |

2.1 Coronal picture for spectral line emission



Reactions:

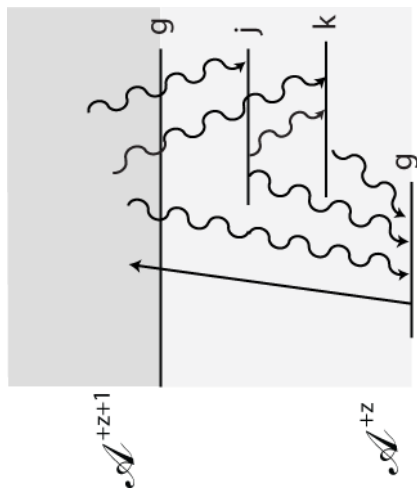


Statistical balance: $N_j = N_e N_g q_{g \rightarrow j} / (A_{j \rightarrow k} + A_{j \rightarrow g})$

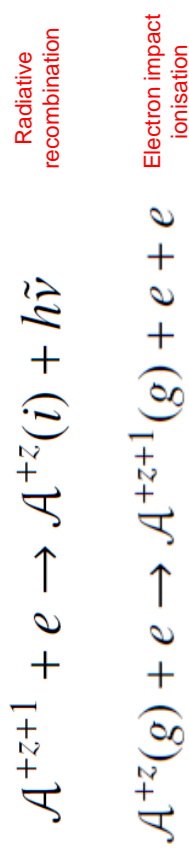
Emissivity: $\epsilon_{j \rightarrow k} = A_{j \rightarrow k} N_j = N_e N_g A_{j \rightarrow k} q_{g \rightarrow j} / (A_{j \rightarrow k} + A_{j \rightarrow g})$

Photon emissivity coefficient: $\mathcal{P}\mathcal{E}\mathcal{C}_{j \rightarrow k} = A_{j \rightarrow k} q_{g \rightarrow j} / (A_{j \rightarrow k} + A_{j \rightarrow g})$

2.2 Coronal picture for ionisation



Reactions:



$$\text{Statistical balance: } \alpha_{tot}^{(z+1 \rightarrow z)} N_e N^{+z+1}(g) \equiv (\alpha_j + \alpha_k + \alpha_g) N_e N^{+z+1}(g)$$

$$= q_{g \rightarrow e} N_e N^{+z}(g)$$

$$\equiv S_{tot}^{(z \rightarrow z+1)} N_e N^{+z}(g)$$

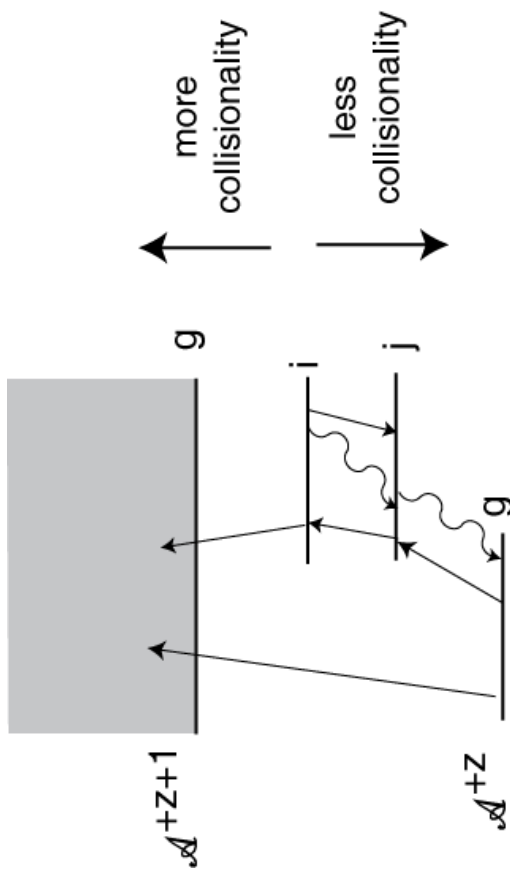
$$\frac{N^{+z+1}(g)}{N^{+z}(g)} = \frac{S_{tot}^{(z \rightarrow z+1)}}{\alpha_{tot}^{(z+1 \rightarrow z)}}$$

Ionisation balance ratio:

2.3 Collisional-radiative picture for line emission and ionisation

Reactions:

At higher densities, collisional excitation and de-excitation between excited levels compete with spontaneous emission.



Indirect pathways lead to line emission and ionisation may occur in a stepwise manner.

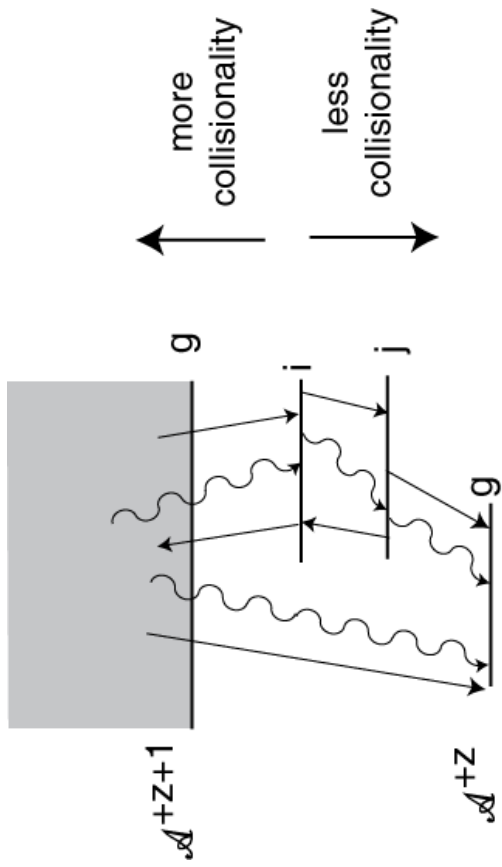
2.4 Collisional-radiative picture for line emission and recombination

Reactions:

Three-body recombination must be added to the reactions which pairs with collisional ionisation from excited states



Not all recombinations lead to growth of the ground population of the recombined ion.



2.5 Population equations

In statistical equilibrium:

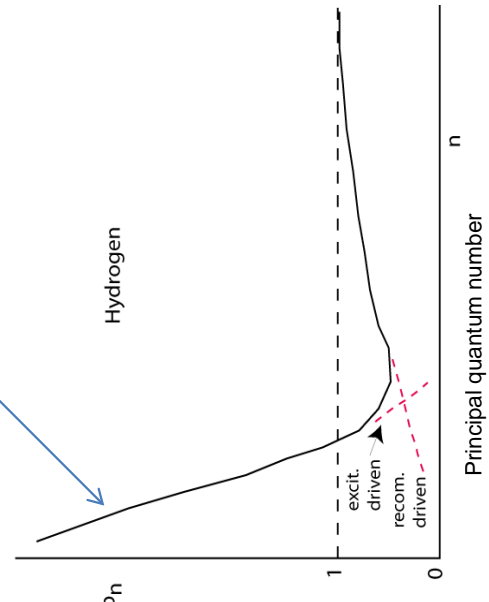
$$\begin{aligned}
 0 = \frac{dN_i}{dt} &= \sum_{I_{i'} < I_i} [A_{i' \rightarrow i} + N_e q_{i' \rightarrow i}] N_{i'} + \sum_{I_{i''} > I_i} N_e q_{i'' \rightarrow i} N_{i''} \\
 &+ N_e N_+ \alpha_i^{(r)} + N_e N_+ \alpha_i^{(d)} + N_e^2 N_+ \alpha_i^{(3)} \\
 &- (\sum_{I_{i''} > I_i} N_e q_{i'' \rightarrow i} + \sum_{I_{i'} < I_i} [A_{i' \rightarrow i} + N_e q_{i' \rightarrow i}] N_{i'} + N_e q_{i \rightarrow e})
 \end{aligned}$$

Introduce Saha-Boltzmann deviation factors, b_i

$$\frac{N_i}{N_+ N_e} = \left(\frac{N_i^{(saha)}}{N_+ N_e} \right) b_i = 8 \left(\frac{\pi a_0^2 I_H}{k T_e} \right)^{3/2} \frac{\omega_i}{2\omega_+} e^{I_i/kT_e} b_i$$

Solve for $b_i : i=1, \dots, \infty$

Bundle-n model for hydrogen at low density and temperature



Algebraic matrix representation:

$$\sum_j C_{ij} N_j = r_i N_e N_1^+ \quad i = 1, \dots$$

$$\text{Collisional-radiative matrix} \quad \frac{N_j}{N_e N_1} = \sum_{k, k \neq 1} \bar{C}_{jk}^{-1} \bar{C}_{k1} \left(\frac{1}{N_e} \right) + \sum_{k, k \neq 1} \bar{C}_{jk}^{-1} r_k \left(\frac{N_1^+}{N_1} \right) \quad j = 2, \dots$$

3.1 Radiative processes: bound-bound

$$\mathcal{A}^{+z}(i) \rightarrow \mathcal{A}^{+z}(j) + h\tilde{\nu}$$

line strength

There are various useful quantities related to the Einstein A-value. The line strength is symmetric between initial and final states.

$$\begin{aligned} \omega_i A_{i \rightarrow j} &= \frac{1}{6} \frac{\alpha^4 c}{a_0} \left(\frac{h\tilde{\nu}}{I_H} \right)^3 \frac{S_{ij}}{e^2 a_0^2} \\ &= \frac{1}{2} \frac{\alpha^4 c}{a_0} \left(\frac{h\tilde{\nu}}{I_H} \right)^2 \omega_j f_{j \rightarrow i} \end{aligned}$$

The oscillator strength is only applicable to dipole allowed transitions.

$$f_{j \rightarrow i} = f'_{j \rightarrow i} g_{ij}^J$$

bound-bound Gaunt factor

$$A_{i \rightarrow j} = \frac{16\alpha^4 c}{3\sqrt{3}\pi a_0} \frac{1}{\omega_i} \frac{1}{\nu_i^3} \frac{1}{\left| \frac{1}{\nu_i^2} - \frac{1}{\nu_j^2} \right|} g_{ij}^J$$

$$\frac{16\alpha^4 c}{3\sqrt{3}\pi a_0} = 1.57456 \times 10^{10} \text{ s}^{-1}$$

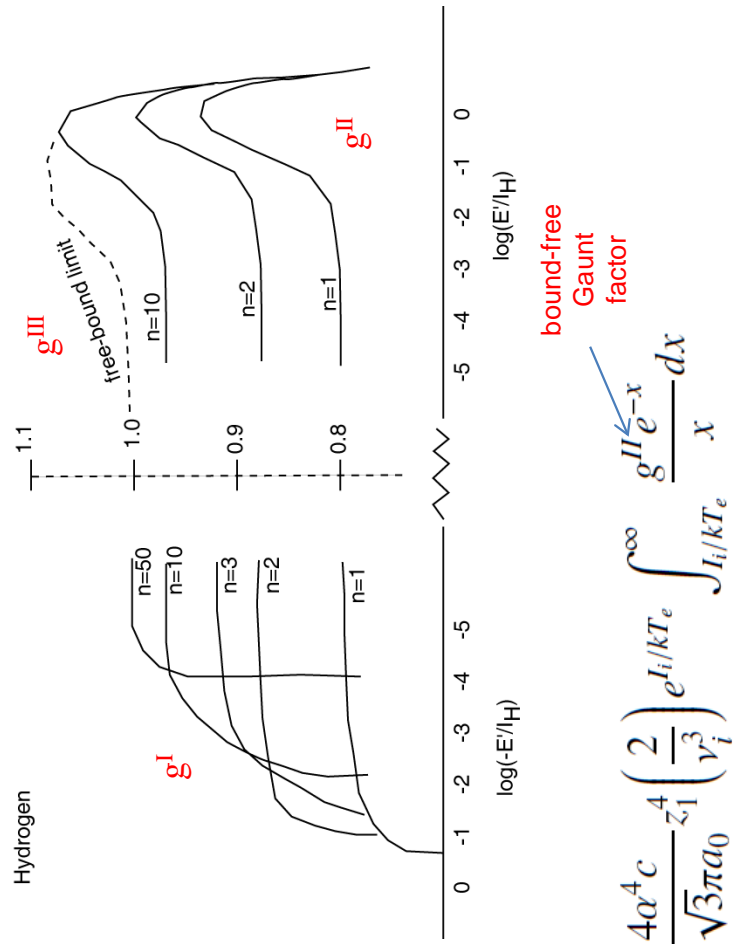
ν_i is the effective principal quantum number for level i. The Gaunt factor is usually fairly close to unity.

3.2 Radiative processes: bound-free



The Milne relation connects the photo-ionisation cross-section and the capture cross-section

$$Q_c(\tilde{\nu}) = \left(\frac{h\tilde{\nu}}{mv^c} \right)^2 \frac{\omega_i}{\omega_+} a(\tilde{\nu})$$



radiative recombination coefficient to level i.

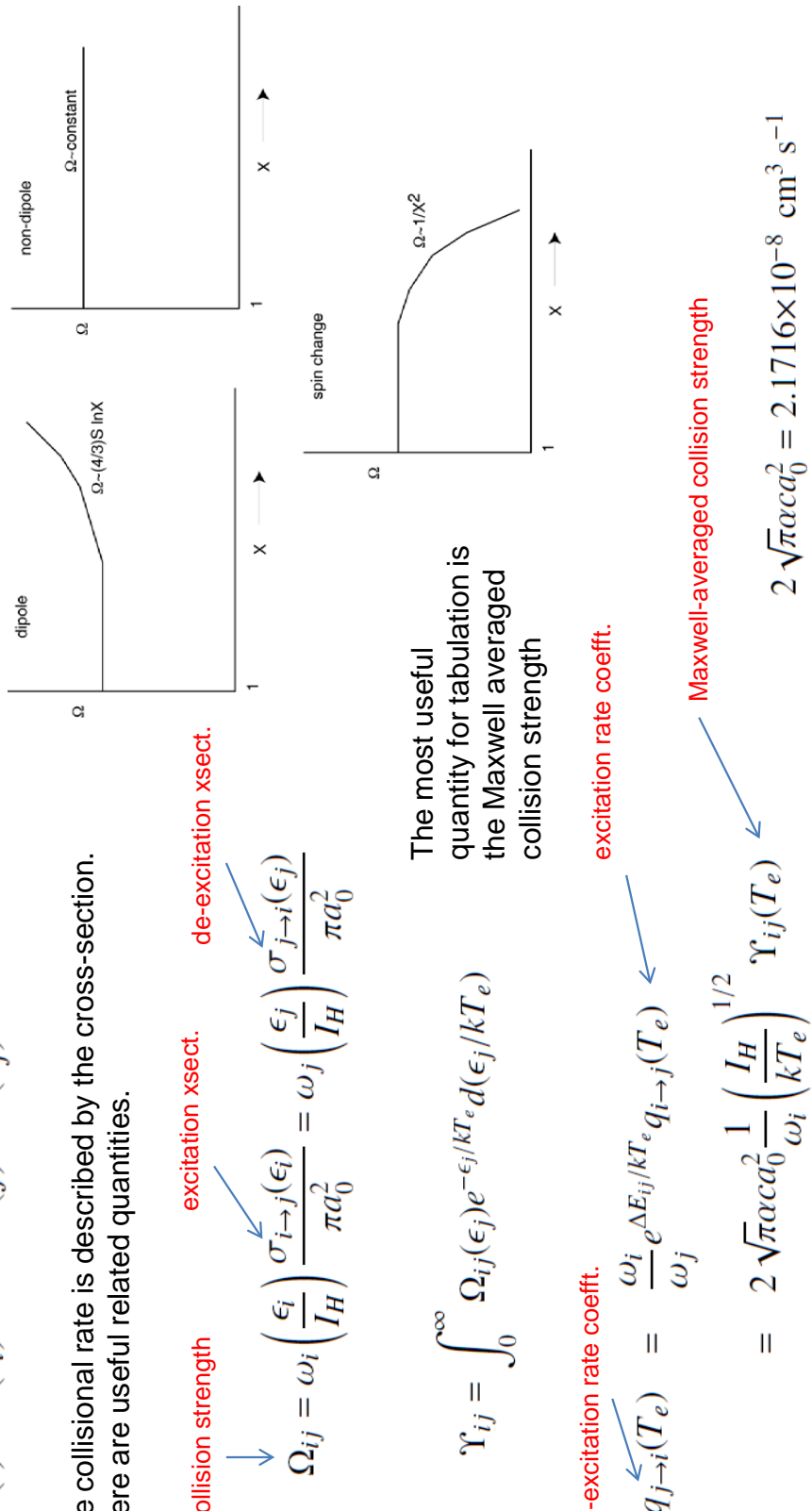
$$\alpha_i(T_e) = 8 \left(\frac{\pi a_0^2 I_H}{kT_e} \right)^{3/2} \frac{4\alpha^4 c}{3\sqrt{3}\pi a_0} z_1^4 \left(\frac{2}{\nu_i^3} \right) e^{I_i/kT_e} \int_{I_i/kT_e}^{\infty} \frac{g^{II} e^{-x}}{x} dx$$

Radiative recombination coefficients are archived in [adf08](#) and prepared by code [ADAS211](#).

3.3 Collisional processes: bound-bound

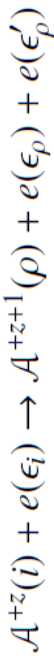


The collisional rate is described by the cross-section.
There are useful related quantities.



Comprehensive datasets of bound-bound radiative and collisional and energy level data are archived in [adf04](#).

3.4 Collisional processes: bound-free



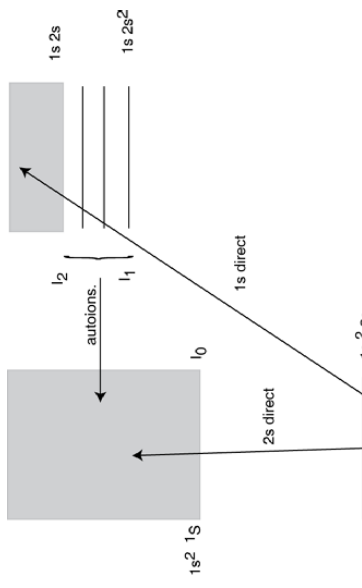
Excitation-autoionisation
must be included along with direct ionisation



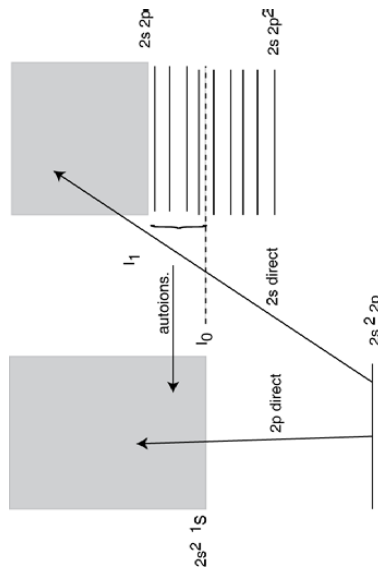
Thompson classical ionisation cross-section

$$\sigma_{i \rightarrow \rho+}(\epsilon_i) = 4\zeta\pi a_o^2 \left(\frac{I_H}{I_i} \right) \left(\frac{I_H}{\epsilon_i} \right) \left(1 - \frac{I_H}{\epsilon_i} \right)$$

$$\begin{aligned} \sigma_{i \rightarrow \rho+}^{tot} &= \sigma_{i \rightarrow \rho+} + \sum_k \sigma_{i \rightarrow k} \left(\frac{A_a}{A_a + A_r} \right) \\ &\sim \sigma_{i \rightarrow \rho+} + \sum_k \sigma_{i \rightarrow k} \end{aligned}$$



Li-like ionisation - case(a) example

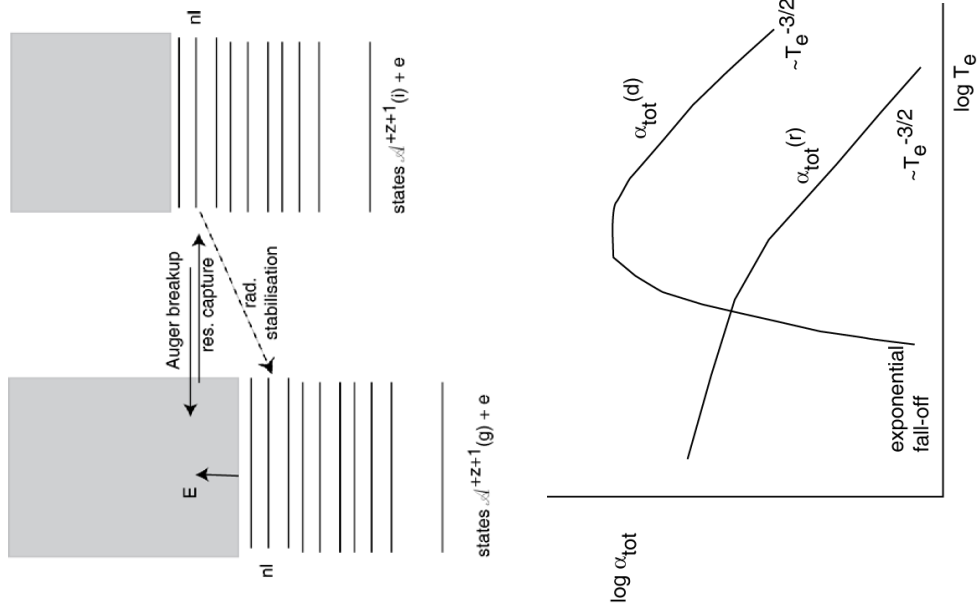


B-like ionisation - case(b) example

$$\sigma_{tot}^{BCHID}(z, \epsilon) = \sum_{i=1}^n \sigma^{BCHID}(z, I_i, \zeta_i, \epsilon)$$

ADAS collisional-ionisation data are archived in [adf23](#) and [adf07](#) and prepared offline with [ADAS8#2](#).

3.5 Dielectronic recombination

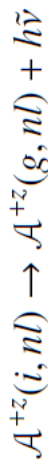


Reactions:

Resonance capture



Auger breakup



Radiative stabilisation

Doubly excited populations:

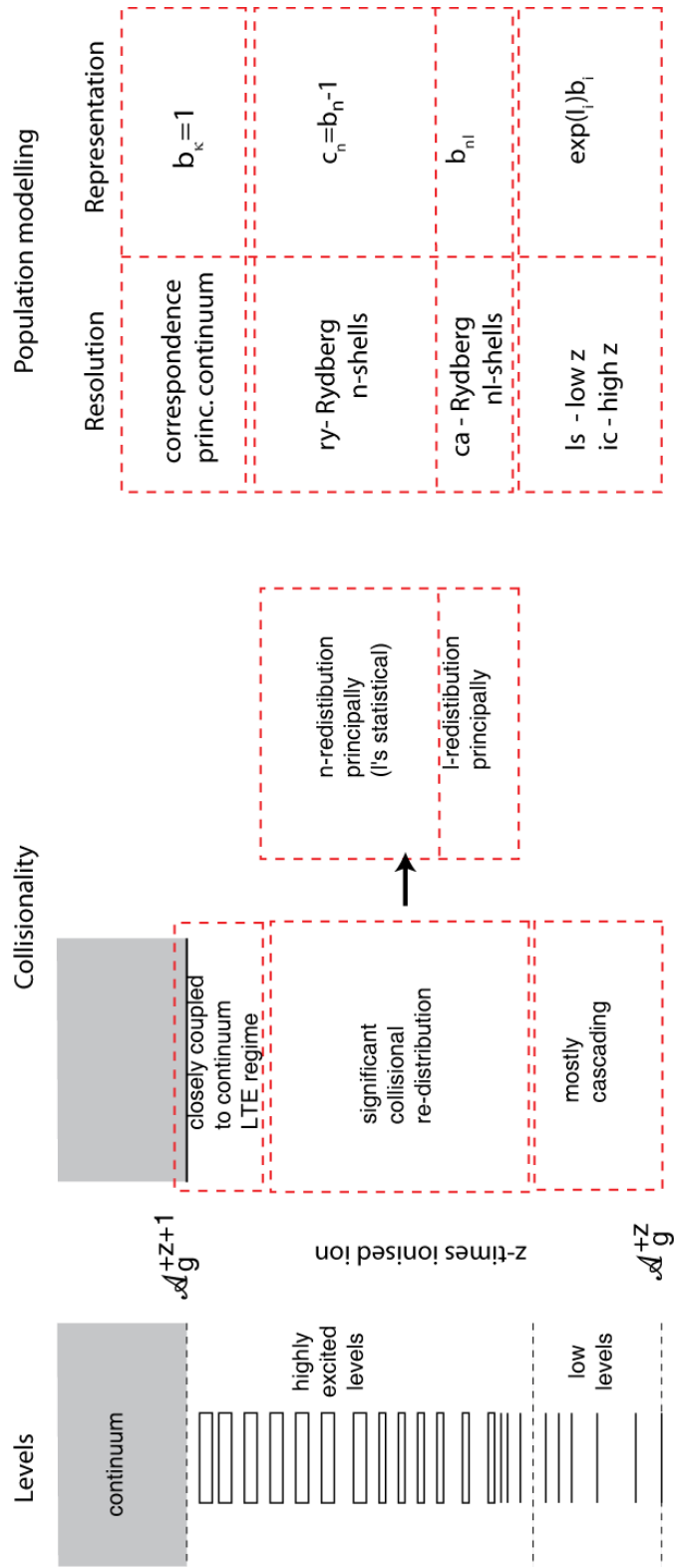
$$b(i, nl) = \frac{A_a}{A_a + A_r}$$

$$\alpha_{\text{tot}}^{(d)} = \sum_{i, nl} \alpha^{(d)}(g, i; nl) = \sum_{i, nl} A_r N_{i, nl} / N_e N_g^+$$

At high density there may be redistribution before stabilisation

State selective dielectronic data are archived in [adf09](#), prepared by Autostructure codes ([ADAS series 7](#))

4.1 Collisionality regimes, grouping and level nomenclatures



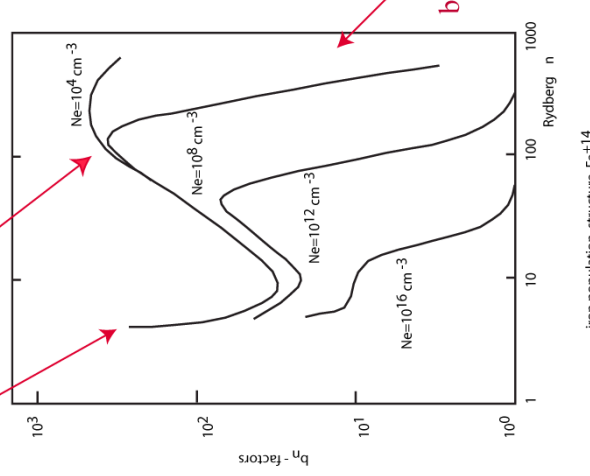
4.2 Bundle-n (ry) and bundle-nl (ca) populations

b_i -factor defined in term of population $N_i = N_i(\text{Saha}) b_i = 8 (\pi a_0^2 I_H/kT_e)^{3/2} (\omega_l/2\omega_+) \exp(I_l/kT_e) b_i$

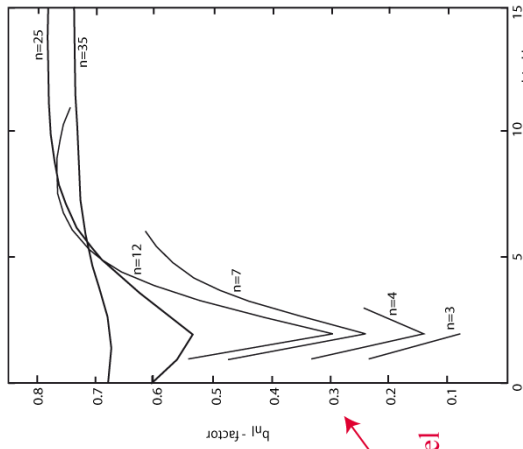
$$c_i = b_{i-1} \quad , \quad \exp b_i = \exp(I_l/kT_e) b_i \rightarrow b_i, c_i, \exp b_i \text{ representations}$$

$\exp b_i$ representation required for very low T_e

c_i representation required



Hydrogen population structure Case B depopulated $Ne=10^4 \text{ cm}^{-3} Te=1 \text{ eV}$



Hydrogen population structure Case B depopulated $Ne=10^4 \text{ cm}^{-3} Te=1 \text{ eV}$

Interactive code ADAS316 is the bundle-n model and ADAS317 is the bundle-nl model

4.3 Low level population structure

Spectroscopy is usually associated with transitions between low lying levels of ions, typically up to the 2nd or 3rd principal quantum shells.

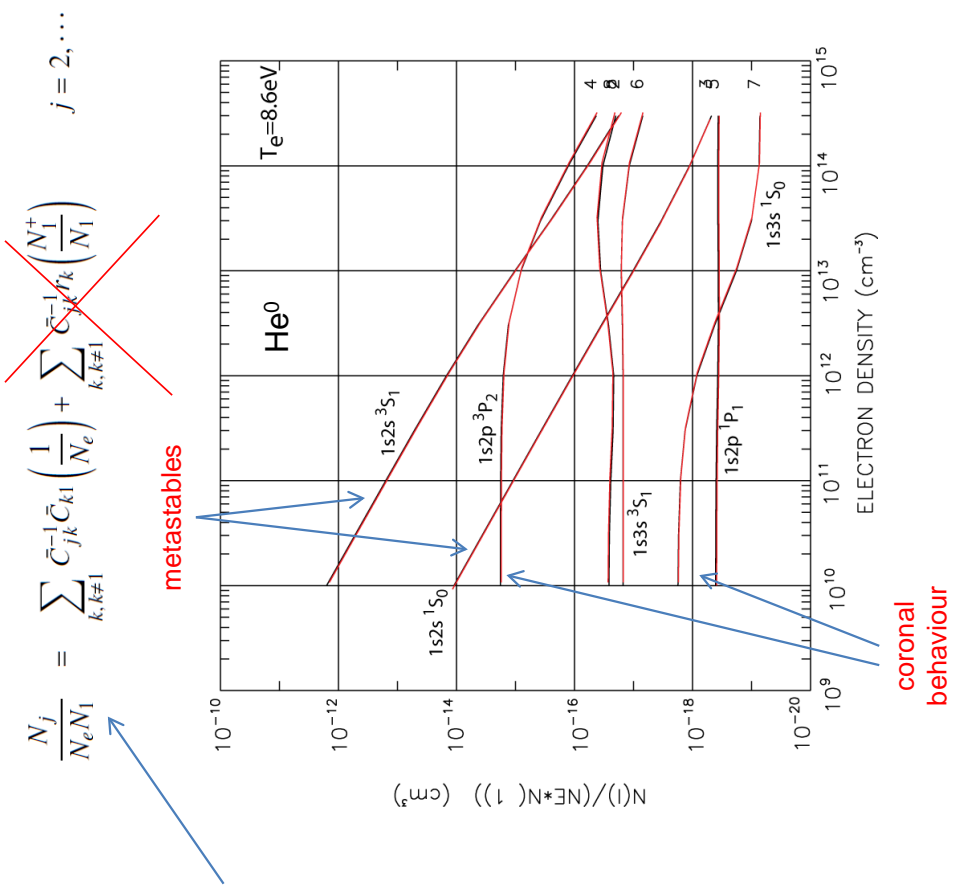
Identify a set of low levels for which all the reactions are available and calculate the population structure for them alone in statistical equilibrium

Some level populations are large ($\sim N_1$) and do not approach coronal behaviour at low densities. These are **metastables**.

Ordinary excited levels can be treated in **quasi-equilibrium** with the instantaneous metastable populations. The metastables must be treated as **dynamic**, in the same manner as the ground states.

Metastables need effective recombination and ionisation coefficients so that their populations can be worked out dynamically in the plasma transport equations.

This is the basis of **generalised-collisional-radiative** (GCR) modelling.



4.4 Generalised collisional-radiative picture

Quasi-static assumption and condensation onto metastables

Time dependent population equations take the form below, where focus is restricted to the metastable (indexed by ρ, σ) and ordinary excited (indexed by i, j) populations of \mathcal{A}^{+z} .

$$\frac{d}{dt} \begin{bmatrix} N_\mu^{+z-1} \\ N_\rho^{+z} \\ N_i^{+z} \\ N_\nu^{+z+1} \end{bmatrix} = \begin{bmatrix} \mathcal{C}_{\mu\mu'} & N_e \mathcal{R}_{\mu\sigma} & 0 & 0 \\ N_e S_{\mu\rho'} & C_{\rho\sigma} & C_{\rho j} & N_e r_{\rho\nu'} \\ 0 & C_{i\sigma} & C_{ij} & N_e r_{i\nu'} \\ 0 & N_e S_{\nu\sigma} & N_e S_{\nu j} & \mathcal{C}_{\nu\nu'} \end{bmatrix} \begin{bmatrix} N_{\mu'}^{+z-1} \\ N_\sigma^{+z} \\ N_j^{+z} \\ N_{\nu'}^{+z+1} \end{bmatrix}$$

Make the quasi-static assumption \rightarrow $\begin{bmatrix} N_\mu^{+z-1} \\ N_\sigma^{+z} \\ N_j^{+z} \\ N_{\nu'}^{+z+1} \end{bmatrix} = \begin{bmatrix} 1 & 0 & 0 & 0 \\ 0 & 1 & 0 & 0 \\ 0 & -C_{ji}^{-1} C_{ip} & -N_e C_{ji}^{-1} r_{i\nu} & 1 \\ 0 & 0 & 0 & 1 \end{bmatrix} \begin{bmatrix} N_\mu^{+z-1} \\ N_\sigma^{+z} \\ N_j^{+z} \\ N_{\nu'}^{+z+1} \end{bmatrix}$

The time-dependence of the metastables is then $\Rightarrow \frac{d}{dt} \begin{bmatrix} N_\mu^{+z-1} \\ N_\rho^{+z} \\ N_{\nu'}^{+z+1} \end{bmatrix} = \begin{bmatrix} \mathcal{C}_{\mu\mu'} & N_e \mathcal{R}_{\mu\sigma} & 0 \\ N_e S_{\rho\mu'} & \mathcal{C}_{\rho\sigma} & N_e \mathcal{R}_{\rho\nu'} \\ 0 & N_e S_{\nu\sigma} & \mathcal{C}_{\nu\nu'} \end{bmatrix} \begin{bmatrix} N_{\mu'}^{+z-1} \\ N_\sigma^{+z} \\ N_{\nu'}^{+z+1} \end{bmatrix}$

4.5 Generalised collisional-radiative coefficients

| | | | | |
|--|------------------------------------|---------------------------------------|---|---------------------------|
| Metastable cross-coupling coefficients | $Q_{\sigma \rightarrow \rho}^{cd}$ | $\equiv \mathcal{C}_{\rho\sigma}/N_e$ | $= (C_{\rho\sigma} - C_{\rho j}C_{ji}^{-1}C_{i\sigma})/N_e$ | $\mathcal{QC}\mathcal{D}$ |
| Effective recombination coefficients | $A_{\nu' \rightarrow \rho}^{cd}$ | $\equiv \mathcal{R}_{\rho\nu'}$ | $= I_{\rho\nu'} - C_{\rho j}C_{ji}^{-1}I_{i\nu'}$ | $\mathcal{AC}\mathcal{D}$ |
| Effective ionisation coefficients | $S_{\sigma \rightarrow \nu}^{cd}$ | $\equiv \mathcal{S}_{\nu\sigma}$ | $= S_{\nu\sigma} - S_{\nu j}C_{ji}^{-1}C_{i\sigma}.$ | $\mathcal{IC}\mathcal{D}$ |

$\mathcal{N}\mathcal{D}$
Parent metastable cross-coupling coefficients

The photon emissivity coefficients also generalize as:

$$A_{j \rightarrow k} N_j^{+z} = \sum_{\sigma} \mathcal{P} \mathcal{E} \mathcal{C}_{\sigma, j \rightarrow k}^{(exc)} N_{\sigma}^{+z} + \sum_{\nu} \mathcal{P} \mathcal{E} \mathcal{C}_{\nu, j \rightarrow k}^{(rec)} N_{\nu}^{+z+1}$$

recombination

excitation

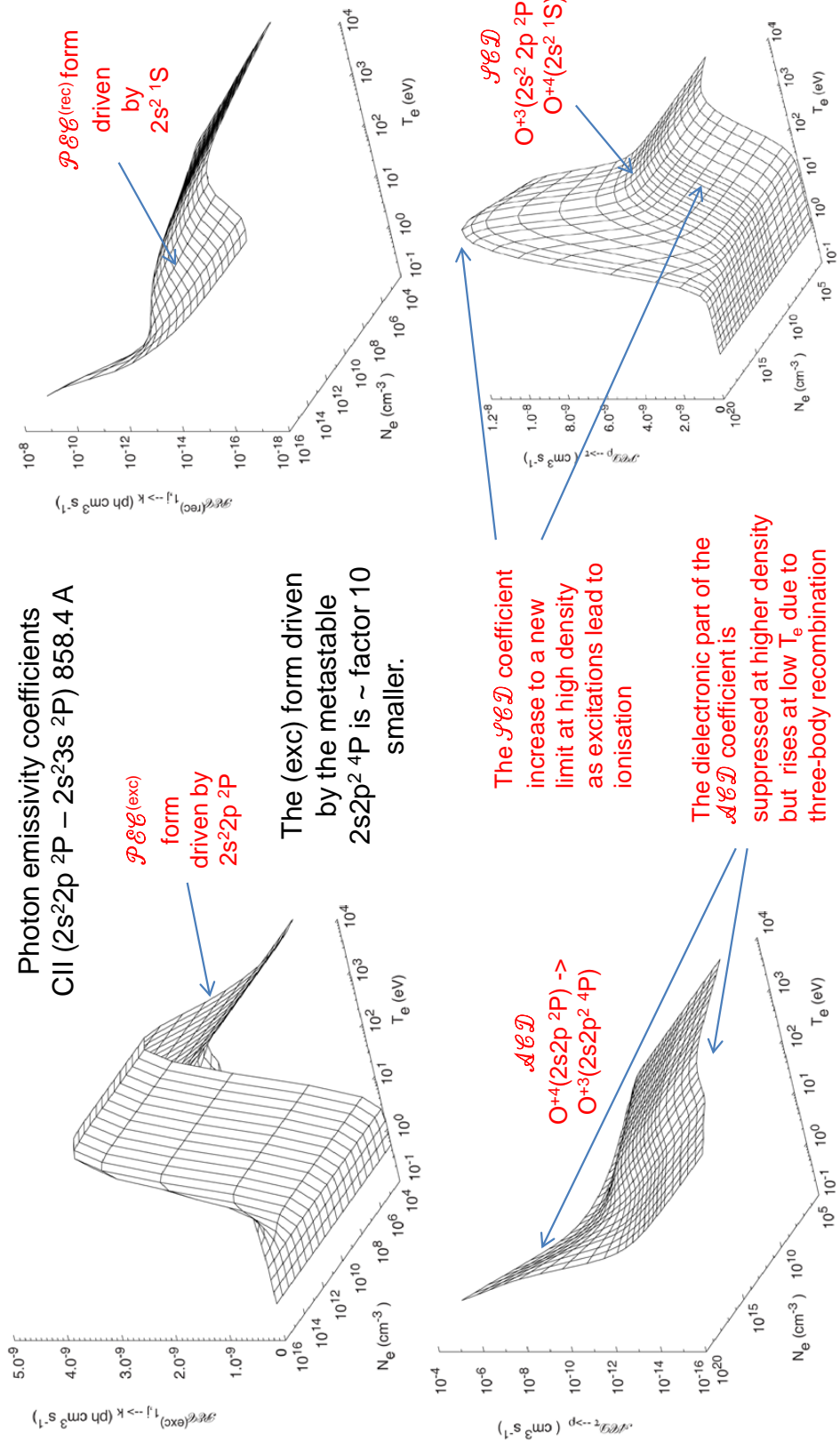
The generalised power coefficients are also obtained

$$\mathcal{PRB}_\nu^{(rec)} = \sum_{j,k} \Delta E_{jk} \mathcal{PEC}_{\sigma,j \rightarrow k}^{(exc)}$$

Recombination + bremsstrahlung power coefficients

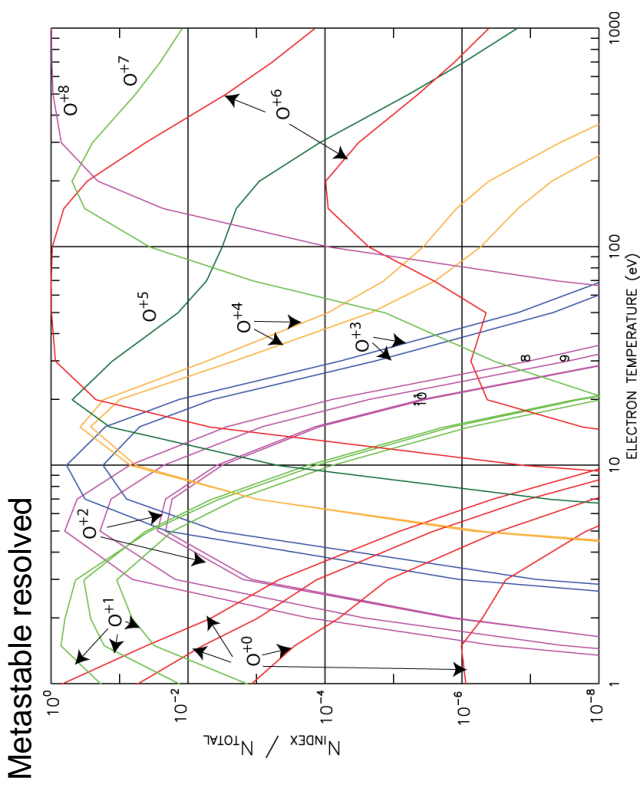
Low-level line power coefficients

4.6 Coefficient illustrations

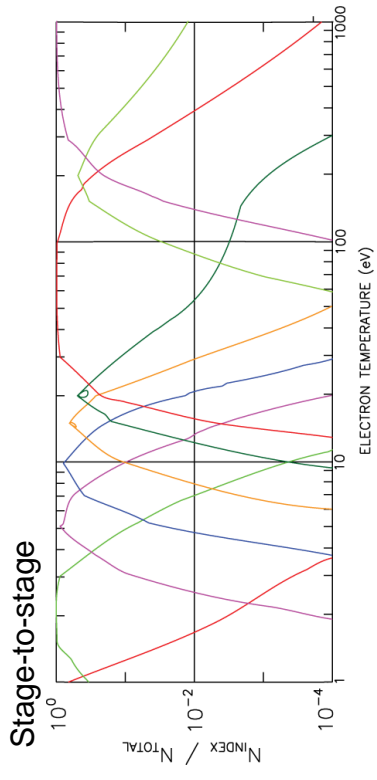
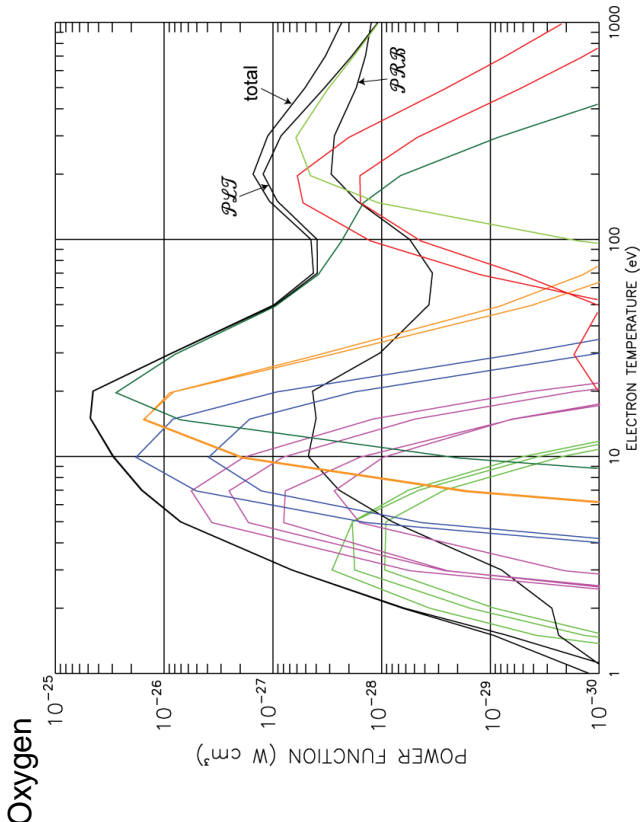


Interactive ADAS208 and offline run_adas208.pro generate the GCR (adf11), PEC (adf15) and SXB (adf13) data

4.7 Ionisation balance and radiated power



Stage-to-stage



Interactive [ADAS405](#) and off-line [run_adas405.pro](#) for ionisation balance. A simple transient model is provided by [ADAS406](#) and [run_adas406.pro](#).

Usually GCR and PEC coefficients enter transport codes [SANCO](#), [EDGE2D](#) and [UTC](#).

5.1 Conclusions

- This has been rather a race through basic atomic physics of atoms in plasmas. I have made up much more substantial notes for the lecture which are available to participants. I hope these will clarify and expand on points which I have treated cursorily.
- Module 2 builds upon this foundation, seeking to bring population and ionisation state modelling fully up-to-date and particularly addressing the complex issues raised by heavy species such as tungsten in fusion plasma.
- We shall now move on to showing how ADAS is used to calculate the various quantities described here, or at least where to find them and interrogate them in the ADAS databases.
- ADAS has comprehensive CR and GCR data to study all the light elements hydrogen to neon, and silicon. The GCR database will be extended to all elements up to argon in the near future.
- Our decision to number ADAS data formats and codes makes things a little difficult for the newcomer to ADAS. One does get used to these numbers and most people in the international fusion community, working towards ITER, now know what at least [adf11](#) and [adf15](#) data are.
- I draw your attention to the annual ADAS course which follows the ADAS Workshop each year. It is a more leisurely course, of one or two weeks, on ADAS, which some of your colleagues have attended. The notes and tutorial sheets from these courses are available in the ADAS documentation. These may help if our three-day visit is a bit too short to answer all the questions.

B.2 module_2



Module 2

Complex species in the core and edge of the fusion plasma. Describing and calculating their characteristics - the current state.

Lecture viewgraphs

Hugh Summers, Martin O'Mullane and Alessandra Giunta

University of Strathclyde

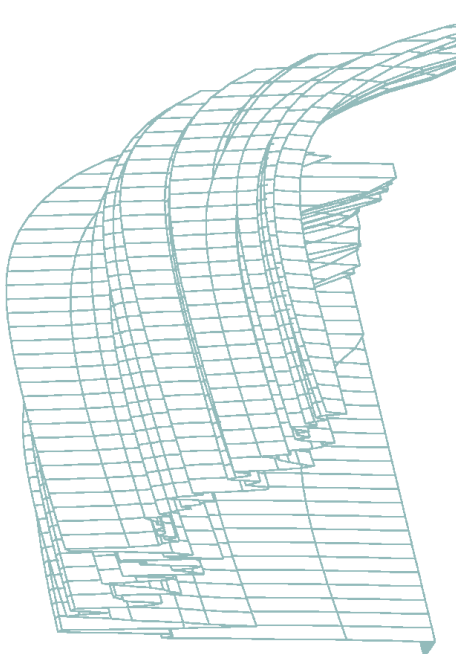
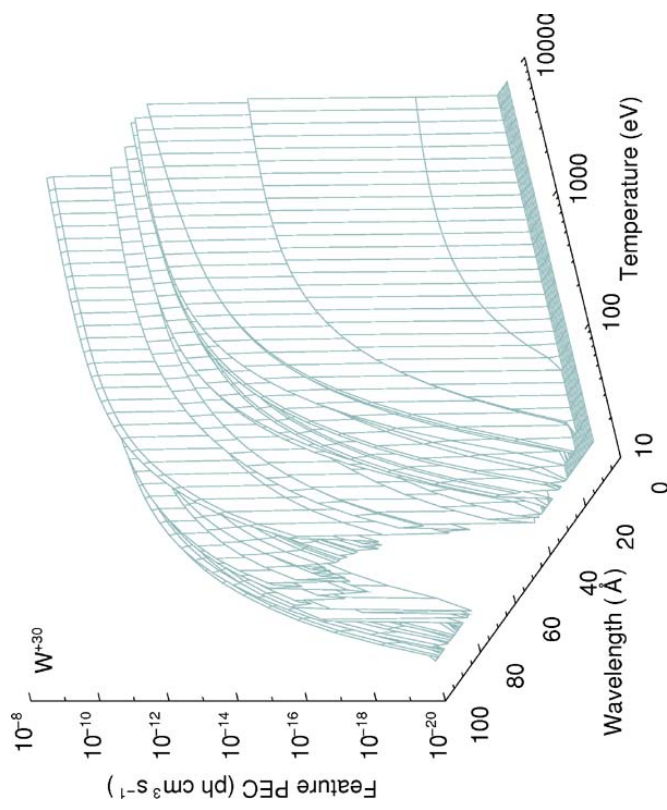
Contents

1. Preliminaries.
2. The whole atom, truncation, collisionality and top-up
3. Ionisation state, partitions, condensations and superstages
4. Supplementary modelling for dielectric recombination and ionisation
5. Conclusions

1.1 Key ADAS data formats

- ***adf04***: A specific ion file is sufficient for the calculation of the excited populations of an ion. It is complete in itself, with energy levels and rate coefficients spanning a set of states beginning with the ground level.
- ***adf11***: A set of element master files is sufficient for the calculation of the ionisation state of an element, that is the fractional abundances of the ions of the element and their radiated power.
- ***adf15***: A photon emissivity coefficient file contains the predicted emissivity coefficients of a set of spectrum lines of an ion, spanned by an adf04 dataset, as a function of plasma parameters Te and Ne . Combined with the ionisation state above, it allows prediction of absolute spectral line emissivities.
- ***adf40***: A feature photon emissivity file is the photon emissivity coefficient per pixel in a pixellated spectral range as a function of plasma parameters Te and Ne , due to all the spectrum lines of an ion spanned by an adf04 dataset. It is a construct for the efficient handling of a complex ion which may have hundreds of thousands of spectral lines.

1.2 Feature photon emissivity coefficients, \mathcal{FPEC} .



\mathcal{FPEC} for W^{+20} in the spectral range of the XUV ('SOXMOS' - KT4) spectrometer at the JET facility versus electron temperature at the fixed electron density of 10^{13} cm^{-3} . (a) View from the low temperature side. (b) View from the high temperature side showing the broadening into an envelope feature (see [ADAS810](#)).

1.3 Configuration string representations

Configuration string: $\Gamma \equiv n_1 l_1^{q_1} n_2 l_2^{q_2} \cdots n_m l_m^{q_m}$

Cowan form: $1s2\ 2s2\ 2p6\ 3s2\ 3p6\ 3d10\ 4s2\ 4p6\ 4d10\ 4f13\ 5s2\ 5p6$

alphabetic

Standard form: $1s2\ 2s2\ 2p6\ 3s2\ 3p6\ 3da\ 4s2\ 4p6\ 4da\ 4fd\ 5s2\ 5p6$

10 ≡a , 11 ≡b , 12 ≡c , 13 ≡d , 14 ≡e .
Standard coding

Eissner form:
 $52152256352456560652756860963A52B56C$
 $2152256352456560652756860963A52B56C$

1 ≡1s , 2 ≡2s , 3 ≡2p , 4 ≡3s , 5 ≡3p , 6 ≡3d , 7 ≡4s , 8 ≡4p ,
9 ≡4d , A ≡4f , B ≡5s , C ≡5p , D ≡5d , E ≡5f , F ≡5g .
Eissner coding

Leading 5 omitted

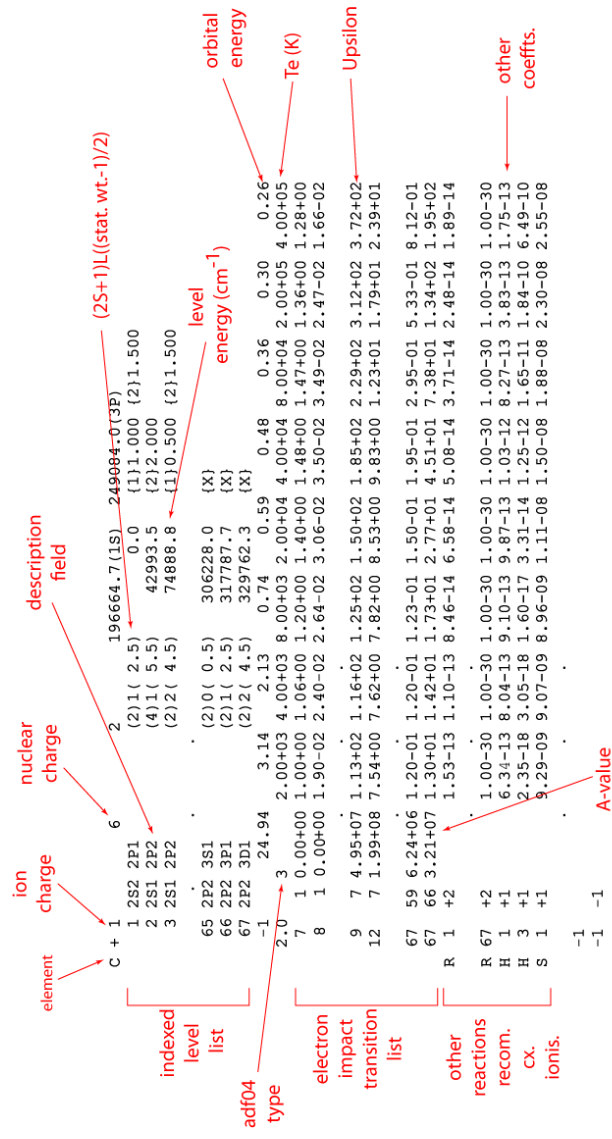
Use `read_adf00.pro` to obtain the ground configurations of ions. Use `xxcftr.pro` to convert between standard and Eissner configuration forms.

1.4 The adf04 data format

There are five **types** of adf04 dataset:

- 1 - coll. strength v X
 - 2 - currently not in use
 - 3 - Maxwellian. aver. coll. strength v T
 - 4 - non-Maxwellian ups/downsilicon v .
 - 5 - coll. strength v final state energy.

The level **description field** is free for the use of the adf04 dataset creator. With the move to heavier species and the very large automatic production of fundamental data for the ADAS/ADAS-EU projects, the descriptor is used for the **configuration string**.



There are ~ 3500 adf04 datasets in the ADAS database in iso-electronic and iso-nuclear collections. These include preferred collections, fully expanded with supplementary reaction data. The adf04 collection is expanding rapidly with the heavy species production (see [module 7](#)).

1.5 W^{+9} adf04 datasets of different resolution

Portions of the level lists
at the top of four adf04
datasets for the same
ion, W^{+9} , are shown.

$(2S+1)L$
unspecified

| | | | | | | |
|---------|---|-------|-----------------|--------|-----------|----------|
| span | [| W + 9 | 74 | 10 | 1443732.5 | |
| | | 1 | 60963A52B54C | (0) 0(| 104.0) | |
| | | 2 | 60963A52B53C51D | (0) 0(| 1399.5) | 0.0 |
| configs |] | 3 | 60963A52B53C51E | (0) 0(| 1959.5) | 425681.8 |

ADAS works with adf04
datasets of different
resolution:
 ca – config. resolution
 ls – term resolution
 ic – level resolution

$(2S+1)L$
config.
weight

| | | | | | | |
|---------|---|-------|--------------------------|-------------|---------|-----------|
| span | [| W + 9 | 74 | 101443732.5 | | |
| | | 1 | 60963A52B54C | (0) 0(| 104.0) | 0.0 |
| configs |] | 27 | 60652755860963A52B54C51E | (0) 0(| 8819.5) | 4302227.3 |

$(2S+1)L$
config.
weight

| | | | | | | |
|-------|---|-------|-----------------|--------|-----------|-----------|
| span | [| W + 9 | 74 | 10 | 1443732.5 | |
| | | 1 | 60963A52B54C | (2) 4(| 8.5) | 0.0 |
| terms |] | 318 | 60963A52B53C51E | (2) 1(| 2.5) | 1066425.0 |

Eissner
form

$(2S+1)L$
level
weight

/adf04/arf40#74/cl#w9.dat

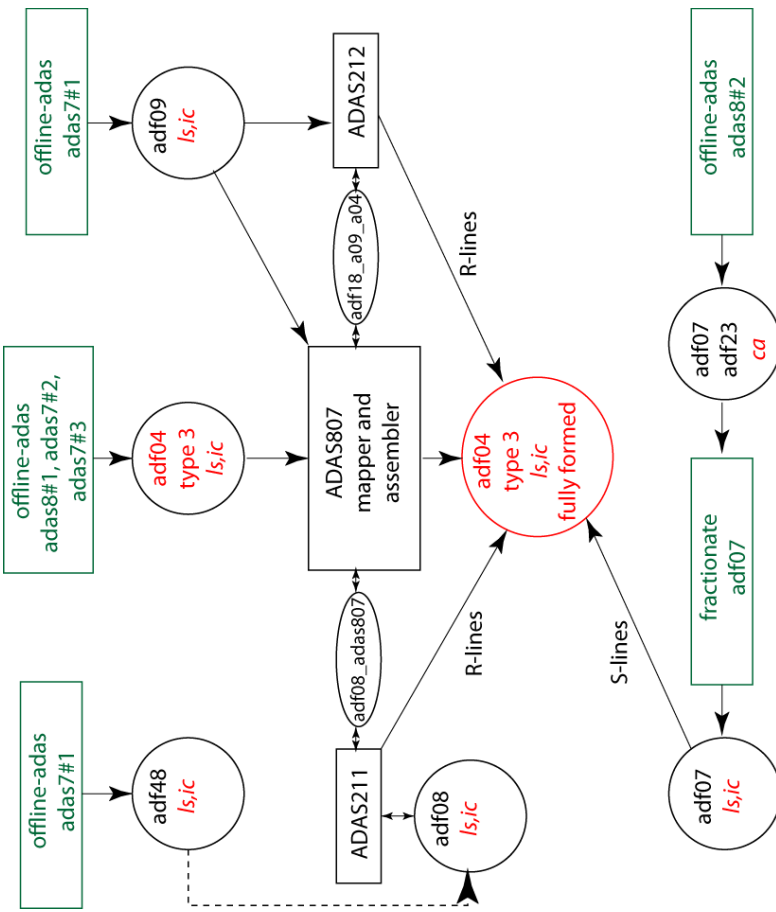
/adf04/arf40#74/ca#w9.dat

/adf04/arf40#74/ls#w9.dat

The first dataset is a small ca case with 3 configurations. These three configuration have 318 terms given in the third dataset (which is ls) and 855 levels given in the fourth dataset (which is ic). The fourth dataset yields a population solution of much higher precision. The second dataset is a large ca case with 27 configurations. It has large coverage but at low resolution. In ic it would span >10000 levels and overwhelm computers.

1.6 Assembling the high precision *ic* adf04 dataset

The schematic shows the interconnected production codes and pathways which are used to form adf04 datasets for light and medium weight ions of elements at the highest precision.



The ADAS codes containing '#' are non-interactive offline-adas codes executed in distributed processing by script. Available in ADAS, they require setting up for a specific site and multi-node computing environments. The methodologies and operation of these codes is described in [module 7](#).

Codes in black letter capitals are part of interactive ADAS . Their use is included in the tutorial materials and example sheets presented at the full ADAS training course and are available from the ADAS and ADAS-EU websites. ADAS staff will be available after the ADAS-EU workshop to give further guidance.

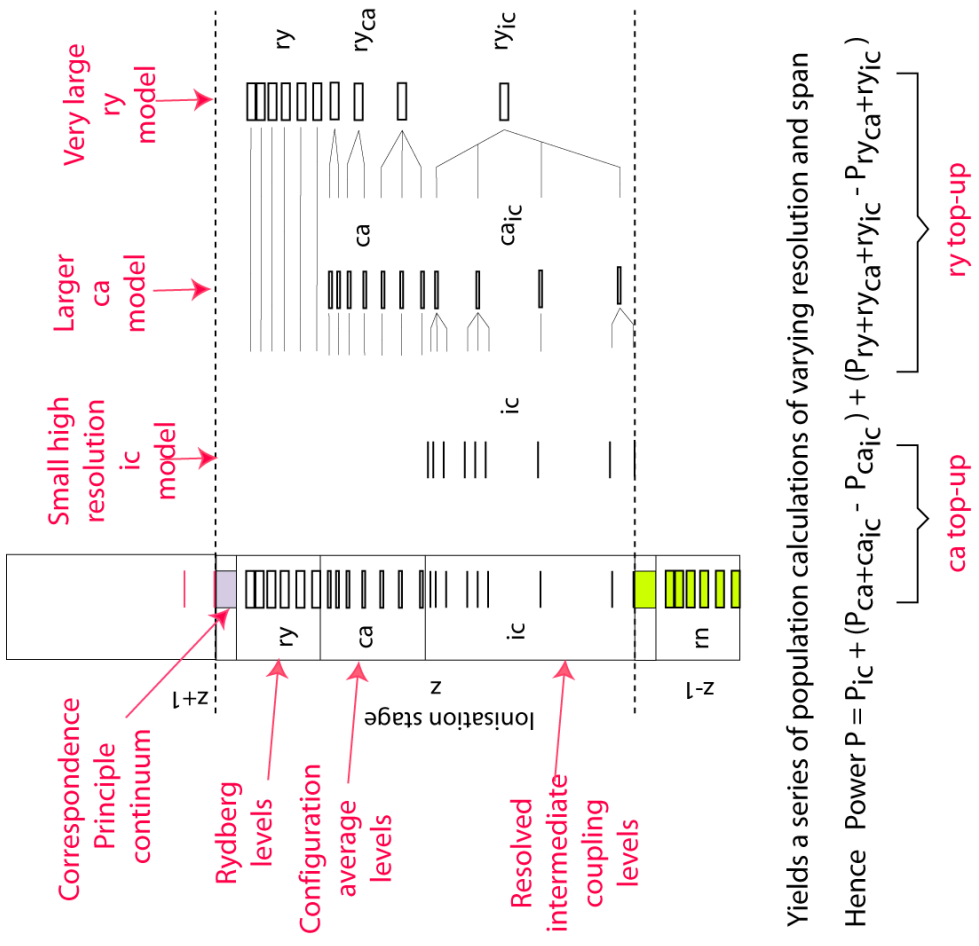
2.1 Exploiting completeness and precision of adf04 datasets

The production of the **ca**, **cl**, **ls** and **ic** categories of *adf04* dataset has been automated for any element. This is done in multi-node distributed computation for all the ions of an element at the one time, optimised for precision in total radiated power. It has been particularly useful for creating the ADAS baseline for heavy species.

For the above purposes, the schematic outlines how the categories of *adf04* datasets are exploited, processing through to baseline *adf11* (see [ADAS407](#) and [ADAS408](#)).

A more sophisticated procedure called **bn-is projection**, also requiring the *adf04*, *ls* datasets has been used for the light elements. It is being extended to argon with completion so-far to silicon.

Current large scale, high precision *adf04* and other fundamental data production is in support of a new **bni-ic projection** procedure for use through to zinc/zinc-like and selectively thereafter (see section 2 of module 2).



2.2 Projection and condensation

For precision with light/medium weight elements, we have not dealt carefully enough with the **truncation problem** of the true atom with its infinite number of **Rydberg states**.

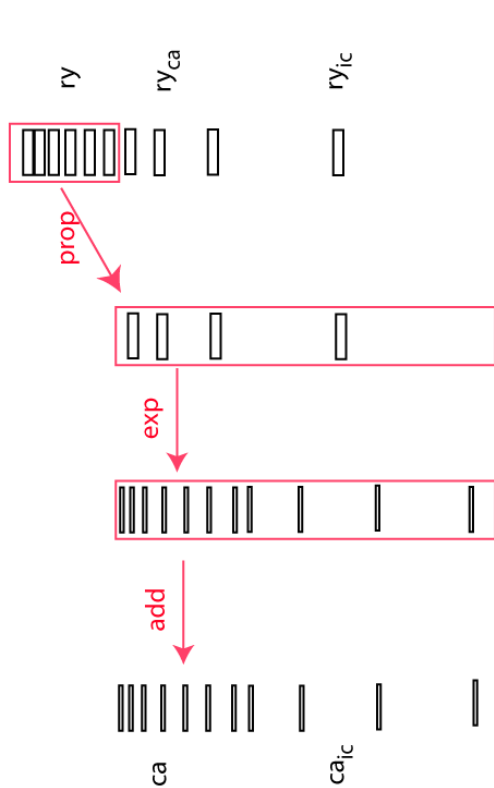
The study of dielectronic recombination of module 1 showed the importance of high Rydberg states and true population solutions for it with the **bundle-n** and **bundle-nl** models. So these models should be used to fill in the gap.

The matrix method used in module 1 to obtain the CR and GCR coefficients can be used again, as shown in the schematic, and again repeatedly.

Setup the bundle-n collisional-radiative matrix for the whole system. Use the inverse sub-matrix propagator for the **ry** n-shells to project onto the **ry_{ca}** and **ry_{ic}** n-shells. Eliminate the direct couplings and expand statistically over the **ca** and **ca_{ic}** nl-shell substructure and add to the more exact collisional-radiative matrix for **ca + ca_{ic}**

Repeat down to the high precision **IC** collisional-radiative matrix we need for spectroscopy.

More complete
ca
model



ry collisional-radiative matrix propagated onto the **ry_{ca} + ry_{ic}** manifold, expanded over the higher resolution **ca + ca_{ic}** manifold and added to the direct **ca + ca_{ic}** collisional-radiative matrix.

2.3 Algebra of projection

Collisional-radiative matrices of progressively greater span (all **ic** levels, all **ca** levels, all **bn** levels) but lower resolution.

$$\left[\begin{array}{c} C_{ij}^{(ic)} \\ C_{i'j'}^{(ca)} \end{array} \right], \left[\begin{array}{c} C_{\bar{i}\bar{j}}^{(ca)} \\ C_{i'j'}^{(ca)} \end{array} \right], \left[\begin{array}{cc} C_{\bar{\bar{i}}\bar{\bar{j}}}^{(bn)} & C_{\bar{i}\bar{j}'}^{(bn)} \\ C_{\bar{i}'\bar{j}}^{(bn)} & C_{\bar{i}'\bar{j}'}^{(bn)} \end{array} \right]$$

not bundled

bundled over outer quantum numbers

$$\bar{C}_{\bar{i}\bar{j}}^{(ca)} = \bar{C}_{\bar{i}\bar{j}}^{(ca)} - C_{\bar{i}j'}^{(ca)}(C_{j'i'}^{(ca)})^{-1}C_{i'\bar{j}}^{(ca)}$$

remove direct couplings

ic span

ca span

$C_{ij}^{(ic)} \rightarrow \bar{C}_{\bar{i}\bar{j}}^{(ca)}$

complete ic resolution with indirect full ca span

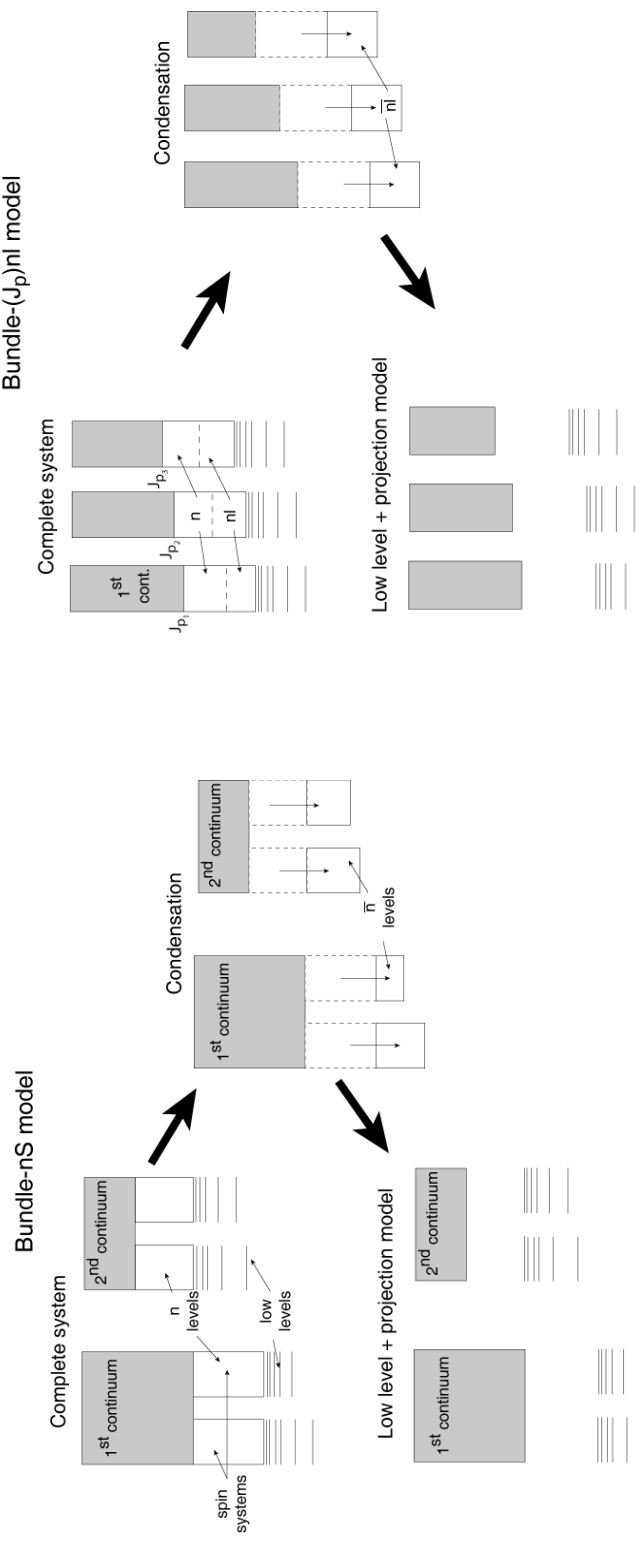
$C_{ij}^{(ic)} \rightarrow C_{ij}^{(ic)} + W_{i\bar{i}} \bar{C}_{\bar{i}\bar{j}}^{(ca)} U_{\bar{j}j}$

expansion

W_{īī} is ω_{ī}/ω̄_{ī} if ī ∈ ī̄ otherwise 0

U_{j̄j̄} is 1 if j̄ ∈ j̄̄ otherwise 0

2.4 Bundle-nS and Bundle-(J_p)nl projection

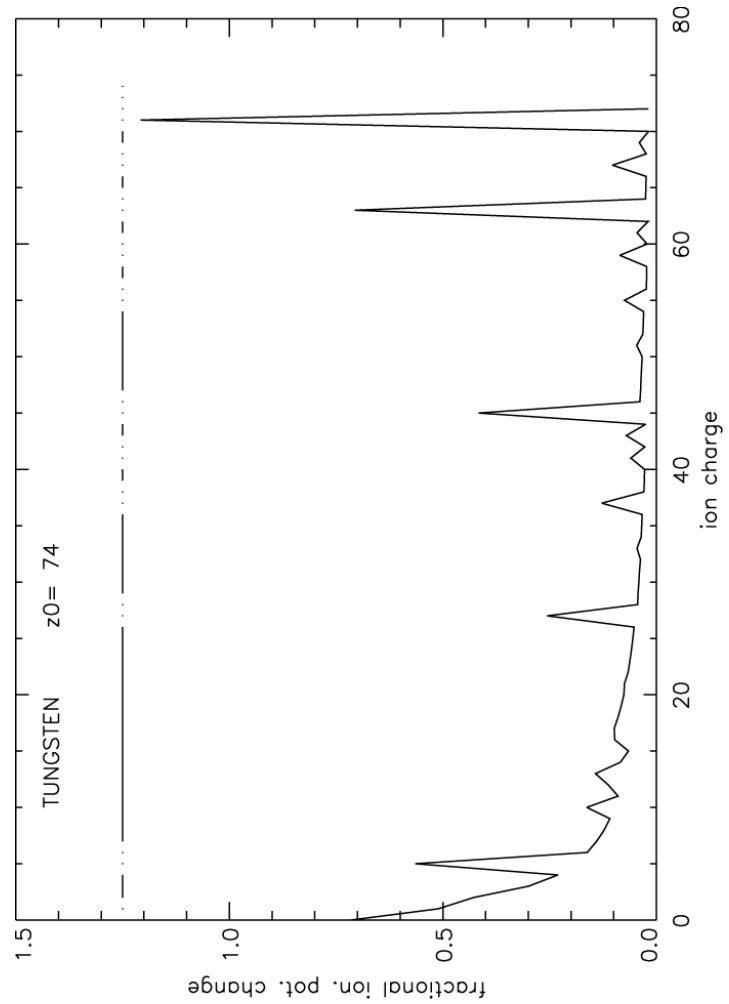


The projection/condensation system used by ADAS for light elements. Projection matrices are archived in format [adf17](#). Mapping files are archived in [adf18](#). (see also code [ADAS204](#)).

The projection/condensation system being completed by ADAS for medium-weight elements. It will also be used selectively for heavy elements.

3.1 Ionisation state – the problem of heavy species

A heavy element such as tungsten with 74 ionisation stages overwhelms computer resources in 2-d impurity transport modelling. Typically elements with only up to about 15 ionisation stages can be handled.



Intermediate ions such as W^{+20} emit so many spectrum lines that they form a **quasi-continuum**. Almost none will ever be identified. A few ionisation stages (nearly closed shells or one or two electrons outside closed shells) emit simpler spectra with a modest number of strong lines.

The fractional ionisation potential change plot is helpful. The ionisation stages at and adjacent to the peak are the key stages for spectroscopy. They are the targets for the highest quality atomic modelling. Other ionisation stages might as well be grouped together, since they have narrow emission shells.

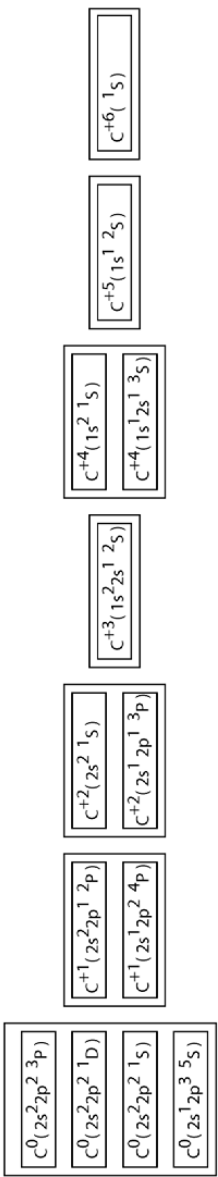
The broken bar at the top of the figure shows a possible grouping of ionisation stages, which also separates the individual spectroscopic stages. The process is called **partitioning** and the **natural partition** is shown for tungsten.

3.2 The new terminology and notation of superstages

Root partition for GCR modelling

metastables

Root partition layer #00: Number of partitions = 13
Connection vector = [4, 2, 2, 1, 2, 1, 1]
Label successive metastables as: 00 01 02 03 04 05 06 07 08 09 10 11 12



Root partition for CR modelling

stages

Form child partition #01 defined by
 $/p00/00 01 02 03/ p01/04 05/ p02/06 07/ p03/08/ p04/09 10/ p05/11/ p06/12/$

Root partition layer #01 Number of partitions = 7
Connection vector = [1, 1, 1, 1, 1, 1]
 C^0 C^{+1} C^{+2} C^{+3} C^{+4} C^{+5} C^{+6}

Form child partition #02 defined by
 $/p00/00/ p01/01 02 03/ p02/04 05/ p03/06/$

superstages

Partition layer #02 Number of partitions = 4
Connection vector = [1, 1, 1, 1]
 C^0 C^{+1} C^{+2} C^{+3} C^{+4} C^{+5} C^{+6}

3.3 Algebra of superstage compression

$$N^{[\#02](j)} = \sum_{i=i_0}^{i_1} N^{[\#01](i)}$$

Partition j of layer #02 composed of partitions i_0 to i_1 of layer #01.

Impose equilibrium ratios on partitions i_0 to i_1 of layer #01.



$$\begin{aligned} N^{[\#01](i_0)} \Big|_{eq} &= (\alpha_{cr}^{[\#01](i_0+1 \rightarrow i_0)} / S_{cr}^{[\#01](i_0 \rightarrow i_0+1)}) N^{[\#01](i_0+1)} \Big|_{eq} \\ N^{[\#01](i_0+1)} \Big|_{eq} &= (\alpha_{cr}^{[\#01](i_0+2 \rightarrow i_0+1)} / S_{cr}^{[\#01](i_0+1 \rightarrow i_0+2)}) N^{[\#01](i_0+2)} \Big|_{eq} \\ &\dots \\ N^{[\#01](i_1-1)} \Big|_{eq} &= (\alpha_{cr}^{[\#01](i_1 \rightarrow i_1-1)} / S_{cr}^{[\#01](i_1-1 \rightarrow i_1)}) N^{[\#01](i_1)} \Big|_{eq} \end{aligned}$$

Gives definition of recombination and ionisation coefficients connecting $j \rightarrow j+1$ and $j \rightarrow j-1$ for layer #02.

$$\begin{aligned} \alpha_{cr}^{[\#02](j \rightarrow j-1)} &= \alpha_{cr}^{[\#01](i_0 \rightarrow i_0-1)} \left(N^{[\#01](i_0)} / N^{[\#02](j)} \right) \Big|_{eq} \\ S_{cr}^{[\#02](j \rightarrow j+1)} &= S_{cr}^{[\#01](i_1 \rightarrow i_1+1)} \left(N^{[\#01](i_1)} / N^{[\#02](j)} \right) \Big|_{eq} \end{aligned}$$

$$\begin{aligned} \frac{dN^{[\#02](j)}}{dt} &= N_e S_{cr}^{[\#01](i_0-1 \rightarrow i_0)} N^{[\#01](i_0-1)} \\ &\quad - N_e \alpha_{cr}^{[\#01](i_0 \rightarrow i_0-1)} N^{[\#01](i_0)} \\ &\quad - N_e S_{cr}^{[\#01](i_1 \rightarrow i_1+1)} N^{[\#01](i_1)} \\ &\quad + N_e \alpha_{cr}^{[\#01](i_1+1 \rightarrow i_1)} N^{[\#01](i_1+1)} \end{aligned}$$

Sum time-dependent ionisation balance equations for partitions i_0 to i_1 of layer #01.

Matrix algebra (see module 2 lecture notes) makes the handling simpler and universal.

Impurity transport modelling needs ionisation potentials, charge(z) and squared charge (z^2). For superstages these become **collisional-radiative quantities**, which vary with T_e and N_e written as: \mathcal{ECD} , \mathcal{ZCD} and \mathcal{YCD} .

Some care is required with the formation energy of the first superstage – analogous to a **work function** (see the module 2 lecture notes).

Transport code have been modified to work with superstages.

3.4 ADAS adf11 dataset classes

| ADF11 Subclass | Character | CR | GCR | Superstage |
|-------------------------------------|--|-----|-----|------------|
| ACD | effective recombination coefft. | x | x | x |
| SCD | effective ionisation coefft. | x | x | x |
| CCD | effective CX recom. coefft. | (x) | | (x) |
| PLT | effective excit. power coefft. | x | x | x |
| PRB | effective recom./brems. power coefft. | x | x | x |
| PRC | CX recom. power coefft. | (x) | | (x) |
| QCD | effective metas. coupling coefft. | x | | |
| XCD | effective parent metas. coupling coefft. | x | | |
| ZCD | effective superstage charge | | x | x |
| YCD | effective superstage squared charge | | x | x |
| ECD | effective ionisation potential | | x | x |
| ADF15 Subclass | Character | | | |
| P _E C(exc) | excit. photon emiss. coefft. | x | x | x |
| P _E C(rec) | recom. photon emiss. coefft. | | x | x |
| F _P E _C (exc) | feature excit. photon emiss. coefft. | | | |
| F _P E _C (rec) | feature recom. photon emiss. coefft. | | | |

3.5 adf11 datasets of different resolution and partition layers

adf11 datasets occur in up to 12 categories and in two basic forms. These forms are unresolved (CR), the upper case, and resolved (GCR), the lower two cases.

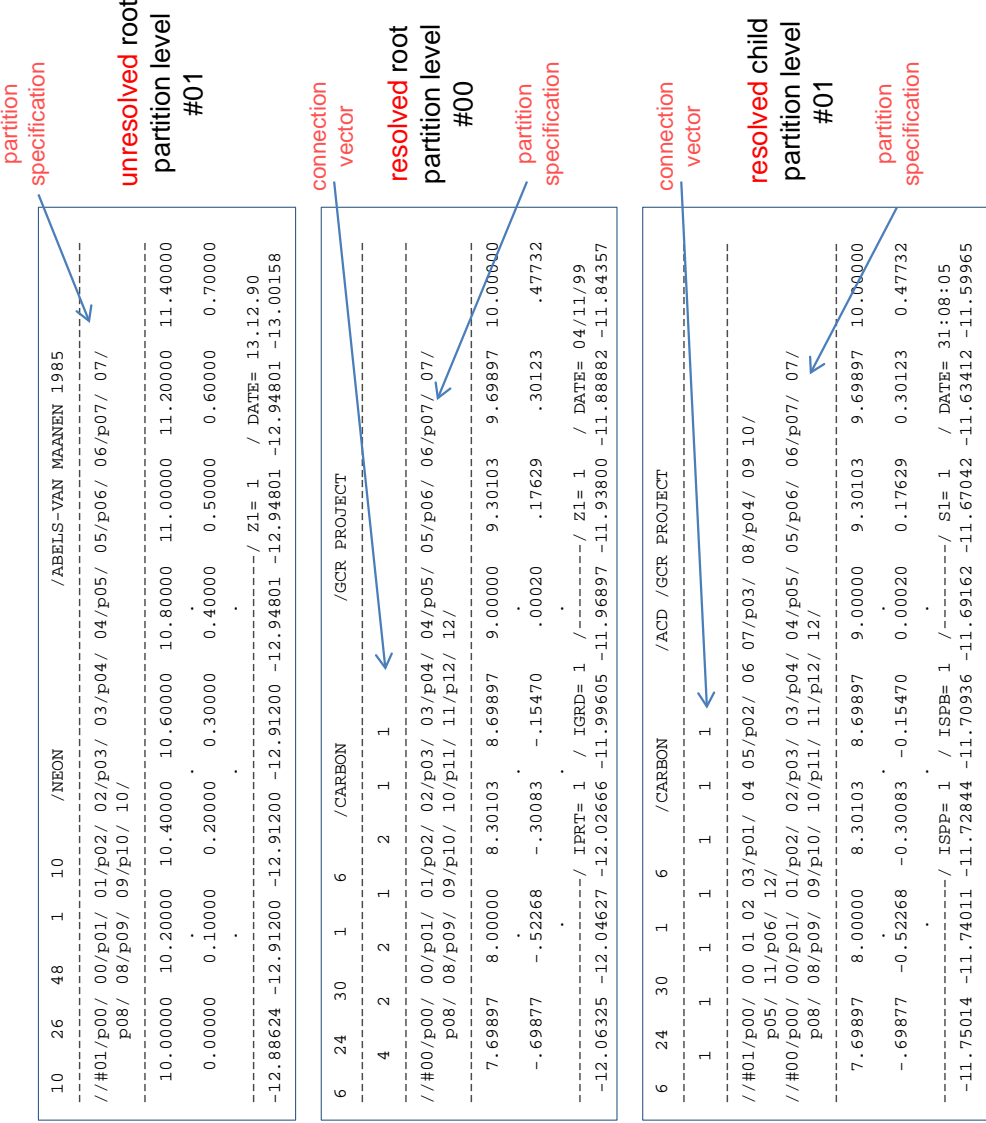
The partition specification may be omitted if it is the root partition of its form, that is #01 for unresolved and #00 for resolved.

The connection vector is required for the resolved form.

The lowest case has two partition layers, a child partition #01 and the resolved #00 root partition

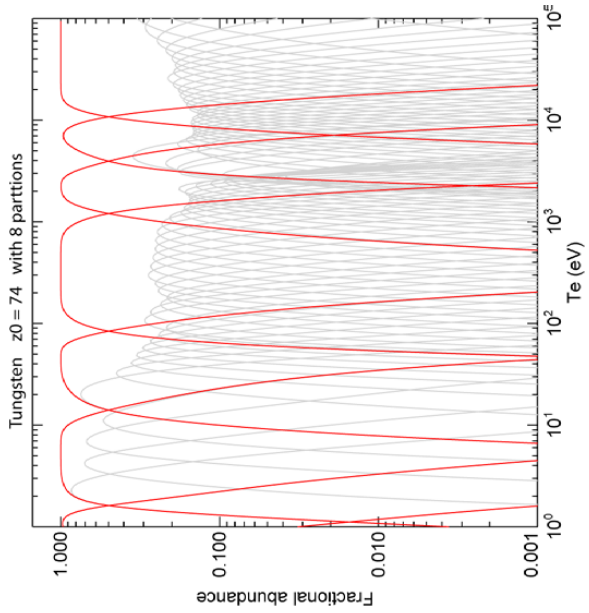
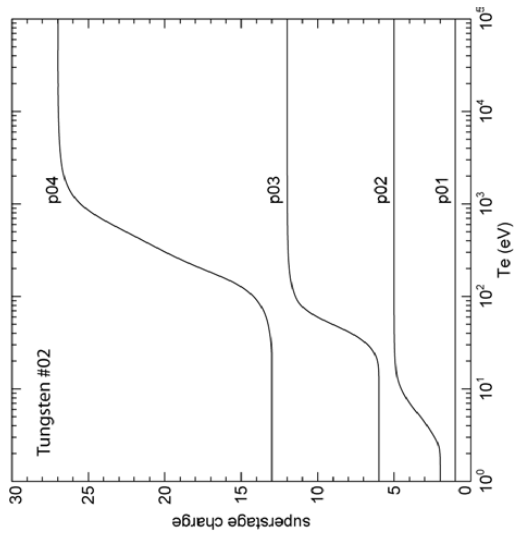
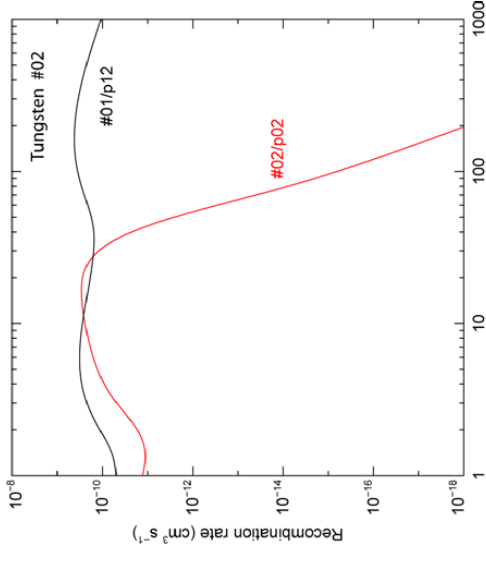
The implementation of a superstage condensation is by the interactive code [ADAS416](#), using a script from the user's [~/adas/scripts416/](#) directory. The script controls the *adf11* categories processed.

adf11 utilisation with simple ionisation stages or superstages is transparent to the user with superstage index **s1** replacing ion charge number **z1**.



3.6 adf11 superstage coefficient behaviours

| p00 | p01 | p02 | p03 | p04 | p05 | p06 | p07 |
|-----------|-----|-----|-----|-----|-----|-----|-----|
| W^{+0} | | | | | | | |
| W^{+1} | | | | | | | |
| W^{+2} | | | | | | | |
| W^{+3} | | | | | | | |
| W^{+4} | | | | | | | |
| W^{+5} | | | | | | | |
| W^{+6} | | | | | | | |
| W^{+7} | | | | | | | |
| W^{+8} | | | | | | | |
| W^{+9} | | | | | | | |
| W^{+10} | | | | | | | |
| W^{+11} | | | | | | | |
| W^{+12} | | | | | | | |
| W^{+13} | | | | | | | |
| W^{+14} | | | | | | | |
| W^{+15} | | | | | | | |
| W^{+16} | | | | | | | |
| W^{+17} | | | | | | | |
| W^{+18} | | | | | | | |
| W^{+19} | | | | | | | |
| W^{+20} | | | | | | | |
| W^{+21} | | | | | | | |
| W^{+22} | | | | | | | |
| W^{+23} | | | | | | | |
| W^{+24} | | | | | | | |
| W^{+25} | | | | | | | |
| W^{+26} | | | | | | | |
| W^{+27} | | | | | | | |
| W^{+28} | | | | | | | |
| W^{+29} | | | | | | | |
| W^{+30} | | | | | | | |
| W^{+31} | | | | | | | |
| W^{+32} | | | | | | | |
| W^{+33} | | | | | | | |
| W^{+34} | | | | | | | |
| W^{+35} | | | | | | | |
| W^{+36} | | | | | | | |
| W^{+37} | | | | | | | |
| W^{+38} | | | | | | | |
| W^{+39} | | | | | | | |
| W^{+40} | | | | | | | |
| W^{+41} | | | | | | | |
| W^{+42} | | | | | | | |
| W^{+43} | | | | | | | |
| W^{+44} | | | | | | | |
| W^{+45} | | | | | | | |
| W^{+46} | | | | | | | |
| W^{+47} | | | | | | | |
| W^{+48} | | | | | | | |
| W^{+49} | | | | | | | |
| W^{+50} | | | | | | | |
| W^{+51} | | | | | | | |
| W^{+52} | | | | | | | |
| W^{+53} | | | | | | | |
| W^{+54} | | | | | | | |
| W^{+55} | | | | | | | |
| W^{+56} | | | | | | | |
| W^{+57} | | | | | | | |
| W^{+58} | | | | | | | |
| W^{+59} | | | | | | | |
| W^{+60} | | | | | | | |
| W^{+61} | | | | | | | |
| W^{+62} | | | | | | | |
| W^{+63} | | | | | | | |
| W^{+64} | | | | | | | |
| W^{+65} | | | | | | | |
| W^{+66} | | | | | | | |
| W^{+67} | | | | | | | |
| W^{+68} | | | | | | | |
| W^{+69} | | | | | | | |
| W^{+70} | | | | | | | |
| W^{+71} | | | | | | | |
| W^{+72} | | | | | | | |
| W^{+73} | | | | | | | |
| W^{+74} | | | | | | | |



4.1 Population modelling for dielectronic resonance states

Zero-density doubly-excited state b-factors

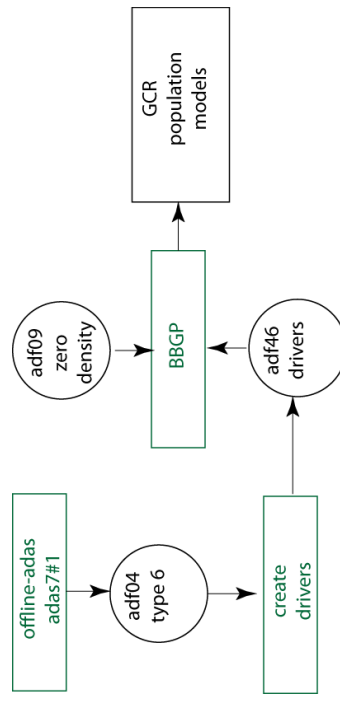
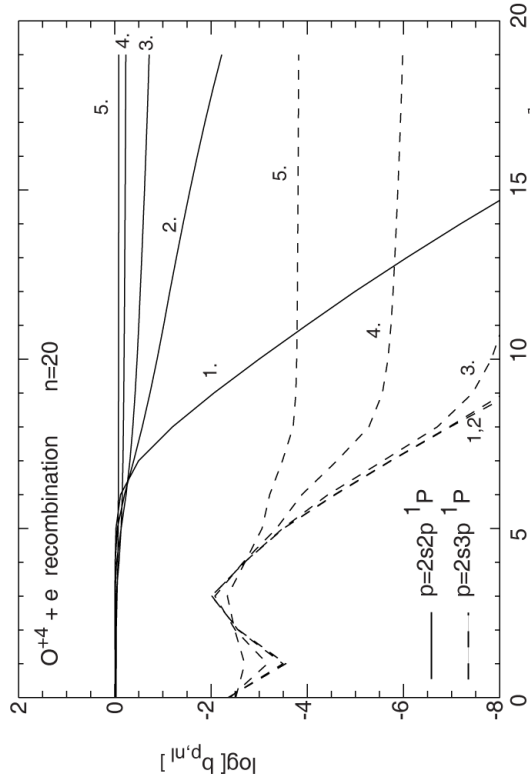
$$b_{p,nl} = \left(\frac{\sum_{l'} A_{p,nl \rightarrow \nu' k'l'}^a}{\sum_{l'} A_{p,nl \rightarrow \nu' k'l'}^a + A_{p,nl \rightarrow \nu',nl}^\Gamma} \right)$$

Finite density-corrected state-selective dielectronic coefficients using the **BBGP** approximation.

$$\alpha_{\nu' \rightarrow \nu',nS}^{(d)IPIRDW}(N_e) = \alpha_{\nu' \rightarrow \nu',nS}^{(d)IPIRDW}(N_e = 0) \frac{\sum_l \alpha_{\nu' \rightarrow \nu',nl}^{(d)BBGP}(N_e)}{\sum_l \alpha_{\nu' \rightarrow \nu',nl}^{(d)BBGP}(N_e = 0)}$$

Double-excited state population equations

$$\begin{aligned}
 & - (N_e d_{nl-1 \rightarrow nl}^e + N_{nl-1 \rightarrow nl}^{z_1} q_{nl-1 \rightarrow nl}^{z_1}) N_{p,nl-1} \\
 & + \left(\sum_{l'=\pm 1} \sum_{l'=l-1}^{l+1} A_{p,nl \rightarrow nl'}^a + \sum_{l'=l-1}^{l+1} A_{p,nl \rightarrow p_1,k'l'}^{\Gamma} + \sum_{p_1=1}^P A_{p,nl \rightarrow p_1,nl}^{\Gamma} \right) N_{p,nl} \\
 & + \sum_{p_1=1}^{P-1} \sum_{l'=l-1}^{l+1} A_{p,nl \rightarrow p_1,k'l'}^{\Gamma} + \sum_{p_1=1}^P A_{p,nl \rightarrow p_1,nl}^{\Gamma} \\
 & - (N_e d_{nl+1 \rightarrow nl}^e + N_{nl+1 \rightarrow nl}^{z_1} q_{nl+1 \rightarrow nl}^{z_1}) N_{p,nl+1} \\
 & = N_e \sum_{p_2=1}^M \sum_{l'=l-1}^{l+1} q_{p_2,k'l' \rightarrow p,nl}^c N_{p_2} + \sum_{p_1=p+1}^P A_{p_1,nl \rightarrow p,nl}^{\Gamma} N_{p_1,nl}
 \end{aligned}$$



4.2 Impurity influx, ionisation pathways and photon efficiencies.

The flux of an impurity is related to the number of ionisations from any ionisation stage along a line-of-sight to the surface which 'burns' through as it flows into the plasma from a surface. This provided there is no lateral loss and no return to the surface.

$$\begin{aligned}
 \Gamma^A &= \sum_{z=0}^Z \Gamma^{(z)}(0) \\
 &= \int_{\zeta=0}^{\infty} N_e \sum_{\sigma} S\mathcal{CD}_{\sigma}^{(Z \rightarrow Z+1)} N_{\sigma}^{(Z)}(\zeta) d\zeta \\
 S\mathcal{CD}_{\sigma}^{(Z \rightarrow Z+1)} &= \sum_{\nu'} S\mathcal{CD}_{\sigma \rightarrow \nu'}^{(Z \rightarrow Z+1)} \\
 \Gamma^A &= \sum_{\sigma, \rho} N_e \left[S\mathcal{CD}_{\sigma}^{(Z \rightarrow Z+1)} W_{\sigma\rho}^{-1} \right] I_{\rho} \\
 &\quad \uparrow \\
 &\quad S\mathcal{X}\mathcal{B}_{\sigma\rho} \quad \text{ionisations per photon - another generalised-collisional-radiative quantity.}
 \end{aligned}$$

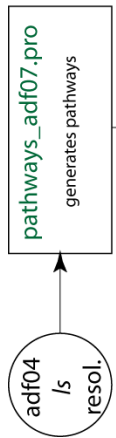
Observe a set of linearly independent spectrum lines equal to the number of metastables of stage Z .

$$\mathcal{PEC}_{\sigma, i \rightarrow j}^{(exc)}$$

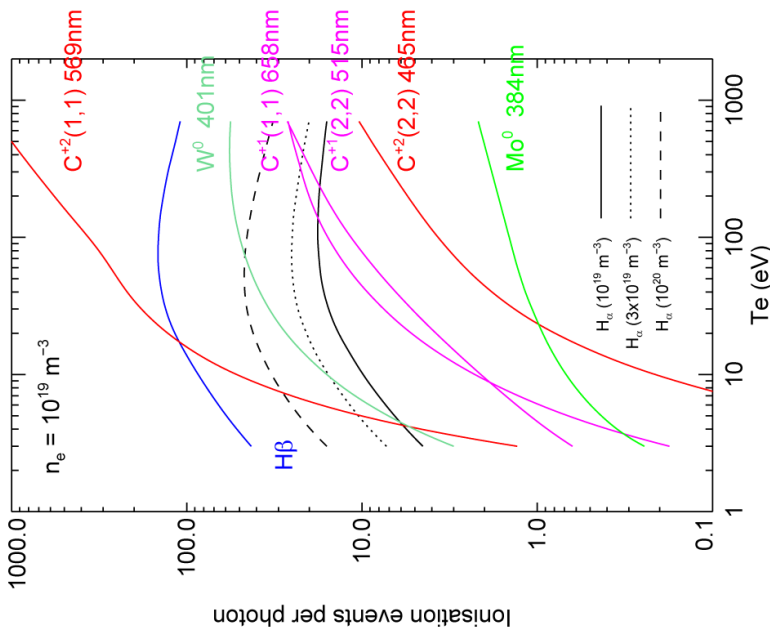
$$\begin{aligned}
 \epsilon_{\rho} &\equiv \epsilon_{\rho, i \rightarrow j} = A_{i \rightarrow j} \sum_k C_{i,k}^{-1} \sum_{\sigma} C_{k\sigma} N_{\sigma}^{(Z)} \\
 \epsilon_{\rho} &= \sum_{\sigma} W_{\rho\sigma} N_{\sigma}^{(Z)} \\
 N_{\sigma}^{(Z)} &= \sum_{\rho} W_{\sigma\rho}^{-1} \epsilon_{\rho} \\
 I_{\rho} &= \int_0^{\infty} \epsilon_{\rho} d\zeta
 \end{aligned}$$

4.3 Metastable resolved ionisation and SXB

ca resolution distorted wave ionisation cross-sections are the preferred ADAS general purpose source at this time. The **ls** resolution is deduced by a fractionation procedure.



The reciprocals of SXB coefficients are sometimes called **photon efficiencies**. The GCR version is necessary for valid influx estimation since metastables are not relaxed.



Details of fundamental data production are given in module 7.

SXB has data format adf13. See [read_adf13.pro](#).

5.1 Conclusions

- Population modelling has been described which can be used at various resolution levels, namely *ic*, *ls* and *ca*, depending on the availability of requisite *adf04* data sets. ADAS fundamental data production for medium/heavy species is tuned to these resolutions.
- The *b_{nl}* and *b_n* very high level population models in ADAS have been designed to solve the truncation problem such that their influence can be projected on the spans of the *adf04* datasets above.
- Progressive **projection/condensation** delivers necessary generalised collisional-radiative (**GCR**) spectroscopic data and plasma transport model data as data formats *adf11* and *adf15*.
- For heavy systems of great complexity, the technique of **superstages** and **feature emissivity coefficients** (*adf40*) has been provided in ADAS, which allows attention to remain focussed on key ions, while still supporting full transport modelling.
- Extension of population modelling to dielectronic resonant states, via the **bbgp** method increases the precision to effective recombination and high densities.
- Inference of impurity influx, including testing of consistent influx from successive ionisation stages, from line-of-sight spectral observations is supported by ADAS in the full GCR framework, including a machinery for ionisation pathways through data classes *adf15* and *adf07*.
- More detail is given in the extended lecture-notes for module 2.

B.3 module_3



Module 3

H₂ molecular emission and collisional-radiative modelling

Lecture viewgraphs

Hugh Summers, Francisco Guzman, Kurt Behringer, Martin O'Mullane and Alessandra Giunta

University of Strathclyde

ADAS/ADAS-EU

Contents

1. Preliminaries and nomenclatures.
2. The molecular H₂ database.
3. Vibronic collisional-radiative modelling.
4. Rovibrational spectral simulation and comparison.
5. Conclusions.

1.1 Preliminaries

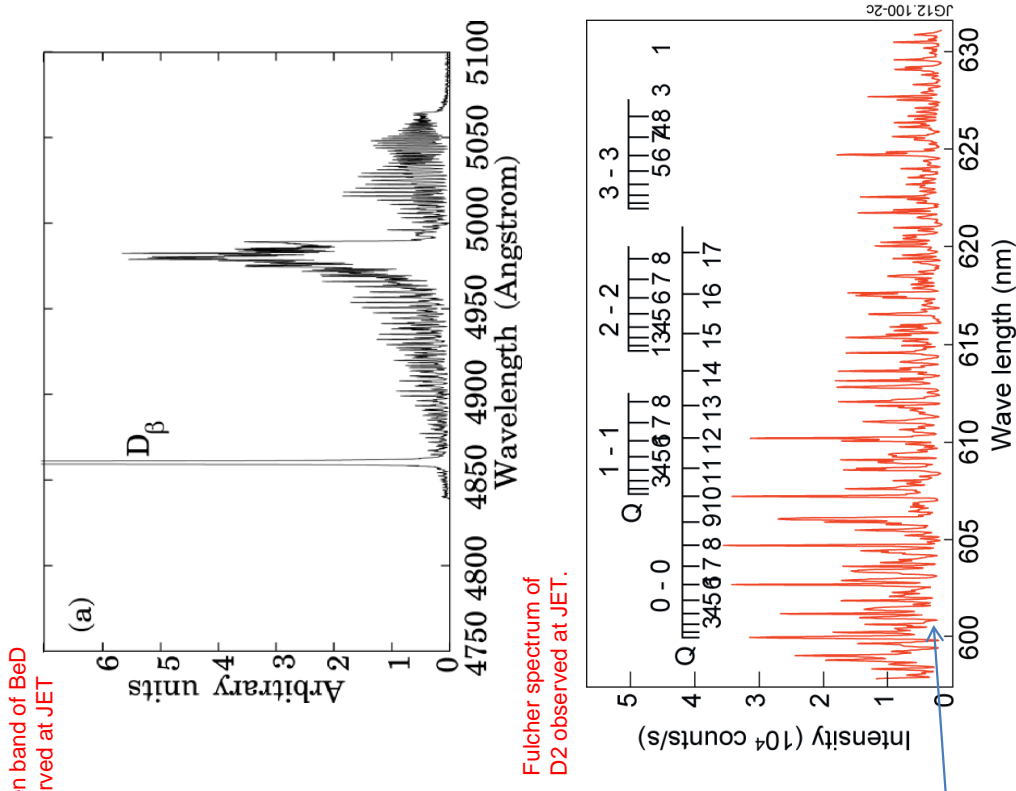
ADAS has restricted interest to diatomic molecules only.

There are two primary motivations:

- (a) analysis of observations of band spectral features at visible wavelengths, which discriminate isotopomers, temperatures (T_r & T_v) and clarify sources.
- (b) Collisional-radiative modelling of H_2 isotopomers for plasma models and quantitative spectroscopy in the visible and UV.

For the former, ADAS models rovibrational band wavelengths between electronic states, with assumptions of upper emitting state populations.

For the latter, ADAS has developed a vibronic collisional radiative model for the H_2 system. This model can provide upper state population information for quantitative/calibrated spectroscopy of hydrogen molecular emission.



Careful comparison with ADAS rovibrational models indicate a weak HD contribution to the primary D_2 spectrum.

1.2 Fundamental molecular constants and data

Following the ADAS practice for atoms and ions, a number of data formats have been introduced for the molecular problem. They are called *molecular data formats* (such as **mdf00**). These fall into the two categories of fundamental data and derived (collisional-radiative) data.

We have tried as far as possible to follow the data format numbering of the atomic case. Thus *mdf00*, *mdf01*, *mdf02* and *mdf04* are fundamental data collections. **mdf04** is a *specific molecular system file* which, as for its atomic counterpart, can support a collisional-radiative (vibrionic) model.

In magnetic confinement fusion research, it is necessary to work with various isotopic combinations, such as H₂, D₂, T₂, HD, HT and DT. It is assumed that the electronic states and their electronic transitions are independent of the nuclear masses. The vibrational and rotational sub-states do reflect the specific isotopic masses.

In practical terms, molecular studies must focus on molecular systems. Thus the D₂ system includes D₂, D₂⁺, D, D⁺ (and in principle D₃ and D₃⁺) and these must be treated together in collisional - radiative modelling. For example, the direct formation of D(n=3) by molecular dissociation is an important parameter.

Molecular constants:

mdf00: enu sub-directories by isotopomer – separate datasets of vibrational substate energies for each electronic state.

pot separate datasets of electronic potential curve for each electronic state.

dip separate datasets of electronic dipole curve for each electronic state.

aval sub-directories by isotopomer – separate datasets of vibrationally resolved A-values for each electronic state pair.

fcl sub-directories by isotopomer – separate datasets of vibrationally resolved Franck-Condon factors for each electronic state pair.

mdf01: nist sub-directories by isotopomer - extract of NIST molecular constant table for selected electronic states.

behr sub-directories by isotopomer - driver parameter file for ADAS908 rovibrational spectral analysis - relevant electronic and vibrational transitions.

pickett sub-directories by isotopomer - driver parameter file for ADAS908 rovibrational spectral analysis - relevant electronic and vibrational transitions.

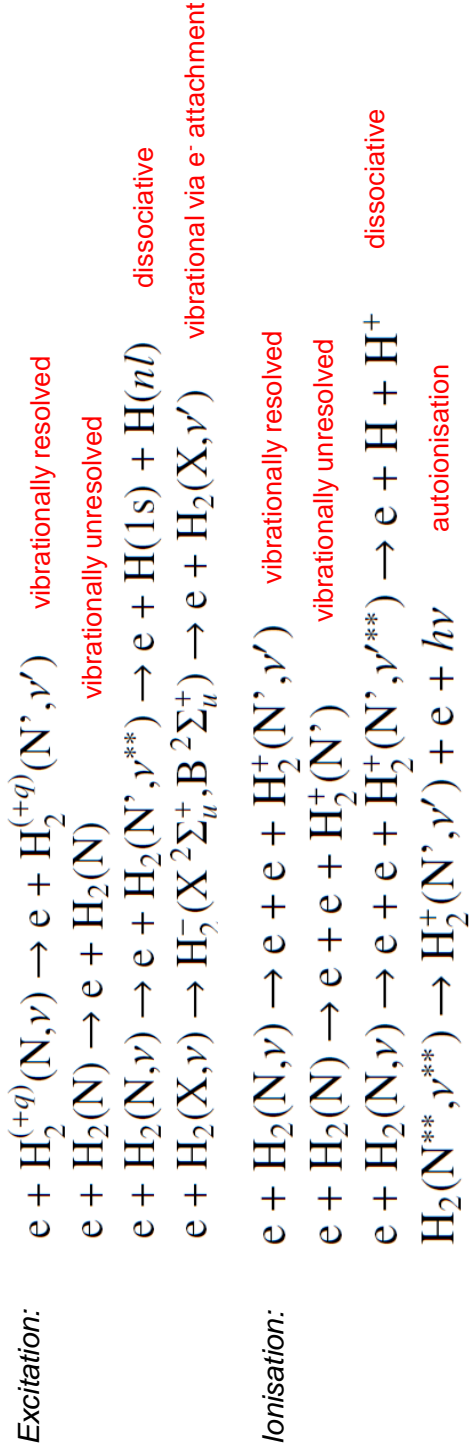
2.1 Electron impact processes with the H₂ molecule

The electron collision processes with the H₂ molecular system has been studied for many years and compilations of reaction cross-sections assembled. A major revision has taken place by Janev, Reiter and Guzman linked to the ADAS-EU project to put these data in a form suitable for ADAS collisional-radiative modelling.

Fundamental data in ADAS data formats are archived as preferred numerical tabulations, with specified asymptotic behaviour. In the molecular collision area, algebraic forms are often used (in certain cases multiple forms) with some lack of clarity in preference. The ADAS database seeks to correct this.

The ADAS impact process molecular data format is [mdf02](#) and it has been designed to have both numerical values and the parameters of the formulaic representation (if available) of each transition.

The primary dataset for electron impact with H₂ is [mdf02/g13_h2#e.dat](#). The groups of processes are summarised below.



2.2 Electron impact processes with the H₂ molecule (contd.)

| | |
|--|---|
| <i>Dissociation:</i> (excluding above) | $e + H_2^+(N, \nu) \rightarrow e + H_2^+(d) \rightarrow e + H(1s) + H(nl)$ vibrationally resolved $e + H_2^+(N) \rightarrow e + H_2^+(d) \rightarrow e + H(1s) + H(nl)$ vibrationally unresolved $e + H_2(N, \nu) \rightarrow H_2^-(X^2\Sigma_u^+) \rightarrow H^- + H(1s)$ diss. e· attachment via H ₂ (X) and H· production $e + H_2(N, \nu) \rightarrow H_2^-(B^2\Sigma_g^+) \rightarrow H^- + H(1s)$ diss. e· attachment via H ₂ (B) and H· production $e + H_2(X, \nu) \rightarrow H_2^-(X/B^2\Sigma_{(u/g)}^+) \rightarrow e + H(1s) + H(1s)$ diss. e· attachment |
| <i>Recombination:</i> | $H + H_2^+(N, \nu) \rightarrow H^+ + H_2(N', \nu')$ vibrationally resolved inverse CX $H + H_2^+(N) \rightarrow H^+ + H_2(N)$ vibrationally unresolved inverse CX $e + H_2^+ \rightarrow H_2^{**} \rightarrow H(n) + H(n)$ dissociative recombination |
| <i>Charge exchange:</i> | $H^+ + H_2(N, \nu) \rightarrow H(1s) + H_2^+(N', \nu')$ vibrationally resolved direct CX $H^+ + H_2(N) \rightarrow H(1s) + H_2^+(N')$ vibrationally unresolved direct CX $H^+ + H_2(N, \nu) \rightarrow H(1s) + H + H^+$ dissociative CX $H^+ + H_2(\nu) \rightarrow H(1s) + H^+ + H^+ + e$ transfer ionisation |

There is a corresponding dataset for H⁺ impact processes with H₂ called *mdf02/fg13_h2#p.dat*

2.3 H₂ system excitation data of format *mdf02*

```

system      → H2 / species / ind_s / ind_e / electr impact / mdf02
species list with characterisations → H2 / H2 / H2+ / H2- / H / H+ / H- / process / process list with descriptions → 11 / 53 / 54 / 55 / states / electronic level list → 1 / 2 / 2 / 3 / 4 / 5
species → identity / e-config / e-coupling / ch_ion / bwno_i / ch_dis / bwno_d
path → e+H2(^+q)(N,v) → e + H2(+q)*(N',v') / e+H2(N,v) → e + H2* (N',v') / H+ + H2(N,v) → H(1s) + H + H+ / H+ + H2(v) → H(1s) + H+ + H+ + e
coupled state → (1)S(+)(g) / (1)S(+)(u) / (2)P(+)(g) / (2)P(+)(u) / (3)P(+)(g) / (2)S(+)(g) / (2)S(+)(u) / (2)P(-)(g) / (2)P(-)(u) / (2)S
wno → 124418. / 124418. / 5386. / 109691. / N / 0. / 427. / 91691.69 / 0.0 / 118509.87 / 0.5 / 0.5 / 0.5 / 148030.30
wno_d → 36117.00 / 36117.00 / 21380.21 / 0.0000.00 / N / 0.0000.00 / 0.0000.00 / 120595.97 / 0.0 / 135837.26 / 1.2418.00 / 0.5 / 0.5 / 148030.30
description → excitation / vib resolved exc. / dissociative CX transfer ion. / other CX processes / values
comments → ground state X / r / dissociative state / dissociative state / ion H+

```

2.4 Transition data and the ADAS901 processing screen

transition data

| /ch_in | ind_p | ch_out | ch_dis | parameters & values | codes and information |
|--------|-------|--------|--------|---|---|
| s e v | 14 | s e v | | categ=4 te= 1.000 1.200 1.400 numer=28 2.400 2.600 2.800 3.000 7.000 8.000 9.000 10.00 40.00 50.00 60.00 70.00 rate= 0.6124E-07 0.5456E-07 0.4877E-07 0.3953E-07 0.2989E-07 0.2746E-07 0.2531E-07 0.2341E-07 0.7480E-08 0.6063E-08 0.5004E-08 0.4191E-08 0.2487E-09 0.1444E-09 0.9086E-10 0.6057E-10 par_val= -7.5980 -1.5006e-1 2.3448 1.0147 -8.0417 7.9813e-2 | DE=0.00000e+00 EX 1.600 1.800 4.000 5.000 2.000 6.000 30.00 100.0 0.3267E-07 0.3586E-07 0.1224E-07 0.1474E-08 0.4829E-09 0.2255E-10 |

fit form parameters

It is helpful to be able to interrogate *mdf02* data and graph the collision data.

The interactive ADAS code **ADAS901** provides this facility. A numerical tabulation at the user's choice of range may also be returned.

process type selector

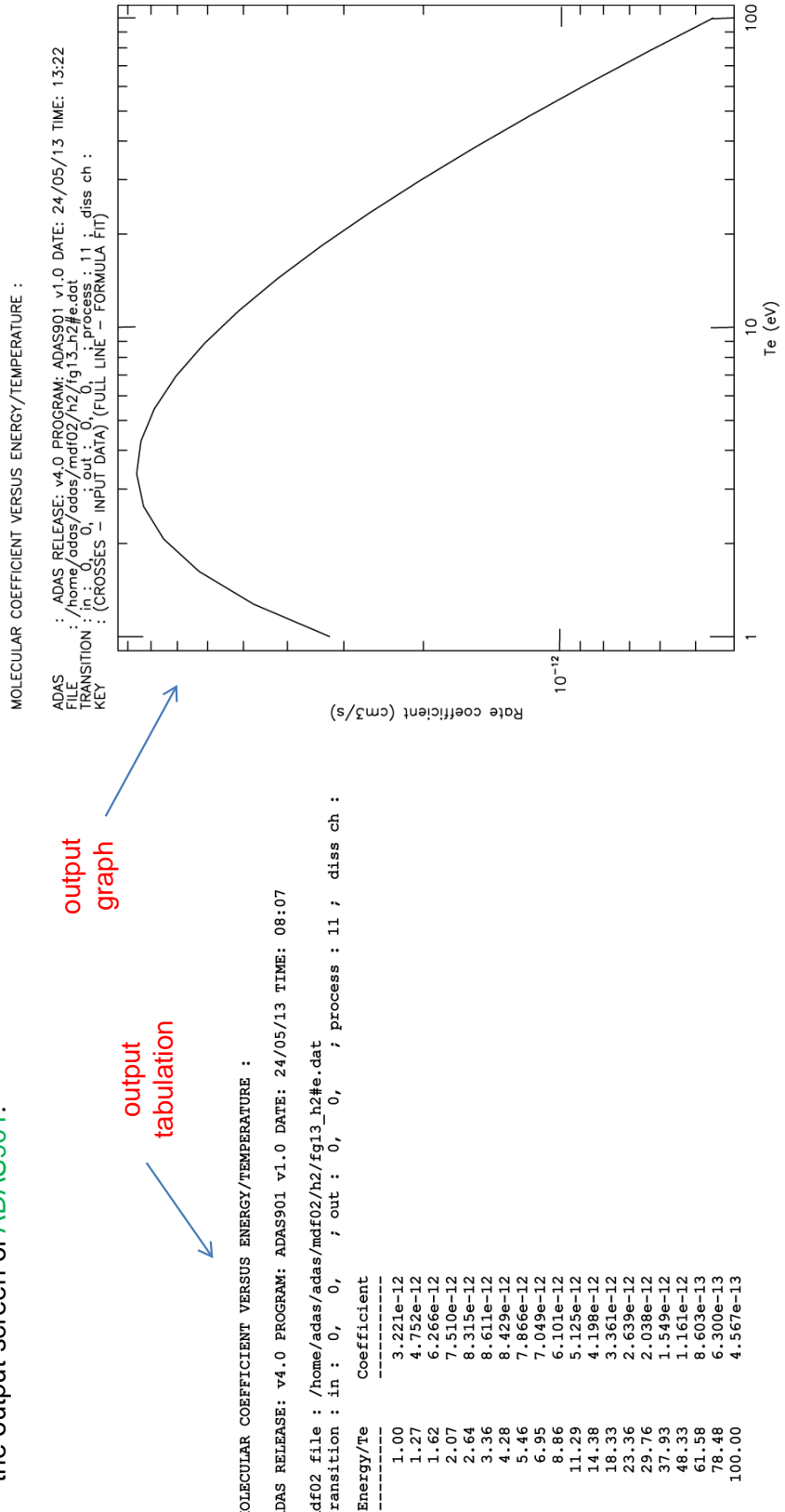
details of selected transition

The screenshot shows the ADAS901 processing interface. It includes:

- A title bar: ADAS901 : PROCESSING OPTIONS (on ferro.phys.strath.ac.uk)
- An input section with fields for Title for run, Number of species (6), Number of electronic states (27), Number of transitions (150), and choose Process (11 : vib resolved exc.).
- A preview window showing a plot of energy (eV) versus index, with a legend for incoming channel and outgoing channel.
- A table titled "Process: incoming channel - outgoing channel" with columns for INDEX, To/Energy (eV), and values for indices 1 through 14.
- A table titled "Select Temperatures/Energies:" with a formula field containing $\text{ferH}_2(N, \nu) \rightarrow e + \text{H}_2^2(N, \nu)$.
- Buttons for Edit Table, Default: mdf02 range, and Clear Table.
- A bottom panel with a formula field (Formula : 201), x-type (temperature (eV)), y-type (Maxwell averaged rate coefficient (cm³/s)), Range (1.00e+00 - 1.00e+02), and Details, along with Cancel and Done buttons.

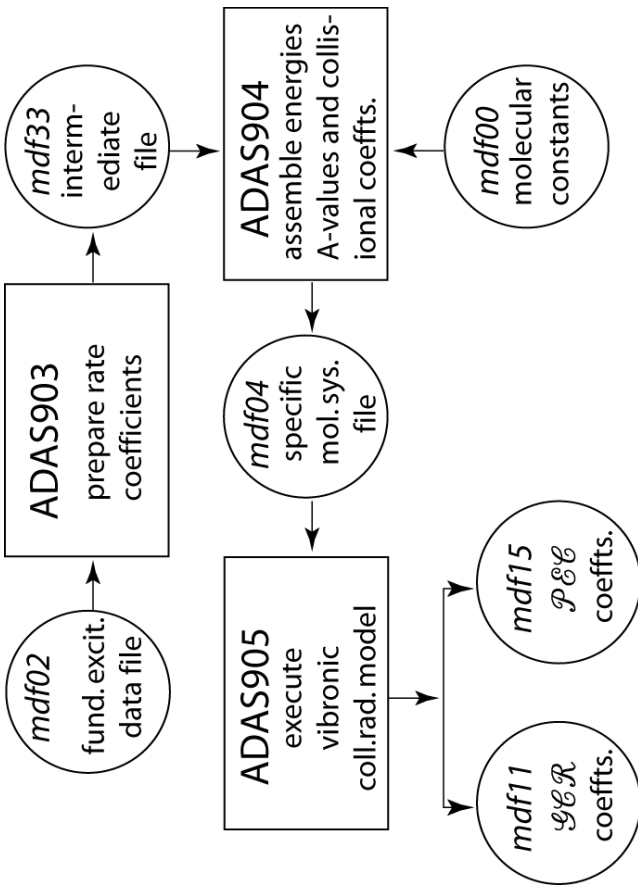
2.5 Text and graphical output from ADAS901

The familiar outputs are available on the output screen of **ADAS901**.



3.1 H₂ vibronic collisional-radiative

The ADAS codes **ADAS903** and **ADAS904** operate in sequence. From *mdf02*, **ADAS903** converts cross-sections to rate coefficients. It prepares an intermediate dataset of format *mdf33* structurally similar to *mdf02*.



ADAS904 gathers the level list and reaction data from *mdf33* and includes A-values and vibrationally-energies from *mdf00* to prepare the vibrationally-resolved specific molecule file *mdf04*.

Formally, *mdf04* is similar to *adf04*. It is sufficient to support a vibronic population calculation.

ADAS905 executes the vibronic collisional-radiative model for the population solution. It generates the generalised collisional-radiative coefficients of format *mdf11* which couple metastable states of species together and the associated emissivity coefficients *mdf15*. These names parallel the *adf11* and *adf15* formats for atoms and ions.

3.2 H₂ generalised collisional-radiative algebra

The generalised collisional matrix reductions follow broadly the same path as for atoms and ions. But there are some new coefficients

$$\frac{dN_\rho}{dt} = \mathcal{MC}_{\rho\sigma}N_\sigma + \mathcal{M}Q_{\rho\nu}^{\text{ICX}}N_\nu N_H + \mathcal{MR}_{\rho\nu}N_\nu N_H$$

$$\begin{aligned}\mathcal{MC}_{\rho\sigma} &= \left[C_{\rho\sigma} - C_{\rho j}C_{ji}^{-1}C_{i\sigma} \right] / N_e & \mathcal{MDEC}\mathcal{D} \\ \mathcal{MR}_{\rho\nu} &= r_{\rho\nu} - C_{\rho j}C_{ji}^{-1}r_{i\nu} & \mathcal{MAD}\mathcal{D} \\ \mathcal{M}Q_{\rho\nu}^{\text{ICX}} &= Q_{\rho\nu}^{\text{ICX}} - C_{\rho j}C_{ji}^{-1}Q_{i\nu}^{\text{ICX}} & \mathcal{MCXIGAEC}\mathcal{D}\end{aligned}$$

New **inverse charge exchange recombination coefficient**

$$\mathcal{MS}_{\nu\sigma} = S_{\nu\sigma} - S_{\nu j}C_{ji}^{-1}C_{i\sigma}$$

$$\mathcal{MQ}_{\nu\sigma}^{\text{CX}} = Q_{\nu\sigma}^{\text{CX}} - Q_{\nu j}C_{ji}^{-1}C_{i\sigma}$$

$\mathcal{MCXEC}\mathcal{D}$

$\mathcal{MCXEC}\mathcal{D}$

New **dissociative** coefficients.

$$\mathcal{PD}_{\mu\sigma} = \mathcal{D}_{\mu\sigma} - C_{\mu j''}C_{j'' i''}^{-1}\mathcal{D}_{i''\sigma}$$

$\mathcal{PDEC}\mathcal{D}$

$$\mathcal{PARD}_{uv} = -\mathcal{D}_{ui}C_{ii}^{-1}Q_{iv}^{\text{ICX}}N_H - \mathcal{D}_{ui}C_{ii}^{-1}r_{iv}N_e$$

$\mathcal{PAD}\mathcal{D}\mathcal{E}\mathcal{D}$

$$\mathcal{PDS}_{\mu^+\sigma} = -N_e \left[S_{\mu^+ j''}C_{j'' i''}^{-1}D_{i''\sigma} \right]$$

$\mathcal{PDEG}\mathcal{D}$

$$\mathcal{PARD}S_{\mu^+\nu} = -N_e S_{\mu^+ j''}C_{j'' i''}^{-1}D_{i'' j}C_{ji}^{-1} \left[Q_{iv}^{\text{ICX}}N_H + r_{iv}N_e \right] \quad \mathcal{PADD}\mathcal{E}\mathcal{D}$$

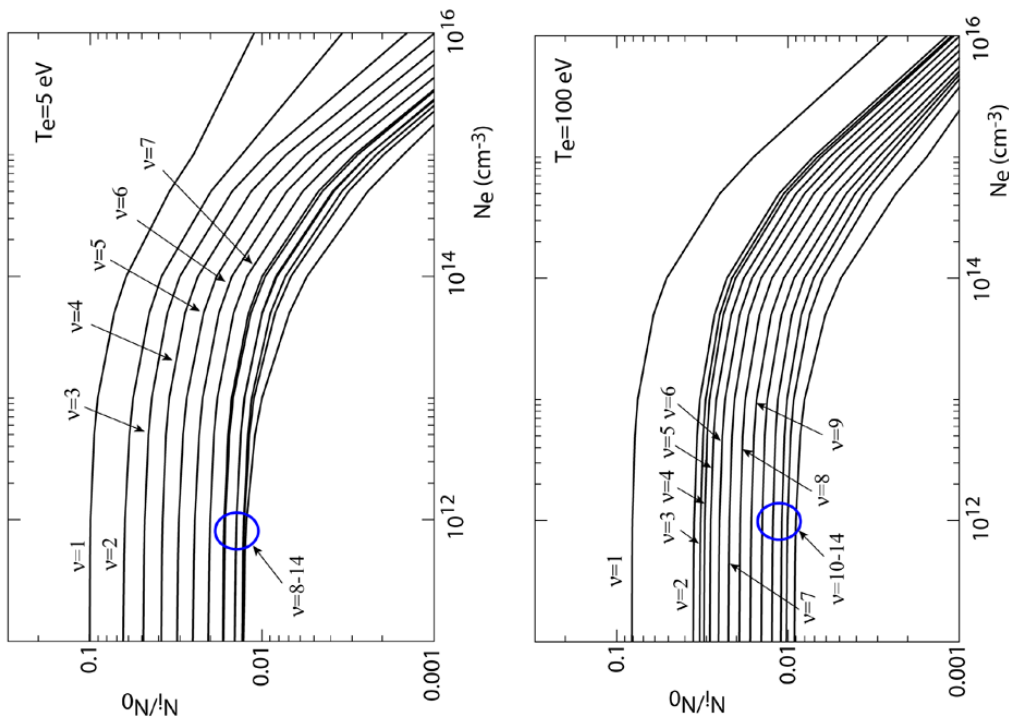
3.3 H₂ ground state vibrational population structure

In the H₂ system, **all** the vibrational states of the ground electronic state H₂ ($X^1S_g^+$) are **metastable**, since they cannot radiate to the lowest vibrational state.

The figures to the right show the vibrational sub-state populations of the ground state in equilibrium.

The vibrational states of the excited electronic states are not metastable. They are **ordinary** states in the generalised collisional-radiative description.

The set of generalised collisional-radiative coefficients is therefore **much larger** for the molecular case. This can be a bit overwhelming for basic studies, so the coefficients are often summed and averaged over the vibrational sub-states of the ground electronic state.



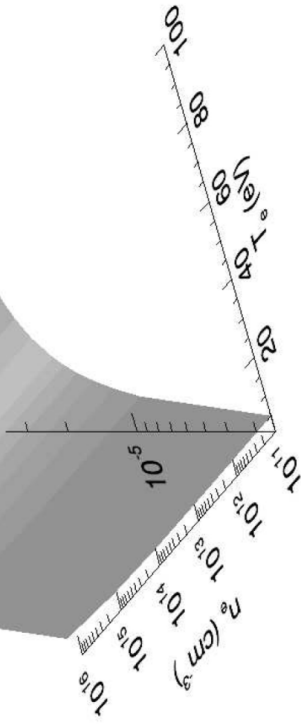
3.3 H₂ collisional-radiative coefficients

The coefficients shown here have been summed over the ground vibrational substates. In the most consistent practice the separate vibrational sub-states of the H₂ (X ¹S_g⁺) ground electronic state are all metastable and should be explicit.

Dissociation coefficient \mathcal{PDEC} for the effective dissociation pathway:
 $H_2 (X ^1\Sigma_g^+) \rightarrow H + H(H^+)$



Ionisation coefficient \mathcal{MDEC} for the pathway :
 $H_2 (X ^1\Sigma_g^+) \rightarrow H_2^+ (X ^2\Sigma_g^+) + e$

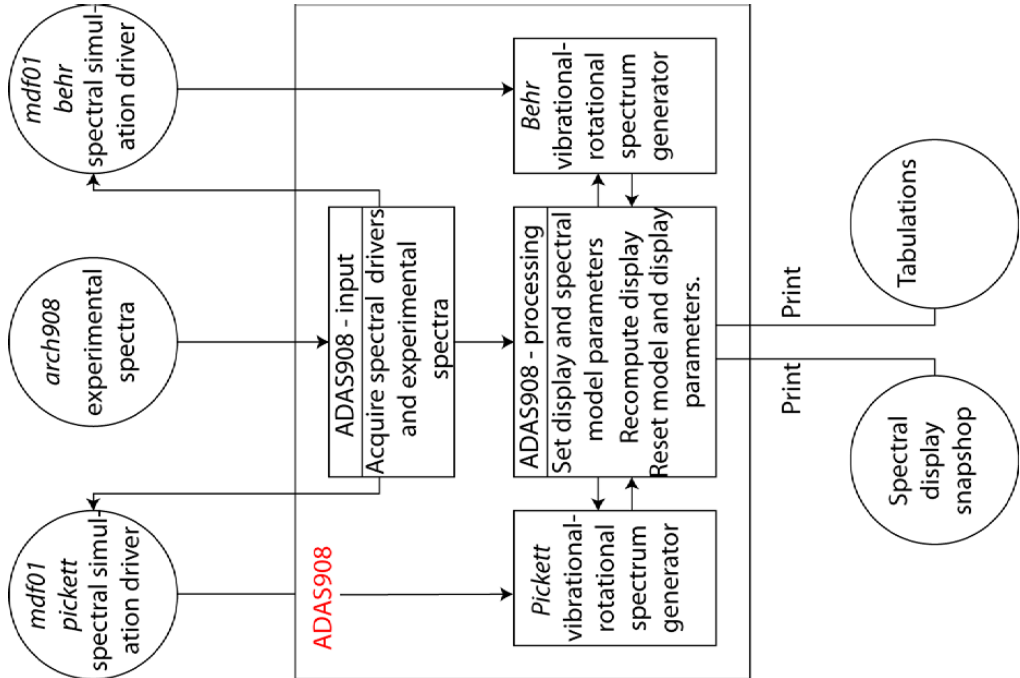


4.1 Spectral analysis using ADAS908

Practical spectral analysis for complex molecular rovibrational spectra often proceeds by comparison and matching of theoretical and experimental spectra over wavelength intervals.

If a convincing match can be obtained, then the variation of relative intensities as a function of effective rotational and vibrational temperatures can be exploited.

ADAS908 is provided to assist in such investigation. It can work with several spectra (experimental and theoretical) simultaneously. Control values appropriate to the experimental spectra and to the theoretical spectra and to the display can be adjusted giving substantial flexibility.



4.2 Some theoretical issues

The usual parametric expansion of a rovibrational level energy is written as:

$$\begin{aligned} T_{\nu,J} &= G(\nu) + F_{\nu}(J) \\ &= \omega_e(\nu + 1/2) - \omega_e x_e(\nu + 1/2)^2 + \omega_e y_e(\nu + 1/2)^3 + \dots \\ &\quad + B_{\nu} J(J + 1) - D_{\nu} J^2(J + 1)^2 + H_{\nu} J^3(J + 1)^3 + \dots \end{aligned}$$

where the rotational parameters may have the supplementary expansions:

$$\begin{aligned} B_{\nu} &= B_e - \alpha_e(\nu + 1/2) + \beta_e(\nu + 1/2)^2 + \dots \\ D_{\nu} &= D_e - \gamma_e(\nu + 1/2) + \dots \end{aligned}$$

If there is no upper electronic state vibrational sub-population collisional-radiative model, then upward projection of the ground and/or metastable thermal vibrational distributions is assumed according to Franck-Condon factors. This can be handled by adjusting B_{ν} values and populations as

$$\begin{aligned} \bar{B}'_{k,\nu'} &= \left[\sum_{\nu_g} B_{g,\nu_g} F_{g\nu_g}^{k,\nu'} N_{g,\nu_g} + \sum_{\nu_m} B_{m,\nu_m} F_{m\nu_m}^{k,\nu'} N_{m,\nu_m} \right] / \left[\sum_{\nu_g} N_{g,\nu_g} + \sum_{\nu_m} N_{m,\nu_m} \right] \\ N_{k,\nu',J} &= \omega_J \exp(-\bar{B}'_{k,\nu'} J(J + 1)/kT_r) N_{k,\nu'} / \sum_J \omega_J \exp(-\bar{B}'_{k,\nu'} J(J + 1)/kT_r) \end{aligned}$$

which most conveniently is presented as a modified rotational temperature $T'_r = B'_{k,\nu'} T_r / \bar{B}'_{k,\nu'}$

4.3 The mdf01/beh driver for H₂

The *mdf01/beh* drivers have been specially tuned to the H₂ molecular case.

The nuclear spin specification is required for homonuclear systems so that the intensity alternation of successive rotational transitions may be correctly determined.

Specific rotational parameters for vibrational substates support the high wavelength precision needed for H₂ rovibrational identification.

```
HH; mdf01 Behringer format; etrans = all; vtrans = all
KS1   = 0.5
KS2   = 0.5
```

| | | | |
|---|-------------------|-----------|-------------------|
| 1 | X singlet Sigma g | 0.000 | electronic states |
| 2 | B singlet Sigma u | 91700.000 | |
| 3 | a triplet Sigma g | 95936.1 | |
| 4 | d triplet Pi u | 112700.3 | |

| | | | | | | |
|----|----------|---|---|---------|---------|-----------|
| -1 | e=1 v= 0 | 1 | 2179.586 | 59.3634 | 0.0455 | 0.0000465 |
| . | e=1 v=14 | . | 38154.391 | 8.7701 | 0.08467 | 0.0 |
| 15 | e=2 v= 0 | 2 | 682.321 | 19.4563 | 0.0156 | 0.0000163 |
| 16 | e=2 v=* | . | 16139.337 | 11.375 | 0.0035 | 0.0000127 |
| 30 | e=2 v=14 | 2 | 0. | 0. | 0. | |
| 31 | e=3 v=* | 3 | 0. | 0. | 0. | |
| 32 | e=4 v=* | 4 | 0. | 0. | 0. | |
| -1 | 2 1 | 1 | electronic transition pairs for spectral generation | | | |
| 1 | 2 4 | 3 | | | | |
| -1 | | | | | | |

| | | | | | | |
|----------------|---|---|---|--|--|--|
| state = "X" | | | | | | |
| vmax = 14 | | | | | | |
| jmax = 20 | | | | | | |
| om = 4401.2654 | | | | | | |
| omx = 120.602 | | | | | | |
| omy = 0.7242 | | | | | | |
| Be = 60.8477 | | | | | | |
| De = 0.04653 | | | | | | |
| alp = 3.0513 | | | | | | |
| bet = 0.0 | | | | | | |
| He = 5.168E-05 | | | | | | |
| Te = 0.0 | | | | | | |
| +++ | . | . | . | | | |
| -1 | | | | | | |

base rovibrational parameter set for each electronic state

improved rotational parameters for specific vibronic states

vibrational states

electronic states

4.4 The mdf01/pickett driver for BeD

The method is best suited to diatomics with heavier nuclei than H₂ for which vibrational and rotational energy separation is better.

Examination and selection of parameters was carried out by Duxbury for JET experiments. ADAS has such special data for CH, CD, C₂, BeH, BeD and BeT.

The capabilities of the Pickett package are very large, but expert knowledge is required for full utilisation. The ADAS mdf01/pickett database will be extended as needed.

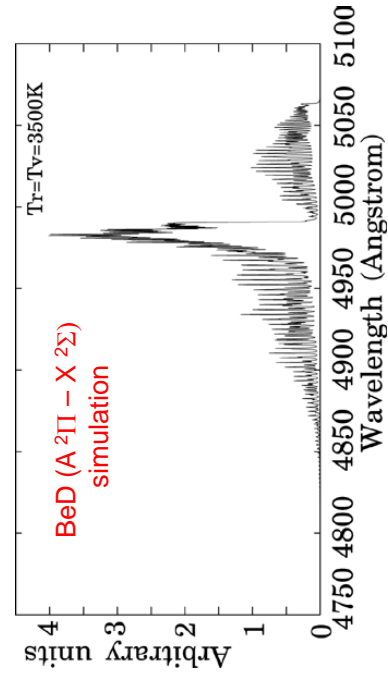
Bed; mdf01 Pickett format; etrans = 2 Sigma - 2 Pi
 1 doublet Sigma 0.000 electronic states
 2 doublet Pi 20037.910
 -1

| | | | |
|----|---------|---|---------------------|
| 1 | e=1 v=0 | 1 | 0.000 |
| 1 | . | . | . |
| 7 | e=1 v=6 | 1 | 8292.458 |
| 8 | e=2 v=0 | 2 | 0.000 |
| 1 | . | . | . |
| 14 | e=2 v=6 | 2 | 8320.162 |
| -1 | | | |
| 1 | 8 | 1 | vibronic pairs with |
| 2 | 9 | 2 | detailed parameters |
| 3 | 10 | 3 | following |
| 4 | 11 | 4 | |
| -1 | | | |

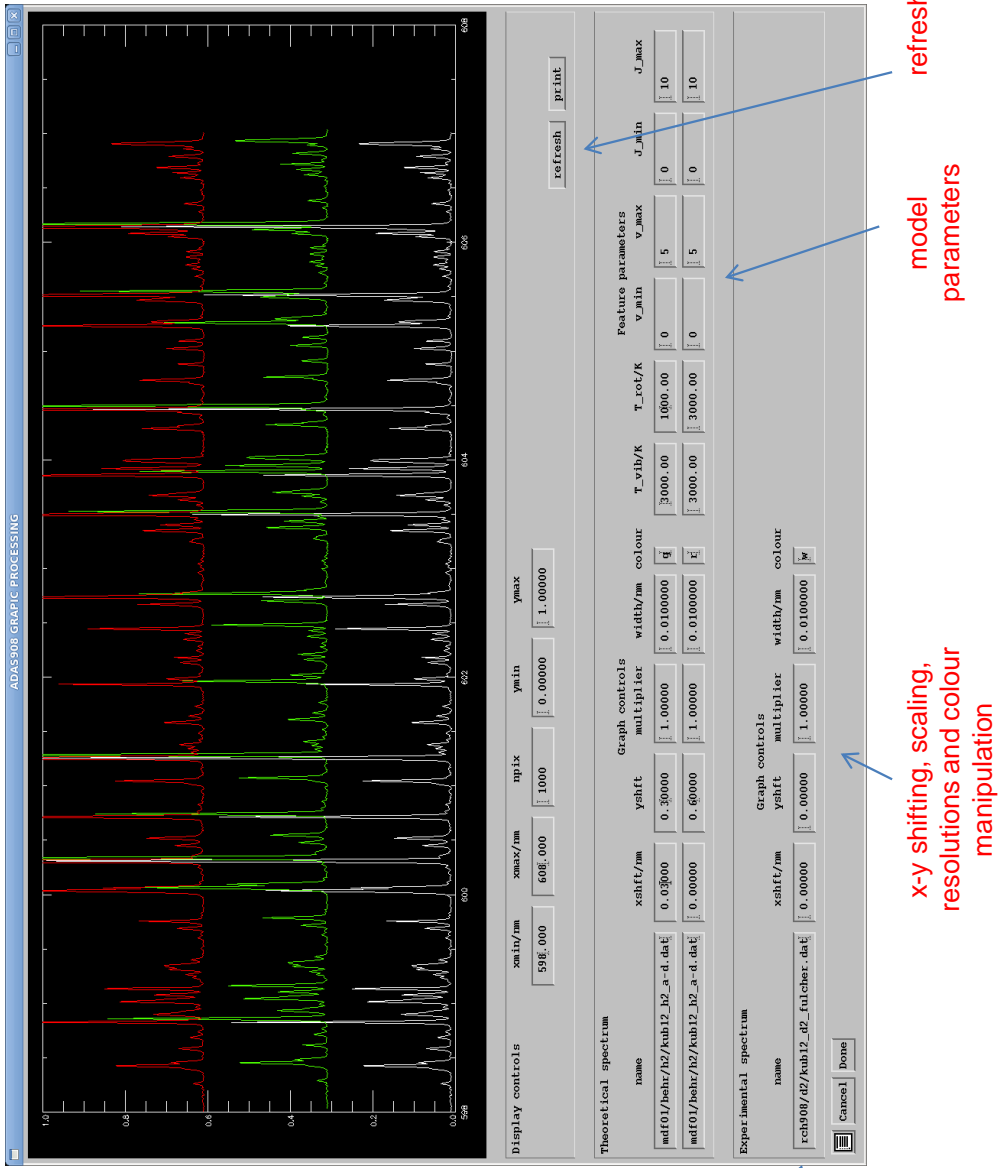
beryllium deuteride 2pi:2sig 14-Oct-2003
 1010 79002 494.139 0 120 -45.0 -45.0 600000 TTTTT
 013 0.0100

| | | |
|-----|---|--------------------|
| --- | Beryllium deuteride 0-0 band 2pi-2sigma 14 Oct 2003 | 1.000 |
| 'a' | 16 600 3 0 1.122000E-10 | 1000.000 |
| 'a' | -2 2 0 0 2 1 -1 1 | 1 |
| 'a' | -2 1 1 1 0 1 0 1 | 1 |
| 'a' | 11 20037.68888 -.05 | 0 |
| 'a' | 100 5.62479800 9.59E-8 | 1 E' (Band Centre) |
| 'a' | 111 5.69574400 9.59E-8 | ! Bbar" (1sg) |
| 'a' | 200 -3.1176800E-4 2.00E-10 | ! Bbar' (1pi) |
| 'a' | 211 -3.1670100E-4 2.00E-10 | ! D0" (1sg) |
| 'a' | 300 1.623800E-4 2.00E-10 | ! D0' (1pi) |
| 'a' | 311 1.5743000E-8 2.00E-10 | ! HJ" (1pi) |
| 'a' | 400 -0.8746000E-12 2.00E-10 | ! HJ0" (1sg) |
| 'a' | 411 -0.9078000E-12 2.00E-10 | ! LJ" (1pi) |
| 'a' | 40011 2.1096000E-3 2.00E-10 | ! q/2 lambda |
| 'a' | 40111 -4.586000E-7 2.00E-10 | ! dq/2 lambda |
| 'a' | 40211 2.6995000E-11 2.00E-10 | ! hq/2 lambda |
| 'a' | 10010011 2.1592000 2.00E-10 | ! Aso 2pi |
| 'a' | 10000111 -0.8015000E-2 2.00E-10 | ! gamma 2pi |
| 'a' | 10001111 0.8069000E-5 2.00E-10 | ! dgamma 2pi |
| 'a' | 10002111 -2.218000E-9 2.00E-10 | ! hgamma 2pi |

Pickett
 int
 data
 Pickett
 par
 data
 +++ parameter values



4.5 ADAS908 plot and analyse window



5.1 Conclusions

- A revision and update of the reaction process for the H₂ molecular system has been carried out and assembled in a new ADAS molecular data format *mdf02*.
- Supplementary molecular vibrational energy levels, A-values, Franck-Condon factors and other fundamental data have been assembled in molecular data format *mdf00*.
- A code machinery has been set up in ADAS series **ADAS9xx** to prepare the specific molecule dataset of format *mdf04*.
- A generalised collisional-radiative model of the H₂ system in vibronic resolution has been implemented called **ADAS905**.
- The rovibrational relative spectral prediction of diatomic band structure has been set based on two models the *Behringer model* and the *Pickett model* suited to the H₂ system and non-homogenous diatomics respectively. These use driver datasets of molecular data format *mdf01*.
- A code **ADAS908** has been set up for comparative assessment of experimental diatomic spectra and theoretical spectra created with *mdf01/behr* and *mdf01/pickett* drivers.

B.4 module_4



Module 4

Modelling and analysing special spectral features – A unified approach

Lecture viewgraphs

Hugh Summers, Christopher Nicholas, Andy Meigs, Martin O'Mullane and
Alessandra Giunta

University of Strathclyde

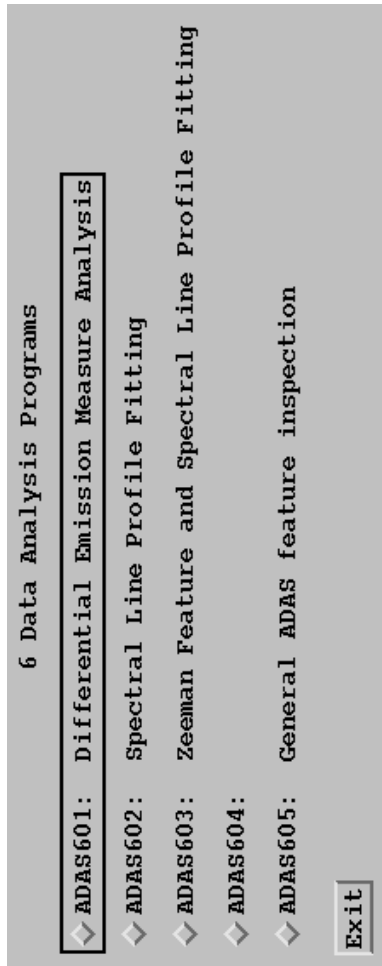
ADAS/ADAS-EU

Contents

1. Preliminaries and nomenclatures.
2. ADAS special feature – applications programming interface (API) and AFG.
3. ADAS605.
4. Combination of functions for spectral fitting - FFS.
5. Conclusions

1.1 Preliminaries

Spectral fitting and analysis is part of the capabilities of all fusion laboratories. It is also a natural adjunct to an atomic data and analysis structure. ADAS, at an early stage in its development, added some spectral analysis codes in series 6.



Basic analysis of spectra by fitting the individual line profiles and background in a spectral interval is the minimum provided in ADAS by [ADAS602](#). Also, a dedicated code, [ADAS603](#), for handling Zeeman features was prepared built on the *xPasschen* code of IPR Forschungszentrum Juelich.

At JET, some spectral intervals of special importance and/or complexity became the focus of dedicated fitting and analysis methods (e.g. [CXSFT](#)). Some, to which ADAS developers have contributed, are maintained as independent codes by ADAS.

1.2 Preliminaries

In the planning the principal themes for ADAS-EU, it was decided to develop a general approach to spectral fitting, closely linked to the atomic population modelling capabilities of ADAS, including complex composite features.

ADAS and its databases primarily operate as a **forward modelling** system, establishing populations of ions, ionisation state, emissivities etc. as a function of key plasma parameters such as T_e , N_e , magnetic field, beam energy and so on.

By contrast, spectral analysis is usually a **reverse analysis** system, fitting amplitude, width and shape of spectrum lines individually and independently of their origin. These extractions are later examined and contrasted with predictions.

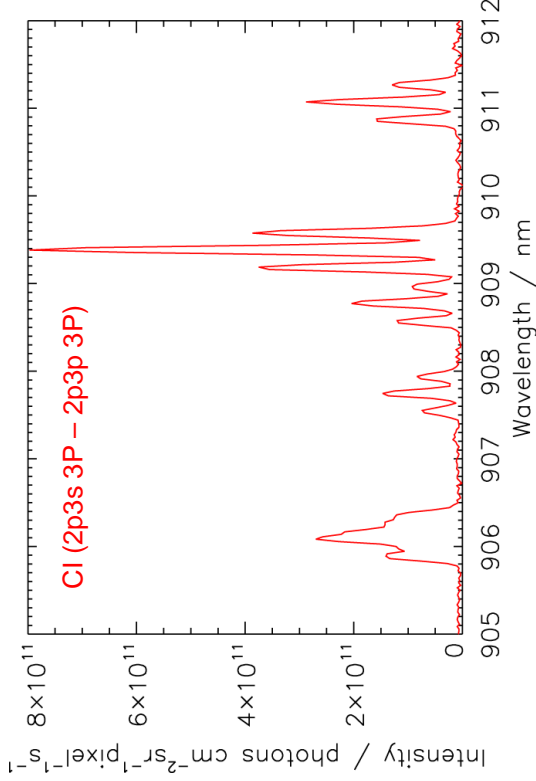
A derived data format of ADAS, such as an *adf15* dataset for an ion, is (or closely related to) an abstract numerical representation of the relative intensities of a whole set of spectrum lines as a function of the plasma parameters, which are the ultimate objective of reverse spectral analysis. With the *adf40* feature emissivity coefficients for complex heavy ions, this is even more obvious. Equally, this is true of ADAS codes such as [ADAS305](#).

We view these ADAS datasets and ADAS codes as **special spectral features** or more exactly as ADAS **special feature generators**, which can be used as a whole in spectral analysis for the direct extraction of plasma parameters in the fitting process.

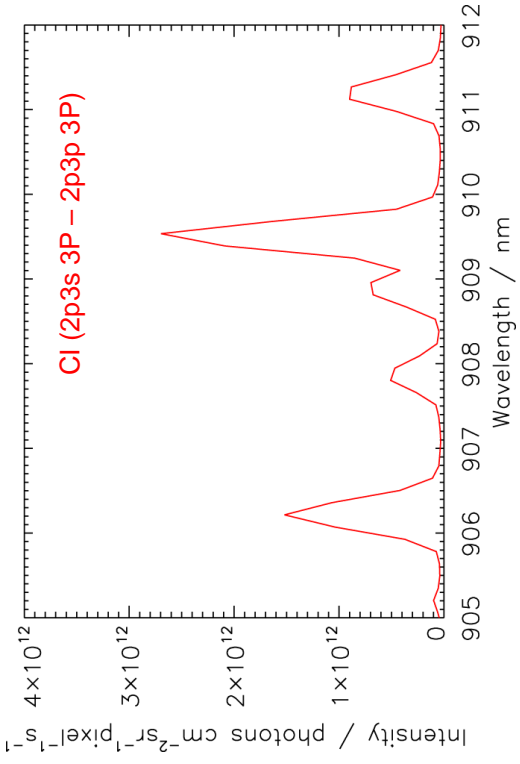
1.3 Preliminaries

The development is quite complex in design, using different coding techniques (object-oriented) from the remainder of ADAS. Also, the whole system is still in the final stages of completion and incorporation.

In this brief introduction, the Zeeman spectra below from JET will be used illustratively.



Zeeman split carbon line emission, from JET pulse #75989 ($R = 2.8$ m, $t = 46.25$ s, diagnostic KT3C mm⁻¹ grating) recorded at sufficient resolution to resolve several component lines of the feature.



Zeeman split carbon line emission, from JET pulse #70574, ($R = 2.68$ m, $t = 60.28$ s, diagnostic KT3C using 300 lines mm⁻¹ grating) at lower resolution. Individual components are no longer resolved, instead they appear blended together.

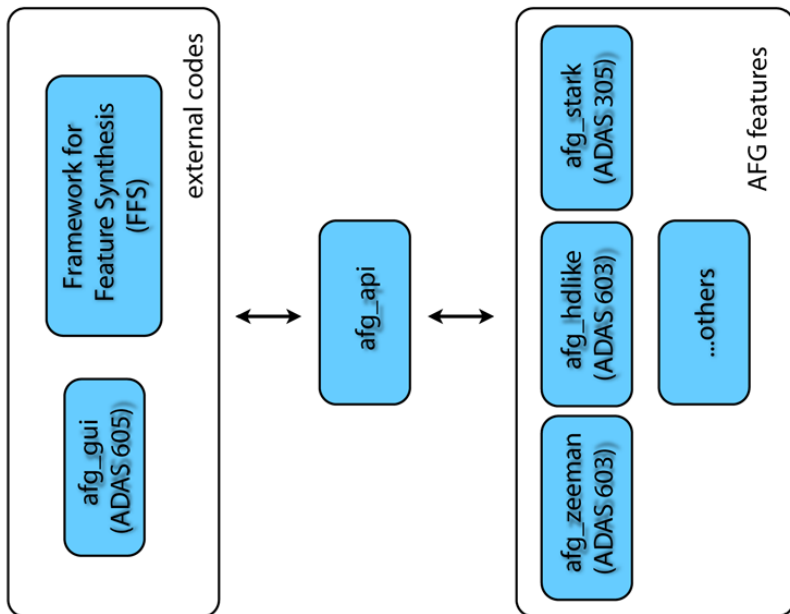
2.1 Accessing ADAS special features - AFG

The main drive behind the *ADAS Feature Generator* (**AFG**) is to ease access to the ADAS special feature routines such that they are easily incorporated into any external modelling code (see **FFS** later). **AFG** enables this to be done through a series of simple commands — now common to all of the ADAS special features. This is the *Applications Program Interface* (**API**).

The **API** provides a common access point to the ADAS special features

The approach means that all external programs can access ADAS special features in a structured, consistent manner for each of the special features.

AFG is made more accessible via a graphical user interface (**GUI**). This code, which also fulfills a pedagogical role, is known as **ADAS605**.



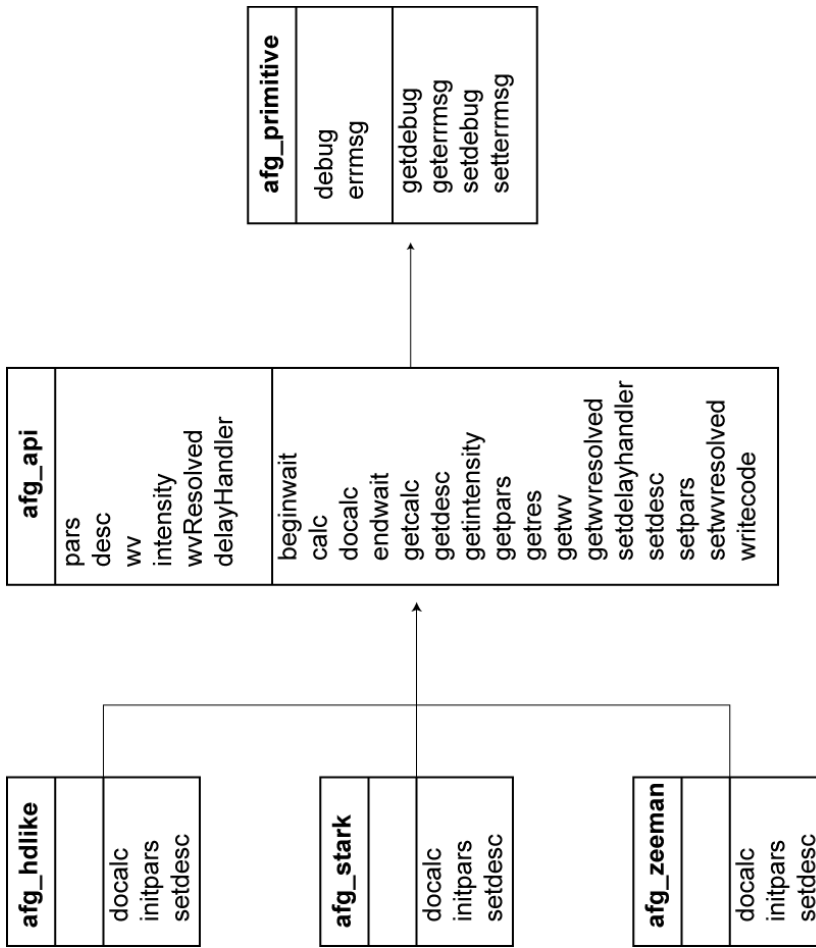
2.2 Class diagram for AFG

AFG is constructed using the **object oriented programming** capabilities of IDL.

As illustrated on the right, each **class** is represented by a rectangular box, split into three compartments.

The upper division is the **class name**, the middle section contains the **class attributes** (data members) and the lower segment holds the names of the available **class methods** (operations).

The arrows, pointing from one class to another, indicate the **inheritance hierarchy**.



2.3 AFG description structures, accessed through the ‘getdesc’ method

```
| IDL> zeeman = obj_new('afg_zeeman')
IDL> desc = zeeman->getdesc()
IDL> help , desc , /str
** Structure <95adba4>, 3 tags , length=1060, data
length=1060, refs=2:
NAME          'Zeeman Feature '
TEXT          'ADAS implementaion of Zeeman
features base ...
PARAMETERS   STRUCT -> <Anonymous> Array [1]
|  
  
| IDL> help , desc . parameters , /str
** Structure <96877a4>, 4 tags , length=1036, data
length=1036, refs=2:
POL           STRUCT -> <Anonymous> Array [1]
OBSANGLE     STRUCT -> <Anonymous> Array [1]
BVALUE        STRUCT -> <Anonymous> Array [1]
FINDEX        STRUCT -> <Anonymous> Array [1]
|  
  
| IDL> help , desc . parameters . bvalue , /str
** Structure <96989b4>, 8 tags , length=60, data
length=60, refs=2:
DESC          STRING 'Magnetic field strength (T)'
TYPE          STRING ,float ,
UNITS         STRING 'T,
MIN           FLOAT 0.00000
MAX           FLOAT 20.0000
DISPYPE       STRING ,continuous ,
LOG            INT    0
ALTERSLIMITS INT    0
|
```

Command line interaction with AFG, retrieving the description structure for the Zeeman feature.

Examination of an AFG description structure, for the Zeeman feature, at the command line.

AFG feature parameter sub-structure for the magnetic field strength, for the Zeeman feature.

3.1 ADAS605 – input and processing screens

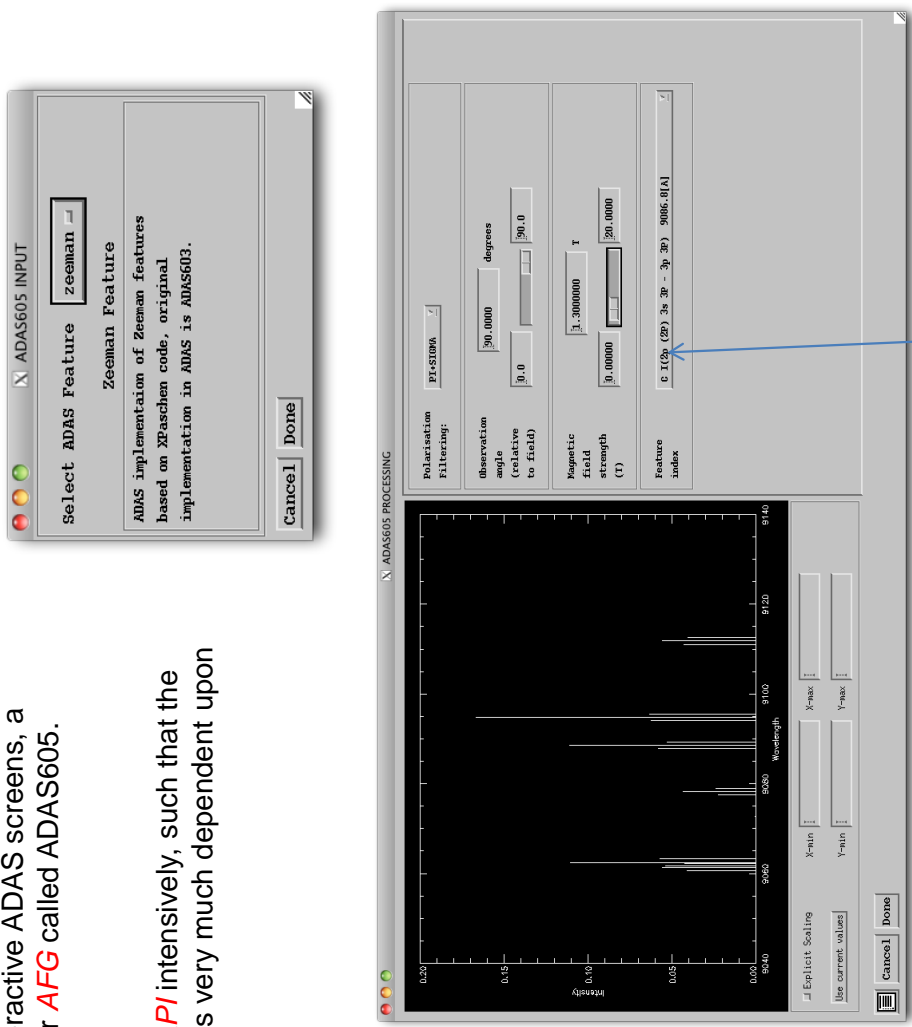
In keeping with the pedagogical role of the interactive ADAS screens, a graphical user interface has been prepared for **AFG** called ADAS605.

ADAS605 has been designed to use the **AFG API** intensively, such that the interface is highly dynamic (i.e. its appearance is very much dependent upon the feature under consideration).

The processing screen is split into two main segments; the left hand side is consistently the same regardless of the feature selected — it is a *graphical display area*.

The right hand side is comprised of a set of *control widgets* to alter the special feature parameters and will therefore adapt to the particular feature selected from the input screen.

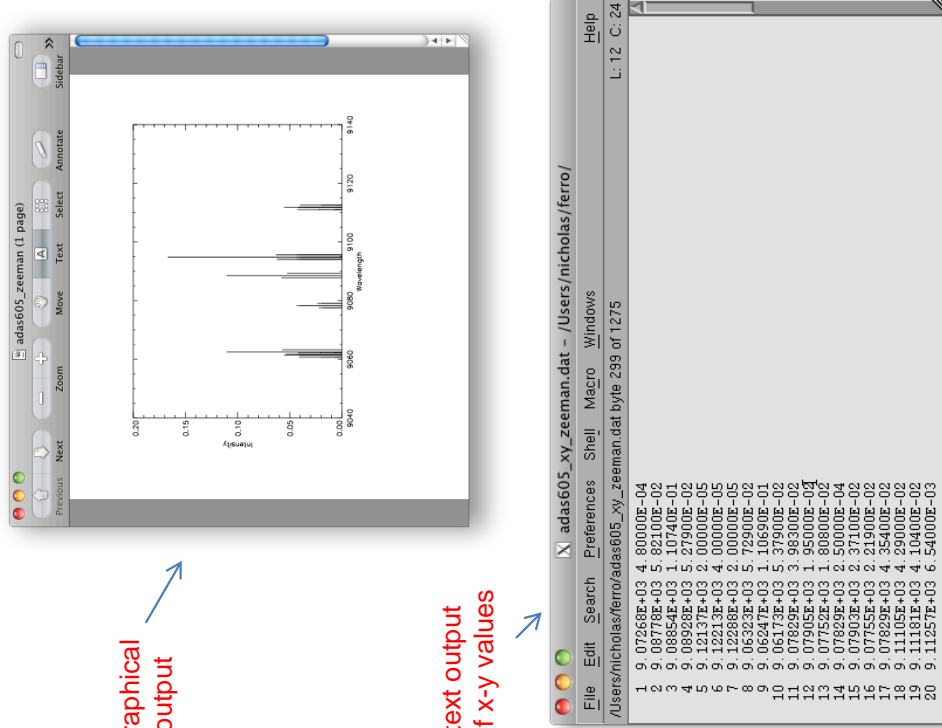
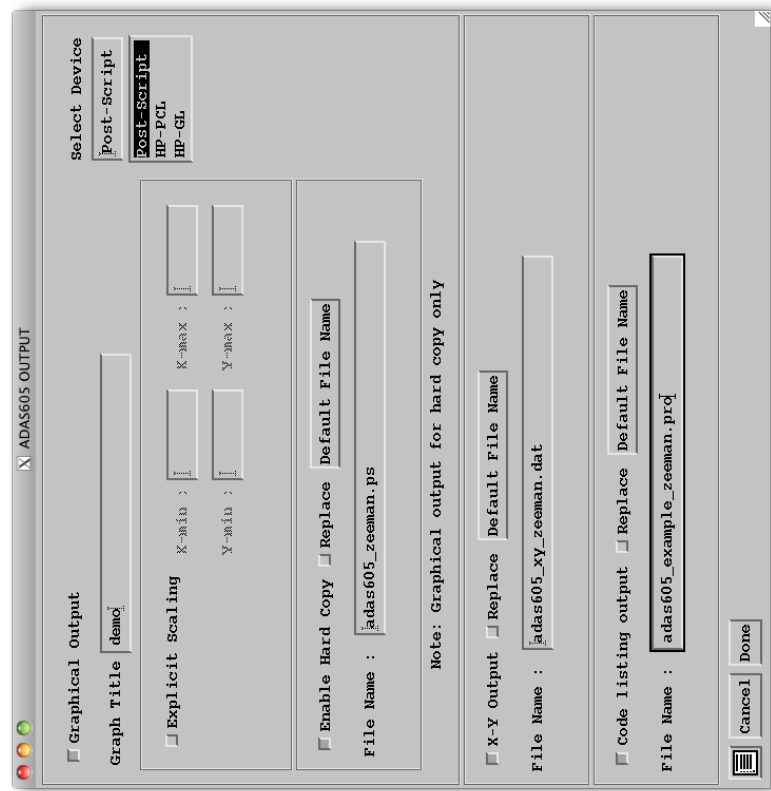
The control panel is not predefined in a static fashion. Instead, **ADAS605** is examining the parameter description structures returned from method calls to the **API**.



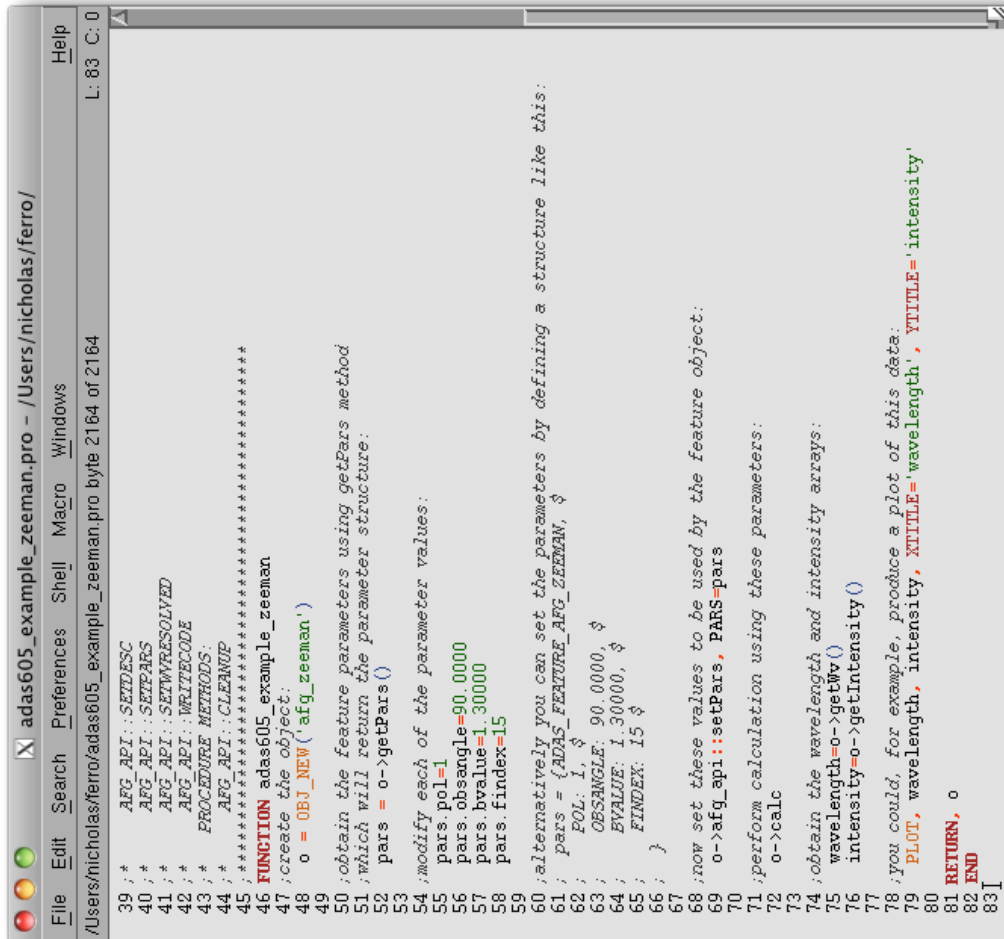
C1 (2p3s 3P – 2p3p 3P)

3.2 ADAS605 – output screen

The output screen provides the familiar ADAS graphical and text outputs, along with a further output called *Code listing output*.



3.3 ADAS605 code listing output



```
File Edit Search Preferences Shell Macro Windows Help
/Users/nicholasferro/adas605_example_zeeman.pro - /Users/nicholas/ferro/
L: 83 C: 0
39 ; * AFG API::SETDESC
40 ; * AFG API::SETPARS
41 ; * AFG API::SEMWRESOLVED
42 ; * AFG API::WRITECODE
43 ; * PROCEDURE METHODS:
44 ; * AFG API::CLEARAPI
45 ; ****
46 FUNCTION adas605_example_zeeman
47 ;create the object
48 o = OBJ_NEW('afg.zeeman')
49 ;obtain the feature parameters using getPars method
50 ;which will return the parameter structure:
51 pars = o->getPars()
52
53 ;modify each of the parameter values:
54 pars.p0l=1
55 Pars.Obangle=90.0000
56 pars.bvalue=1.30000
57 pars.findIndex=15
58
59 ;alternatively you can set the parameters by defining a structure like this:
60 pars = {ADAS_FEATURE_AFG_ZEEMAN,
61   F0L: 1, $}
62   OBSANGLE: 90.0000, $
63   EVALUE: 1.30000, $
64   FINDEX: 15 $}
65
66 ;
67
68 ;now set these values to be used by the feature object:
69 o->afg_api::setPars, PARS=pars
70
71 ;perform calculation using these parameters:
72 o->calc
73
74 ;obtain the wavelength and intensity arrays:
75 wavelength=o->getW()
76 intensity=o->getIntensity()
77
78 ;you could, for example, produce a plot of this data:
79 PLOT, wavelength, intensity, XTITLE='wavelength', YTITLE='intensity'
80
81 RETURN, o
82 END
83 I
```

AFG will auto-generate the appropriate IDL source code (including in-line comments) to generate the feature using the **API** directly, rather than via the **GUI**. It is envisaged that production of this template source code will serve as an entry point to most users looking to utilise AFG in their own codes.

4.1 Setting up spectral fitting with complex features

In order to model complex spectra, it is useful to consider a composite structure in which various model elements are assembled together to represent the various features present in the data.

In a mathematical sense, these **model elements** provide a set of **basis functions** for the model.

A useful analysis system requires a reasonable set of these elements, from basic spectral feature representations, such as a Gaussian line, to complex features coming from specialised modelling codes.

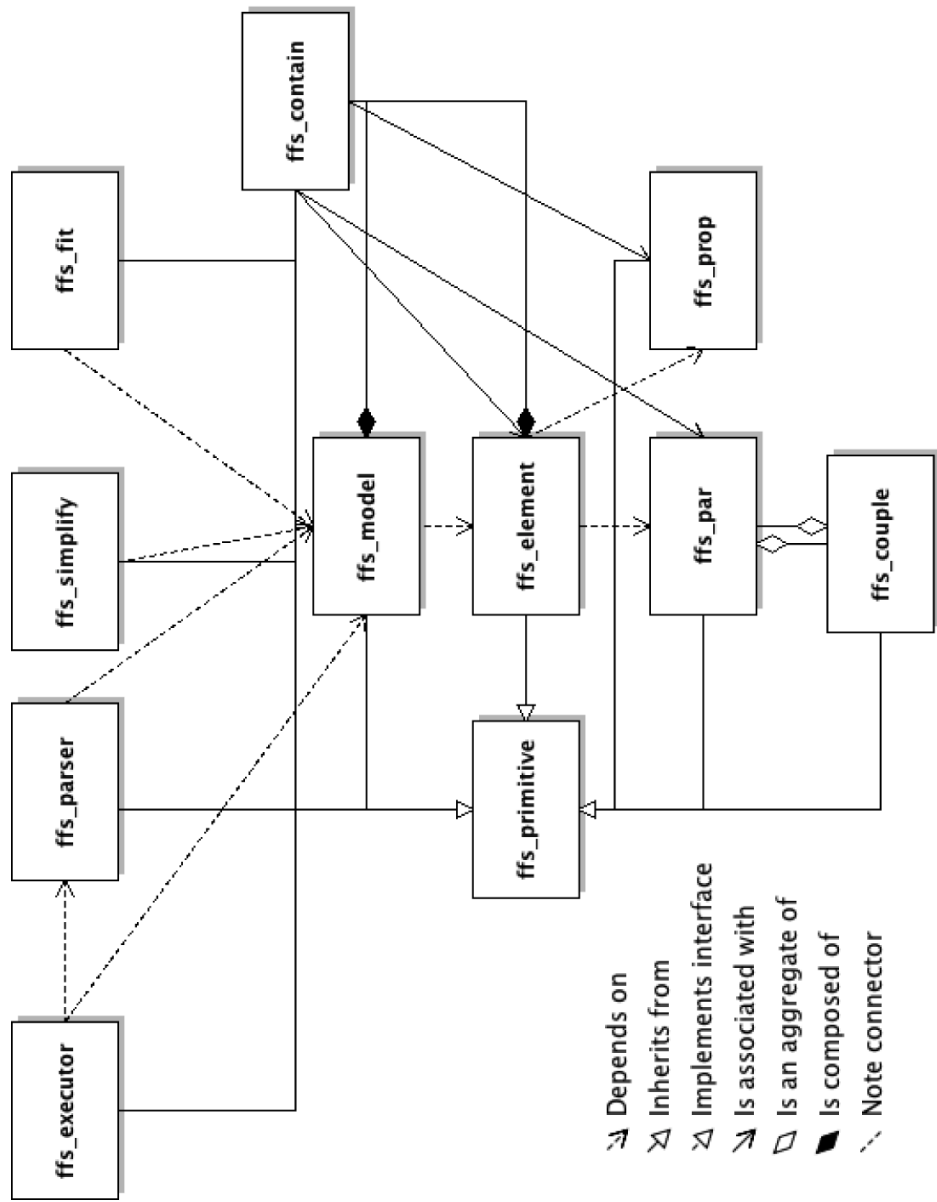
ADAS (via **AFG**) provides the complex features coming from specialised modelling codes.

Attention is given to the mathematical formulations for the calculation of the most commonly occurring features and their partial derivatives.

The analytic representations of the partial derivatives provide substantial improvements in performance for the fitting algorithm.

Each of the functions defined here (including intermediates such as the broadening functions) are implemented, programmatically in the *Framework for Feature Synthesis (FFS)* system.

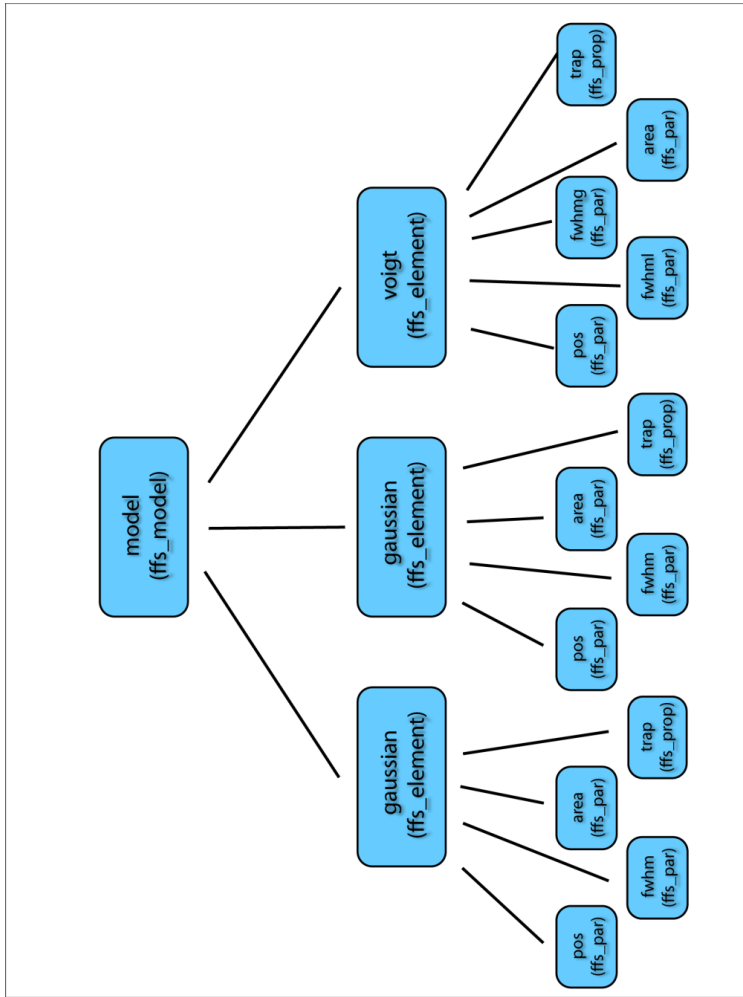
4.3 Class diagram for FFS



4.4 FFS

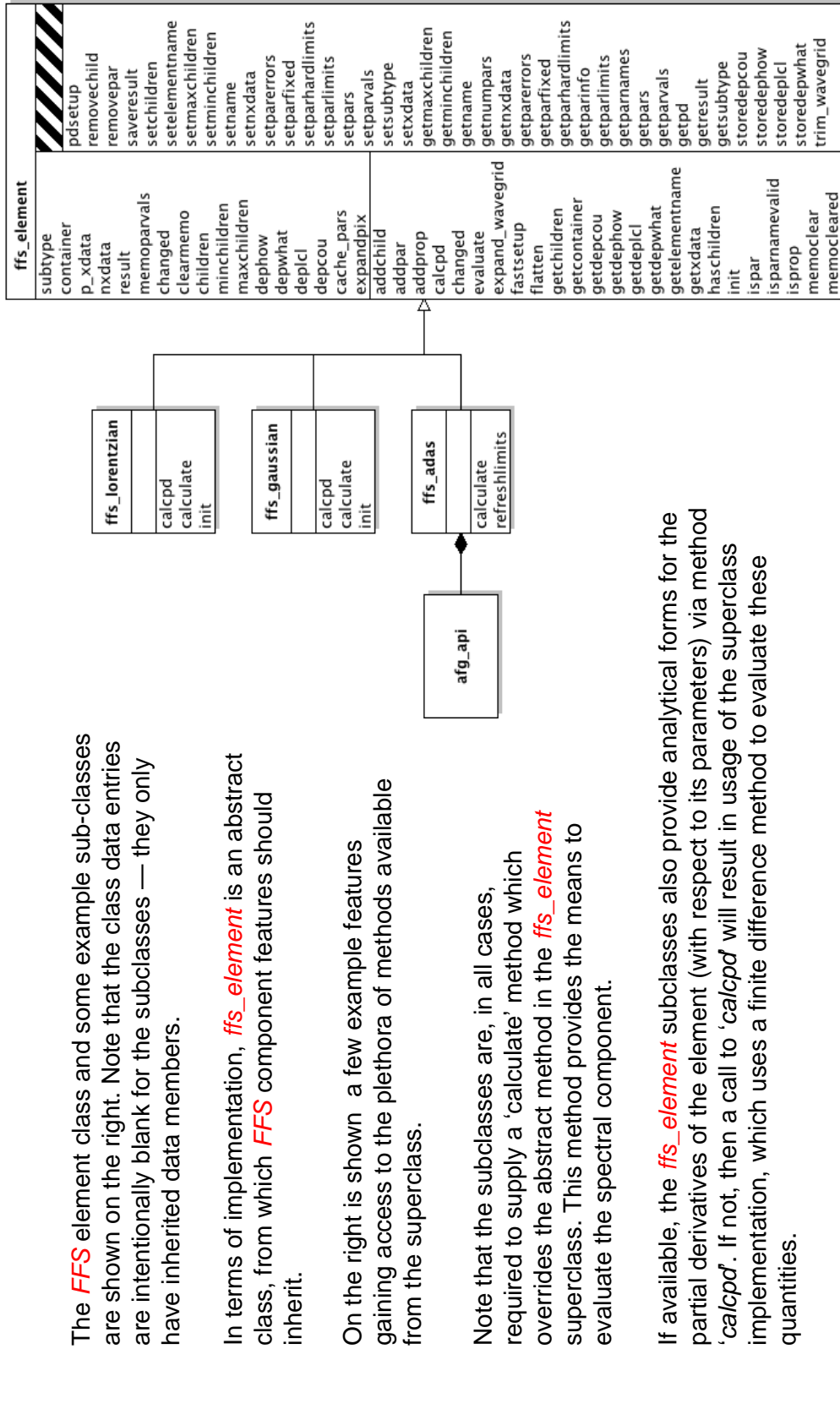
On the right, the model-element-par hierarchy for a simple model in **FFS**, consisting of two Gaussian lines and a Voigt line shape is shown. The Gaussian shapes have three parameters: position, full-width at half maximum and area. The Voigt has four: position, Lorentzian component of width, Gaussian component of width and area. The three elements, in this case also have a property ‘trap’.

The model on the right has only a single layer of elements in the tree structure—elements that are independent of each other



FFS is not limited to this case — there is support for operator elements that take the output of one or more of the other elements as input. To manage this in a generalised way, the **ffs_element** class caters for the storage of ‘child elements’ i.e. those elements on which it is dependent. By storing a reference to a ‘root’ element, the **ffs_model** element can then initiate recursive traversal of the tree to ensure that element results are calculated in the correct order.

4.5 FFS element class



4.6 MDF model definition language and syntax

To specify the construct for an arbitrarily complex model spectra, it was helpful to set out a *Model Definition Language* (*MDL*).

The expressions defining elements take the form shown on the right where ‘elementclass’ is the name of the class type of the element.

‘operands’ (as noted above) is optional and can in fact be a list of element definition expressions.

The model is defined by a set of nested element definition expressions, each enclosed in a set of brackets. The expressions themselves are of prefix notation i.e. an operator followed by a set of operands. It should be noted that one, or indeed all, of the operands can be further *MDL* expressions.

```
( model
  (+ (broaden-gauss
    (+ (gaussian g)
      (lorentzian 1)
    )
    brdg)
    (background-linear bg)
  )
  example )
```

FFS provides a system for handling complex coupling between parameters, specified by the model definition. In the coupling expression form, shown on the right, ‘parname’ is the name of the parameter being coupled and ‘elementname’ is the name of the element to which it belongs.

```
( couple elementname . parname cexpression )
```

4.7 The model optimisation

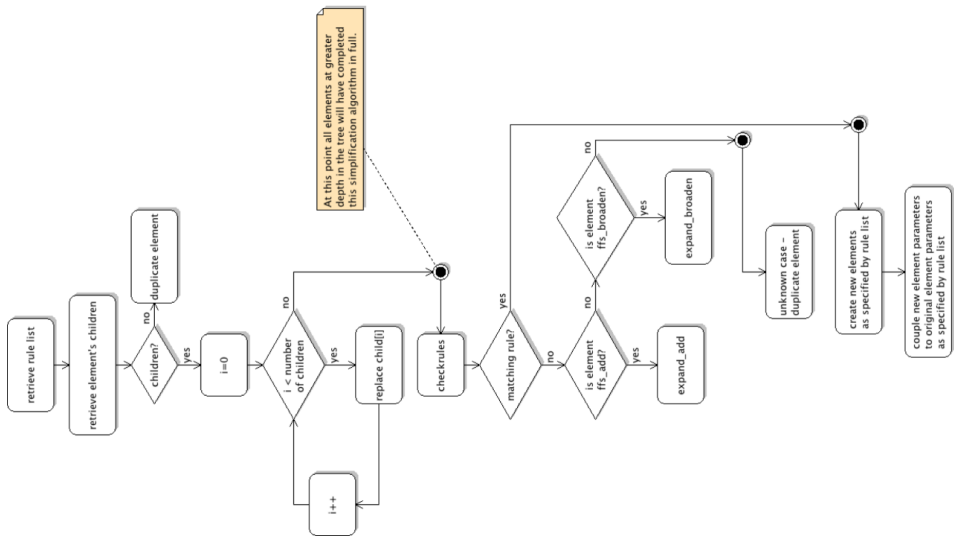
It is possible that some models will possess combinations of elements that can be readily reduced to a more optimum representation.

This is the case if, for example, there is a well known analytic solution for an operator element acting on some other element, that provides more efficient function evaluation.

The possibility of using analytic expressions for the parameter partial derivatives is an important such case.

A simple illustration is below.

```
(model
(+ (broaden-gauss
(+ (gaussian g)
(lorentzian 1)
) optimized)
brdg)
(background-linear bg)
)
example)
```



The model optimisation, by the `fs_simplify` routine, in practice, uses a reference table of rules defining more efficient representations for a set of operator element-element pairs. The whole scheme is shown on the right.

4.8 FFS_FIT

Non-linear least squares fitting:

The fitting algorithm implemented for use in this work, is a version of that developed by Marquardt. The method has become one of the most widely used in optimisation problems. The advantage of this algorithm is that it manages to smoothly vary between two methods of minimising a function mentioned above: steepest descent and the Gauss-Newton method. The two methods complement each other in that each is effective under conditions that are less favourable for the other.

A custom fitting code:

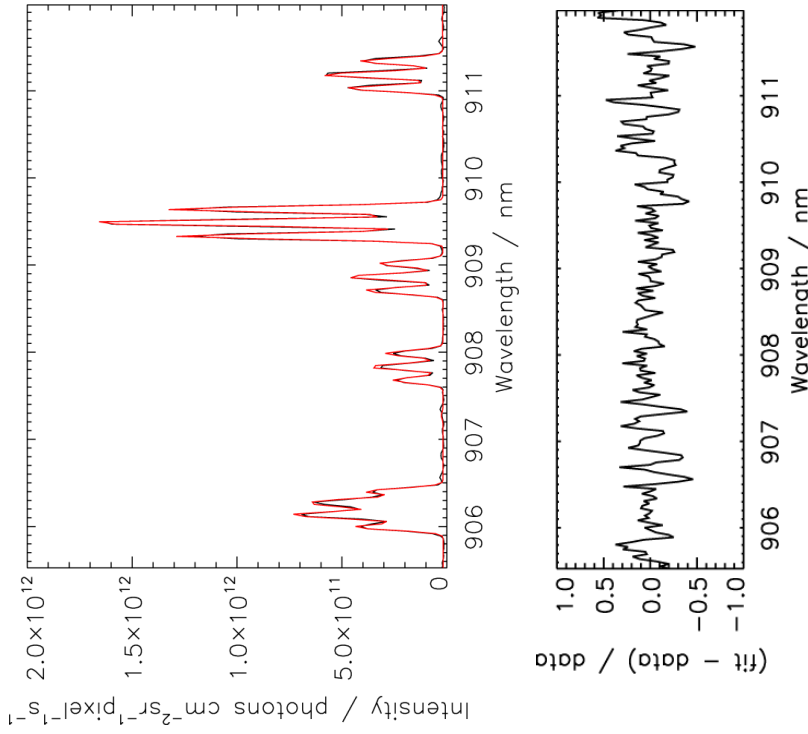
FFS is a computational framework for provision of complex spectral model specification. The spectral fitting process itself, however, is handled by a separate module to allow for flexibility for the user. Despite this design decision, it should be noted that FFS was originally intended to be used in conjunction with the readily available fitting program MPFIT. This package has, at its core, the Levenberg-Marquardt algorithm detailed above. MPFIT provides some additional machinery around the core algorithm such as setting some parameters in the model to be fixed, or imposing boundary constraints, basic parameter coupling and suggested step sizes (for numerical partial derivatives). These facilities influenced the parameter structure for FFS, thus it remains compatible with the routine, but FFS retains control of these properties as they are considered to be part of the model definition, rather than the concern of a fitting program.

Batch fitting:

It is often the case that an experiment will record multiple spectra—usually a series of spectra in time, space or both. It is desirable to fit all of the spectra in a systematic, automated scheme to identify trends in the derived parameters across the series. To this end, scripts exist as part of FFS which cycle through the frames of spectra performing fits using a single model definition.

4.7 An example

```
(model zeeman
(+ (shift -lambda
(+ (* (broaden-gauss
(adas-zeeman cizeemansi)
bgpi)
cimultipi)
(* (broaden-gauss
(adas-zeeman cizeemansi)
bgsig)
cimultisig)
)
sh)
(background-linear backg)
)
)
(seval sh_lambda 0.01)
(seval backg_m -8.0e9)
(seval backg_c 1.0e11)
(seval bgpi.fwhm 0.1)
(setlimits bgpi.fwhm 0.05 1.0)
(seval cizeemansi.findex 15)
(seval cizeemansi.obsangle 90.0)
(fixed cizeemansi.obsangle)
(seval cizeemansi.bvalue 2.0)
(setlimits cizeemansi.bvalue 1.0 4.0)
(seval cizeemansi.pol_2)
(seval cimultipi.factor 1.0e13)
(setlimits cimultipi.factor 1.0e11 1.0e15)
(seval bgsig.fwhm 0.1)
(setlimits bgsig.fwhm 0.05 1.0)
(couple bgsig.fwhm = bgpi.fwhm)
(seval cizeemansi.findex 15)
(seval cizeemansi.obsangle 90.0)
(fixed cizeemansi.obsangle)
(seval cizeemansi.bvalue 2.0)
(setlimits cizeemansi.bvalue 1.0 4.0)
(couple cizeemansi.bvalue = cizeemansi.bvalue)
(seval cizeemansi.pol_3)
(seval cimultisig.factor 1.0e13)
(setlimits cimultisig.factor 1.0e11 1.0e15)
```



C I (2s22p3s 3P - 2s22p3p 3P) emission at 909 nm as recorded by KT3C at JET, pulse #78658 ($R = 2.749$ m, $t = 61.3$ s). The fitted model is shown in red, with the fit residual shown in the lower plot

5.1 Conclusions

The outcome of this work is the provision of two useful tools for analysis of atomic and molecular spectra. Firstly, the ADAS Feature Generator (**AFG**) facilitates ease of access to a range of special feature models within ADAS.

Secondly, the Framework for Feature Synthesis (**FFS**) package accomplishes its task by providing a highly flexible, modular model representation that can draw upon ADAS provided special features (via **AFG**) in addition to a basis set of familiar mathematical functions.

The FFS implementation goes beyond that offered by existing packages by allowing for specification of arbitrarily complex functional dependence between parameters via the model definition language.

A model ‘simplification’ module optimises any inefficient representations using the derived analytic solutions to form a new model, yet connects the new parameter set, via the coupling system, to the originally specified set.

The system has proved effective across the range of studies considered and the design of the framework remains flexible enough such that it can be used in support of analysis of any fusion or astrophysical spectra — a new special feature model is easily integrated by means of a lightweight AFG wrapper to an external modelling code.

The system is not yet complete. A number of areas are receiving further attention and the scope of models is being increased.

B.5 module_5



Module 5

Charge exchange and beam emission spectroscopy. Modelling emitter populations, beam stopping and analysing spectra.

Lecture viewgraphs

Hugh Summers, Martin O'Mullane and Alessandra Giunta

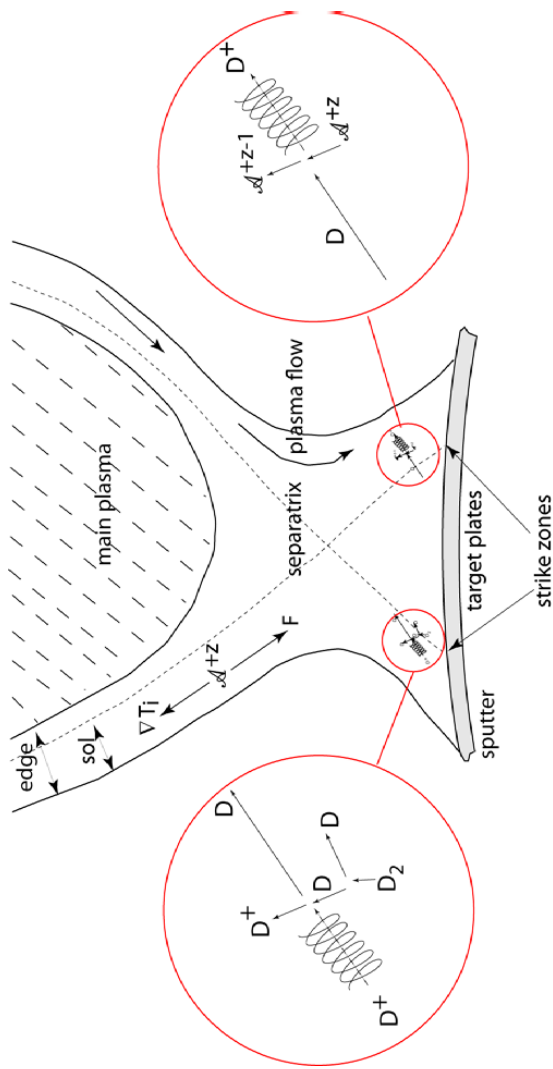
University of Strathclyde

Contents

1. Preliminaries.
2. Modelling populations and emission following charge transfer
3. Charge exchange spectroscopy
4. Modelling beam stopping and beam emission
5. Integrated analysis
6. Conclusions

1.1 The edge-divertor plasma environment

The expanded schematic on the left shows the migration of deuterium into the plasma, starting from the release of molecular deuterium from the target zone.

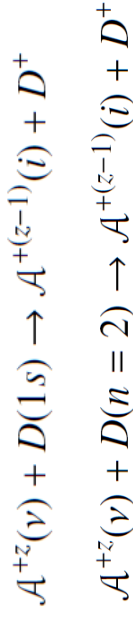


The migration of D^0 into the plasma is more efficient than expected since the CX reaction rate is larger than the electron impact ionisation rate for D^0 .

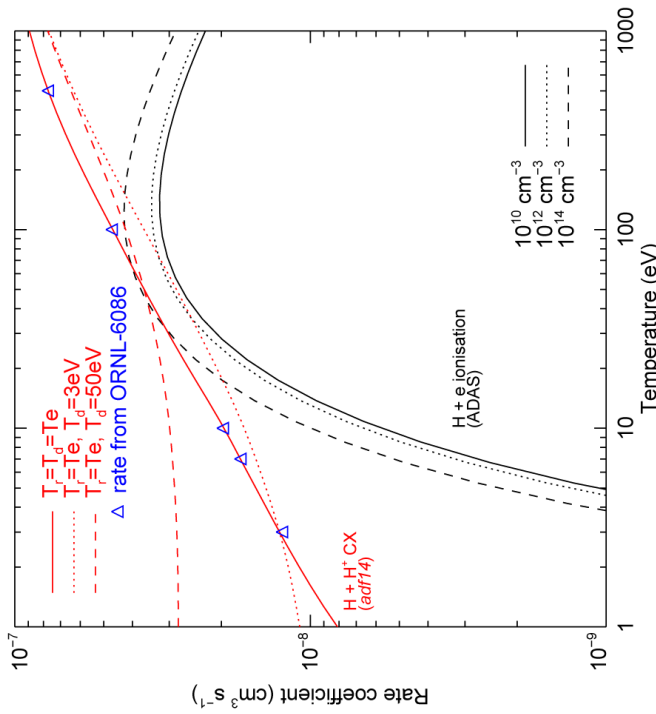


The partially ionised impurities near the wall have shells of existence which can overlap that of D^0 . The charge transfer at thermal speeds is very strongly state-selective with only one or two states significantly populated. The reaction is in competition with electron impact excitation from the ground or metastable levels.

Ratios of spectrum lines emitted by \mathcal{A}^{+z-1} can be altered modestly. The bigger effect is the change of ionisation state. The ADAS codes [ADAS208](#) and [ADAS405](#), including H-lines in the [adf04](#) dataset model this emission.

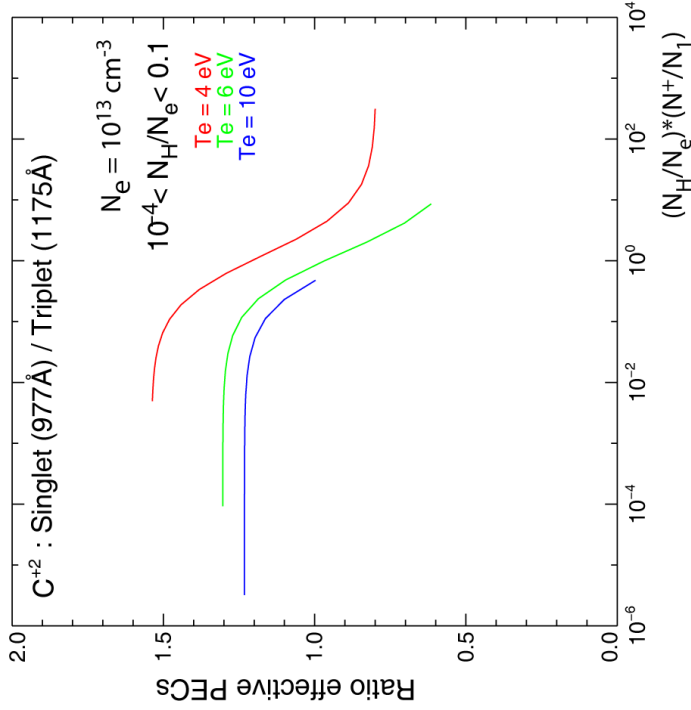


1.2 CX reaction rates and impurity spectral emission in divertors



Comparative reaction data electron impact and ion impact are available in ADAS. With ion/atom rates, the distribution functions of both reactants matter.

ADAS data formats [adf14](#) and [adf24](#) are relevant to charge exchange in thermal conditions. [ADAS509](#) and the procedure [ceevth.pro](#) are helpful.



Thermal charge transfer from hydrogen to impurity ions is a very state-selective process. It competes with the generally stronger electron impact excitation. Depending on divertor conditions, emission measures may be favourable for diagnostic line ratios. [adf15](#) includes CX contributions.

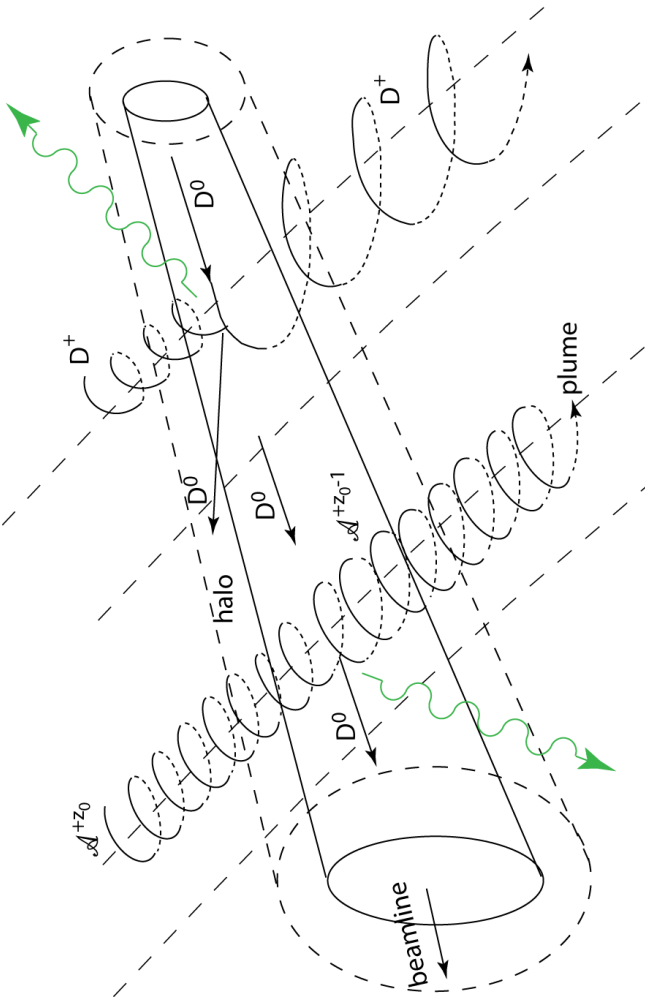
1.3 The beam plasma environment

The injected neutral atoms, usually isotopes of hydrogen, have speeds comparable to the Bohr orbital speed ($\approx 25\text{keV/amu}$).

Positive ion sources have acceleration voltages $\sim 40\text{-}160\text{keV}$. For hydrogen isotopes, the neutral beam contains three energy fractions, E_b , $E_b/2$ and $E_b/3$ of varying proportions. These energies are well suited to CXRS.

^2D is the most commonly injected hydrogen isotope. Also ^3He and ^4He have been used, usually as minority admixtures to hydrogen. All can be handled with ADAS.

Negative ion sources (hydrogen isotopes) usually operate at acceleration voltages $>200\text{keV}$ and give mono-energetic neutral beams. These energies are less suited to CXRS.



$\lambda^{+z_0 - 1}$ is the CX emitter. The halo radius is an ionisation length. The key plume length is a radiative decay length.

In the core plasma, with $T_i \sim 6\text{keV}$, a carbon nucleus has average energy $0.5\text{keV/amu} < E_b$ so the beam speed usually determines the collision speed of projectile (D^0 **donor**) and target (λ^{+z_0} **receiver**). This situation is reversed for electron collisions with both donors and receivers.

1.4 Reactions in the beam plasma region

- Charge exchange spectroscopy is driven by reactions of the form.



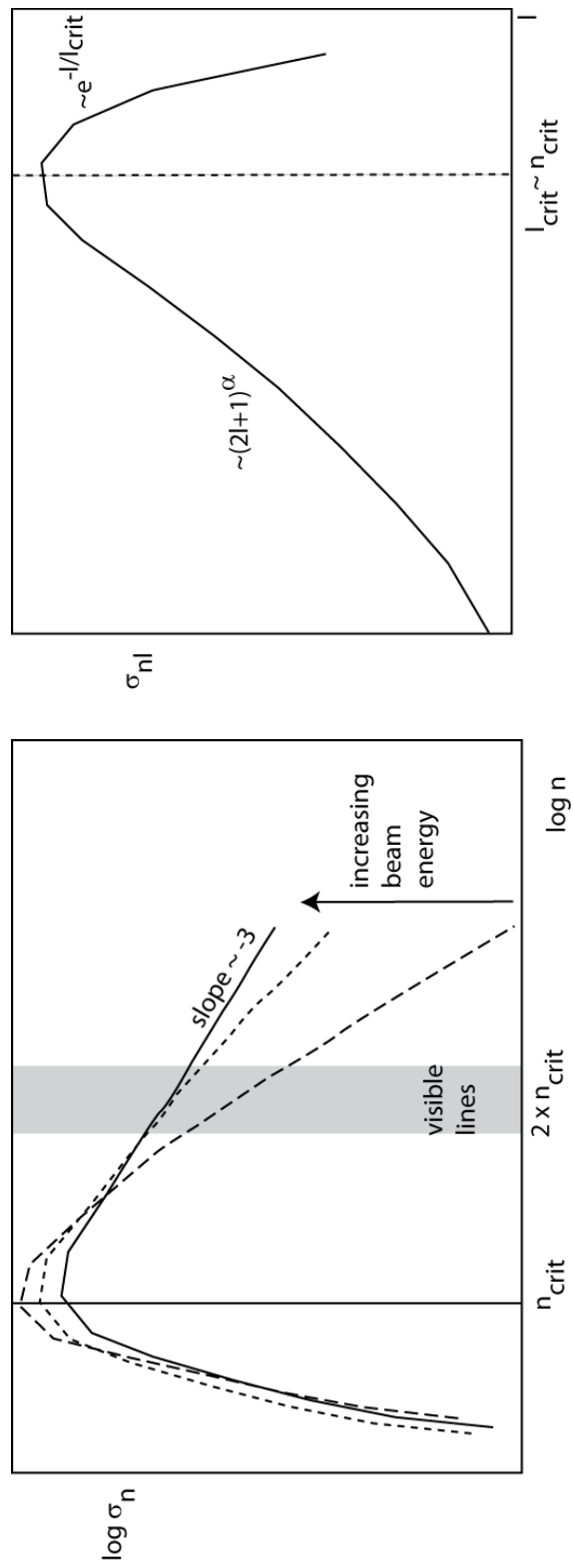
- The principal application is to capture by the bare nuclei of impurity atoms in the plasma from the ground state of deuterium in fast neutral beams. The hydrogen-like impurity ion radiates as



- Composite spectral line features of the form $n' \rightarrow n''$ are observed made up of unresolved multiplet components. Charge exchange line features often involve high principal quantum shells and occur over wide spectral ranges including the visible.
- In general the populations of receiver levels are modified by redistributive collisions with plasma ions, electrons and fields before radiation emission occurs.

1.5 Partial capture cross-section behaviours.

Partial n and partial nl CX cross-sections



- Asymptotic slope in n at higher beam energies means that cascading contributions to populating of emitting levels are significant.

1.6 adf01 format and extrapolation parameters

n-shells above the numerical tabulation contribute substantially to effective emission in visible CX lines.

Asymptotically

$$\sigma_{nl}(E_u) = \left(\frac{n_t}{n} \right)^{\alpha(E_u)} \sigma_{nl}(E_u)$$

for $n > n_t$

| Receiver | | Donor | | | |
|----------|-----------|---------------------------------------|----------|------------|----------|
| c + 6 | H + 0 (1) | / receiver, donor (donor state index) | | / LPARMs / | |
| 9 | | / number of energies | | | |
| 2 | | / min | | | |
| 6 | 1.00 | 1.50 | 2.00 | 3.00 | 5.00 |
| | 10.00 | 10.00 | 10.00 | 10.00 | 9.30 |
| | 8 | 8 | 8 | 8 | 8 |
| | 6.29D+00 | 6.27D+00 | 6.26D+00 | 6.25D+00 | 6.25D+00 |
| | 3.00D+01 | 4.30D+01 | 5.20D+01 | 6.40D+01 | 8.00D+01 |
| | 0.00D+00 | 8.80D-01 | 1.15D+00 | 2.60D+00 | 4.00D+00 |
| | 4.20D+15 | 4.30D+15 | 4.80D+15 | 5.00D+15 | 5.00D+15 |
| 1 | m | | | | |
| 2 | 4.71D-18 | 6.03D-18 | 7.50D-18 | 9.65D-18 | 1.29D-17 |
| 2 | 1.97D-18 | 2.32D-18 | 2.71D-18 | 3.20D-18 | 3.78D-18 |
| 2 | 2.74D-18 | 3.71D-18 | 4.79D-18 | 6.45D-18 | 9.12D-18 |
| 3 | 2.94D-16 | 3.72D-16 | 4.54D-16 | 5.48D-16 | 6.47D-16 |
| | . | . | . | . | . |
| 8 | 1.02D-18 | 1.28D-18 | 1.46D-18 | 2.41D-18 | 3.96D-18 |
| 8 | 7.20D-20 | 7.02D-20 | 6.63D-20 | 5.82D-20 | 6.19D-20 |
| 8 | 1.00D-19 | 1.13D-19 | 1.14D-19 | 1.18D-19 | 1.24D-19 |
| 8 | 1.17D-19 | 1.40D-19 | 1.54D-19 | 1.63D-19 | 2.25D-19 |
| 8 | 1.29D-19 | 1.62D-19 | 1.84D-19 | 2.03D-19 | 2.35D-19 |
| 8 | 1.39D-19 | 1.81D-19 | 2.11D-19 | 2.40D-19 | 3.67D-19 |
| 8 | 1.48D-19 | 2.00D-19 | 2.38D-19 | 2.82D-19 | 4.54D-19 |
| 8 | 1.56D-19 | 2.16D-19 | 2.65D-19 | 3.15D-19 | 5.18D-19 |
| 8 | 1.58D-19 | 1.99D-19 | 2.26D-19 | 2.41D-19 | 5.27D-19 |
| 7 | | | | | |

| parms | | | | | |
|-------|---|--|--|--|--|
| 1 | m | | | | |
| 2 | 0 | | | | |
| 2 | 1 | | | | |
| 3 | | | | | |

| Shells n & nl | | | | | |
|---------------|---|--|--|--|--|
| 8 | 0 | | | | |
| 8 | 1 | | | | |
| 8 | 2 | | | | |
| 8 | 3 | | | | |
| 8 | 4 | | | | |
| 8 | 5 | | | | |
| 8 | 6 | | | | |
| 8 | 7 | | | | |

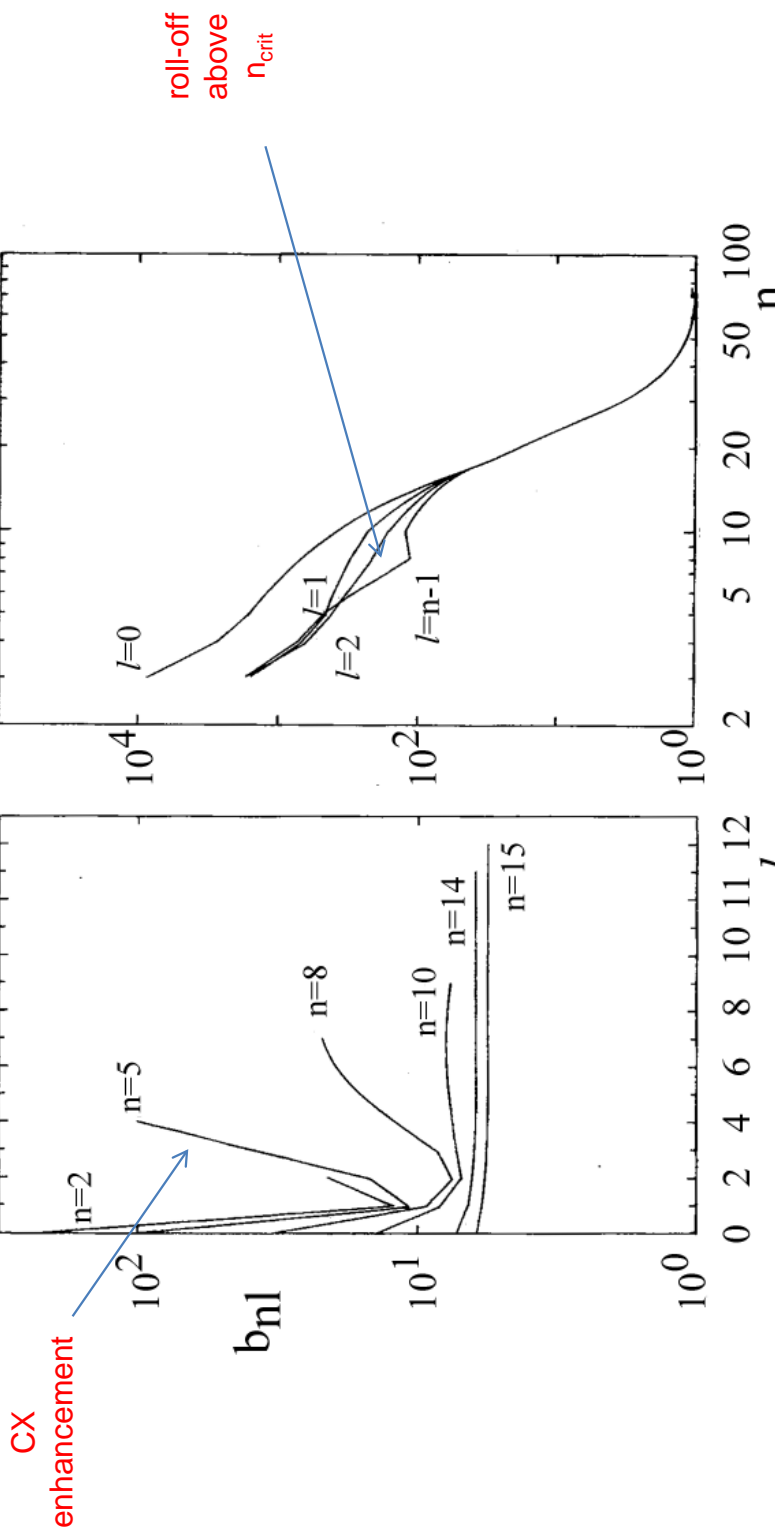
To a reasonable approximation, there is universal scalable behaviour in l so that for the capture cross-sections.

$$\sigma_{nl}(E_u) = f_{(n)l}^{(theor)} \sigma_n(E_u)$$

$$f_{(n)l}^{(theor)} = \left(\frac{1}{2} [1 - \tanh(w(l - l_{cut}))] \left(\frac{2l + 1}{2l_{cut} + 1} \right)^{p_2} + \left(\frac{1}{2} [1 + \tanh(w(l - l_{cut}))] \exp(p_3(1 - l/l_{cut})) \right) \right)$$

with $w = 1.2$, $p_2 \equiv p12a$, $p_3 \equiv p13a$, $l_{cut} \equiv xlcuta$
Of various forms investigated the preferred one for ADAS is shown on the right (lforma = 8).

2.1 Population structure: bundle-nl with CX



O^{+7} : $T_e = T_p = 6.4 \times 10^6$, $N_e = N_p = 5 \times 10^{13} \text{ cm}^{-3}$,
 $E_H = 25 \text{ keV/amu}$, $N_H = 5 \times 10^8 \text{ cm}^{-3}$

O^{+5} : $T_e = T_p = 3.6 \times 10^6$, $N_e = N_p = 5 \times 10^{13} \text{ cm}^{-3}$,
 $E_H = 25 \text{ keV/amu}$, $N_H = 5 \times 10^8 \text{ cm}^{-3}$

2.2 The redistribution-cascade population model

- With the dominant collisional-radiative processes state selective capture, collisional redistribution by ions within each n-shell and cascade, the effective emission coefficient determination simplifies. It can be implemented recursively downwards. Relevant matrices may be stored to enable a multi-line experimental confrontation.

Since no collisional excitation from lower to higher n-shells is allowed, the populations of the l_j sub-levels of the principal quantum shell $n' \geq n + 1$ may be written as

$$N_{n'l_j} = N_H N^+ \sum_{n'' \geq n+1} W_{n'l_j'n''} q_{n''}^{(CX)}$$

Then the equations determining the populations of the sub-shells of the principal quantum shell n are

$$\sum_{l''j''} M_{(n)l_jl''j''} N_{nl''j''} = N_H N^+ f_{(n)lj}^{(theor)} q_n^{(CX)} + \sum_{n' \geq n+1} A_{nl_jn'l_j} N_{n'l_j}$$

so that

$$N_{nl_j} = N_H N^+ W_{nl_jn} q_n^{(CX)} + N_H N^+ \sum_{n'' \geq n+1} W_{nl_jn''} q_{n''}^{(CX)}$$

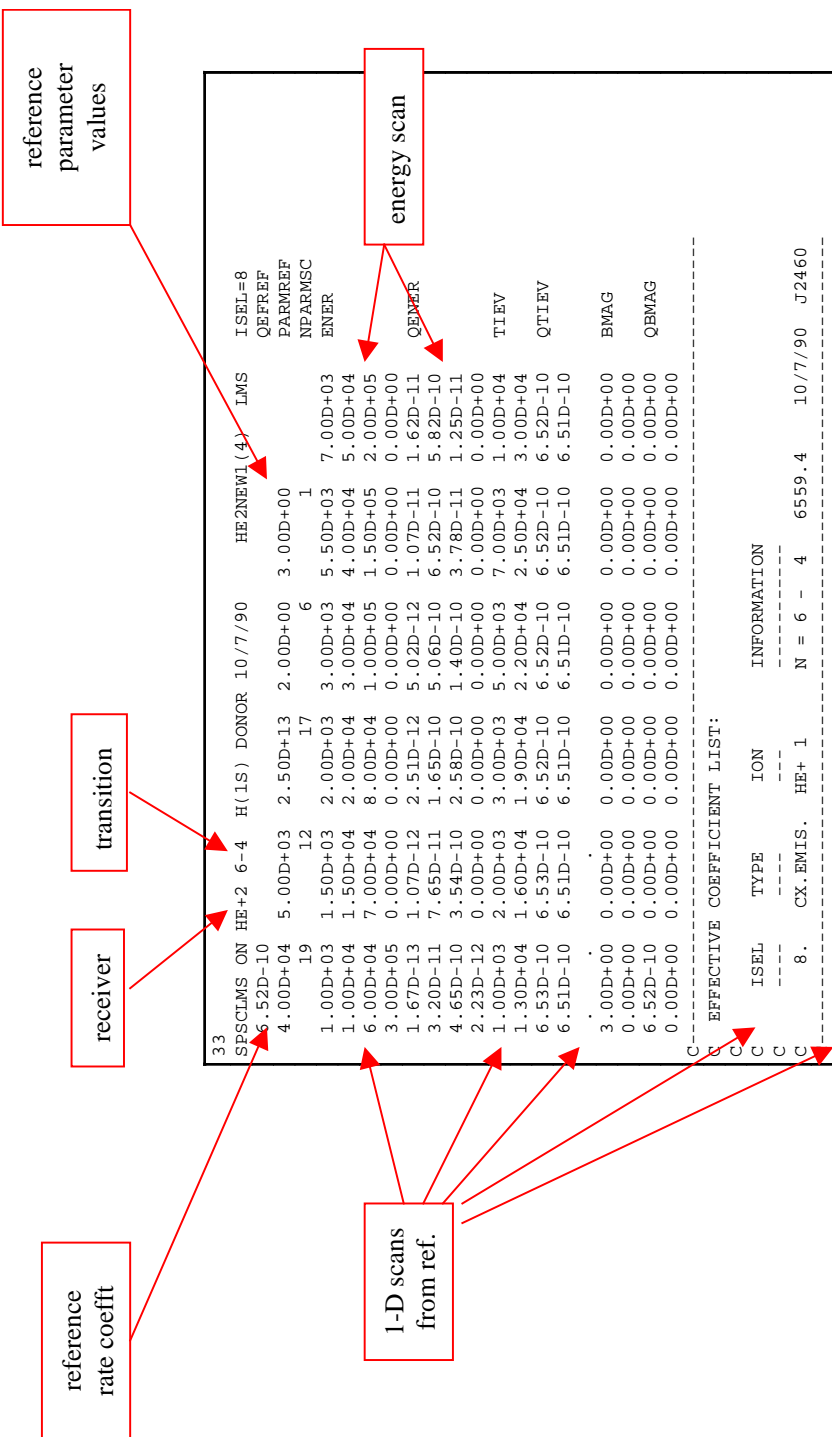
with

$$W_{nl_jn} = [\sum_{l'',j''} M_{(n)l_jl''j''}^{-1} f_{(n)lj}^{(theor)}] q_n^{(CX)}$$

and

$$W_{nl_jn''} = \sum_{l'',j'',l',j'} M_{(n)l_jl''j''}^{-1} A_{nl''j''n'l_j} W_{nl'l_jn''}$$

2.3 *adf12* charge exchange effective emission coefficients



3.1 Line-of-sight emission

- The line-of-sight integrated photon emissivity of a charge exchange driven line may be written as

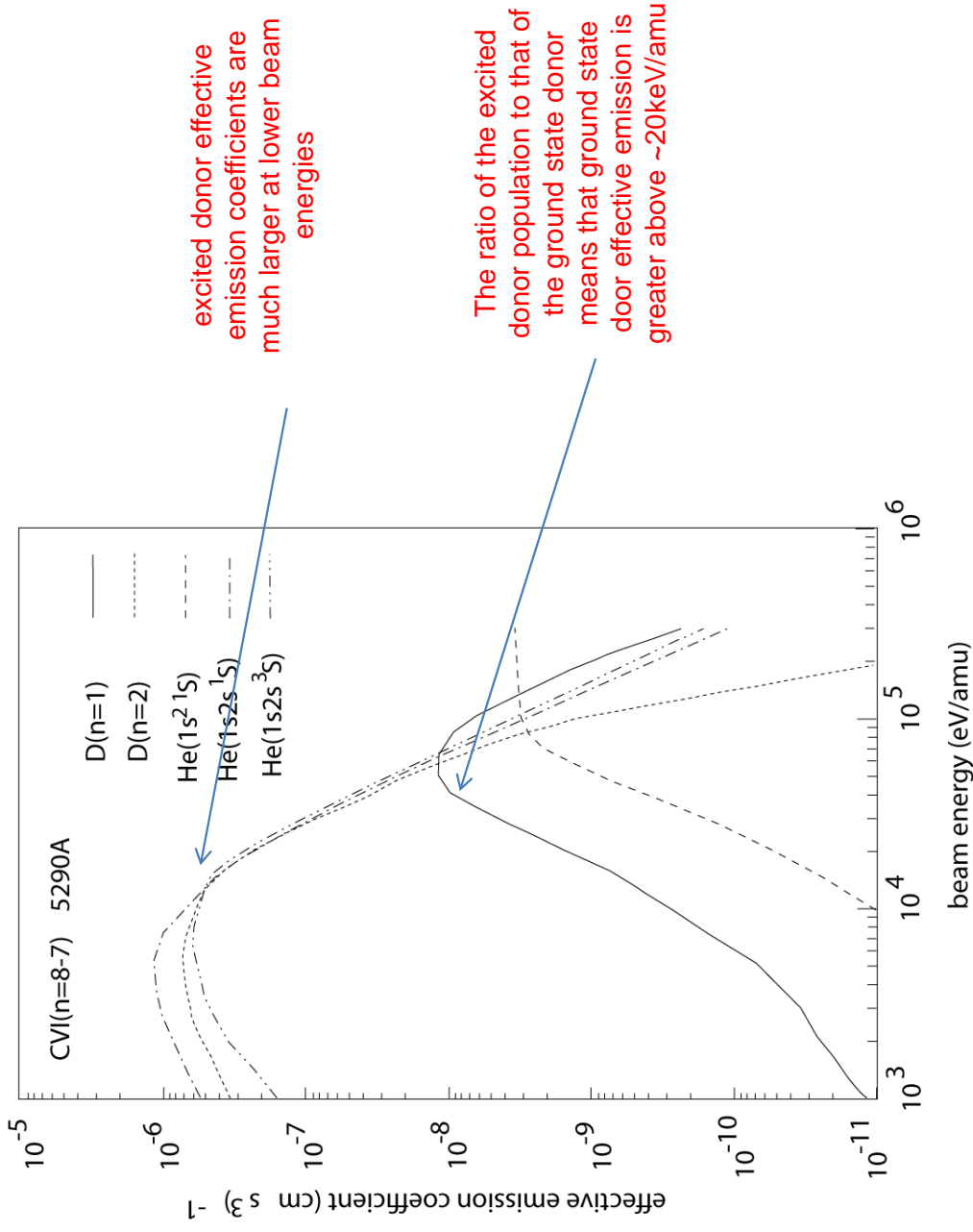
$$\begin{aligned}
 I_{n \rightarrow n'}^{(z_0-1)} &= \sum_{l,l'} I_{nl \rightarrow n'l'}^{(z_0-1)} \\
 &= \int \sum_S A_{nl \rightarrow n'l'} N_{nl}^{(z_0-1)} ds \\
 &= \int [\sum_S A_{nl \rightarrow n'l'} (N_{nl}^{(z_0-1)} / N_D N^{(z_0)})] N_D N^{(z_0)} ds \\
 &= \int [\sum_S q_{nl \rightarrow n'l'}^{(eff)}] N_D N^{(z_0)} ds \\
 &= \int q_{n \rightarrow n'}^{(eff)} N_D N^{(z_0)} ds \\
 &\approx q_{n \rightarrow n'}^{(eff)} \int_S N_D N^{(z_0)} ds
 \end{aligned}$$

- $\int_S N_D N^{(z_0)} ds$ is the emission measure
- $q_{n \rightarrow n'}^{(eff)}$ is the effective emission coefficient

3.2 Charge exchange emission measure

- The effective emission coefficient may be obtained theoretically from a collisional-radiative population calculation.
- If it is approximately constant over the emitting volume, then measurement of a charge exchange line intensity $I_{n \rightarrow n'}^{(z_0-1)}$ allows deduction of the emission measure
 - .
- $\int_S N_D N^{(z_0)} ds$
- If neutral beam attenuation to the observed volume is known or calculable then the local impurity number density may be inferred.
- With the effective emission coefficients calculated theoretically, comparison with one charge exchange line intensity allows deduction of the emission measure. Then all other lines are predictable.
- If more than one line intensity is observed then a mean emission measure may be deduced and some comment made on the ratios of experimental to theoretical effective emission coefficients.

3.3 Effective emission coefficients for various beam donors



3.4 Consistency of observed spectral intensities

In general observable spectrum lines are associated with upper principal quantum shells $n \leq n_1$. If M_{rep} , lines are identified each with a distinct upper n -shells $\bar{n}_{irep} : irep = 1, \dots, M_{rep}$, then a 'condensation' may be imposed such that

$$q_n^{(CX)} = \sum_{irep=1}^{M_{rep}} L_{n,irep} q_{\bar{n}_{irep}}^{(CX)}$$

and

$$q_n^{(CX)} = (n / n_1)^\alpha q_{n_1}^{(CX)}$$

giving, after integration along the line-of-sight, a matrix relation

$$\begin{bmatrix} I_{\bar{n}_1 \rightarrow \bar{n}_1'} \\ \vdots \\ I_{\bar{n}_{M_{rep}} \rightarrow \bar{n}'_{M_{rep}}} \end{bmatrix} = \left(\int_S N_D N^+ ds \right) \begin{bmatrix} a_{11} & \cdots & a_{1M_{rep}} \\ \vdots & \ddots & \vdots \\ a_{M_{rep}1} & \cdots & a_{M_{rep}M_{rep}} \end{bmatrix} \begin{bmatrix} q_{\bar{n}_1}^{(CX)} \\ \vdots \\ q_{\bar{n}_{M_{rep}}}^{(CX)} \end{bmatrix}$$

The coefficients of the matrix are theoretically calculated quantities. The equations may be solved for the the $q_{\bar{n}_i}^{(CX)}$ and the emission measure $\int_S N_D N^+ ds$ subject to the constraint

$$\sum_{irep=1}^{M_{rep}} q_{\bar{n}_{irep}}^{(CX)} = \sum_{irep=1}^{M_{rep}} q_{\bar{n}_{irep}}^{(CX)(theor)}$$

- This casts the theory/experiment challenge in terms of the partial n-shell charge exchange cross-sections – an important issue as CXS with heavier species is contemplated.

4.1 Beam stopping and emission

To progress further with charge exchange spectral analysis, that is to unfold the emission measure, it is necessary to know the local number density of beam atoms in the plasma at each point along the beam. The hydrogen isotopes species H, D and T and the helium isotopes ^3He and ^4He must be addressed for comprehensive coverage of fusion needs.

The isotope mass influences the beam speed. The **fundamental collision cross-sections, as a function of relative collision speed are the same**. So rate coefficients, for atom-ion collisions must use the correct speeds. Otherwise beam population and collisional-radiative modelling **are the same**.

Hydrogen isotope beams: collisionality is strong, the collision limit is typically $\sim n=4$, I-sub-shells are strongly mixed.

Bundle-n modelling is appropriate for the beam populations. The stopping coefficient is the $S_{\text{CR}, 1s^2 2S}$ coefficient (including charge exchange losses) of the ground level. Excited beam populations are solved as

$$b_n = F_n^{(1)} \frac{N_1}{N_+} + F_n^{(2)} + F_n^{(3)} \frac{\cancel{N_H}}{\cancel{N_e}}$$

Helium isotope beams: collisionality is strong, the collision limit is typically $n \sim 4$, I-sub-shells are less strongly mixed. There are two effective metastables, the ground $1s^2 1S$ and the triplet $1s2s 3S$ (often $1s2s 1S$ is also treated as metastable for consistency with other applications). The singlet and triplet sides behave like two almost independent beams with stopping coefficients $S_{\text{CR}, 1s^2 1S}$ and $S_{\text{CR}, 1s2s 3S}$. **Bundle-nl** modelling is appropriate. Excited populations are solved as

$$b_{n^2 S+1L} = FI_{(nlS)}^{(1)} \left(\frac{N_{1^1 S}}{N_+} \right) + FI_{(nlS)}^{(1)} \left(\frac{N_{2^1 S}}{N_+} \right) + FIII_{(nlS)}^{(1)} \left(\frac{N_{2^3 S}}{N_+} \right) + FIII_{(nlS)}^{(1)} \left(\frac{N_{3^3 S}}{N_+} \right) + F^{(2)} \cancel{\left(\frac{N_H}{N_e} \right)} + F^{(3)} \cancel{\left(\frac{N_H}{N_e} \right)}$$

4.2 Beam atom population modelling and stopping

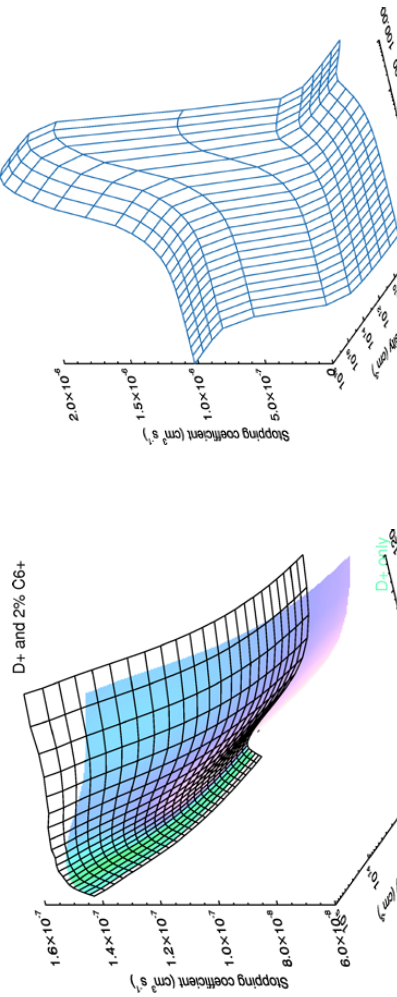
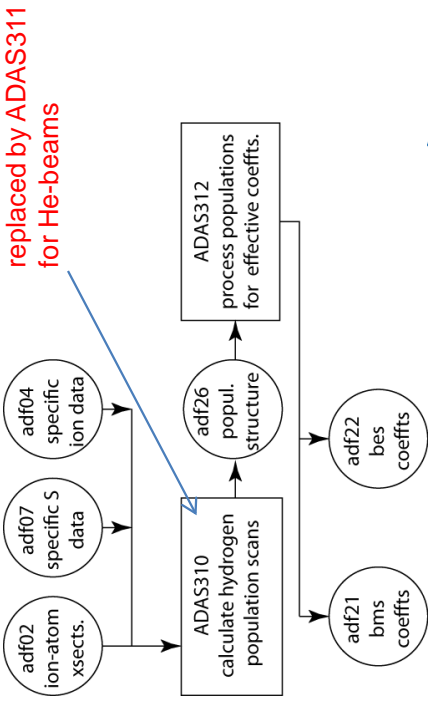
For beam atom populations, collisions with impurity ions must be added to the rate equations and the beam translational speed added to collision dynamics to form the rate coefficients. In ADAS, [adf02](#) provides the ion impact cross-section data. [adf07](#) provides the most accurate electron impact direct ionisation coefficients.

The ADAS data format [adf21](#) and [adf22](#) archive the beam stopping and beam emission coefficients. They are held in libraries for the different beam species in datasets for each individual impurity species which contributes to the stopping (see next viewgraph).

The beam energy and impurity number density are the primary parameters, with other secondary. This determines the organisation of the [adf21](#) and [adf22](#) archives.

Beam stopping by a composite of impurities and electrons is usually assembled as a linear superposition of pure stopping species.

The beam stopping coefficient is defined in terms of the electron density.



Stopping coefficient for D-beam in 2×10^3 eV D^+ + 2% C^{+6} plasma.

Stopping coefficient for the He-beam triplet metastable by a pure D^+ plasma at 2×10^3 eV.

Stopping coefficient for the He-beam triplet metastable by a pure D^+ plasma at 2×10^3 eV.

4.3 Assembling beam stopping coefficients

Let the stopping coefficient for the impurity species X^{+z_0} be $S_{CR}^{(\alpha, X)}$ then the loss rate is

$$\begin{aligned} N_e S_{CR}^{(\alpha, X)}(E_B, N^{(z_0)}, T^{(z_0)}) &= N_e S_{CR}^{(\alpha, e)}(E_B, N^{(z_0)}, T^{(z_0)}) \\ &\quad + N^{(z_0)} S_{CR}^{(\alpha, \bar{z}_0)}(E_B, N^{(z_0)}, T^{(z_0)}) \end{aligned}$$

distinguishing parts driven by excitation from the ground state of A by electron collisions and by X^{+z_0} ions respectively. The coefficient is

$$\begin{aligned} S_{CR}^{(\alpha, X)}(E_B, N^{(z_0)}, T^{(z_0)}) &= S_{CR}^{(\alpha, e)}(E_B, N^{(z_0)}, T^{(z_0)}) \\ &\quad + (1/z_0) S_{CR}^{(\alpha, \bar{z}_0)}(E_B, N^{(z_0)}, T^{(z_0)}) \end{aligned}$$

The density dependence of the collisional-radiative coefficient is written in terms of the impurity ion density $N^{(z_0)}$ since ion collisions primarily determine the collisional redistribution..

Consider a set of species $\{X_i^{+z_{0i}} : i = 1, \dots, I\}$ with fractions $\{f_i : i = 1, \dots, I\}$, in the plasma causing a composite stopping. The loss rate may be written approximately as

$$\begin{aligned} N_e S_{CR}^{(\alpha)}(E_B, N_I, T_I) &\approx N_e S_{CR}^{(\alpha, e)}(E_B, N_I, T_I) + \\ &\quad \sum_{i=1}^I N_i^{(z_{0i})} S_{CR}^{(\alpha, z_{0i})}(E_B, N_I, T_I) \\ &= \sum_{i=1}^I N_{e,i} [S_{CR}^{(\alpha, e)}(E_B, N_I, T_I) + \\ &\quad (1/z_{0i}) S_{CR}^{(\alpha, z_{0i})}(E_B, N_I, T_I)] \end{aligned}$$

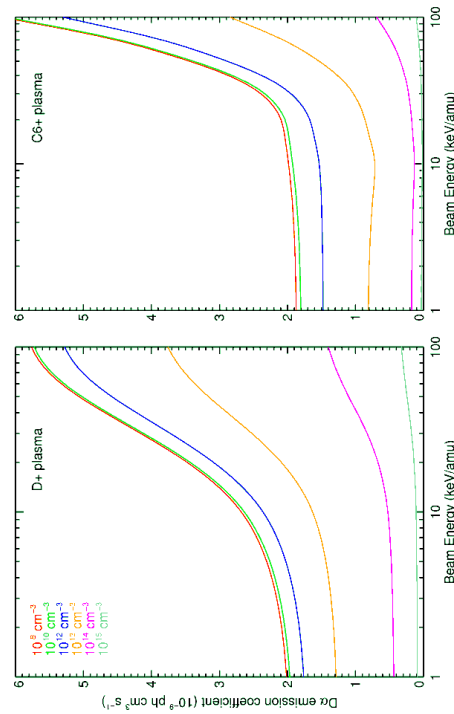
where

$$N_e = \sum_{i=1}^I N_{e,i} = \sum_{i=1}^I z_{0i} N^{(z_{0i})} = N_I \left(\sum_{i=1}^I z_{0i} f_i \right)$$

defines the proportions of the electron density contributed by each impurity species.

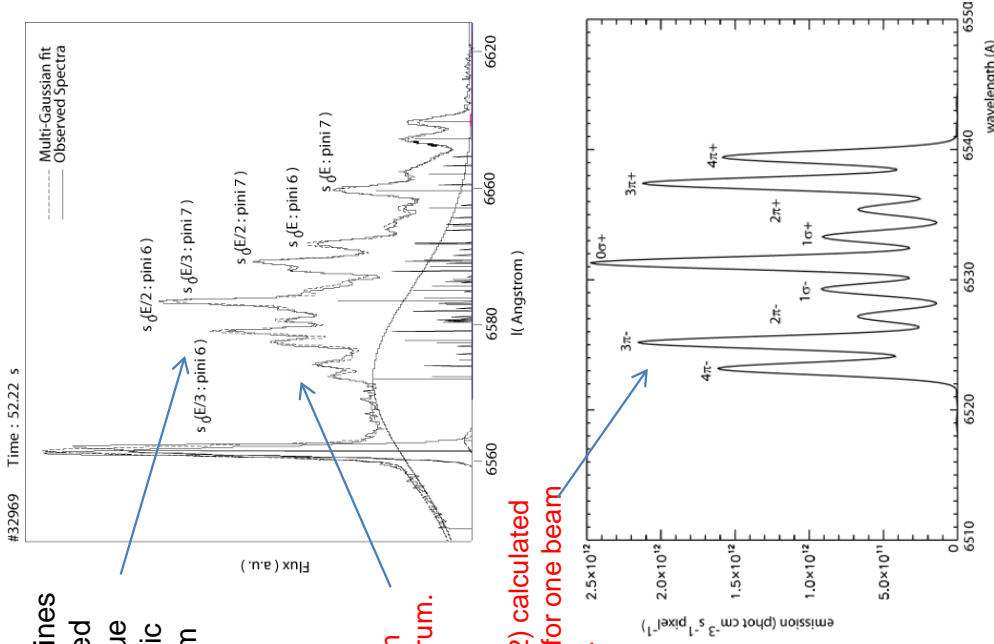
ADAS304 interrogates the data formats adf21 and adf22 and assembles mixtures.

4.4 D(n=3-2) beam emission



The beam emission lines appear Doppler shifted as Stark multiplets due to the motional electric field in the beam atom frame.

Observed beam emission spectrum.



The bundle-n model works well for overall H-beam Balmer line intensities and ratios. Although l-mixing is substantially complete at most densities, the subtlety of the motional Stark features justifies more elaborate studies, linked to MSE spectroscopy.

D(n=3-2) calculated pattern for one beam fraction.

Stark resolved collisional radiative models seek to describe the precise wavelengths, the polar distribution and polarisation of emission and the collisional mixing for the low n-shell emission (Balmer and Paschen). See for example [adas305_get_stark.pro](#).

4.5 Calculating Stark manifold populations and emission

The Hamiltonian for the beam hydrogen atom crossing the magnetic field strength \vec{B} with velocity \vec{v}_b is

$$H = H_0 - e\vec{\mathcal{E}}_m \cdot \vec{r} - e\vec{\mathcal{E}} \cdot \vec{r} - \vec{\mu} \cdot \vec{B}$$

where $\vec{\mathcal{E}}_m = \vec{v}_b \wedge \vec{B}$ is the motional Stark electric field. $\vec{\mu} = \mu_0(\vec{L} + 2\vec{S})$ is the magnetic moment of the electron in the atom. H_0 is the isolated atom Hamiltonian.

Diagonalise this Hamiltonian in a basis of zeroth order wave functions of the isolated atom. In ADAS, this is done for each n-shell separately. With only the $\vec{\mathcal{E}}_m$ field, we obtain Stark states as labelled below, where the axis of quantisation is along $\vec{\mathcal{E}}_m$.
 $n=3$ energy levels of hydrogen in Stark field

Stark states

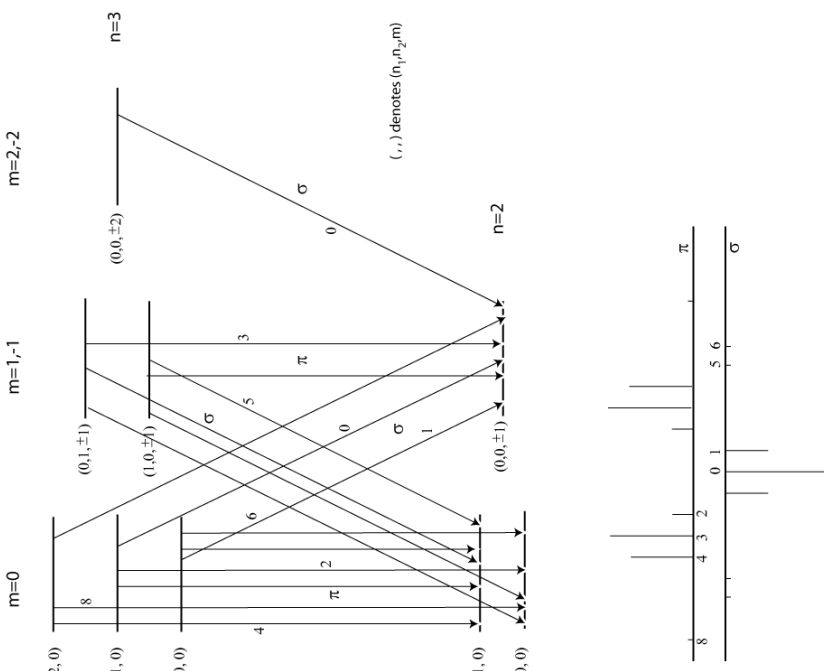
| (n_1, n_2, m) | (k, m) | (l, m) |
|-----------------|---------------|----------|
| $(0, 2, 0)$ | $(-2, 0)$ | — |
| $(0, 1, \pm 1)$ | $(-1, \pm 1)$ | — |
| $(1, 1, 0)$ | $(0, 0)$ | — |
| $(0, 0, \pm 2)$ | $(0, \pm 2)$ | — |
| $(1, 0, \pm 1)$ | $(1, \pm 1)$ | — |
| $(2, 0, 0)$ | $(2, 0)$ | — |

Angular states

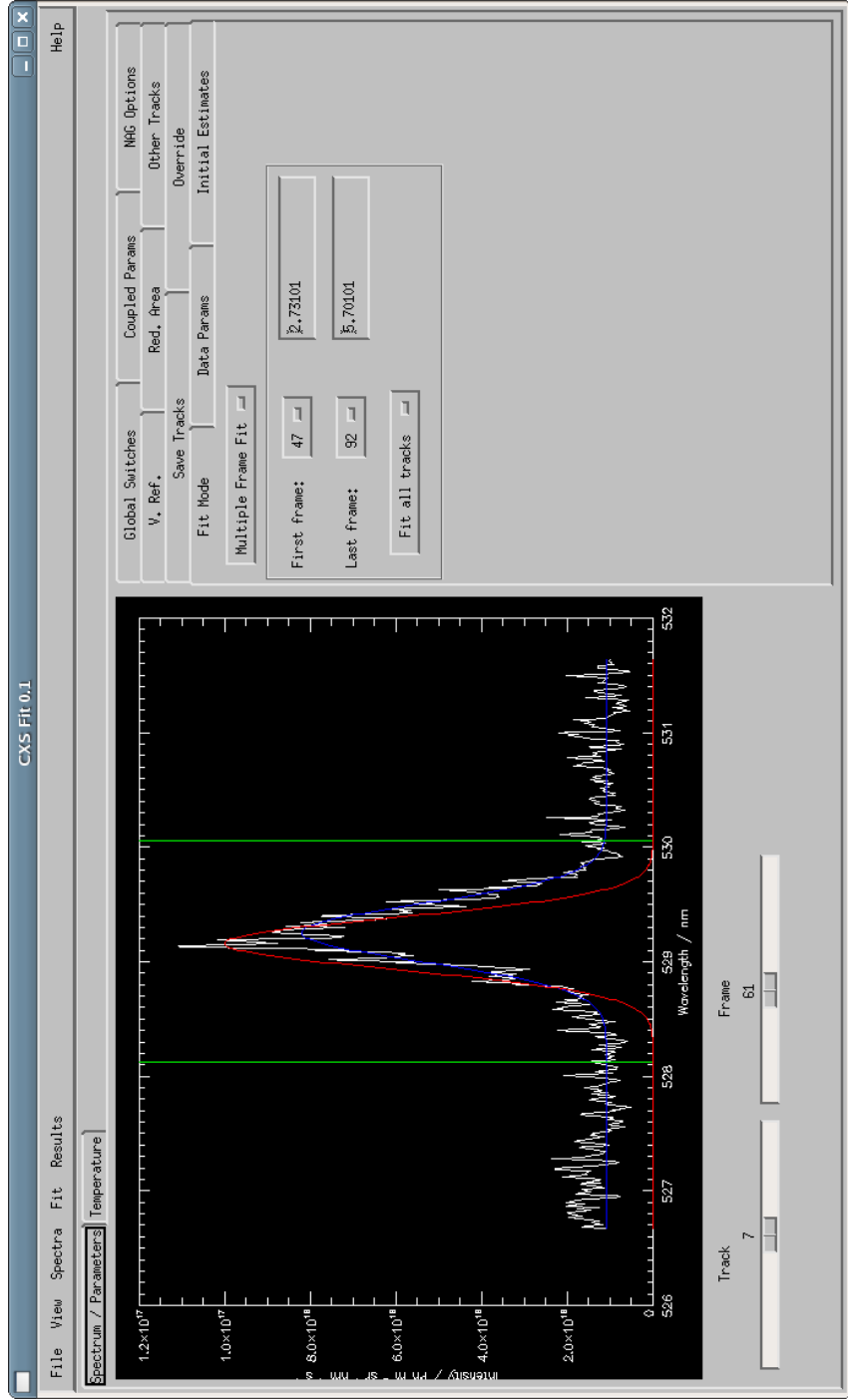
| (n_1, n_2, m) | (k, m) | (l, m) |
|-----------------|---------------|----------|
| $(0, 2, 0)$ | $(-2, 0)$ | — |
| $(0, 1, \pm 1)$ | $(-1, \pm 1)$ | — |
| $(1, 1, 0)$ | $(0, 0)$ | — |
| $(0, 0, \pm 2)$ | $(0, \pm 2)$ | — |
| $(1, 0, \pm 1)$ | $(1, \pm 1)$ | — |
| $(2, 0, 0)$ | $(2, 0)$ | — |

For the pure Stark field case the $n=3-2$ transitions are as above giving the spectrum shown on the previous viewgraph. The code `adas305_get_stark.pro` does this for arbitrary fields and orientations.

{....} denotes a superposition



5.1 Integrated analysis

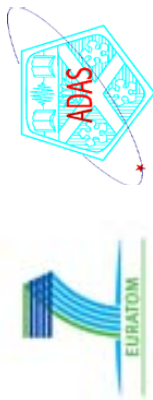


The codes **CXSFIT**, **UTC** and **CHEAP**, maintained by the ADAS team, assist in diagnostic analysis using charge exchange driven spectral features.

6.1 Conclusions

- Charge exchange is a key atomic reaction in fusion plasmas with special diagnostic impact when the donor atom, usually hydrogen or helium isotopes, is in a fast beam.
- Charge exchange in the thermal edge-divertor plasma is a strongly state selective process which can modify line ratios and ionisation balance of light impurities.
- Charge transfer from fast beam atoms can populate subdominant levels of the receiver ions in the plasma giving visible emission and enabling charge exchange spectroscopy (CXS).
- Collisional-radiative modelling is required to predict CXS emission. Special models and analysis tools allow diagnostic insight and extraction of plasma parameters. ADAS has extensive data collections and models to support such analysis and for preparation of new derived data.
- Beam stopping and beam emission are key consequences of the interaction of the beam atoms with the plasma. The beam emission is of special diagnostic importance, enabling beam emission spectroscopy (BES).
- Collisional-radiative models for beam atoms are strongly affected by ion collisions. ADAS has extensive data collections and models to support these situations and analyses.
- The influence of the motional Stark electric field on beam atoms crossing the containment magnetic field of the plasma is an exotic effect and powerfully diagnostic. Special ADAS models allow exploration of this and related effects – see also module 6.

B.6 module_6



Module 6

Advanced charge exchange plasma receiver and beam donor modelling
– the current state.

Lecture viewgraphs

Hugh Summers, Luis Menchero, Martin O'Mullane and Alessandra Giunta

University of Strathclyde

Contents

1. Charge exchange data for medium weight and heavy receiver ions.
2. Extending population models for medium-weight receivers.
3. Exact Stark atom representations and field ionisation.
4. Collisions, directionality and orientation.
5. Conclusions.

1.1 Patterns of CXS lines in the visible

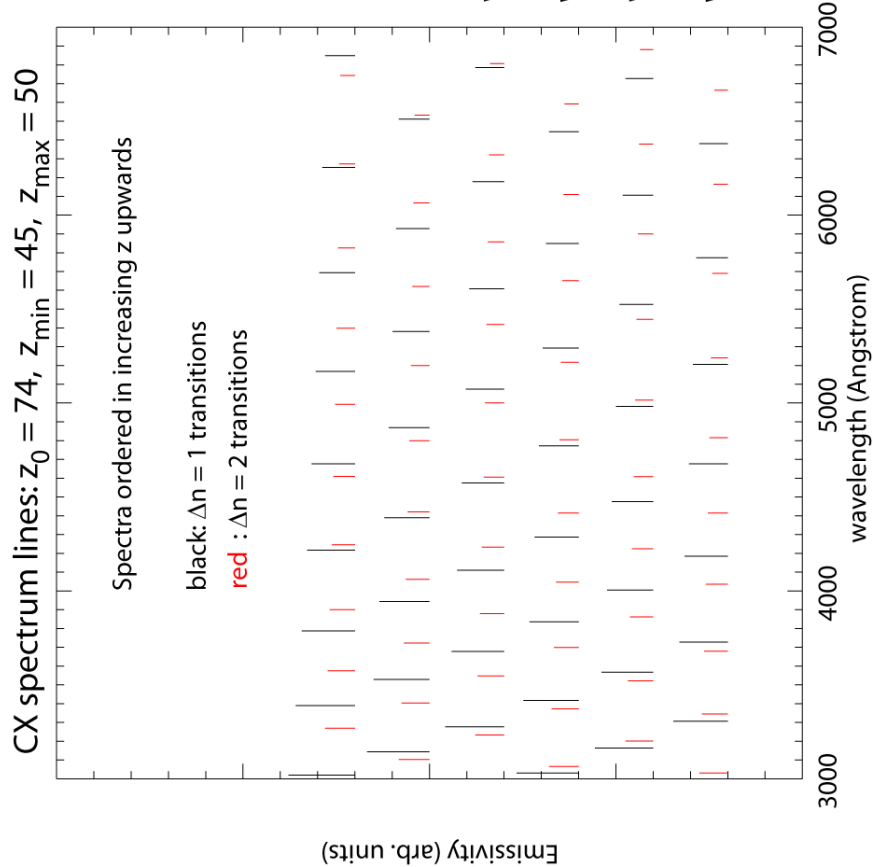
For light elements bare nucleus charge exchange receivers, up to neon, only one or two CX lines occur in the visible spectral range.

As the nuclear charge of the receiver increases, $n_{\text{crit}} \sim Z_0^{3/4}$ increases. The number of lines in the visible increases and they become weaker.

The weakening of the lines means that the possibility of individual line CX spectroscopy, in the manner adopted for light elements, can only continue up to about Fe^{+26} .

With heavy elements of high nuclear charge, the partially stripped ions occur in the confined plasma, so they are also possible charge exchange receivers. By tungsten, a very large number of weak charge exchange lines are expected in the visible.

Although weak, their presence can disturb other diagnostic inferences. So it remains necessary to be able to calculate them.



1.2 Z-scaling of total CX xsects: H(1s) donor

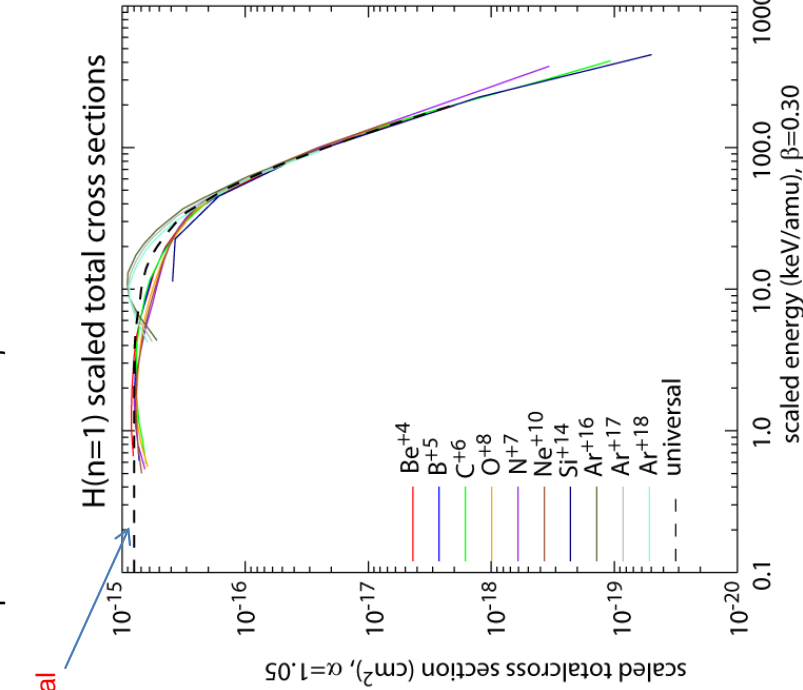
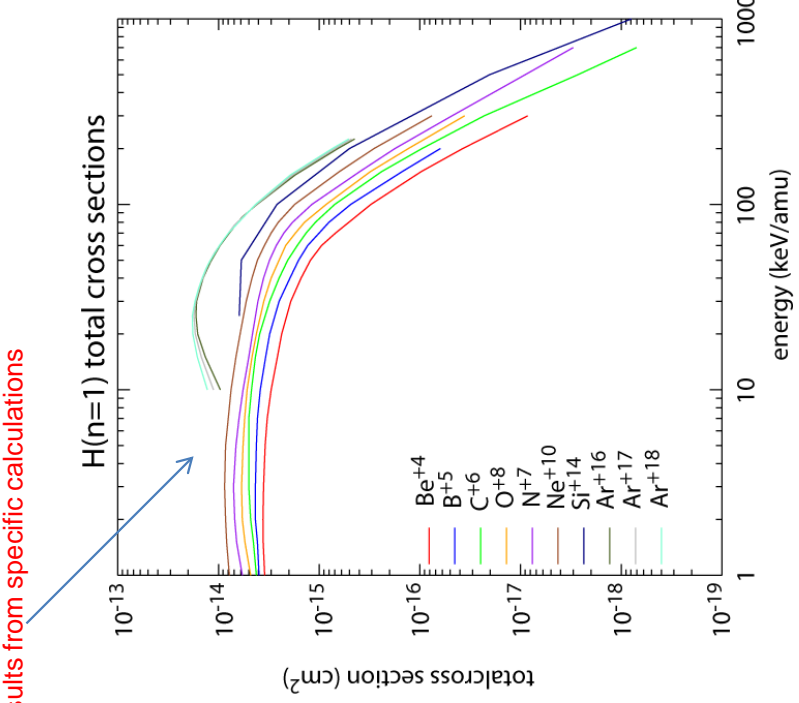
For CX capture by heavier species into higher n-shells, the receiver core is passive. Only the receiver ion charge z_1 matters. The scaling $n_{crit} \sim z_0^{3/4}$ suggests a z-scaled approach for the cross-sections.

Results from specific calculations

Introduce scaled energy \bar{E} and scaled total cross-section $\bar{\sigma}_{tot}$ as:

$$\bar{E} = E z_1^{-\beta} \quad \bar{\sigma}_{tot} = \sigma_{tot} z_1^{-\alpha}$$

The parameters α and β are chosen for best convergence



1.3 Z-scaling of partial-n CX xsects: H(1s) donor

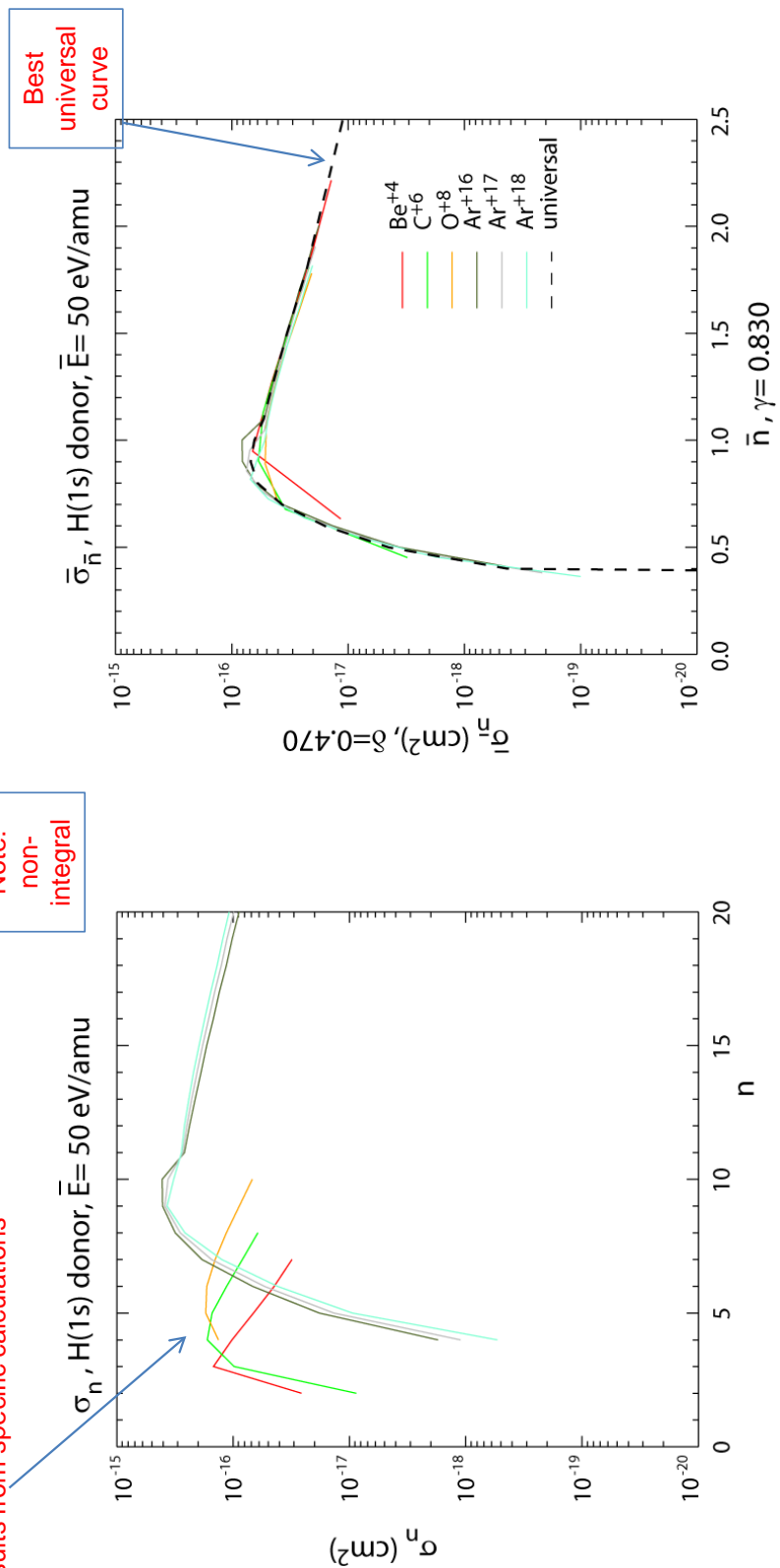
Likewise, the scaling $n_{crit} \sim z_0^{3/4}$ suggests the same approach for the partial-n cross-sections.

For each E , that is at its corresponding \bar{E} , choose z-scaling parameters γ and δ for best convergence for the different ions as:

Results from specific calculations

Note:
non-integral

$$\bar{n} = n z_1^{-\gamma(\bar{E})} \quad \bar{\sigma}_n = \sigma_n z_1^{-\delta(\bar{E})}$$



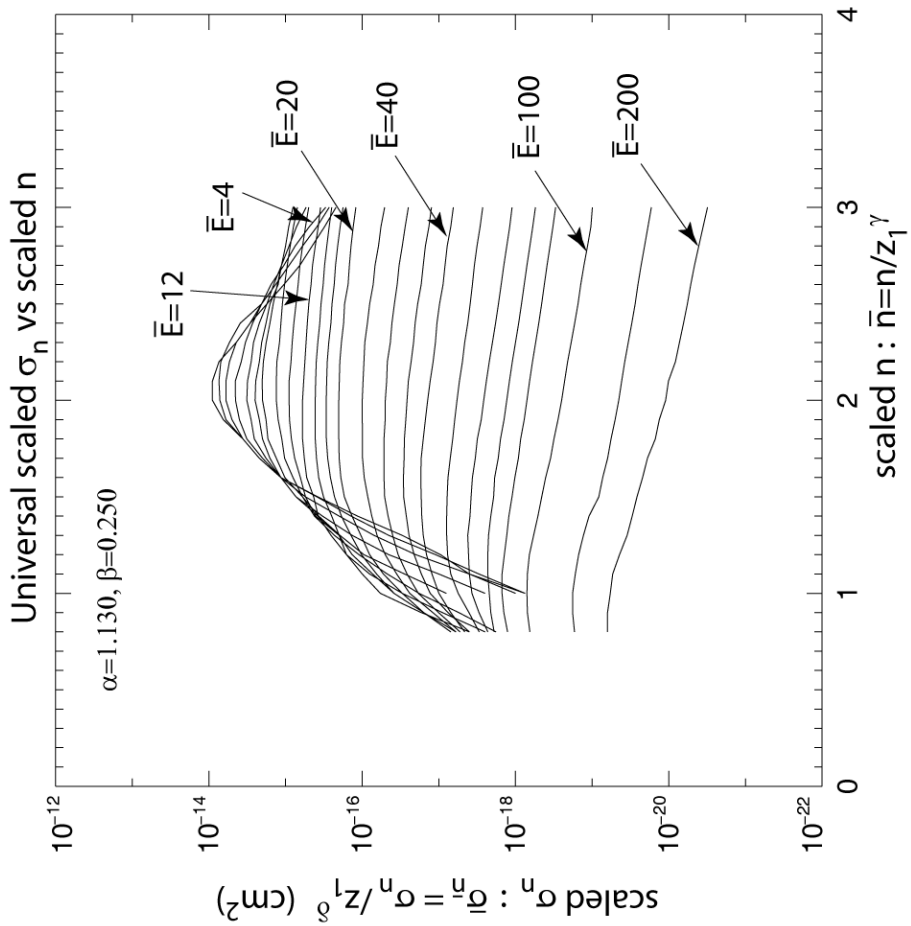
1.4 Universal scaled σ_n Vs scaled n for selected scaled E.

The scaling parameters for the final universal semi-empirical data and formulae are optimised fits to the available specific receiver ion data.

Completion of the final values require extrapolation to high n-shells outside the range of the source data using the procedures of module 5. Partial-n results are normalised to optimised total cross-sections.

The above procedure has been carried out for both H(1s) and H(2s,2p) donors.

Calculations have recently been completed for ADAS-EU including new data for B^{+5} , N^{+7} , O^{+8} , Ar^{+18} and Kr^{+36} . A revised optimisation of the universal formula will be issued in a subsequent ADAS release.



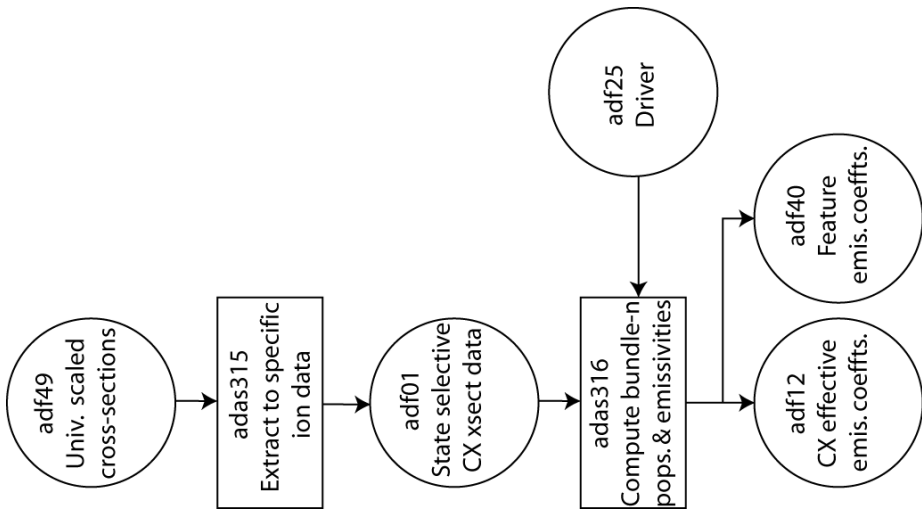
1.5 Universal scaling and heavy receiver CXS emissivities

An ADAS data format [adf49](#) has been assigned to the universal CX scaled cross-section data.

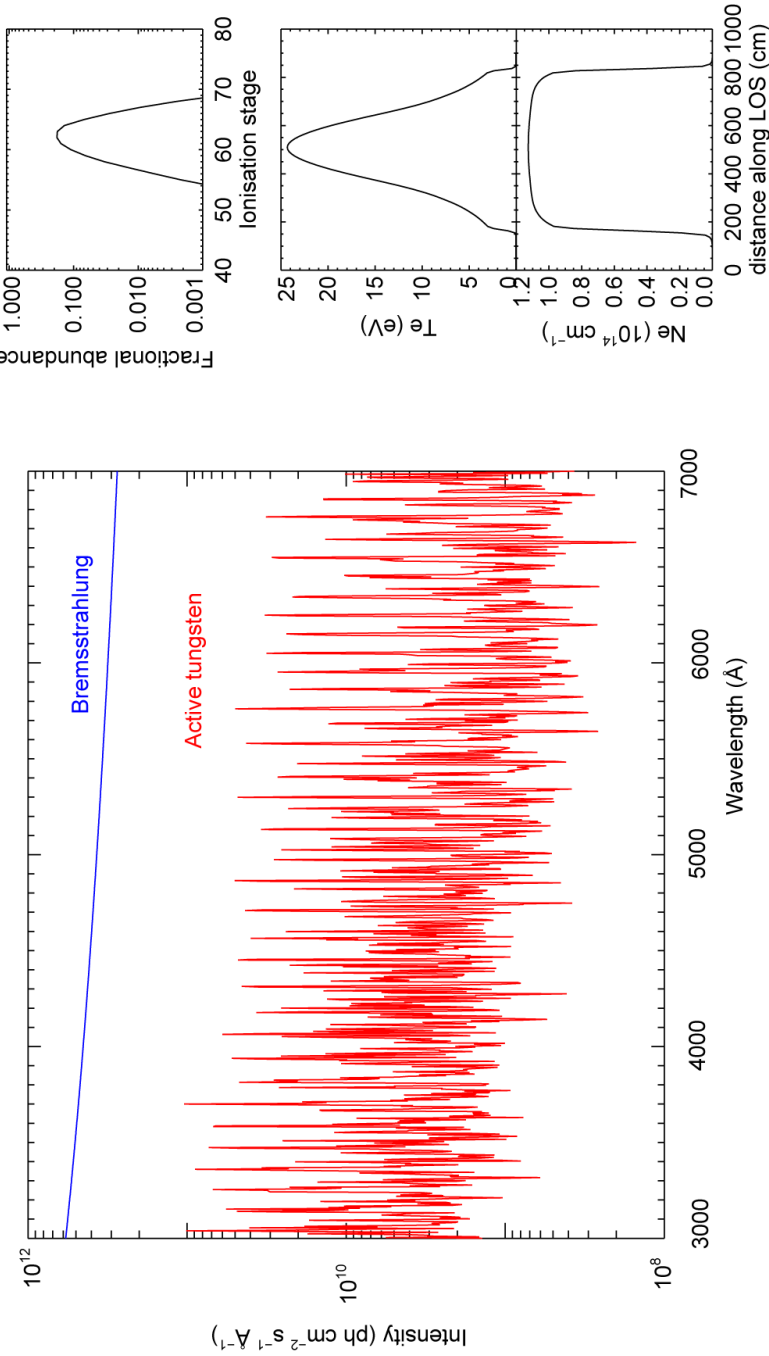
The interactive ADAS series 3 code [ADAS315](#) extracts from adf49, producing a standard charge exchange cross-section dataset of format [adf01](#) for any ion (that is residual ion charge).

For heavy ion receivers, the special algorithms and codes ADAS306 – ADAS309 are less appropriate. Refined individual line CXS is at this point less likely. Consistency in the handling of suppression of the populations of the highest n-shells (in the collisional-radiative sense) by stepwise ionisation is important.

The processing chain to effective emission coefficients ([adf12](#) and [adf40](#)) is completed with the bundle-n population model [ADAS316](#) as shown in the schematic.



1.6 ITER: tungsten CX emission compared with Bremsstrahlung



- 50 keV/amu D beam (diagnostic NB), $|JNB| = 300 \text{ A/m}^2$, $|INBI| = 60 \text{ A}$
- Using ITER scenario 2 ($T_e = 24 \text{ keV}$ core, $N_e = 1 \times 10^{14} \text{ cm}^{-3}$)
- No transport – steady state ionisation balance
- Assume looking vertically down on the beam at the core.
- No beam attenuation effects taken into account.
- W concentration = 1×10^{-6} of N_H

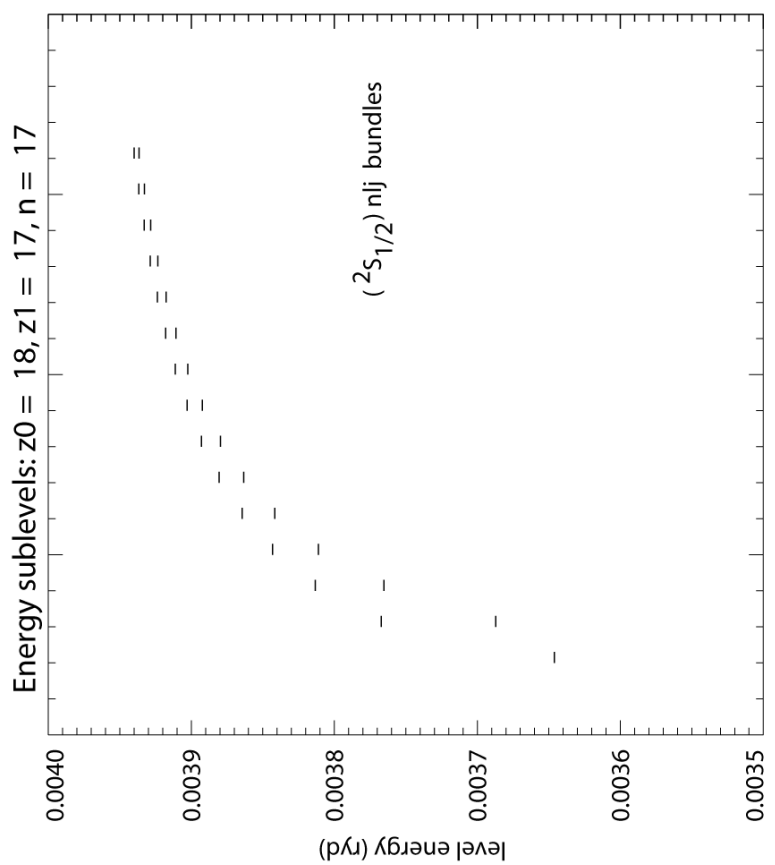
2.1 High n-shell fine structure in $(J_p)nlj$, $(J_p)nl$ and $(J_p)n$ for bundles

For the medium weight elements between argon and iron, further CXS spectroscopy may be anticipated. For these elements, the few-electron (1-6) electron receivers may be expected as well as the bare nucleus

Whereas the core of the receiver ion is of little influence on the charge exchange capture (only the residual ion charge matters), this is not so for redistribution in l -shell after capture and before emission. The fine energy separations are influential, especially towards low l .

There are four steps:

1. The precise energy levels
2. Assigning $(J_p)nlj$ quantum numbers
3. Bundling for population models
4. The population model



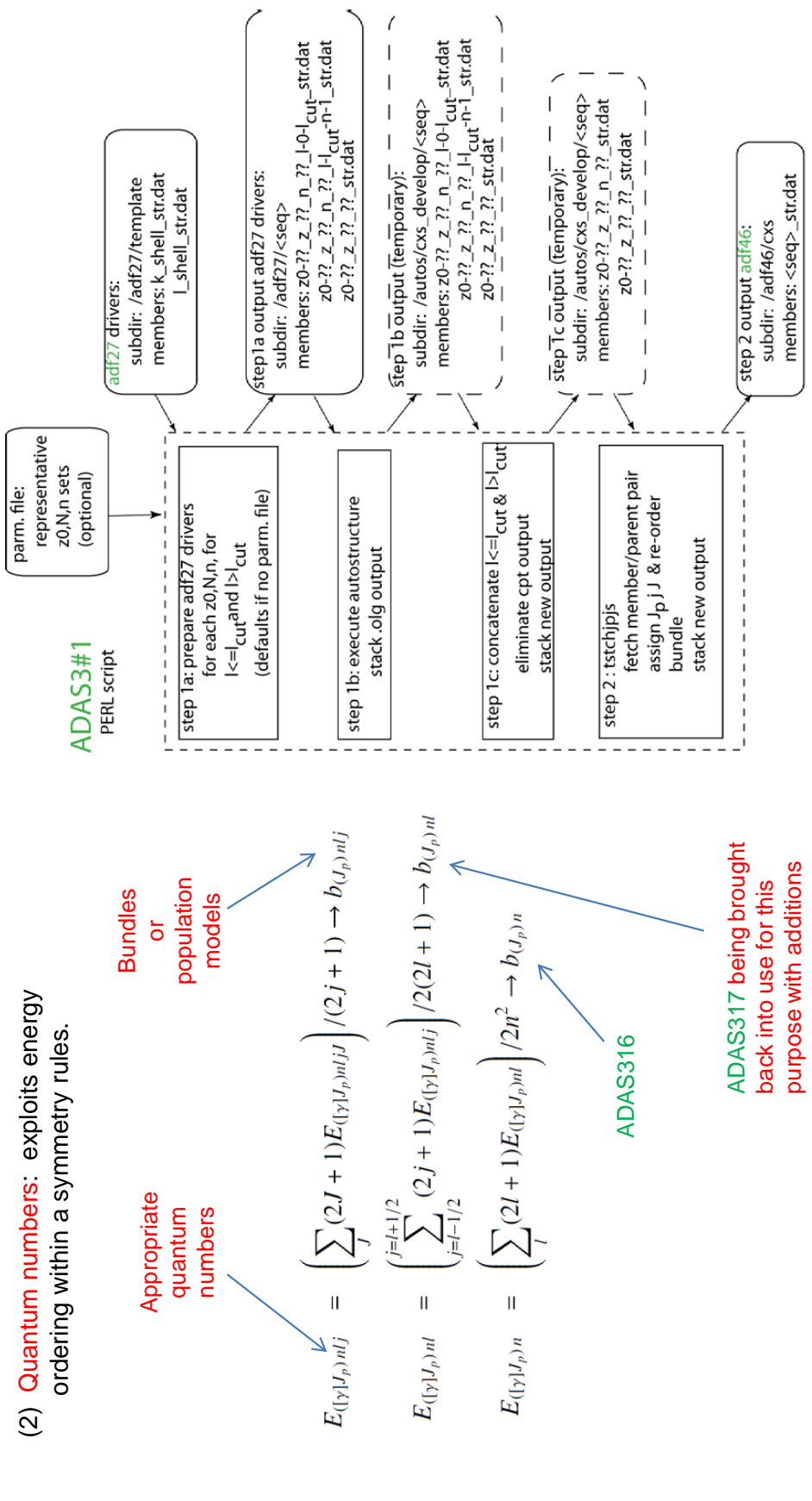
(1) **Energy levels:** Autostructure, multi-config, *ic*, scripted

$$\begin{aligned} & \left[1s^2 2s^2 2p^q nl : l = 0, \dots, \min(l_{\text{cut}}, n-1) \right] \\ & \left[1s^2 2s 2p^{q+1} nl : l = 0, \dots, \min(l_{\text{cut}}, n-1) \right] \\ & \left[1s^2 2p^{q+2} nl : l = 0, \dots, \min(l_{\text{cut}}, n-1) \right] \\ & \left[1s^2 2s^2 2p^q nl, 1s^2 2s 2p^{q+1} nl, 1s^2 2p^{q+2} nl \right] : l = l_{\text{cut}}, \dots, (n-1) \end{aligned}$$

20
15
10
5
0
orbital I for valence electron

2.2 Handling medium-weight receivers in $(J_p)nlj$, $(J_p)nl$ and $(J_p)n$ bundles

(2) **Quantum numbers:** exploits energy ordering within a symmetry rules.

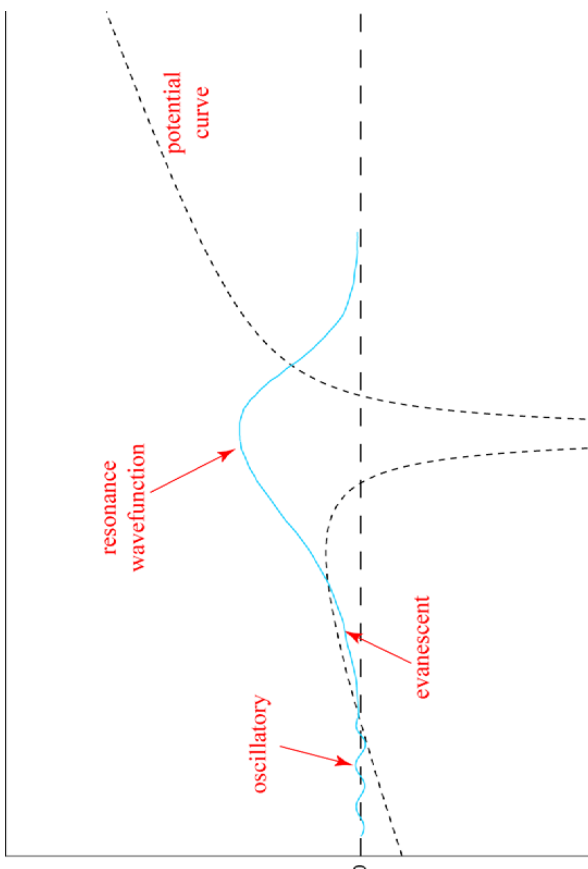


3.1 Stark state – resonance character

Although a hydrogen atom state in a Stark field is often treated as a bound state, its wave-function is non-vanishing at infinity on the low-field side. Properly it is a **resonance** embedded in a continuum sea.

In the simpler viewpoint, it is argued that the bound electron can tunnel through the potential barrier in -ve z-direction, resulting a **field ionisation rate**. Also the energy levels of the Stark atom are calculated as a 1st order perturbation of the isolated atom.

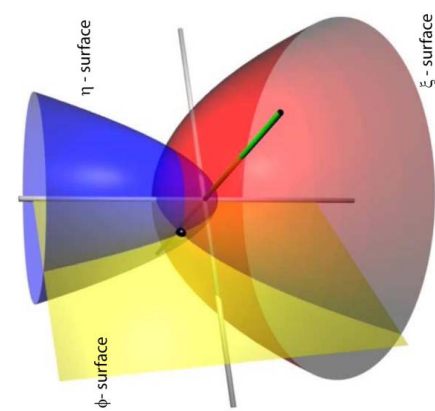
Working in parabolic coordinates



Electric field strength

The Hamiltonian is

$$H = -\frac{2}{\xi + \eta} \frac{\partial}{\partial \xi} \left(\xi \frac{\partial}{\partial \xi} \right) - \frac{2}{\xi + \eta} \frac{\partial}{\partial \eta} \left(\eta \frac{\partial}{\partial \eta} \right) - \frac{1}{2\xi\eta} \frac{\partial^2}{\partial \phi^2} - \frac{\xi}{\xi + \eta} + \frac{1}{2} F(\xi - \eta)$$



3.2 The complex coordinate rotation

By a rotation in the complex plane through a variable angle ϑ as $r' = r e^{i\vartheta}$ the resonant states and their character may be determined.

The Hamiltonian in the rotated coordinate is no longer Hermitian and its eigenvalues are complex.

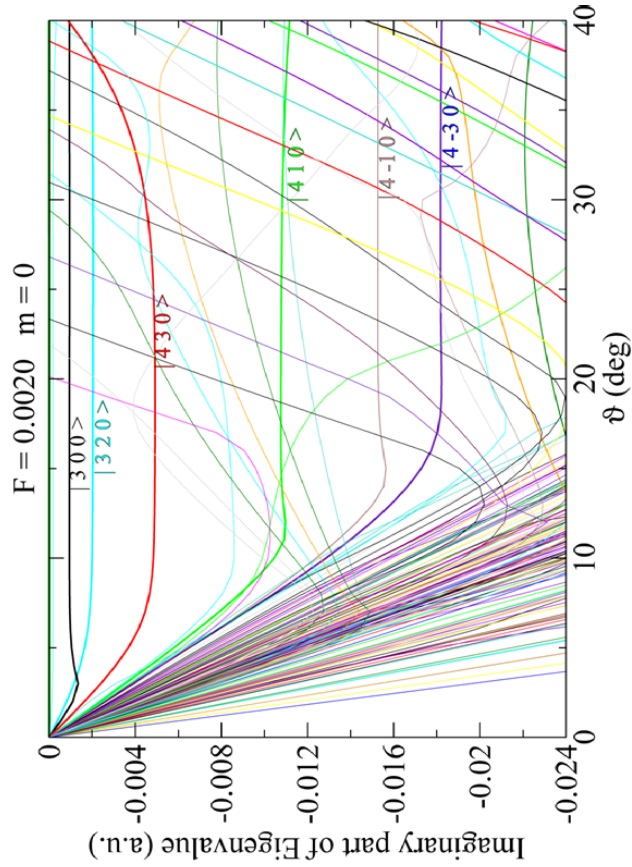
There are three types of effect of the transformation on the eigenvalues:

- bound states are unchanged
- continuum branches are rotated at an angle 2ϑ with the real axis with origin at the threshold energy.
- resonances are exposed in the complex plane when the rotation angle ϑ is greater than the complex root of the resonance.

Let the complex energy of the resonance be.

$$E = E_r - i \frac{\Gamma}{2} = |E| e^{i\beta}$$

E_r



The figure shows the resonances being exposed as the angle ϑ is varied against the continuous background. Their trajectories become horizontal when the angle ϑ is greater than the argument β .

3.3 Solving the secular equation, the Laguerre basis and matrix handling

Expand the wavefunction in a basis set separating the coordinate variables ξ and η as:

$$\Psi(\xi, \eta, \varphi) = \frac{1}{\sqrt{2\pi}} e^{im\varphi} \sum_{k=1}^N \sum_{l=1}^N c_{klm} g_k(\xi) g_l(\eta)$$

The Hamiltonian becomes

$$\begin{aligned} H_{kk'lm}(\vartheta) &= \langle g_k g_l | H(\vartheta) | g_{k'} g_{l'} \rangle \\ &= \int_0^\infty d\xi \int_0^\infty d\eta \frac{1}{4} (\xi + \eta) g_k^*(\xi) g_l^*(\eta) H(\vartheta) g_k(\xi) g_l(\eta) \\ &= -\frac{e^{-2i\vartheta}}{2} (\mathcal{T}_{kk'} \mathcal{I}_{ll'} + \mathcal{I}_{kk'} \mathcal{T}_{ll'}) - \frac{e^{-i\vartheta}}{2} \mathcal{I}_{kk'} \mathcal{I}_{ll'} + \frac{e^{i\vartheta}}{8} F (\mathcal{T}_{kk'} \mathcal{I}_{ll'} - \mathcal{I}_{kk'} \mathcal{T}_{ll'}) \end{aligned}$$

and the overlap integral become

$$\begin{aligned} S_{kk'lm} &= \langle g_k g_l | g_{k'} g_{l'} \rangle \\ &= \int_0^\infty d\xi \int_0^\infty d\eta \frac{1}{4} (\xi + \eta) g_k^*(\xi) g_l^*(\eta) g_{k'}(\eta) g_{l'}(\xi) g_l(\eta) \\ &= \frac{1}{4} (\mathcal{S}_{kk'} \mathcal{I}_{ll'} + \mathcal{I}_{kk'} \mathcal{S}_{ll'}) \end{aligned}$$

leading to solution of the secular equation $(\mathbf{H} - \mathbf{E}\mathbf{S})\mathbf{C} = 0$ efficiently for any F and ϑ in terms of the matrices $\mathcal{T}_{kk'}$, $\mathcal{F}_{kk'}$ and $\mathcal{I}_{kk'}$.

In practice, a finite basis of Laguerre mesh polynomials is used as:

$$\Lambda_{Ni}(x) = (-1)^i \sqrt{x_i} \sum_{j=0}^{N-1} \frac{(-1)^{j+1}}{(j+1)!} L_{N-j-1}^{j+1}(x_i) (x - x_i)^j$$

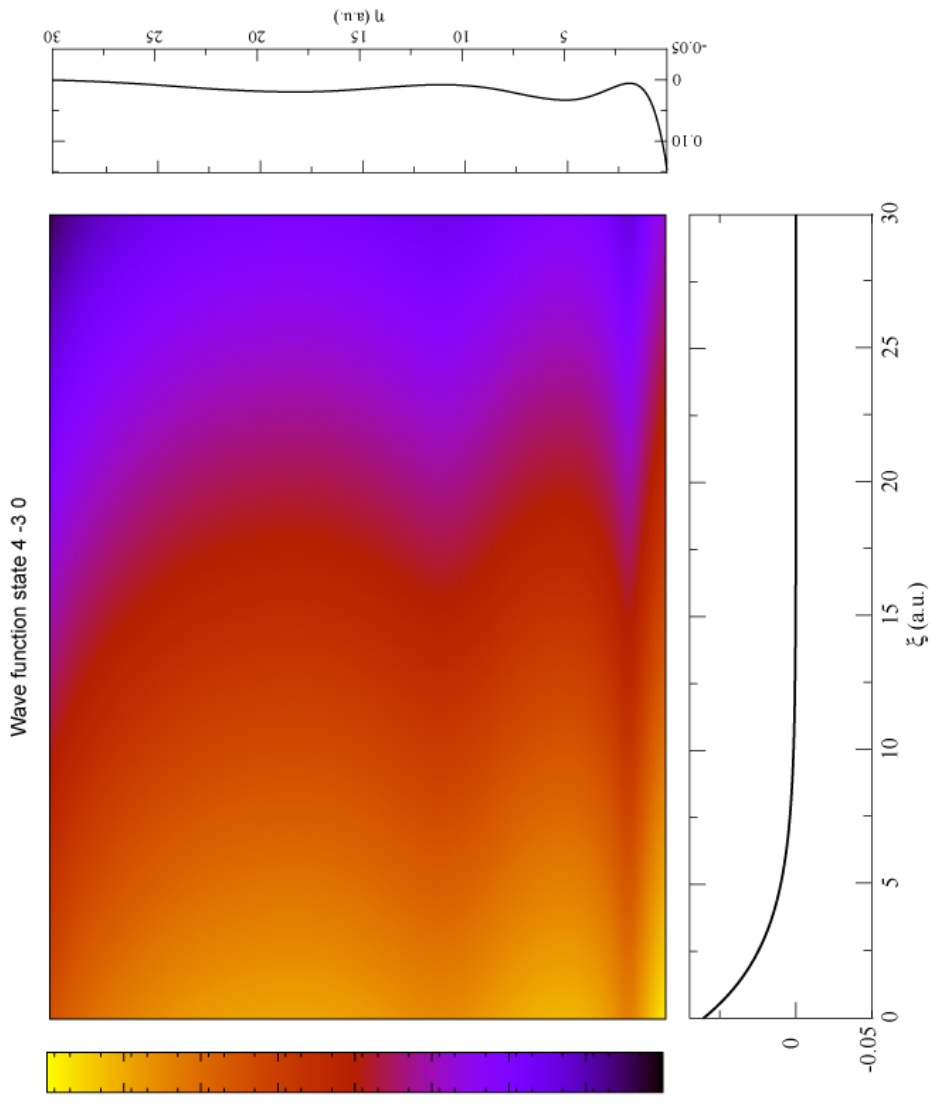
3.4 Stark state wave functions in ξ , η space

States are labelled $|\tilde{n} \tilde{k} m\rangle$ with the approximate quantum numbers \tilde{n}_1 and \tilde{n}_2 which correspond to the quasi-nodes of the modulus of the partially integrated wavefunctions.

$$\begin{aligned}\psi_\xi(\xi) &= \int_0^\infty d\eta \psi(\xi, \eta) \\ \psi_\eta(\eta) &= \int_0^\infty d\xi \psi(\xi, \eta)\end{aligned}$$

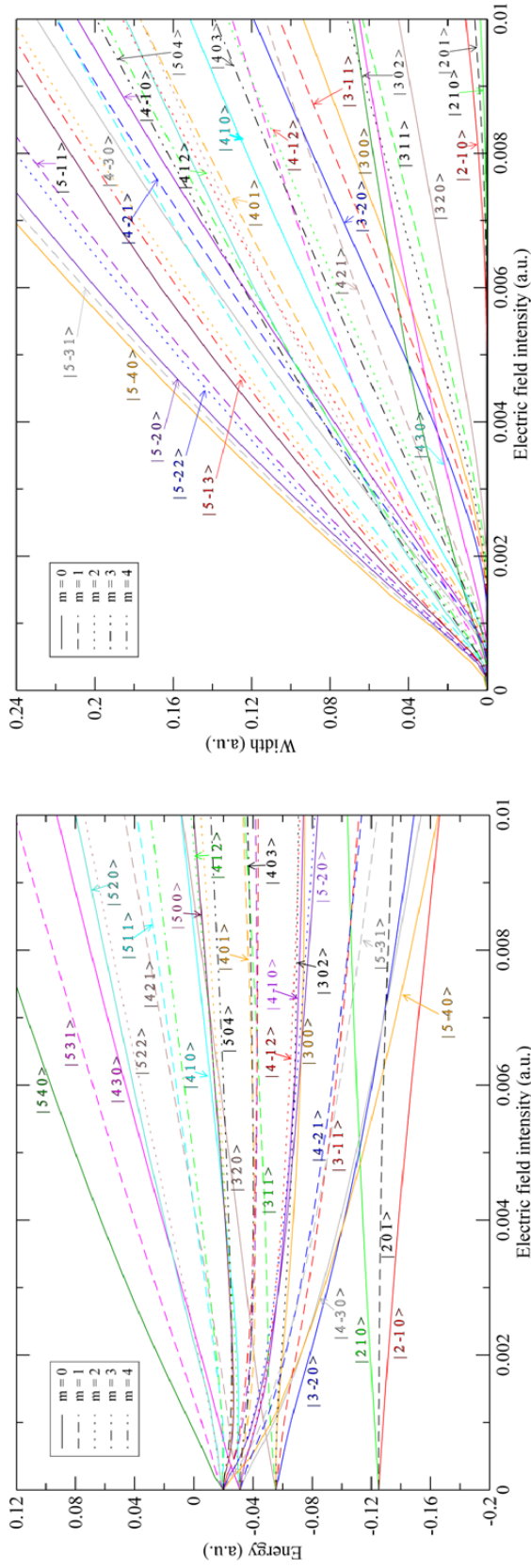
Note that

$$\begin{aligned}\tilde{n} &= \tilde{n}_1 + \tilde{n}_2 + |m| + 1 \\ \tilde{k} &= \tilde{n}_1 - \tilde{n}_2 \\ &\tilde{k}\end{aligned}$$



The figure is of the $n=4$, $k=-3$, $m=0$ wavefunction. For given n , the level energies increase with increasing k .

3.5 Energies and widths



Energies of the resonances up to n=5 for the hydrogen atom vs electric field strength. Note that: 0.01 a.u. = 5.1×10^9 V/m.

Widths of the resonances up to n=5 for the hydrogen atom vs electric field strength. Note that: 0.01 a.u. = 5.1×10^9 V/m.

The solution above together with its archive of the matrix elements and others required for transition probabilities, angular momentum, Runge-Lenz etc. permits a return to the code [ADAS305](#) described in [module 5](#). Now only secondary interactions due to magnetic moment and minor electric fields are treated in 1st order perturbation theory.

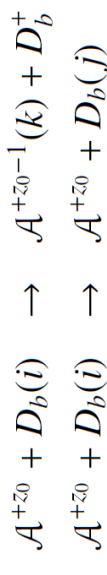
The revision of [ADAS305](#), to be called [ADAS316](#), is in progress. Useful fundamental atomic data such as the energies, widths (field ionisation lifetimes) and A-values are being archived in format [adf50](#).

4.1 Ion and electron collisions with neutral beam atoms

In the core plasma $|\vec{V}_e - \vec{V}_{beam}| \sim V_e$ where \vec{V}_e represents a mean thermal electron velocity, whereas $|\vec{V}_i - \vec{V}_b| \sim V_b$ where \vec{V}_i represents a mean thermal ion velocity. Thus electron collisions are effectively isotropic but ion collisions are not. \vec{V}_b is the beam velocity.

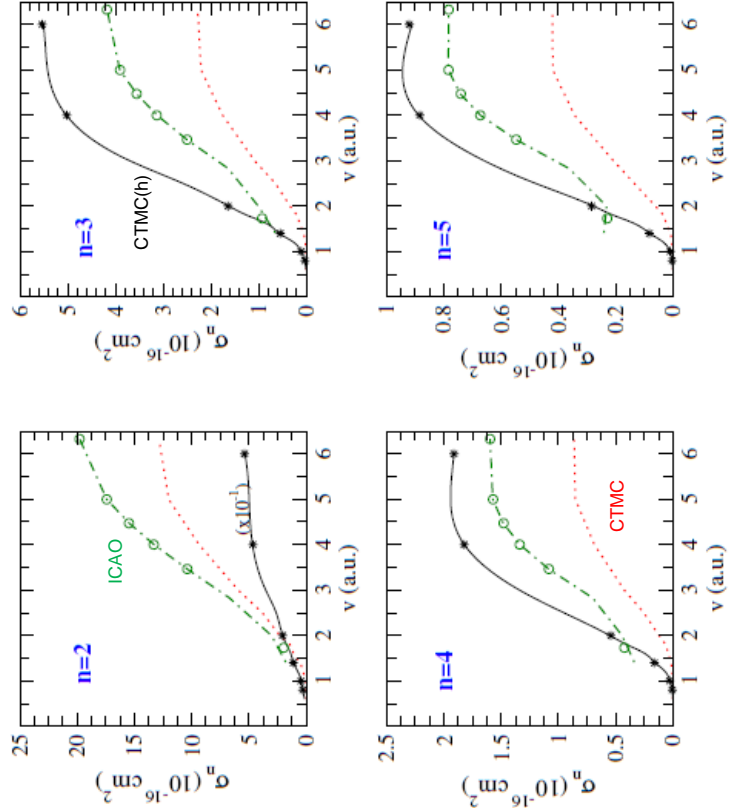
Because of the speed of the beam and electrons in the thermal core of the plasma, electron-impact collision cross-sections for beam-atom excitation are generally much smaller than ion-impact cross-sections.

For ion collisions with beam atoms, the charge transfer and beam excitation reactions are complementary.



Both should be evaluated consistently in the one close-coupled calculation. This is often not done.

The recent calculations of B (CCMO), N, O and Ar (CCAO) for state selective charge transfer cross-sections do not include the beam atom excitation cross-sections. On the other hand the CTMC improved calculations for Ne, Ar and Kr do. The latter can act as a basis for a universal approximation similar to charge transfer.



4.2 Impact parameter approaches

The treatment of the collider as travelling on a classical trajectory is frequently used in atomic collision physics. It has wide validity for ion colliders and is useful for electron collisions.

The trajectory is hyperbolic (attractive or repulsive for electron or ion respectively) if both projectile and target are charged (as shown in the schematic), otherwise it is a straight line. The latter is the situation for excitation of neutral beams.

The probability of inducing the transition $i \rightarrow j$ in the target by a collider on the trajectory of impact parameter R_i is $P_{ij}(R_i)$. Then the cross-section is

$$Q(i \rightarrow j) = \int_0^\infty P_{ij}(R_i) 2\pi R_i dR_i$$

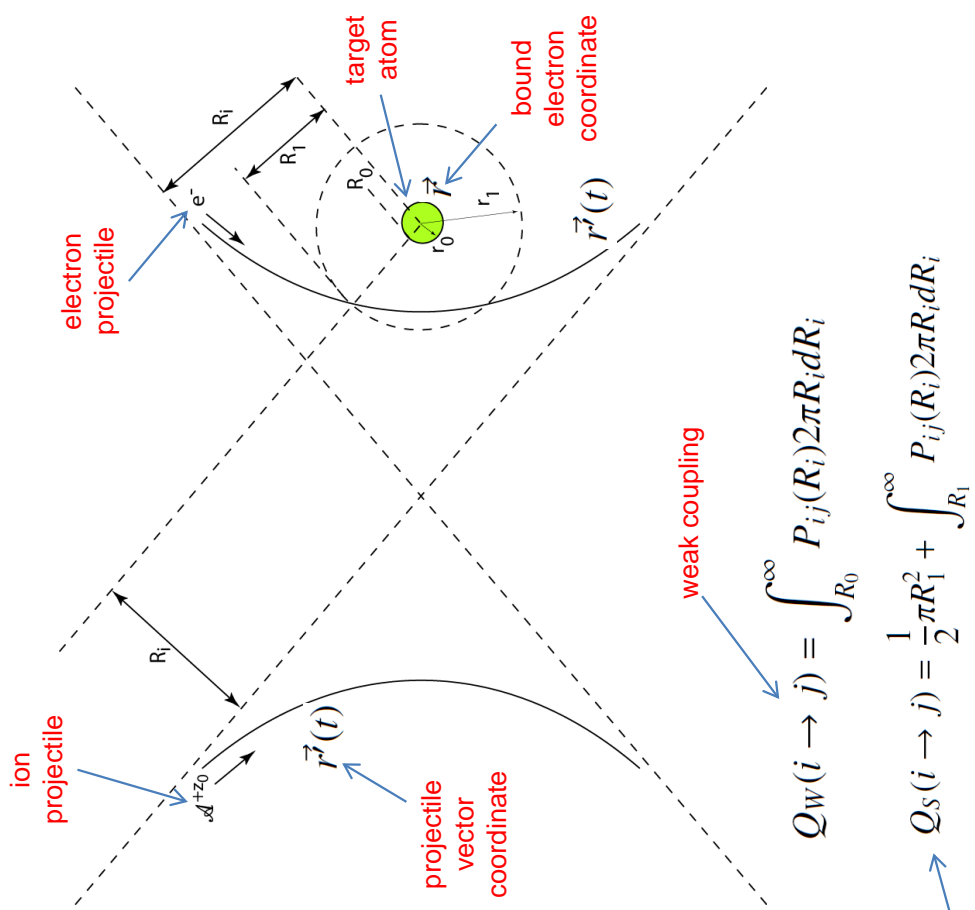
Considerations of whether the trajectory penetrates the atom, R_0 , or if the probability exceeds $1/2$, R_1 , leads to so-called **weak coupling** and **strong coupling** versions of the cross-section. Simplified approximations for those are shown on the right.

weak coupling

$$Q_W(i \rightarrow j) = \int_{R_0}^\infty P_{ij}(R_i) 2\pi R_i dR_i$$

strong coupling

$$Q_S(i \rightarrow j) = \frac{1}{2} \pi R_1^2 + \int_{R_1}^\infty P_{ij}(R_i) 2\pi R_i dR_i$$



4.3 Working with path integrals

The probability of transition from time-dependent perturbation theory is

$$P_{ij} = \frac{1}{\hbar^2 \omega_i} \left| \int_{-\infty}^{+\infty} e^{ipt} V_{ij}(t) dt \right|^2$$

with the interaction potential

$$V_{ij} = \int \phi^*(\vec{r}) \frac{e^2}{|\vec{r}(t) - \vec{r}|} \phi(\vec{r}) d^3 \vec{r}$$

This can be expanded in multipoles, most simply retaining only the dipole term and assuming no penetration of the collider closer to the nucleus than the bound electron. With these restrictions and assuming an orbit in the x-y plane, P_{ij} is expressible in terms of two path integrals which yield modified K Bessel functions. In the isotropic case

$$P_{i \rightarrow j} = 4 \left(\frac{I_H}{\Delta E_{ij}} f_{i \rightarrow j} \right) \frac{k_i k_j}{(k_i k_j R_c + z z' / a_0)^2} X(\xi, \delta)$$

$$X(\xi, \delta) = \exp(\pi\xi)(\xi\epsilon)^2 \left[K_{i\xi}^2(\xi\epsilon) + \frac{\epsilon^2 - 1}{\epsilon^2} K_{i\xi}^2(\xi\epsilon) \right]$$

$$\text{and } \xi = \frac{zz'}{a_0} \left| \frac{1}{k_i} - \frac{1}{k_j} \right| \quad \delta = R_c |k_i - k_j|$$

$$\text{with } \delta = \xi\epsilon - \xi.$$

ADAS has subroutines for these cross-sections and related functions `eqip.for`, `xip.for`, `yip.for` together with many other cross-section approximations.

The form and evaluation of the path integrals has been used to handle degenerate transitions, allow penetration of the atom, include higher multipoles and so on. **It is an active area at this time.**

In the present context of collisional excitation and redistribution of fast beam atoms, the ADAS team is testing these methods for the oriented Stark atom, experiencing **highly directional collisions**.

4.4 Directional and orientation issues

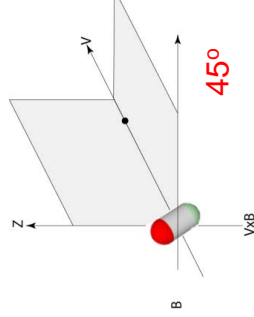
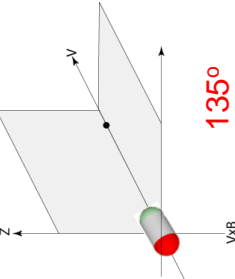
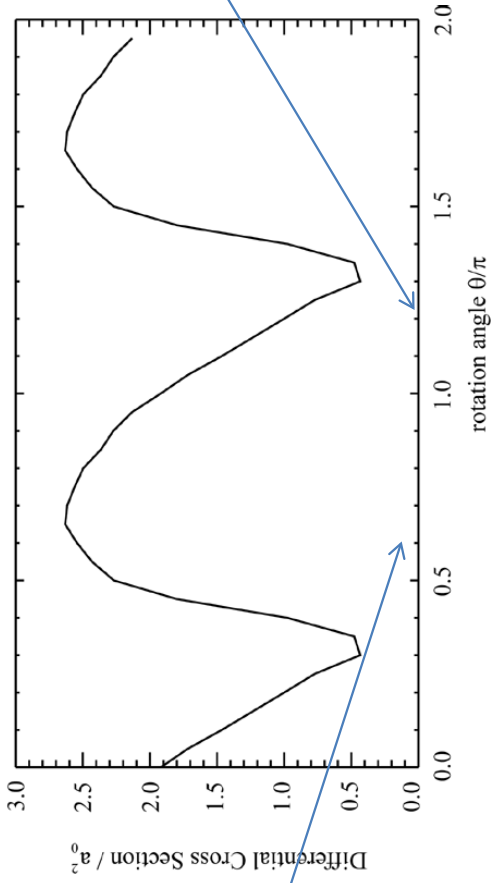
The probability generalises in the directional/ oriented case requires the **three component path integrals** and three matrix elements between **Stark states**.

The cross-section is an integral over the **cone of attack** and the strong coupling circle is now a more complex area

$$\begin{aligned} P_{s \rightarrow s'} &= \frac{e^4}{(4\pi\epsilon_0)^2 \hbar^2} \left| \int_{-\infty}^{\infty} \exp(i\Delta E_{s,s'} t/\hbar) \left(\frac{x'(t)}{r'^3(t)} < \psi_s | x | \psi_{s'} > \right. \right. \\ &\quad + \left. \left. \frac{y'(t)}{r'^3(t)} < \psi_s | y | \psi_{s'} > + \frac{z'(t)}{r'^3(t)} < \psi_s | z | \psi_{s'} > \right) dt \right|^2 \end{aligned}$$

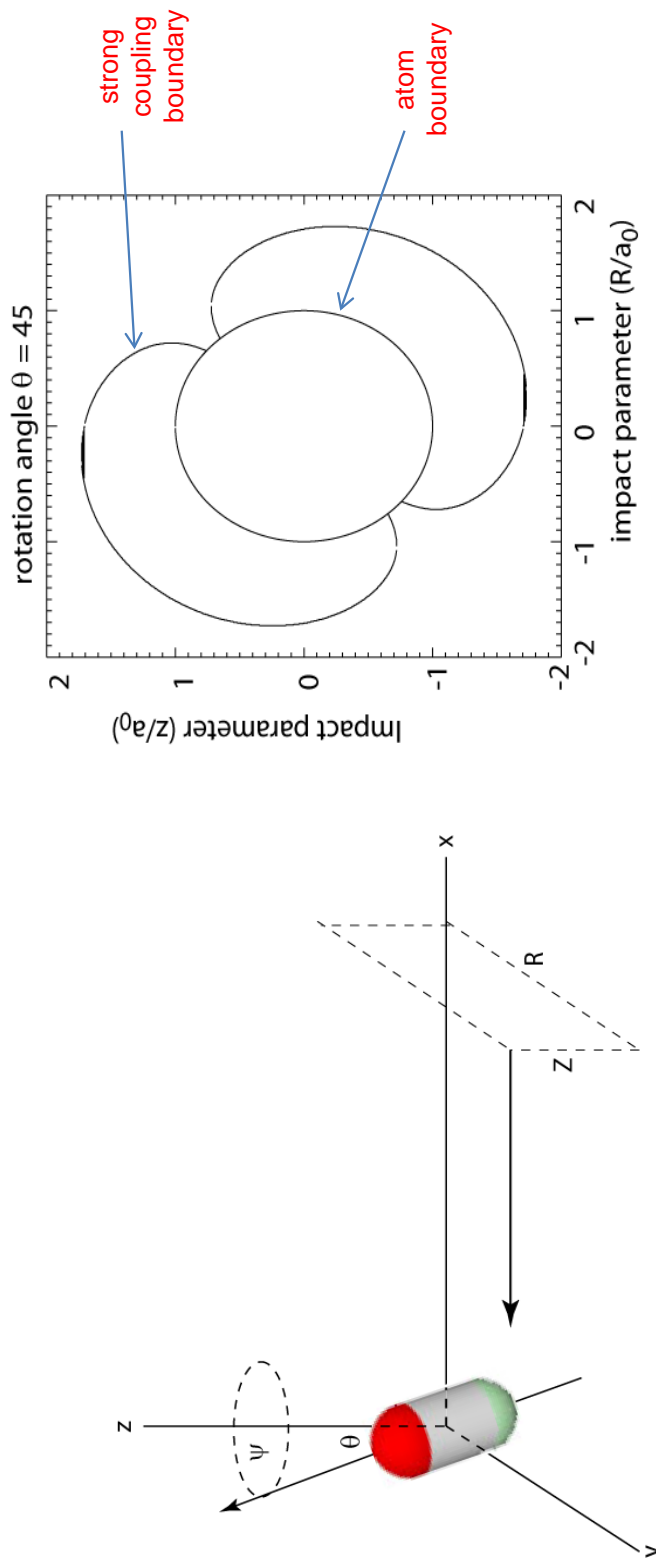
$$Q_{i\sigma j\eta}^{tot} = \frac{1}{2\pi\theta_0} \int_0^{\theta_0} \left[A(\vec{r}_1, \theta) + \int_0^{2\pi} \int_0^{\infty} \int_{R_1}^{\infty} (P_{i\sigma j\eta}(\theta, \psi, Z, R) dR dZ d\psi \right] \sin\theta d\theta$$

The schematic and an illustrative graph below shows the broad type of behaviour.



4.5 Strong coupling zones

The shape of the strong coupling area is illustrated below with a schematic of the impact parameters.



The brief discussion above summarises [work in progress](#) for the neutral beam description, utilising the zeroth order Stark states and matrix elements evaluated in section 4. The cross-sections will be normalised at zero field in the isotropic case to the CTMC (h) data of viewgraph 5.1.

5.1 Conclusions

- The database of state selective charge transfer from H($n=1$) and H($n=2$) donors to fully ionised impurity nuclei up to argon has allowed preparation of a universal semi-empirical approximation for all charged receivers.
- Current utilisation for derived effective emission is through the b_n -model.
- New state selective charge transfer data, calculated for ADAS-EU confirms the broad behaviour, although some ambiguity on l-shell capture remains, and extends the available data to krypton. The universal approximation is being re-optimised using these data.
- More precise high nl-shell energies allows more precise l-distribution modelling for medium-weight partially ionised receivers. This is being enabled in the b_{nl} -model.
- Exact solutions of the motional-Stark modified beam atom have been prepared, yielding field ionisation and other quantities at high precision for arbitrary field strengths. They are being embedded in a revised beam emission model.
- Directional ion and electron collisions with the oriented Stark beam atom have been addressed in the impact parameter formalism. Modified cross-sections will be incorporated in the revised beam emission model.

B.7 module_7



Module 7

Calculating fundamental atomic structure and electron impact
cross-section data – Autostructure and R-Matrix.

Lecture viewgraphs

Hugh Summers, Nigel Badnell, Martin O'Mullane and Alessandra Giunta

University of Strathclyde

Contents

1. Preliminaries.
2. Atomic Structure and collision cross-sections with the COWAN code
3. Atomic structure and collision cross-sections with the AUTOSTRUCTURE code
4. Mass production of data with scripts
5. Collision cross-sections with the R-matrix code
6. Conclusions

1.1 Atomic structure codes in general use

| Code | Method | Usual application | Precision (E%, A%) | Comments |
|---------------|--|--|---|---|
| AUTOSTRUCTURE | Multi-config, Breit-Pauli, Thomas-Fermi and Slater-type parametric potential | General + Auger rates + Born integrals | (~2,~5) typically dependent on CI scope. | Recently extended to multiply- occupied f-shells. Extended experience of use up to M-shell. Limited coupling scheme information. Specially tuned for dielectronic and radiative recombination. Can separate term, level and configuration average resolution calculations. A preferred code for ADAS. |
| COWAN | Multi-config, Breit-Pauli, Hartree-Fock potential | General + Auger rates + Born | (~2,~5) typically dependent on CI scope and tuning. | Handles multiply-occupied f-states. Extended experience in many complex systems. Flexible coupling scheme information. Easy access to configuration average information. Executes level resolution calculation and averages to terms. A preferred code for ADAS. |
| HULLAC | Multi-configuration, Dirac Hamiltonian; j-j coupled basis, Breit and QED | General, but extensive use with EBIT measurements. | (~2,~5) typically dependent on CI scope. | Proprietary code package; structure code part matched to distorted wave collision code and collisional-radiative modelling. |
| FAC | As for HULLAC | General, but mostly astrophysics. | (~2,~5) typically dependent on CI scope and tuning. | Public domain variant of HULLAC. Use increasing and experience building up. |
| GRASP | Multi-configuration, Dirac/ Breit Hamiltonian; MCDHF or parametric potential; various couplings and optimizations. | General. | (<1,<3) with extensive core/ valence CI. | High grade code, but MCDHF not always able to converge on potential. Tuned to DARC fully relativistic version of R-matrix collision code. A preferred code for ADAS level 2 in relativistic region. |

1.2 Electron impact collision codes in general use

| Code | Method | Usual application | Precision (%) | Comments |
|-------------------------|--|--|---------------|--|
| AUTOSTRUCTURE/ COWAN | Born with modified threshold region. | Low - medium/ high z. | (<40%) | Very general, stable and enabled by all structure codes with a free electron wave-function generator. No spin change. CA, LS and IC coupling. Suitable for ADAS baseline. |
| CCC / CCC-R | Convergent close-coupling. | Low - medium/ high z; 1-2 valence electrons | (<5%) | Highest precision, inefficient for very many energies and delimiting resonances. Limited ion scope. Currently being extended to Dirac relativistic. |
| DARC/ DRMPS | Relativistic R-matrix close-coupling / with pseudo-states. | Low - high z. | (~ 5-10%) | Very high precision, tuned to GRASP structure and shared algebra. Resonances included. Recent pseudo-state extension increases heavy element near neutral scope. Use also for ionization. Intermediate coupling. Suitable for ADAS level 2 at low and high z. |
| HULLAC / FAC | Distorted wave. | Medium - high z. | (~20%) | Intermediate coupling, includes spin change, no resonances. Efficient algebra – but now used universally. Matched to HULLAC structure part. |
| AUTOSTRUCTURE | Distorted wave | Medium - high z with some use at low z | (~20%) | Very stable. In continuing development. CA, LS and IC coupling. Integrated in ADAS and suitable for level 1 increase from baseline. |

1.3 Electron impact collision codes in general use (contd)

| Code | Method | Usual application | Precision (%) | Comments |
|-------------------|---|-------------------------------|---------------|--|
| RM / RMPS | R-matrix close-coupling / with pseudo-states. | Low - med | | High precision, tuned to AUTOSTRUCTURE and shared algebra. Resonances included. Use also for ionization. Implemented for isoelectronic sequences with scripts. LS coupling. Parallelized versions. Suitable for ADAS level 1,2 medium-scale mass production. |
| RM - ICFT / RM-II | R-matrix close-coupling with intermediate-coupling frame transformations/ R-matrix close-coupling with IC inner region. | Medium - medium/ high z. | (~ 5-10%) | As for RM, but extends to higher z ions in intermediate coupling. Suitable for ADAS level 1, 2 medium-scale mass production. R-matrix inner region IC gives improved higher z treatment. Suitable for ADAS level 2 and benchmarking of RM-ICFT. |
| RM-RD / DARC-RD | R-matrix close-coupling with radiation damping. | Medium - high z. | (~ 5-10%) | As for RM, but extends to high z ions with significant radiative/ Auger branching of resonances. Suitable for ADAS level 1,2. |
| TDCC | Time-dependent close coupling. | Low z; 1-2 valence electrons. | (<5%) | Highest precision. Benchmark for low-z ionization. Used for ADAS level 2. |
| UCL-DW / JAJOM | LS distorted wave with IC transformation. | Medium -medium/ high z. | (~20%) | Matched to AUTOSTRUCTURE. Extension to IC via algebraic transformation. Includes spin change. No resonances. Can isolate calculation of cross-sections starting with selected metastables. Now inefficient and falling out of use in comparison with RM. |

* depends on precision of multi-configuration multi-electron structure calculation and/or close-coupled set and/or pseudo-state span and completeness.

2.1 Driving the Cowan code for ADAS

```
adf34 config. file:
2 -5 2 10 1.0 5.d-11-2 0130 1.0 0.65 0.0 0.5
4 2 Be 2s1
4 2 Be 3s1
4 2 Be 4s1
.
.
4 2 Be 4f1
4 2 Be 5f1
-1

control parameters
config. list,
1st parity then
2nd parity
```

RCN2 instruction file:

```
z0 74 W0
zi 0
parity-1 11 : 2 1 2
parity-2 9 : 2 1 7
E2 3
M1 3
scale 85 85 85 50
temperature 25
1.00e+03 1.47e+03 2.15e+03 3.16e+03 4.64e+03 6.81e+03 1.00e+04 1.47e+04
2.15e+04 3.16e+04 4.64e+04 6.81e+04 1.00e+05 1.47e+05 2.15e+05 3.16e+05
4.64e+05 6.81e+05 1.00e+06 1.47e+06 2.15e+06 3.16e+06 4.64e+06 6.81e+06
1.00e+07
```

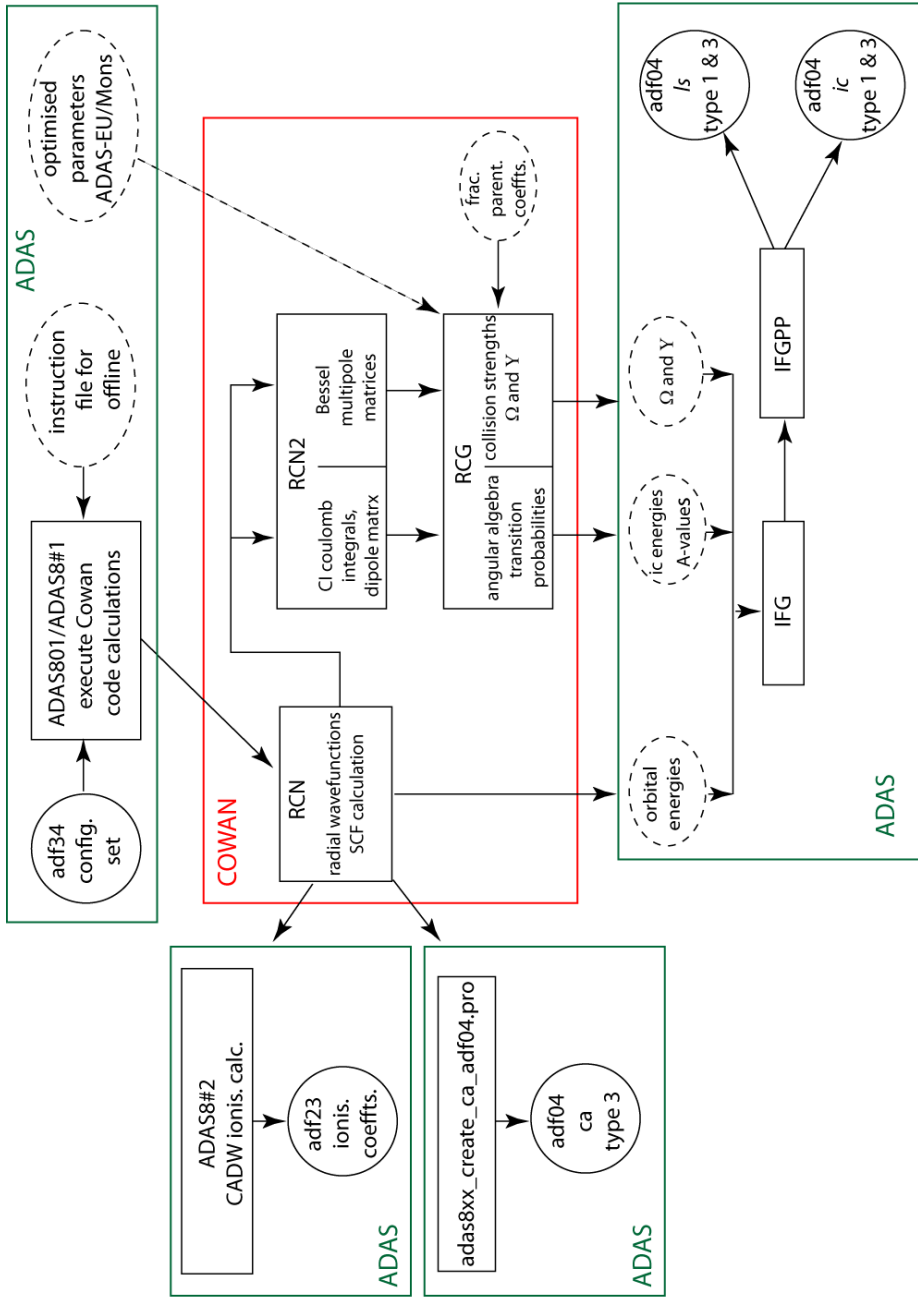
reduced T_e set
for adf04

```
1 Martin O'Mullane
5 03-08-2012
```

comments to be
 appended to adf04
 dataset

```
&FILES ifgfile = 'ifg!w0#a.adf34.dat' , outfile = 'wlike_mons11#w0.dat' &END
&OPTIONS ip = 63427.7, coupling = 'IC' , aval = 'YES' ,
isnuclear = 'NO' , quantity = 'RATES' , lweight = 'NO' ,
comments = 2, numtemp = 14 , &END
1 2 3 5 7 9 11 12 13 14 15 17 19 20
parity-1 11 : 2 1 2
parity-2 9 : 2 1 7
```

2.2 Cowan code schematic and ADAS utilisation



3.1 Basis atomic structure using AUTOSTRUCTURE

At the command line, the AUTO-STRUCTURE code requires a driver dataset. Results are returned to the initial directory as for example:

```
> ../../bin/as25lm_hps.x < das_2
```

The main summary results are returned in the dataset called *olg*.

| <i>das_2</i> | | intermediate coupling | | electric dipole transition probabilities | |
|--------------|----------|--|----------------------------------|--|----------------------------|
| 1s orbital | configs. | A.S. Be-like Cstructure &SAIGEB CUP='IC' RAD='E1' 1 0 2 0 2 1 2 2 0 1 1 2 0 2 &END | valence orbitals | energies + radiative rates MXCONF=3 MXVORB=3 &END | number of valence orbitals |
| | | &SMINIM NZION=6 &END | configuration occupation numbers | number of configurations | number of configurations |
| | | | nuclear charge | quantum numbers | |
| | | | | | level energies |
| | | | | | algebraic term indexing |

olg (last part)

| K | IV | T | K*CM | 2*S+1 | L | 2J | CF | (EK-E1)/RY | E1/RY = | -72.87735554 |
|----|----|---|---------|-------|---|----|----|------------|---------|--------------|
| 1 | 8 | 5 | 0. | -1 | 0 | 0 | 1 | 0.00000000 | | |
| 2 | 10 | 3 | 53644. | -3 | 1 | 0 | 2 | 0.48884297 | | |
| 3 | 5 | 3 | 53686. | -3 | 1 | 2 | 2 | 0.48921835 | | |
| 4 | 3 | 3 | 53768. | -3 | 1 | 4 | 2 | 0.48997075 | | |
| 5 | 6 | 4 | 110586. | -1 | 1 | 2 | 2 | 1.00773254 | | |
| 6 | 7 | 2 | 138633. | 3 | 1 | 0 | 3 | 1.26331362 | | |
| 7 | 4 | 2 | 138674. | 3 | 1 | 2 | 3 | 1.26369166 | | |
| 8 | 2 | 2 | 138756. | 3 | 1 | 4 | 3 | 1.26444154 | | |
| 9 | 1 | 1 | 154402. | 1 | 2 | 4 | 3 | 1.40701900 | | |
| 10 | 9 | 6 | 191560. | 1 | 0 | 0 | 3 | 1.74562274 | | |

3.2 Control of AUTOSTRUCTURE with namelist parameters

The AUTOSTRUCTURE code has been in continuing development for more than 30 years. It is now one of the most versatile codes of its kind in the world.

Much of its operation in recent years has been tuned to ADAS needs. It writes directly to ADAS formats such as *adf04*, *adf09*, *adf38*, *adf39* and *adf48*.

controls type of calculation and coupling scheme

```
&SALGEB RUN='DE' CUP='ICR' KCOR1=1 NMETA,I=1028 MXCONF=18 MXVORB=9 &END  
salgeb namelist:  
DR dielectronic recombination  
RR radiative recombination  
DE distorted wave xsects  
PI photoionisation  
BBGP partial wave for bbgp
```

controls optimisation of scaling parameters

```
&SMINIM NZION=15 INCLUD=20 NLAM=16 NVAR=6 LL0WMN=1 JI0WMX=1 JI0WMN=1 JI0WMX=1 &END  
smimin namelist:  
1.0 1.0  
1.0 1.0 1.0  
1.0 1.0 1.0 1.0  
1.0 1.0 1.0 1.0 1.0  
1.0 1.0 1.0 1.0 1.0 1.0  
1.0 1.0 1.0 1.0 1.0 1.0  
1.0 1.0 1.0 1.0 1.0 1.0  
4,5,6,7,8,11
```

It can be used from the command line or via the interactive ADAS code **ADAS701**.

controls free electron energy ranges and grid for cross-sections

```
&SRADDON MENG=-14 EMIN=0.003 EMAX=3 NDE=4 MENG=-1 &END  
sraddcon namelist:  
0.110518 0.167285 0.77000 3.00000
```

3.3 Using AUTOSTRUCTURE for dielectric recombination

An original purpose of AUTOSTRUCTURE was the calculation of state selective dielectronic recombination coefficients.

The input data set is a driver of data format *adf27* of sub-category *dr*. It is designed to create dielectric data tuned to bundle-n and bundle-nl population models.

The dataset name:
`./adf27/dr/lilike/jc00#li/mg9ic22-n.dat`

informs that it is a lithium-like Mg^{+9} which is recombining via **2-2** parent transitions capturing into higher n states.

The driver can be used interactively by the code **ADAS701** or offline by **ADAS7#1**. It creates a number of datasets including the **o/g** file and the **o/s** and **o/ic** files of Auger rates in **/s** and **/ic** coupling.

The code **ADAS702** assembles energy level, transition probability and Auger data to obtain dielectronic coefficients of format *aaafg9.*

The ADAS project has a long history dating from ~1990 of dielectronic data preparation to the *adf09* format. Originally prepared in /s coupling, since 2000, it has been prepared also in /ic coupling. Isoelectronic sequences up to Al-like have been completed spanning elements up to zinc. The drivers are archived similarly in format *adf27/dr*.

```

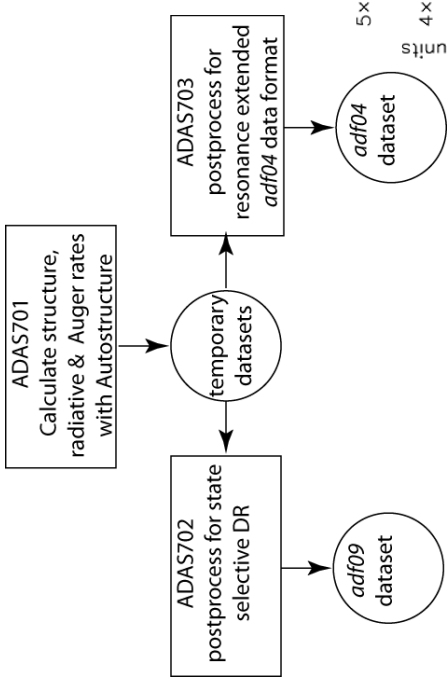
S.S.          'Mg9+ 2-2,n'
dielectronic 13517
case          12518 1251A
              13519
              22 12513 23 12517
              10 20 21      801900901902
              &SALGEB RUN='DR' RAD='YES' CUP='IC' KORB2=1 &END
              &DRR NMIN=3 NMAX=15 JND=14 LMIN=0 LMCON=3 &END
              16    25 35 45 55 70 100 140 200 300 450 700 999
              &SMINIM NZIN= 12 PRINT='UNIFORM' MCFMX=8 &END
              1     8   1   0   0   1   2
              &SRADCON MENG= 1.5 &END ranges for
              0.00000 3.00000 nL electron

```

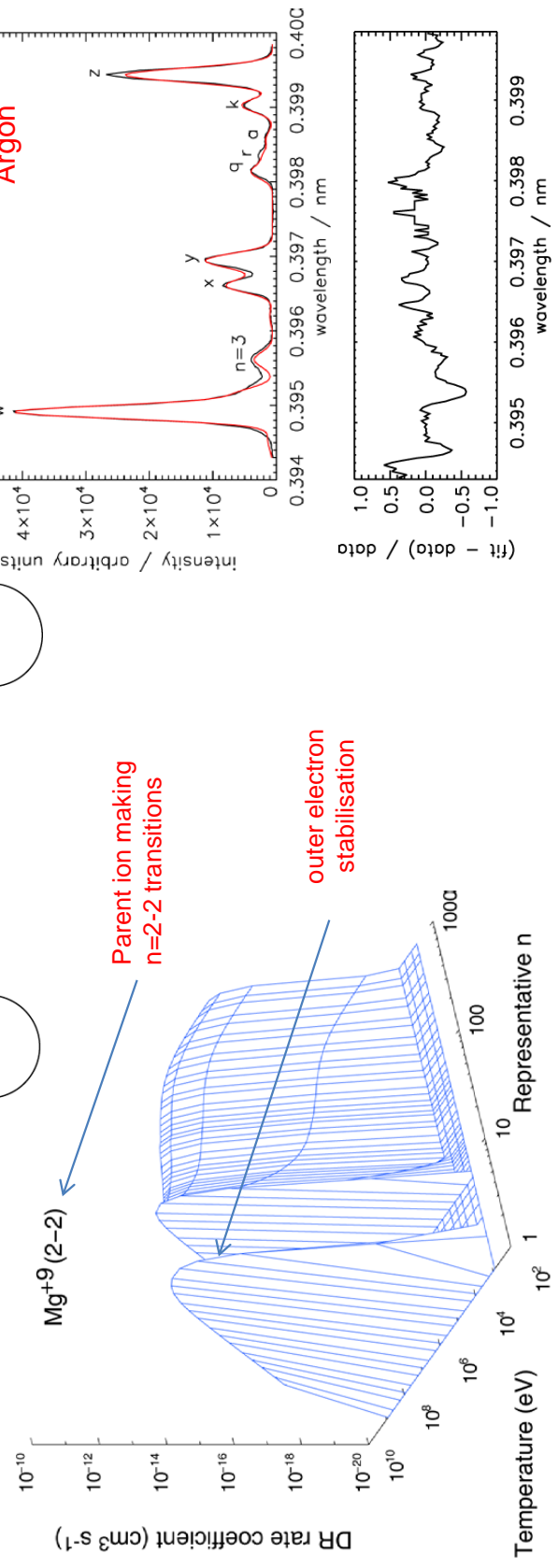
JND representative
bundle-n shells

3.4 Postprocessing Auger data for ADAS applications

The adf09 database is one of the most important parts of ADAS. It is noted that correct modelling of dielectronic recombination in plasmas requires attention to capture to quantum shells as high as $n \sim 1000$.



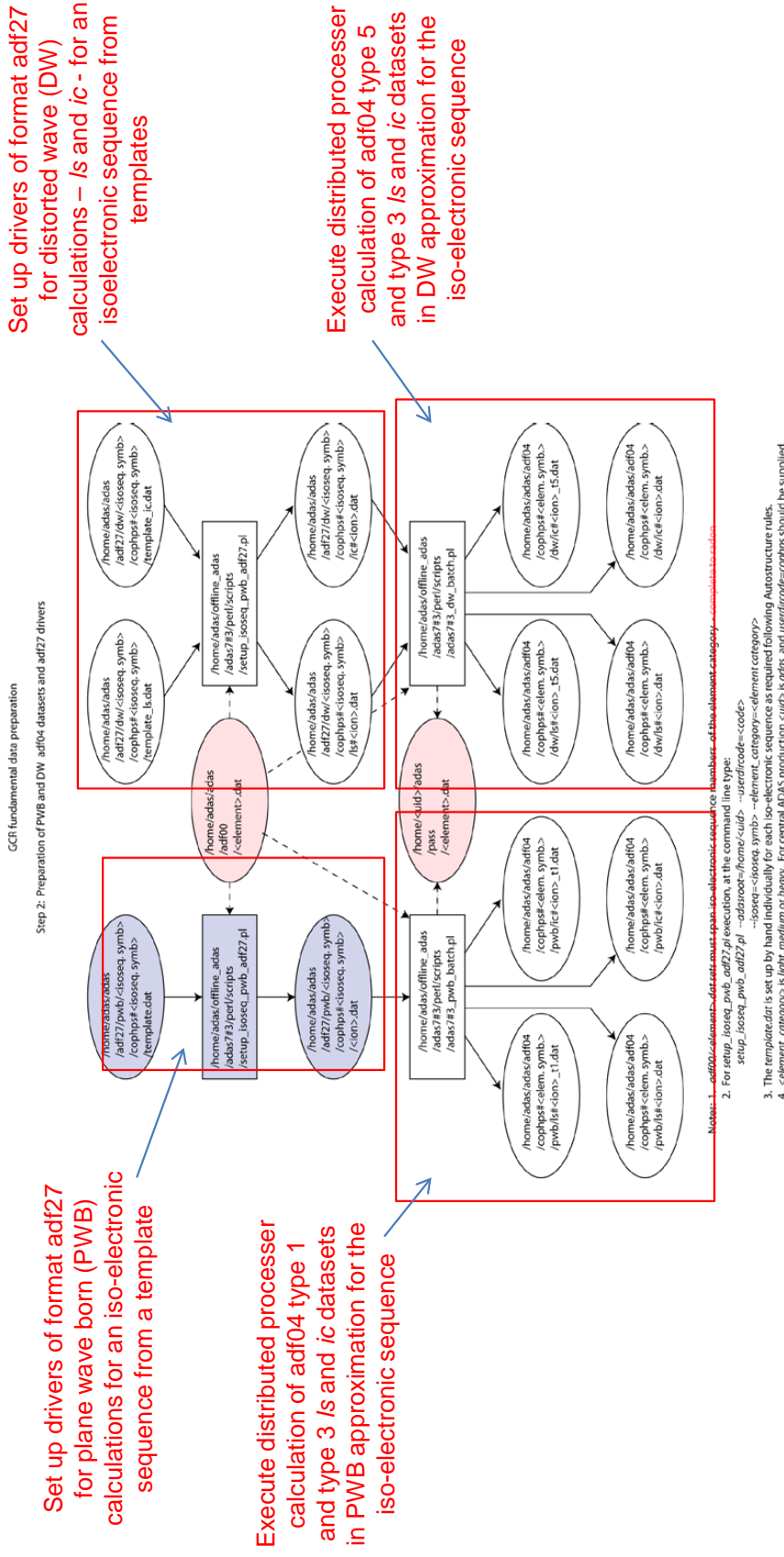
The ADAS703 processing path creates an enhanced adf04 dataset which includes resonance capture and Auger breakup transition data lines. So satellite line modelling is enabled. Results below are from [ADAS605](#).



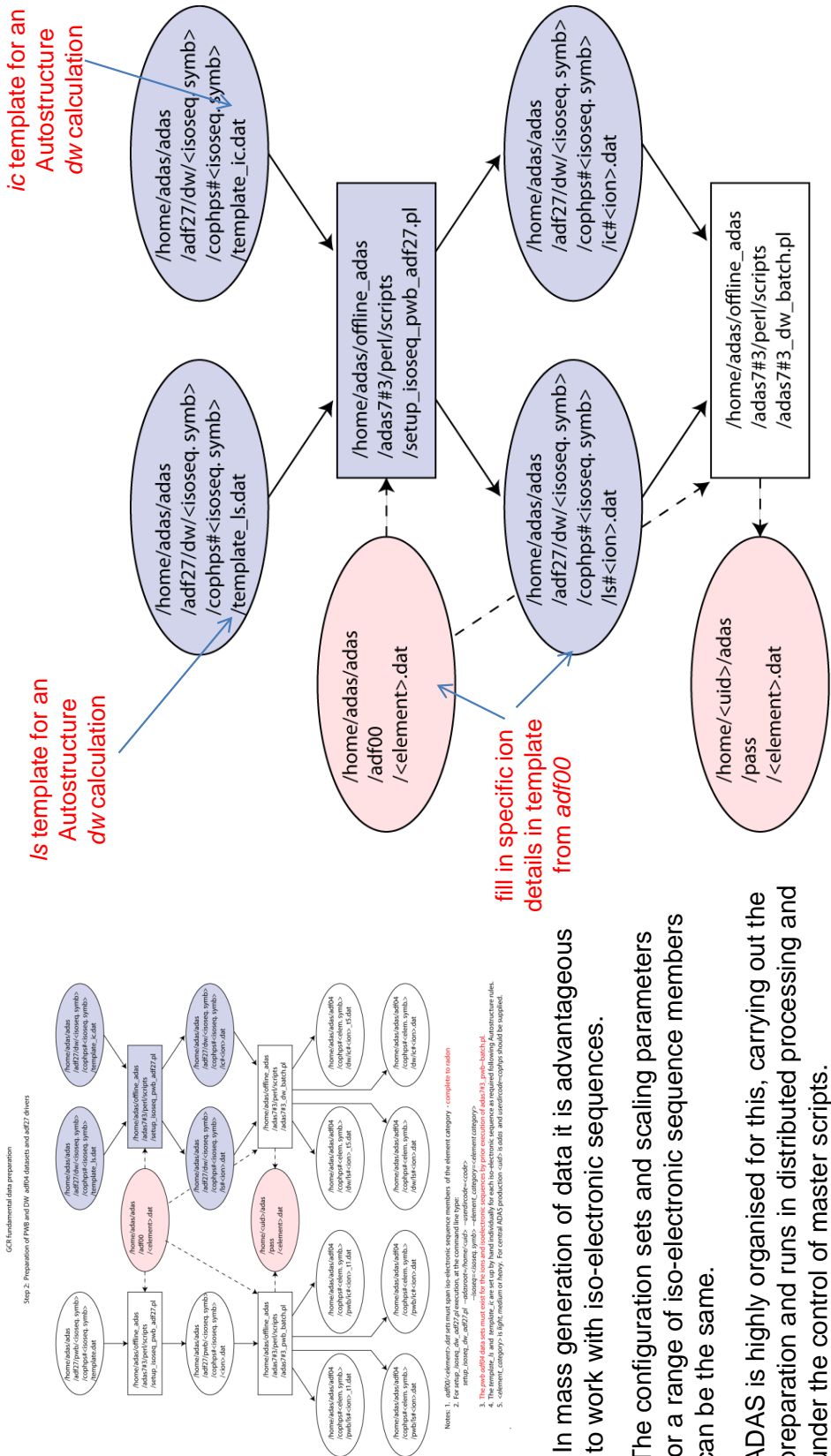
3.5 Current extensions of dielectronic calculations

- On progressing to systems with more electrons, the size of *adf09* datasets has increased markedly. It is unlikely that further large scale production in the standard *adf09* **ic** pattern will be produced.
- The complexity of heavy element ions has caused us to introduce a new hybrid approximation, combining an **ic** parent description with a configuration average intermediate state representation. This is much more economical in space requirements and ideally tuned to the bundling population models to be used for heavy species ions. This method will be introduced in ADAS and AUTOS releases in the near future.
- Dielectronic recombination at very low electron temperatures, typical of **photo-ionised** plasmas has been under extensive revision in recent years. The general assumption that dielectronic recombination gives way to radiative recombination at very low temperatures is not sustained, due to the common occurrence of ‘at threshold’ dielectronic resonances.
- Special measurements for W⁺²⁰ obtained for ADAS-EU reveal extremely large resonance contributions which influence effective recombination markedly even up to electron-excited plasma temperatures.
- Theoretical examination of the problem, suggest that its origin lies in strong interaction of many configurations best described as an ergodic-like spreading of Auger rates amongst very many doubly excited states. Current calculations, near threshold begin to reproduce the experimental results. We anticipate these effects being introduced into the dielectronic data as we progress into the difficult heavy element ions.

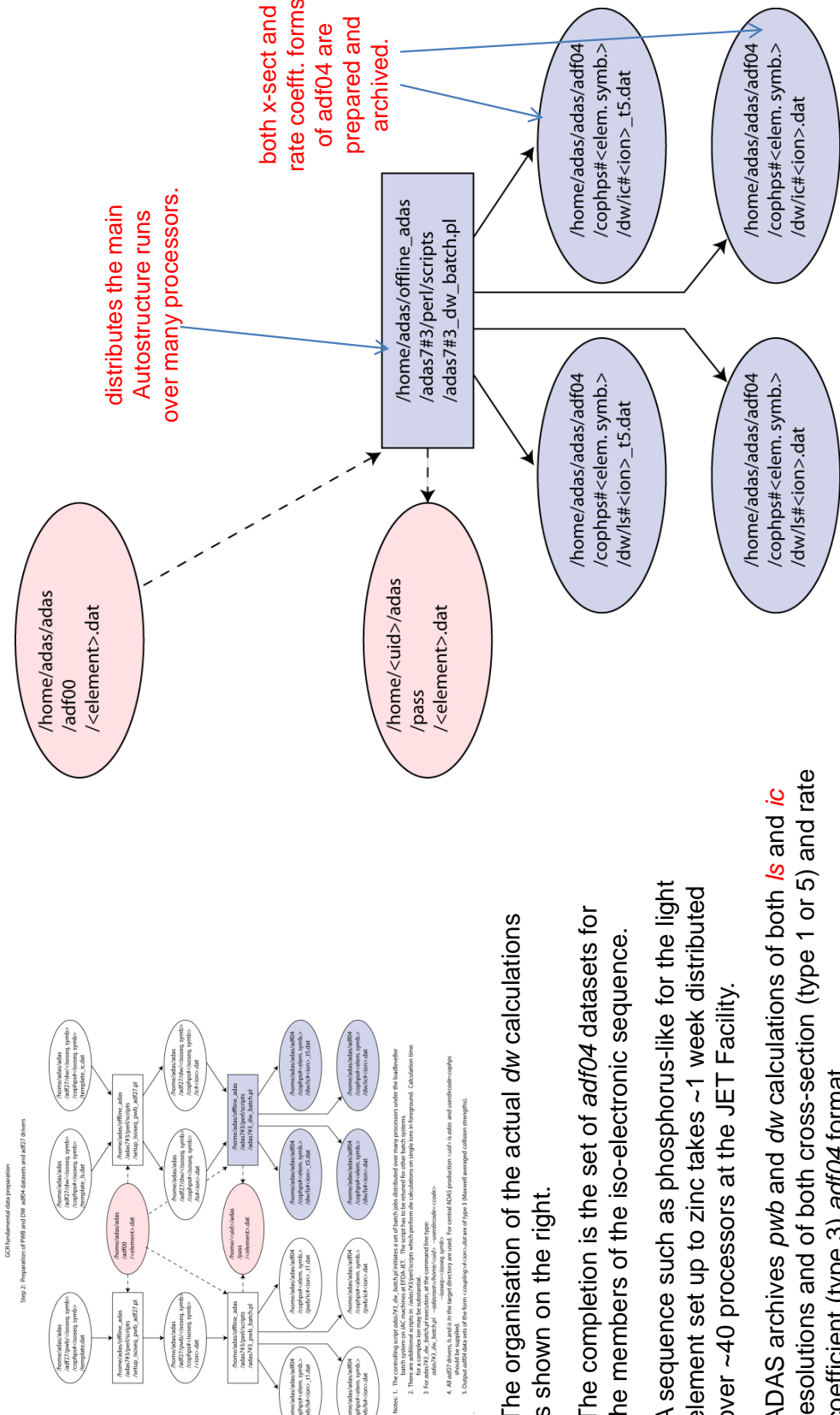
4.1 AUTOSTRUCTURE PWB and DW mass production



4.2 Creation of adf27 DW drivers from templates



4.3 Production of adf04 type 5 and type 3 datasets from adf27 driver



4.4 Neutral and near neutral ion level adjustments

The neutral and near-neutral atoms are the most difficult systems to calculate, since the electron-electron Coulomb potential is not dominated by the Coulomb interaction with the nucleus.

Much more extensive configuration interaction must be included and optimisation of potential scaling parameters. In spite of this, level energies are insufficiently precise for spectroscopy and must be adjusted.

The National Institute of Standards and Technology (NIST) is the primary atomic energy level source. ADAS uses periodic automatic scanning of NIST to assemble ***ls*** and ***ic adf04*** data sets of energy levels without collisional data archived element directories as:

`/.../adas/adf04/nist#<at: numb.>/`

ADAS uses these data for Autostructure adjustment. ADAS also has special codes for matching and merging *adf04* datasets: [/adas705/q5mrg4for](#)

A.S. P-like p0 structure - energies + radiative rates + dw adi04 type 5
 45HGES RUN=1DE-4 CUP='ICM' RAD=511 RACONF=3 MAXORB=13 KCORR=1 KCORR2=3
 RCUP=23

ICFG=2 NMETA=194 KPOL=8 REND

3.0 3 1 3 2 4 0 4 1 4 2 3 5 0 5 1 5 2 5 3 5 4 6 0

0 0 0 10*0
 2 5 3 10*0 3
 1 2 0 10*0
 2 3 0 10*1
 2 3 0 10*0 1
 0 0 0 10*0
 2 5 3 10*1
 1 4 0 10*1 1

1.4 0 10*0 1
 ECORR=0. 848 END

1.0 1.0 1.0
 1.09735 1.11768 -32293
 1.12729 -11851 1.32293 1.00000
 1.13058 1.11835 1.32293 1.00000 1.00000

1.110558
 0.110518 0.167285 0.77000 3.00000

6SRDCON MENG=-14 EMTN=0.003 EMXN=3 NDE=4 MENGI=-1 &END

dw run

ic coupling

optimised scaling parameters

SHFTLS file of term adjustments from NIST

NIST wave numbers

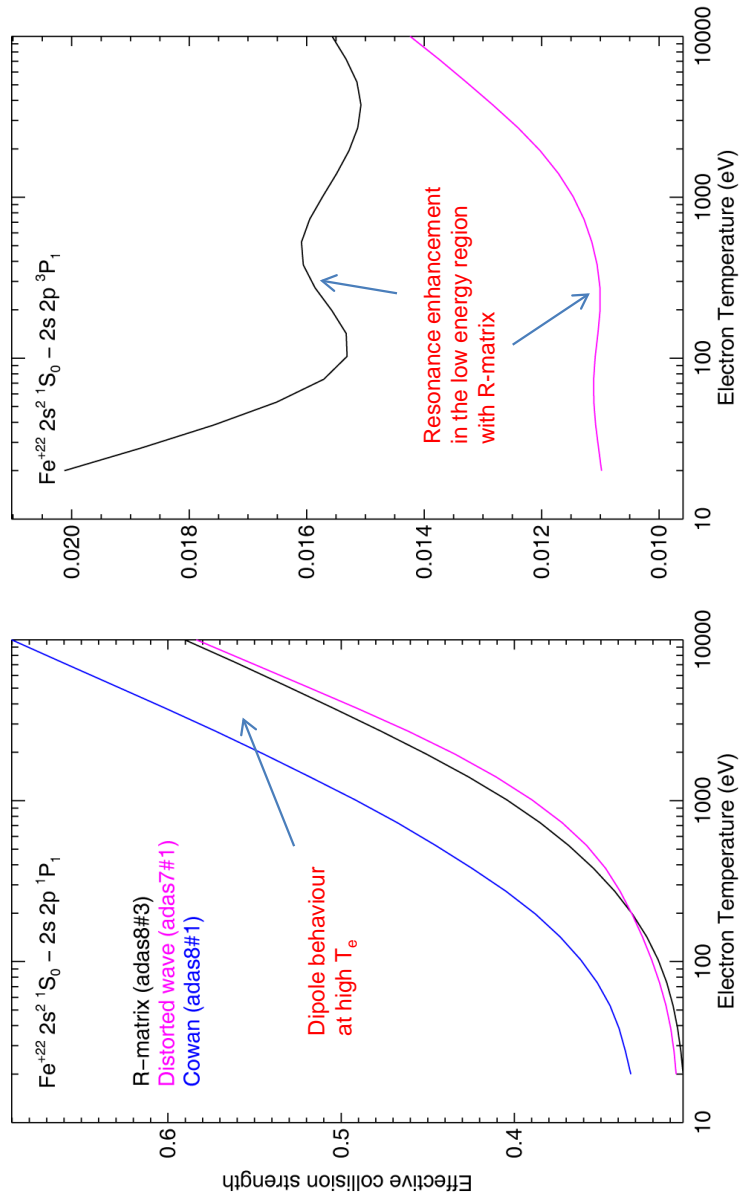
adf04 type 5

spin-changing transition

term algebraic index T

4.5 Cross-section illustrations and comparisons

There is no valid Born cross-section for this spin change transition although residual weak spin breakdown does give a non-zero cross-section



5.1 The R-matrix method and electron impact cross-sections

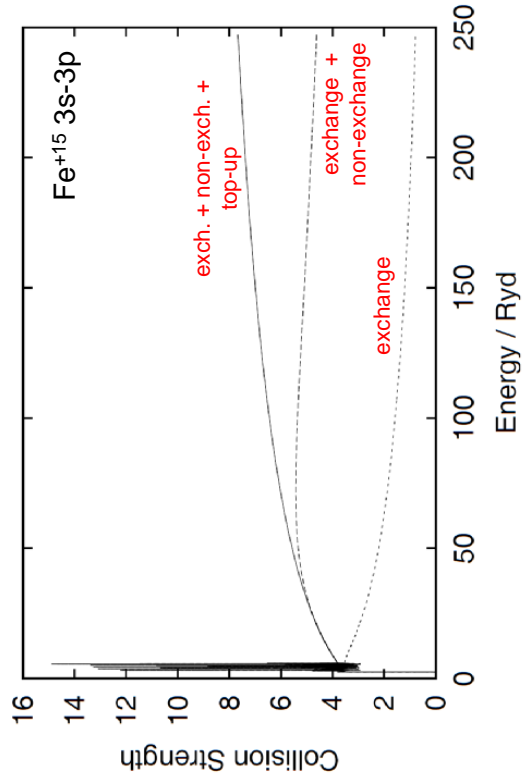
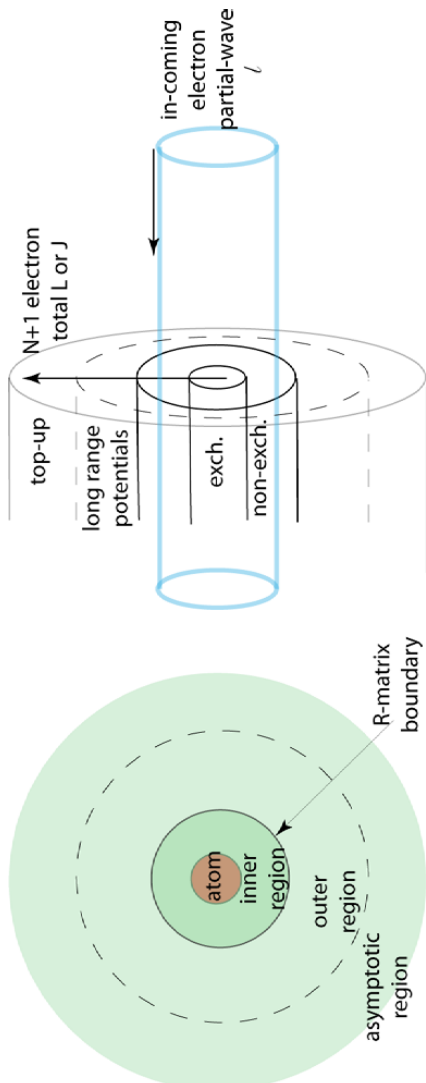
The R-matrix method is the most versatile, high precision method available for calculation of electron impact excitation cross-sections.

It treats resonant structure in the N+1-electron system correctly at root, but is a complex method which is demanding on computer resources.

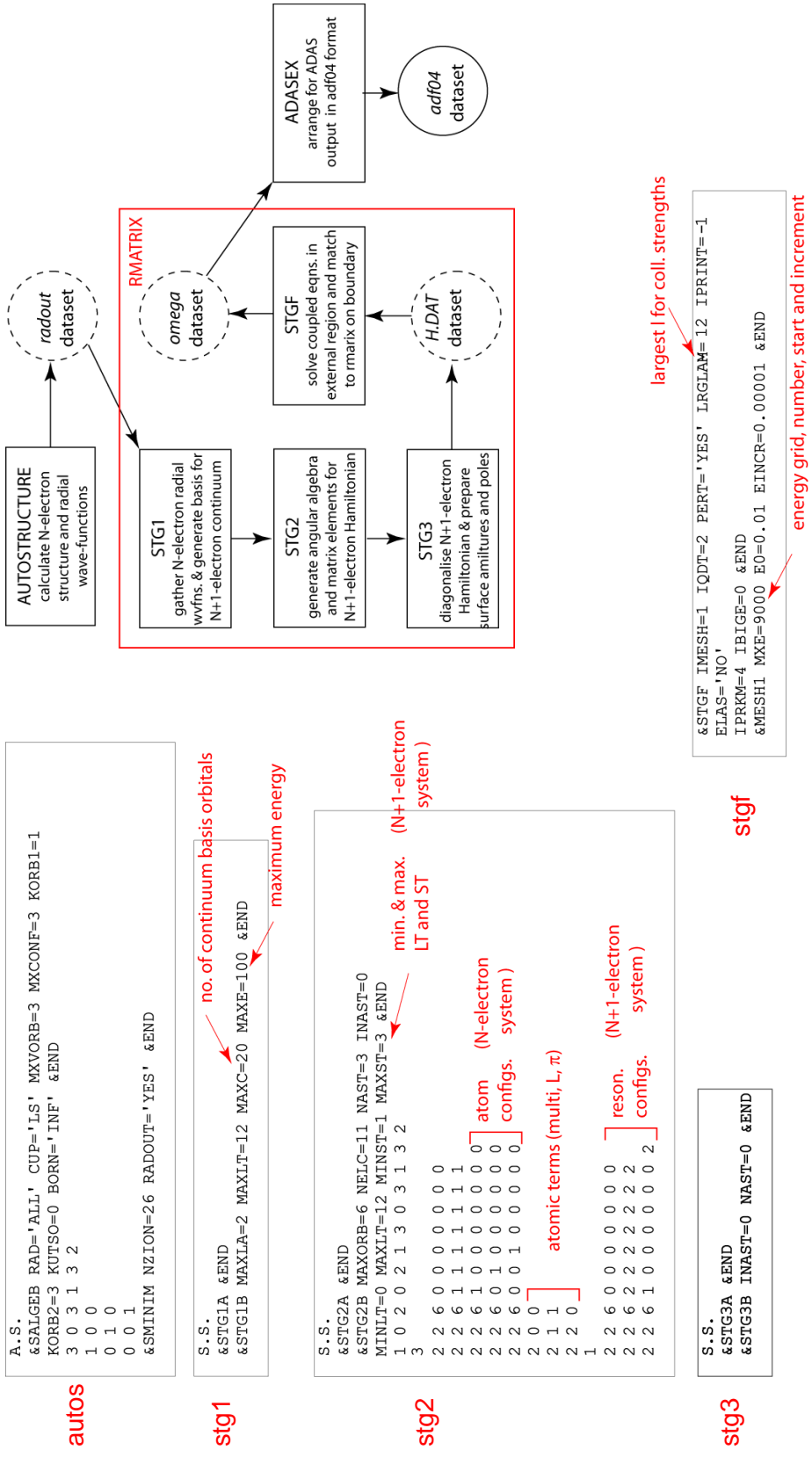
The variants are able to handle light systems in **1s** coupling, semi-relativistic systems in Breit-Pauli **1C** coupling and fully relativistic systems in the Dirac formalism.

With inclusion of pseudo-states, it can address neutral and near-neutral systems – including ionising collisions.

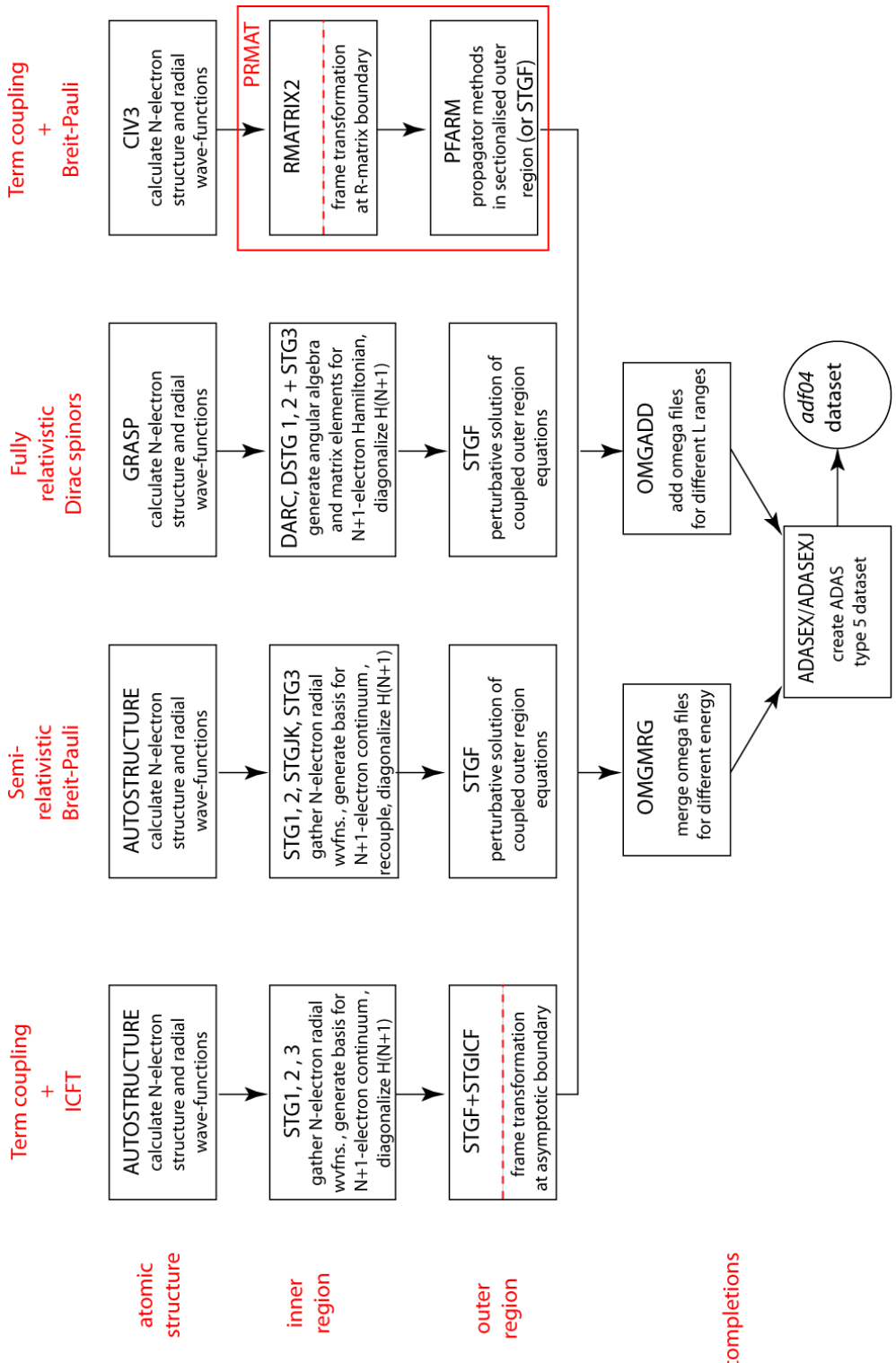
Most current development and production using R-matrix methods are coordinated between Strathclyde University, Auburn University and Queen's University of Belfast and are closely linked to the ADAS Project.



5.2 Using the R-matrix method with ADAS: Fe⁺¹⁵



5.3 The current family of R-matrix method implementations



5.4 Participation in R-matrix calculations

The preparations and infrastructure required for R-matrix calculations for the new species and ions of current interest for fusion are substantially beyond the usual needs of ADAS codes. Most calculations require parallel computing capabilities and often the power of massively parallel supercomputers.

It has usually been most fruitful and likely of success, to work closely with the Strathclyde/Auburn/ADAS teams in a first development, so that insight and experience can be communicated efficiently and work coordinated. Thereafter, trained researchers can progress satisfactorily back in their home laboratories.

Further information on the R-matrix codes is available <http://amdp.phys.strath.ac.uk/tamoc/>. The recent user manual for the current parallel R-matrix codes, prepared by Ballance and Griffin, is added as an appendix to the lecture notes for module 7.

The ADAS implementation is to be found in the directory `/home/adas/offline_adas/adas8#3/`. A *Makefile* downloads the current code versions and creates and compiles the codes. A user password is required to access the download site. A PERL script for execution of a basic R-matrix run is available as `adas8#3.pl`. These require adjustment for specific local conditions and computer resources.

6.1 Conclusions

- The ADAS team and its coworkers have built up a very large capability for the calculation of the atomic structure of arbitrary atoms and ions and of electron impact collisional cross-sections with them.
- The ADAS fundamental data formats, including *adf04*, *adf07*, *adf08*, *adf09* provide one of the largest resources of such data in the world.
- ADAS can bring to bear three major atomic structure codes and four major cross-section calculation codes. These collectively provide very wide species coverage at baseline precision through to highest precision, leading-edge calculations for specific high-priority ions.
- ADAS-EU sub-contracting collaborations have been of major importance in refining treatments of special cases, such as neutral atoms and in clarifying behaviour in the most complex systems. The going ADAS research program is extending these collaborative linkages and enabling greater penetration of special studies into the collisional domain.
- Fundamental data production by ADAS and its coworkers is tuned to exploitation in the various collisional-radiative models of ADAS and to the production of the derived data required for application.
- ADAS can at some level address all elements and their ions occurring in the present fusion plasma environments and in the expected ITER environments.

B.8 module_8



Module 8

Spectral diagnostics for special environments – the interface between
fusion and astrophysics

Lecture viewgraphs

Hugh Summers, Martin O'Mullane and Alessandra Giunta

University of Strathclyde

Contents

1. Introduction.
2. Emissivities, line ratio studies and contribution functions.
3. Differential emission measure (DEM) analysis.
4. Escape probabilities and opacity.
5. Non-Maxwellian electron distributions.

1.1 Atomic physics of astrophysical plasmas – the connection to fusion

Atomic physics of plasmas has application in many areas of astrophysics:

1. The solar upper atmosphere
 2. Gaseous and diffuse nebulae
 3. Emission from cometary plasma
 4. Black hole accretion disks and columns
- a. Electron-excited or photo-excited
- b. Tenuous or dense
- c. Optically thick or thin
- d. Transient or stationary
- e. Thermal or non-thermal electrons

These areas emphasise particular plasma atomic physics scenarios, such as

We wish to explore if the ADAS studies of astrophysical plasmas can assist in analysing new situations of concern for current fusion plasma and ITER. It is evident that the **solar plasma** has exceptional spectral observations from spacecraft such as SOHO and can give us special insight.

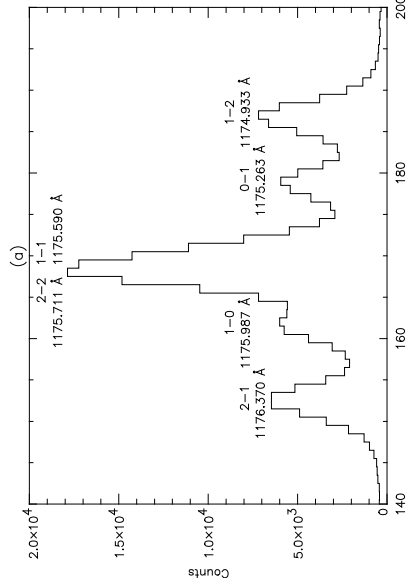
This means atomic physics parameter space of: a - **electron excited**; b - **low to intermediate density**; c - **mostly thin**; d - **both**; e - **mostly thermal**.

1.2 SUMER spectrum lines form CIII

The top figure shows a small portion of a spectrum from the SUMER UV spectrometer on the SOHO spacecraft looking at the sun.

It shows J-resolved components of the CIII ($2s2p\ ^3P - 2p^2\ ^3P$) multiplet.

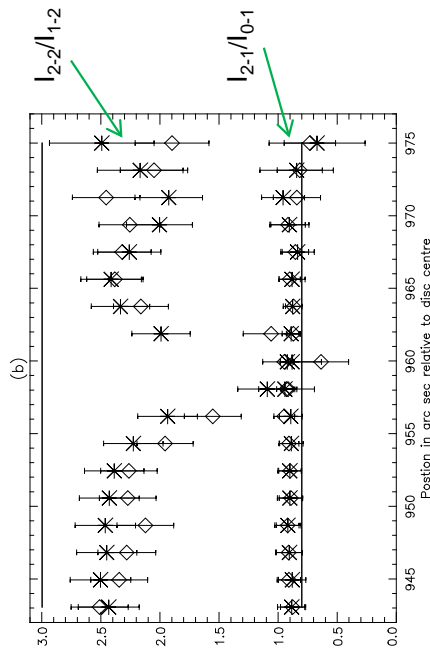
CIII lines are important in deducing lower chromosphere density/variation with height, that is **emission measure**.



The lower figure shows two ratios of different component line intensities - the upper is I_{2-2}/I_{1-2} and the lower I_{0-1}/I_{1-2} .

Observations are made at different positions scanning across the limb of the sun.

Both the lines of each ratio originate from the same upper level.

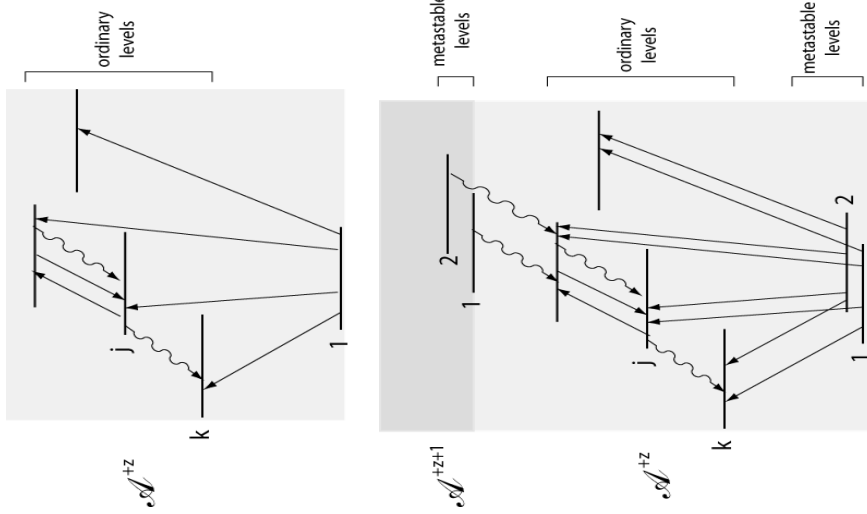


These are **electron-excited** lines and one ratio shows the effects of **opacity** at the limb.

1.3 Approximate photon emissivities

Excited population modelling solves the statistical balance equations of an ion \mathcal{A}^{+z} . Most simply, the excited populations N_j are solved in equilibrium with respect to the ground population N_1 . Then the emissivity in a transition j to k is

$$\epsilon_{j \rightarrow k} = A_{j \rightarrow k} N_j = \mathcal{P} \mathcal{E} \mathcal{C}_{j \rightarrow k} N_e N_1$$



Properly

$$\epsilon_{j \rightarrow k} = A_{j \rightarrow k} \left(\sum_{\sigma=1}^{M^{(z)}} \mathcal{F}_{j\sigma}^{(exc)} N_e N_\sigma + \sum_{\nu'=1}^{M^{(z+1)}} \mathcal{F}_{j\nu'}^{(rec)} N_e N_{\nu'}^+ + \sum_{\mu'=1}^{M^{(z-1)}} \mathcal{F}_{j\mu'}^{(CX)} N_H N_{\nu'}^+ + \sum_{\mu'=1}^{M^{(z+1)}} \mathcal{F}_{j\mu'}^{(ion)} N_e N_{\mu'}^- \right)$$

where excited, N_j , and metastable, N_σ , populations are distinguished, and solution is for excited populations in quasi-equilibrium with metastables. Recombination, charge exchange and inner shell ionisation are included – called generalised-collisional-radiative , *GCR*, modelling.

1.4 Generalised collisional-radiative photon emissivities

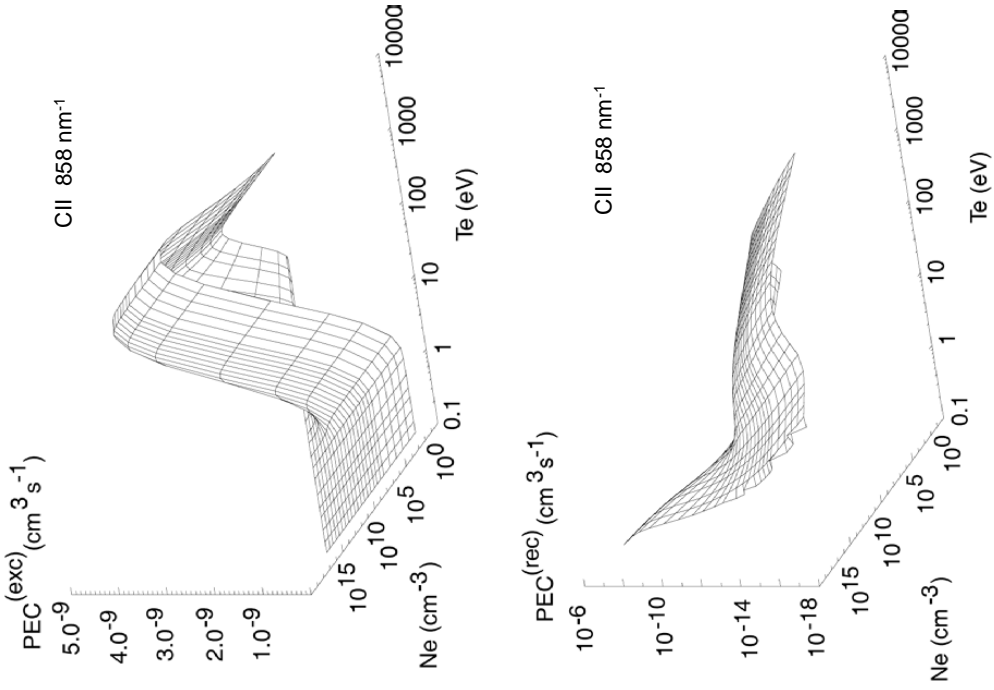
The partial photon emissivity coefficients are prepared and archived as ADAS data format ADF15.

$$\mathcal{PEC}_{\sigma,j \rightarrow k}^{(exc)} = A_{j \rightarrow k} \mathcal{F}_{j\sigma}^{(exc)}$$

$$\mathcal{PEC}_{\nu',j \rightarrow k}^{(rec)} = A_{j \rightarrow k} \mathcal{F}_{j\nu'}^{(rec)}$$

$$\mathcal{PEC}_{\nu',i \rightarrow k}^{(CX)} = A_{j \rightarrow k} \mathcal{F}_{i\nu'}^{(CX)}$$

$$\mathcal{PEC}_{\sigma,j \rightarrow k}^{(ion)} = A_{j \rightarrow k} \mathcal{F}_{j\mu'}^{(ion)}$$



They are resolved by transition, primary driver, metastable and depend on T_e and N_e in general.

2.1 Emissivities and line ratio studies.

For two lines driven primarily by excitation, the intensity ratio is simpler for diagnostic deductions.
It is usually helpful to work with line sets. If recombination is ignored

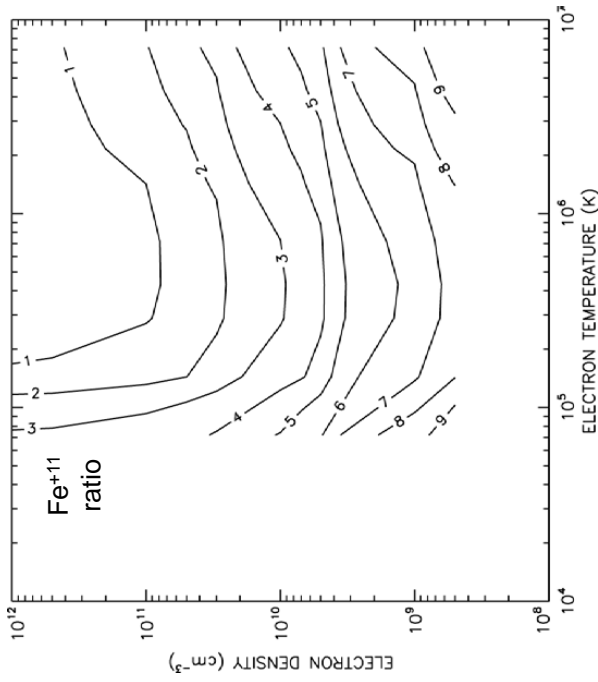
$$\frac{\epsilon_{G_1}}{\epsilon_{G_2}} = \frac{\sum_{j \in J_G, k \in K_G} \mathcal{PEC}_{1,j \rightarrow k}^{(exc)} + N_e N_1 \sum_{j \in J_G, k \in K_G} \sum_{\sigma, \sigma \neq 1} \mathcal{PEC}_{\sigma, j \rightarrow k}^{(exc)} \left(\frac{N_\sigma}{N_1} \right)}{\sum_{j' \in J'_G, k' \in K'_G} \mathcal{PEC}_{1,j' \rightarrow k'}^{(exc)} + N_e N_1 \sum_{j' \in J'_G, k' \in K'_G} \sum_{\sigma', \sigma' \neq 1} \mathcal{PEC}_{\sigma', j' \rightarrow k'}^{(exc)} \left(\frac{N_{\sigma'}}{N_1} \right)}$$

Then, the character of the metastables must be considered. If

$$\left(\frac{N_\sigma}{N_1} \right) \approx \left(\frac{N_\sigma}{N_1} \right)_{eq} \quad \text{or} \quad \approx 0$$

a ratio depending only on T_e and N_e results.
Contour plots of the ratio show the important sensitivities. See [ADAS205](#), [ADAS207](#).

More careful approaches uses the PECs directly.
See [run_adas208.pro](#), [read_adf15.pro](#).



2.2 Line-of-sight intensity

The intensity of emission in the spectrum line j to k from a column of plasma of area A .

$$I_{j \rightarrow k} = \frac{1}{4\pi A} \int \varepsilon_{j \rightarrow k} dV \text{ [photons cm}^{-2}\text{s}^{-1}\text{sr}^{-1}\text{]}$$

Consider the ionisation stages, \mathcal{A}^{+z} of element \mathcal{A} of nuclear charge z_0 . With $N_\sigma \equiv N_\sigma^{(z)}$

$$N_{tot} = \sum_{z=0}^{z_0} N^{(z)} = \sum_{z=0}^{z_0} \sum_{\sigma=1}^{M^{(z)}} N_\sigma^{(z)}$$

$$N_\sigma^{(z)} = \frac{N_\sigma^{(z)}}{N^{(z)}} \frac{N^{(z)}}{N_{tot}} \frac{N_{tot}}{N_H} \frac{N_H}{N_e} N e$$

Then neglecting recombination contributions to emissivity

$$I_{j \rightarrow k} = \frac{1}{4\pi A} \int_V \left(A_{j \rightarrow k} \sum_{\sigma=1}^{M^{(z)}} \mathcal{F}_{j\sigma}^{(exc)} \frac{N_\sigma^{(z)}}{N^{(z)}} \frac{N^{(z)}}{N_{tot}} \right) \frac{N_{tot}}{N_H} \frac{N_H}{N_e} N_e^2 dV$$

$$\approx \frac{1}{4\pi A} \left(\frac{N_{tot}}{N_H} \right) \left(\frac{N_H}{N_e} \right) \int_V \left(A_{j \rightarrow k} \sum_{\sigma=1}^{M^{(z)}} \mathcal{F}_{j\sigma}^{(exc)} \frac{N_\sigma^{(z)}}{N^{(z)}} \frac{N^{(z)}}{N_{tot}} \right) N_e^2 dV$$

2.3 Contribution functions

The excitation contribution function or GTN-function for a general plasma is

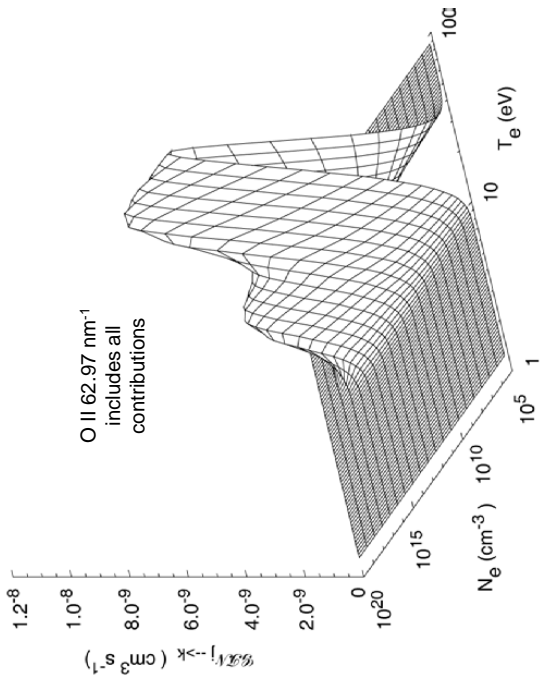
$$GJN_{j \rightarrow k}^{(exc)}(T_e, N_e) = \left(A_{j \rightarrow k} \sum_{\sigma=1}^{M^{(z)}} \mathcal{F}_{j\sigma}^{(exc)} \frac{N_\sigma^{(z)}}{N^{(z)}} \frac{N^{(z)}}{N_{tot}} \right)_{eq}$$

2-parm. family

The solar astrophysical contribution function or GTe-function is

$$G_{j \rightarrow k}(T_e, N_e(T_e)) = \left(A_{j \rightarrow k} \sum_{\sigma=1}^{M^{(z)}} \mathcal{F}_{j\sigma}^{(exc)} \frac{N_\sigma^{(z)}}{N^{(z)}} \frac{N^{(z)}}{N_{tot}} \right)_{eq} \left(\frac{N_H}{N_e} \right)$$

1-parm. family



ADAS has facilities for preparing GTe-functions in format [adf20](#). See [ADAS412](#). It can select GTe-functions from [adf20](#) into a collection file ready for DEM analysis. See [ADAS506](#).

ADAS can prepare GTN-functions of format [adf16](#) at the same time as executing an ionisation balance . See [ADAS405](#).

3.1 Differential emission measure (DEM) analysis.

Since $\frac{1}{A} \int N_e^2 dV \approx \int N_e^2 \frac{dh}{dT_e} dT_e$ define the differential emission measure as $\Phi(T_e) = N_e^2 \frac{dh}{dT_e}$

If $\mathcal{A}(z_0) = \frac{N_{tot}}{N_H}$ is the fractional abundance of the element of nuclear charge z_0 , then for a suitable set of observed spectral intensities $I_i : i = 0, \dots, m$ with known theoretical GTE-functions

The integral equation $I_i = \frac{1}{4\pi} \int_{T_1}^{T_2} \mathcal{A}(z_0) G_i(T_e) \Phi(T_e) dT_e$ can be solved for the differential emission measure.

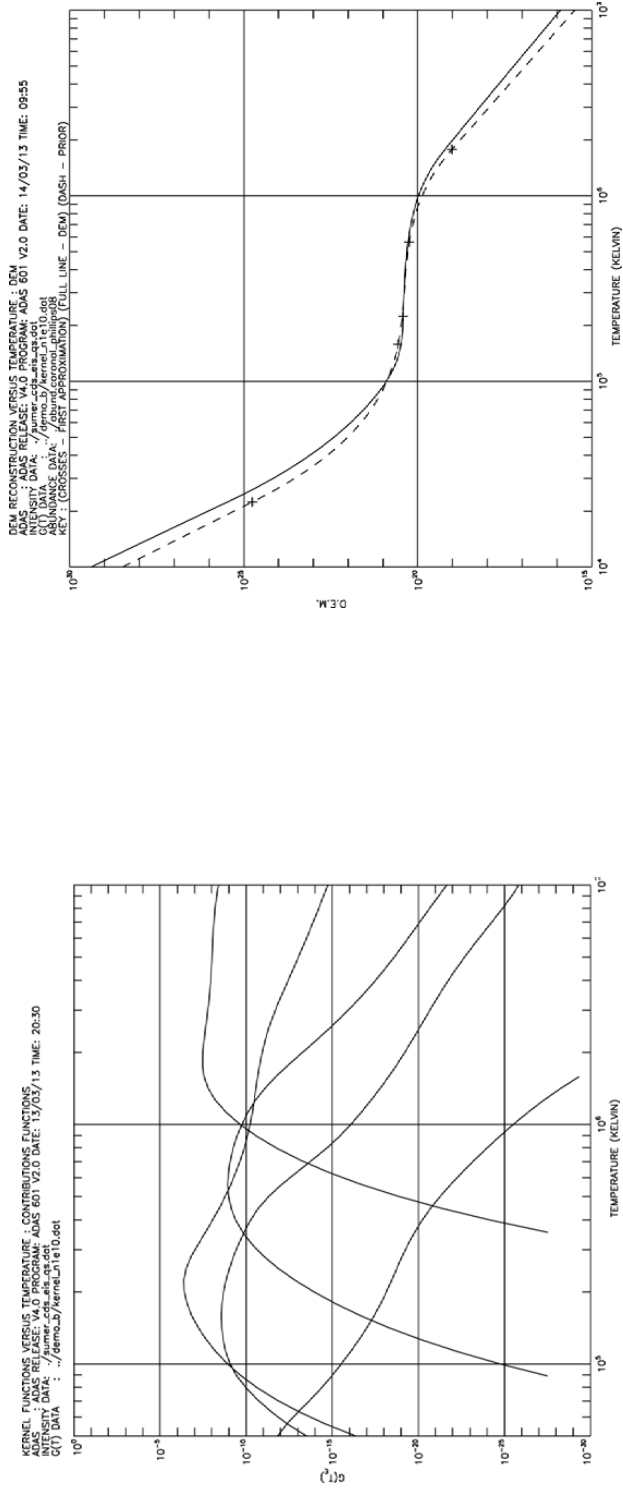
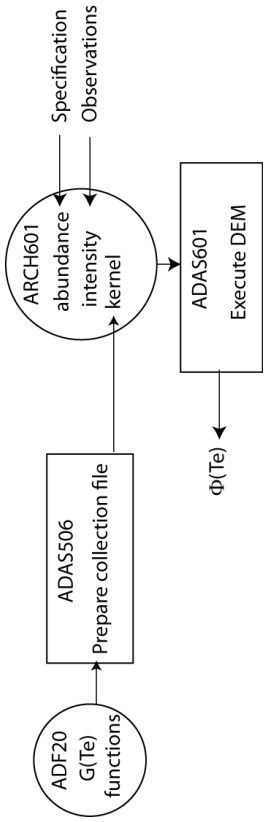
There is an extensive history of study and implementation of solutions of this system. ADAS uses the methodology of Thompson. ADAS staff and collaborators (Giunta & Lanzafame) have worked intensively on refinement of the method, implemented as code [ADAS601](#) - summarised in the notes for the lecture.

3.2 DEM implementation.

The schematic shows the principal ADAS steps, datasets and codes.

1. Collection of a targetted set of $G(T_e)$ functions spanning the required T_e range – shown below.

2. The final DEM – shown below right



4.1 Escape probabilities and opacity.

The emission from an optically thick plasma is characterised by the equations of radiative transfer and of statistical balance.

$$\frac{dI_\nu(s)}{ds} = J_\nu(s) - \kappa_\nu(s)I_\nu(s)$$

$$\frac{dN_u(\vec{r})}{dt} = -A_{u\rightarrow l}N_u(\vec{r}) + \frac{4\pi}{c}B_{l\rightarrow u}N_l(\vec{r}) \int \bar{I}_\nu(\vec{r})\phi_a(\nu)d\nu$$

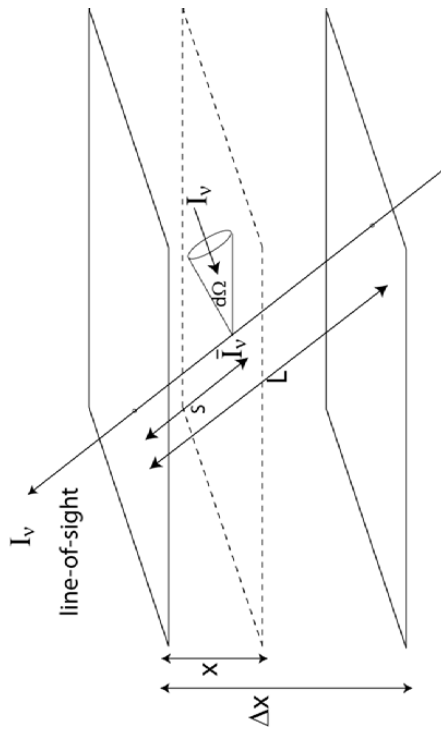
emission coefficient

absorption coefficient

The equations can be rewritten as

$$\frac{dI_\nu(s)}{ds} = \frac{1}{4\pi}A_{u\rightarrow l}N_u(s)g(s)$$

$$\frac{dN_u(\vec{r})}{dt} = -A_{u\rightarrow l}N_u(\vec{r})\Lambda(\vec{r}) + \text{other terms}$$



$g(s)$ is the **emergent flux escape factor**.

$\Lambda(\vec{r})$ is the **absorption factor** or
population escape factor.

4.2 Line-of-sight averaged escape probability, $\bar{g}\{\tau_0\}$.

For Doppler emission and absorption profiles of Doppler width $\Delta\nu_D$

$$\phi_e(\nu) = \phi_a(\nu) \equiv \phi(\nu) = \frac{1}{\sqrt{\pi\Delta\nu_D}} \exp\left\{-\left(\frac{\nu - \nu_0}{\Delta\nu_D}\right)^2\right\}$$

With a line-of-sight $s : 0 \rightarrow L$

$$g(s) = \frac{1}{\sqrt{\pi}} \int_{-\infty}^{\infty} e^{-u^2} \exp\left\{-\tau_0(s)e^{-u^2}\right\} du$$

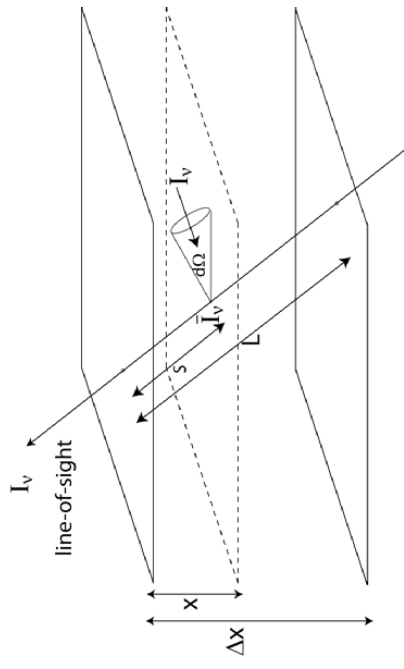
where $\tau_0(s) = \kappa_{0,l \rightarrow u}(L - s)$ is the line centre optical depth.

The total intensity, integrating through the layer, assuming constant density, is

$$I = \frac{1}{4\pi} A_{u \rightarrow l} N_u \bar{g}\{\tau_0\} L \quad \text{with} \quad \bar{g}\{\tau_0\} = \frac{1}{\sqrt{\pi}} \int_{-\infty}^{\infty} \left[\frac{1 - \exp\{-\tau_0 e^{-u^2}\}}{\tau_0} \right] du$$

and $\tau_0 \equiv \tau_0(s=0) = 1.16^{-6} \sqrt{M/T_i} \lambda_0 N_l f_{l \rightarrow u} L$

[T_i in K, M in amu, lengths in cm]



4.3 The absorption factor, $\Lambda(\vec{r})$

$$\begin{aligned}
 \bar{I}_\nu &= \frac{1}{4\pi} \int_0^{4\pi} I_\nu(\theta, \phi) d\Omega \\
 &= \frac{1}{4\pi} \int_0^{4\pi} \frac{\kappa_\nu}{j_\nu} [1 - e^{-\tau_\nu(\theta, \phi)}] d\Omega \\
 &= \frac{\kappa_\nu}{j_\nu} \overline{[1 - e^{-\tau_\nu(\theta, \phi)}]} \\
 &= \frac{\kappa_\nu}{j_\nu} \left[1 - e^{\overline{-\tau_\nu(\theta, \phi)}} \right]
 \end{aligned}$$

$$\text{where } \overline{\tau_\nu(\theta, \phi)} = \kappa_0 \phi(\nu) \bar{L} = \bar{\tau}_0 \phi(\nu)$$

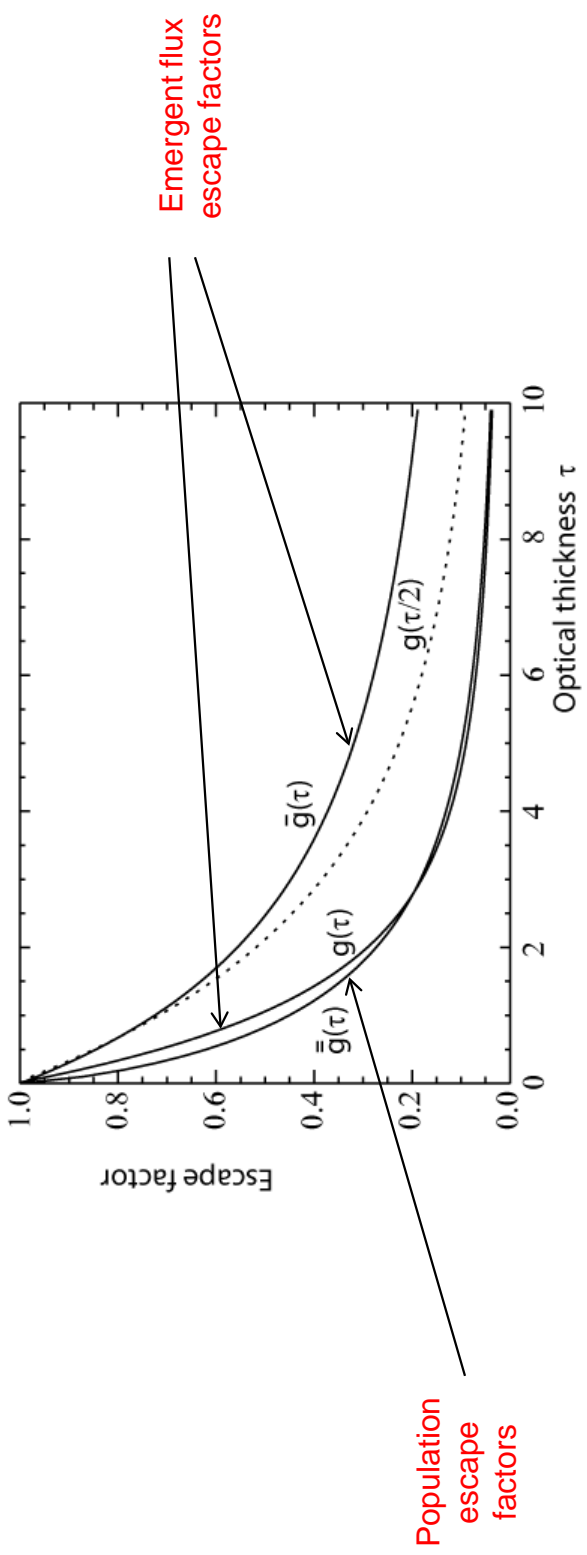
$$\text{Then } \Lambda(\vec{r}) = 1 - \frac{N_l(\vec{r}) \omega_u}{N_u(\vec{r}) \omega_l} \frac{c^2}{2\nu_0^2} \int \bar{I}_\nu(\vec{r}) \phi_a(\nu) d\nu$$

$$\Lambda(\vec{r}) = 1 - \frac{1}{\sqrt{\pi}} \int_{-\infty}^{\infty} [1 - \exp\{-\bar{\tau}_0 e^{-u^2}\} e^{-u^2}] du \equiv g\{\bar{\tau}_0\}$$

4.4 Various escape factors

For a semi-infinite layer of thickness D and perpendicular optical thickness τ_0 , at layer centre

$$\Lambda(\vec{r}) = \frac{1}{\sqrt{\pi}} \int_{-\infty}^{\infty} e^{-u^2} \left[\exp\left\{ \frac{-\tau_0 e^{-u^2}}{2} \right\} - \left\{ \frac{\tau_0 e^{-u^2}}{2} E_1\left\{ \frac{\tau_0 e^{-u^2}}{2} \right\} \right\} \right] du \equiv \bar{g}\{\tau_0/2\}$$



4.5 Application to solar observations

For two lines with common upper level u and lower levels l_1 and l_2 , the observed intensity ratio is

$$\frac{\bar{I}_{u \rightarrow l_1}}{\bar{I}_{u \rightarrow l_2}} = \frac{A_{u \rightarrow l_1} \bar{g}\{\tau_{0,l_1 \rightarrow u}\}}{A_{u \rightarrow l_2} \bar{g}\{\tau_{0,l_2 \rightarrow u}\}}$$

$$\text{but } \tau_{0,l_1 \rightarrow u} = \tau_{0,l_2 \rightarrow u} \frac{N_{l_1} f_{l_1 \rightarrow u}}{N_{l_2} f_{l_2 \rightarrow u}}$$

then find the $\tau_{0,l_1 \rightarrow u}$ which satisfies the intensity ratio taking the $\bar{g}(\tau)$ value ratio from the previous figure.

Infer the emergent flux escape factors and population escape factors for all other transitions from the ground or metastables.

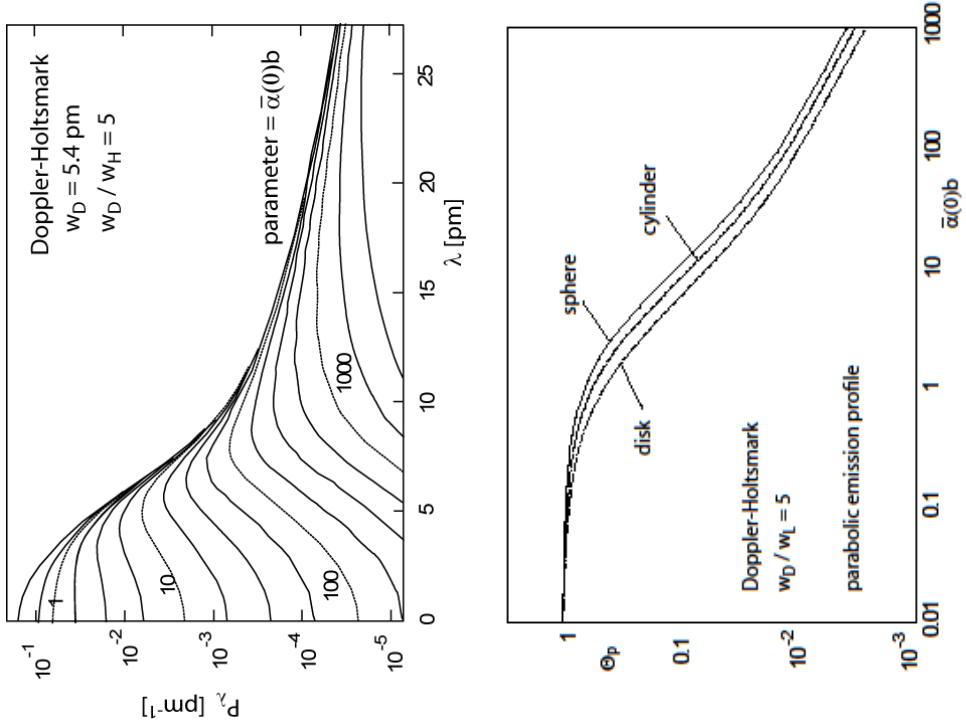
4.6 ADAS predictive modelling

ADAS214 calculates escape factors for emergent flux and for population calculations for simple plasma models and spectral line profiles.

Spectral profiles include Doppler, Lorentz, Holtsmark and convolutions of pairs of these.

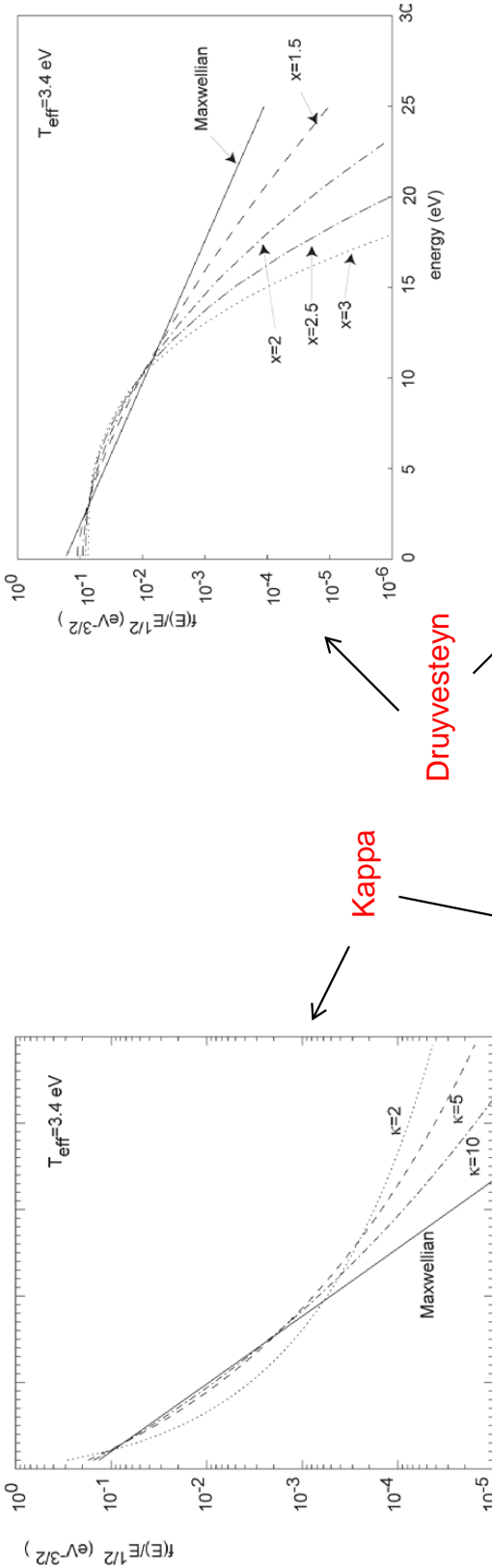
The population escape factor can be calculated in the centre of a plasma sphere, in the mid-plane of a disk and on the axis of a cylinder.

The code can be run for constant emission, linear or parabolic decrease from the plasma centre (or axis).



5.1 Non-Maxwellian electron distributions.

$$f_{T_e}(E) = \frac{1}{kT_e} \frac{2}{\sqrt{\pi}} \left(\frac{E}{kT_e} \right)^{1/2} \exp \left(-\frac{E}{kT_e} \right) \xleftarrow{\text{Maxwellian}}$$



$$f_{\kappa, E_\kappa}(E) = \frac{1}{E_\kappa} \frac{2}{\sqrt{\pi}} \left(\frac{E}{E_\kappa} \right)^{1/2} \kappa^{-3/2} \frac{\Gamma(\kappa+1)}{\Gamma(\kappa - \frac{1}{2})} \left(1 + \frac{E}{\kappa E_\kappa} \right)^{-(\kappa+1)} f_{x, E_x}(E) = \frac{x}{E_x^{3/2}} \frac{\Gamma(5/2x)^{3/2}}{\Gamma(3/2x)^{5/2}} E^{1/2} \exp \left(- \left[\frac{E \Gamma(5/2x)}{E_x \Gamma(3/2x)} \right]^x \right)$$

5.2 Reaction cross-sections and rate coefficients.

Consider the reaction



Maxwellian: detailed balance

$$\Upsilon_{ij}(T_e) = \int_0^{\infty} \Omega_{ij}(\varepsilon_j) \exp\left(-\frac{\varepsilon_j}{kT_e}\right) d\left(\frac{\varepsilon_j}{kT_e}\right)$$

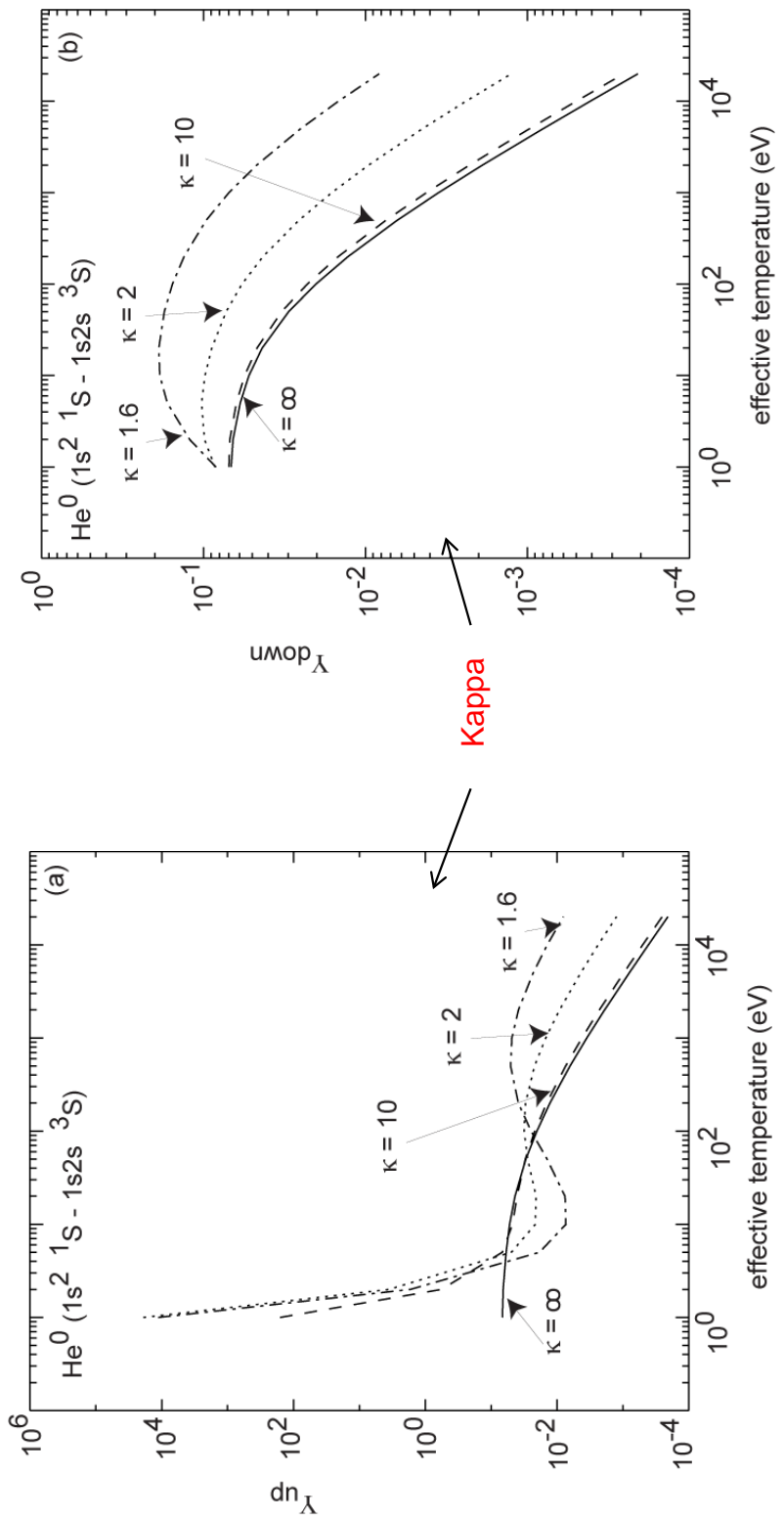
Non-Maxwellian: no detailed balance

$$\begin{aligned} \Upsilon_{i \rightarrow j}(T_{eff}) &= \frac{\sqrt{\pi}}{2} \exp\left(\frac{\Delta E_{ij}}{kT_{eff}}\right) \int_0^{\infty} \Omega_{ij}(\varepsilon_i) \left(\frac{\varepsilon_i}{kT_{eff}}\right)^{-1/2} f(\varepsilon_i) d\varepsilon_i \\ \mathcal{J}_{j \rightarrow i}(T_{eff}) &= \frac{\sqrt{\pi}}{2} \int_0^{\infty} \Omega_{ij}(\varepsilon_j) \left(\frac{\varepsilon_j}{kT_{eff}}\right)^{-1/2} f(\varepsilon_j) d\varepsilon_j \end{aligned}$$

$$\begin{aligned} q_{i \rightarrow j}(T_{eff}) &= 2 \sqrt{\pi \alpha c a_0} \left(\frac{I_H}{kT_{eff}}\right)^{1/2} \frac{1}{\omega_i} \exp\left(-\frac{\Delta E_{ij}}{kT_e}\right) \Upsilon_{ij}(T_e) \\ q_{j \rightarrow i}(T_{eff}) &= 2 \sqrt{\pi \alpha c a_0} \left(\frac{I_H}{kT_{eff}}\right)^{1/2} \frac{1}{\omega_j} \mathcal{J}_{j \rightarrow i}(T_{eff}) \end{aligned}$$

Effective mean energy parameter

5.3 Upsilonons and downsilons



5.4 Other rate coefficients

Dielectronic recombination and radiative recombination coefficients are straightforward.
Electron impact ionisation and three-body recombination are more complicated.

Fowler relation is the starting point

$$\omega_i E Q_{i \rightarrow+}(E; E', E'') = \frac{16\pi m}{h^3} \omega_+ E' E'' Q_{+ \rightarrow i}(E', E''; E)$$

Collisional ionisation

$$q_{i \rightarrow+} = \int_{I_i}^{\infty} \sqrt{\frac{2E}{m}} Q_{i \rightarrow+}(E; E', E'') f(E) dE \int dE' \int dE''$$

E is the incident energy,
E' and E'' the scattered
and ejected energies

$$\alpha_{+ \rightarrow i}^{(3)} = 8 \left(\frac{\pi a_0^2 I_H}{k T_{eff}} \right)^{3/2} \frac{\omega_i}{2\omega_+} e^{I_i/kT_{eff}}$$

Three-body recombination

$$\times \int_{I_i}^{\infty} \sqrt{\frac{2E}{m}} Q_{i \rightarrow+}(E; E', E'') f(E) dE$$

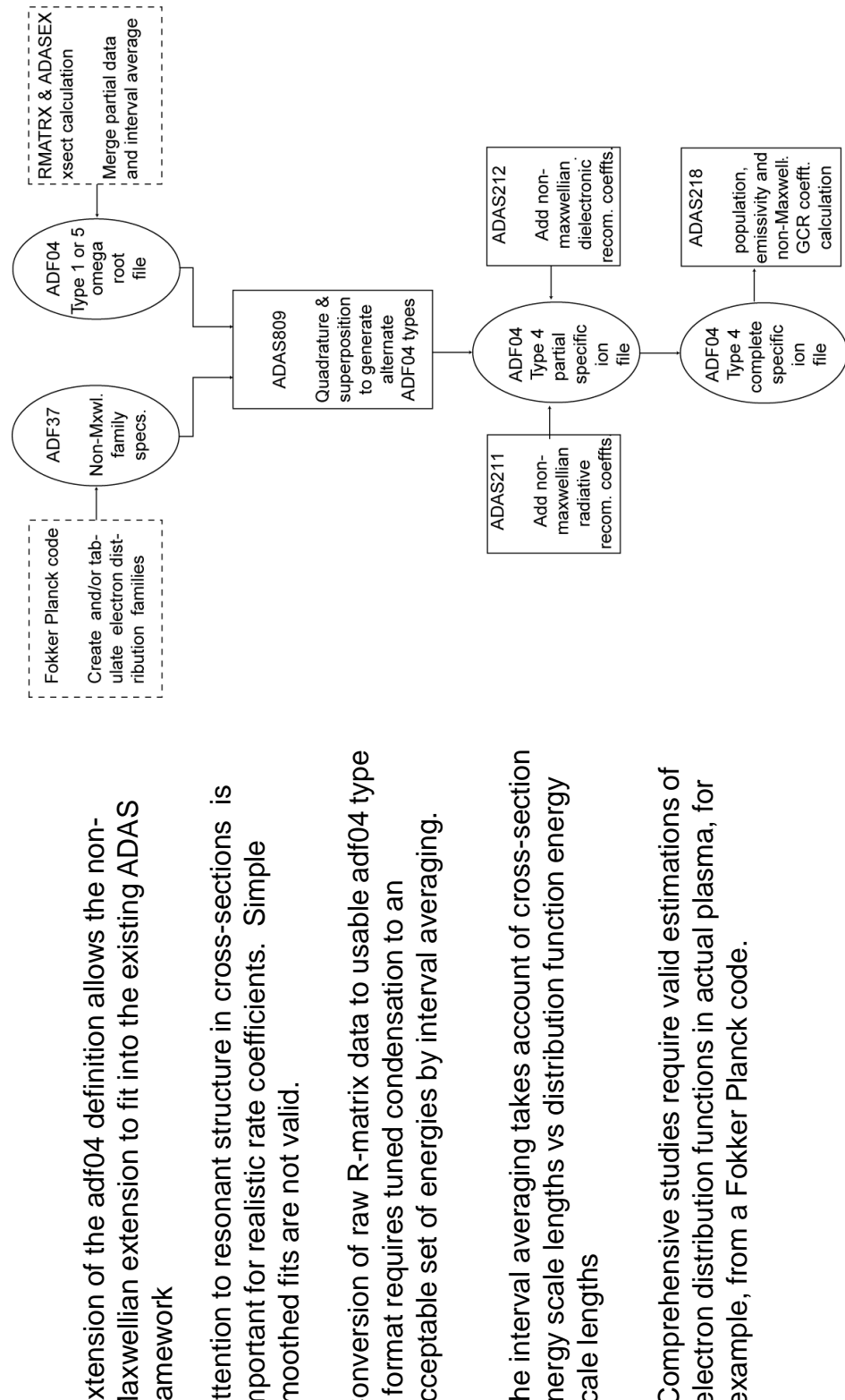
$$\times \int \int \left[\frac{\sqrt{\pi}}{2} (k T_{eff})^{3/2} e^{-I_i/kT_{eff}} \right]$$

$$\times \sqrt{\frac{E}{E' E''}} \frac{f(E') f(E'')}{f(E)} \right] dE' dE''$$

Thompson cross-section allows
evaluation

$$Q_{i \rightarrow+}(E; E', E'') = 4\pi a_0^2 \zeta I_H^2 \frac{1}{E E'^2} \delta(E - E' - E'' - I_i)$$

5.5 ADAS code schematics

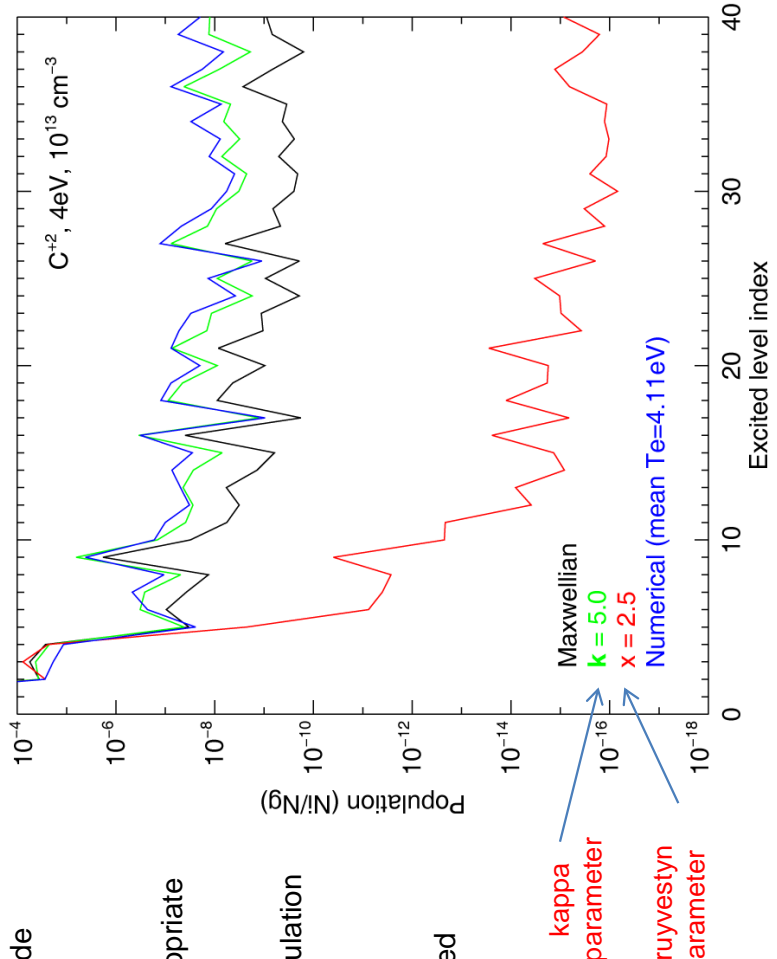


5.6 Non-Maxwellian populations

Non-Maxwellian populations evaluated using code
[ADAS218](#).

Differential variation of populations according to
enhancement or depletion of regions of the appropriate
distribution functions.

The numerical non-Maxwellian is from a JET simulation
near the divertor plate by Tskhakaya.



The non-Maxwellian adf04 datasets were prepared
for the appropriate distribution functions using
[offline_adas/adas7#3/adf04_om2ups](#)

ADAS has wide coverage of type 5 adf04 datasets for non-Maxwellian studies in directory
[..../adas/adf04/cophtps#<ionseq>/dw/<coupling>#<ion>_t5.dat](#).

6.1 Conclusions.

- Spectral analysis of fusion plasma environments has strong similarities with that of the solar upper atmosphere, but with the unique advantages of independent knowledge (from Thompson scattering) of the electron density and temperature profiles across the plasma and multiple lines-of-sight through the plasma.
- The line-of-sight issue has necessitated a technique of analysis in the solar case called differential emission measure analysis (DEM) for inferring the variation of temperature and effective emitting volume with height in the solar atmosphere.
- Attempts to model more complex outer fusion plasma regions of strong gradients, possibly with transient island formation, suggests an extended DEM approach, called ‘double-differential emission measure’ which can be supported with precisions of atomic data attainable by ADAS GCR modelling.
- Transient events are common to both solar and fusion scenarios and the associated non-linear ionisation state issues are amenable to ADAS modelling and inclusion in a DEM framework.
- Opacity has been of low relevance in fusion (except for hydrogen Lyman lines) but the extended path lengths and low temperatures of divertor scenarios raise this issue for low ionisation stages of light elements, especially carbon. Low to moderate opacity studies, addressed in the escape factor approach has a record of success in solar astrophysics, using ADAS models and data. This is ready for transfer to the fusion case.
- Non-Maxwellian distributions are certainly present in both fusion and astrophysical plasmas and with a need in both to make progress in spectroscopic diagnostic deduction of non-Maxwellian character. ADAS development in this area is comprehensive and is enabling fusion and solar astrophysics to share knowledge and experience.

Appendix C

ADAS-EU WATC: demonstration scripts

C.1 module_1

MODULE 1

Impurity atomic species in fusion plasma, their ionisation state and radiating characteristics - the ADAS approach.

Demonstration script

Hugh Summers, Martin O'Mullane and Alessandra Giunta

September 29, 2013

Contents

| | |
|--|-----------|
| 1 Demo (a) Finding about ADAS | 3 |
| 1.1 Demo (a) Figures | 4 |
| 1.1.1 Demo (a-1) demo_a/demo_a1_adaseu_web.png | 4 |
| 1.1.2 Demo (a-1) demo_a/demo_a1_adas_web.png | 5 |
| 1.1.3 Demo (a-1) demo_a/demo_a1_adas_web_series.png | 6 |
| 1.1.4 Demo (a-1) demo_a/demo_a1_adas_web_adf.png | 7 |
| 1.1.5 Demo (a-2) demo_a/demo_a2_open_adas_search.png | 8 |
| 1.1.6 Demo (a-2) demo_a/demo_a2_open_adas_z.png | 9 |
| 2 Demo (b) The code and data organisation | 10 |
| 3 Demo (c) Fundamental data collections | 13 |
| 3.1 Demo (c) Figures | 15 |
| 3.1.1 Demo (c-1) demo_c/demo_c_1.pdf | 15 |
| 3.1.2 Demo (c-2) demo_c/demo_c_2.pdf | 16 |
| 3.1.3 Demo (c-3) demo_c/demo_c_3.pdf | 17 |
| 3.2 Demo (c) Procedures | 18 |
| 3.2.1 Demo (c-1) demo_c/demo_c_1.pro | 18 |
| 3.2.2 Demo (c-2) demo_c/demo_c_2.pro | 19 |
| 3.2.3 Demo (c-3) demo_c/demo_c_3.pro | 21 |
| 4 Demo (d) Executing population calculations | 22 |
| 4.1 Demo (d) Figures | 25 |
| 4.1.1 Demo (d-1) demo_d/demo_d_1.pdf | 25 |
| 4.1.2 Demo (d-2) demo_d/demo_d_2_acd.pdf | 26 |
| 4.1.3 Demo (d-2) demo_d/demo_d_2_pec.pdf | 27 |
| 4.1.4 Demo (d-3) demo_d/demo_d_3_intv_ion_res.pdf | 28 |

| | | |
|--------|---|----|
| 4.1.5 | Demo (d-3) demo_d/demo_d_3.intv.ion.unres.pdf | 29 |
| 4.1.6 | Demo (d-3) demo_d/demo_d_3.intv.power.res.pdf | 30 |
| 4.1.7 | Demo (d-3) demo_d/demo_d_3.intv.power.unres.pdf | 31 |
| 4.1.8 | Demo (d-3) demo_d/demo_d_3.ion.res.pdf | 32 |
| 4.1.9 | Demo (d-3) demo_d/demo_d_3.ion.unres.pdf | 33 |
| 4.1.10 | Demo (d-3) demo_d/demo_d_3.power.res.pdf | 34 |
| 4.2 | Demo (d) Procedures | 35 |
| 4.2.1 | Demo (d-3) demo_d/demo_d_3.pro | 35 |

1 Demo (a) Finding about ADAS

DEMO A: Finding about ADAS

PURPOSE: Look at the ADAS, ADAS-EU and OPEN-ADAS websites and their structure.

EXAMPLE: There are three main websites related to ADAS:

1. <http://www.adas.ac.uk>: this website contains all information about ADAS, its history, news. It includes the online manual, which gives an overview of the theory behind and detailed explanation of all ADAS series and data formats. All material related to dissemination (e.g. bulletins, publications, theses) is available in the website, together with information about past and future ADAS courses and workshops. Links to ADAS-EU and OPEN-ADAS are also present.
2. <http://www.adas-fusion.eu>: this website is strictly related to the ADAS-EU project in support of fusion laboratories in Europe and for ITER (Euratom Framework 7 Support Action). It provides all information about the work packages supporting fusion research and implemented by ADAS. It also gives details on ADAS-EU courses and links to ADAS and OPEN-ADAS websites.
3. <http://open.adas.ac.uk>: this website enables non members to download and use ADAS data. It allows one multiple research choice:
 - a freedom research (e.g. typing the name of the elements or ion or wavelength range of interest);
 - a research according to the wavelength of interest
 - a research based on ion selecting the element from the periodic table.

DEMO a1: The ADAS and ADAS-EU websites
ADAS website

1. Open an internet browser and type <http://www.adas.ac.uk>.
2. Click on "Manual"
3. Look at the different ADAS series (ADAS102, ADAS102, etc.)
4. Scrolling down, look at the different ADAS data formats (adf00, adf01, etc.)
(Example files: demo_a1_adas_web.png, demo_a1_adas_web_series.png, demo_a1_adas_web_adf.png)

ADAS-EU website

5. Click on "ADAS-EU" and, in the webpage which appears, click to the link <http://www.adas-fusion.eu>. Alternatively, type directly on the browser <http://www.adas-fusion.eu>.
6. Look at the ADAS-EU website.
(Example files: demo_a1_adaseu_web.png)

DEMO a2: OPEN-ADAS

1. Type on the browser <http://open.adas.ac.uk>.
2. Click on "Freedom" to look at the freedom research.
3. Then click on "Ion" and choose an element from the periodic table.
(Example files: demo_a2_open_adas_search.png, demo_a2_open_adas_z.png)

1.1 Demo (a) Figures

1.1.1 Demo (a-1) demo_a/demo_a1_adaseu_web.png

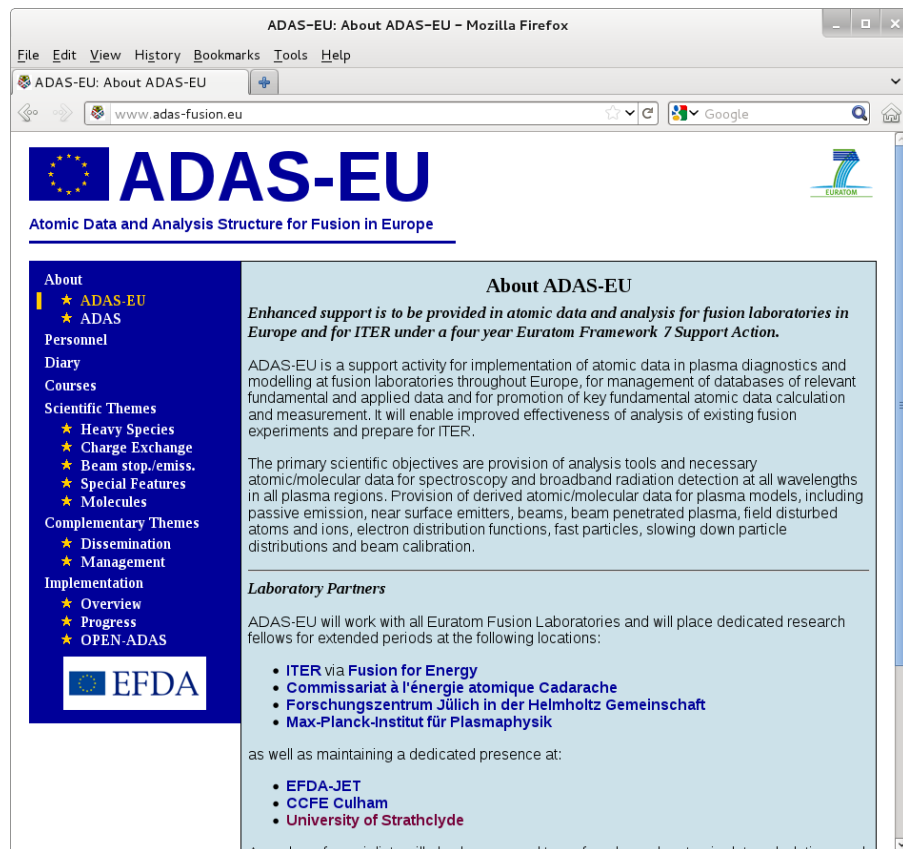


Figure 1: ADAS-EU website - first page

1.1.2 Demo (a-1) demo_a/demo_a1_adas_web.png

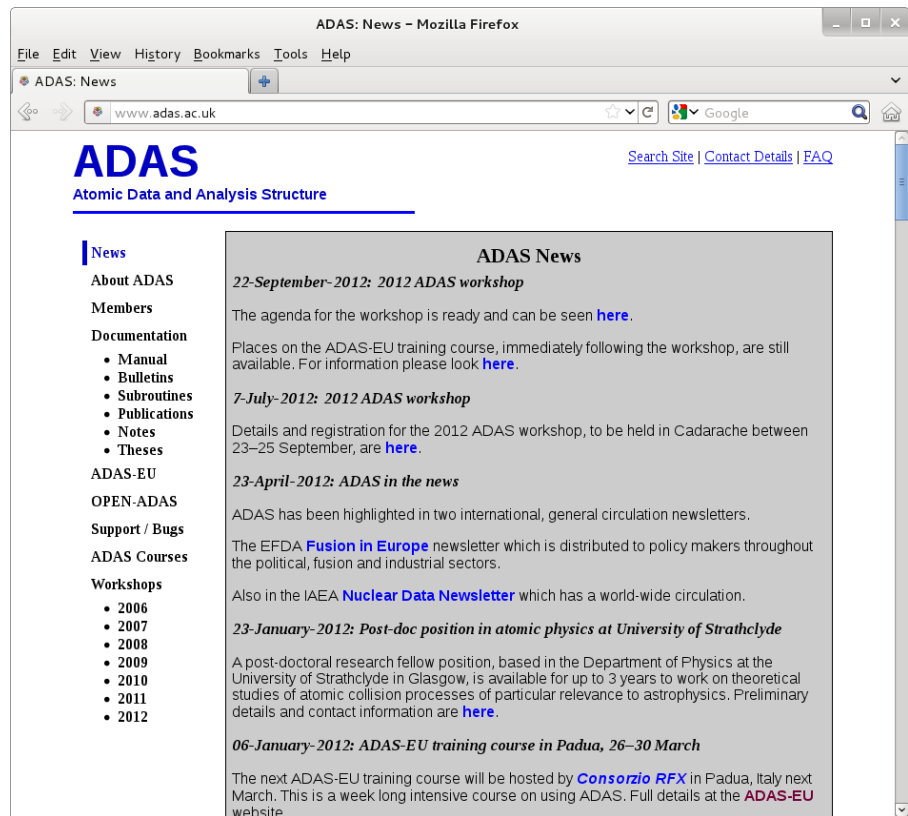


Figure 2: ADAS website - first page

1.1.3 Demo (a-1) demo_a/demo_a1_adas_web_series.png

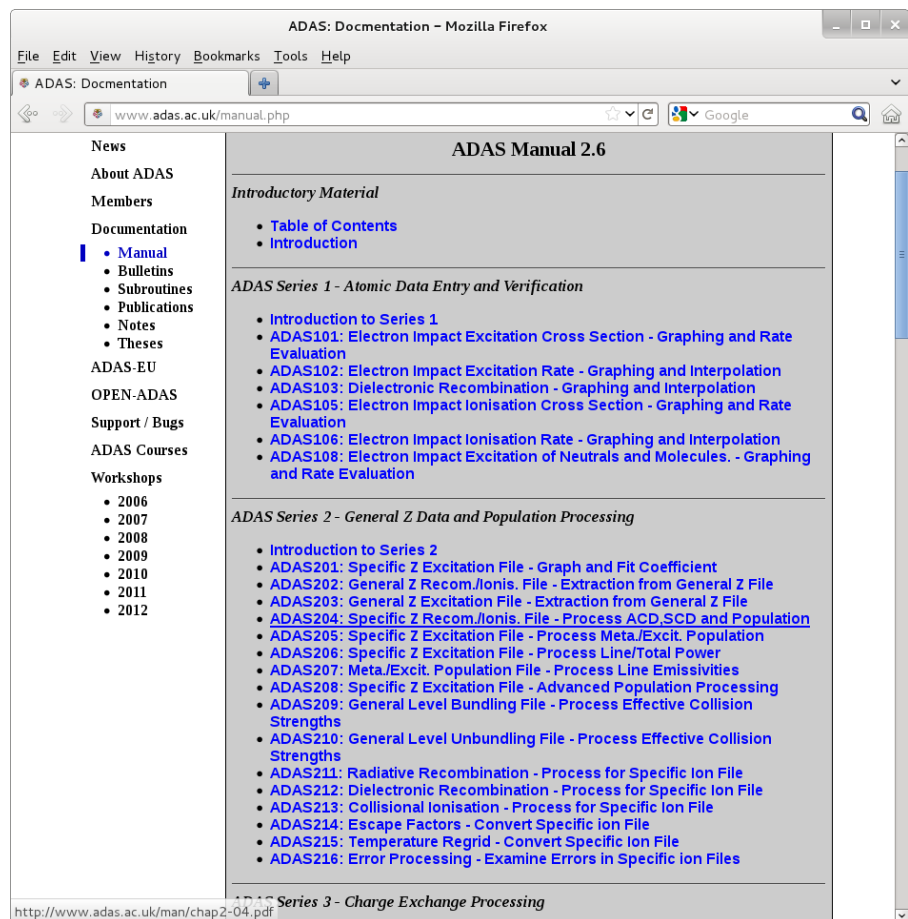


Figure 3: ADAS - code series

1.1.4 Demo (a-1) demo_a/demo_a1_adas_web.adf.png

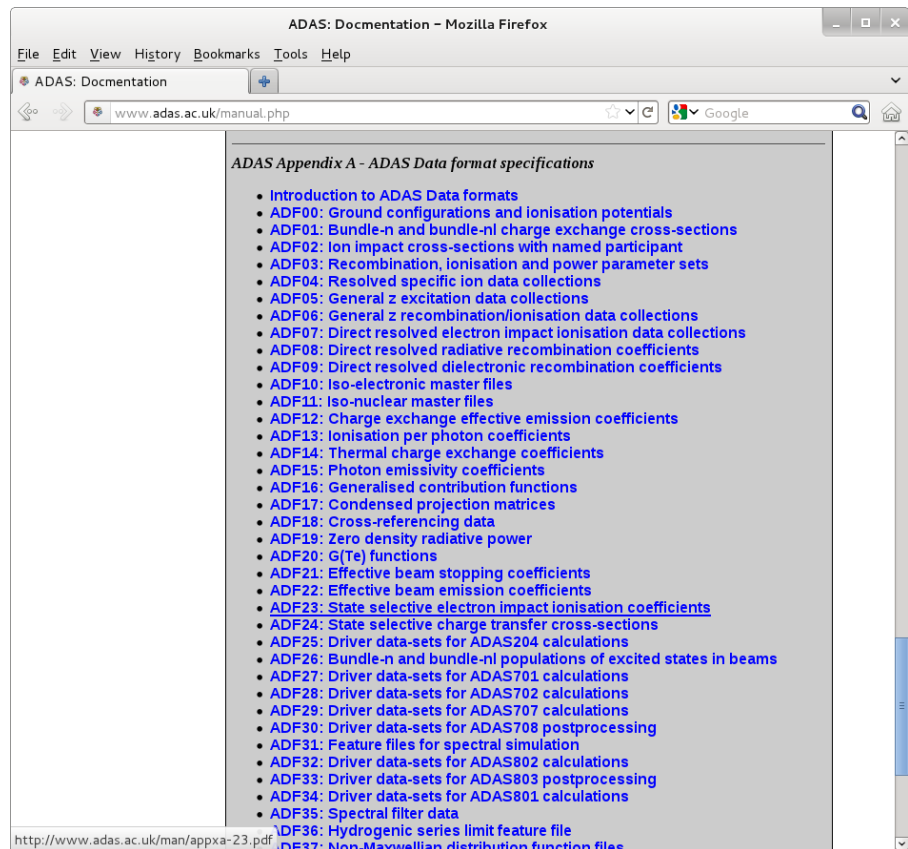


Figure 4: ADAS data formats

1.1.5 Demo (a-2 demo.a/demo.a2_open_adas_search.png)

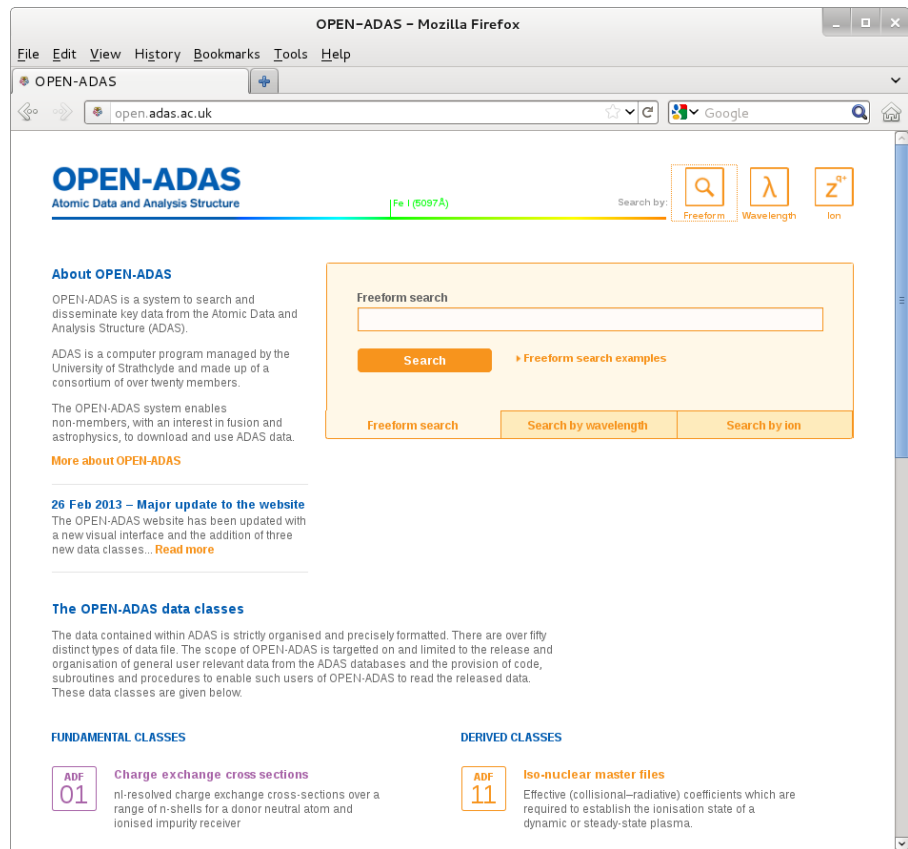


Figure 5: OPEN-ADAS - freeform search

1.1.6 Demo (a-2 demo.a/demo.a2_open.adas.z.png)

The screenshot shows the OPEN-ADAS website in Mozilla Firefox. The URL bar shows `open.adas.ac.uk`. The main content area features the OPEN-ADAS logo and navigation links for About, Data, Tools, and Help. A banner at the top indicates a 'Ra II (4533.1 Å)' event. On the right, there's a search interface titled 'Select an element from the periodic table' with a grid of elements (H, He, Li, Be, Na, Mg, etc.) and a 'Search by ion' section with three buttons: 'Freeform', 'Wavelength', and 'Ion'. Below the search is a section titled 'The OPEN-ADAS data classes' with a note about data organization.

Figure 6: OPEN-ADAS - search by ion

2 Demo (b) The code and data organisation

DEMO B: The code and data organisation

PURPOSE: Overview of ADAS database and code organisation. This demo shows the interactive and non-interactive capabilities of ADAS. It also illustrates how to access the atomic and molecular database and look at the different libraries and codes (fortran,idl, etc.).

EXAMPLE: ADAS provides atomic data as well as sets of codes for modelling the radiating properties of ions and atoms in plasmas and for assisting in the interpretation and analysis of spectral measurements. It is addressed to a large variety of plasmas, ranging from astrophysical (from solar atmosphere to interstellar medium) to laboratory devices (from fusion to technological plasmas).

Documentations: The entire ADAS manual and related documentation are in the directory /home/adas/doc/

Components of ADAS structure:

1. an extensive database of fundamental and derived atomic data. They are collected in the directory /home/adas/adas/

```
adf00  adf06  adf12  adf18  adf24  adf34  adf48    arch103  arch603  scripts409
adf01  adf07  adf13  adf19  adf25  adf35  adf49    arch105  arch804  scripts416
adf02  adf08  adf14  adf20  adf26  adf38  adf54    arch106  mdf00
adf03  adf09  adf15  adf21  adf27  adf39  adf56    arch108  mdf02
adf04  adf10  adf16  adf22  adf28  adf40  arch101  arch601  scripts405
adf05  adf11  adf17  adf23  adf32  adf42  arch102  arch602  scripts406
```

adf is ADAS data file
mdf is molecular data format
arch are archives
scripts are drivers

2. a large set of libraries, routines and utilities (including FORTRAN, C,C++, IDL and MATLAB) for accessing the database, delivering data, performing calculation of fundamental data and spectroscopic analysis (ADAS series, e.g. ADAS201). Some of the most relevant directories are the following:

- /home/adas/fortran/
which contains:

```
adas1xx  adas3xx  adas5xx  adas7xx  adas9xx
adas2xx  adas4xx  adas6xx  adas8xx  adaslib
```

-/home/adas/C/
which contains:

```

adas5xx adas6xx adaslib

-/home/adas/idl/
which contains:

adas1xx adas3xx adas5xx adas7xx adas9xx write_adf
adas2xx adas4xx adas6xx adas8xx adaslib read_adf

The subdirectories adaslib, write_adf and read_adf include utility and reading
routines.

Each of the subdirectories of the type adas1xx,adas2xx etc are related to the ADAS
series: e.g. adas2xx is ADAS series 2 for the investigation of "General Z data and
Population Processing". In turn this includes the directories:

adas201 adas203 adas205 adas207 adas209 adas211 adas213 adas215 adaslib
adas202 adas204 adas206 adas208 adas210 adas212 adas214 adas216

for specific displaying or analysis purposes: e.g. adas201 contains a set of
routines which allows one to graph and fit coefficients for specific Z excitation.

```

Capabilities of ADAS structure:

1. the interactive part, which provides immediate display of fundamental and derived data used in analysis and allow one to explore parameter dependencies and diagnostic predictions of atomic population and plasma models;
2. the non-interactive part, provides a set of subroutines than can be accessed from the users and embedded in their own codes.

COMMENTS: The use of ADAS and its full capabilities, as described by this demo, is reserved to the members. However, the database (fundamental and derived atomic data) and the fortran reading routines for the ADAS data files are available also in the OPEN-ADAS website (see demo a) and free from the restriction of ADAS membership..

DEMO b1: Language and library structure

1. Open the directory /home/adas/doc/ to look at the documentation.
2. Open the directory /home/adas/adas/ to look at the location of the atomic and molecular database.
3. Open the directory /home/adas/idl/ to look at the ADAS series.
4. Open the directory /home/adas/fortran/ to look at the ADAS series (as point 3.).

DEMO b2: ADAS data formats

1. Open the directory /home/adas/adas/adf04 to look at an example of ADAS data file.

DEMO b3: Interactive ADAS menus and starting code

1. Go into the directory /home/adas/pass/.
2. Run adas.

3. Click on series 2: "2 General Z Data and Population Processing".
4. Click on "ADAS201: Specific Z Excitation File - Graph and Fit Coefficient"
5. Select a data set, e.g. from /home/adas/adas/adf04/adas#6/mom97_ls#c1.dat and start the program.

3 Demo (c) Fundamental data collections

DEMO C: Fundamental data collections

PURPOSE: Look at the fundamental data collection.

EXAMPLE: This demo gives examples of how look at some of the fundamental data collected in the ADAS data files (adf).

Three samples are provided:

1. adf04: These ADAS data files are collections of energy levels (or terms or configuration arrays according to the resolution adopted), radiative transitions probabilities (A-values) and rate coefficients for specified low states of an ion. There are five types of adf04: a) Type 1: electron collision transition line Omega (collision strength) as a function of the threshold parameter X. X, with $1 < X < \infty$, is defined as $e_i/(E_j - E_i)$, where e_i is the incident electron energy, E_j the energy of the upper state of the transition and E_i the energy of the lower state (Note that $e_i + E_i = e_j + E_j$, where e_j is the energy of the scattered electron). b) Type 3: electron collision transition line Upsilon (effective collision strength) as a function of electron temperature. c) Type 4: electron collision transition line Upsilon and Downpsilon as a function of energy (see Bryans 2005 - http://www.adas.ac.uk/theses/bryans_thesis.pdf). d) Type 5: electron collision transition line Omega as a function of the final state energy (which is the energy of scattered electron e_j). e) Type 6: electron collision transition line Omega_1 as a function of 1.

For the demo a distorted wave adf04 for Be-like oxygen (O+4) has been chosen: /home/adas/adas/adf04/cophps#be/dw/ls#o4_t5.dat

This is a type 5 adf04 in ls resolution. The term configurations are in the Eissner notation.

Three different transitions, which involve the ground term, have been chosen: 1) a dipole transition: 2s2 1S - 2s 3p 1P (corresponding to indices 1-9) 2) a spin change transition: 2s2 1S - 2s 3p 3P (corresponding to indices 1-10) 3) a monopole transition: 2s2 1S - 2p 3p 1S (corresponding to indices 1-24)

The three transitions show three characteristic behaviour (see viewgraphs).

2. adf08: This data file set contains the radiative recombination coefficients. For ionised H which recombines to neutral H, the adf08 is: /home/adas/adas/adf08/rrc98##/rrc98##_h1.dat. This is in LS resolution. Consider the first three shells n=2,3,4. For n=2 shell the corresponding terms are 2s 2S and 2p 2P, with indices 2 and 3 respectively. For n=3 shell the corresponding terms are 3s 2S, 3p 2P and 3d 2D with indices 4, 5 and 6 respectively. Finally, for n=4 shell the corresponding terms are 4s 2S, 4p 2P, 4d 2D and 4f 2F with indices 7, 8, 9 and 10 respectively. The

contribution of radiative recombination to each shell is given by the sum of the term contributions.

3. adf09: This data file provides final state level-resolved dielectronic recombination rate coefficients into final terms (LS resolution) or levels (J -resolved). For Be-like \rightarrow B-like carbon ($C+2 \rightarrow C+1$), in LS resolution and considering the recombination from $n=2$ shell of recombining ion into $n=2$ shell of recombined ion, the adf09 is:
`/home/adidas/adidas/adf09/nrbjc00#be/nrb00#be_c2ls22.dat` The total contribution due to dielectronic recombination is calculated for each metastable of the recombining ion. In this case the recombining ion is $C+2$ and the metastable terms are $2s2\ 1S$ and $2s\ 2p\ 3P$ (see also MODULE 2 DEMO a: Identifying metastables).

COMMENTS: Note that an adf04 type 5 has been used in DEMO 1c instead of an adf04 type 1. Therefore the final energy e_j (energy of scattered electron) has been converted into the X parameter for each transitions, which is $X=(e_j+\delta_E)/\delta_E$, where δ_E is the equals to E_j-E_i , that is the energy difference between level j and level i of the corresponding transition.

DEMO c1: Looking at adf04: understanding the cross sections

1. Look at the adf04 type 5 for $O+4$ and select three transitions: e.g. dipole, spin change and monopole.
2. Use `read_adf04.pro` to read the adf04 selected.
3. Convert type 5 in type 1 adf04 to show the behaviour of the collision strength of each transition as a function of the threshold parameter.
4. Plot the Omega for the three transitions.

Program: `demo_c_1.pro`

Sample of output file: `demo_c_1.ps`

DEMO c2: Looking at adf08: radiative recombination data.

1. Look at the adf08 for H to select the appropriate level indices.
2. Use `read_adf08.pro` to read the selected adf08.
3. Sum over the shell ($n=2$, $n=3$, $n=4$).
4. Plot the radiative recombination coefficients into $n=2$, $n=3$ and $n=4$ shells for H as a function of electron temperature.

Program: `demo_c_2.pro`

Sample of output file: `demo_c_2.ps`

DEMO c3: Looking at adf09: dielectronic recombination data

1. Use `xxdata_09.pro` to read adf09.
2. Plot the total contribution of dielectronic recombination from the two metastables of recombining ion.

Program: `demo_c_3.pro`

Sample of output file: `demo_c_3.ps`

3.1 Demo (c) Figures

3.1.1 Demo (c-1) demo_c/demo_c_1.pdf

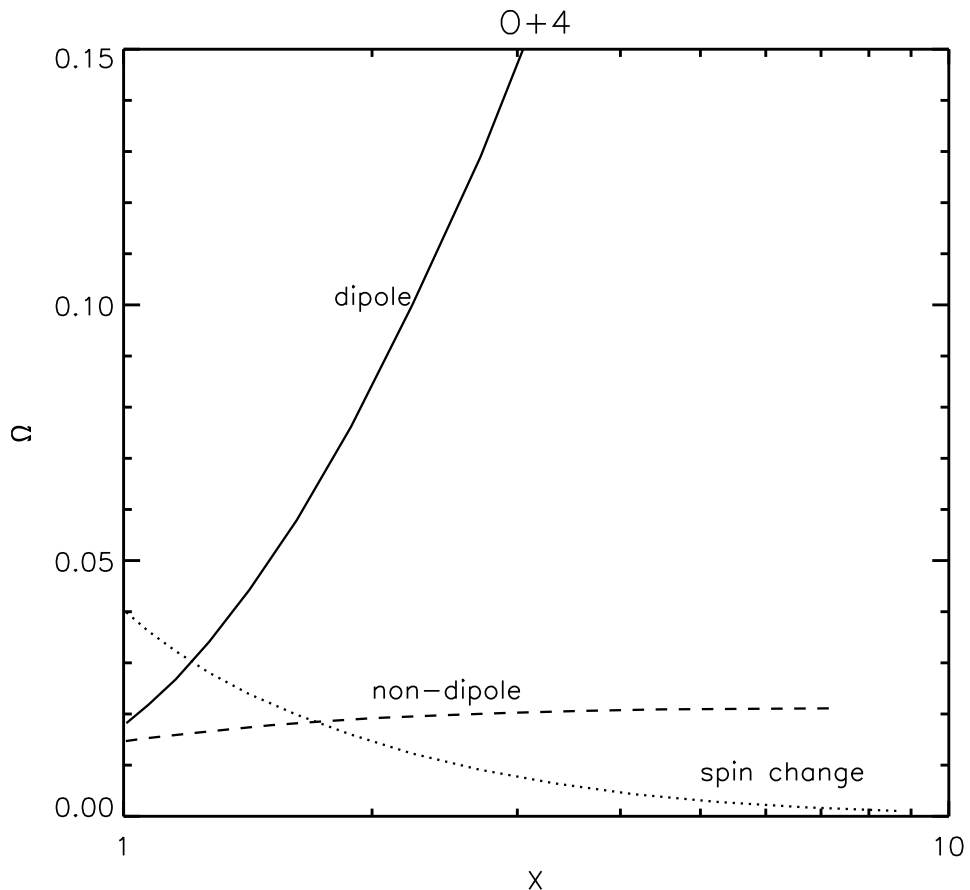


Figure 7:

3.1.2 Demo (c-2) demo_c/demo_c_2.pdf

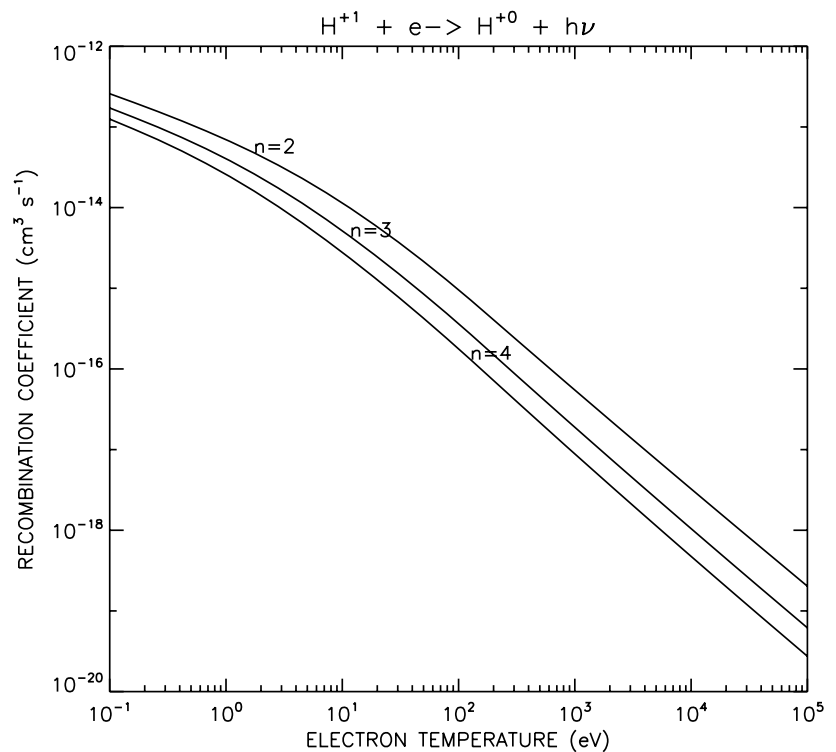


Figure 8:

3.1.3 Demo (c-3) demo_c/demo_c_3.pdf

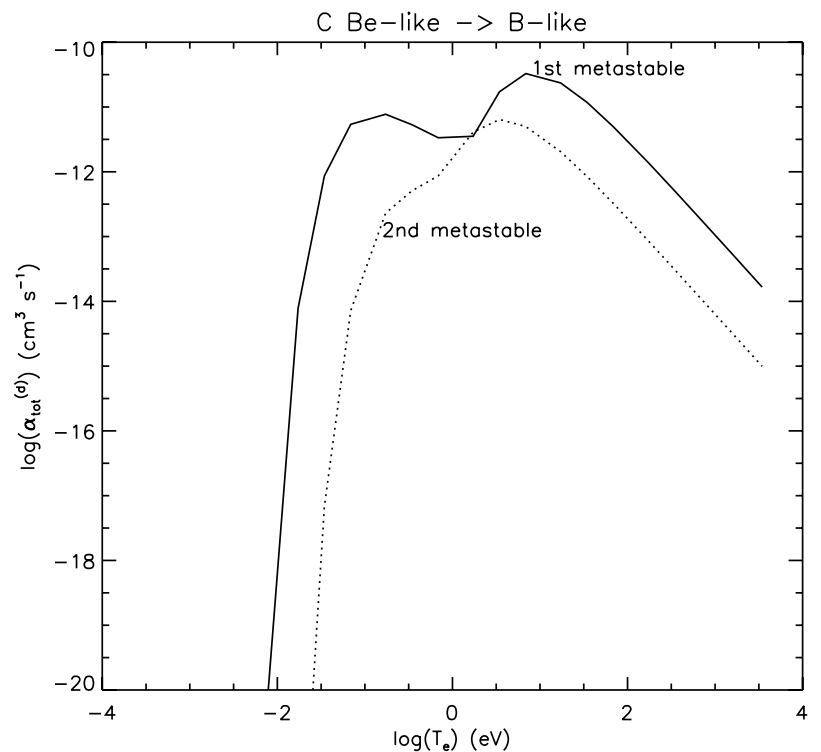


Figure 9:

3.2 Demo (c) Procedures

3.2.1 Demo (c-1) demo_c/demo_c_1.pro

```
pro demo_c_1
;Use read_adf04.pro to read type 5 adf04 for 0+4 (Be-like)
;select three different transitions (e.g. dipole, spin change and monopole)
;plot the omega as a function of the threshold parameter [X=ei/(Ej-Ei)]  
  
;adf04 type 5 in ls resolution
adf04='/home/agiuanta/adas/adf04/cophps#be/dw/ls#o4_t5.dat'  
  
;read the adf04 using read_adf04.pro
read_adf04,file=adf04,fulldata=data  
  
;dipole transition: e.g. 2s2 1S - 2s 3p 1P
dd=where(data.lower eq 1 and data.upper eq 9)  
  
;spin exchange transition: e.g. 2s2 1S - 2s 3p 3P
ee=where(data.lower eq 1 and data.upper eq 10)  
  
;monopole transition: e.g. 2s2 1S - 2p 3p 1S
mm=where(data.lower eq 1 and data.upper eq 24);8)  
  
ej=data.te  
  
;Derive the X parameter for the three transitions  
  
;1. Dipole transition
;identify the levels
d1=where(data.ia eq 1)
d2=where(data.ia eq 9)
;Values of energy in cm-1 corresponding to the previous levels
Ej_d=data.wa[d2]
Ei_d=data.wa[d1]
;calculate the delta_E for the dipole transition and convert to eV
delta_E_d=(Ej_d-Ei_d)/8066.0
;convert eV to Ryd
delta_E_d=delta_E_d/13.6
X_d=dblarr(n_elements(ej))
for i=0,n_elements(ej)-1 do X_d[i]=(ej[i]+delta_E_d)/delta_E_d  
  
;2. Spin exchange transition
;identify the levels
s1=where(data.ia eq 1)
s2=where(data.ia eq 10)
;Values of energy in cm-1 corresponding to the previous levels
Ej_s=data.wa[s2]
Ei_s=data.wa[s1]
```

```

;calculate the delta_E for the dipole transition and convert to eV
delta_E_s=(Ej_s-Ei_s)/8066.0
;convert eV to Ryd
delta_E_s=delta_E_s/13.6
X_s=dblarr(n_elements(ej))
for i=0,n_elements(ej)-1 do X_s[i]=(ej[i]+delta_E_s)/delta_E_s

;3. Monopole transition
;identify the levels
m1=where(data.ia eq 1)
m2=where(data.ia eq 24)
;Values of energy in cm-1 corresponding to the previous levels
Ej_m=data.wa[m2]
Ei_m=data.wa[m1]
;calculate the delta_E for the dipole transition and convert to eV
delta_E_m=(Ej_m-Ei_m)/8066.0
;convert eV to Ryd
delta_E_m=delta_E_m/13.6
X_m=dblarr(n_elements(ej))
for i=0,n_elements(ej)-1 do X_m[i]=(ej[i]+delta_E_m)/delta_E_m

;plot Omega as a function of the threshold parameter X
set_plot,'ps'
device, /isolatin1, font_index=8
device, bits=8, filename='demo_c_1.ps',  $
    font_size = 14, xsize=18.0, ysize=16.0, $
    yoffset=7.0, /color
device, /helvetica

;using a normalisation factor to show the behaviour of the three transitions
plot_oi,X_d,data.gamma[dd,*],xrange=[1.,10.],yrange=[0.,0.15],$ 
    title='0+4',xtitle='X',ytitle='!7X!3'
plots,X_s,data.gamma[ee,*],line=1
plots,X_m,data.gamma[mm,*],line=2

xyouts,1.8,0.1,'dipole'
xyouts,5.,0.007,'spin change'
xyouts,2.,0.023,'non-dipole'

device, /close
set_plot,'X'
!p.font=-1

end

3.2.2 Demo (c-2) demo_c/demo_c_2.pro
pro demo_c_2

```

```

;Use read_adf08 to read adf08 for H
;and extract and plot state selective radiative
;recombination coefficients for H into n=2, n=3 and n=4 shells

adf08='/home/adas/adas/adf08/rrc98##/rrc98##_h1.dat'
parent=1
;define the level indices looking at the adf08 selected
level=[2,3,4,5,6,7,8,9,10]
nlev=n_elements(level)

;define electron temperature (eV)
te=adas_vector(low=0.1,high=1.e5,num=30)
nte=n_elements(te)

rec=fltarr(nte,nlev)

;read the adf08 selected using read_adf08.pro
for i=0,nlev-1 do begin
    read_adf08,file=adf08,parent=parent,level=level[i],te=te,data=data
    rec[*,i]=data
endfor

;sum over the shell
;n=2: level=2 -> 2s 2S; level+3 -> 2p 2P
recn2=total(rec[*,0:1],2)

;n=3: level=4 -> 3s 2S;level=5 -> 3p 2P;level=6 -> 2d 2D
recn3=total(rec[*,2:4],2)

;n=4: level=7 -> 4s 2S;level=8 -> 4p 2P;level=9 -> 4d 2D; level=10 -> 4f 2F
recn4=total(rec[*,5:8],2)

;plot recombination coefficients to n=2, n=3 and n=4
set_plot,'ps'
device, /isolatin1, font_index=8
device, bits=8, filename='demo_c_2.ps',  $
    font_size = 14, xsize=18.0, ysize=16.0, $
    yoffset=7.0, /color
device, /helvetica

plot_oo,te,recn2,title='H!u+1!n + e-> H!u+0!n + h!7m!3', $
    xtitle='ELECTRON TEMPERATURE (eV)', $
    ytitle='RECOMBINATION COEFFICIENT (cm!u3!n s!u-1!n)'

oplot,te,recn3
oplot,te,recn4

xyouts,te[nte/5],recn2(nte/5),'n=2'
xyouts,te[nte/3],recn3(nte/3),'n=3'

```

```

xyouts,te[ntr/2],recn4(ntr/2),'n=4'

device, /close
set_plot,'X'
!p.font=-1

end

3.2.3 Demo (c-3) demo_c/demo_c_3.pro

pro demo_c_3
;Use xxdata_09.pro to read adf09 for C Be-like -> B-like
;in ls resolution from n=2 -> n=2

adf09='/home/adas/adas/adf09/nrbjc00#be/nrb00#be_c2ls22.dat'

;read adf09 using use xxdata_09.pro
xxdata_09,file=adf09,fulldata=data

;convert electron temperature units from Kelvin to eV
te=data.tea/11604.5

;plot the total contribution of dielectronic recombination
;from the two metastables of recombining ion
set_plot,'ps'
device, /isolatin1, font_index=8
device, bits=8, filename='demo_c_3.ps',           $
          font_size = 14, xsize=18.0, ysize=16.0, $ 
          yoffset=7.0, /color
device, /helvetica
plot,alog10(te),alog10(data.diel_tot[0,*]),      $
          yrang=[-20.,-10.],           $
          title='C Be-like -> B-like',   $
          xtitle='log(T!de!n) (eV)',    $
          ytitle='log(17a!3!dtot!n!u(d)!n) (cm!u3!n s!u-1!n)' $
oplot,alog10(te),alog10(data.diel_tot[1,*]),line=1

xyouts,0.9,-10.5,'1st metastable'
xyouts,-0.8,-13.0,'2nd metastable'

device, /close
set_plot,'X'
!p.font=-1

end

```

4 Demo (d) Executing population calculations

DEMO D: Executing population calculations

PURPOSE: Perform population calculations, look at the different coefficients and calculate ionisation balance and radiated power.

The population of excited levels is calculated by ADAS205 and ADAS208. The input dataset is a specific ion file in the adf04 format. ADAS208 is an extension of ADAS205 and includes in the population calculation: a) metastable parents; b) condensed influenced of very highly excited level populations; c) inner shell ionisation forming excited states; d) three body recombination.

Additionally, ADAS208 generates the Generalised Collisional-Radiative (GCR) coefficients:

- 1) adf15, which is the Photon Emissivity Coefficients, PEC;
- 2) adf11, which includes the following coefficients:

```
scd= ionisation coefficients
acd= free electron recombination coefficients
ccd= charge exchange recombination coefficients
xcd= metastable cross-coupling coefficients
qcd= parent metastable cross-coupling coefficients

plt= total excitation line power coefficients
prb= free electron recombination cascade bremsstrahlung power coefficients
prc= charge exchange power coefficients
pls= specific line excitation power coefficients

ecd= effective ionisation potential
zcd= effective superstage charge
ycd= effective superstage square of effective charge
```

The units of first group are cm³ s⁻¹, while for the power coefficients the units are ergs cm³ s⁻¹. The last group is used for heavy species.

The adf11 data files are identified by year (e.g. 85, 89, 93, 96).
96 -> full GCR (also 93 is GCR, however they are available only for a small set of elements)

Once all the GCR coefficients adf11 are available (metastable resolved and stage to stage), fractional abundances and radiated power may be calculated using ADAS405 at equilibrium and ADAS406 using a simple transient model.

EXAMPLE: For the population calculation, this demo provides an example of the use of ADAS205 applied to neutral helium. The population of excited levels is calculated with respect to the ground or metastable level population.

The behaviour of the ratio between excited level population and ground level population as a function of electron density helps to identify:

- 1) different plasma regimes: coronal, CR, LTE
- 2) metastable levels or terms (see also MODULE 2 DEMO a: Identifying metastables).

The adf04 selected for the demo is:
`/home/adas/adas/adf04/adas#2/mom97_ls#he0.dat`

The temperature chosen is 8.6 eV.

Two outputs from the advanced calculation performed by ADAS208 are included in the demo:

- 1) adf15 for C+1 (excitation PEC):
`/home/adas/adas/adf15/pec96#c/pec96#c_pjr#c1.dat`
 spectral line: 858.4 Ang. 2s2 2p 2P - 2s2 3s 2P
 C+1 has two metastable terms: 2s2 2p 2P, which is the ground term, and 2s 2p2 4P.
 The excitation PECs driven by the two metastables have been chosen for the demo.
- 2) adf11 for O+3 (free electron recombination coefficient, acd):
 In central ADAS the data file is:
`/home/adas/adas/adf11/acd96r/acd96r_o.dat`
 However, if one wants to investigate the behaviour at high density, it would be better to increase the electron density range at which the coefficient is calculated. This is done running ADAS404 interactively for oxygen and editing the electron temperature and density range. The output file used as example has been saved locally and named acd404_o.pass.

O+4 has 2 metastable terms, 2s2 1S and 2s 2p 3P, as well as O+3 which has the 2 metastable terms 2s2 2p 2P and 2s 2p2 4P.
 The recombination coefficient from the second metastable of O+4 (iprt=2) to the second metastable of O+3 (igrd=2) has been selected for this demo.

The adf11 data files are of two types: stage to stage or unresolved (also called standard type) and metastable resolved - e.g. the file
`/home/adas/adas/adf11/acd96r/acd96r_o.dat`, mentioned above provides metastable resolved recombination coefficients, while the file
`/home/adas/adas/adf11/acd96/acd96_o.dat` gives stage to stage recombination coefficients. Once the adf11 files (scd, acd, etc) are available for an element, it is possible to calculate the fractional abundances and the radiated power at equilibrium using ADAS405.

For oxygen the inputs are the following:

```
Element symbol= o
Year=96
Default year=96
Isonuclear master classes: scd, acd, prb, plt (for stage to stage)
                           scd, acd, qcd, xcd prb, plt (for metastable resolved)
```

COMMENTS: Note that the full GCR adf15 used for the demo is in LS resolution.

DEMO d1: Running ADAS205 for populations

1. Use ADAS205 with the interactive ADAS windows.
(sample of output file: demo_d1.ps)

DEMO d2: Looking at adf15 and adf11

1. Look at the adf15 selected to identify blocks corresponding to the line chosen (C II 858.4 Ang.).
2. Use read_adf15.pro to read the metastable resolved PEC data file adf15
3. Plot a surface of the excitation PEC as a function of Te and Ne comparing the behaviour due to the two metastables of C+1.
3. Look at the adf11 year 96 resolved for oxygen. Look at the electron temperature and density range. If it is not appropriate, run the interactive ADAS404, with a wider range of Te and Ne, to produce a new adf11 for oxygen and save it locally.
4. Use read_adf11.pro to read the selected adf11.
5. Plot a surface of ACD as a function of electron temperature and density.

Program: demo_d_2.pro

Output files: demo_d_2_pec.ps, demo_d_2_acd.ps

DEMO d3: Running ADAS405 interactively and offline

1. Using the input defined above run ADAS405 using the interactive windows:
 - a. Select -> Type of master files: Standard
 - b. Select -> Data file: NULL
 - c. Produce a fractional abundance plot and a power function plot
(output files: demo_d_3_intv_ion_unres.ps, demo_d_3_intv_power_unres.ps)
 - d. Repeat a.- c. selecting Type of master files: Partial - Resolved
(output files: demo_d_3_intv_ion_res.ps, demo_d_3_intv_power_res.ps)
2. Use run_adas405.pro from the command line for oxygen.
3. Plot stage to stage fractional abundances as a function of electron temperature for a fixed electron density (e.g. dens=1.e10 cm-3).
4. Plot metastable resolved fractional abundances as a function of electron temperature for a fixed electron density (e.g. dens=1.e10 cm-3).
5. Plot metastable resolved radiated power (total, plt, prb and ion) as a function of electron temperature for a fixed electron density (e.g. dens=1.e10 cm-3).

Program: demo_d_3.pro

Output files: demo_d_3_ion_unres.ps, demo_d_3_ion_res.ps, demo_d_3_power_res.ps

4.1 Demo (d) Figures

4.1.1 Demo (d-1) demo.d/demo_d_1.pdf

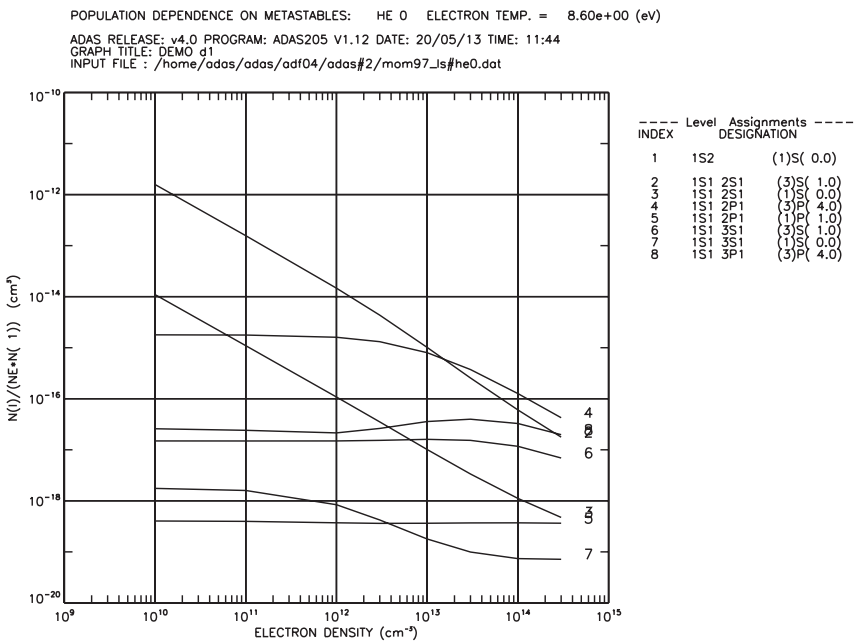


Figure 10:

4.1.2 Demo (d-2) demo_d/demo_d_2.acd.pdf

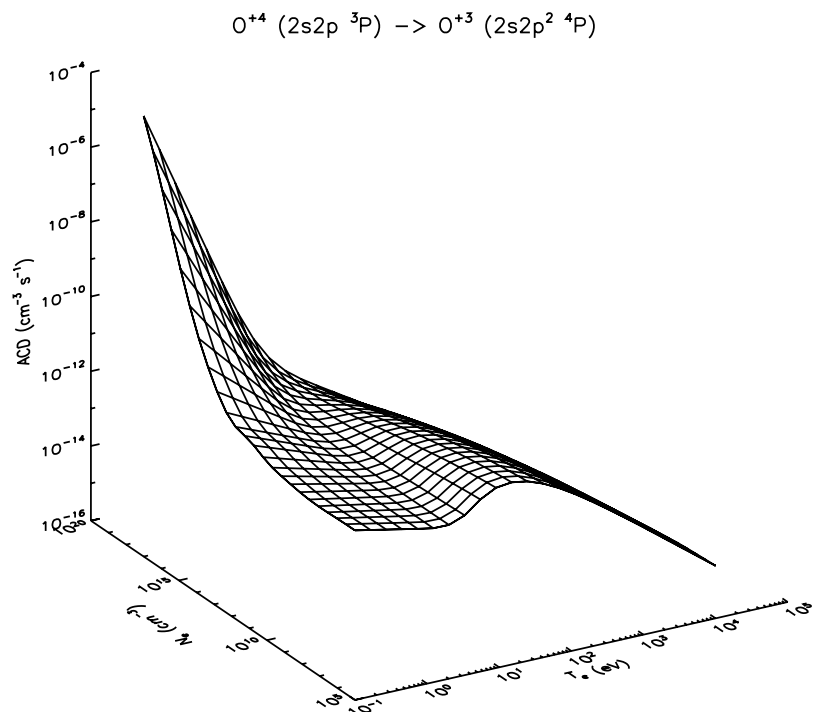


Figure 11:

4.1.3 Demo (d-2) demo_d/demo_d_2_pec.pdf

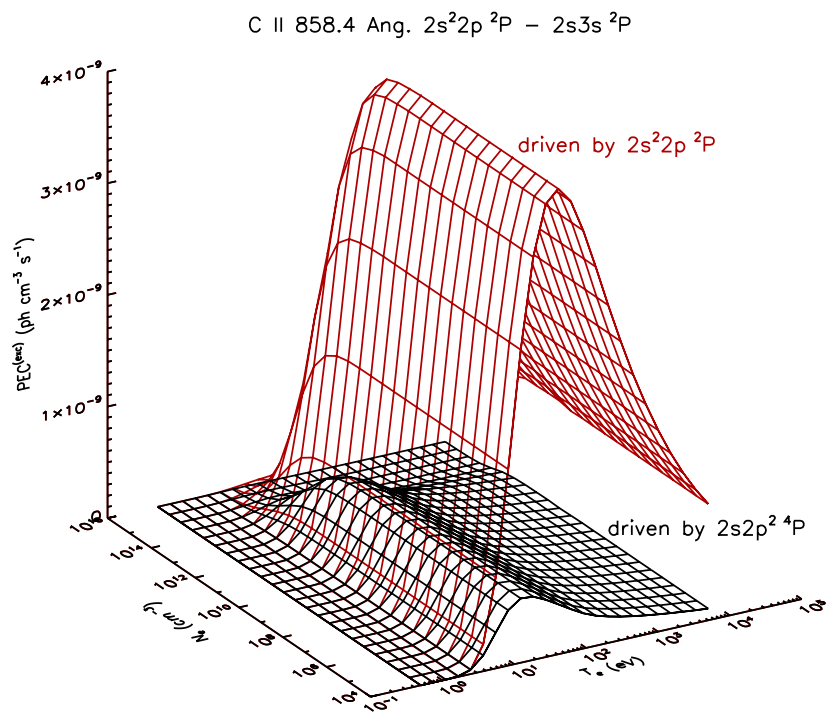


Figure 12:

4.1.4 Demo (d-3) demo_d/demo_d_3_intv.ion_res.pdf

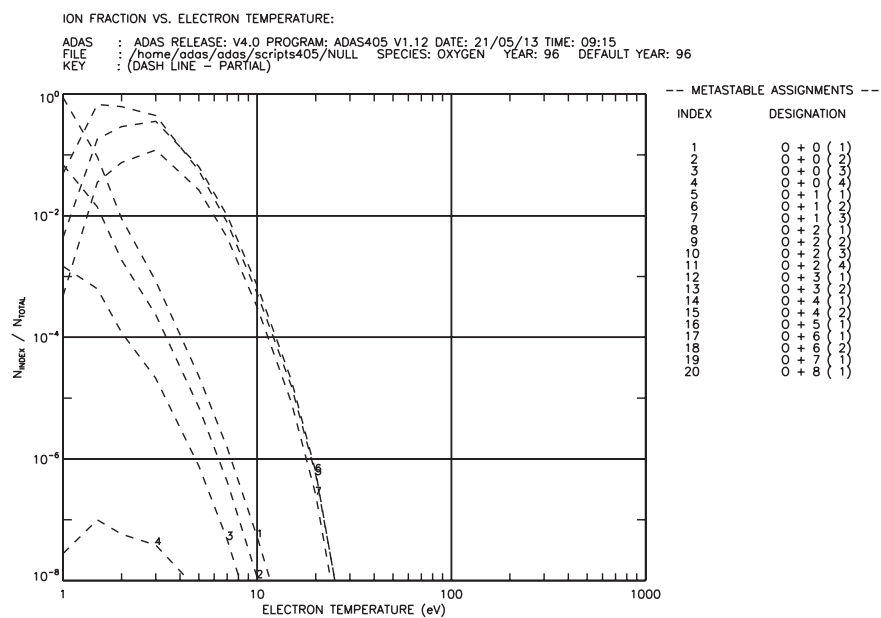


Figure 13:

4.1.5 Demo (d-3) demo_d/demo_d_3_intv_ion_unres.pdf

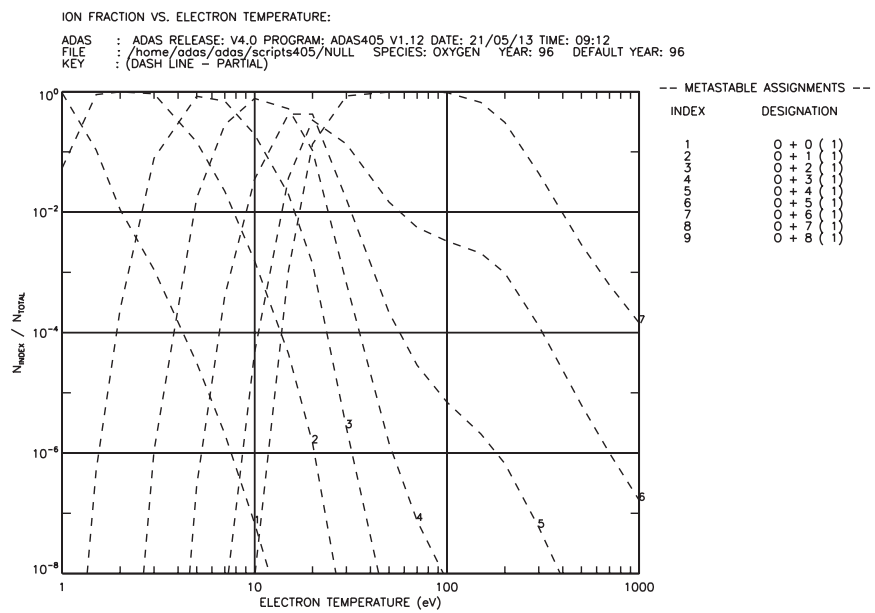


Figure 14:

4.1.6 Demo (d-3) demo_d/demo_d_3_intv_power_res.pdf

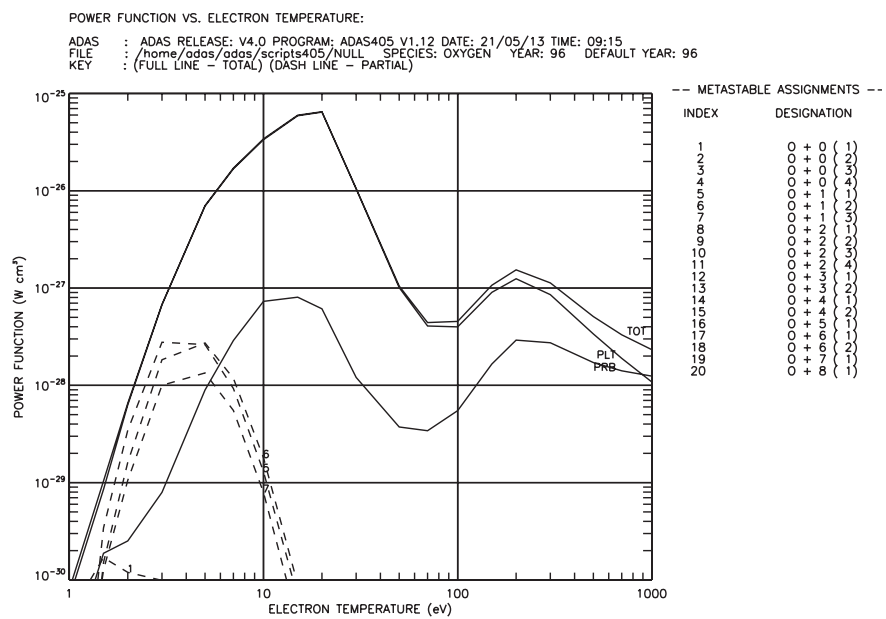


Figure 15:

4.1.7 Demo (d-3) demo_d/demo_d_3_intv_power_unres.pdf

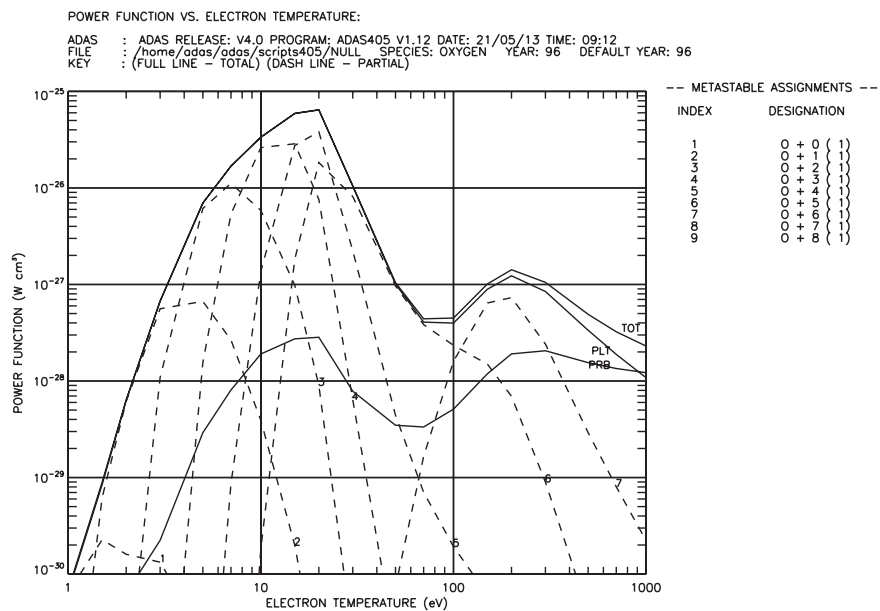


Figure 16:

4.1.8 Demo (d-3) demo_d/demo_d_3_ion_res.pdf

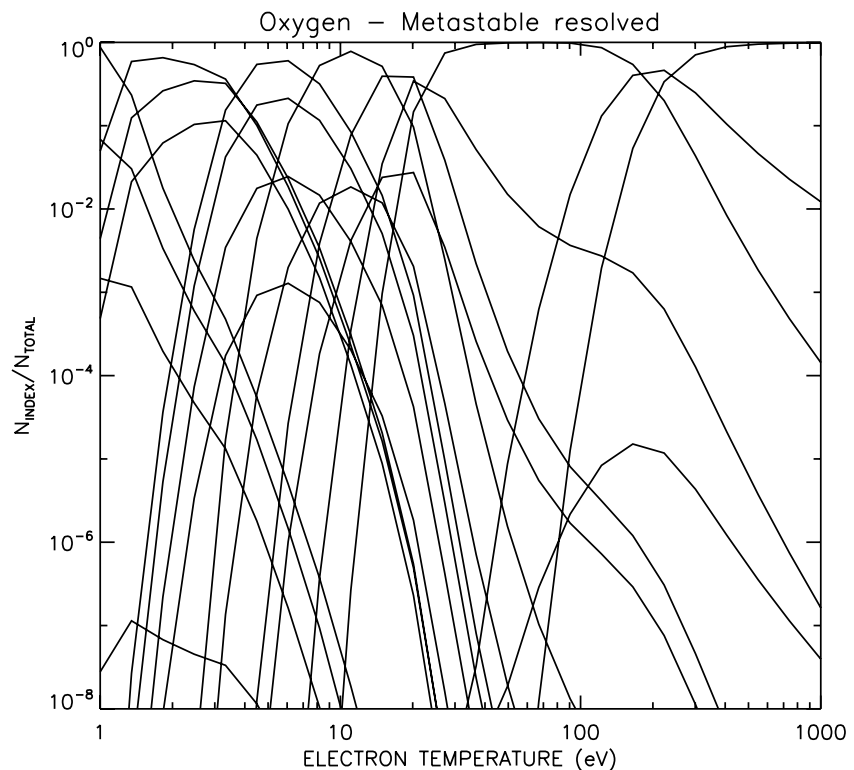


Figure 17:

4.1.9 Demo (d-3) demo_d/demo_d_3_ion_unres.pdf

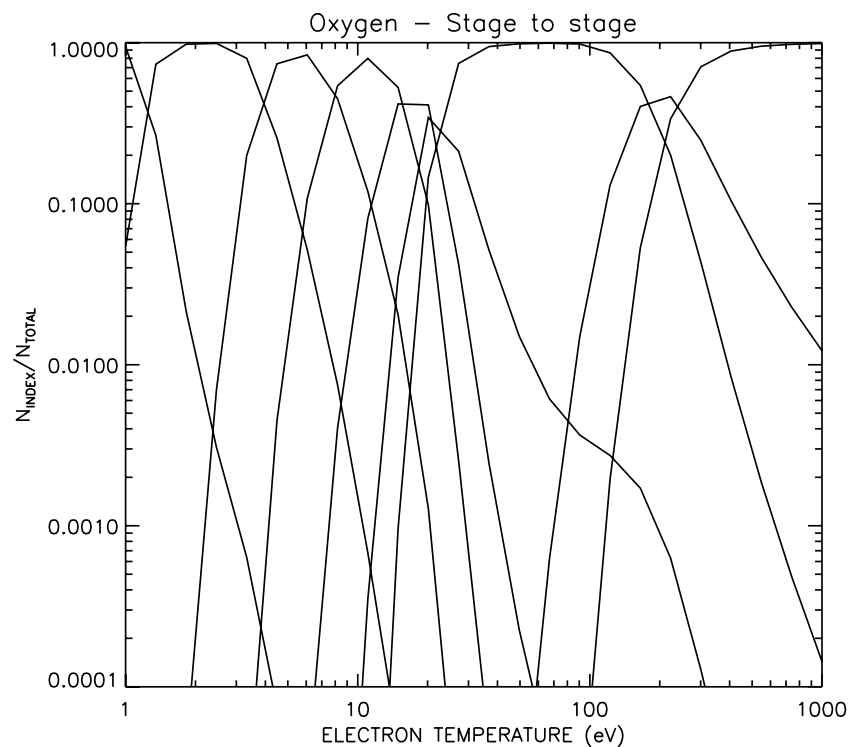


Figure 18:

4.1.10 Demo (d-3) demo_d/demo_d_3.power_res.pdf

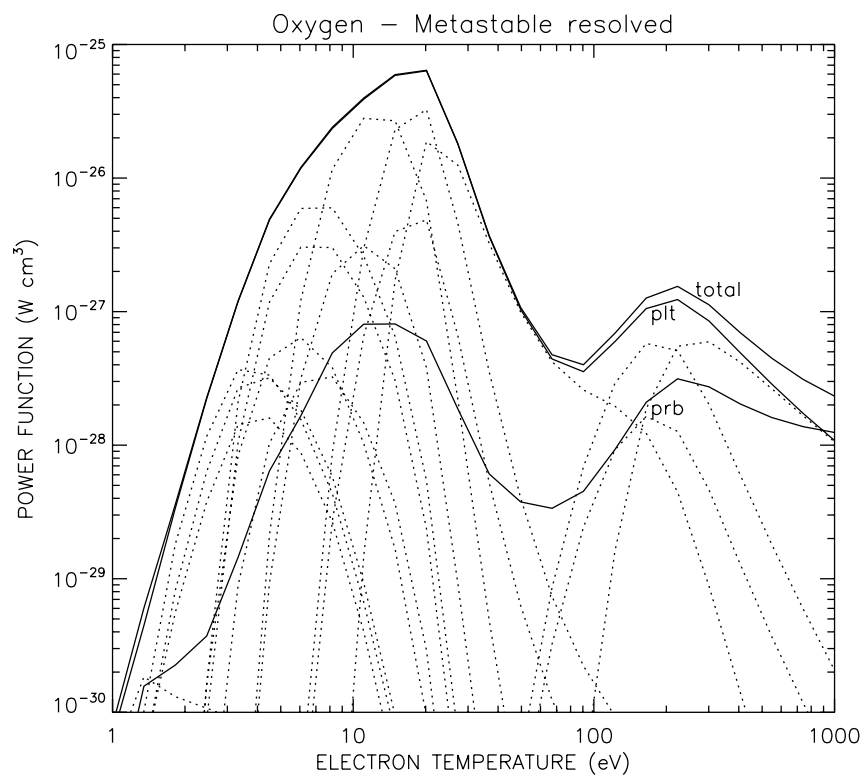


Figure 19:

4.2 Demo (d) Procedures

4.2.1 Demo (d-3) demo.d/demo_d_3.pro

```
pro demo_d_3
;Use run_adas405.pro to produce stage to stage and metastable resolved
;fractional abundances and radiated power for oxygen

;Define electron temperature (eV) array
te=adas_vector(low=1.,high=1000.,num=24)

;Define a constant electron density (cm-3)
dens=1.e10

;Set up source (central ADAS or user directory),
;element, year and default year

uid='adas'
elem='o'
year=96
defyear=96

;Run run_adas405.pro to produce both fractional abundances and power
;in the unresolved or standard (stage to stage) case
run_adas405, uid=uid, year=year, defyear=defyear, elem=elem, te=te,$
dens=dens, frac=frac_unres, power=power_unres,/all

;Run run_adas405.pro to produce both fractional abundances and power
;in the metastable resolved case
run_adas405, uid=uid, year=year, defyear=defyear, elem=elem, te=te,$
dens=dens, partial=1, frac=frac_res, power=power_res,/all

;Plot oxygen fractional abundances for stage to stage case
set_plot,'ps'
device, /isolatin1, font_index=8
device, bits=8, filename='demo_d_3_ion_unres.ps',           $
font_size = 14, xsize=18.0, ysize=16.0, $ 
yoffset=7.0, /color
device, /helvetica

plot_oo,te,frac_unres.ion[0,*,0],xrange=[1.,1000.],yrange=[1.e-4,1.],$ 
title='Oxygen - Stage to stage',$
xtitle='ELECTRON TEMPERATURE (eV)',$
ytitle='N!dINDEX!n/N!dTOTAL!n' ,/nodata
for i=0,n_elements(frac_unres.stage)-1 do oplot,te,frac_unres.ion[0,*,i]

device, /close
set_plot,'X'
```

```

!p.font=-1

;Plot oxygen fractional abundances for metastable resolved case
set_plot,'ps'
device, /isolatin1, font_index=8
device, bits=8, filename='demo_d_3_ion_res.ps',           $
      font_size = 14, xsize=18.0, ysize=16.0,   $
      yoffset=7.0, /color
device, /helvetica

plot_oo,te,frac_res.ion[0,*,0],xrange=[1.,1000.],yrange=[1.e-8,1.],$
      title='Oxygen - Metastable resolved',$
      xtitle='ELECTRON TEMPERATURE (eV)',$
      ytitle='N!dINDEX!n/N!dTOTAL!n' ,/nodata
for i=0,n_elements(frac_res.stage)-1 do oplot, te,frac_res.ion[0,*,i]

device, /close
set_plot,'X'
!p.font=-1

;Plot oxygen radiated power for metastable resolved case
set_plot,'ps'
device, /isolatin1, font_index=8
device, bits=8, filename='demo_d_3_power_res.ps',           $
      font_size = 14, xsize=18.0, ysize=16.0,   $
      yoffset=7.0, /color
device, /helvetica

plot_oo,te,power_res.plt[0,*],xrange=[1.,1000.],yrange=[1.e-30,1.e-25],$
      title='Oxygen - Metastable resolved',$
      xtitle='ELECTRON TEMPERATURE (eV)',$
      ytitle='POWER FUNCTION (W cm!u3!n)'
oplot,te,power_res.prb[0,*]
oplot,te,power_res.total[0,*] ,thick=3
for i=0,n_elements(power_res.stage)-1 do oplot,te,power_res.ion[0,*,i],line=1

xyouts,0.8,0.63,'total',/normal
xyouts,0.75,0.6,'plt',/normal
xyouts,0.75,0.48,'prb',/normal

device, /close
set_plot,'X'
!p.font=-1

end

```

C.2 module_2

MODULE 2

Complex species in the core and edge of the fusion plasma. Describing and calculating their characteristics - the current state.

Demonstration script

Hugh Summers, Martin O'Mullane and Alessandra Giunta

September 29, 2013

Contents

| | |
|---|-----------|
| 1 Demo (a) Identifying metastables | 3 |
| 1.1 Demo (a) Figures | 4 |
| 1.1.1 Demo (a-1) demo_a/demo_a_1.pdf | 4 |
| 1.2 Demo (a) IDL procedures | 5 |
| 1.2.1 Demo (a-2) demo_a_2.pro | 5 |
| 2 Demo (b) Computing 'bn' and 'ca'/'ls'/'ic' populations | 7 |
| 2.1 Demo (b) Figures | 9 |
| 2.1.1 Demo (b-1) demo_b/adas316.plot.pdf | 9 |
| 2.1.2 Demo (b-4) demo_b/demo_b_4.pdf | 10 |
| 2.2 Demo (b) Procedures | 11 |
| 2.2.1 Demo (b-4) demo_b/demo_b_4.pro | 11 |
| 2.3 Demo (b) Tables and datasets | 12 |
| 2.3.1 Demo (b-2) demo_b/adas204.adf17.pass | 12 |
| 2.3.2 Demo (b-3) demo_b/exp96#na_si3ls.dat | 13 |
| 3 Demo (c) Producing and examining a mapping file | 14 |
| 3.1 Demo (c) Tables and datasets | 14 |
| 3.1.1 Demo (c-1) demo_c/adas807_a09_a04.pass | 14 |
| 4 Demo (d)Evaluating metastable pathways for ionisation cross-sections | 16 |
| 4.1 Demo (d) Tables and datasets | 16 |
| 4.1.1 Demo (d-1) demo_d/pathways.b1_b2.dat | 16 |
| 4.1.2 Demo (d-1) demo_d/fractionation_b.csv | 17 |
| 4.1.3 Demo (d-1) demo_d/boron_adf07.dat | 17 |

| | |
|--|-----------|
| 5 Demo (e)Making up partitions and executing superstage compression | 19 |
| 5.1 Demo (e) Figures | 20 |
| 5.1.1 Demo (e-1) demo_e/demo_e_1.pdf | 20 |
| 5.1.2 Demo (e-2) demo_e/adas416_plot.pdf | 21 |
| 5.1.3 Demo (e-3) demo_e/demo_e_3.acd.pdf | 22 |
| 5.1.4 Demo (e-3) demo_e/demo_e_3_zeff.pdf | 23 |
| 5.2 Demo (e) Procedures | 24 |
| 5.2.1 Demo (e-1) demo_e_1.pro | 24 |
| 5.2.2 Demo (e-3) demo_e_3.pro | 24 |
| 5.3 Demo (e) Tables and datasets | 27 |
| 5.3.1 Demo (e-2) demo_d/adf11/acd50/acd50_w_02.dat | 27 |

1 Demo (a) Identifying metastables

DEMO A: Identifying metastables

PURPOSE: Identify the metastable terms or levels using population calculations and from adf00 file, which contains ionisation potentials and normalised energies for ground and metastable terms (ls-resolution) or levels (ic-resolution).

EXAMPLE: For demo a1 see also Module 1 Demo d1.
The input file is the following adf04 for neutral helium:
`/home/adas/adas/adf04/adas#2/mom97_ls#he0.dat`
The temperature chosen is 8.6 eV.

The element chosen for Demo a2 is silicon. There are 3 adf00 files for this element:

1. unresolved adf00: `/home/adas/adas/adf00/si.dat`
2. ls resolved adf00: `/home/adas/adas/adf00/si_ls.dat`
3. ic resolved adf00: `/home/adas/adas/adf00/si_ic.dat`

DEMO a1: Examine an ADAS205 graph

1. Use ADAS205 interactively (see Module 1 Demo d1 - demo_d1.ps)
 2. Look at the behaviour of the population of different terms.
- Sample of output file: `demo_a_1.ps`

DEMO a2: Interrogate adf00 '_ls' and '_ic' forms

1. Look at the 3 adf00 data files for Silicon.
2. Read the 3 adf00 using `read-adf00.pro`.
3. Plot ionisation potential as a function of ionisation stage for the unresolved case.
4. List metastable states in the different resolutions.

Program: `demo_a_2.pro`

Sample of output file: `demo_a_2.ps, demo_a_2.txt`

1.1 Demo (a) Figures

1.1.1 Demo (a-1) demo_a/demo_a_1.pdf

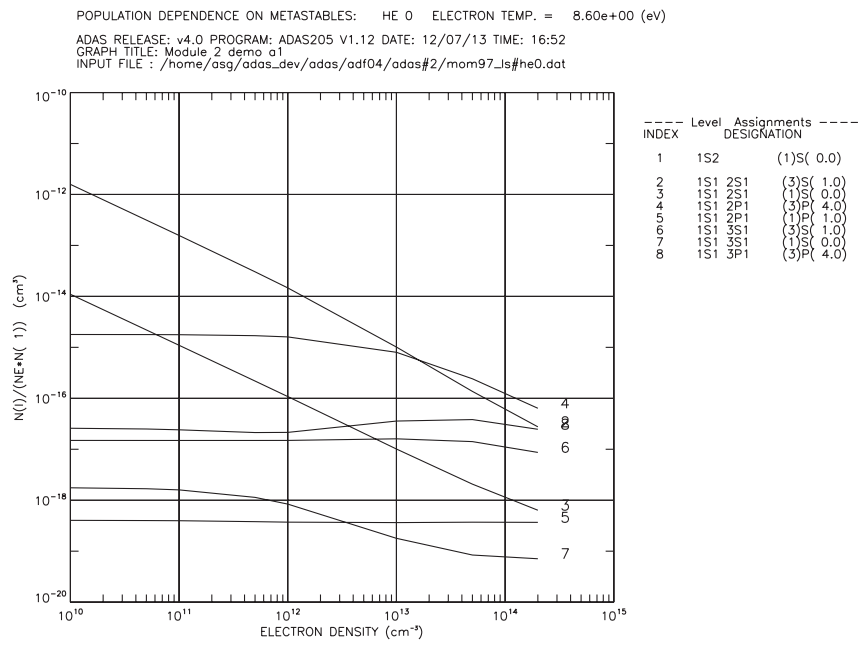


Figure 1: demo_a/demo_a_1.pdf

1.2 Demo (a) IDL procedures

1.2.1 Demo (a-2) demo_a_2.pro

Demonstration IDL procedure using *read.adf00*.

```
pro demo_a_2

;Define file paths
file_unres='/home/adas/adas/adf00/si.dat'
file_ls='/home/adas/adas/adf00/si_ls.dat'
file_ic='/home/adas/adas/adf00/si_ic.dat'

;Use read_adf00.pro in the unresolved case and using ls and ic resolutions
read_adf00,file=file_unres,z1=z1,$
    ionpot=ionpot_unres,nmeta=nmeta_unres,config=config_unres,/all
read_adf00,file=file_ls,z1=z1,$
    ionpot=ionpot_ls,nmeta=nmeta_ls,config=config_ls,isa=isa_ls,$
    ila=ila_ls,xja=xja_ls,/all,/ls
read_adf00,file=file_ic,z1=z1,$
    ionpot=ionpot_ic,nmeta=nmeta_ic,config=config_ic,isa=isa_ic,$
    ila=ila_ic,xja=xja_ic,/all,/ic

;plot ionisation potential as a function of ionisation stage

set_plot,'ps'
device, /isolatin1, font_index=8
device, bits=8, filename='demo_a_2.ps',           $
    font_size = 14, xsize=18.0, ysize=16.0, $ 
    yoffset=7.0, /color
device, /helvetica
plot_io,z1,ionpot_unres,title='Silicon',$
    xtitle='Ionisation stage', $
    ytitle='Ionisation potential'

device,/close
set_plot,'x'

;Print the number of metastables in each resolution in a file
openw,lun,'demo_a_2.txt',/get_lun
printf, lun,' ion.stage  unres  ls      ic'
for j = 0, 13 do printf,lun, ' Si' + string(j,format='(i2.2)'),  $ 
    nmeta_unres[j], nmeta_ls[j], nmeta_ic[j]

;For Si+9 identify the metastables

printf,lun, ''
printf,lun, 'Unresolved : ' + config_unres[9]
printf,lun, ''
printf,lun, 'LS resolution'
```

```

for j = 1, nmeta_ls[9] do printf,lun, strtrim(strmid(config_ls[9,j],4),2),' ', $
strtrim(string(isa_ls[9,j]),2),$
'('+strtrim(string(ila_ls[9,j]),2)+')', '$
strtrim(string(xja_ls[9,j]),2)

printf,lun, ''
printf,lun, 'IC resolution'
for j = 1, nmeta_ic[9] do printf,lun, strtrim(strmid(config_ic[9,j],4),2),' ', $
strtrim(string(isa_ic[9,j]),2),$
'('+strtrim(string(ila_ic[9,j]),2)+')', '$
strtrim(string(xja_ic[9,j]),2)

close,lun
free_lun,lun

end

```

2 Demo (b) Computing 'bn' and 'ca'/'ls'/'ic' populations

DEMO B: Computing 'bn' and 'ca'/'ls'/'ic' populations

PURPOSE: To evaluate the populations at different resolutions. Furthermore, this demo shows how to create and locate the projection file and the effect on the low levels.

This is required in the Generalised Collisional-Radiative (GCR) modelling for the solution of the whole population structure.
In ADAS the GCR model is implemented as "ls resolution", that is to say the population structure is evaluated for LS terms.
This is appropriate for light element ions for which the fine structure separation of levels is small. Although fine structure separation may be observable through distinct components in high resolution spectroscopy, the levels are in relative statistical proportion.

As one moves to heavier species and more highly ionised ions, the fine structure separations become larger and the relative population deviates from relative statistical. This is called "ic resolution". On the other hand, in finite density plasma, as one moves to higher quantum shells collisional redistribution becomes more efficient and populations move progressively towards the LTE regime. Firstly, terms of the same nl-shell move into relative statistical proportions. This is called "ca resolution". Finally 1-subshells of the same n-shell move into relative statistical populations. This is referred to as "bn resolution". These mnemonics indicate that at bn resolution it is only necessary to work with whole n-shell population whereas at ic resolution it is necessary to work with individual level population.

A high precision study must deal with all the levels of an atom, but it is only required to treat the low levels, particularly which are observed spectroscopically in high resolution, higher level population may be treated in coarser resolution. This leads to a sequence of condensation and projection extended down to the low levels (See Module 2 notes).

EXAMPLE: The input file for ADAS316, which shows the behaviour of bn resolution as a function of representative n-shell, is adf25_bn#14_si3.dat.

For producing the projection file, Si3+ is used as example. The input for ADAS204 is bns96#na_si3.dat. The output is adas204_adf17.pass in the adf17 format.

The data file exp96#na_si3ls.dat in the adf18 format is a mapping file which relate the adf17 produced by ADAS204 to the adf04.
The populations of excited states are calculated by ADAS208 (run_adas208.pro from the command line). Demo b4 uses run_adas208.pro to compute the

populations of excited states for Si3+ including the projection file and without it.

The input are the following:

- adf04: asg09_lgy09_ls#si3.dat
- adf18: exp96#na_si3ls.dat

COMMENTS: The file used as driver for ADAS316 and ADAS204 have been copied from central ADAS and changed according to the purpose (e.g. adding the correct paths etc.).

DEMO b1: 'bn' population with ADAS316

1. Run ADAS316 interactively.

Sample of output file: adas316_plot.ps

DEMO b2: Using ADAS204 to produce a projection file

1. Run ADAS204 interactively to produce the projection file of the adf17 format.

Sample of output file: adas204_adf17.pass

DEMO b3: Locating projection/expasion matrices of type adf17

1. Look at the projection file produced bu ADAS204 and build up the mapping file in the adf18 format.

Sample of output file: exp96#na_si3ls.dat

DEMO b4: Use run_adas208.pro with and without projection file

1. define the input file in the adf04 and adf18 formats.

2. Use run_adas208.pro including the adf18 data file (projection mapping file).

3. Use run_adas208.pro without the adf18 data file.

4. Plot the populations as a function of excited states in case 2. and 3.

Program: demo_b_4.pro

Output files: demo_b_4.ps

2.1 Demo (b) Figures

2.1.1 Demo (b-1) demo.b/adas316_plot.pdf

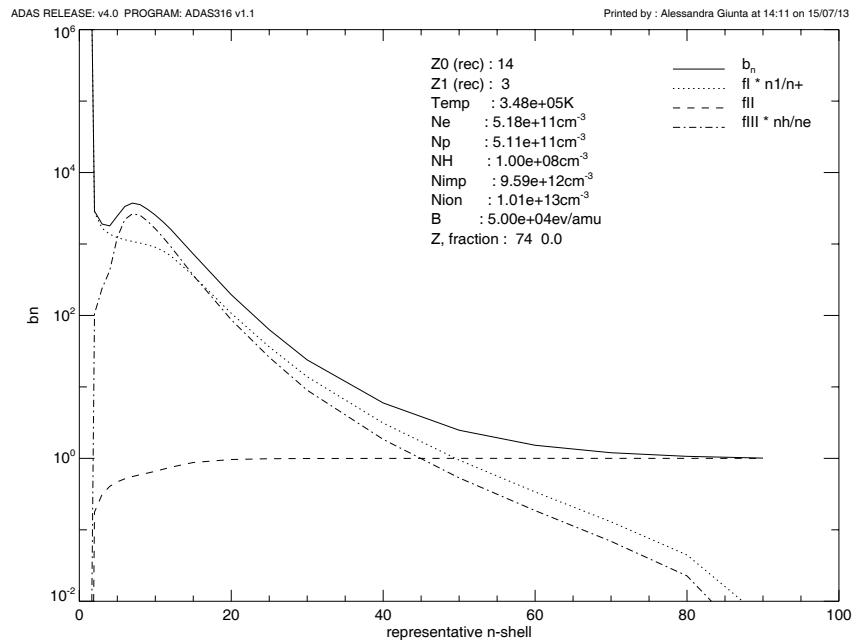


Figure 2: GTe-function plot vs Te for an O⁺⁴ transition

2.1.2 Demo (b-4) demo_b/demo_b_4.pdf

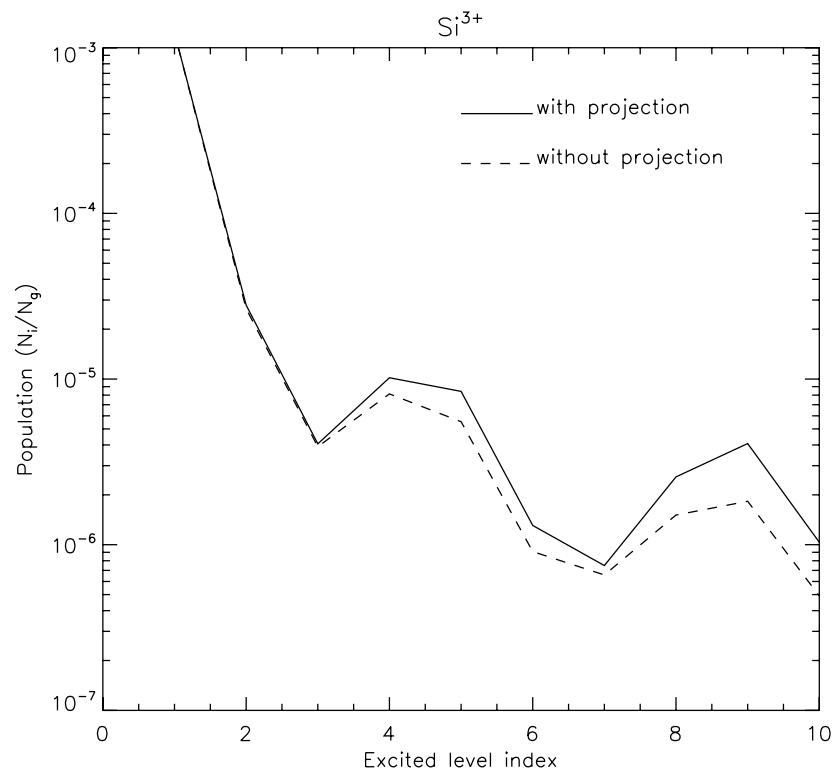


Figure 3: demo_b/demo_b_4.pdf

2.2 Demo (b) Procedures

2.2.1 Demo (b-4) demo.b/demo_b_4.pro

```
pro demo_b_4
;to compare the population obtained from the adf04 for Si3+ using the projection
;file and without it

te      = 13.0
dens   = 1e13
unit_te = 'ev'
unid_dens = 'cm-3'
meta_list = [1]

adf04 = 'asg09_lgy09_ls#si3.dat'
adf18 = 'exp96#na_si3ls.dat'

;use run_adas208.pro to calculate the populations with the projection file
run_adas208, adf04=adf04, adf18=adf18,
              te=te, dens=dens, unit_te=unit_te, unit_dens=unit_dens,
              meta=meta_list,
              pass_dir='.', pop=pop_pju, log='paper.txt'

;use run_adas208.pro without the projection file
run_adas208, adf04=adf04,
              te=te, dens=dens, unit_te=unit_te, unit_dens=unit_dens,
              meta=meta_list,
              pass_dir='.', pop=pop_llu

;-----
; Plot populations
;-----

index    = indgen(pop_pju.numlev) + 1
dep_pju  = pop_pju.dependence
dep_llu  = pop_llu.dependence

xmin = 1
xmax = 10
ymin = 1e-7
ymax = 1e-3

set_plot,'ps'
device, /isolatin1, font_index=8
device, bits=8, filename='demo_b_4.ps',  $
          font_size = 14, xsize=18.0, ysize=16.0, $
```

```

yoffset=7.0, /color
device, /helvetica
plot_io, [xmin, xmax], [ymin, ymax], /nodata, ystyle=1,$
    title='Si!u3+!n', $
    xtitle = 'Excited level index', $
    ytitle = 'Population (N!di!n/N!dg!n)'

oplot, index, dep_pju, thick=3
oplot, index, dep_llu, line=2, thick=3

plots,[5.,6.],[4.e-4,4.e-4], thick=3
xyouts,6.05,4.e-4,'with projection'
plots,[5.,6.],[2.e-4,2.e-4], thick=3,line=2
xyouts,6.05,2.e-4,'without projection'

```

```

device, /close
set_plot,'X'
!p.font=-1

```

```
end
```

2.3 Demo (b) Tables and datasets

2.3.1 Demo (b-2) demo.b/adas204.adf17.pass

```

SEQUENCE = na   NUCCHG =14   NPARNT = 2   MAXD =24   MAXT =24
IEDMAT = 0   IECION = 0   IETREC = 0   IEDREC = 0   IERREC = 0   IEXREC = 0   IERSYS = 0
NE(CM-3) =   1.64D+05   1.64D+06   1.64D+07   1.64D+08   1.64D+09   1.64D+10   4.92D+10   1.64D+11
               4.92D+13   1.64D+14   4.92D+14   1.64D+15   4.92D+15   1.64D+16   4.92D+16   1.64D+17
TE(K)      =   8.00D+03   1.12D+04   1.60D+04   2.40D+04   3.20D+04   4.80D+04   8.00D+04   1.12D+05
               8.00D+05   1.12D+06   1.60D+06   2.40D+06   3.20D+06   4.80D+06   8.00D+06   1.12D+07
IPRT = 1   TRMPRT = (1S)   SPNPRT = 1.
-----
SPNSYS = 2.   NSHEL = 3
-----
ID= 1 IT= 1 N= 3   9.3737513787D-13-2.5881195019D+09-6.2892858578D+08
               N= 4   -9.3732071464D-13 2.5881195019D+09-7.2243053977D+08
               N= 5   -5.4423231613D-17-5.8160151830D-06 1.3513591255D+09
(DIR) N= 3   9.3737489303D-13-2.5881195019D+09-6.2892858578D+08
               N= 4   -9.3732060783D-13 2.5881195019D+09-7.2243053977D+08
               N= 5   -5.4285198554D-17-5.8031868604D-06 1.3513591255D+09
(PRB)          4.2567599516D-22
.
.
.
ID= 1 IT= 2 N= 3   6.6555125989D-10-2.5881195019D+09-6.2892858578D+08
               N= 4   -6.6509918273D-10 2.5881195019D+09-7.2243053977D+08
               N= 5   -4.5207702277D-13-6.0327599846D-05 1.3513591255D+09
(DIR) N= 3   6.6554400139D-10-2.5881195019D+09-6.2892858578D+08
               N= 4   -6.6509599877D-10 2.5881195019D+09-7.2243053977D+08
               N= 5   -4.4800261554D-13-5.9867220145D-05 1.3513591255D+09
(PRB)          3.3778496536D-22
.
.
.
ID=24 IT=24 N= 3   1.9035247633D+11-8.5202879688D+10-1.0056202220D+10
               N= 4   -1.4628947181D+11 1.1544201549D+12-5.3447206624D+11
               N= 5   -2.5724447421D+10-8.3267586993D+11 3.9016749836D+12
(DIR) N= 3   1.6895371708D+11-8.5163410268D+10-8.8547709432D+09
               N= 4   -1.4622619208D+11 8.8410431550D+11-5.1277901425D+11
.
.
.
0.00000000000D+00

```

```
N= 5 -2.2727524999D+10-7.9894090523D+11 5.2163378519D+11
(PRB) 1.4013878323D-22
```

2.3.2 Demo (b-3) demo.b/exp96#na_si3ls.dat

```
&SEQINF SEQ='Na',
DSNREF='asg09_lgy09_ls#si3.dat',
DSNCMP='/home/asg/adas_modules/module_2/demo_b/adas204_adf17.pass ',
NPARNT=2,
NSHEL=5,
NLEV= 12,
&END

PARENT      :(1S)      :(3P)      :
SPINRPT    :1          :3          :
NSPNSYS    :1          :1          :

PARENT = 1
-----
SPINSYS   :2          :
LOWESTN   :3          :
IMAX      :1          :
LOWESTP   :1.0000     :
FRPARNT   :0.2500     :

PARENT = 2
-----
SPINSYS   :2          :
LOWESTN   :3          :
IMAX      :1          :
LOWESTP   :1.0000     :
FRPARNT   :0.7500     :

RESOLVED NL <-- BUNDLE-N           N:1      N:2      N:3      N:4      N:5
INDX CODE      SZD SP SH PT  N-SHELL NORMALISED WEIGHTS
----- -----
1 3S      (2)0( 0.5) 0 2 3 1 :  :  : 0.1111:  :
1 3S      (2)0( 0.5) 0 2 3 2 :  :  : 1.0000:  :
2 3P      (2)1( 2.5) 0 2 3 1 :  :  : 0.3333:  :
3 3D      (2)2( 4.5) 0 2 3 1 :  :  : 0.5556:  :
4 4S      (2)0( 0.5) 0 2 4 1 :  :  : 0.0625:  :
5 4P      (2)1( 2.5) 0 2 4 1 :  :  : 0.1875:  :
6 4D      (2)2( 4.5) 0 2 4 1 :  :  : 0.3125:  :
7 4F      (2)3( 6.5) 0 2 4 1 :  :  : 0.4375:  :
8 5S      (2)0( 0.5) 0 2 5 1 :  :  : 0.0400:  :
9 5P      (2)1( 2.5) 0 2 5 1 :  :  : 0.1200:  :
10 5D     (2)2( 4.5) 0 2 5 1 :  :  : 0.2000:  :
11 5F     (2)3( 6.5) 0 2 5 1 :  :  : 0.2800:  :
12 5G     (2)4( 8.5) 0 2 5 1 :  :  : 0.3600:  :

C-----
C
C ADF04 FILE FOR PARENT ION:
C adf04/ada#14/asg09_ls#si4.dat
C
C ADF04 FILE FOR RECOMBINED ION:
C adf04/ada#14/asg09_lgy09_ls#si3.dat
C
C Code      : ADAS07
C Producer : Alessandra Giunta
C Date     : 22/10/10
C
```

3 Demo (c) Producing and examining a mapping file

DEMO C: Producing and examining a mapping file

PURPOSE: Create a mapping file to connect the specific ion file in the adf04 format to the dielectronuc data in the af09 format.

EXAMPLE: Li0+ is used as example. The input file for the ADAS807 running are the following:

- adf04: /home/adas/adas/adas#3/cpb02_ls#li0.dat
- adf09: /home/adas/adas/adf09/nrb93#he/nrb93#he_li1ls12.dat
/home/adas/adas/adf09/nrb93#he/nrb93#he_li1ls22.dat

DEMO c1: Using ADAS807 to produce a mapping file

1. Run ADAS807 interactively to produce a mapping file for Li0+.
2. Examine the mapping file.

Sample of output files: adas807_a09_a04.pass

3.1 Demo (c) Tables and datasets

3.1.1 Demo (c-1) demo_c/adas807_a09_a04.pass

Specific ion input file

"ADASCENT"/adf04/adas#3/cpb02_ls#li0.dat : specific ion file

Badnell dielectronic files

/home/adas/adas/adf09/nrb93#he/nrb93#he_li1ls12.dat : 1st. Badnell file
/home/adas/adas/adf09/nrb93#he/nrb93#he_li1ls22.dat : 2nd. Badnell file

Output files

"ADASUSER"/pass/postllev.pass : supplemented spec. ion file
"ADASUSER"/pass/postllev.pass1 : dielectronic data for MAINCL codes

Level cross-reference lists for specific ion and badnell files

| sp. | bd1. | bd2. | bd3. | bd4. | bd5. | bd6. |
|-----|------|------|------|------|------|------|
| --- | ---- | ---- | ---- | ---- | ---- | ---- |
| 1 | 1 | 1 | | | | |
| 2 | 34 | 34 | | | | |
| 3 | 2 | 2 | | | | |
| 4 | 3 | 3 | | | | |
| 5 | 4 | 4 | | | | |
| 6 | 5 | 5 | | | | |
| 7 | 6 | 6 | | | | |
| 8 | 8 | 8 | | | | |
| 9 | 7 | 7 | | | | |

| C----- | # specific ion | Badnell 1 | Badnell 2 |
|--------|----------------|---------------|--------------|
| C 1 | 2S1 | 2S 1/2--> 2S1 | 2S 1/2 2S1 |
| C 2 | 2P1 | 2P 5/2--> 2P1 | 2P 5/2 2P1 |
| C 3 | 3S1 | 2S 1/2--> 3S1 | 2S 1/2 3S1 |
| C 4 | 3P1 | 2P 5/2--> 3P1 | 2P 5/2 3P1 |
| C 5 | 3D1 | 2D 9/2--> 3D1 | 2D 9/2 3D1 |
| C 6 | 4S1 | 2S 1/2--> 4S1 | 2S 1/2 4S1 |
| C 7 | 4P1 | 2P 5/2--> 4P1 | 2P 5/2 4P1 |
| C 8 | 4D1 | 2D 9/2--> 4D1 | 2D 9/2 4D1 |
| C 9 | 4F1 | 2F13/2--> 4F1 | 2F13/2 4F1 |

```
C-----  
C-----  
C ADF04 FILE :  
C      /home/asg/adas_dev/adas/adf04/adas#3/cpb02_ls#li0.dat  
C  
C ADF09 FILE(S) FOR RECOMBINED ION:  
C      /home/adas/adas/adf09/nrb93#he/nrb93#he_li1ls12.dat  
C      /home/adas/adas/adf09/nrb93#he/nrb93#he_li1ls22.dat  
C  
C  
C Code      : ADAS807  
C Producer : Alessandra Giunta  
C Date     : 19/06/13  
C-----
```

4 Demo (d)Evaluating metastable pathways for ionisation cross-sections

DEMO D: Evaluating metastable pathways for ionisation cross-sections

PURPOSE: Convert an unresolved adf07 data file in a ls resolved adf07.
The adf07 data files provide electron impact ionisation rate coefficients for each ion of an element. The baseline within ADAS is calculated using the offline ADAS8#2 using the Configuration Average Distorted Wave (CADW) method, which gives stage to stage ionisation rates. The GCR picture requires metastable resolved ionisation rates and so a resolved adf07.
This can be produced using the following idl routines, stored in /home/adas/adas/idl/adaslib/proc_adf/:
- pathways_adf07.pro
- fractionate_adf07.pro
- split_adf07.pro.

EXAMPLE: For this demo Boron is considered. The resolved ionisation rates for B1+→B2+ are derived.

The input files are the following:

- input adf04 for B1+: /home/adas/adas/adf04/belike/belike_nrb03#b1.dat
- input adf04 for B2+: /home/adas/adas/adf04/lilike/lilike_dvb02#b2.dat
- unresolved adf07 for B: /home/adas/adas/adf07/szd93#b/szd93#b_b.dat

DEMO d1:Convert adf07 from unresolved to resolved

1. Create the pathway file from the adf04 data files.
2. Generate an ionisation pathway spreadsheet.
3. Produce the resolved adf07.
4. Compare the resolved and unresolved adf07.

Program: demo_d.pro

Sample of output files: pathways_b1_b2.dat, fractionation_b.csv (use oocalc to view), boron_adf07.dat

4.1 Demo (d) Tables and datasets

4.1.1 Demo (d-1) demo.d/pathways.b1.b2.dat

| | |
|------------------------|-----------------------------------|
| B+1 | |
| B+1 Metastable Number: | 2 |
| B+2 Metastable Number: | 1 |
| Orbital Number: | 3 |
| Pathway Numbers: | 2 2 |
| ----- | |
| Orbital | Energy(Ryd) |
| ----- | |
| 1s | 16.418 |
| 2s | 1.919 |
| 2p | 1.462 |
| ----- | |
| B+1 → B+2 | |
| ----- | |
| Pathways | I.P.(cm ⁻¹) I.P.(Ryd) |
| ----- | |
| 1s2 2s2 1s → 2s | 1s2 2s1 2s 202888.0 1.84885 |

| | | | | | | | |
|-----|-----|-----|-----|-----|----|----------|----------|
| | | 1s | 1s1 | 2s2 | 2S | -1.0 | -1.00000 |
| 1s2 | 2s1 | 2p1 | 3P | -> | | | |
| | | 2p | 1s2 | 2s1 | 2S | 165544.0 | 1.50855 |
| | | 2s | 1s2 | 2p1 | 2P | 213916.0 | 1.94935 |

4.1.2 Demo (d-1) demo.d/fractionation.b.csv

```
"Transition","Metastable","Index","Purpose","Formula","Shell 1","","Shell 2","","Shell 3",
,"Shell 4","","Shell 5","","Shell 6","","Shell 7","","Scale factor"
,,,"I(is) (Ryd)","z(is) (Ryd)","I(2s) (Ryd)","z(2s) (Ryd)","I(2p) (Ryd)","z(2p) (Ryd)","I(3s)(Ryd)",
,"z(3s)","I(3p)(Ryd)","z(3p)","I(4s)(Ryd)","z(4s)","I(3d)(Ryd)","z(3d)",
,"B+1 -> B+2","","f1",,,14.4990,2.00000,1.84885,2.00000,,...,1.000
,,,"RATE comparison","ratio=RATE/f1",,,,...,,
,"1s2 2s2(1S)","f2","2s via 2S direct",,,,1.84885,2.00000,,...,1.00000
,,,"f3","is +auto",,,14.4990,2.00000,,...,1.00000
,,,"f4","is direct",,,16.4180,2.00000,,...,1.00000
,,,"1s2 2s2(1S) total","(f2+f3)*ratio",,,,...,,
,"#","1s2 2s2(1S)->1s2 2s1(2S)","(f2+f3)*ratio",,,,...,,
,"1s2 2s1 2p1(3P)","f5","2p via 2S direct",,,,1.50855,1.00000,,...,1.00000
,,,"f6","2s via 2P +auto",,,1.50855,1.00000,,...,1.00000
,,,"f7","is +auto",,,14.4990,2.00000,,...,1.00000
,,,"f8","is direct",,,16.4180,2.00000,,...,1.00000
,,,"1s2 2s1 2p1(3P) total","(f5+f6+f7)*ratio",,,,...,,
,"#","1s2 2s1 2p1(3P)->1s2 2s1(2S)","(f5+f6+f7)*ratio",,,,...,,
```

4.1.3 Demo (d-1) demo.d/boron.adf07.dat

```
4 /B IONISATION RATE COEFFICIENTS /
B + 1/B + 2/ 24/I.P. = 202887.2/ICODE = 1/FCODE = 0/ISEL = 1
1.000E+00 2.000E+00 3.000E+00 4.000E+00 5.000E+00 7.000E+00
1.000E+01 1.500E+01 2.000E+01 3.000E+01 4.000E+01 5.000E+01
7.000E+01 1.000E+02 1.500E+02 2.000E+02 3.000E+02 4.000E+02
5.000E+02 7.000E+02 1.000E+03 2.000E+03 5.000E+03 1.000E+04
2.629E-12 3.189E-10 1.803E-09 4.520E-09 8.059E-09 1.618E-08
2.832E-08 4.526E-08 5.807E-08 7.539E-08 8.620E-08 9.339E-08
1.019E-07 1.079E-07 1.110E-07 1.111E-07 1.088E-07 1.058E-07
1.028E-07 9.758E-08 9.128E-08 7.803E-08 6.079E-08 4.915E-08
B + 1/B + 2/ 24/I.P. = 202887.2/ICODE = 1/FCODE = 1/ISEL = 2
1.000E+00 2.000E+00 3.000E+00 4.000E+00 5.000E+00 7.000E+00
1.000E+01 1.500E+01 2.000E+01 3.000E+01 4.000E+01 5.000E+01
7.000E+01 1.000E+02 1.500E+02 2.000E+02 3.000E+02 4.000E+02
5.000E+02 7.000E+02 1.000E+03 2.000E+03 5.000E+03 1.000E+04
2.629E-12 3.189E-10 1.803E-09 4.520E-09 8.059E-09 1.618E-08
2.832E-08 4.526E-08 5.807E-08 7.539E-08 8.620E-08 9.339E-08
1.019E-07 1.079E-07 1.110E-07 1.111E-07 1.088E-07 1.058E-07
1.028E-07 9.758E-08 9.128E-08 7.803E-08 6.079E-08 4.915E-08
B + 1/B + 2/ 24/I.P. = 165543.8/ICODE = 2/FCODE = 0/ISEL = 3
1.000E+00 2.000E+00 3.000E+00 4.000E+00 5.000E+00 7.000E+00
1.000E+01 1.500E+01 2.000E+01 3.000E+01 4.000E+01 5.000E+01
7.000E+01 1.000E+02 1.500E+02 2.000E+02 3.000E+02 4.000E+02
5.000E+02 7.000E+02 1.000E+03 2.000E+03 5.000E+03 1.000E+04
4.047E-10 4.817E-09 1.252E-08 2.123E-08 2.990E-08 4.574E-08
6.504E-08 8.806E-08 1.037E-07 1.231E-07 1.342E-07 1.411E-07
1.485E-07 1.526E-07 1.529E-07 1.507E-07 1.450E-07 1.396E-07
1.347E-07 1.267E-07 1.176E-07 9.936E-08 7.655E-08 6.151E-08
B + 1/B + 2/ 24/I.P. = 165543.8/ICODE = 2/FCODE = 1/ISEL = 4
1.000E+00 2.000E+00 3.000E+00 4.000E+00 5.000E+00 7.000E+00
1.000E+01 1.500E+01 2.000E+01 3.000E+01 4.000E+01 5.000E+01
7.000E+01 1.000E+02 1.500E+02 2.000E+02 3.000E+02 4.000E+02
5.000E+02 7.000E+02 1.000E+03 2.000E+03 5.000E+03 1.000E+04
4.047E-10 4.817E-09 1.252E-08 2.123E-08 2.990E-08 4.574E-08
6.504E-08 8.806E-08 1.037E-07 1.231E-07 1.342E-07 1.411E-07
1.485E-07 1.526E-07 1.529E-07 1.507E-07 1.450E-07 1.396E-07
1.347E-07 1.267E-07 1.176E-07 9.936E-08 7.655E-08 6.151E-08
C-----
C
C
C
C Resolved adf07 : /home/adas/adas/adf07/szd93#b/szd93#b_b.dat
C
C
```

```

C
C
C
C   ISEL  INITIAL MET.    DESIG.          FINAL  MET.    DESIG.
C           ION      CODE
C   -----
C   1   B + 1    1    1s2 2s2 (1S)        B + 2    0    Total
C   2   B + 1    1    1s2 2s2 (1S)        B + 2    1    1s2 2s1 (2S)
C   3   B + 1    2    1s2 2s1 2p1 (3P)    B + 2    0    Total
C   4   B + 1    2    1s2 2s1 2p1 (3P)    B + 2    1    1s2 2s1 (2S)
C
C
C
C   Code   : split_adf07.pro
C   Author : Alessandra Giunta
C   Date   : 16/07/13
C
C-----

```

5 Demo (e) Making up partitions and executing superstage compression

DEMO E: Making up partitions and executing superstage compression

PURPOSE: To build up a partition and execute a superstage compression.
In the GCR picture, each element is described by the fractional abundances of every ionisation stage, derived by the effective ionisation and recombination coefficients. From a dynamic point of view the whole set of populations may be tracked in transport modelling. However, for heavy species, the complete set of populations is large. Since not all populations are of equal importance, grouping of populations may be appropriate and reduces the problem of dealing with a too large number of ionisation stages. The specification of grouping is called "partition", while the members of partition are called "superstages".

EXAMPLE: Tungsten is used for this demo. The input file for the ADAS416 run is w_partition_7groups.dat. The output provides the whole set of effective coefficients for the superstages. These files can be read by read_adf11.pro to show the effective coefficients.

COMMENTS: In demo_e_3.pro, the paths which define the adf11 produced by ADAS416 depend on the user.

DEMO e1: Examine a natural partition

1. Use preview_natural_partition.pro to show the
 - fractional ionisation potential change
 - partition fractional abundance
 - fractional abundances for all 74 W ionisation stages
 - fractional abundances for 35 partitions of W

Programs: demo_e_1.pro

Sample of output files: demo_e_1.ps

DEMO e2: Apply superstage compression with ADAS416

1. Use ADAS416 interactively.

Samples of output files: adas416_plot.ps

All set of adf11 data files: acd50 ccd50 ecd50 plt50 prb50
prc50 scd50 ycd50 zcd50

DEMO e3: Show the superstage coefficient behaviour.

1. Define input files.
2. Use read_adf1.pro to read:
 - recombination rates
 - effective charge

Program: demo_e_3.pro

Sample of output files: demo_e_3_acd.ps, demo_e_3_zeff.ps

5.1 Demo (e) Figures

5.1.1 Demo (e-1) demo_e/demo_e_1.pdf

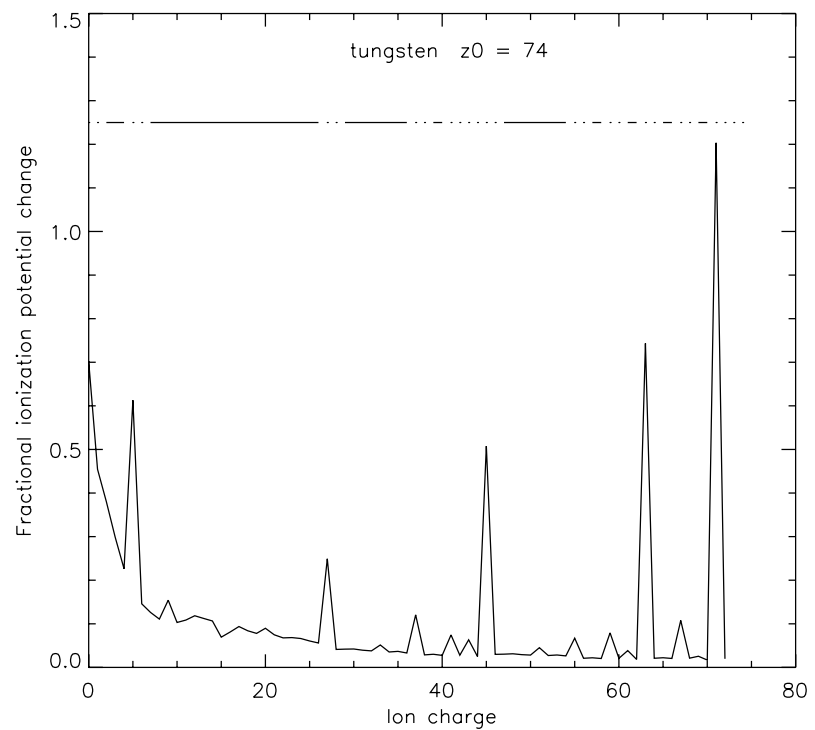


Figure 4: Natural partition for tungsten

5.1.2 Demo (e-2) demo_e/adas416.plot.pdf

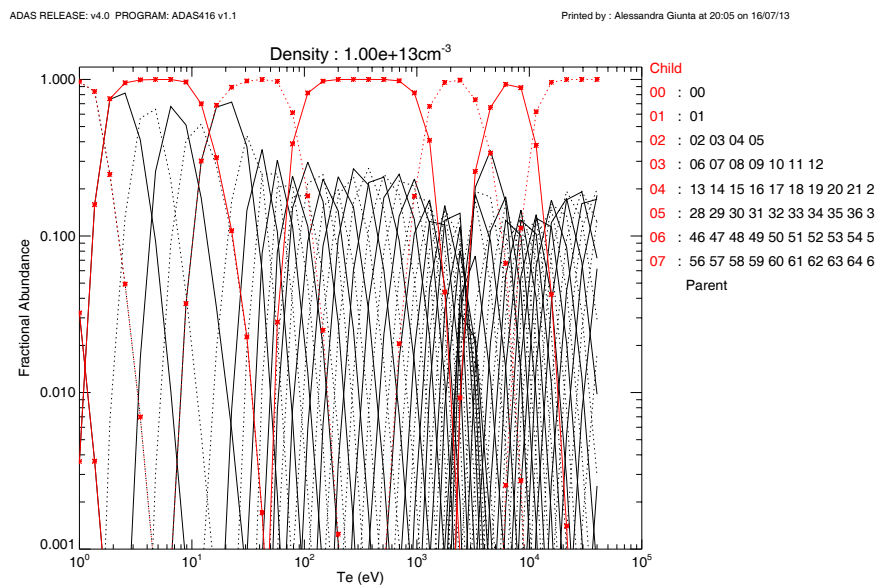


Figure 5: Superstage ionisation balance for tungsten

5.1.3 Demo (e-3) demo_e/demo_e_3.acd.pdf

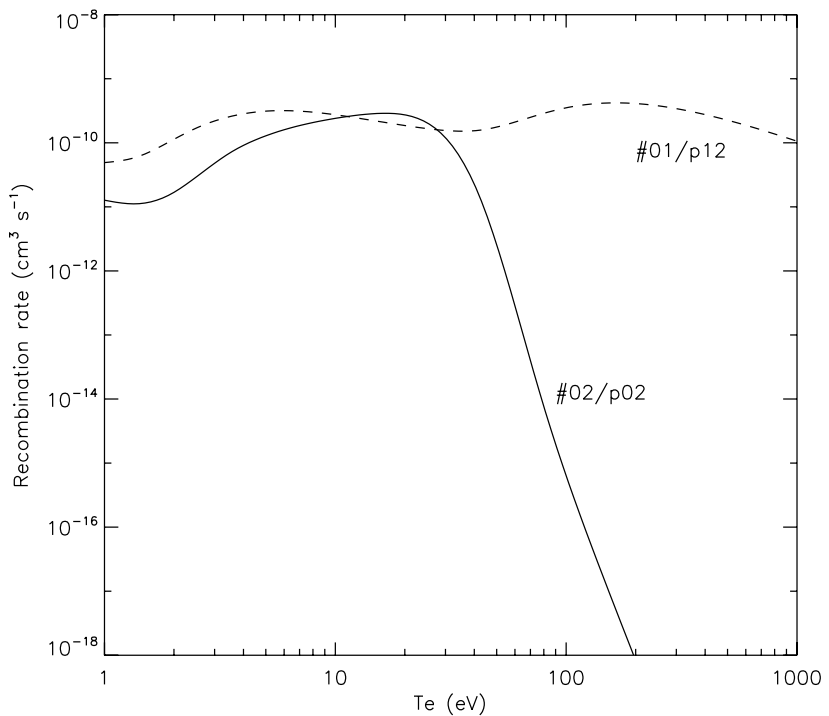


Figure 6: Superstage recombination coefficients for tungsten

5.1.4 Demo (e-3) demo_e/demo_e_3_zeff.pdf

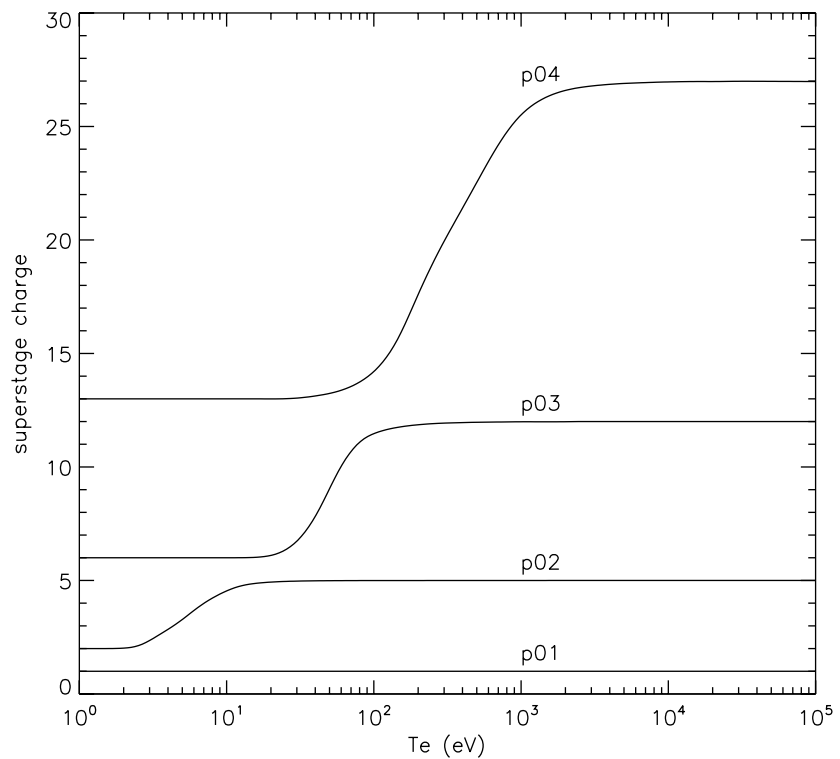


Figure 7: Superstage charges for tungsten

5.2 Demo (e) Procedures

5.2.1 Demo (e-1 demo_e_1.pro)

Demonstration IDL procedure for preliminary examination of superstage partitions.

```
pro demo_e_1
;to identify the natural partition for W and plot the superstages

set_plot,'ps'
device, /isolatin1, font_index=8
device, bits=8, filename='demo_e_1.ps', $
    font_size = 14, xsize=18.0, ysize=16.0, $
    yoffset=7.0, /color
device, /helvetica

preview_natural_partition, z0=74, te_min=10, te_max=50000, plot_type=1
preview_natural_partition, z0=74, te_min=10, te_max=50000, plot_type=2
preview_natural_partition, z0=74, te_min=10, te_max=50000, plot_type=3
preview_natural_partition, z0=74, te_min=10, te_max=50000, plot_type=4

device, /close
set_plot,'X'
!p.font=-1

end
```

5.2.2 Demo (e-3 demo_e_3.pro)

To show the effective coefficients for W after a superstage compression.

```
pro demo_e_3
;To show the effective coefficients for W after a superstage compression has been
applied.

; Conditions

itval = 200
te   = adas_vector(low=1, high=1e5, num=itval)
dens = fltarr(itval) + 1e13

; files

files   =
{ acd : '/home/asg/adas_modules/module_2/demo_e/adf11/acd50/acd50_w.dat', $
  scd : '/home/asg/adas_modules/module_2/demo_e/adf11/scd50/scd50_w.dat', $
  plt : '/home/asg/adas_modules/module_2/demo_e/adf11/plt50/plt50_w.dat', $
  prb : '/home/asg/adas_modules/module_2/demo_e/adf11/prb50/prb50_w.dat' }
```

```

files_ss =
{ acd : '/home/asg/adas_modules/module_2/demo_e/adf11/acd50/acd50_w_02.dat', $
  scd : '/home/asg/adas_modules/module_2/demo_e/adf11/scd50/scd50_w_02.dat', $
  plt : '/home/asg/adas_modules/module_2/demo_e/adf11/plt50/plt50_w_02.dat', $
  prb : '/home/asg/adas_modules/module_2/demo_e/adf11/prb50/prb50_w_02.dat' }

; Recombination rates

read_adf11, file=files_ss.acd, class='acd', iz0=74, iz1=3, $
              te=te, dens=dens, data=acd_ss

read_adf11, file=files.acd, class='acd', iz0=74, iz1=13, $
              te=te, dens=dens, data=acd

xmin = min(te, max=xmax)
xmax = 1e3
ymin = 1e-18
ymax = 1e-8

set_plot,'ps'
device, /isolatin1, font_index=8
device, bits=8, filename='demo_e_3_acd.ps',  $
          font_size = 14, xsize=18.0, ysize=16.0, $
          yoffset=7.0, /color
device, /helvetica

plot_oo, [xmin, xmax], [ymin, ymax], /nodata, ystyle=1,  $
          xtitle = 'Te (eV)', $
          ytitle = 'Recombination rate (cm!u3!n s!u-1!n)'

oplot, te, acd_ss, thick=3

oplot, te, acd, thick=3, line=2

xyouts, 90, 1e-14, '#02/p02'
xyouts, 200, 6e-11, '#01/p12'

device, /close
set_plot,'X'
!p.font=-1

; Effective charge

file = '/home/asg/adas_modules/module_2/demo_e/adf11/zcd50/zcd50_w_02.dat'

read_adf11, file=file, class='zcd', iz0=74, iz1=1, $

```

```

        te=te, dens=dens, data=zcd_p0
read_adf11, file=file, class='zcd', iz0=74, iz1=2, $
        te=te, dens=dens, data=zcd_p1
read_adf11, file=file, class='zcd', iz0=74, iz1=3, $
        te=te, dens=dens, data=zcd_p2
read_adf11, file=file, class='zcd', iz0=74, iz1=4, $
        te=te, dens=dens, data=zcd_p3
read_adf11, file=file, class='zcd', iz0=74, iz1=5, $
        te=te, dens=dens, data=zcd_p4

xmin = min(te, max=xmax)
ymin = min(zcd_p0)
ymax = max(zcd_p4)

set_plot,'ps'
device, /isolatin1, font_index=8
device, bits=8, filename='demo_e_3_zeff.ps',  $
        font_size = 14, xsize=18.0, ysize=16.0, $
        yoffset=7.0, /color
device, /helvetica

plot_oi, [xmin, xmax], [ymin, ymax], /nodata, ystyle=0,  $
        xtitle = 'Te (eV)', $
        ytitle = 'superstage charge'

oplot, te, zcd_p0, thick=3
oplot, te, zcd_p1, thick=3
oplot, te, zcd_p2, thick=3
oplot, te, zcd_p3, thick=3
oplot, te, zcd_p4, thick=3

xyouts, 1000, 1.5, 'p01'
xyouts, 1000, 5.5, 'p02'
xyouts, 1000, 12.5, 'p03'
xyouts, 1000, 27, 'p04'

device, /close
set_plot,'X'
!p.font=-1

end

```

5.3 Demo (e) Tables and datasets

5.3.1 Demo (e-2) demo_d/adf11/adc50/adc50_w_02.dat

```

    74      5     35      1     7      /TUNGSTEN          /ACD /GCR PROJECT      ADF11
-----
//#02/p00/ 00 /
p01/ 01/
p02/ 02 03 04 05/
p03/ 06 07 08 09 10 11 12/
p04/ 13 14 15 16 17 18 19 20 21 22 23 24 25 26 27/
p05/ 28 29 30 31 32 33 34 35 36 37 38 39 40 41 42 43 44 45/
p06/ 46 47 48 49 50 51 52 53 54 55/
p07/ 56 57 58 59 60 61 62 63 64 65 66 67 68 69 70 71 72 73 74/
-----//#01/p00/ 00/p01/ 01/p02/ 02/p03/ 03/p04/ 04/p05/ 05/p06/ 06/p07/ 07/
p08/ 08/p09/ 09/p10/ 10/p11/ 11/p12/ 12/p13/ 13/p14/ 14/p15/ 15/
p16/ 16/p17/ 17/p18/ 18/p19/ 19/p20/ 20/p21/ 21/p22/ 22/p23/ 23/
p24/ 24/p25/ 25/p26/ 26/p27/ 27/p28/ 28/p29/ 29/p30/ 30/p31/ 31/
p32/ 32/p33/ 33/p34/ 34/p35/ 35/p36/ 36/p37/ 37/p38/ 38/p39/ 39/
p40/ 40/p41/ 41/p42/ 42/p43/ 43/p44/ 44/p45/ 45/p46/ 46/p47/ 47/
p48/ 48/p49/ 49/p50/ 50/p51/ 51/p52/ 52/p53/ 53/p54/ 54/p55/ 55/
p56/ 56/p57/ 57/p58/ 58/p59/ 59/p60/ 60/p61/ 61/p62/ 62/p63/ 63/
p64/ 64/p65/ 65/p66/ 66/p67/ 67/p68/ 68/p69/ 69/p70/ 70/p71/ 71/
p72/ 72/p73/ 73/p74/ 74/
-----
11.00000 12.00000 13.00000 14.00000 15.00000
 0.00000 0.13535 0.27071 0.40606 0.54142 0.67677 0.81213 0.94748
 1.08284 1.21819 1.35355 1.48890 1.62426 1.75961 1.89497 2.03032
 2.16568 2.30103 2.43638 2.57174 2.70709 2.84245 2.97780 3.11316
 3.24851 3.38387 3.51922 3.65458 3.78993 3.92529 4.06064 4.19600
 4.33135 4.46671 4.60206
-----/ ISPP= 1 / ISPB= 1 /-----/ S1= 1 / DATE= 16:07:13
-11.66843 -11.68984 -11.70588 -11.71774 -11.72646
-11.52151 -11.59021 -11.64720 -11.69306 -11.72901
-11.29994 -11.40750 -11.50442 -11.58920 -11.66132
-11.08599 -11.21833 -11.34420 -11.46009 -11.56388
-10.92868 -11.07716 -11.22298 -11.36081 -11.48740
-10.81161 -10.97420 -11.13840 -11.29643 -11.44335
-10.73620 -10.90971 -11.08948 -11.26557 -11.43106
-10.70565 -10.88643 -11.07782 -11.26838 -11.44958
-10.71961 -10.90458 -11.10375 -11.30484 -11.49815
-10.77329 -10.96022 -11.16421 -11.37247 -11.57451
-10.85983 -11.04725 -11.25397 -11.46690 -11.67499
-10.97215 -11.15911 -11.36714 -11.58301 -11.79516
-11.10252 -11.28845 -11.49694 -11.71464 -11.92959
-11.24088 -11.42552 -11.63416 -11.85333 -12.07072
-11.37526 -11.55864 -11.76761 -11.98862 -12.20907
-11.49888 -11.68110 -11.89069 -12.11414 -12.33859
-11.61440 -11.79538 -12.00557 -12.23161 -12.46047
-11.73011 -11.90957 -12.11998 -12.34815 -12.58100
-11.85346 -12.03106 -12.24114 -12.47069 -12.70664
-11.98796 -12.16341 -12.37263 -12.60283 -12.84091
-12.13402 -12.30708 -12.51502 -12.74527 -12.98467
-12.29040 -12.46091 -12.66726 -12.89709 -13.13718
-12.45533 -12.62316 -12.82769 -13.05675 -13.29708
-12.62709 -12.79215 -12.99467 -13.22270 -13.46292
-12.80421 -12.96643 -13.16680 -13.39362 -13.63347
-12.98548 -13.14483 -13.34294 -13.56838 -13.80769
-13.16999 -13.32642 -13.52218 -13.74612 -13.98473
-13.35701 -13.51048 -13.70382 -13.92617 -14.16397
-13.54599 -13.69649 -13.88733 -14.10800 -14.34490
-13.73647 -13.88399 -14.07228 -14.29119 -14.52713
-13.92813 -14.07267 -14.25835 -14.47543 -14.71032
-14.12074 -14.26228 -14.44531 -14.66051 -14.89431
-14.31410 -14.45263 -14.63298 -14.84623 -15.07889
-14.50894 -14.64358 -14.82119 -15.03245 -15.26390
-14.70251 -14.83506 -15.00991 -15.21910 -15.44931
-----/ ISPP= 1 / ISPB= 1 /-----/ S1= 2 / DATE= 16:07:13
-11.43897 -11.45854 -11.47317 -11.48398 -11.49191
-11.22838 -11.30461 -11.36954 -11.42320 -11.46625
-10.91068 -11.02587 -11.13353 -11.23227 -11.32061
-10.64807 -10.78941 -10.93270 -11.07665 -11.21821
-10.65524 -10.84518 -11.04928 -11.26819 -11.49887
-11.02404 -11.26858 -11.53654 -11.83362 -12.16029

```

```
-11.74823 -12.04148 -12.36408 -12.72787 -13.13952  
C-----  
C  
C   Rate coefficients: adf11 class acd  
C   Units           : cm3 s-1  
C   Status          : partition applied  
C   Parent dataset  : /home/asg/adas_modules/module_2/demo_e/adf11/acd50/acd50_w.dat  
C  
C   Code            : adas416  
C   Producer        : Alessandra Giunta  
C   Date            : 16/07/13  
C-----
```

C.3 module_3

MODULE 3

H₂ molecular emission and collisional-radiative modelling.

Demonstration script

Hugh Summers, Francisco Guzman, Kurt Behringer,
Martin O'Mullane and Alessandra Giunta

October 14, 2013

Contents

| | |
|--|----------|
| 1 Demo (a) Looking at molecular data | 2 |
| 1.1 Demo (a) Figures | 4 |
| 1.1.1 Demo (a-1) demo_a/demo_a_1_avalue.pdf | 4 |
| 1.1.2 Demo (a-1) demo_a/demo_a_1_fcordon.pdf | 5 |
| 1.1.3 Demo (a-2) demo_a/adas901.pdf | 6 |
| 1.2 Demo (a) Procedures | 7 |
| 1.2.1 Demo (a-1) demo_a/demo_a.pro | 7 |
| 2 Demo (b) Rovibronic emission from heteronuclear diatomics | 9 |
| 2.1 Demo (b) Figures | 11 |
| 2.1.1 Demo (b-1) demo_b/demo_b_1_BeD.temp.ps | 11 |
| 2.1.2 Demo (b-1) demo_b/demo_b_1_BeD.BeT.ps | 12 |
| 2.2 Demo (b) Procedures | 13 |
| 2.2.1 Demo (b-1) demo_b/demo_b.pro | 13 |

1 Demo (a) Looking at molecular data

DEMO A: Looking at molecular data

PURPOSE: Look at H₂ fundamental molecular constants and data.
As for atoms and ions, ADAS includes data format for molecules called mdf
(molecular data formats).
This demo shows how to look and extract data from mdf00 and mdf02 data files.

The data files mdf00 contain the following molecular constants, collected in different subdirectories:

- emu: vibrational substate energies for each electronic state;
- pot: electronic potential curve for each electronic state;
- dip: electronic dipole curve for each electronic state;
- aval: vibrationally resolved A-values for each electronic state pair;
- fcf: vibrationally resolved Franck-Condon factors for each electronic state pair.

The data files mdf02 provide the impact process molecular data and are designed to have both the numerical and parameters of the formulaic representation (if available) of each transition.

As for the atomic data, there are routines and interactive programs which deal with the molecular data files.

The idl routine to read and extract data from mdf00 is xxdatm_00.pro.
ADAS901 deals interactively with mdf02 files.

EXAMPLE: For this demo, data for H₂ molecule are considered. These data are read and extracted using the idl routine xxdatm_00.pro to look at A-values (/home/adas/adas/mdf00/aval/h2/aval0112_0109.dat) and Franck-Condon factors (/home/adas/adas/mdf00/fcf/h2/fc0101_0102.dat).

The input file for the ADAS901 run is
/home/adas/adas/mdf02/h2/fg13_h2#e.dat. The process 11 is selected for this example.

DEMO a1: Extract data from mdf00: understanding the molecular data format
1. Use xxdatm_00.pro to read the A-values.

2. Plot a surface of A-values as a function of the lower and upper vibrational levels.

3. Use xxdatm_00.pro to read the Franck-Condon factors.

2. Plot a surface of Franck-Condon factors as a function of the lower and upper vibrational levels.

Program: demo_a.pro

Samples of output: demo_a_1_avelue.ps, demo_a_1_fcondon.ps

DEMO a2: Running ADAS901 interactively

1. Use ADAS901 interactively.
2. Select the process number.
Sample of output: adas901.ps

1.1 Demo (a) Figures

1.1.1 Demo (a-1) demo.a/demo.a_1 aValue.pdf

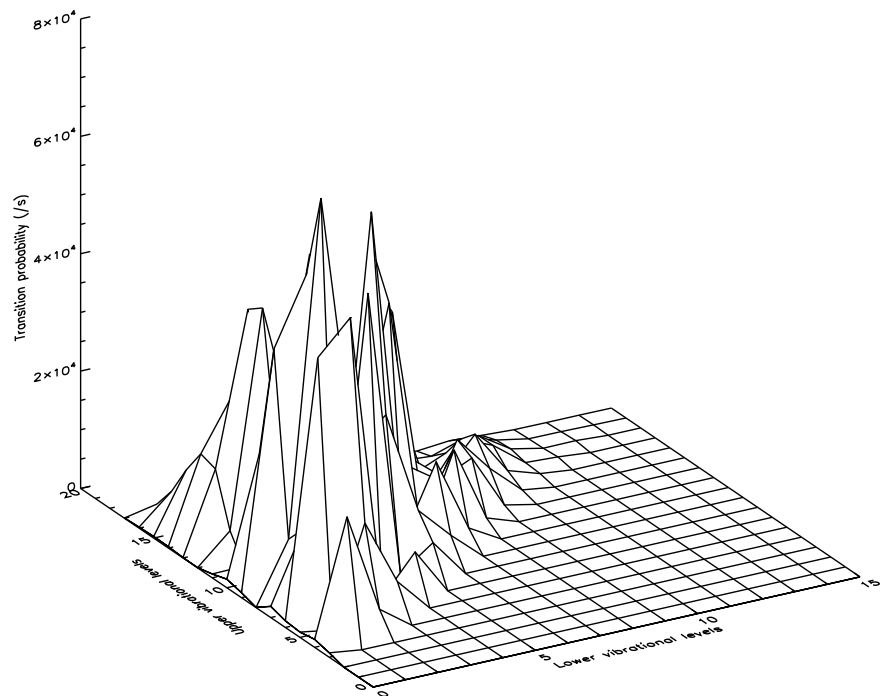


Figure 1: A-value surface from mdf00

1.1.2 Demo (a-1) demo_a/demo_a_1.fcondon.pdf

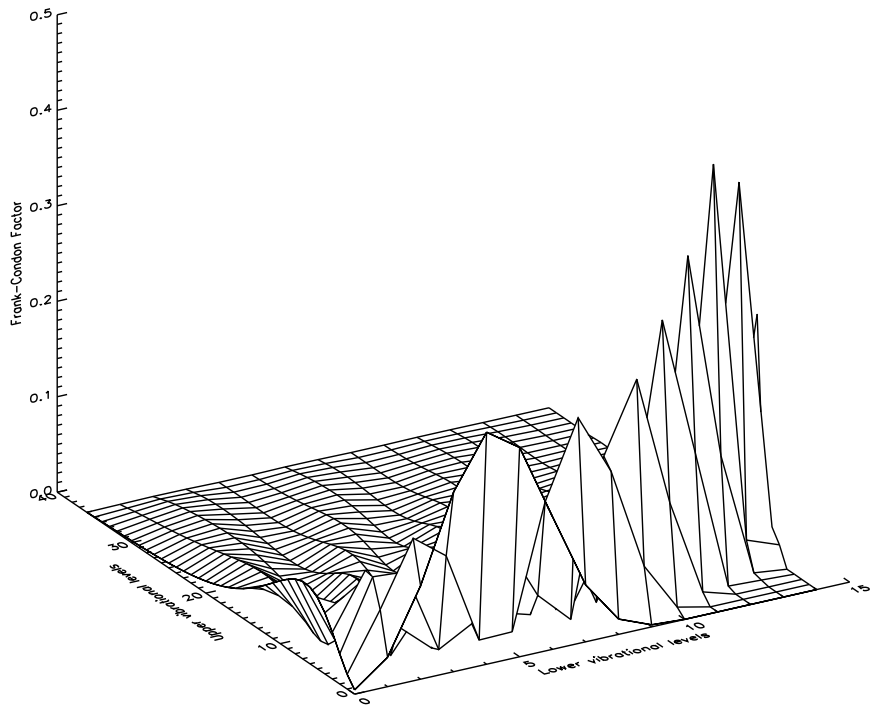


Figure 2: Franck-Condon factor surface from mdf00

1.1.3 Demo (a-2) demo_a/adas901.pdf

MOLECULAR COEFFICIENT VERSUS ENERGY/TEMPERATURE :

```
ADAS      : ADAS RELEASE: v4.0 PROGRAM: ADAS901 v1.0 DATE: 18/06/13 TIME: 16:01
FILE     : /home/giunto/adas/mdf02/h2/fg13_h2#e.dot
TRANSITION : in : 0, 0; out : 0, 0; process : 11; diss ch :
KEY      : (CROSSES - INPUT DATA) (FULL LINE - FORMULA FIT)
```

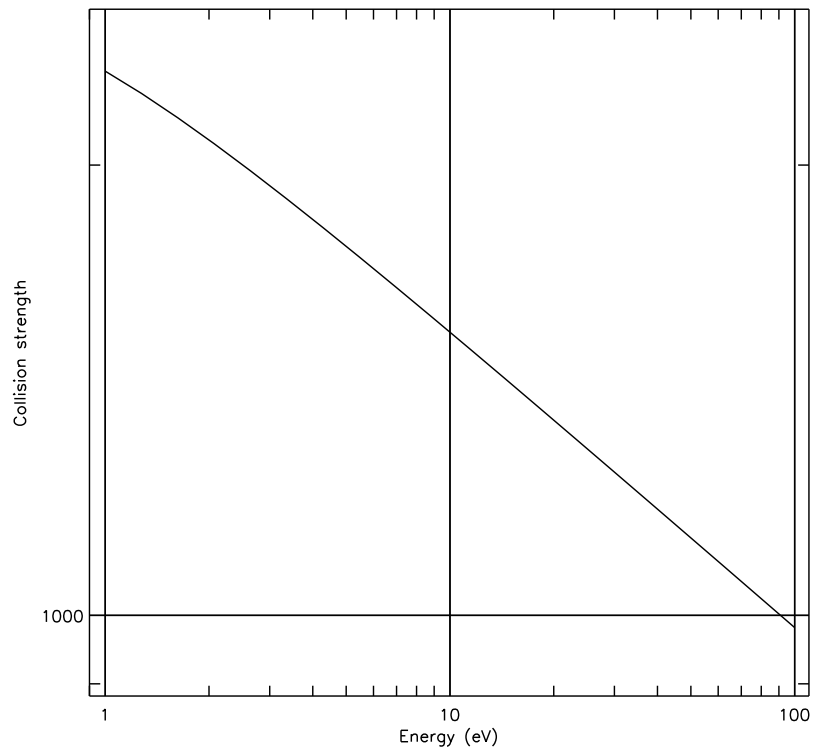


Figure 3: Cross-section output graph from ADAS901

1.2 Demo (a) Procedures

1.2.1 Demo (a-1) demo_a/demo_a.pro

```
pro demo_a

; Extract A-values for H2 A-value between state 9 and 12

;Define the mdf00 file using aval directory
file ='/home/adas/adas/mdf00/aval/h2/aval0112_0109.dat'

;Use xxdatm_00.pro to read the mdf00/aval selected
xxdatm_00, file=file, fulldata=all_aval

x = indgen(all_aval.max_vib_l+1)
y = indgen(all_aval.max_vib_u+1)

;Plot the A-values as a function of lower and upper vibrational levels
set_plot,'ps'
device, /islatin1, font_index=8
device, bits=8, filename='demo_a_1_avalue.ps',  $
    font_size = 14, xsize=18.0, ysize=16.0,  $
    yoffset=7.0, /color
device, /helvetica

surface, all_aval.data, x, y, $
    xtitle ='Lower vibrational levels', $
    ytitle ='Upper vibrational levels', $
    ztitle = 'Transition probability (/s)'

device,/close
set_plot,'x'

; Frank-Condon factor for

;Define the mdf00 file using fcf directory
file = '/home/adas/adas/mdf00/fcf/h2/fc0101_0102.dat'

;Use xxdatm_00.pro to read the mdf00/fcf selected
xxdatm_00, file=file, fulldata=all_fcf

x = indgen(all_fcf.max_vib_l+1)
y = indgen(all_fcf.max_vib_u+1)

;Plot the Franck-Condon fractors as a function of lower and upper
;vibrational levels
set_plot,'ps'
```

```
device, /islatin1, font_index=8
device, bits=8, filename='demo_a_1_fcondon.ps',  $
    font_size = 14, xsize=18.0, ysize=16.0, $
    yoffset=7.0, /color
device, /helvetica

surface, all_fcf.data, x, y, $
    xtitle ='Lower vibrational levels', $
    ytitle ='Upper vibrational levels', $
    ztitle = 'Frank-Condon Factor'

device,/close
set_plot,'x'

end
```

2 Demo (b) Rovibronic emission from heteronuclear diatomics

DEMO B: Rovibronic emission from heteronuclear diatomics

PURPOSE: To calculate rovibrational band features for heteronuclear diatomics using the Pickett method.

This demo use as input the mdf01 molecular data format.

The data files mdf01 are grouped in the following subdirectories:

- nist: extract of NIST molecular constant table for selected electronic state;
- behr: driver parameter file for ADAS908 rovibrational spectra analysis (relevant electronic and vibrational transitions from Behringer method for H2)
- pickett: driver parameter file for ADAS908 rovibrational spectra analysis (relevant electronic and vibrational transitions from Pickett method for heteronuclear diatomics)

Different formats are used for the three types of mdf01 and so also different reading routines are used:

- readf_mdf01p.pro for /mdf01/pickett
- readf_mdf01b.pro for /mdf01/behr

The program to execute the Pickett calculations is wrapper_pickett.pro. This program calls the routine readf_mdf01p.pro to read the mdf01 in the Pickett format.

EXAMPLE: For this example the molecules BeD and BeT are analysed.

The input files are the following:

- /home/adas/adas/mdf01/pickett/bed.dat
 - /home/adas/adas/mdf01/pickett/bet.dat
- Three rotational and vibrational temperatures are specified for BeD, assuming that rotational temperature, Tr, is equals to vibrational temperature, Tv:
- 1000 K
 - 3500 K
 - 9000 K

One temperature (Tr=Tv=3500 K) has been selected to compare BeD with BeT.

DEMO b1: Calculate rovibrational band features using the Pickett method

1. Specify the wavelength range.
2. Define three different sets of rotational and vibrational temperatures.

3. Use wrapper_pickett.pro to execute the Pickett calculations for BeD at the three sets of temperatures.
4. Plot the normalised emissivity as a function of pixel.
5. Compare the emissivity of BeD at the three temperatures.
6. Use wrapper_pickett.pro to execute the Pickett calculations for BeT at one temperature.
7. Comapre BeD emissivity with BeT emissivity.

Program: demo_b.pro

Samples of output: demo_b_1_BeD_temp.ps, demo_b_1_BeD_BeT.ps

2.1 Demo (b) Figures

2.1.1 Demo (b-1) demo.b/demo.b.1.BeD.temp.ps

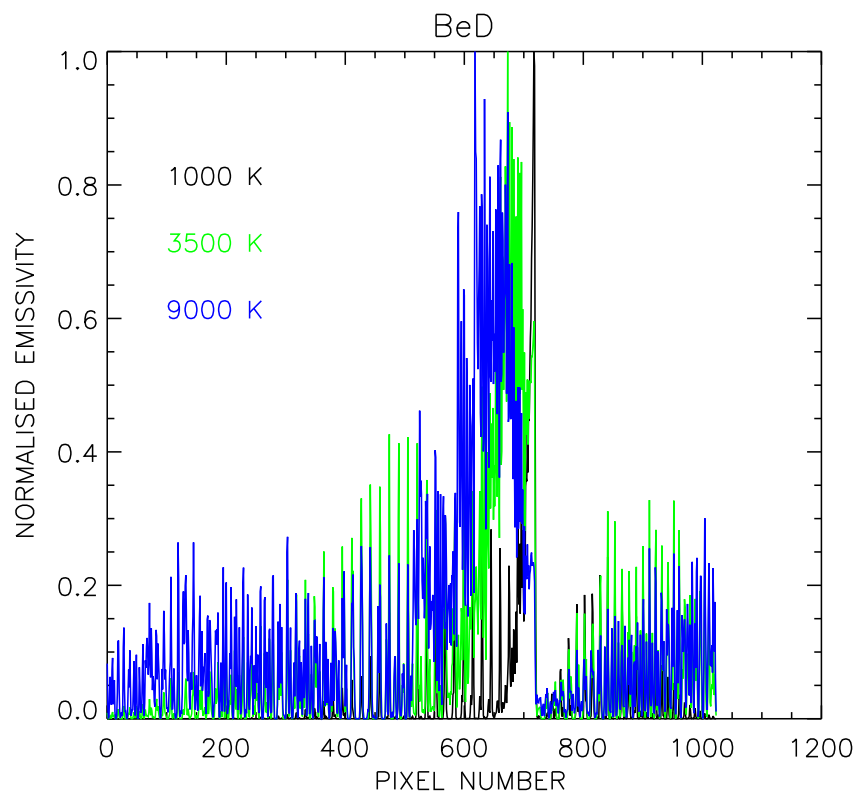


Figure 4: Simulation of the superposed 0-0, 1-1 and 2-2 sequence bands of BeD A₂ Π - X² Σ at three different temperatures, Tr=Tv=1000 K, 3500 K and 9000 K.

2.1.2 Demo (b-1) demo_b/demo_b_1_BeD_BeT.ps

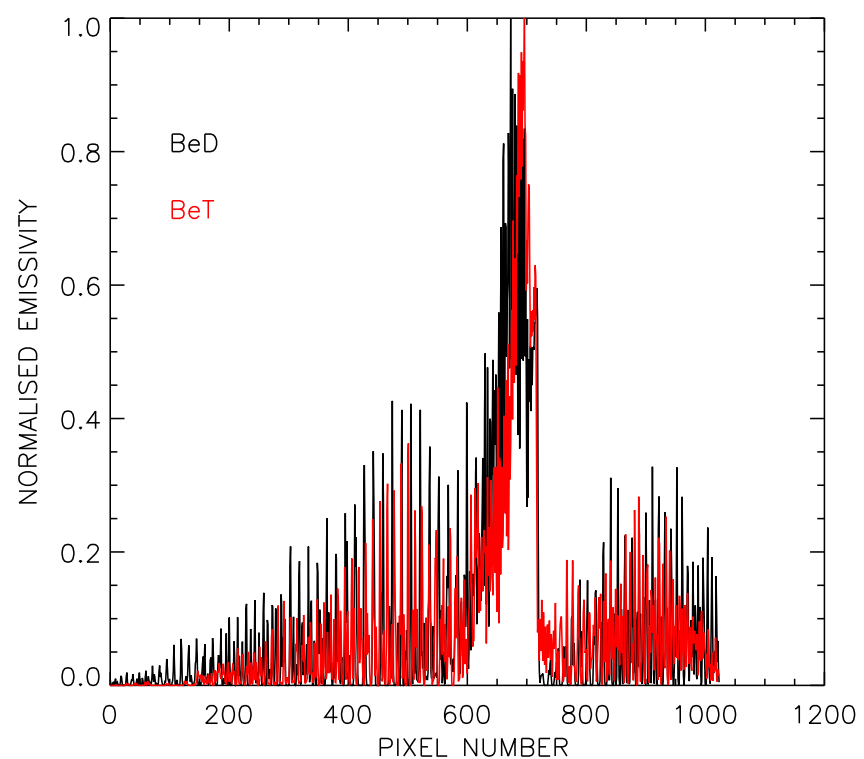


Figure 5: Comparison between BeD and BeT bands at $Tr=Tv=3500$ K.

2.2 Demo (b) Procedures

2.2.1 Demo (b-1) demo.b/demo.b.pro

```
pro demo_b
;To calculate rovibrational band features for heteronuclear diatomics
;using the Pickett method
;The program accesses driver datasets of format mdf01/pickett using
;read_mdf01p.pro. The dataset contains a dedicated set of parameters in the
;Pickett format for a specific molecule such as BeD
;The first step is specify the name of the dataset for input

adas_colors, colors=colors

;Specify the input dataset in the mdf01/pickett format
infiled='/home/adas/adas/mdf01/pickett/bed.dat'
infilet='/home/adas/adas/mdf01/pickett/bet.dat'

;Define wavelength range in nm
xmin=485.d0
xmax=505.d0

;Define rotational temperature in K
ktr=3500.d0
ktr_low=1000.d0
ktr_high=9000.d0

;define vibrational temperature in K
ktv=3500.d0
ktv_low=1000.d0
ktv_high=9000.d0

;Use wrapper_pickett.pro to execute the Pickett calculations
;for BeD at three different rotational and vibrational temperatures
wrapper_pickett, infiled, xmin=xmin, xmax=xmax, $
    ktr=ktr_low, ktv=ktv_low,$
    digi_spec=digi_specd_low

wrapper_pickett, infiled, xmin=xmin, xmax=xmax, $
    ktr=ktr, ktv=ktv,$
    digi_spec=digi_specd

wrapper_pickett, infiled, xmin=xmin, xmax=xmax, $
    ktr=ktr_high, ktv=ktv_high,$
    digi_spec=digi_specd_high

;Use wrapper_pickett.pro to execute the Pickett calculations
```

```

;for BeT
wrapper_pickett, infilet, xmin=xmin, xmax=xmax, $
    ktr=ktr, ktv=ktv,$
    digi_spec=digi_spect

!p.thick=1.3
!p.charsize=1.4
!p.charthick=1.3

;Look at the behaviour of BeD as a function of rotational and
;vibrational temperature
;Plot the normalised emissivity spectrum of BeD
;as a function of pixel number for three temperatures

set_plot,'ps'
device, /isolatin1, font_index=8
device, bits=8, filename='demo_b_1_BeD_temp.ps',  $
    font_size = 14, xsize=18.0, ysize=16.0, $
    yoffset=7.0, /color
device, /helvetica

plot, digi_specd_low, title='BeD', xtitle=' PIXEL NUMBER', $
    ytitle='NORMALISED EMISSIVITY'
xyouts,100.,0.8,'1000 K'

oplot,digi_specd, color=colors.green
xyouts,100.,0.7,'3500 K',color=colors.green

oplot,digi_specd_high,color=colors.blue
xyouts,100.,0.6,'9000 K',color=colors.blue

device,/close
set_plot,'x'

;Compare BeD and BeT ata specified temperature

set_plot,'ps'
device, /isolatin1, font_index=8
device, bits=8, filename='demo_b_1_BeD_BeT.ps',  $
    font_size = 14, xsize=18.0, ysize=16.0, $
    yoffset=7.0, /color
device, /helvetica

plot, digi_specd, xtitle=' PIXEL NUMBER', $
    ytitle='NORMALISED EMISSIVITY'
xyouts,100.,0.8,'BeD'

```

```
 oplot, digi_spect, color=colors.red  
 xyouts,100.,0.7,'BeT', color=colors.red  
  
 device,/close  
 set_plot,'x'  
  
 stop  
 end
```

C.4 module_4

MODULE 4

Modelling and analysing special spectral features

- A unified approach.

Demonstration script

Hugh Summers, Christopher Nicholas,
Martin O'Mullane and Alessandra Giunta

September 29, 2013

Contents

| | |
|---|----------|
| 1 Demo (a) Show spectral features | 2 |
| 1.1 Demo (a) Figures | 3 |
| 1.1.1 Demo (a-1) demo_a/demo_a_adas605.pdf | 3 |
| 2 Demo (b) Fitting spectral features | 4 |
| 2.1 Demo (b) Figures | 5 |
| 2.1.1 Demo (b-1) demo_b/demo_b.pdf | 5 |
| 2.2 Demo (b) Procedures | 6 |
| 2.2.1 Demo (b-1) demo_b/demo_b.pro | 6 |
| 2.3 Demo (b) Drivers | 9 |
| 2.3.1 Demo (b-1) demo_b/simplify_output.mdl | 9 |
| 2.3.2 Demo (b-1) demo_b/zeeman_be2.mdl | 10 |

1 Demo (a) Show spectral features

DEMO A: Show spectral features

PURPOSE: To explore the behaviour of the Stark split manifold of the (beam) hydrogen Balmer-alpha emission as a function of beam energy, plasma parameters and external electric field.

COMMENTS: ADAS605 is a pedagogical tool to interactively see the effect of varying the conditions which affect a spectral feature. The afg framework (ADAS feature generator) supplies the feature and the appropriate widgets, and their ranges, are automatically generated thus making it simple to add new features. Note that the available features are limited to beam Stark features and Zeeman-split line emission for now.

DEMO a: Using ADAS605 with the interactive ADAS windows

1. Run interactively ADAS605 for Stark feature.
(output file: demo_a_adas605.ps).

1.1 Demo (a) Figures

1.1.1 Demo (a-1) demo_a/demo_a_adas605.pdf

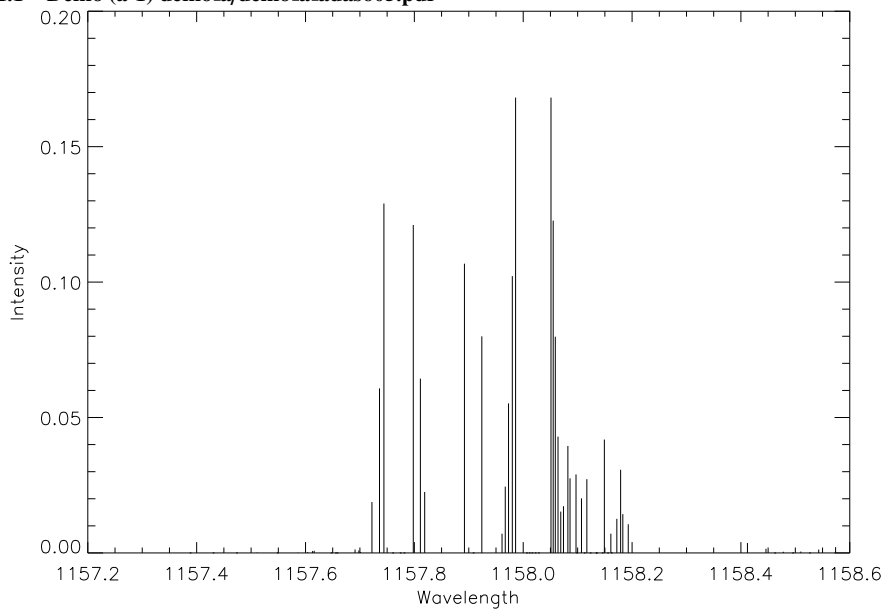


Figure 1: Stark feaures from ADAS605.

2 Demo (b) Fitting spectral features

DEMO B: Fitting spectral features.

PURPOSE: Use the FFS (Framework for Feature Synthesis) routines to fit a Zeeman feature.

EXAMPLE: A sample JET spectrum, distributed in adas/arch603, is the BeIII multiplet, 1s 2s 3S - 1s 2p 3P at 372.17nm, on a relatively clean background with a nearby interfering line. The purpose of the demonstration is to setup a model, fit the spectrum with ffs and deduce the local magnetic field.

COMMENTS: The FFS framework is an optimized, least squares fitting system based on physics-based parametrized spectral features. Individual lines, background models and broadening operators are also part of the system to allow a sophisticated description of the target spectrum, specified with a bespoke model definition language (MDL). Multiple features and coupling of parameters are fundamental to the design of the system.

DEMO b: Fit Zeeman features using FFS routines

1. Take an experimental spectra (example from JET).
2. Setup a ffs model defined by the MDL file 'zeeman_be2.mdl'.
3. Plot the data with the model fit.

Program: demo_b.pro

Samples of input files: simplify_output.mdl, zeeman_be2.mdl

Sample of output file:.demo_b.ps

2.1 Demo (b) Figures

2.1.1 Demo (b-1) demo.b/demo_b.pdf

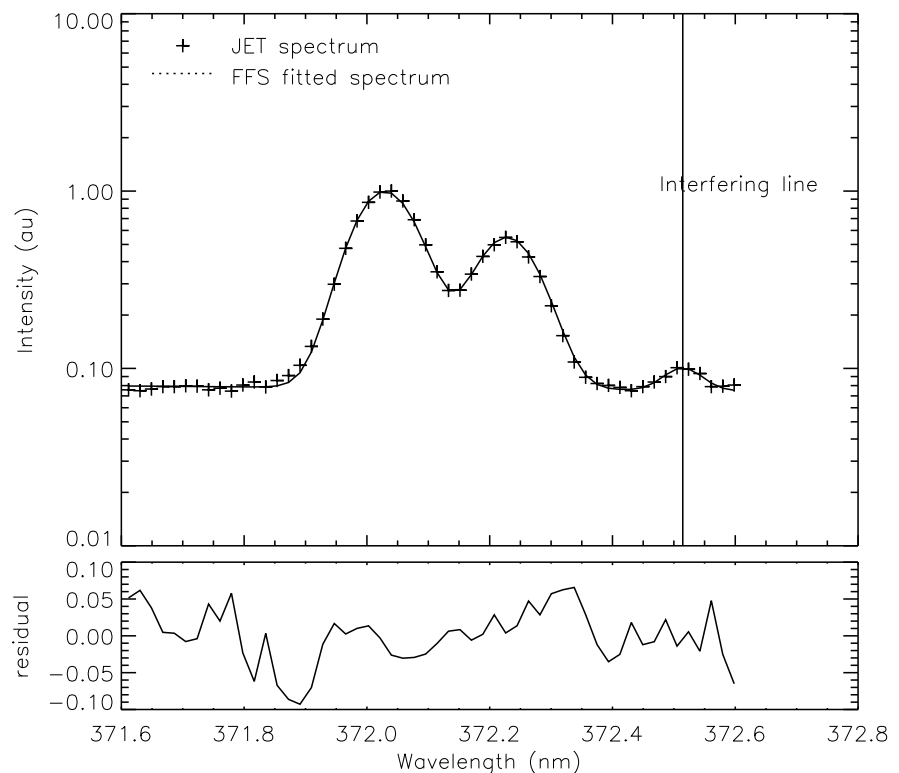


Figure 2: JET spectrum fitted using FFS fit.

2.2 Demo (b) Procedures

2.2.1 Demo (b-1) demo.b/demo_b.pro

```
;-----  
; Using FFS (Framework for Feature Synthesis) routines  
; fit a Zeeman feature (with a background and interfering  
; ordinary line) to a sample spectrum, of the multiplet  
; BeIII 1s 2s 3S - 1s 2p 3P (372.17nm).  
;-----  
  
pro demo_b  
  
; Example JET spectrum from central ADAS  
  
adascent = getenv('ADASCENT')  
restore, adascent + '/arch603/jet_test.dat'  
  
; Get the wavelength in nm and restrict to +/- 0.5nm about the feature  
; Set the error to be square root of the counts  
  
x = adas_vector(low=header.wavemin, high=header.wavemax, num=header.nsize,/linear)  
x = x / 10.0  
y = spectrum  
  
ind = where(x GT 371.6 and x LT 372.6, count)  
x = x[ind]  
y = y[ind]  
err = sqrt(y)  
  
; Setup a ffs model defined by the MDL file 'zeeman_be2.mdl'  
;  
; 1. make a model object (container)  
; 2. parse the MDL file  
; 3. add the parsed MDL to the model  
; 4. Set the independent x values in the model  
; 5. make a fit object and a data structure with wavelength, intensity and error  
; 6. fit the model to the data  
  
model = obj_new('ffs_model', modelname='zeeman_be2', /debug)  
parser = obj_new('ffs_parser', file='zeeman_be2.mdl', /debug)  
  
tmp = parser->apply(model)  
tmp = model->setxdata(x)  
  
tmp = model->pdsetup()  
tmp = model->pdsetup()
```

```

fit = obj_new('ffs_fit')
data = {x:x, y:y, error:err}
tmp = fit->apply(model, data)

; Parameters of fit

parnames = model->getparnames(/free, /full)
parvals = model->getparvals(/free)
errors = fit->geterrors()

; Plot the data with the model fit and print the fitted parameters

;set_plot,'ps'
;device, /isolatin1, font_index=8
;device, bits=8, filename='demo_b.ps', $
;           font_size = 14, xsize=18.0, ysize=16.0, $
;           yoffset=7.0, /color
;device, /helvetica

window,0,ret=2

fitspec = *(model->getresult())
residual = (fitspec.intensity - y) / y

plot_io, [371.6, 372.6], [0.01,2], /nodata, xtickname=replicate(' ', 10), $
ytitle = 'Intensity (au)', position=[0.15, 0.3, 0.95, 0.95]

oplot, x, y, psym=1

oplot, fitspec.wavelength, fitspec.intensity

; Label graph

plots, [371.7], [6.6], psym=1
oplot, [371.65, 371.75], [4.6, 4.6], line=1

xyouts, 371.78, 6, 'JET spectrum'
xyouts, 371.78, 4, 'FFS fitted spectrum'

; Plot fitted position of the ordinary line

oplot, [parvals[6],parvals[6]], [0.01, 10]
xyouts, 0.9999 * parvals[6], 1.0, 'Interfering line'

; Plot residuals

```

```

plot, [371.6, 372.6], [-0.1, 0.1], /nodata, $
      xtitle = 'Wavelength (nm)', $
      ytitle = 'residual', position=[0.15, 0.10, 0.95, 0.28], /noerase
      oplot, x, residual

;device,/close
;set_plot,'x'

; Print out the fitted parameters

for j = 0, n_elements(parnames)-1 do $
  print, j, parnames[j], parvals[j], errors[j], $
    format = '(i2, " : ", a20, " = ", 2f12.4)'
; Write the parsed model to a file in order to see all the limits

isok = parser->writedefinition(model, 'simplify_output.mdl')

stop
end

```

2.3 Demo (b) Drivers

2.3.1 Demo (b-1) demo.b/simplify_output.mdl

Model written automatically by FFS

Editing this file by hand is ok but please
note that FFS will not retain any comments
or formatting changes which you may add if
asked to read and then re-save this model.

```
(model
  (add
    (background-linear backg)
    (multiply (broaden_gauss (shift (adas-zeeman be2zeeman) sh) bg) be2mult)
    (gaussian g1)
  )
)

(setval backg.c 0.079600883)
(setval backg.m -0.0048565742)
(setval be2zeeman.obsangle 0.0000000)
(setval be2zeeman.bvalue 1.8503528)
(setval sh.lambda -0.069918945)
(setval bg.fwhm 0.10742071)
(setval be2mult.factor 0.058118828)
(setval g1.pos 372.51450)
(setval g1.fwhm 0.070975998)
(setval g1.area 0.0019231882)

(setval be2zeeman.pol 0)
(setval be2zeeman.findex 8)
(setval bg.trap 10.000000)
(setval g1.trap 5.0000000)

(setmin backg.c -Infinity)
(setmax backg.c Infinity)
(setmin backg.m -Infinity)
(setmax backg.m Infinity)
(setmin be2zeeman.obsangle 0.0000000)
(setmax be2zeeman.obsangle 90.000000)
(setmin be2zeeman.bvalue 0.97000000)
(setmax be2zeeman.bvalue 4.0000000)
(setmin sh.lambda -0.10000000)
(setmax sh.lambda 0.20000000)
(setmin bg.fwhm 0.050000000)
(setmax bg.fwhm 1.0000000)
(setmin be2mult.factor 0.010000000)
(setmax be2mult.factor 100.00000)
```

```

(setmin g1.pos 372.40000)
(setmax g1.pos 372.60000)
(setmin g1.fwhm 0.0000000)
(setmax g1.fwhm Infinity)
(setmin g1.area 1.000000e-05)
(setmax g1.area Infinity)

(free backg.c backg.m be2zeeman.bvalue sh.lambda
    bg.fwhm be2mult.factor g1.pos g1.fwhm g1.area)

(fixed be2zeeman.obsangle)

```

2.3.2 Demo (b-1) demo.b/zeeman.be2.mdl

Setup model of BeIII Zeeman feature on a liner background with one contaminating ordinary line around 372.5nm

The Zeeman feature

- can be shifted in wavelength (sh - constrained to -0.1 to 0.2 nm)
- is Doppler broadened with a Gaussian with FVWM constrained to 0.05 to 1.0
- is multiplied by a factor constrained to 0.01 to 100.0
- the field is constrained between 1-4T
- all pi and sigma components are used
- the observation angle is 0 degrees

The ordinary line

- position is constrained between 372.4 - 372.6 nm
- fwhm and area are not constrained

The background

- is linear
- unconstrained constant value and slope

```

(model
  (add
    (background-linear backg)
    (* (broaden_gauss (shift-lambda (adas-zeeman be2zeeman) sh) bg) be2mult)
       (gaussian g1)
    )
  zeeman)

  (setval backg.m 0.01)
  (setval backg.c 0.1)

  (setval g1.pos 372.5)
  (setlimits g1.pos 372.4 372.6)

  (setval g1.area 1.0)

```

```
(setval g1.fwhm 0.07)

(setval sh.lambda -0.06)
(setlimits sh.lambda -0.1 0.2)

(setval be2zeeman.findex 8)
(setval be2zeeman.pol 0)
(setval be2zeeman.obsangle 0.0)
(fixed be2zeeman.obsangle)
(setval be2zeeman.bvalue 1.0)
(setlimits be2zeeman.bvalue 1.0 4.0)

(setval be2mult.factor 1.0e-1)
(setlimits be2mult.factor 1.0e-2 1.0e2)

(setval bg.fwhm 0.07)
(setlimits bg.fwhm 0.05 1.0)
```

C.5 module_5

MODULE 5

Charge exchange and beam emission spectroscopy. Modelling emitter populations, beam stopping and analysing spectra

Demonstration script

Hugh Summers, Martin O'Mullane and Alessandra Giunta

September 29, 2013

Contents

| | |
|--|-----------|
| 1 Demo (a) Looking at basic charge exchange and ion impact cross-section data | 3 |
| 1.1 Demo (a-1) Figures | 4 |
| 1.2 Demo (a-2) IDL procedure | 7 |
| 1.3 Demo (a-2) Figures | 8 |
| 1.4 Demo (a-3) IDL procedure | 12 |
| 1.5 Demo (a-3) Figures | 14 |
| 2 Demo (b) Obtaining charge exchange receiver populations driven by beams | 16 |
| 2.1 Demo (b-1) Figures | 17 |
| 2.2 Demo (b-2) IDL procedure | 19 |
| 2.3 Demo (b-2) Figures | 20 |
| 3 Demo (c) Obtaining beam stopping and beam coefficients | 22 |
| 3.1 Demo (c-1) IDL procedure | 24 |
| 3.2 Demo (c-1) datasets | 27 |
| 3.2.1 adf26_h1.pass | 27 |
| 3.2.2 adf26_c6.pass | 29 |
| 3.2.3 adf21_h1.pass | 30 |
| 3.2.4 adf21_c6.pass | 32 |
| 3.3 Demo (c-2) IDL procedure | 35 |
| 3.4 Demo (c-2) datasets | 35 |
| 3.4.1 /bme10#/h/bme10#/h_h1.dat | 35 |
| 3.4.2 /bme10#/h/bme10#/h_c6.dat | 37 |
| 3.5 Demo (c-3) procedure | 40 |
| 3.6 Demo (c-3) Figures | 43 |

| | |
|--|-----------|
| 4 Demo (d) Looking at Stark multiplet emission for the H-beam | 46 |
| 4.1 Demo (d-1) procedure | 47 |
| 4.2 Demo(d-1) Figures | 49 |

1 Demo (a) Looking at basic charge exchange and ion impact cross-section data

DEMO A: Looking at basic charge exchange and ion impact cross-section data

PURPOSE: Looking at ion impact and charge exchange data. Furthermore a comparison between ionisation and charge exchange reactions is shown.

Ion-atom impact cross sections are collected in the adf02 files, which provide data for different reactions.

Selective Charge Exchange (CX) cross sections are stored in the adf01 data files, while ad state selective charge exchangecross sections for partially stripped receivers. Thermally averaged total chiarge exchange rate coefficients are given by adf14 files. They Maxwellian averages over the receiver and donor temperatures.

EXAMPLE: The adf02 for ion-atom cross section selected for this demo is the following:

/home/adas/adas/adf02/sia#h/sia#h_j99#h.dat

Three reactions have been chosen with corresponding blocks:

- 1) total charge exchange (cx) transfer: H+0 impact Li+3 -> Li+2
block=3
- 2) ionisation: Li+3 target H+0 -> H+
block=13
- 3) excitation: Li+3 target H+0 -> H(n=2)
block=28

Isotopic mass number of primary specie (deuterium has been chosen)=2
Isotopic mass number of secondary specie (lithium)=7

Two adf01s for CX are selected for this demo:

- 1) Oxygen: O8+ + H(is) -> O7+ + H+
/home/adas/adas/adf01/qcx#h0/qcx#h0_old#o8.dat
For nl-resolved cross section the chosen quantum numbers are:
n=5, l=1.
- 2) Lithium: Li3+ + H(1s) -> Li2+ + H+
/home/adas/adas/adf01/ext#h0/arf07#3/ext#h0_arf07#li3.dat
For nl-resolved cross section the chosen quantum numbers are:
n=3, l=0.

For the comparison between charge exchange and electron impact rate coefficients the following reactions are considered:

- 1) IONISATION: H+e -> H+ + e + e electron impact rate from adf11
/home/adas/adas/adf11/scd12/scd_h.dat
Two electron density values are selected: 1.e10 cm-3 and 1.e14 cm-3
- 2) CHARGE EXCHANGE: H + H+ -> H+ + H+ cx rate from

a) adf14
 /home/adas/adas/adf14/tcx#h0/tcx#h0_h.dat
 Two cases are shown: - no beam -> when the temperature of receiver (Tr) is equal to the temperature of donor (Td) and both are equal to the electron temperature (Te).
 - cold beam -> Tr = Te and Td = 3 eV
 b) cx cross section in the adf24 format, converted into cx rate by ceevth.pro
 The adf24 used is the following:
 /home/adas/adas/adf24/scx#h0/scx#h0_ornl#h1.dat

DEMO a1: Extract and graph adf02 data interactively with ADAS302
 1. Look at the selected adf02 for specifying the blocks corresponding to the reactions.
 2. Use ADAS302 with the interactive ADAS window for the selected species, selecting different reactions (e.g. cx, ionisation, excitation).
 3. Compare the different cross sections.
 (output files: demo_a_1_cx.ps, demo_a_1_ion.ps, demo_a_1_exc.ps)

DEMO a2: Extract adf01 data with ADAS301, use read_adf01.pro offline
 1. Use ADAS301 with the interactive windows for O and Li
 (outputs: demo_a_2_oxygen.ps, demo_a_2_oxygen_nl.ps,
 demo_a_2_lithium.ps, demo_a_2_lithium_nl.ps).
 2. Using the command line:
 a) Use rea_adf01.pro to read the selected adf01 files.
 b) Find the indices corresponding to the n and l specified.
 c) Plot total and selective cx cross sections as a function of energy (eV/amu).
 Program: demo_a_2.pro
 Output file: demo_a_2.ps

DEMO a3: Comparison between ion impact/cx and electron impact reactions
 1. Use read_adf11.pro to read the selected ionisation rate coefficients adf11 for H.
 2. Use read_adf14.pro to read thermal cx rate coefficients.
 3. Use read_adf24.pro to read the cx cross sections adf24.
 4. Use ceevth.pro to produce cx rate for H from adf24 data.
 5. Compare the results (adf11 with adf14 and output of ceevth.pro)
 Program: demo_a_3.pro
 Output file: demo_a_3.ps

1.1 Demo (a-1) Figures

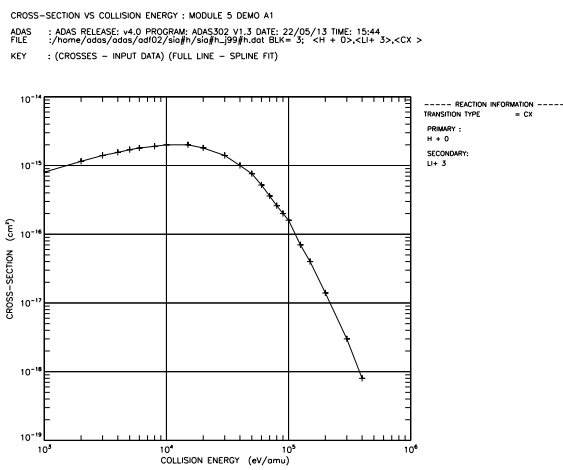


Figure 1: demo_a/demo_a_1_cx.pdf

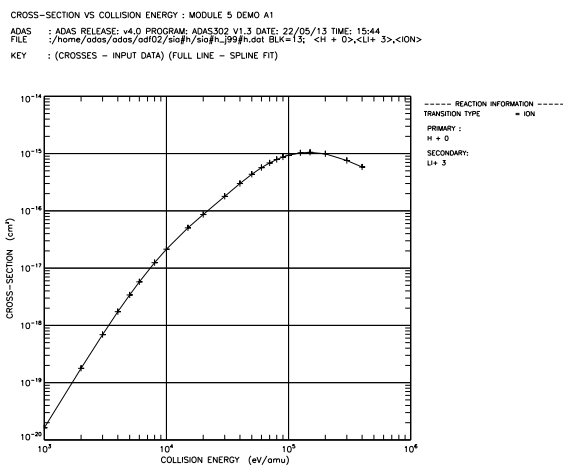


Figure 2: demo_a/demo_a_1_ion.pdf

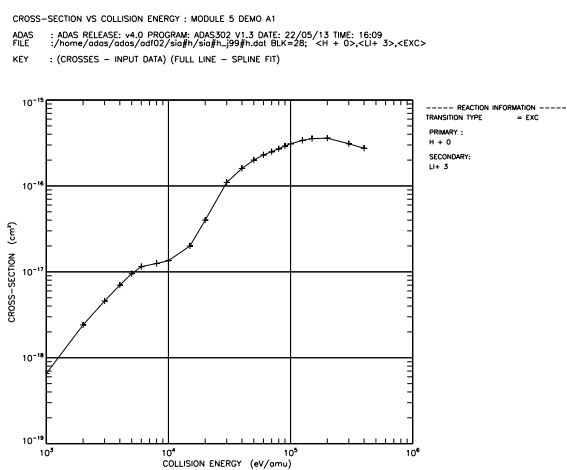


Figure 3: demo_a/demo_a_1.exc.pdf

1.2 Demo (a-2) IDL procedure

```
pro demo_a_2
;Use read_adf01.pro to read selective charge exchange cross section
;for O8+ + H(1s) -> O7+ + H+
;and for Li3+ + H(1s) -> Li2+ + H+

adf01_o='/home/adas/adas/adf01/qcx#h0/qcx#h0_old#o8.dat'
adf01_li='/home/adas/adas/adf01/ext#h0/arf07#3/ext#h0_arf07#li3.dat'

;Use read_adf01.pro to read the selected adf01 for O+8 and Li+3
read_adf01,file=adf01_o,fulldata=cx_o
read_adf01,file=adf01_li,fulldata=cx_li

;specify principal and angular quantum numbers for oxygen
n_o=5
l_o=1
;find the index corresponding to n=5 and l=1 (l-resolved) for oxygen
index_o=i4idfl(n_o,l_o,/idl_index)

;specify principal and angular quantum numbers for lithium
n_li=3
l_li=0
;find the index corresponding to n=3 and l=0 (l-resolved) for lithium
index_li=i4idfl(n_li,l_li,/idl_index)

loadct,3
;Plot total and selective cx cross sections as a function of energy (eV/amu)
set_plot,'ps'
device, /isolatin1, font_index=8
device, bits=8, filename='demo_a_2.ps',           $
    font_size = 14, xsize=18.0, ysize=16.0, $           $
    yoffset=7.0, /color
device, /helvetica

plot_o0,cx_o.enrgya,cx_o.sigta,xrange=[5.e3,5.e5],yrange=[1.e-17,1.e-14],$           $
    title='Total and selective CX cross sections',$           $
    xtitle='ENERGY (eV/amu)',ytitle='CROSS-SECTION (cm!u2!n)'
oplot,cx_o.enrgya,cx_o.sigta,psym=1
oplot,cx_o.enrgya,cx_o.sigta[*,index_o],line=1

plots,cx_li.enrgya,cx_li.sigta,color=120
plots,cx_li.enrgya,cx_li.sigta,color=120,psym=1
plots,cx_li.enrgya,cx_li.sigta[*,index_li]>1.e-17,color=120,line=1

xyouts,0.63,0.9,'O!u8+!n + H!u0+!n -> O!u7+!n + H!u1+!n',/normal
```

```

xyouts,0.63,0.85,'Li!u3+!n + H!u0+!n -> Li!u2+!n + H!u1+!n',color=120,/normal
xyouts,0.73,0.6,'total',/normal
xyouts,0.47,0.7,'total',color=120,/normal
xyouts,0.2,0.6,'n=5 l=1',/normal
xyouts,0.43,0.3,'n=3 l=0',color=120,/normal

device, /close
set_plot,'X'
!p.font=-1

end

```

1.3 Demo (a-2) Figures

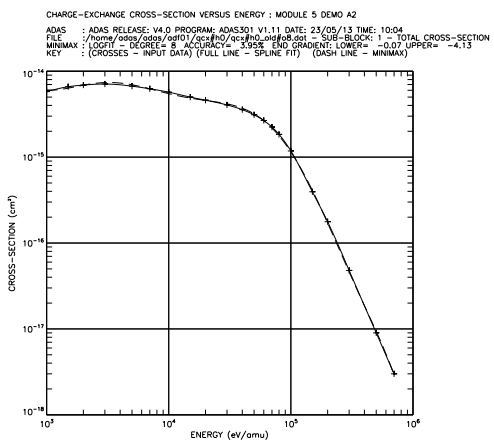


Figure 4: demo_a/demo_a_2_oxygen.pdf

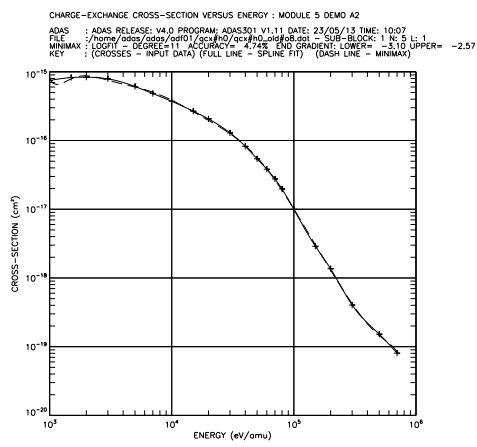


Figure 5: demo_a/demo_a_2.oxygen_nl.pdf

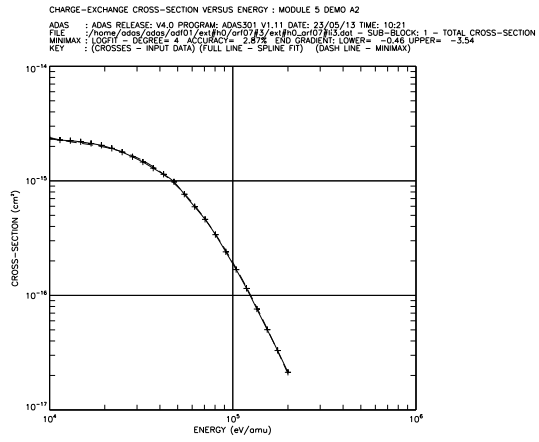


Figure 6: demo_a/demo_a_2.lithium.pdf

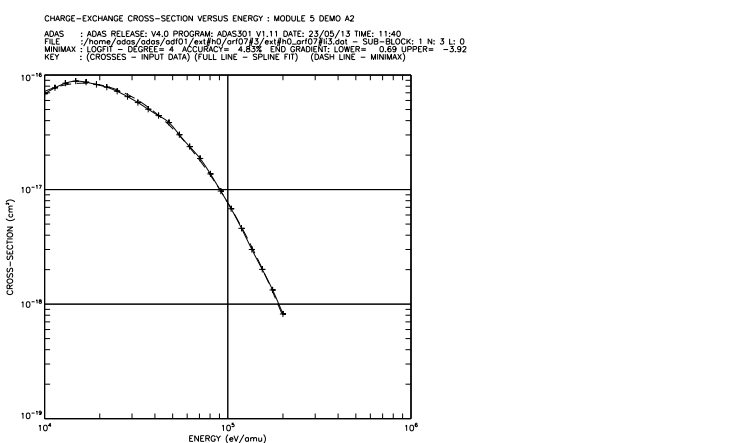


Figure 7: demo_a/demo_a_2_lithium_nl.pdf

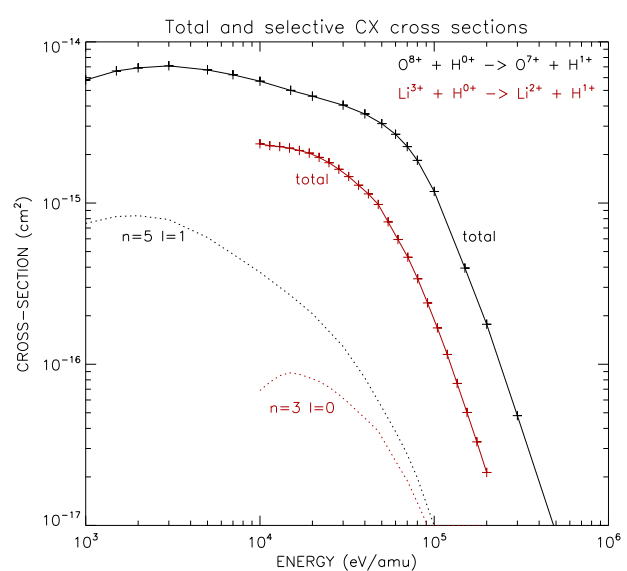


Figure 8: demo_a/demo_a_2.pdf

1.4 Demo (a-3) IDL procedure

```
pro demo_a_3
;Compare electron impact excitation vs thermal CX for H.
;Contrast the ORNL red book rates against forming the double
;Maxwellian with the ceevth.pro library routine.

;define electron temperature range
itval =30
te=adas_vector(low=1., high=1000., num=itval)

;Ionisation rates from adf11 for two different electron densities

file_scd = '/home/adas/adas/adf11/scd12/scd12_h.dat'

read_adf11, file=file_scd, class='scd', iz0=1, iz1=1, $
    te=te, dens=fltarr(itval)+1e10, data=scd_10

read_adf11, file=file_scd, class='scd', iz0=1, iz1=1, $
    te=te, dens=fltarr(itval)+1e14, data=scd_14

;Thermal CX rates from adf14
;Note isotope is hydrogen, not deuterium, H + H+
adf14='/home/adas/adas/adf14/tcx#h0/tcx#h0_h.dat'

;use read_adf14.pro to read the selected adf14
;case of temperature of receiver=temp.of donor=electron temp.
read_adf14, file=adf14, block=1, t_rec=te, t_don=te, $
    m_rec = 1.0, m_don=1.0, data=tctx_eq
;case of temperature of receiver=electron temp. and temp.of donor=3eV
read_adf14, file=adf14, block=1, t_rec=te, t_don=fltarr(itval)+3.0, $
    m_rec = 1.0, m_don=1.0, data=tctx_3

;Form H CX rate from the adf24 cross section
adf24='/home/adas/adas/adf24/scx#h0/scx#h0_ornl#h1.dat'

read_adf24, file=adf24, fulldata=all

eng = reform(all.teea[*,0]) ; block 1
sig = reform(all.scx[*,0])
ind = where(eng GT 0.0) ; remove zeros
eng = eng[ind]
sig = sig[ind]

amdon = 1.0001 ; Hydrogen as before
amrec = 1.0001
catyp = 'tt'
```

```

iextyp = 2

te_comp = [3, 7, 10, 100, 500]

;use ceevth.pro to produce cx rate for H
ceevth, amdon = amdon, $
    amrec = amrec, $
    catyp = catyp, $
    iextyp = iextyp, $
    enin = eng, $
    sgin = sig, $
    enout = te_comp, $
    rcout = cx_rate

; Plot the results
set_plot,'ps'
device, /isolatin1, font_index=8
device, bits=8, filename='demo_a_3.ps',           $
    font_size = 14, xsize=18.0, ysize=16.0, $ 
    yoffset=7.0, /color
device, /helvetica

xmin = 1
xmax = 1000
ymin = 1e-9
ymax = 1e-7

plot_oo, [xmin, xmax], [ymin, ymax], /nodata, $
    xtitle = 'Temperature (eV)', $
    ytitle = 'Rate coefficient (cm!u3!n s!u-1!n)'

oplot, te, scd_10
oplot, te, scd_14, linestyle=2

loadct,3
oplot, te, tcx_eq, color=120
oplot, te, tcx_3, linestyle=1, color=120

loadct,1
oplot, te_comp, cx_rate, psym=5, color=120

plots, 3.8, 4.5e-8, psym=5, color=120
xyouts, 4.7, 4.2e-8, 'rate from ceevth.pro', color=120

loadct,3
xyouts, 1.2, 7e-9, 'H + H!u+!n CX', color=120
xyouts, 10.0, 3e-9, 'H + e ionisation'

xyouts,70.,2.e-9, 'N!de!n=10!u10!n cm!u-3!n'

```

```

plots,[300.,600.],[2.e-9,2.e-9]
xyouts,70.,1.5e-9,'N!de!n=10!u14!n cm!u-3!n'
plots,[300.,600.],[1.5e-9,1.5e-9],line=2

plots, [1.5,3.8],[8.e-8,8.e-8], color=120
xyouts, 4.7, 8.e-8, 'T!dr!n=T!dd!n=T!de!n', color=120
plots, [1.5,3.8],[6.e-8,6.e-8], color=120, line=1
xyouts, 4.7, 6.e-8, 'T!dr!n=T!de!n, T!dd!n=3 eV', color=120

device, /close
set_plot,'X'
!p.font=-1

end

```

1.5 Demo (a-3) Figures

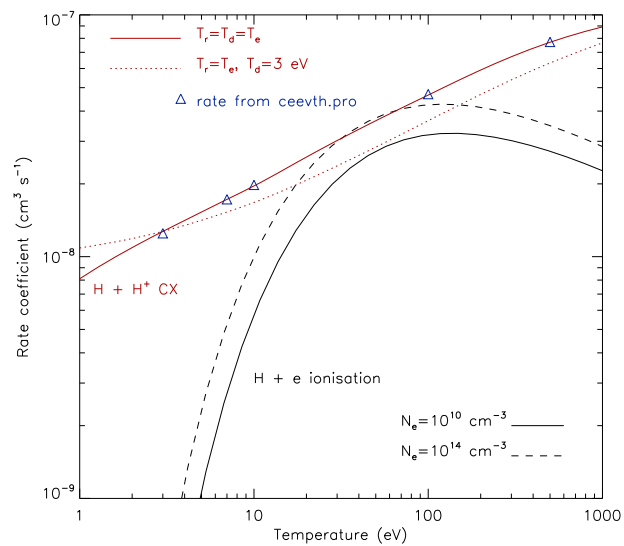


Figure 9: demo_a/demo_a_3.pdf

2 Demo (b) Obtaining charge exchange receiver populations driven by beams

DEMO B: Obtaining charge exchange receiver populations driven by beams

PURPOSE: Produce and analyse charge exchange effective emission coefficients associated by a particula donor.

The charge exchange effective emission coefficients are produced by ADAS306 (in the j-resolved case) and stored in the adf12 format. This format is read and analysed by ADAS303.

EXAMPLE: For this demo C VI n=8-7 at 5290.7 Ang. has been chosen.

The adf12 selected are the following:

- adf12 for n=1 is : /home/adas/adas/adf12/qef93#h/qef93#h_c6.dat
- adf12 for n=2 is : /home/adas/adas/adf12/qef97#h/qef97#h_en2_kvi#c6.dat

The plasma parameters are:

Ion temperature (eV): 1.e3

Ion density(cm⁻³): 1.e13

Effective charge: 2.0

Magnetic field (Tesla): 3.0

DEMO b1: Examine adf12 data with ADAS303 interactively.

1. Use ADAS303 with interactive windows.

(Output files: demo_b_1_interactive_n1.ps, demo_b_1_interactive_n2.ps)

DEMO b2: Examine adf12 using read_adf12.pro.

1. Define plasma parameters.

2. Use read_adf12.pro fro n=1 and n=2

3. Plot the effective emission coefficients as a function of beam energy.

4. Compare the results withe the interactive run.

Program: demo_b_2.pro

Output files: demo_b_2.ps

2.1 Demo (b-1) Figures

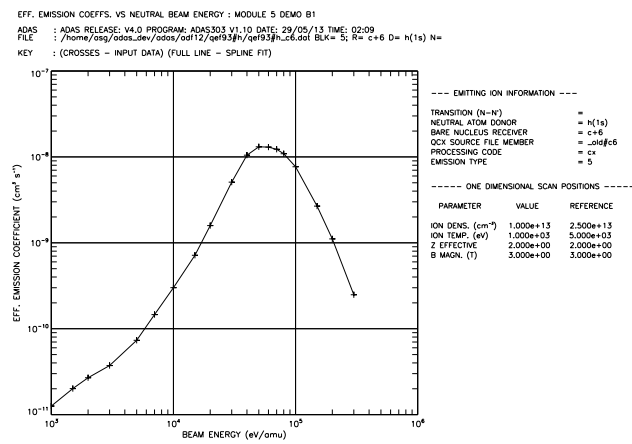


Figure 10: demo_b/demo_b_1_interactive_n1.pdf

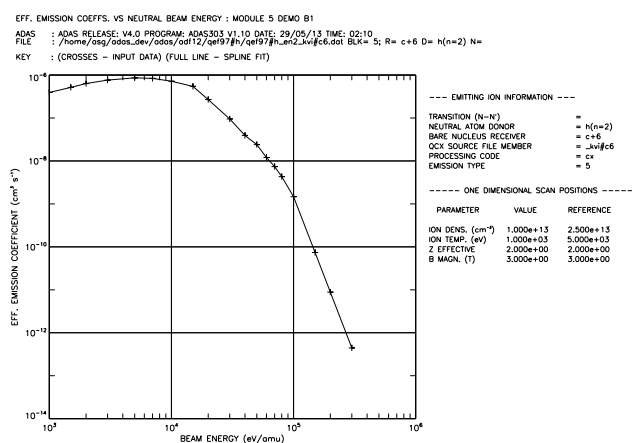


Figure 11: demo_b/demo_b_1_interactive_n2.pdf

2.2 Demo (b-2) IDL procedure

```
pro demo_b_2
;Use read_adf12.pro to read adf12 files for C5+ with different donors:
;- D in n=1
;- D in n=2

;Plasma and beam conditions
ein      = adas_vector(low=2e3, high=1e5, num=100)
dion     = 1.e13
tion     = 1.e3
zeff     = 2.0
bmag     = 3.0

;n=1 and n=2 adf12 files for CVI(n=8-7) 5290.7 Ang.

adf12_n1 = '/home/adas/adas/adf12/qef93#h/qef93#h_c6.dat'
read_adf12, file=adf12_n1, block=5,                      $
    tion=tion, dion=dion, zeff=zeff, bmag=bmag,   $
    ein=ein, data=data_n1

adf12_n2 = '/home/adas/adas/adf12/qef97#h/qef97#h_en2_kvi#c6.dat'
read_adf12, file=adf12_n2, block=5,                      $
    tion=tion, dion=dion, zeff=zeff, bmag=bmag,   $
    ein=ein, data=data_n2

;Plot the effective emission coefficients as a function of beam energy.
set_plot,'ps'
device, /isolatin1, font_index=8
device, bits=8, filename='demo_b_2.ps',                  $
    font_size = 14, xsize=14.0, ysize=16.0,   $
    yoffset=7.0, /color
device, /helvetica
plot_oo, ein, data_n1, xtitle='Energy (eV/amu)',   $
    ytitle='Effective emission coefficient (cm!u3!n s!u-1!n)',   $
    yrange=[1.e-11,1.e-5]
oplot, ein, data_n2, linestyle=2

xyouts, 2.3e3,8e-11, 'D(n=1)'
xyouts, 4.e3,3e-7, 'D(n=2)'
xyouts,0.4,0.9,'C VI (n=8-7) 5290 Ang.',/normal

device, /close
set_plot,'X'
!p.font=-1

end
```

2.3 Demo (b-2) Figures

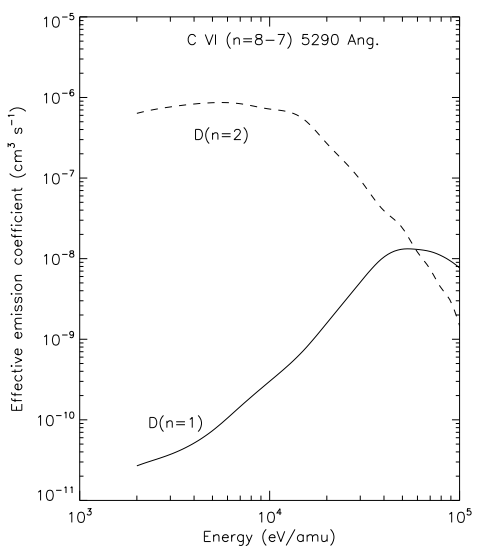


Figure 12: demo_b/demo_b_2.pdf

3 Demo (c) Obtaining beam stopping and beam coefficients

DEMO C: Obtaining beam stopping and beam coefficients

PURPOSE: Compute the populations (excited population structure, effective ionisation and recombination) for hydrogen atoms or hydrogenic ions in a plasma with impurities using a bundle-n approximation and tabulate beam stopping and beam emission coefficients.

Starting from an adf01 (selecting cx cross section) and an adf18 (cross-referencing data - beam emission and stopping coefficients in the adf21 and adf22 formats are shown by ADAS30

EXAMPLE: The input files for ADAS310 used for this demo are the following:

- adf01: /home/adas/adas/adf01/qcx#h0/qcx#h0_e2p#h1.dat
- adf18: /home/adas/adas/adf18/p310_a17/bndlen_exp#h0.dat

The beam emission and beam stopping coefficients are calculated for D1+ and C6+ plasmas. Plasma parameters are defined in the script demo_d_1.pro.

The output files from ADAS310 in the adf26 and adf21 formats are:

- for D1+: adf26_h1.pass, adf21_h1.pass
- for C6+: adf26_c6.pass, adf21_c6.pass

These are the input file for the ADAS312 ru, which gives the following outputs:

- adf22 for D1+: ./bme10#h/bme10#h_h1.dat
- adf22 for C6+: ./bme10#h/bme10#h_c6.dat

COMMENTS: Note that for H beams a bundle-n modelling is suitable (ADAS310), while for He be

DEMO c1: Processing H-beam stopping and emission with ADAS310

1. Define parameters for run_adas310.pro.
2. Use run_adas310.pro for calculating beam emission coefficients and stopping coefficients.
3. Write adf21 and adf26 files.

Program: demo_c_1.pro

Output files: adf26_h1.pass, adf26_c6.pass, adf21_h1.pass, adf21_c6.pass

DEMO c2: Convert adf26 to adf22 using ADAS312

1. Create a directory called "bme10#h".
2. Use run_adas312.pro to produce beam emission coefficients for D1+ and C6+.

Program: demo_c_2.pro

Input files: adf26_h1.pass, adf26_c6.pass

Output files: /bme10#h/bme10#h_h1.dat, /bme10#h/bme10#h_c6.dat

DEMO c3: Examine adf22 with ADAS304 and use read_adf21.pro and read_adf22.pro

1. Using ADAS304 with interactive windows:

- a) Run ADAS304 interactively, taking the adf22 stored locally.
 - b) Plot emission coefficients for a pure D1+ plasma and a pure C6+ plasma.
(Output files: demo_d_3_beam_emission_h.ps, demo_d_3_beam_emission_c.ps)
2. Using read_adf21.pro and read_adf22.pro with command line:
- a) Use read_adf22.pro to read the adf22 stored locally.
 - b) Plot emission coefficients for a pure D1+ plasma and a pure C6+ plasma at different densities.
 - c) Compare the results with the interactive outputs.
 - d) Use read_adf21.pro to read beam stopping coefficients for D1+ and C6+ plasmas.
 - e) Plot a surface of beam stopping coefficients as a function of beam energy and density.
 - f) Compare beam stopping coefficients for a pure D1+ plasma and a plasma with D1+ and a 2% concentration of C6+.
- Program: demo_c_3.pro
Output files: demo_c_3_emission.ps, demo_c_3_stopping.ps

3.1 Demo (c-1) IDL procedure

```
pro demo_c_1
;Use run_adas310.pro to make an adf21 (stopping coefficients for an H
;beam) and an adf26 tabulation over a wide range of densities and beam
;energies(which is needed to make and adf22 for beam
;emission coefficients) for H+1 and C+6

;Input files for run_adas310.pro
adf18 = '/home/adas/adas/adf18/p310_a17/bndlen_exp#h0.dat'
adf01 = '/home/adas/adas/adf01/qcx#h0/qcx#h0_e2p#h1.dat'

iz0      = 1          ; Nuclear charge of beam species
iz1      = 0          ; Recombining ion charge
ts       = 8617.00    ; Radiation field temperature (ev)
wdil     = 0.00000    ; External radiation field dilution factor
cion     = 1.00000    ; Multiplier of ground level e-impact ionisation rate
cpy      = 1.00000    ; Multiplier of ground level e-impact excitation rate
wdpi     = 1.0e+08   ; External radiation field dilution factor photo-ionisation
bsim     = 1.00000    ; Beam species isotope mass
nip      = 2          ; Range of delta n for impact parameter cross sections
intd     = 3          ; Order of maxwell quadrature for cross sections
iprs     = 1          ; Beyond nip - 0 van regemorter, 1 percival-richards
ilow     = 1          ; Access special low level data
ionip    = 1          ; Include ion impact collisions
nionip   = 4          ; Delta n for ion impact excitation cross sections
ilprs    = 1          ; Lodge-percival-richards or vainshtein default
ivdisp   = 1          ; Use of beam energy in calculation of cross section

; 1-110, make sure nrep is below 110 to avoid negative F's

nmin   = 1
nmax   = 110
nrep   = [ 1, 2, 3, 4, 5, 6, 7, 8, 9, 10, 11, 12, 15, 20, $
           30, 40, 50, 60, 70, 80, 90, 100]

;define a density and temperature arrays
dens = adas_vector(low=1e8, high=1e18, num=24)

denp = fltarr(24) + 1.0

te   = [100.000, 200.000, 300.000, 500.000, 600.000, 700.000, $
        800.000, 900.000, 1000.00, 2000.00, 3000.00, 5000.00, $
        6000.00, 7000.00, 8000.00, 9000.00, 10000.0, 20000.0, $
        30000.0, 50000.0]

tp   = te


```

```

bmeng = [ 5.000E+03, 1.000E+04, 1.500E+04, 2.000E+04, 2.500E+04, 3.000E+04, 3.500E+04, $  

        4.000E+04, 4.500E+04, 5.000E+04, 5.500E+04, 6.000E+04, 6.500E+04, 7.000E+04, $  

        7.500E+04, 8.000E+04, 8.500E+04, 9.000E+04, 9.500E+04, 1.000E+05, 1.050E+05, $  

        1.100E+05, 1.150E+05, 1.200E+05, 1.250E+05]

;Reference values
tref = 2000.0
dref = dens[11]
bref = 6.5e4
bdens = 1.0e7

;Define ion features: H+1, C+6
z_list = [1, 6]
m_list = [1.0, 12]
n_list = ['h1', 'c6']

for j = 0, n_elements(z_list)-1 do begin

    print, 'Generating...' + n_list[j]
    izimp = z_list[j]
    amimp = m_list[j]
    frimp = 1.0D0

;Use run_adas310.pro to calculate adf21 and adf26
    if izimp EQ 1 then denp_in = dens else denp_in = denp ; Different for Hydrogen

    run_adas310, iz0 = iz0, $
                  iz1 = iz1, $
                  adf18 = adf18, $
                  adf01 = adf01, $
                  ts = ts, $
                  wdil = wdil, $
                  cion = cion, $
                  cpy = cpy, $
                  wdpi = wdpi, $
                  bsim = bsim, $
                  nip = nip, $
                  intd = intd, $
                  iprs = iprs, $
                  ilow = ilow, $
                  ionip = ionip, $
                  nionip = nionip, $
                  ilprs = ilprs, $
                  ivdisp = ivdisp, $
                  izimp = izimp, $
                  amimp = amimp, $
                  frimp = frimp, $
                  nmin = nmin, $
                  nmax = nmax, $
                  nrep = nrep, $

```

```
    te      = te,      $  
    tp      = tp,      $  
    dens   = dens,    $  
    denp   = denp_in,$  
    bmeng  = bmeng,   $  
    tref   = tref,    $  
    dref   = dref,    $  
    bref   = bref,    $  
    bdens  = bdens,   $  
    log    = log,     $  
    adf21  = 'adf21_+'+n_list[j]+'.pass', $  
    adf26  = 'adf26_+'+n_list[j]+'.pass'  
  
endfor  
  
end
```

3.2 Demo (c-1) datasets

3.2.1 adf26.h1.pass

1

EFFECTIVE CONTRIBUTION TABLE FOR ION PRINCIPAL QUANTUM SHELL POPULATIONS IN THERMAL PLASMA

```
Generated by run_adas310 Z0 = 1.00E+00          Z1 = 1.00E+00
TRAD = 1.00E+08 K      TE = 2.32E+07 K      TP = 2.32E+07 K
W = 0.00E+00          NE = 1.00E+08 CM-3      NP = 1.00E+08 CM-3
EH = 5.00E+03 EV/AMU  NH = 1.00E+07 CM-3      NH/NE = 1.00E-01  FLUX = 9.78E+14 CM-2 SEC-1

CHARGE EXCHANGE OFF : N1/N+ = 1.20636E-09 RECOMB COEFF = 1.44370E-16 CM+3 SEC-1  IONIZ COEFF = 1.19674E-07 CM+3 SEC-1
CHARGE EXCHANGE ON  : N1/N+ = 5.07543E-01 RECOMB COEFF = 6.07398E-08 CM+3 SEC-1  IONIZ COEFF = 1.19674E-07 CM+3 SEC-1
```

| I | N | F1 | F2 | F3 | B(CHECK) | B(ACTUAL) | NN/(BN*N+) |
|----|-----|-------------|-------------|-------------|-------------|-------------|-------------|
| 1 | 1 | 0.00000E+00 | 3.23307E+09 | 1.36023E+19 | 1.36027E+18 | 1.36027E+18 | 3.73131E-19 |
| 2 | 2 | 3.77374E+09 | 3.67088E+00 | 7.29101E+10 | 9.20635E+09 | 9.20635E+09 | 1.48493E-18 |
| 3 | 3 | 1.56414E+09 | 2.67814E+00 | 4.78802E+10 | 5.58189E+09 | 5.58189E+09 | 3.33793E-18 |
| 4 | 4 | 1.09994E+09 | 2.32591E+00 | 1.00100E+10 | 1.55926E+09 | 1.55926E+09 | 5.93213E-18 |
| 5 | 5 | 8.69960E+08 | 2.13763E+00 | 3.07331E+09 | 7.48874E+08 | 7.48874E+08 | 9.26753E-18 |
| 6 | 6 | 7.02215E+08 | 2.01525E+00 | 1.18814E+09 | 4.75218E+08 | 4.75218E+08 | 1.33441E-17 |
| 7 | 7 | 6.38332E+08 | 1.92564E+00 | 5.35483E+08 | 3.77529E+08 | 3.77529E+08 | 1.81619E-17 |
| 8 | 8 | 5.89970E+08 | 1.85360E+00 | 2.68896E+08 | 3.26325E+08 | 3.26325E+08 | 2.37209E-17 |
| 9 | 9 | 5.49073E+08 | 1.79067E+00 | 1.46075E+08 | 2.93286E+08 | 2.93286E+08 | 3.00211E-17 |
| 10 | 10 | 5.12139E+08 | 1.73306E+00 | 8.42682E+07 | 2.68360E+08 | 2.68360E+08 | 3.70626E-17 |
| 11 | 11 | 4.94781E+08 | 1.70356E+00 | 5.30325E+07 | 2.56426E+08 | 2.56426E+08 | 4.48452E-17 |
| 12 | 12 | 4.59388E+08 | 1.64894E+00 | 3.36139E+07 | 2.36521E+08 | 2.36521E+08 | 5.33690E-17 |
| 13 | 15 | 3.20687E+08 | 1.44505E+00 | 9.65185E+06 | 1.63728E+08 | 1.63728E+08 | 8.33876E-17 |
| 14 | 20 | 1.26779E+08 | 1.17233E+00 | 1.35438E+06 | 6.44813E+07 | 6.44813E+07 | 1.48243E-16 |
| 15 | 30 | 2.02429E+07 | 1.02717E+00 | 1.62966E+05 | 1.02905E+07 | 1.02905E+07 | 3.33543E-16 |
| 16 | 40 | 4.89611E+06 | 1.00653E+00 | 3.57972E+04 | 2.48857E+06 | 2.48857E+06 | 5.92963E-16 |
| 17 | 50 | 1.55678E+06 | 1.00207E+00 | 1.08745E+04 | 7.91221E+05 | 7.91221E+05 | 9.26503E-16 |
| 18 | 60 | 5.87660E+05 | 1.00078E+00 | 3.99779E+03 | 2.98664E+05 | 2.98664E+05 | 1.33416E-15 |
| 19 | 70 | 2.43975E+05 | 1.00032E+00 | 1.62790E+03 | 1.23992E+05 | 1.23992E+05 | 1.81594E-15 |
| 20 | 80 | 1.02940E+05 | 1.00014E+00 | 6.72652E+02 | 5.23150E+04 | 5.23150E+04 | 2.37184E-15 |
| 21 | 90 | 3.82958E+04 | 1.00005E+00 | 2.40014E+02 | 1.94618E+04 | 1.94618E+04 | 3.00186E-15 |
| 22 | 100 | 5.97491E+03 | 1.00001E+00 | 2.55108E+01 | 3.03608E+03 | 3.03608E+03 | 3.70601E-15 |

```
BN = F1*(N1/N+) + F2 + F3*(NH/NE)
N1 = POPULATION OF GROUND STATE OF ION
N+ = POPULATION OF GROUND STATE OF NEXT IONISATION STAGE
NN = POPULATION OF PRINCIPAL QUANTUM SHELL N OF ION
BN = SAHA-BOLTZMANN FACTOR FOR PRINCIPAL QUANTUM SHELL N
EH = NEUTRAL HYDROGEN BEAM ENERGY
W = RADIATION DILUTION FACTOR
Z0 = NUCLEAR CHARGE
Z1 = ION CHARGE+1
```

```
NIP = 2      INTD = 3      IPRS = 1      ILOW = 1      IONIP = 1      NIONIP= 4      ILPRS = 1      IVDISP= 1
ZEFF = 1.0    TS = 1.00D+08     W = 0.00D+00      CION = 1.0      CPY = 1.0      W1 = 1.00D+08      ZIMP = 0.0 ( 0.00D+00)
1
```

EFFECTIVE CONTRIBUTION TABLE FOR ION PRINCIPAL QUANTUM SHELL POPULATIONS IN THERMAL PLASMA

```
Generated by run_adas310 Z0 = 1.00E+00          Z1 = 1.00E+00
TRAD = 1.00E+08 K      TE = 2.32E+07 K      TP = 2.32E+07 K
```

$W = 0.00E+00$ $NE = 2.72E+08 \text{ CM}^{-3}$ $NP = 2.72E+08 \text{ CM}^{-3}$
 $EH = 5.00E+03 \text{ EV/AMU}$ $NH = 1.00E+07 \text{ CM}^{-3}$ $NH/NE = 3.68E-02$ $FLUX = 9.78E+14 \text{ CM}^{-2} \text{ SEC}^{-1}$

CHARGE EXCHANGE OFF : $N1/N+ = 1.20494E-09$ RECOMB COEFF = $1.44278E-16 \text{ CM}^{+3} \text{ SEC}^{-1}$ IONIZ COEFF = $1.19739E-07 \text{ CM}^{+3} \text{ SEC}^{-1}$
 CHARGE EXCHANGE ON : $N1/N+ = 1.86491E-01$ RECOMB COEFF = $2.23303E-08 \text{ CM}^{+3} \text{ SEC}^{-1}$ IONIZ COEFF = $1.19739E-07 \text{ CM}^{+3} \text{ SEC}^{-1}$

| I | N | F1 | F2 | F3 | B(CHECK) | B(ACTUAL) | NN/(BN*N+) |
|----|-----|---------------|---------------|---------------|---------------|---------------|---------------|
| 1 | 1 | $0.00000E+00$ | $1.18723E+09$ | $4.99800E+18$ | $1.83756E+17$ | $1.83756E+17$ | $1.01492E-18$ |
| 2 | 2 | $3.77015E+09$ | $3.66585E+00$ | $7.29093E+10$ | $3.38359E+09$ | $3.38359E+09$ | $4.03900E-18$ |
| 3 | 3 | $1.55969E+09$ | $2.67192E+00$ | $4.78787E+10$ | $2.05111E+09$ | $2.05111E+09$ | $9.07916E-18$ |
| 4 | 4 | $1.09402E+09$ | $2.31763E+00$ | $1.00078E+10$ | $5.71959E+08$ | $5.71959E+08$ | $1.61354E-17$ |
| 5 | 5 | $8.61886E+08$ | $2.12636E+00$ | $3.07028E+09$ | $2.73612E+08$ | $2.73612E+08$ | $2.52077E-17$ |
| 6 | 6 | $6.91108E+08$ | $1.99951E+00$ | $1.18426E+09$ | $1.72424E+08$ | $1.72424E+08$ | $3.62960E-17$ |
| 7 | 7 | $6.22372E+08$ | $1.90297E+00$ | $5.30925E+08$ | $1.35586E+08$ | $1.35586E+08$ | $4.94005E-17$ |
| 8 | 8 | $5.66427E+08$ | $1.82004E+00$ | $2.63792E+08$ | $1.15332E+08$ | $1.15332E+08$ | $6.45210E-17$ |
| 9 | 9 | $5.14238E+08$ | $1.74092E+00$ | $1.40729E+08$ | $1.01075E+08$ | $1.01075E+08$ | $8.16575E-17$ |
| 10 | 10 | $4.64629E+08$ | $1.66533E+00$ | $7.95062E+07$ | $8.95722E+07$ | $8.95722E+07$ | $1.00810E-16$ |
| 11 | 11 | $4.43672E+08$ | $1.63119E+00$ | $5.06610E+07$ | $8.46032E+07$ | $8.46032E+07$ | $1.21979E-16$ |
| 12 | 12 | $3.90259E+08$ | $1.55182E+00$ | $3.16133E+07$ | $7.39419E+07$ | $7.39419E+07$ | $1.45164E-16$ |
| 13 | 15 | $2.19032E+08$ | $1.30490E+00$ | $8.35559E+06$ | $4.11546E+07$ | $4.11546E+07$ | $2.26814E-16$ |
| 14 | 20 | $6.70459E+07$ | $1.09155E+00$ | $9.63736E+05$ | $1.25389E+07$ | $1.25389E+07$ | $4.03220E-16$ |
| 15 | 30 | $9.95771E+06$ | $1.01345E+00$ | $1.13632E+05$ | $1.86120E+06$ | $1.86120E+06$ | $9.07236E-16$ |
| 16 | 40 | $2.35270E+06$ | $1.00316E+00$ | $2.49380E+04$ | $4.39674E+05$ | $4.39674E+05$ | $1.61286E-15$ |
| 17 | 50 | $7.40186E+05$ | $1.00099E+00$ | $7.57556E+03$ | $1.38317E+05$ | $1.38317E+05$ | $2.52009E-15$ |
| 18 | 60 | $2.77744E+05$ | $1.00037E+00$ | $2.78514E+03$ | $5.19000E+04$ | $5.19000E+04$ | $3.62892E-15$ |
| 19 | 70 | $1.14814E+05$ | $1.00015E+00$ | $1.13416E+03$ | $2.14545E+04$ | $2.14545E+04$ | $4.93937E-15$ |
| 20 | 80 | $4.82228E+04$ | $1.00006E+00$ | $4.68667E+02$ | $9.01133E+03$ | $9.01133E+03$ | $6.45142E-15$ |
| 21 | 90 | $1.77809E+04$ | $1.00002E+00$ | $1.67250E+02$ | $3.32312E+03$ | $3.32312E+03$ | $8.16507E-15$ |
| 22 | 100 | $2.58867E+03$ | $1.00000E+00$ | $1.78030E+01$ | $4.84418E+02$ | $4.84418E+02$ | $1.00803E-14$ |

$BN = F1 * (N1/N+) + F2 + F3 * (NH/NE)$
 $N1 = \text{POPULATION OF GROUND STATE OF ION}$
 $N+ = \text{POPULATION OF GROUND STATE OF NEXT IONISATION STAGE}$
 $NN = \text{POPULATION OF PRINCIPAL QUANTUM SHELL N OF ION}$
 $BN = \text{SAHA-BOLTZMANN FACTOR FOR PRINCIPAL QUANTUM SHELL N}$
 $EH = \text{NEUTRAL HYDROGEN BEAM ENERGY}$
 $W = \text{RADIATION DILUTION FACTOR}$
 $Z0 = \text{NUCLEAR CHARGE}$
 $Z1 = \text{ION CHARGE}+1$

$NIP = 2$ $INTD = 3$ $IPRS = 1$ $ILOW = 1$ $IONIP = 1$ $NIONIP= 4$ $ILPRS = 1$ $IVDISP= 1$
 $ZEFF = 1.0$ $TS = 1.00D+08$ $W = 0.00D+00$ $CION = 1.0$ $CPY = 1.0$ $W1 = 1.00D+08$ $ZIMP = 0.0 (0.00D+00)$

EFFECTIVE CONTRIBUTION TABLE FOR ION PRINCIPAL QUANTUM SHELL POPULATIONS IN THERMAL PLASMA

Generated by run_adas310 $Z0 = 1.00E+00$ $Z1 = 1.00E+00$
 $TRAD = 1.00E+08 \text{ K}$ $TE = 2.32E+07 \text{ K}$ $TP = 2.32E+07 \text{ K}$
 $W = 0.00E+00$ $NE = 7.41E+08 \text{ CM}^{-3}$ $NP = 7.41E+08 \text{ CM}^{-3}$
 $EH = 5.00E+03 \text{ EV/AMU}$ $NH = 1.00E+07 \text{ CM}^{-3}$ $NH/NE = 1.35E-02$ $FLUX = 9.78E+14 \text{ CM}^{-2} \text{ SEC}^{-1}$

CHARGE EXCHANGE OFF : $N1/N+ = 1.20281E-09$ RECOMB COEFF = $1.44141E-16 \text{ CM}^{+3} \text{ SEC}^{-1}$ IONIZ COEFF = $1.19836E-07 \text{ CM}^{+3} \text{ SEC}^{-1}$
 CHARGE EXCHANGE ON : $N1/N+ = 6.83959E-02$ RECOMB COEFF = $8.19632E-09 \text{ CM}^{+3} \text{ SEC}^{-1}$ IONIZ COEFF = $1.19836E-07 \text{ CM}^{+3} \text{ SEC}^{-1}$

| I | N | F1 | F2 | F3 | B(CHECK) | B(ACTUAL) | NN/(BN*N+) |
|---|---|---------------|---------------|---------------|---------------|---------------|---------------|
| 1 | 1 | $0.00000E+00$ | $4.35029E+08$ | $1.83303E+18$ | $2.47379E+16$ | $2.47379E+16$ | $2.76490E-18$ |
| 2 | 2 | $3.76477E+09$ | $3.65825E+00$ | $7.29071E+10$ | $1.24140E+09$ | $1.24140E+09$ | $1.10033E-17$ |

| | | | | | | | |
|----|-----|-------------|-------------|-------------|-------------|-------------|-------------|
| 3 | 3 | 1.55298E+09 | 2.66243E+00 | 4.78747E+10 | 7.52301E+08 | 7.52301E+08 | 2.47340E-17 |
| 4 | 4 | 1.08489E+09 | 2.30477E+00 | 1.00023E+10 | 2.09186E+08 | 2.09186E+08 | 4.39571E-17 |
| 5 | 5 | 8.48879E+08 | 2.10808E+00 | 3.06233E+09 | 9.93868E+07 | 9.93868E+07 | 6.86724E-17 |
| 6 | 6 | 6.72236E+08 | 1.97241E+00 | 1.17418E+09 | 6.18241E+07 | 6.18241E+07 | 9.88800E-17 |
| 7 | 7 | 5.93201E+08 | 1.86106E+00 | 5.19299E+08 | 4.75806E+07 | 4.75806E+07 | 1.34580E-16 |
| 8 | 8 | 5.20641E+08 | 1.75414E+00 | 2.51360E+08 | 3.90019E+07 | 3.90019E+07 | 1.75772E-16 |
| 9 | 9 | 4.46152E+08 | 1.64310E+00 | 1.28948E+08 | 3.22551E+07 | 3.22551E+07 | 2.22457E-16 |
| 10 | 10 | 3.77770E+08 | 1.54120E+00 | 7.03891E+07 | 2.67878E+07 | 2.67878E+07 | 2.74634E-16 |
| 11 | 11 | 3.46421E+08 | 1.49330E+00 | 4.51569E+07 | 2.43032E+07 | 2.43032E+07 | 3.32303E-16 |
| 12 | 12 | 2.83793E+08 | 1.40198E+00 | 2.76968E+07 | 1.97840E+07 | 1.97840E+07 | 3.95464E-16 |
| 13 | 15 | 1.29182E+08 | 1.18054E+00 | 6.81864E+06 | 8.92755E+06 | 8.92755E+06 | 6.17902E-16 |
| 14 | 20 | 3.19573E+07 | 1.04383E+00 | 6.64381E+05 | 2.19472E+06 | 2.19472E+06 | 1.09848E-15 |
| 15 | 30 | 4.53750E+06 | 1.00617E+00 | 7.68456E+04 | 3.11384E+05 | 3.11384E+05 | 2.47155E-15 |
| 16 | 40 | 1.05718E+06 | 1.00143E+00 | 1.68550E+04 | 7.25355E+04 | 7.25355E+04 | 4.39386E-15 |
| 17 | 50 | 3.30482E+05 | 1.00045E+00 | 5.12058E+03 | 2.26737E+04 | 2.26737E+04 | 6.86539E-15 |
| 18 | 60 | 1.23557E+05 | 1.00017E+00 | 1.88274E+03 | 8.47722E+03 | 8.47722E+03 | 9.88615E-15 |
| 19 | 70 | 5.09416E+04 | 1.00007E+00 | 7.66751E+02 | 3.49554E+03 | 3.49554E+03 | 1.34561E-14 |
| 20 | 80 | 2.13355E+04 | 1.00003E+00 | 3.16871E+02 | 1.46454E+03 | 1.46454E+03 | 1.75754E-14 |
| 21 | 90 | 7.82329E+03 | 1.00001E+00 | 1.13101E+02 | 5.37607E+02 | 5.37607E+02 | 2.22438E-14 |
| 22 | 100 | 1.08761E+03 | 1.00000E+00 | 1.20652E+01 | 7.55505E+01 | 7.55505E+01 | 2.74615E-14 |

BN = F1*(N1/N+) + F2 + F3*(NH/NE)
 N1 = POPULATION OF GROUND STATE OF ION
 N+ = POPULATION OF GROUND STATE OF NEXT IONISATION STAGE
 NN = POPULATION OF PRINCIPAL QUANTUM SHELL N OF ION
 BN = SAHA-BOLTZMANN FACTOR FOR PRINCIPAL QUANTUM SHELL N
 EH = NEUTRAL HYDROGEN BEAM ENERGY
 W = RADIATION DILUTION FACTOR
 Z0 = NUCLEAR CHARGE
 Z1 = ION CHARGE+1

```

NIP = 2      INTD = 3      IPRS = 1      ILOW = 1      IONIP = 1      NIONIP= 4      ILPRS = 1      IVDISP= 1
ZEFF = 1.0    TS = 1.000D+08    W = 0.00D+00      CION = 1.0      CPY = 1.0      W1 = 1.00D+08      ZIMP = 0.0 ( 0.00D+00)
1
.....
```

BN = F1*(N1/N+) + F2 + F3*(NH/NE)
 N1 = POPULATION OF GROUND STATE OF ION
 N+ = POPULATION OF GROUND STATE OF NEXT IONISATION STAGE
 NN = POPULATION OF PRINCIPAL QUANTUM SHELL N OF ION
 BN = SAHA-BOLTZMANN FACTOR FOR PRINCIPAL QUANTUM SHELL N
 EH = NEUTRAL HYDROGEN BEAM ENERGY
 W = RADIATION DILUTION FACTOR
 Z0 = NUCLEAR CHARGE
 Z1 = ION CHARGE+1

```

NIP = 2      INTD = 3      IPRS = 1      ILOW = 1      IONIP = 1      NIONIP= 4      ILPRS = 1      IVDISP= 1
ZEFF = 1.0    TS = 1.000D+08    W = 0.00D+00      CION = 1.0      CPY = 1.0      W1 = 1.00D+08      ZIMP = 0.0 ( 0.00D+00)
```

```

C-----
C
C  Code      : run_adas310
C  Producer   : Alessandra Giunta
C  Date       : 27/05/13
C
C-----
```

3.2.2 adf26_c6.pass

1

EFFECTIVE CONTRIBUTION TABLE FOR ION PRINCIPAL QUANTUM SHELL POPULATIONS IN THERMAL PLASMA

```

Generated by run_adas310  Z0 = 1.00E+00          Z1 = 1.00E+00
TRAD = 1.00E+08 K        TE = 2.32E+07 K        TP = 2.32E+07 K

```

```

W = 0.00E+00          NE = 1.00E+08 CM-3          NP = 1.00E+00 CM-3
EH = 5.00E+03 EV/AMU   NH = 1.00E+07 CM-3          NH/NE = 1.00E-01   FLUX = 9.78E+14 CM-2 SEC-1

CHARGE EXCHANGE OFF : N1/N+ = 1.53030E-09 RECOMB COEFF = 1.44336E-16 CM+3 SEC-1 IONIZ COEFF = 9.43188E-08 CM+3 SEC-1
CHARGE EXCHANGE ON : N1/N+ = 6.43981E-01 RECOMB COEFF = 6.07395E-08 CM+3 SEC-1 IONIZ COEFF = 9.43188E-08 CM+3 SEC-1

      I      N            F1            F2            F3        B(CHECK)        B(ACTUAL)        NN/(BN*N+)
1      1    0.00000E+00  4.10125E+09  1.72588E+19  1.72594E+18  1.72594E+18  3.73131E-19
2      2    3.12743E+09  3.66905E+00  7.29100E+10  9.30501E+09  9.30501E+09  1.48493E-18
3      3    1.30553E+09  2.67589E+00  4.78799E+10  5.62873E+09  5.62873E+09  3.33793E-18
4      4    9.26108E+08  2.32297E+00  1.00095E+10  1.59735E+09  1.59735E+09  5.93213E-18
5      5    7.79429E+08  2.13388E+00  3.07305E+09  8.09243E+08  8.09243E+08  9.26753E-18
6      6    6.98798E+08  2.01056E+00  1.18790E+09  5.68803E+08  5.68803E+08  1.33441E-17
7      7    6.34125E+08  1.91983E+00  5.35176E+08  4.61882E+08  4.61882E+08  1.81619E-17
8      8    5.84756E+08  1.84640E+00  2.68472E+08  4.03419E+08  4.03419E+08  2.37209E-17
9      9    5.42440E+08  1.78147E+00  1.45495E+08  3.63871E+08  3.63871E+08  3.00211E-17
10     10   5.02788E+08  1.72002E+00  8.34769E+07  3.32134E+08  3.32134E+08  3.70626E-17
11     11   4.79956E+08  1.68280E+00  5.20095E+07  3.14283E+08  3.14283E+08  4.48452E-17
12     12   4.35230E+08  1.61510E+00  3.23641E+07  2.83516E+08  2.83516E+08  5.33690E-17
13     15   2.65677E+08  1.36899E+00  8.18657E+06  1.71910E+08  1.71910E+08  8.33876E-17
14     20   8.16708E+07  1.11095E+00  5.33217E+05  5.26478E+07  5.26478E+07  1.48243E-16
15     30   1.08689E+07  1.01460E+00  5.50221E+04  7.00487E+06  7.00487E+06  3.33543E-16
16     40   2.38810E+06  1.00319E+00  1.11508E+04  1.53901E+06  1.53901E+06  5.92963E-16
17     50   7.10059E+05  1.00095E+00  3.18844E+03  4.57585E+05  4.57585E+05  9.26503E-16
18     60   2.53500E+05  1.00034E+00  1.11267E+03  1.63361E+05  1.63361E+05  1.33416E-15
19     70   9.93969E+04  1.00013E+00  4.28977E+02  6.40537E+04  6.40537E+04  1.81594E-15
20     80   3.86460E+04  1.00005E+00  1.63567E+02  2.49047E+04  2.49047E+04  2.37184E-15
21     90   1.17210E+04  1.00002E+00  4.71438E+01  7.55382E+03  7.55382E+03  3.00186E-15
22    100   -1.35648E+03  9.99998E-01  -8.99322E+00  -8.73445E+02  -8.73445E+02  3.70601E-15

```

BN = F1*(N1/N+) + F2 + F3*(NH/NE)
 N1 = POPULATION OF GROUND STATE OF ION
 N+ = POPULATION OF GROUND STATE OF NEXT IONISATION STAGE
 NN = POPULATION OF PRINCIPAL QUANTUM SHELL N OF ION
 BN = SAHA-BOLTZMANN FACTOR FOR PRINCIPAL QUANTUM SHELL N
 EH = NEUTRAL HYDROGEN BEAM ENERGY
 W = RADIATION DILUTION FACTOR
 Z0 = NUCLEAR CHARGE
 Z1 = ION CHARGE+1

BN = F1*(N1/N+) + F2 + F3*(NH/NE)
 N1 = POPULATION OF GROUND STATE OF ION
 N+ = POPULATION OF GROUND STATE OF NEXT IONISATION STAGE
 NN = POPULATION OF PRINCIPAL QUANTUM SHELL N OF ION
 BN = SAHA-BOLTZMANN FACTOR FOR PRINCIPAL QUANTUM SHELL N
 EH = NEUTRAL HYDROGEN BEAM ENERGY
 W = RADIATION DILUTION FACTOR
 Z0 = NUCLEAR CHARGE
 Z1 = ION CHARGE+1

```

NIP = 2      INTD = 3      IPRS = 1      ILOW = 1      IONIP = 1      NIONIP= 4      ILPRS = 1      IVDISP= 1
ZEFF = 6.0    TS = 1.00D+08   W = 0.00D+00    CION = 1.0      CPY = 1.0      W1 = 1.00D+08    ZIMP = 6.0 ( 1.01D+12)

C-----
C
C Code      : run_adas310
C Producer  : Alessandra Giunta
C Date      : 27/05/13
C
C-----

```

3.2.3 adf21.h1.pass

```
1 /SVREF=9.132E-08 /SPEC=H /DATE=27/05/13 /CODE=ADAS310
```

25 24 /TREF=2.000E+03

| | | | | | | | |
|-----------|-----------|-----------|-----------|-----------|-----------|-----------|-----------|
| 5.000E+03 | 1.000E+04 | 1.500E+04 | 2.000E+04 | 2.500E+04 | 3.000E+04 | 3.500E+04 | 4.000E+04 |
| 4.500E+04 | 5.000E+04 | 5.500E+04 | 6.000E+04 | 6.500E+04 | 7.000E+04 | 7.500E+04 | 8.000E+04 |
| 8.500E+04 | 9.000E+04 | 9.500E+04 | 1.000E+05 | 1.050E+05 | 1.100E+05 | 1.150E+05 | 1.200E+05 |
| 1.250E+05 | | | | | | | |
| 1.000E+08 | 2.720E+08 | 7.410E+08 | 2.020E+09 | 5.480E+09 | 1.490E+10 | 4.060E+10 | 1.110E+11 |
| 3.010E+11 | 8.190E+11 | 2.230E+12 | 6.060E+12 | 1.650E+13 | 4.490E+13 | 1.220E+14 | 3.320E+14 |
| 9.050E+14 | 2.460E+15 | 6.700E+15 | 1.820E+16 | 4.960E+16 | 1.350E+17 | 3.670E+17 | 1.000E+18 |
| ----- | | | | | | | |
| 1.197E-07 | 1.212E-07 | 1.190E-07 | 1.156E-07 | 1.116E-07 | 1.074E-07 | 1.032E-07 | 9.897E-08 |
| 9.500E-08 | 9.127E-08 | 8.795E-08 | 8.493E-08 | 8.236E-08 | 8.009E-08 | 7.816E-08 | 7.651E-08 |
| 7.505E-08 | 7.380E-08 | 7.268E-08 | 7.167E-08 | 7.077E-08 | 6.993E-08 | 6.917E-08 | 6.846E-08 |
| 6.781E-08 | | | | | | | |
| 1.197E-07 | 1.213E-07 | 1.191E-07 | 1.157E-07 | 1.117E-07 | 1.075E-07 | 1.032E-07 | 9.902E-08 |
| 9.506E-08 | 9.133E-08 | 8.800E-08 | 8.499E-08 | 8.241E-08 | 8.015E-08 | 7.821E-08 | 7.656E-08 |
| 7.510E-08 | 7.384E-08 | 7.273E-08 | 7.172E-08 | 7.081E-08 | 6.998E-08 | 6.921E-08 | 6.851E-08 |
| 6.786E-08 | | | | | | | |
| 1.198E-07 | 1.214E-07 | 1.192E-07 | 1.158E-07 | 1.118E-07 | 1.076E-07 | 1.033E-07 | 9.911E-08 |
| 9.514E-08 | 9.141E-08 | 8.808E-08 | 8.506E-08 | 8.248E-08 | 8.022E-08 | 7.828E-08 | 7.663E-08 |
| 7.517E-08 | 7.391E-08 | 7.279E-08 | 7.179E-08 | 7.088E-08 | 7.004E-08 | 6.928E-08 | 6.858E-08 |
| 6.792E-08 | | | | | | | |
| 1.200E-07 | 1.215E-07 | 1.193E-07 | 1.159E-07 | 1.119E-07 | 1.077E-07 | 1.034E-07 | 9.923E-08 |
| 9.526E-08 | 9.152E-08 | 8.819E-08 | 8.517E-08 | 8.259E-08 | 8.032E-08 | 7.838E-08 | 7.672E-08 |
| 7.527E-08 | 7.401E-08 | 7.289E-08 | 7.188E-08 | 7.097E-08 | 7.013E-08 | 6.937E-08 | 6.866E-08 |
| 6.801E-08 | | | | | | | |
| 1.202E-07 | 1.217E-07 | 1.195E-07 | 1.161E-07 | 1.121E-07 | 1.079E-07 | 1.036E-07 | 9.940E-08 |
| 9.542E-08 | 9.168E-08 | 8.834E-08 | 8.531E-08 | 8.273E-08 | 8.046E-08 | 7.852E-08 | 7.686E-08 |
| 7.540E-08 | 7.413E-08 | 7.301E-08 | 7.200E-08 | 7.109E-08 | 7.026E-08 | 6.949E-08 | 6.878E-08 |
| 6.813E-08 | | | | | | | |
| 1.204E-07 | 1.220E-07 | 1.198E-07 | 1.164E-07 | 1.123E-07 | 1.081E-07 | 1.039E-07 | 9.964E-08 |
| 9.566E-08 | 9.190E-08 | 8.856E-08 | 8.552E-08 | 8.293E-08 | 8.065E-08 | 7.871E-08 | 7.704E-08 |
| 7.558E-08 | 7.431E-08 | 7.319E-08 | 7.218E-08 | 7.126E-08 | 7.042E-08 | 6.965E-08 | 6.895E-08 |
| 6.829E-08 | | | | | | | |
| 1.207E-07 | 1.223E-07 | 1.201E-07 | 1.167E-07 | 1.127E-07 | 1.085E-07 | 1.042E-07 | 1.000E-07 |
| 9.601E-08 | 9.225E-08 | 8.889E-08 | 8.584E-08 | 8.324E-08 | 8.095E-08 | 7.900E-08 | 7.733E-08 |
| 7.586E-08 | 7.458E-08 | 7.345E-08 | 7.244E-08 | 7.152E-08 | 7.067E-08 | 6.990E-08 | 6.919E-08 |
| 6.853E-08 | | | | | | | |
| 1.211E-07 | 1.227E-07 | 1.207E-07 | 1.173E-07 | 1.133E-07 | 1.091E-07 | 1.048E-07 | 1.006E-07 |
| 9.660E-08 | 9.282E-08 | 8.945E-08 | 8.639E-08 | 8.377E-08 | 8.147E-08 | 7.950E-08 | 7.782E-08 |
| 7.634E-08 | 7.505E-08 | 7.391E-08 | 7.289E-08 | 7.196E-08 | 7.111E-08 | 7.033E-08 | 6.961E-08 |
| 6.895E-08 | | | | | | | |
| 1.216E-07 | 1.234E-07 | 1.214E-07 | 1.181E-07 | 1.142E-07 | 1.100E-07 | 1.058E-07 | 1.015E-07 |
| 9.754E-08 | 9.375E-08 | 9.037E-08 | 8.730E-08 | 8.466E-08 | 8.235E-08 | 8.037E-08 | 7.867E-08 |
| 7.717E-08 | 7.588E-08 | 7.472E-08 | 7.369E-08 | 7.275E-08 | 7.189E-08 | 7.110E-08 | 7.037E-08 |
| 6.970E-08 | | | | | | | |
| 1.223E-07 | 1.243E-07 | 1.224E-07 | 1.193E-07 | 1.154E-07 | 1.114E-07 | 1.072E-07 | 1.030E-07 |
| 9.897E-08 | 9.519E-08 | 9.181E-08 | 8.873E-08 | 8.609E-08 | 8.376E-08 | 8.177E-08 | 8.006E-08 |
| 7.855E-08 | 7.724E-08 | 7.607E-08 | 7.502E-08 | 7.407E-08 | 7.320E-08 | 7.240E-08 | 7.166E-08 |
| 7.098E-08 | | | | | | | |
| 1.233E-07 | 1.255E-07 | 1.238E-07 | 1.209E-07 | 1.172E-07 | 1.132E-07 | 1.091E-07 | 1.050E-07 |
| 1.010E-07 | 9.730E-08 | 9.393E-08 | 9.086E-08 | 8.822E-08 | 8.589E-08 | 8.388E-08 | 8.216E-08 |
| 8.064E-08 | 7.932E-08 | 7.815E-08 | 7.708E-08 | 7.612E-08 | 7.524E-08 | 7.442E-08 | 7.367E-08 |
| 7.298E-08 | | | | | | | |
| 1.246E-07 | 1.271E-07 | 1.258E-07 | 1.231E-07 | 1.197E-07 | 1.159E-07 | 1.119E-07 | 1.079E-07 |
| 1.040E-07 | 1.003E-07 | 9.700E-08 | 9.395E-08 | 9.132E-08 | 8.900E-08 | 8.700E-08 | 8.527E-08 |
| 8.375E-08 | 8.242E-08 | 8.123E-08 | 8.016E-08 | 7.918E-08 | 7.828E-08 | 7.746E-08 | 7.670E-08 |
| 7.599E-08 | | | | | | | |
| 1.265E-07 | 1.295E-07 | 1.286E-07 | 1.263E-07 | 1.232E-07 | 1.197E-07 | 1.160E-07 | 1.121E-07 |
| 1.084E-07 | 1.048E-07 | 1.015E-07 | 9.850E-08 | 9.591E-08 | 9.361E-08 | 9.162E-08 | 8.991E-08 |
| 8.839E-08 | 8.706E-08 | 8.586E-08 | 8.478E-08 | 8.380E-08 | 8.289E-08 | 8.205E-08 | 8.127E-08 |
| 8.055E-08 | | | | | | | |
| 1.293E-07 | 1.329E-07 | 1.326E-07 | 1.308E-07 | 1.282E-07 | 1.251E-07 | 1.217E-07 | 1.182E-07 |
| 1.146E-07 | 1.112E-07 | 1.081E-07 | 1.052E-07 | 1.027E-07 | 1.004E-07 | 9.848E-08 | 9.679E-08 |
| 9.529E-08 | 9.398E-08 | 9.279E-08 | 9.171E-08 | 9.072E-08 | 8.980E-08 | 8.895E-08 | 8.816E-08 |
| 8.742E-08 | | | | | | | |
| 1.335E-07 | 1.380E-07 | 1.385E-07 | 1.375E-07 | 1.356E-07 | 1.332E-07 | 1.303E-07 | 1.272E-07 |
| 1.241E-07 | 1.210E-07 | 1.181E-07 | 1.153E-07 | 1.129E-07 | 1.108E-07 | 1.089E-07 | 1.073E-07 |
| 1.059E-07 | 1.046E-07 | 1.034E-07 | 1.024E-07 | 1.014E-07 | 1.005E-07 | 9.958E-08 | 9.878E-08 |
| 9.802E-08 | | | | | | | |
| 1.392E-07 | 1.444E-07 | 1.457E-07 | 1.455E-07 | 1.445E-07 | 1.429E-07 | 1.409E-07 | 1.385E-07 |
| 1.360E-07 | 1.335E-07 | 1.310E-07 | 1.286E-07 | 1.265E-07 | 1.246E-07 | 1.230E-07 | 1.215E-07 |
| 1.202E-07 | 1.190E-07 | 1.180E-07 | 1.170E-07 | 1.160E-07 | 1.151E-07 | 1.143E-07 | 1.135E-07 |
| 1.127E-07 | | | | | | | |

```

1.446E-07 1.499E-07 1.515E-07 1.519E-07 1.516E-07 1.507E-07 1.495E-07 1.480E-07
1.462E-07 1.443E-07 1.424E-07 1.405E-07 1.389E-07 1.373E-07 1.360E-07 1.348E-07
1.337E-07 1.327E-07 1.318E-07 1.310E-07 1.302E-07 1.294E-07 1.286E-07 1.279E-07
1.272E-07
1.479E-07 1.530E-07 1.548E-07 1.554E-07 1.555E-07 1.551E-07 1.544E-07 1.534E-07
1.521E-07 1.507E-07 1.492E-07 1.477E-07 1.463E-07 1.451E-07 1.440E-07 1.430E-07
1.421E-07 1.413E-07 1.406E-07 1.399E-07 1.392E-07 1.385E-07 1.378E-07 1.372E-07
1.366E-07
1.494E-07 1.544E-07 1.562E-07 1.570E-07 1.572E-07 1.570E-07 1.566E-07 1.558E-07
1.548E-07 1.536E-07 1.523E-07 1.510E-07 1.498E-07 1.487E-07 1.477E-07 1.469E-07
1.461E-07 1.454E-07 1.448E-07 1.441E-07 1.435E-07 1.429E-07 1.422E-07 1.416E-07
1.411E-07
1.500E-07 1.550E-07 1.568E-07 1.576E-07 1.578E-07 1.578E-07 1.574E-07 1.567E-07
1.559E-07 1.547E-07 1.536E-07 1.523E-07 1.512E-07 1.501E-07 1.492E-07 1.484E-07
1.477E-07 1.474E-07 1.464E-07 1.458E-07 1.452E-07 1.446E-07 1.440E-07 1.435E-07
1.429E-07
1.503E-07 1.552E-07 1.570E-07 1.578E-07 1.581E-07 1.581E-07 1.578E-07 1.571E-07
1.563E-07 1.552E-07 1.540E-07 1.528E-07 1.517E-07 1.507E-07 1.498E-07 1.490E-07
1.483E-07 1.477E-07 1.471E-07 1.465E-07 1.459E-07 1.453E-07 1.447E-07 1.442E-07
1.436E-07
1.504E-07 1.553E-07 1.571E-07 1.579E-07 1.582E-07 1.582E-07 1.579E-07 1.572E-07
1.564E-07 1.553E-07 1.542E-07 1.530E-07 1.519E-07 1.509E-07 1.500E-07 1.493E-07
1.485E-07 1.479E-07 1.473E-07 1.468E-07 1.462E-07 1.456E-07 1.450E-07 1.444E-07
1.439E-07
1.504E-07 1.553E-07 1.571E-07 1.579E-07 1.582E-07 1.582E-07 1.579E-07 1.573E-07
1.565E-07 1.554E-07 1.543E-07 1.530E-07 1.520E-07 1.510E-07 1.501E-07 1.493E-07
1.486E-07 1.480E-07 1.474E-07 1.468E-07 1.463E-07 1.457E-07 1.451E-07 1.445E-07
1.440E-07
1.504E-07 1.553E-07 1.571E-07 1.579E-07 1.582E-07 1.582E-07 1.579E-07 1.573E-07
1.566E-07 1.554E-07 1.543E-07 1.531E-07 1.520E-07 1.510E-07 1.501E-07 1.494E-07
1.487E-07 1.480E-07 1.475E-07 1.469E-07 1.463E-07 1.457E-07 1.451E-07 1.446E-07
1.440E-07
-----20 /EREF=6.500E+04 /NREF=6.060E+12-----
1.000E+02 2.000E+02 3.000E+02 5.000E+02 6.000E+02 7.000E+02 8.000E+02 8.966E+02
1.000E+03 2.000E+03 3.000E+03 5.000E+03 6.000E+03 7.000E+03 8.000E+03 8.966E+03
1.000E+04 2.000E+04 3.000E+04 5.000E+04
-----1.082E-07 1.076E-07 1.056E-07 1.021E-07 1.006E-07 9.942E-08 9.836E-08 9.745E-08
9.658E-08 9.132E-08 8.852E-08 8.530E-08 8.418E-08 8.325E-08 8.245E-08 8.176E-08
8.109E-08 7.639E-08 7.308E-08 6.821E-08
-----C-----
C
C Code      : run_adas310
C Producer  : Alessandra Giunta
C Date      : 27/05/13
C
C-----
```

3.2.4 adf21_c6.pass

```

6 /SVREF=1.781E-07 /SPEC=C /DATE=27/05/13 /CODE=ADAS310
-----25 24 /TREF=2.000E+03
5.000E+03 1.000E+04 1.500E+04 2.000E+04 2.500E+04 3.000E+04 3.500E+04 4.000E+04
4.500E+04 5.000E+04 5.500E+04 6.000E+04 6.500E+04 7.000E+04 7.500E+04 8.000E+04
8.500E+04 9.000E+04 9.500E+04 1.000E+05 1.050E+05 1.100E+05 1.150E+05 1.200E+05
1.250E+05
1.000E+08 2.720E+08 7.410E+08 2.020E+09 5.480E+09 1.490E+10 4.060E+10 1.110E+11
3.010E+11 8.190E+11 2.230E+12 6.060E+12 1.650E+13 4.490E+13 1.220E+14 3.320E+14
9.050E+14 2.460E+15 6.700E+15 1.820E+16 4.960E+16 1.350E+17 3.670E+17 1.000E+18
-----9.432E-08 1.141E-07 1.231E-07 1.285E-07 1.325E-07 1.366E-07 1.408E-07 1.452E-07
1.499E-07 1.548E-07 1.598E-07 1.648E-07 1.700E-07 1.750E-07 1.800E-07 1.848E-07
1.894E-07 1.938E-07 1.981E-07 2.020E-07 2.056E-07 2.090E-07 2.123E-07 2.154E-07
2.184E-07
9.439E-08 1.142E-07 1.232E-07 1.286E-07 1.326E-07 1.367E-07 1.409E-07 1.453E-07
1.500E-07 1.549E-07 1.598E-07 1.649E-07 1.700E-07 1.751E-07 1.801E-07 1.849E-07
1.895E-07 1.939E-07 1.981E-07 2.021E-07 2.057E-07 2.091E-07 2.123E-07 2.154E-07
-----
```

2.184E-08
 9.448E-08 1.143E-07 1.233E-07 1.287E-07 1.327E-07 1.368E-07 1.409E-07 1.454E-07
 1.501E-07 1.549E-07 1.599E-07 1.650E-07 1.701E-07 1.752E-07 1.802E-07 1.850E-07
 1.896E-07 1.940E-07 1.982E-07 2.022E-07 2.058E-07 2.092E-07 2.124E-07 2.155E-07
 2.185E-07
 9.462E-08 1.144E-07 1.234E-07 1.288E-07 1.328E-07 1.369E-07 1.411E-07 1.455E-07
 1.502E-07 1.551E-07 1.600E-07 1.651E-07 1.702E-07 1.753E-07 1.803E-07 1.851E-07
 1.897E-07 1.941E-07 1.984E-07 2.023E-07 2.059E-07 2.093E-07 2.125E-07 2.156E-07
 2.186E-07
 9.479E-08 1.146E-07 1.236E-07 1.289E-07 1.330E-07 1.371E-07 1.412E-07 1.457E-07
 1.504E-07 1.552E-07 1.602E-07 1.653E-07 1.704E-07 1.755E-07 1.804E-07 1.852E-07
 1.899E-07 1.943E-07 1.985E-07 2.025E-07 2.061E-07 2.095E-07 2.127E-07 2.158E-07
 2.188E-07
 9.502E-08 1.148E-07 1.238E-07 1.292E-07 1.332E-07 1.373E-07 1.414E-07 1.459E-07
 1.506E-07 1.554E-07 1.604E-07 1.655E-07 1.706E-07 1.757E-07 1.807E-07 1.855E-07
 1.901E-07 1.945E-07 1.987E-07 2.027E-07 2.063E-07 2.097E-07 2.129E-07 2.160E-07
 2.190E-07
 9.532E-08 1.151E-07 1.241E-07 1.294E-07 1.335E-07 1.376E-07 1.417E-07 1.462E-07
 1.509E-07 1.557E-07 1.607E-07 1.658E-07 1.709E-07 1.760E-07 1.810E-07 1.858E-07
 1.904E-07 1.949E-07 1.991E-07 2.031E-07 2.067E-07 2.101E-07 2.133E-07 2.164E-07
 2.194E-07
 9.571E-08 1.155E-07 1.244E-07 1.298E-07 1.339E-07 1.379E-07 1.421E-07 1.466E-07
 1.513E-07 1.562E-07 1.612E-07 1.663E-07 1.714E-07 1.765E-07 1.815E-07 1.864E-07
 1.910E-07 1.955E-07 1.997E-07 2.037E-07 2.074E-07 2.108E-07 2.140E-07 2.172E-07
 2.202E-07
 9.623E-08 1.160E-07 1.250E-07 1.304E-07 1.344E-07 1.385E-07 1.427E-07 1.472E-07
 1.519E-07 1.568E-07 1.619E-07 1.670E-07 1.722E-07 1.773E-07 1.824E-07 1.872E-07
 1.919E-07 1.964E-07 2.007E-07 2.047E-07 2.084E-07 2.119E-07 2.152E-07 2.183E-07
 2.214E-07
 9.691E-08 1.168E-07 1.257E-07 1.311E-07 1.352E-07 1.393E-07 1.435E-07 1.481E-07
 1.528E-07 1.578E-07 1.629E-07 1.681E-07 1.733E-07 1.785E-07 1.837E-07 1.886E-07
 1.934E-07 1.979E-07 2.023E-07 2.064E-07 2.101E-07 2.136E-07 2.170E-07 2.202E-07
 2.233E-07
 9.781E-08 1.179E-07 1.269E-07 1.322E-07 1.363E-07 1.405E-07 1.448E-07 1.494E-07
 1.543E-07 1.593E-07 1.645E-07 1.698E-07 1.752E-07 1.805E-07 1.857E-07 1.908E-07
 1.957E-07 2.004E-07 2.048E-07 2.090E-07 2.129E-07 2.165E-07 2.199E-07 2.232E-07
 2.264E-07
 9.902E-08 1.194E-07 1.285E-07 1.340E-07 1.381E-07 1.423E-07 1.467E-07 1.515E-07
 1.565E-07 1.618E-07 1.671E-07 1.726E-07 1.781E-07 1.836E-07 1.890E-07 1.943E-07
 1.994E-07 2.042E-07 2.089E-07 2.133E-07 2.173E-07 2.210E-07 2.246E-07 2.281E-07
 2.315E-07
 1.006E-07 1.215E-07 1.310E-07 1.366E-07 1.407E-07 1.451E-07 1.496E-07 1.546E-07
 1.598E-07 1.653E-07 1.710E-07 1.767E-07 1.825E-07 1.883E-07 1.939E-07 1.995E-07
 2.048E-07 2.100E-07 2.149E-07 2.195E-07 2.238E-07 2.278E-07 2.316E-07 2.354E-07
 2.389E-07
 1.028E-07 1.246E-07 1.347E-07 1.405E-07 1.447E-07 1.492E-07 1.539E-07 1.591E-07
 1.646E-07 1.704E-07 1.764E-07 1.825E-07 1.887E-07 1.949E-07 2.009E-07 2.069E-07
 2.126E-07 2.182E-07 2.235E-07 2.285E-07 2.331E-07 2.375E-07 2.417E-07 2.457E-07
 2.497E-07
 1.062E-07 1.291E-07 1.396E-07 1.456E-07 1.500E-07 1.547E-07 1.597E-07 1.652E-07
 1.711E-07 1.774E-07 1.840E-07 1.906E-07 1.973E-07 2.040E-07 2.105E-07 2.170E-07
 2.233E-07 2.294E-07 2.353E-07 2.409E-07 2.460E-07 2.508E-07 2.555E-07 2.600E-07
 2.644E-07
 1.109E-07 1.339E-07 1.443E-07 1.504E-07 1.551E-07 1.601E-07 1.654E-07 1.714E-07
 1.779E-07 1.847E-07 1.918E-07 1.990E-07 2.063E-07 2.134E-07 2.206E-07 2.276E-07
 2.345E-07 2.412E-07 2.477E-07 2.538E-07 2.594E-07 2.648E-07 2.699E-07 2.749E-07
 2.798E-07
 1.152E-07 1.373E-07 1.473E-07 1.534E-07 1.583E-07 1.636E-07 1.693E-07 1.757E-07
 1.825E-07 1.898E-07 1.973E-07 2.049E-07 2.125E-07 2.201E-07 2.276E-07 2.350E-07
 2.422E-07 2.494E-07 2.562E-07 2.627E-07 2.687E-07 2.744E-07 2.799E-07 2.853E-07
 2.905E-07
 1.179E-07 1.390E-07 1.487E-07 1.548E-07 1.598E-07 1.653E-07 1.712E-07 1.777E-07
 1.848E-07 1.923E-07 2.001E-07 2.079E-07 2.156E-07 2.234E-07 2.311E-07 2.387E-07
 2.461E-07 2.534E-07 2.605E-07 2.672E-07 2.734E-07 2.792E-07 2.849E-07 2.904E-07
 2.958E-07
 1.191E-07 1.397E-07 1.493E-07 1.553E-07 1.604E-07 1.660E-07 1.719E-07 1.786E-07
 1.858E-07 1.934E-07 2.012E-07 2.091E-07 2.170E-07 2.248E-07 2.325E-07 2.402E-07
 2.478E-07 2.552E-07 2.623E-07 2.691E-07 2.753E-07 2.813E-07 2.870E-07 2.926E-07
 2.980E-07
 1.196E-07 1.400E-07 1.495E-07 1.556E-07 1.607E-07 1.662E-07 1.722E-07 1.789E-07
 1.862E-07 1.938E-07 2.017E-07 2.096E-07 2.175E-07 2.253E-07 2.331E-07 2.408E-07
 2.484E-07 2.558E-07 2.630E-07 2.698E-07 2.761E-07 2.820E-07 2.878E-07 2.934E-07
 2.989E-07
 1.198E-07 1.401E-07 1.496E-07 1.556E-07 1.608E-07 1.663E-07 1.724E-07 1.791E-07

```

1.863E-07 1.940E-07 2.018E-07 2.098E-07 2.177E-07 2.255E-07 2.333E-07 2.410E-07
2.486E-07 2.561E-07 2.633E-07 2.701E-07 2.764E-07 2.823E-07 2.881E-07 2.937E-07
2.992E-07
1.199E-07 1.402E-07 1.496E-07 1.557E-07 1.608E-07 1.664E-07 1.724E-07 1.791E-07
1.864E-07 1.940E-07 2.019E-07 2.098E-07 2.177E-07 2.256E-07 2.334E-07 2.411E-07
2.487E-07 2.562E-07 2.634E-07 2.702E-07 2.765E-07 2.824E-07 2.882E-07 2.938E-07
2.994E-07
1.199E-07 1.402E-07 1.496E-07 1.557E-07 1.608E-07 1.664E-07 1.724E-07 1.791E-07
1.864E-07 1.940E-07 2.019E-07 2.098E-07 2.178E-07 2.256E-07 2.334E-07 2.411E-07
2.487E-07 2.562E-07 2.634E-07 2.702E-07 2.765E-07 2.825E-07 2.883E-07 2.939E-07
2.994E-07
1.199E-07 1.402E-07 1.496E-07 1.557E-07 1.608E-07 1.664E-07 1.724E-07 1.791E-07
1.864E-07 1.940E-07 2.019E-07 2.099E-07 2.178E-07 2.256E-07 2.334E-07 2.412E-07
2.488E-07 2.562E-07 2.634E-07 2.702E-07 2.765E-07 2.825E-07 2.883E-07 2.939E-07
2.994E-07
-----20 /EREF=6.500E+04 /NREF=6.060E+12-----
1.000E+02 2.000E+02 3.000E+02 5.000E+02 6.000E+02 7.000E+02 8.000E+02 8.966E+02
1.000E+03 2.000E+03 3.000E+03 5.000E+03 6.000E+03 7.000E+03 8.000E+03 8.966E+03
1.000E+04 2.000E+04 3.000E+04 5.000E+04
-----1.927E-07 1.924E-07 1.905E-07 1.872E-07 1.859E-07 1.847E-07 1.838E-07 1.830E-07
1.822E-07 1.781E-07 1.767E-07 1.761E-07 1.764E-07 1.768E-07 1.774E-07 1.780E-07
1.787E-07 1.858E-07 1.925E-07 2.029E-07
-----C-----
C
C  Code      : run_adas310
C  Producer   : Alessandra Giunta
C  Date       : 27/05/13
C
C-----

```

3.3 Demo (c-2) IDL procedure

```
pro demo_c_2
;Use run_adas312.pro to make an adf22 (Beam emission coefficients)
;from an adf26 for H+1 and C+6

;Define ion features: H+1, C+6
z_list = [1, 6]
n_list = ['h1', 'c6']

for j = 0, n_elements(z_list)-1 do begin
    run_adas312, adf26='adf26_'+n_list[j]+'\.pass', nlow=2, nup=3,$
        outfile='./bme10#h/bme10#h_' + n_list[j] + '.dat'
endfor

end
```

3.4 Demo (c-2) datasets

3.4.1 /bme10#h/bme10#h.h1.dat

```
1 /ECREF=3.647E-09 /SPEC=H /DATE=27/05/13 /CODE=ADAS312
-----
25   24 /TREF=2.000E+03
-----
5.000E+03 1.000E+04 1.500E+04 2.000E+04 2.500E+04 3.000E+04 3.500E+04 4.000E+04
4.500E+04 5.000E+04 5.500E+04 6.000E+04 6.500E+04 7.000E+04 7.500E+04 8.000E+04
8.500E+04 9.000E+04 9.500E+04 1.000E+05 1.050E+05 1.100E+05 1.150E+05 1.200E+05
1.250E+05
1.000E+08 2.720E+08 7.410E+08 2.020E+09 5.480E+09 1.490E+10 4.060E+10 1.110E+11
3.010E+11 8.190E+11 2.230E+12 6.060E+12 1.650E+13 4.490E+13 1.220E+14 3.320E+14
9.050E+14 2.460E+15 6.700E+15 1.820E+16 4.960E+16 1.350E+17 3.670E+17 1.000E+18
-----
2.304E-09 2.677E-09 3.080E-09 3.475E-09 3.838E-09 4.161E-09 4.443E-09 4.684E-09
4.890E-09 5.063E-09 5.208E-09 5.327E-09 5.426E-09 5.507E-09 5.574E-09 5.628E-09
5.673E-09 5.710E-09 5.739E-09 5.763E-09 5.782E-09 5.797E-09 5.808E-09 5.817E-09
5.824E-09
2.298E-09 2.671E-09 3.073E-09 3.468E-09 3.832E-09 4.155E-09 4.437E-09 4.678E-09
4.885E-09 5.058E-09 5.203E-09 5.321E-09 5.421E-09 5.502E-09 5.569E-09 5.624E-09
5.668E-09 5.705E-09 5.734E-09 5.758E-09 5.778E-09 5.792E-09 5.804E-09 5.813E-09
5.819E-09
2.288E-09 2.661E-09 3.063E-09 3.458E-09 3.822E-09 4.146E-09 4.428E-09 4.670E-09
4.876E-09 5.050E-09 5.195E-09 5.314E-09 5.414E-09 5.495E-09 5.561E-09 5.617E-09
5.661E-09 5.698E-09 5.728E-09 5.752E-09 5.771E-09 5.786E-09 5.797E-09 5.806E-09
5.812E-09
2.273E-09 2.646E-09 3.048E-09 3.444E-09 3.808E-09 4.132E-09 4.415E-09 4.657E-09
4.864E-09 5.038E-09 5.183E-09 5.303E-09 5.403E-09 5.484E-09 5.551E-09 5.606E-09
5.651E-09 5.688E-09 5.718E-09 5.742E-09 5.762E-09 5.777E-09 5.788E-09 5.797E-09
5.804E-09
2.254E-09 2.626E-09 3.028E-09 3.423E-09 3.787E-09 4.112E-09 4.396E-09 4.638E-09
4.846E-09 5.021E-09 5.167E-09 5.287E-09 5.388E-09 5.469E-09 5.537E-09 5.592E-09
5.637E-09 5.675E-09 5.705E-09 5.729E-09 5.749E-09 5.764E-09 5.775E-09 5.785E-09
5.791E-09
2.228E-09 2.599E-09 2.999E-09 3.393E-09 3.758E-09 4.083E-09 4.367E-09 4.611E-09
4.820E-09 4.995E-09 5.142E-09 5.263E-09 5.365E-09 5.447E-09 5.515E-09 5.571E-09
5.617E-09 5.655E-09 5.685E-09 5.710E-09 5.730E-09 5.745E-09 5.757E-09 5.766E-09
5.773E-09
2.193E-09 2.558E-09 2.955E-09 3.347E-09 3.710E-09 4.035E-09 4.320E-09 4.565E-09
4.776E-09 4.953E-09 5.102E-09 5.224E-09 5.327E-09 5.411E-09 5.480E-09 5.537E-09
5.583E-09 5.622E-09 5.653E-09 5.679E-09 5.699E-09 5.715E-09 5.727E-09 5.737E-09
5.744E-09
2.141E-09 2.496E-09 2.884E-09 3.270E-09 3.629E-09 3.953E-09 4.238E-09 4.484E-09
4.697E-09 4.876E-09 5.027E-09 5.152E-09 5.257E-09 5.343E-09 5.414E-09 5.473E-09
5.521E-09 5.561E-09 5.593E-09 5.620E-09 5.642E-09 5.659E-09 5.672E-09 5.683E-09
```

5.691E-09
 2.062E-09 2.396E-09 2.767E-09 3.139E-09 3.490E-09 3.809E-09 4.092E-09 4.339E-09
 4.553E-09 4.735E-09 4.889E-09 5.017E-09 5.125E-09 5.214E-09 5.288E-09 5.350E-09
 5.400E-09 5.443E-09 5.478E-09 5.506E-09 5.530E-09 5.548E-09 5.563E-09 5.576E-09
 5.585E-09
 1.931E-09 2.227E-09 2.566E-09 2.912E-09 3.245E-09 3.553E-09 3.831E-09 4.076E-09
 4.292E-09 4.476E-09 4.634E-09 4.766E-09 4.878E-09 4.972E-09 5.050E-09 5.116E-09
 5.170E-09 5.217E-09 5.255E-09 5.287E-09 5.313E-09 5.335E-09 5.353E-09 5.367E-09
 5.379E-09
 1.707E-09 1.938E-09 2.219E-09 2.520E-09 2.818E-09 3.104E-09 3.369E-09 3.608E-09
 3.822E-09 4.008E-09 4.169E-09 4.306E-09 4.424E-09 4.523E-09 4.607E-09 4.679E-09
 4.739E-09 4.791E-09 4.835E-09 4.872E-09 4.903E-09 4.929E-09 4.951E-09 4.970E-09
 4.986E-09
 1.345E-09 1.483E-09 1.681E-09 1.909E-09 2.150E-09 2.392E-09 2.627E-09 2.846E-09
 3.048E-09 3.229E-09 3.388E-09 3.526E-09 3.647E-09 3.751E-09 3.840E-09 3.918E-09
 3.984E-09 4.042E-09 4.092E-09 4.136E-09 4.173E-09 4.205E-09 4.233E-09 4.257E-09
 4.278E-09
 8.827E-10 9.378E-10 1.051E-09 1.196E-09 1.361E-09 1.537E-09 1.716E-09 1.891E-09
 2.057E-09 2.211E-09 2.349E-09 2.473E-09 2.583E-09 2.680E-09 2.765E-09 2.840E-09
 2.906E-09 2.965E-09 3.016E-09 3.061E-09 3.101E-09 3.136E-09 3.167E-09 3.195E-09
 3.219E-09
 4.841E-10 5.014E-10 5.597E-10 6.416E-10 7.400E-10 8.495E-10 9.658E-10 1.083E-09
 1.199E-09 1.308E-09 1.409E-09 1.501E-09 1.584E-09 1.658E-09 1.725E-09 1.785E-09
 1.838E-09 1.886E-09 1.929E-09 1.967E-09 2.001E-09 2.032E-09 2.058E-09 2.083E-09
 2.104E-09
 2.424E-10 2.480E-10 2.773E-10 3.210E-10 3.754E-10 4.383E-10 5.074E-10 5.793E-10
 6.514E-10 7.211E-10 7.865E-10 8.470E-10 9.024E-10 9.528E-10 9.985E-10 1.040E-09
 1.077E-09 1.111E-09 1.142E-09 1.169E-09 1.193E-09 1.215E-09 1.234E-09 1.252E-09
 1.268E-09
 1.158E-10 1.165E-10 1.300E-10 1.513E-10 1.790E-10 2.121E-10 2.495E-10 2.895E-10
 3.305E-10 3.708E-10 4.093E-10 4.454E-10 4.788E-10 5.096E-10 5.377E-10 5.635E-10
 5.869E-10 6.082E-10 6.274E-10 6.448E-10 6.604E-10 6.745E-10 6.871E-10 6.985E-10
 7.088E-10
 5.113E-11 5.029E-11 5.572E-11 6.494E-11 7.734E-11 9.253E-11 1.101E-10 1.292E-10
 1.492E-10 1.692E-10 1.885E-10 2.068E-10 2.239E-10 2.398E-10 2.544E-10 2.680E-10
 2.804E-10 2.917E-10 3.020E-10 3.114E-10 3.199E-10 3.275E-10 3.345E-10 3.408E-10
 3.465E-10
 2.074E-11 2.008E-11 2.212E-11 2.578E-11 3.079E-11 3.702E-11 4.431E-11 5.233E-11
 6.079E-11 6.932E-11 7.763E-11 8.557E-11 9.304E-11 1.000E-10 1.065E-10 1.125E-10
 1.180E-10 1.231E-10 1.277E-10 1.319E-10 1.358E-10 1.393E-10 1.424E-10 1.453E-10
 1.479E-10
 7.946E-12 7.630E-12 8.384E-12 9.767E-12 1.168E-11 1.407E-11 1.689E-11 2.000E-11
 2.330E-11 2.663E-11 2.990E-11 3.302E-11 3.597E-11 3.874E-11 4.131E-11 4.369E-11
 4.589E-11 4.792E-11 4.978E-11 5.148E-11 5.302E-11 5.442E-11 5.570E-11 5.687E-11
 5.794E-11
 2.974E-12 2.847E-12 3.124E-12 3.640E-12 4.355E-12 5.250E-12 6.307E-12 7.477E-12
 8.719E-12 9.978E-12 1.121E-11 1.239E-11 1.351E-11 1.456E-11 1.553E-11 1.644E-11
 1.728E-11 1.805E-11 1.876E-11 1.940E-11 1.999E-11 2.053E-11 2.102E-11 2.146E-11
 2.187E-11
 1.098E-12 1.050E-12 1.152E-12 1.342E-12 1.605E-12 1.936E-12 2.327E-12 2.760E-12
 3.219E-12 3.685E-12 4.142E-12 4.581E-12 4.995E-12 5.384E-12 5.746E-12 6.083E-12
 6.394E-12 6.681E-12 6.944E-12 7.184E-12 7.403E-12 7.603E-12 7.784E-12 7.951E-12
 8.103E-12
 4.045E-13 3.864E-13 4.239E-13 4.937E-13 5.909E-13 7.127E-13 8.566E-13 1.016E-12
 1.185E-12 1.357E-12 1.526E-12 1.688E-12 1.840E-12 1.984E-12 2.117E-12 2.242E-12
 2.357E-12 2.462E-12 2.560E-12 2.648E-12 2.729E-12 2.803E-12 2.870E-12 2.931E-12
 2.988E-12
 1.489E-13 1.422E-13 1.560E-13 1.817E-13 2.175E-13 2.623E-13 3.153E-13 3.741E-13
 4.364E-13 4.997E-13 5.618E-13 6.214E-13 6.777E-13 7.305E-13 7.798E-13 8.256E-13
 8.679E-13 9.068E-13 9.427E-13 9.753E-13 1.005E-12 1.032E-12 1.057E-12 1.080E-12
 1.100E-12
 5.467E-14 5.222E-14 5.727E-14 6.671E-14 7.984E-14 9.630E-14 1.158E-13 1.373E-13
 1.602E-13 1.835E-13 2.062E-13 2.281E-13 2.488E-13 2.682E-13 2.863E-13 3.031E-13
 3.186E-13 3.330E-13 3.461E-13 3.581E-13 3.691E-13 3.790E-13 3.881E-13 3.964E-13
 4.040E-13

20 /EREF=6.500E+04 /NREF=6.060E+12

1.000E+02 2.000E+02 3.000E+02 5.000E+02 6.000E+02 7.000E+02 8.000E+02 8.966E+02
 1.000E+03 2.000E+03 3.000E+03 5.000E+03 6.000E+03 7.000E+03 8.000E+03 8.966E+03
 1.000E+04 2.000E+04 3.000E+04 5.000E+04

4.168E-09 4.242E-09 4.211E-09 4.108E-09 4.058E-09 4.012E-09 3.970E-09 3.933E-09
 3.895E-09 3.647E-09 3.510E-09 3.341E-09 3.284E-09 3.237E-09 3.198E-09 3.167E-09

```

3.138E-09 2.996E-09 2.957E-09 2.952E-09
-----
C
C
C ADAS file type : adf22 (bme)
C Source file    : adf26_h1.pass
C
C A-VALUE       : 4.413E+07 S-1
C
C
C CODE      : ADAS312
C PRODUCER  : Alessandra Giunta
C DATE      : 27/05/13
C
C
-----
```

3.4.2 /bme10#h/bme10#h_c6.dat

```

6 /ECREF=2.407E-09 /SPEC=C /DATE=27/05/13 /CODE=ADAS312
-----
25   24 /TREF=2.000E+03
-----
5.000E+03 1.000E+04 2.000E+04 2.500E+04 3.000E+04 3.500E+04 4.000E+04
4.500E+04 5.000E+04 5.500E+04 6.000E+04 6.500E+04 7.000E+04 7.500E+04 8.000E+04
8.500E+04 9.000E+04 9.500E+04 1.000E+05 1.050E+05 1.100E+05 1.150E+05 1.200E+05
1.250E+05
1.000E+08 2.720E+08 7.410E+08 2.020E+09 5.480E+09 1.490E+10 4.060E+10 1.110E+11
3.010E+11 8.190E+11 2.230E+12 6.060E+12 1.650E+13 4.490E+13 1.220E+14 3.320E+14
9.050E+14 2.460E+15 6.700E+15 1.820E+16 4.960E+16 1.350E+17 3.670E+17 1.000E+18
-----
1.923E-09 1.985E-09 2.036E-09 2.096E-09 2.216E-09 2.389E-09 2.609E-09 2.869E-09
3.150E-09 3.438E-09 3.721E-09 3.990E-09 4.257E-09 4.533E-09 4.818E-09 5.111E-09
5.406E-09 5.689E-09 5.950E-09 6.197E-09 6.439E-09 6.680E-09 6.920E-09 7.160E-09
7.400E-09
1.916E-09 1.978E-09 2.029E-09 2.089E-09 2.209E-09 2.382E-09 2.602E-09 2.863E-09
3.143E-09 3.431E-09 3.714E-09 3.983E-09 4.250E-09 4.526E-09 4.812E-09 5.105E-09
5.399E-09 5.682E-09 5.943E-09 6.190E-09 6.432E-09 6.673E-09 6.913E-09 7.153E-09
7.393E-09
1.906E-09 1.969E-09 2.020E-09 2.079E-09 2.200E-09 2.373E-09 2.593E-09 2.853E-09
3.134E-09 3.421E-09 3.705E-09 3.974E-09 4.241E-09 4.517E-09 4.802E-09 5.095E-09
5.390E-09 5.672E-09 5.934E-09 6.181E-09 6.423E-09 6.664E-09 6.904E-09 7.144E-09
7.384E-09
1.893E-09 1.956E-09 2.007E-09 2.067E-09 2.187E-09 2.361E-09 2.581E-09 2.841E-09
3.122E-09 3.409E-09 3.692E-09 3.961E-09 4.228E-09 4.504E-09 4.790E-09 5.083E-09
5.377E-09 5.660E-09 5.921E-09 6.168E-09 6.410E-09 6.651E-09 6.891E-09 7.131E-09
7.371E-09
1.874E-09 1.938E-09 1.990E-09 2.050E-09 2.171E-09 2.344E-09 2.564E-09 2.824E-09
3.105E-09 3.392E-09 3.675E-09 3.944E-09 4.211E-09 4.487E-09 4.772E-09 5.065E-09
5.359E-09 5.642E-09 5.903E-09 6.150E-09 6.392E-09 6.633E-09 6.873E-09 7.113E-09
7.352E-09
1.848E-09 1.914E-09 1.966E-09 2.026E-09 2.148E-09 2.321E-09 2.540E-09 2.800E-09
3.081E-09 3.368E-09 3.650E-09 3.919E-09 4.186E-09 4.461E-09 4.746E-09 5.038E-09
5.332E-09 5.614E-09 5.875E-09 6.122E-09 6.363E-09 6.603E-09 6.843E-09 7.083E-09
7.322E-09
1.812E-09 1.878E-09 1.931E-09 1.993E-09 2.114E-09 2.286E-09 2.506E-09 2.764E-09
3.044E-09 3.330E-09 3.611E-09 3.879E-09 4.144E-09 4.418E-09 4.702E-09 4.993E-09
5.285E-09 5.566E-09 5.826E-09 6.071E-09 6.311E-09 6.550E-09 6.789E-09 7.027E-09
7.265E-09
1.758E-09 1.823E-09 1.878E-09 1.941E-09 2.061E-09 2.233E-09 2.450E-09 2.706E-09
2.983E-09 3.266E-09 3.545E-09 3.809E-09 4.072E-09 4.342E-09 4.622E-09 4.916E-09
5.198E-09 5.475E-09 5.731E-09 5.972E-09 6.209E-09 6.445E-09 6.681E-09 6.916E-09
7.151E-09
1.674E-09 1.733E-09 1.793E-09 1.857E-09 1.976E-09 2.144E-09 2.357E-09 2.608E-09
2.878E-09 3.154E-09 3.425E-09 3.683E-09 3.939E-09 4.202E-09 4.474E-09 4.754E-09
5.034E-09 5.302E-09 5.550E-09 5.784E-09 6.014E-09 6.244E-09 6.472E-09 6.701E-09
6.929E-09
1.535E-09 1.577E-09 1.645E-09 1.713E-09 1.830E-09 1.990E-09 2.191E-09 2.429E-09
2.684E-09 2.944E-09 3.199E-09 3.441E-09 3.683E-09 3.931E-09 4.187E-09 4.449E-09
4.712E-09 4.963E-09 5.195E-09 5.414E-09 5.629E-09 5.844E-09 6.058E-09 6.273E-09
6.486E-09
1.305E-09 1.313E-09 1.390E-09 1.465E-09 1.574E-09 1.716E-09 1.893E-09 2.101E-09
2.324E-09 2.550E-09 2.772E-09 2.984E-09 3.196E-09 3.414E-09 3.638E-09 3.866E-09
```

```

4.093E-09 4.310E-09 4.510E-09 4.699E-09 4.886E-09 5.072E-09 5.258E-09 5.444E-09
5.629E-09
9.596E-10 9.304E-10 1.010E-09 1.085E-09 1.176E-09 1.286E-09 1.421E-09 1.579E-09
1.746E-09 1.915E-09 2.082E-09 2.244E-09 2.407E-09 2.574E-09 2.744E-09 2.916E-09
3.087E-09 3.249E-09 3.398E-09 3.540E-09 3.680E-09 3.821E-09 3.961E-09 4.101E-09
4.240E-09
5.736E-10 5.338E-10 5.964E-10 6.557E-10 7.189E-10 7.891E-10 8.732E-10 9.716E-10
1.076E-09 1.180E-09 1.284E-09 1.388E-09 1.492E-09 1.599E-09 1.708E-09 1.817E-09
1.924E-09 2.026E-09 2.121E-09 2.212E-09 2.301E-09 2.391E-09 2.480E-09 2.570E-09
2.659E-09
2.877E-10 2.590E-10 2.953E-10 3.314E-10 3.680E-10 4.066E-10 4.520E-10 5.049E-10
5.607E-10 6.172E-10 6.744E-10 7.323E-10 7.915E-10 8.519E-10 9.133E-10 9.746E-10
1.035E-09 1.093E-09 1.147E-09 1.200E-09 1.252E-09 1.304E-09 1.356E-09 1.408E-09
1.460E-09
1.337E-10 1.158E-10 1.323E-10 1.506E-10 1.696E-10 1.893E-10 2.123E-10 2.389E-10
2.671E-10 2.959E-10 3.254E-10 3.558E-10 3.869E-10 4.187E-10 4.511E-10 4.835E-10
5.155E-10 5.467E-10 5.767E-10 6.057E-10 6.342E-10 6.625E-10 6.909E-10 7.193E-10
7.480E-10
6.028E-11 4.895E-11 5.525E-11 6.334E-11 7.215E-11 8.145E-11 9.225E-11 1.047E-10
1.180E-10 1.317E-10 1.457E-10 1.602E-10 1.751E-10 1.903E-10 2.058E-10 2.213E-10
2.368E-10 2.520E-10 2.667E-10 2.811E-10 2.951E-10 3.090E-10 3.229E-10 3.368E-10
3.510E-10
2.566E-11 1.949E-11 2.169E-11 2.494E-11 2.862E-11 3.255E-11 3.713E-11 4.240E-11
4.805E-11 5.387E-11 5.985E-11 6.604E-11 7.237E-11 7.881E-11 8.538E-11 9.201E-11
9.862E-11 1.051E-10 1.115E-10 1.177E-10 1.237E-10 1.297E-10 1.357E-10 1.417E-10
1.478E-10
1.022E-11 7.449E-12 8.222E-12 9.463E-12 1.089E-11 1.244E-11 1.423E-11 1.631E-11
1.853E-11 2.083E-11 2.318E-11 2.561E-11 2.810E-11 3.063E-11 3.322E-11 3.582E-11
3.843E-11 4.100E-11 4.351E-11 4.595E-11 4.834E-11 5.070E-11 5.305E-11 5.543E-11
5.786E-11
3.887E-12 2.777E-12 3.055E-12 3.517E-12 4.055E-12 4.636E-12 5.314E-12 6.096E-12
6.936E-12 7.802E-12 8.690E-12 9.608E-12 1.055E-11 1.150E-11 1.247E-11 1.346E-11
1.444E-11 1.541E-11 1.636E-11 1.728E-11 1.818E-11 1.907E-11 1.996E-11 2.086E-11
2.178E-11
1.451E-12 1.029E-12 1.130E-12 1.301E-12 1.500E-12 1.716E-12 1.968E-12 2.259E-12
2.572E-12 2.894E-12 3.224E-12 3.566E-12 3.914E-12 4.269E-12 4.631E-12 4.997E-12
5.362E-12 5.723E-12 6.076E-12 6.420E-12 6.755E-12 7.086E-12 7.417E-12 7.751E-12
8.093E-12
5.351E-13 3.782E-13 4.152E-13 4.781E-13 5.516E-13 6.311E-13 7.240E-13 8.311E-13
9.463E-13 1.065E-12 1.187E-12 1.312E-12 1.441E-12 1.571E-12 1.705E-12 1.839E-12
1.974E-12 2.107E-12 2.237E-12 2.364E-12 2.487E-12 2.609E-12 2.731E-12 2.854E-12
2.980E-12
1.970E-13 1.391E-13 1.526E-13 1.758E-13 2.028E-13 2.321E-13 2.662E-13 3.056E-13
3.480E-13 3.917E-13 4.365E-13 4.827E-13 5.300E-13 5.780E-13 6.270E-13 6.766E-13
7.261E-13 7.751E-13 8.230E-13 8.695E-13 9.150E-13 9.599E-13 1.005E-12 1.050E-12
1.096E-12
7.251E-14 5.117E-14 5.616E-14 6.467E-14 7.461E-14 8.538E-14 9.796E-14 1.125E-13
1.281E-13 1.441E-13 1.606E-13 1.776E-13 1.950E-13 2.127E-13 2.308E-13 2.490E-13
2.672E-13 2.852E-13 3.029E-13 3.200E-13 3.367E-13 3.532E-13 3.697E-13 3.864E-13
4.035E-13
2.662E-14 1.878E-14 2.061E-14 2.374E-14 2.739E-14 3.134E-14 3.596E-14 4.128E-14
4.700E-14 5.290E-14 5.895E-14 6.520E-14 7.159E-14 7.807E-14 8.470E-14 9.140E-14
9.809E-14 1.047E-13 1.112E-13 1.175E-13 1.236E-13 1.297E-13 1.357E-13 1.418E-13
1.481E-13
-----
20 /EREF=6.500E+04 /NREF=6.060E+12
-----
1.000E+02 2.000E+02 3.000E+02 5.000E+02 6.000E+02 7.000E+02 8.000E+02 8.966E+02
1.000E+03 2.000E+03 3.000E+03 5.000E+03 6.000E+03 7.000E+03 8.000E+03 8.966E+03
1.000E+04 2.000E+04 3.000E+04 5.000E+04
-----
2.894E-09 2.929E-09 2.889E-09 2.791E-09 2.746E-09 2.706E-09 2.670E-09 2.637E-09
2.606E-09 2.407E-09 2.307E-09 2.192E-09 2.155E-09 2.125E-09 2.101E-09 2.082E-09
2.065E-09 1.981E-09 1.960E-09 1.970E-09
-----
C
C
C ADAS file type : adf22 (bme)
C Source file   : adf26_c6.pass
C
C A-VALUE      : 4.413E+07 S-1
C
C
C
```

C CODE : ADAS312
C PRODUCER : Alessandra Giunta
C DATE : 27/05/13
C-----

3.5 Demo (c-3) procedure

```
pro demo_c_3
;Use read_adf22.pro to read beam emission coefficients.
;Use read_adf21.pro to read beam stopping coefficient (adf21.pass).
;Plot the D-alpha emission coefficients in a pure D+ and pure C6+ plasma

;Conditions

ieval=50
te=2000.0
energy=adas_vector(low=1e3, high=1e5, num=ieval)
dens=[1e8, 1e12, 1e15]
idval =n_elements(dens)

file_d='./bme10#h/bme10#h_h1.dat'
file_c='./bme10#h/bme10#h_c6.dat'

;Read data at fixed Te, for different densities s a function of beam energy
data_d = fltarr(ieval,idval)
data_c = fltarr(ieval,idval)

for id=0,idval-1 do begin

    read_adf22, files=file_d, fraction=[1.0], te=fltarr(ieval)+te,      $
        dens=fltarr(ieval) + dens[id], energy=energy, data=tmp
    data_d[*,id] = tmp

    read_adf22, files=file_c, fraction=[1.0], te=fltarr(ieval)+te,      $
        dens=fltarr(ieval) + dens[id], energy=energy, data=tmp
    data_c[*,id] = tmp
endfor

;Plot D and C side by side with same y-axis
set_plot,'ps'
device, /isolatin1, font_index=8
device, bits=8, filename='demo_c_3_emission.ps',           $
    font_size = 14, xsize=20.0, ysize=16.0, $ 
    yoffset=7.0, /color
device, /helvetica

energy_kev = energy / 1000.0

xmin=1
xmax=100
ymin=0
ymax=6
```

```

plot_oi, [xmin, xmax], [ymin, ymax], /nodata, ystyle=1, $
    position=[0.07, 0.09, 0.5, 0.95], $
    title='D!u+!n plasma', $
    xtitle = 'Beam Energy (keV/amu)', $
    ytitle = 'D!7a!3 emission coefficient (10!u-9!n ph cm!u3!n s!u-1!n)'

for id = 0, idval-1 do oplot, energy_kev, data_d[*,id]/1e-9, line=id

plots,[1.3,3.],[5.7,5.7]
xyouts,3.1,5.7,'10!u8!n cm!u-3!n'
plots,[1.3,3.],[5.3,5.3],line=1
xyouts,3.1,5.3,'10!u12!n cm!u-3!n'
plots,[1.3,3.],[4.9,4.9],line=2
xyouts,3.1,4.9,'10!u14!n cm!u-3!n'

plot_oi, [xmin, xmax], [ymin, ymax], /nodata, ystyle=1, $
    title='C!u6+!n plasma', $
    position=[0.55, 0.09, 0.95, 0.95], /noerase, $
    xtitle = 'Beam Energy (keV/amu)'

for id = 0, idval-1 do oplot, energy_kev, data_c[*,id]/1e-9, line=id

device, /close
set_plot,'X'
!p.font=-1

;Use read_adf21.pro to read adf21.pass produced in demo_d_1 and
;compare pure D+1 and D+1 + 2% of C6+
idval = 24
ieval = 20
te = 2000.0
dens = adas_vector(low=1e12, high=1e15, num=idval)
energy = adas_vector(low=5e3, high=1.2e5, num=ieval)
files = ['adf21_h1.pass', $
          'adf21_c6.pass' ]

data_d = fltarr(ieval, idval)
data_dc = fltarr(ieval, idval)

for id = 0, idval-1 do begin
    ; D+ only
    read_adf21, files=files[0], fraction=[1.0], te=fltarr(ieval)+te,      $
        dens=fltarr(ieval) + dens[id], energy=energy, data=tmp
    data_d[*,id] = tmp

```

```

; D+ and C6+
read_adf21, files=files, fraction=[0.98, 0.02], te=fltarr(ieval)+te, $
    dens=fltarr(ieval) + dens[id], energy=energy, data=tmp
data_dc[*,id] = tmp

endfor

energy_kev =energy/1000.0
loadct,3

;Plot total beam stopping coefficient as a function of energy and
;density
;for pure D1+ and D1+ and 2% C6+
set_plot,'ps'
device, /isolatin1, font_index=8
device, bits=8, filename='demo_c_3_stopping.ps',           $
    font_size = 14, xsize=20.0, ysize=16.0, $                \
    yoffset=7.0, /color
device, /helvetica

surface, data_d, energy_kev, dens, /ylog,charsize=1.3,color=120,$
    xrange=[5,120], yrangle=[1e12, 1e15], zrange=[6e-8,1.6e-7],$ \
    xtitle='log(Beam energy) (keV/amu)', $                   \
    ytitle='log(Density) (cm!u-3!n s!u-1!n)', $             \
    ztitle = 'Stopping coefficient (cm!u3!n s!u-1!n)'

surface, data_dc, energy_kev, dens, /ylog,charsize=1.3,/noerase,$
    xrange=[5,120], yrangle=[1e12, 1e15], zrange=[6e-8,1.6e-7],$ \
    xtitle='log(Beam energy) (keV/amu)', $                   \
    ytitle='log(Density) (cm!u-3!n s!u-1!n)', $             \
    ztitle = 'Stopping coefficient (cm!u3!n s!u-1!n)'

xyouts,0.7,0.9,'D!u1+!n only',color=120,/normal
xyouts,0.7,0.85,'D!u1+!n and 2% C!u6+!n',/normal

device, /close
set_plot,'X'
!p.font=-1

end

```

3.6 Demo (c-3) Figures

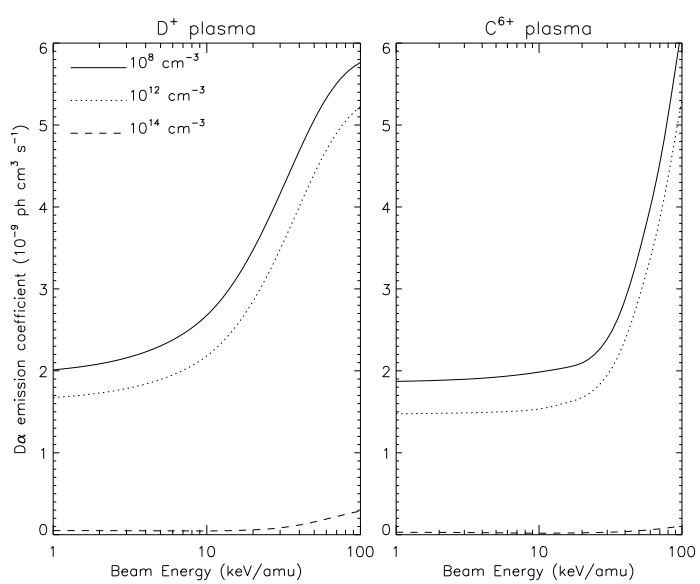


Figure 13: demo_c/demo_c_3_emission.pdf

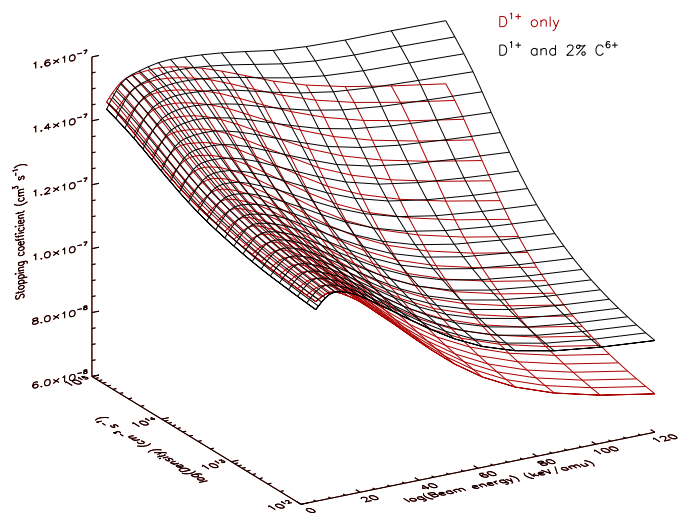


Figure 14: demo_c/demo_c_3_stopping.pdf

4 Demo (d) Looking at Stark multiplet emission for the H-beam

DEMO D: Looking at Stark multiplet emission for the H-beam

PURPOSE: Look at the hydrogen Stark feature as components and as a Doppler broadened feature.

EXAMPLE: For this demo a deuterium beam and a deuterium plasma are considered.

Beam details are the following:

H beam mass (deuterium): 2.0

Energy: 78.0e3e V/amu

Temperature: 10.0 eV

Density: 1.00e10 cm⁻³

Direction cosines for velocity components: x = 0.0, y = 0.0, z = 1.0

Plasma details are the following:

H plasma mass (deuterium): 2.0

Temperature: 4440.0 eV

Density: 2.49e13 cm⁻³

Effective charge: 2.0

Magnetic field details are the following:

Value: 3.3915 Tesla

Direction cosines for components: x = 0.788, y = 0.788, z = 0.0

Electric field details are the following:

Value: 0.0000 Volts

Direction cosines for components: x = 1.000, y = 1.000, z = 0.0

Viewing line of sight details are the following:

Direction cosines for components: x = 0.8701, y = -0.047, z = 0.4905

Specific sigma polarisation: 1.0

Specific pi polarisation: 1.0

H Balmer alpha line is chosen:

n_lower=2

n_upper=3

DEMO d1: Working offline with adas305_get_stark.pro

1. Define beam, plasma, magnetic, electric and observed line of sight details.

2. Use adas305_get_stark.pro to get Stark and Doppler-broadened features for D(n=3-2).

3. Plot Stark line emission and Doppler broadening.

Program: demo_d.pro

Output file: demo_d.ps

4.1 Demo (d-1) procedure

```

pro demo_d
;Use adas305_get_stark.pro to calculate the D(n=3-2) Stark manifold.

;Set all parameters

;Beam details: H beam mass -> 2 for deuterium; energy in eV/amu, te in eV,
;density in cm-3, dc_X,dc_y,dc_z are velocity component directions
beam = {mass : 2.0, energy : 78.0e3, te : 10.0, density : 1.00e10, $
        dc_x : 0.0, dc_y : 0.0, dc_z : 1.0}

;Plasma details
plasma = {mass : 2.0, te : 4440.0, density : 2.49e13, zeff : 2.0}

;Magnetic field details
bfield = {value : 3.3915, dc_x : 0.788, dc_y : 0.788, dc_z : 0.0}

;Electric field details
efield = {value : 0.0000, dc_x : 1.000, dc_y : 1.0000, dc_z : 0.0000}

;Viewing line of sight details
obs = {dc_x : 0.8701, dc_y : -0.047, dc_z : 0.4905, sigma : 1.0, pi : 1.0}

;Number of pixels
npix = 360

;Use adas305_get_stark.pro to get the wavelength components of stark feature
;together with the associated emission and the emission Doppler-bradened on to
;the wavelength grid
adas305_get_stark, beam      = beam,      $
plasma       = plasma,      $
bfield        = bfield,      $
efield        = efield,      $
obs          = obs,          $
n_lower      = 2,           $
n_upper      = 3,           $
wave_comp    = wave_comp,   $
emiss_comp   = emiss_comp,  $
wave_min     = wave_min,   $
wave_max     = wave_max,   $
npix         = npix,         $
adf22        = adf22,        $
emiss_doppler = emiss_doppler, $
wave_doppler  = wave_doppler, $
/doppler,/auto_wave

;Plot Stark line emission and Doppler broadening for D(n=3-2)
loadct,3
set_plot,'ps'
device, /isolatin1, font_index=8
device, bits=8, filename='demo_d.ps',           $
font_size = 14, xsize=18.0, ysize=16.0, $           $
yoffset=7.0, /color
device, /helvetica

plot, wave_comp, emiss_comp,/nodata, $
title='Beam Balmer 17a!3 Stark manifold',xmargin=[12,3],$           $
xtitle='Wavelength (A)', $           $
ytitle = 'Intensity /ion (Photon cm!u-2!n s!u-1!n)'
for i = 0, n_elements(wave_comp)-1 do oplot,[wave_comp[i],wave_comp[i]], [0,emiss_comp[i]]
plots, wave_doppler, emiss_doppler,color=120

xyouts,6524.,8.e12,'Stark emission components'
xyouts,6520.,1.le13,'Doppler-broadened emission',color=120

device, /close
set_plot,'X'
```

```
!p.font=-1
```

```
end
```

4.2 Demo(d-1) Figures

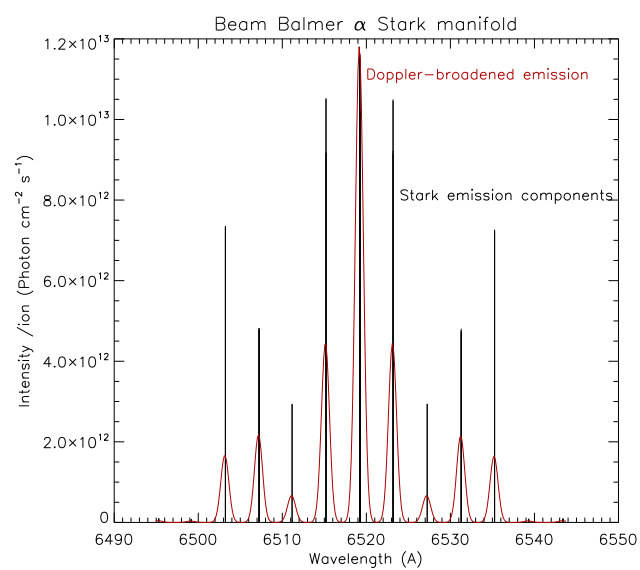


Figure 15: demo_d/demo_d.pdf

C.6 module_6

MODULE 6

Advanced charge exchange plasma receiver and beam donor modelling - the current state.

Demonstration script

Hugh Summers, Martin O'Mullane and Alessandra Giunta

September 29, 2013

Contents

| | |
|--|-----------|
| 1 Demo (a) Using universal charge exchange cross-section data | 3 |
| 1.1 Demo (a) IDL procedures | 4 |
| 1.1.1 Demo (a-2) demo_a_2.pro | 4 |
| 1.2 Demo (a) Tables and datasets | 4 |
| 1.2.1 Demo (a-1) demo_d/adf01_w51_interactive.pass | 4 |
| 1.2.2 Demo (a-1) demo_d/adf01_w51_interactive.pass | 5 |
| 2 Demo (b) Obtaining charge exchange driven 'bn' populations and emissivities | 8 |
| 2.1 Demo (b) Figures | 9 |
| 2.1.1 Demo (b-2) demo_b/adas316_plot_w61.pdf | 9 |
| 2.2 Demo (b) Tables and datasets | 10 |
| 2.2.1 Demo (b-1) demo_b/adf25_bn#74_w61_n1.dat | 10 |
| 2.2.2 Demo (b-1) demo_b/w61_n1.dat | 11 |
| 2.2.3 Demo (b-2) demo_b/adas316_adf12.pass | 12 |
| 2.2.4 Demo (b-2) demo_b/adas316_adf40.pass | 13 |
| 3 Demo (c) Comparing active W emission to bremsstrahlung background | 16 |
| 3.1 Demo (c) Figures | 18 |
| 3.1.1 Demo (c-1) demo_c/demo_c_1_frac.pdf | 18 |
| 3.1.2 Demo (c-1) demo_c/demo_c_1_temp_dens.pdf | 19 |
| 3.1.3 Demo (c-3) demo_c/demo_c_3_active.pdf | 20 |
| 3.1.4 Demo (c-3) demo_c/demo_c_3_compare.pdf | 21 |
| 3.2 Demo (c) IDL procedures | 22 |
| 3.2.1 Demo (c-1) demo_c_1.pro | 22 |
| 3.2.2 Demo (c-2) demo_c_2.pro | 24 |
| 3.2.3 Demo (c-3) demo_c_3.pro | 26 |

| | | |
|----------|--|-----------|
| 4 | Demo (d) Looking at Stark multiplet emission for the H-beam | 30 |
| 4.1 | Demo (d) Figures | 31 |
| 4.1.1 | Demo (d-1) demo_d/demo_d.pdf | 31 |
| 4.2 | Demo (d) IDL procedures | 32 |
| 4.2.1 | Demo (d-1) demo_d/demo_d.pro | 32 |

1 Demo (a) Using universal charge exchange cross-section data

DEMO A: Using universal charge exchange cross-section data

PURPOSE: To prepare an adf01 data file for a specific ion from universal z-scaled charge exchange (CX) cross-section data, collected in the adf49 data format.

The adf01 data files provide state selective CX data.

The adf49 data files give, at the present, the universal scaled CX cross-section for H(n=1) and H(n=2) donors

EXAMPLE: This demo shows how to produce an adf01 from the universal scaled CX data for W51+ with H(n=1) donor.

This can be done using either ADAS315 interactively or run_adas315.pro from the IDL command line.

The adf49 input file is /home/adas/adas/adf49/arf07#h0_n1.dat.

The element chosen is Tungsten: iz0=74

The ionisation stage W51+: iz1=51

DEMO a1: Extract adf01 data for an ion from adf49
with interactive ADAS315

1. Use ADAS315 interactively.

Sample of output file: adf01_w51_interactive.pass

DEMO a2: Extract adf01 using run_adas315.pro

1. Define iz0 and iz1.

2. Define the adf49 for H(n=1) as donor.

3. Use run_adas315.pro to produce the adf01.

Program: demo_a_2.pro

Sample of output file: adf01_w51.pass

1.1 Demo (a) IDL procedures

1.1.1 Demo (a-2) demo_a_2.pro

Use IDL procedure *run_adas315.pro* for tungsten.

```
pro demo_a_2
;Use run_adas315.pro for W, receiver z0=74, donor z1=51
iz0=74
iz1=51

adf49='/home/adas/adas/adf49/arf07#h0_n1.dat'

;Define energy array in eV/amu
energy=adas_vector(low=0.01e3,high=100.e3,num=20)

;Use run_adas315.pro
run_adas315,iz0=iz0,iz1=iz1,energy=energy,adf49=adf49,adf01='adf01_w51.pass'
end
```

1.2 Demo (a) Tables and datasets

1.2.1 Demo (a-1) demo_d/adf01_w51.interactive.pass

```
W +51      H + 0 (1) / receiver, donor (donor state index) /      /
9          / number of energies
17         / nmin
40         / nmax
          0.01    0.02    0.05    0.10    0.20    0.50    1.00    2.00    5.00 / energies      (keV/amu)
          80.90   58.62   45.27   31.04   14.88   9.94   19.34   16.68   11.76 / alpha
4.97E-14 4.97E-14 4.97E-14 4.97E-14 4.97E-14 4.97E-14 4.97E-14 4.97E-14 / total xsects. (cm2)
                                         / partial xsects. (cm2)
n 1 m
17 3.85E-16 3.23E-16 3.75E-16 5.08E-16 6.57E-16 9.25E-16 1.22E-15 1.60E-15 2.59E-15
18 2.56E-15 2.39E-15 2.55E-15 2.89E-15 3.20E-15 3.77E-15 4.37E-15 4.75E-15 5.73E-15
19 7.90E-15 7.64E-15 7.67E-15 7.85E-15 7.96E-15 8.28E-15 8.59E-15 8.42E-15 8.39E-15
20 1.30E-14 1.27E-14 1.23E-14 1.20E-14 1.17E-14 1.11E-14 1.06E-14 1.00E-14 9.11E-15
21 1.32E-14 1.30E-14 1.25E-14 1.21E-14 1.16E-14 1.08E-14 1.01E-14 9.47E-15 8.33E-15
22 8.67E-15 9.03E-15 9.03E-15 8.77E-15 8.51E-15 8.10E-15 7.73E-15 7.41E-15 6.56E-15
23 3.29E-15 3.72E-15 4.07E-15 4.18E-15 4.31E-15 4.48E-15 4.59E-15 4.72E-15 4.47E-15
24 6.30E-16 7.87E-16 1.01E-15 1.18E-15 1.40E-15 1.67E-15 1.85E-15 2.22E-15 2.51E-15
25 5.57E-17 7.66E-17 1.25E-16 1.84E-16 2.72E-16 3.95E-16 4.77E-16 7.49E-16 1.14E-15
26 2.58E-18 4.18E-18 9.45E-18 1.86E-17 3.63E-17 6.78E-17 9.08E-17 2.00E-16 4.56E-16
27 1.05E-19 2.73E-19 9.28E-19 2.26E-18 5.87E-18 1.21E-17 1.54E-17 4.93E-17 1.75E-16
28 4.96E-21 2.99E-20 1.68E-19 4.51E-19 1.45E-18 2.83E-18 3.04E-18 1.36E-17 7.27E-17
29 2.62E-22 3.54E-21 3.24E-20 1.27E-19 4.25E-19 8.67E-19 8.55E-19 4.93E-18 3.58E-17
30 1.53E-23 4.53E-22 6.62E-21 4.27E-20 1.49E-19 3.59E-19 3.99E-19 2.57E-18 2.21E-17
31 9.86E-25 6.21E-23 1.43E-21 1.49E-20 8.07E-20 2.18E-19 2.85E-19 1.83E-18 1.63E-17
32 6.95E-26 9.08E-24 3.23E-22 5.39E-21 5.91E-20 1.75E-19 2.54E-19 1.53E-18 1.29E-17
33 5.32E-27 1.41E-24 7.68E-23 2.01E-21 4.18E-20 1.37E-19 2.26E-19 1.28E-18 1.02E-17
34 4.42E-28 2.32E-25 1.91E-23 7.74E-22 2.64E-20 9.52E-20 1.71E-19 9.55E-19 7.52E-18
35 3.95E-29 4.04E-26 4.94E-24 3.06E-22 1.69E-20 5.23E-20 1.19E-19 6.66E-19 5.39E-18
36 3.78E-30 7.38E-27 1.33E-24 1.25E-22 1.10E-20 3.77E-20 8.37E-20 4.75E-19 3.92E-18
37 3.87E-31 1.42E-27 3.71E-25 5.20E-23 7.24E-21 2.85E-20 6.33E-20 3.58E-19 2.92E-18
38 4.22E-32 2.84E-28 1.07E-25 2.22E-23 4.82E-21 2.17E-20 4.88E-20 2.75E-19 2.20E-18
39 4.88E-33 5.95E-29 3.21E-26 9.70E-24 3.24E-21 1.66E-20 3.29E-20 1.85E-19 1.65E-18
40 5.97E-34 1.30E-29 9.92E-27 4.33E-24 2.20E-21 1.28E-20 1.99E-20 1.20E-19 1.21E-18
9          / number of energies
17         / nmin
40         / nmax
          10.00   15.00   20.00   25.00   30.00   35.00   40.00   45.00   50.00 / energies      (keV/amu)
          8.99    8.69   10.17   9.99    9.04    7.26    5.55    4.60    4.41 / alpha
4.97E-14 4.87E-14 4.70E-14 4.50E-14 4.39E-14 4.28E-14 4.13E-14 3.99E-14 3.81E-14 / total xsects. (cm2)
                                         / partial xsects. (cm2)
n 1 m
17 2.48E-15 2.26E-15 4.41E-16 4.18E-16 4.08E-16 3.98E-16 3.88E-16 3.92E-16 3.92E-16
```

```

18      4.88E-15 4.28E-15 9.51E-16 1.09E-15 1.00E-15 9.66E-16 9.27E-16 9.22E-16 9.01E-16
19      7.09E-15 6.19E-15 1.59E-15 1.78E-15 1.59E-15 1.53E-15 1.46E-15 1.43E-15 1.38E-15
20      8.01E-15 7.05E-15 2.28E-15 2.26E-15 2.02E-15 1.93E-15 1.85E-15 1.79E-15 1.69E-15
21      7.59E-15 6.82E-15 2.98E-15 2.69E-15 2.49E-15 2.29E-15 2.20E-15 2.10E-15 1.97E-15
22      6.40E-15 5.93E-15 3.67E-15 3.19E-15 2.86E-15 2.72E-15 2.60E-15 2.47E-15 2.30E-15
23      4.86E-15 4.74E-15 4.18E-15 3.63E-15 3.26E-15 3.08E-15 2.94E-15 2.78E-15 2.59E-15
24      3.31E-15 3.55E-15 4.38E-15 3.81E-15 3.43E-15 3.22E-15 3.06E-15 2.91E-15 2.72E-15
25      2.05E-15 2.51E-15 4.24E-15 3.70E-15 3.36E-15 3.13E-15 2.90E-15 2.74E-15 2.62E-15 2.48E-15
26      1.19E-15 1.70E-15 3.89E-15 3.41E-15 3.13E-15 2.90E-15 2.74E-15 2.62E-15 2.48E-15
27      6.65E-16 1.13E-15 3.44E-15 3.05E-15 2.86E-15 2.66E-15 2.50E-15 2.38E-15 2.25E-15
28      3.79E-16 7.54E-16 2.96E-15 2.69E-15 2.59E-15 2.42E-15 2.27E-15 2.15E-15 2.02E-15
29      2.30E-16 5.11E-16 2.51E-15 2.36E-15 2.34E-15 2.22E-15 2.07E-15 1.95E-15 1.83E-15
30      1.51E-16 3.56E-16 2.10E-15 2.06E-15 2.12E-15 2.04E-15 1.90E-15 1.79E-15 1.69E-15
31      1.07E-16 2.51E-15 1.73E-15 1.73E-15 1.79E-15 1.91E-15 1.87E-15 1.75E-15 1.66E-15 1.59E-15
32      7.89E-17 1.78E-16 1.41E-15 1.54E-15 1.71E-15 1.70E-15 1.61E-15 1.55E-15 1.49E-15
33      5.90E-17 1.27E-16 1.13E-15 1.32E-15 1.50E-15 1.52E-15 1.47E-15 1.43E-15 1.39E-15
34      4.40E-17 9.27E-17 8.91E-16 1.10E-15 1.29E-15 1.34E-15 1.33E-15 1.31E-15 1.28E-15
35      3.29E-17 6.92E-17 6.83E-16 8.98E-16 1.09E-15 1.17E-15 1.19E-15 1.18E-15 1.16E-15
36      2.47E-17 5.29E-17 5.09E-16 7.07E-16 9.05E-16 1.01E-15 1.05E-15 1.05E-15 1.05E-15
37      1.87E-17 4.09E-17 3.75E-16 5.43E-16 7.38E-16 8.60E-16 9.26E-16 9.47E-16 9.45E-16
38      1.43E-17 3.21E-17 2.77E-16 4.14E-16 5.93E-16 7.27E-16 8.08E-16 8.41E-16 8.46E-16
39      1.13E-17 2.57E-17 2.08E-16 3.17E-16 4.71E-16 6.07E-16 7.03E-16 7.47E-16 7.56E-16
40      8.95E-18 2.05E-17 1.60E-16 2.44E-16 3.72E-16 5.03E-16 6.09E-16 6.63E-16 6.74E-16
2          / number of energies
17          / nmin
40          / nmax
    75.00 100.00          / energies (keV/amu)
    2.58   2.17          / alpha
    2.87E-14 2.18E-14          / total xsects. (cm2)
          / partial xsects. (cm2)
n 1  m
17      3.31E-16 2.81E-16
18      6.85E-16 5.53E-16
19      9.79E-16 7.56E-16
20      1.17E-15 8.66E-16
21      1.36E-15 9.81E-16
22      1.62E-15 1.15E-15
23      1.86E-15 1.32E-15
24      1.96E-15 1.42E-15
25      1.91E-15 1.42E-15
26      1.78E-15 1.34E-15
27      1.63E-15 1.24E-15
28      1.49E-15 1.13E-15
29      1.38E-15 1.04E-15
30      1.29E-15 9.72E-16
31      1.22E-15 9.27E-16
32      1.16E-15 8.87E-16
33      1.09E-15 8.44E-16
34      1.02E-15 7.96E-16
35      9.49E-16 7.49E-16
36      8.82E-16 7.05E-16
37      8.20E-16 6.65E-16
38      7.64E-16 6.28E-16
39      7.14E-16 5.94E-16
40      6.67E-16 5.62E-16
-1      -1

```

1.2.2 Demo (a-1) demo_d/adf01_w51.interactive.pass

```

W +51      H + 0 (1) / receiver, donor (donor state index) / /
9          / number of energies
17          / nmin
40          / nmax
    0.01    0.02    0.03    0.04    0.07    0.11    0.18    0.30    0.48 / energies (keV/amu)
    80.90   64.40   52.44   46.21   44.07   31.01   14.98   14.09   9.98 / alpha
    4.97E-14 4.97E-14 4.97E-14 4.97E-14 4.97E-14 4.97E-14 4.97E-14 4.97E-14 4.97E-14 / total xsects. (cm2)
          / partial xsects. (cm2)
n 1  m
17      3.85E-16 3.33E-16 3.21E-16 3.54E-16 4.33E-16 5.32E-16 6.36E-16 7.64E-16 9.13E-16
18      2.56E-15 2.42E-15 2.38E-15 2.49E-15 2.71E-15 2.95E-15 3.16E-15 3.40E-15 3.75E-15
19      7.90E-15 7.70E-15 7.60E-15 7.63E-15 7.76E-15 7.88E-15 7.95E-15 8.03E-15 8.26E-15
20      1.30E-14 1.28E-14 1.26E-14 1.23E-14 1.21E-14 1.19E-14 1.17E-14 1.15E-14 1.12E-14
21      1.32E-14 1.31E-14 1.29E-14 1.26E-14 1.23E-14 1.20E-14 1.17E-14 1.13E-14 1.08E-14
22      8.67E-15 8.95E-15 9.10E-15 9.07E-15 8.91E-15 8.72E-15 8.54E-15 8.35E-15 8.12E-15
23      3.29E-15 3.60E-15 3.86E-15 4.03E-15 4.13E-15 4.20E-15 4.30E-15 4.39E-15 4.48E-15

```

```

24      6.30E-16 7.38E-16 8.54E-16 9.70E-16 1.09E-15 1.22E-15 1.37E-15 1.54E-15 1.66E-15
25      5.57E-17 6.94E-17 8.80E-17 1.14E-16 1.50E-16 1.96E-16 2.58E-16 3.39E-16 3.92E-16
26      2.58E-18 3.58E-18 5.22E-18 8.11E-18 1.31E-17 2.08E-17 3.31E-17 5.33E-17 6.72E-17
27      1.05E-19 2.05E-19 3.97E-19 7.57E-19 1.42E-18 2.64E-18 5.15E-18 9.87E-18 1.21E-17
28      4.96E-21 1.81E-20 5.49E-20 1.32E-19 2.70E-19 5.41E-19 1.23E-18 2.67E-18 2.87E-18
29      2.62E-22 1.74E-21 8.15E-21 2.47E-20 5.43E-20 1.55E-19 3.55E-19 8.55E-19 8.86E-19
30      1.53E-23 1.81E-22 1.29E-21 4.87E-21 1.16E-20 5.22E-20 1.23E-19 3.21E-19 3.65E-19
31      9.86E-25 2.04E-23 2.19E-22 1.02E-21 2.60E-21 1.82E-20 6.60E-20 1.77E-19 2.20E-19
32      6.95E-26 2.47E-24 3.92E-23 2.24E-22 6.13E-22 6.60E-21 4.85E-20 1.30E-19 1.75E-19
33      5.32E-27 3.20E-25 7.41E-24 5.15E-23 1.51E-22 2.47E-21 3.45E-20 9.19E-20 1.35E-19
34      4.42E-28 4.41E-26 1.48E-24 1.24E-23 3.90E-23 9.50E-22 2.17E-20 5.96E-20 9.37E-20
35      3.95E-29 6.45E-27 3.09E-25 3.13E-24 1.05E-23 3.76E-22 1.39E-20 3.91E-20 5.15E-20
36      3.78E-30 9.97E-28 6.75E-26 8.20E-25 2.91E-24 1.53E-22 9.00E-21 2.60E-20 3.72E-20
37      3.87E-31 1.62E-28 1.54E-26 2.23E-25 8.42E-25 6.39E-23 5.90E-21 1.75E-20 2.81E-20
38      4.22E-32 2.78E-29 3.66E-27 6.29E-26 2.52E-25 2.73E-23 3.92E-21 1.19E-20 2.13E-20
39      4.88E-33 4.99E-30 9.05E-28 1.83E-26 7.78E-26 1.20E-23 2.63E-21 8.16E-21 1.64E-20
40      5.97E-34 9.38E-31 2.32E-28 5.52E-27 2.48E-26 5.34E-24 1.78E-21 5.66E-21 1.26E-20
9          / number of energies
17          / nmin
40          / nmax
        0.78    1.27    2.07    3.36    5.46    8.86   14.38   23.36   37.93 / energies      (keV/amu)
        9.55   18.35   16.55   14.32   11.31   9.78   8.40   10.07   6.19 / alpha
        4.97E-14 4.97E-14 4.97E-14 4.97E-14 4.96E-14 4.88E-14 4.57E-14 4.19E-14 / total xsects. (cm2)
                                / partial xsects. (cm2)
n l m
17      1.10E-15 1.35E-15 1.62E-15 2.02E-15 2.65E-15 2.36E-15 2.42E-15 4.19E-16 3.90E-16
18      4.16E-15 4.54E-15 4.76E-15 5.15E-15 5.74E-15 4.84E-15 4.53E-15 1.12E-15 9.37E-16
19      8.53E-15 8.59E-15 8.41E-15 8.34E-15 8.32E-15 7.20E-15 6.41E-15 1.85E-15 1.48E-15
20      1.08E-14 1.04E-14 1.00E-14 9.53E-15 9.01E-15 8.20E-15 7.20E-15 2.36E-15 1.88E-15
21      1.03E-14 9.88E-15 9.44E-15 8.89E-15 8.23E-15 7.76E-15 6.90E-15 2.82E-15 2.24E-15
22      7.86E-15 7.60E-15 7.40E-15 7.05E-15 6.50E-15 6.53E-15 5.93E-15 3.35E-15 2.65E-15
23      4.55E-15 4.62E-15 4.73E-15 4.70E-15 4.47E-15 4.90E-15 4.68E-15 3.81E-15 2.99E-15
24      1.77E-15 1.95E-15 2.24E-15 2.46E-15 2.56E-15 3.28E-15 3.45E-15 3.99E-15 3.12E-15
25      4.35E-16 5.48E-16 7.66E-16 9.93E-16 1.21E-15 1.97E-15 2.39E-15 3.86E-15 3.02E-15
26      7.79E-17 1.16E-16 2.08E-16 3.36E-16 5.02E-16 1.09E-15 1.59E-15 3.53E-15 2.80E-15
27      1.28E-17 2.20E-17 5.23E-17 1.07E-16 2.02E-16 5.79E-16 1.03E-15 3.14E-15 2.55E-15
28      2.53E-18 4.75E-18 1.47E-17 3.72E-17 8.74E-17 3.15E-16 6.77E-16 2.74E-15 2.33E-15
29      7.07E-19 1.44E-18 5.37E-18 1.59E-17 4.43E-17 1.84E-16 4.54E-16 2.38E-15 2.13E-15
30      3.17E-19 6.99E-19 2.82E-18 9.07E-18 2.77E-17 1.19E-16 3.14E-16 2.05E-15 1.96E-15
31      2.18E-19 5.04E-19 2.00E-18 6.54E-18 2.04E-17 8.35E-17 2.21E-16 1.76E-15 1.80E-15
32      1.90E-19 4.43E-19 1.67E-18 5.29E-18 1.61E-17 6.22E-17 1.57E-16 1.49E-15 1.65E-15
33      1.65E-19 3.89E-19 1.40E-18 4.27E-18 1.26E-17 4.69E-17 1.13E-16 1.25E-15 1.49E-15
34      1.23E-19 2.93E-19 1.04E-18 3.17E-18 9.32E-18 3.52E-17 8.31E-17 1.02E-15 1.34E-15
35      7.86E-20 2.08E-19 7.25E-19 2.25E-18 6.70E-18 2.62E-17 6.23E-17 8.18E-16 1.18E-15
36      5.56E-20 1.47E-19 5.18E-19 1.62E-18 4.90E-18 1.96E-17 4.76E-17 6.31E-16 1.04E-15
37      4.20E-20 1.11E-19 3.90E-19 1.21E-18 3.64E-18 1.47E-17 3.67E-17 4.77E-16 9.05E-16
38      3.23E-20 8.55E-20 2.99E-19 9.24E-19 2.74E-18 1.12E-17 2.88E-17 3.59E-16 7.81E-16
39      2.51E-20 6.04E-20 2.02E-19 6.62E-19 2.06E-18 8.69E-18 2.31E-17 2.73E-16 6.70E-16
40      1.96E-20 3.75E-20 1.31E-19 4.56E-19 1.54E-18 6.74E-18 1.86E-17 2.10E-16 5.70E-16
2          / number of energies
17          / nmin
40          / nmax
        61.58   100.00
        3.47    2.17
        3.36E-14 2.18E-14
                                / energies      (keV/amu)
                                / alpha
                                / total xsects. (cm2)
                                / partial xsects. (cm2)
n l m
17      3.64E-16 2.81E-16
18      7.93E-16 5.53E-16
19      1.18E-15 7.56E-16
20      1.43E-15 8.66E-16
21      1.67E-15 9.81E-16
22      1.96E-15 1.15E-15
23      2.23E-15 1.32E-15
24      2.34E-15 1.42E-15
25      2.29E-15 1.42E-15
26      2.14E-15 1.34E-15
27      1.95E-15 1.24E-15
28      1.76E-15 1.13E-15
29      1.61E-15 1.04E-15
30      1.49E-15 9.72E-16
31      1.40E-15 9.27E-16
32      1.32E-15 8.87E-16
33      1.24E-15 8.44E-16
34      1.16E-15 7.96E-16
35      1.07E-15 7.49E-16

```

36 9.90E-16 7.05E-16
37 9.13E-16 6.65E-16
38 8.39E-16 6.28E-16
39 7.70E-16 5.94E-16
40 7.03E-16 5.62E-16
-1 -1

2 Demo (b) Obtaining charge exchange driven 'bn' populations and emissivities

DEMO B: Obtaining charge exchange driven 'bn' populations and emissivities

PURPOSE: To provide charge exchange (CX) populations and emissivities performing bundle-n population calculations.

The use of ADAS316 has been described in Demo b of Module 2. The plot produced by running ADAS316 interactively show the different contribution to the population structure: 1. excitation part, driven from the ground state of recombined receiver (fI^*n1/n_+); 2. recombination part, driven from free electron capture by the recombining receiver (fII); 3. charge exchange part, driven by neutral beam CX capture ($fIII^*nH/ne$). This last part $fIII$ allows one to build up the CX line emissivity coefficients.
ADAS316 provides the CX effective emission coefficients in the format adf12 and the feature photon emissivity coefficients (FPEC) in the format adf40.

EXAMPLE: For this demo, the input file for ADAS316 population calculation is adf25_bn#74_w61_n1.dat for W61+.

Following Demo a1 an adf01 for W61+ is produced: w61_n1.dat.

This is the input for deriving the adf12 and adf40 using ADAS316 interactively. For producing the adf40 data files the number of pixels and wavelength range must be defined. The values chosen for this demo are the following:

- pixel: 500
- min wave: 3000
- max wave: 5000

COMMENTS: Note that the adf01, w61_n1.dat, has been produced using ADAS315 and it is called within the file adf25_bn#74_w61_n1.dat.

DEMO b1: Examine the structure of adf25/a25_p316 drivers

1. Open adf25_bn#74_w61_n1.dat and examine the file.

Sample of file: adf25_bn#74_w61_n1.dat, w61_n1.dat

DEMO b2: Prepare adf12 and adf40 data for an ion with ADAS316

1. Use ADAS316 interactively.
2. Define pixel number and wavelength range.
3. Generate adf12 and adf40 and look at them.

Samples of output file: adas316_plot_w61.ps, adas316_adf12.pass,
adas316_adf40.pass

2.1 Demo (b) Figures

2.1.1 Demo (b-2) demo_b/adas316_plot_w61.pdf

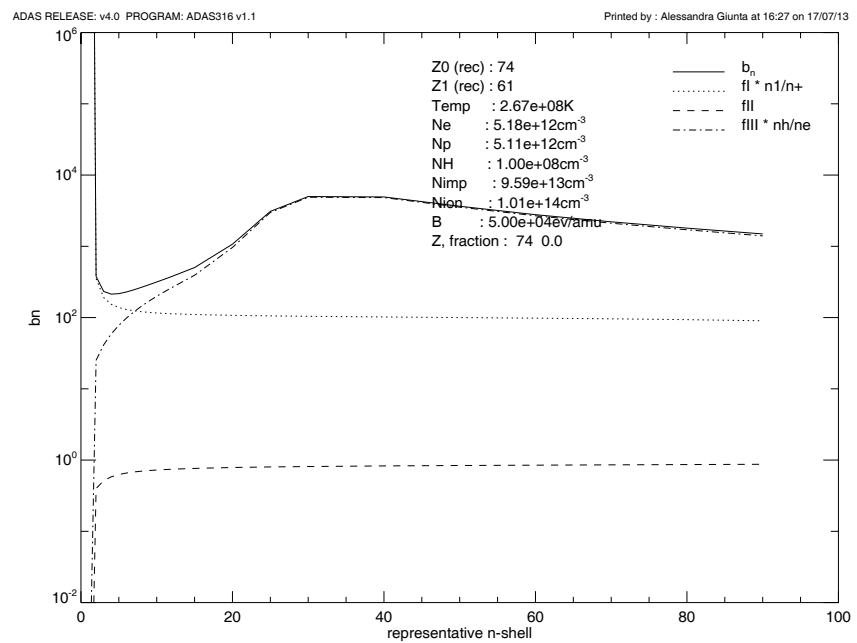


Figure 1:

2.2 Demo (b) Tables and datasets

2.2.1 Demo (b-1) demo.b/adf25.bn#74_w61.n1.dat

```

receiver ion parameters
-----
z0      :          74
z1      :          61
outfmt  : adf40
exfile  : /home/adas/adas/adf18/p310_a17/bndlen_exp#h0.dat
cxfile  : /home/asg/adas_modules/module_6/demo_b/w61_n1.dat

plasma density parameters
-----
ndens   :          1
id_ref  :          1
densa   : 1.01E+14
denpa   : 0.00E+00
denimpa : 0.00E+00
denionia: 1.01E+14

plasma temperature parameters
-----
ntemp   :          5
it_ref  :          3
tea     : 2.67E+08 2.67E+08 2.67E+08 2.67E+08 2.67E+08
tpa     : 2.67E+08 2.67E+08 2.67E+08 2.67E+08 2.67E+08
timpa   : 2.67E+08 2.67E+08 2.67E+08 2.67E+08 2.67E+08
tiona   : 2.67E+08 2.67E+08 2.67E+08 2.67E+08 2.67E+08

plasma zeff parameters
-----
nzef    :          3
iz_ref  :          2
zefa    : 1.00E+00 2.00E+00 3.00E+00

neutral beam donor parameters
-----
nbeam   :         13
ib_ref  :          9
bmena   : 1.00E+04 1.50E+04 2.00E+04 2.50E+04 3.00E+04 3.50E+04 4.00E+04
        : 4.50E+04 5.00E+04 5.50E+04 6.00E+04 6.50E+04 7.00E+04
denha   : 1.00E+08 1.00E+08 1.00E+08 1.00E+08 1.00E+08 1.00E+08 1.00E+08
        : 1.00E+08 1.00E+08 1.00E+08 1.00E+08 1.00E+08 1.00E+08
bmfra   : 1.00E+00 1.00E+00 1.00E+00 1.00E+00 1.00E+00 1.00E+00 1.00E+00
        : 1.00E+00 1.00E+00 1.00E+00 1.00E+00 1.00E+00 1.00E+00

plasma impurity parameters
-----
nimpp   :          1
im_ref  :          1
zimpa   : 7.40E+01
amimpa  : 1.35E+02
frimpa  : 1.00E-05

control parameters - radiation
-----
ts      : 1.00e+08
w       : 0.00e+00
wl     : 1.00e+08

control parameters - collisions
-----
cion   : 1.00e+00
cpy    : 1.00e+00
nip    :          0
intd   :          3
iprs   :          1
ilow   :          1
ionip  :          0
nionip :          2
ilprs  :          1
ivdisp :          0

```

```

representative level parameters
-----
nmin   :          1
nmax   :         110
imax    :         22
nrep   :  1  2  3  4  5  6  7  8  9  10 11 12 15 20
      : 25 30 40 50 60 70 80 90
wbrep  : 0.00E+00 0.00E+00 0.00E+00 0.00E+00 0.00E+00 0.00E+00 0.00E+00
      : 0.00E+00 0.00E+00 0.00E+00 0.00E+00 0.00E+00 0.00E+00 0.00E+00
      : 0.00E+00 0.00E+00 0.00E+00 0.00E+00 0.00E+00 0.00E+00 0.00E+00
jdef   :          1
def    : 0.00E+00 0.00E+00 0.00E+00 0.00E+00 0.00E+00 0.00E+00 0.00E+00
      : 0.00E+00 0.00E+00 0.00E+00 0.00E+00 0.00E+00 0.00E+00 0.00E+00
      : 0.00E+00 0.00E+00 0.00E+00 0.00E+00 0.00E+00 0.00E+00 0.00E+00

dielectronic recombination parameters
-----
jcor   :          4
cor    : 5.00E-02 3.00E-01 7.00E-01 9.00E-01
jmax   :          1
epsil  : 7.50E-01
fij   : 0.00E+00
wij   : 0.00E+00

C---

2.2.2 Demo (b-1) demo.b/w61_n1.dat

W +61   H + 0 (1) / receiver, donor (donor state index) / /
9           / number of energies
20          / nmin
45          / nmax
          0.01    0.02    0.05    0.10    0.20    0.50    1.00    2.00    5.00 / energies (keV/amu)
          83.35   59.91   45.20   42.70   15.33   9.73    8.99   16.58   11.92 / alpha
          5.99E-14 5.99E-14 5.99E-14 5.99E-14 5.99E-14 5.99E-14 5.99E-14 5.99E-14 / total xsects. (cm2)
          / partial xsects. (cm2)

n l m
20 1.15E-15 1.02E-15 1.11E-15 1.37E-15 1.63E-15 2.11E-15 2.66E-15 3.17E-15 4.44E-15
21 4.44E-15 4.20E-15 4.34E-15 4.71E-15 5.02E-15 5.69E-15 6.49E-15 6.76E-15 7.60E-15
22 9.92E-15 9.60E-15 9.51E-15 9.61E-15 9.63E-15 9.82E-15 1.01E-14 9.79E-15 9.57E-15
23 1.41E-14 1.38E-14 1.33E-14 1.30E-14 1.26E-14 1.20E-14 1.15E-14 1.08E-14 9.89E-15
24 1.40E-14 1.38E-14 1.33E-14 1.29E-14 1.24E-14 1.16E-14 1.08E-14 1.02E-14 9.04E-15
25 9.98E-15 1.03E-14 1.03E-14 9.96E-15 9.65E-15 9.12E-15 8.61E-15 8.25E-15 7.35E-15
26 4.75E-15 5.26E-15 5.61E-15 5.66E-15 5.71E-15 5.73E-15 5.67E-15 5.72E-15 5.35E-15
27 1.37E-15 1.65E-15 1.98E-15 2.19E-15 2.43E-15 2.71E-15 2.84E-15 3.20E-15 3.37E-15
28 2.24E-16 2.94E-16 4.18E-16 5.42E-16 7.08E-16 9.11E-16 9.99E-16 1.36E-15 1.78E-15
29 2.02E-17 2.87E-17 5.17E-17 8.47E-17 1.37E-16 2.20E-16 2.61E-16 4.61E-16 8.23E-16
30 1.25E-18 2.15E-18 5.26E-18 1.10E-17 2.30E-17 4.57E-17 5.66E-17 1.35E-16 3.50E-16
31 7.40E-20 2.08E-19 7.45E-19 1.85E-18 4.87E-18 1.06E-17 1.19E-17 3.90E-17 1.49E-16
32 4.81E-21 2.91E-20 1.69E-19 4.55E-19 1.43E-18 3.08E-18 2.91E-18 1.26E-17 6.82E-17
33 3.41E-22 4.34E-21 4.03E-20 1.17E-19 4.81E-19 1.10E-18 9.40E-19 5.00E-18 3.59E-17
34 2.62E-23 6.87E-22 1.00E-20 3.15E-20 1.81E-19 4.76E-19 4.45E-19 2.66E-18 2.26E-17
35 2.18E-24 1.15E-22 2.60E-21 8.81E-21 9.17E-20 2.71E-19 3.03E-19 1.86E-18 1.68E-17
36 1.95E-25 2.02E-23 7.01E-22 2.56E-21 6.40E-20 2.06E-19 2.59E-19 1.53E-18 1.35E-17
37 1.86E-26 3.74E-24 1.96E-22 7.67E-22 5.00E-20 1.72E-19 2.40E-19 1.34E-18 1.12E-17
38 1.90E-27 7.25E-25 5.69E-23 2.38E-22 3.56E-20 1.32E-19 2.07E-19 1.12E-18 8.93E-18
39 2.05E-28 1.47E-25 1.70E-23 7.62E-23 2.36E-20 9.45E-20 1.57E-19 8.47E-19 6.75E-18
40 2.36E-29 3.09E-26 5.27E-24 2.51E-23 1.59E-20 5.42E-20 1.13E-19 6.16E-19 5.03E-18
41 2.86E-30 6.78E-27 1.68E-24 8.53E-24 1.08E-20 4.08E-20 8.28E-20 4.57E-19 3.80E-18
42 3.65E-31 1.55E-27 5.49E-25 2.97E-24 7.38E-21 3.17E-20 6.41E-20 3.54E-19 2.93E-18
43 4.89E-32 3.65E-28 1.85E-25 1.06E-24 5.10E-21 2.51E-20 5.16E-20 2.83E-19 2.29E-18
44 6.89E-33 8.91E-29 6.38E-26 3.89E-25 3.56E-21 1.99E-20 4.18E-20 2.10E-19 1.78E-18
45 1.01E-33 2.25E-29 2.26E-26 1.46E-25 2.50E-21 1.59E-20 3.40E-20 1.43E-19 1.36E-18

9           / number of energies
20          / nmin
45          / nmax
          10.00   15.00   20.00   25.00   30.00   35.00   40.00   45.00   50.00 / energies (keV/amu)
          9.09    7.99   10.66   10.34    9.04    7.23    5.67    4.68    4.28 / alpha
          5.99E-14 5.89E-14 5.72E-14 5.50E-14 5.33E-14 5.23E-14 5.06E-14 4.90E-14 4.71E-14 / total xsects. (cm2)
          / partial xsects. (cm2)

n l m
20 3.83E-15 3.70E-15 7.02E-16 5.11E-16 4.80E-16 4.60E-16 4.25E-16 4.05E-16 3.96E-16
21 6.23E-15 5.75E-15 1.26E-15 1.15E-15 1.01E-15 9.62E-16 8.77E-16 8.26E-16 7.95E-16
22 8.09E-15 7.27E-15 1.94E-15 1.80E-15 1.55E-15 1.45E-15 1.32E-15 1.24E-15 1.17E-15
23 8.73E-15 7.81E-15 2.68E-15 2.27E-15 1.95E-15 1.81E-15 1.66E-15 1.54E-15 1.44E-15

```

```

24      8.28E-15 7.48E-15 3.39E-15 2.65E-15 2.28E-15 2.11E-15 1.94E-15 1.79E-15 1.66E-15
25      7.18E-15 6.59E-15 4.03E-15 3.08E-15 2.66E-15 2.45E-15 2.25E-15 2.07E-15 1.90E-15
26      5.73E-15 5.42E-15 4.51E-15 3.54E-15 3.06E-15 2.81E-15 2.58E-15 2.36E-15 2.16E-15
27      4.20E-15 4.21E-15 4.76E-15 3.89E-15 3.39E-15 3.10E-15 2.83E-15 2.58E-15 2.37E-15
28      2.84E-15 3.12E-15 4.72E-15 4.03E-15 3.53E-15 3.21E-15 2.92E-15 2.67E-15 2.45E-15
29      1.79E-15 2.21E-15 4.45E-15 3.93E-15 3.48E-15 3.14E-15 2.84E-15 2.60E-15 2.40E-15
30      1.07E-15 1.53E-15 4.03E-15 3.67E-15 3.30E-15 2.97E-15 2.68E-15 2.45E-15 2.27E-15
31      6.33E-16 1.04E-15 3.54E-15 3.34E-15 3.06E-15 2.76E-15 2.48E-15 2.27E-15 2.10E-15
32      3.81E-16 7.17E-16 3.05E-15 3.00E-15 2.80E-15 2.56E-15 2.29E-15 2.08E-15 1.92E-15
33      2.41E-16 5.02E-16 2.59E-15 2.66E-15 2.56E-15 2.36E-15 2.12E-15 1.91E-15 1.76E-15
34      1.63E-16 3.61E-16 2.18E-15 2.36E-15 2.33E-15 2.18E-15 1.96E-15 1.77E-15 1.62E-15
35      1.18E-16 2.65E-16 1.82E-15 2.08E-15 2.12E-15 2.03E-15 1.83E-15 1.64E-15 1.51E-15
36      8.93E-17 1.96E-16 1.50E-15 1.83E-15 1.92E-15 1.88E-15 1.70E-15 1.54E-15 1.42E-15
37      6.94E-17 1.46E-16 1.23E-15 1.59E-15 1.74E-15 1.73E-15 1.58E-15 1.44E-15 1.34E-15
38      5.39E-17 1.10E-16 1.00E-15 1.38E-15 1.56E-15 1.57E-15 1.46E-15 1.34E-15 1.27E-15
39      4.18E-17 8.43E-17 8.06E-16 1.18E-15 1.37E-15 1.40E-15 1.33E-15 1.24E-15 1.18E-15
40      3.24E-17 6.55E-17 6.41E-16 9.92E-16 1.20E-15 1.24E-15 1.21E-15 1.14E-15 1.09E-15
41      2.52E-17 5.16E-17 5.05E-16 8.16E-16 1.02E-15 1.09E-15 1.09E-15 1.05E-15 1.00E-15
42      1.96E-17 4.09E-17 3.92E-16 6.55E-16 8.58E-16 9.50E-16 9.70E-16 9.48E-16 9.18E-16
43      1.54E-17 3.28E-17 3.03E-16 5.16E-16 7.10E-16 8.21E-16 8.62E-16 8.54E-16 8.35E-16
44      1.23E-17 2.69E-17 2.35E-16 4.05E-16 5.81E-16 7.03E-16 7.61E-16 7.68E-16 7.57E-16
45      1.00E-17 2.24E-17 1.84E-16 3.20E-16 4.72E-16 5.95E-16 6.68E-16 6.90E-16 6.86E-16
2          / number of energies
20         / nmin
45         / nmax
      75.00   100.00          / energies (keV/amu)
      2.64    2.17            / alpha
      3.63E-14 2.78E-14      / total xsects. (cm2)
                                         / partial xsects. (cm2)
n  l   m
20      2.72E-16 2.02E-16
21      5.00E-16 3.57E-16
22      6.96E-16 4.76E-16
23      8.28E-16 5.46E-16
24      9.41E-16 6.04E-16
25      1.09E-15 6.90E-16
26      1.26E-15 7.94E-16
27      1.40E-15 8.86E-16
28      1.46E-15 9.34E-16
29      1.43E-15 9.30E-16
30      1.35E-15 8.91E-16
31      1.25E-15 8.33E-16
32      1.16E-15 7.71E-16
33      1.08E-15 7.15E-16
34      1.01E-15 6.68E-16
35      9.52E-16 6.34E-16
36      9.05E-16 6.08E-16
37      8.62E-16 5.85E-16
38      8.18E-16 5.61E-16
39      7.73E-16 5.34E-16
40      7.27E-16 5.06E-16
41      6.82E-16 4.79E-16
42      6.40E-16 4.54E-16
43      6.00E-16 4.31E-16
44      5.64E-16 4.10E-16
45      5.30E-16 3.90E-16
-1      -1

```

2.2.3 Demo (b-2) demo_b/adas316_adf12.pass

```

333
E=w  W= 3140.86 D=h(1s) R=w+61 N=30-29 F=#74_w61_n1 M=cx  isel= 1
7.96D-08  qrefref
5.00D+04 2.30D+04 1.01D+14 2.00D+00 3.00D+00  parmrref
13      5      1      3      1
1.00D+04 1.50D+04 2.00D+04 2.50D+04 3.00D+04 3.50D+04  nparmsc
4.00D+04 4.50D+04 5.00D+04 5.50D+04 6.00D+04 6.50D+04  ener
7.00D+04
1.34D-08 2.44D-08 7.97D-08 8.36D-08 8.45D-08 8.37D-08  qener
8.22D-08 8.07D-08 7.96D-08 7.70D-08 7.32D-08 6.91D-08
6.51D-08
2.30D+04 2.30D+04 2.30D+04 2.30D+04 2.30D+04  tiev
7.96D-08 7.96D-08 7.96D-08 7.96D-08 7.96D-08  qtiev
1.01D+14  densi

```

```

7.96D-08 qdensi
1.00D+00 2.00D+00 3.00D+00 zeff
1.55D-06 7.96D-08 4.09D-08 qzeff
3.00D+00 bmag
7.96D-08 qbmag

E=w W= 3471.35 D=h(1s) R=w+61 N=31-30 F=#74_w61_n1 M=cx isel= 2
7.58D-08 qrefref
5.00D+04 2.30D+04 1.01D+14 2.00D+00 3.00D+00 parpref
13 5 1 3 1 nparmsc
1.00D+04 1.50D+04 2.00D+04 2.50D+04 3.00D+04 3.50D+04 ener
4.00D+04 4.50D+04 5.00D+04 5.50D+04 6.00D+04 6.50D+04
7.00D+04
9.13D-09 1.77D-08 7.08D-08 7.72D-08 7.94D-08 7.91D-08 gener
7.79D-08 7.66D-08 7.58D-08 7.34D-08 6.99D-08 6.61D-08
6.24D-08
2.30D+04 2.30D+04 2.30D+04 2.30D+04 2.30D+04 tiev
7.58D-08 7.58D-08 7.58D-08 7.58D-08 7.58D-08 qtiev
1.01D+14 densi
7.58D-08 qdensi
1.00D+00 2.00D+00 3.00D+00 zeff
1.48D-06 7.58D-08 3.89D-08 qzeff
3.00D+00 bmag
7.58D-08 qbmag
.

C-----
C Wavelength ranges:
C
C      wvmin(A)      wvmax(A)
C      -----      -----
C      3000.00      5000.00
C
C      emis_thres =   1.00D-12
C
C
C Effective coefficient list:
C
C      isel      type      ion      transition      wavln.(A)      emis. rank
C      ----      ----      ---      -----      -----      -----
C      1.      cx.emis.      w +60      n = 30- 29      3140.86      1
C      2.      cx.emis.      w +60      n = 31- 30      3471.35      2
C
C      332.      cx.emis.      w +60      n =110- 86      4657.80      319
C      333.      cx.emis.      w +60      n =110- 87      4948.75      315
C
C
C Bundle-n population code parameters:
C
C      nip = 0      intd = 3      iprs = 1      ilow = 1
C      ionip = 0      nionip= 2      ilprs = 1      ivdisp = 0
C      cion = 1.0      cpy = 1.0
C
C      ts(K) = 1.00D+08      w = 0.00D+00      w1 = 1.00D+08
C
C      zimp(1) = 7.40D+01      amimp(1)= 1.35D+02      frimp(1)= 1.00D-05
C
C
C adf25 file : /home/asg/adas_modules/module_6/demo_b/adf25_bn#74_w61_n1.dat
C Code : adas316
C Producer : Alessandra Giunta
C Date : 18/06/13
C
C

```

2.2.4 Demo (b-2) demo_b/adas316_adf40.pass

```
1 /w :60 feature photon emissivity coefficients/
```

```

-----#
//#01/p00/ 00/p01/ 01/p02/ 02/p03/ 03/p04/ 04/p05/ 05/p06/ 06/p07/ 07/p08/ 08/
p09/ 09/p10/ 10/p11/ 11/p12/ 12/p13/ 13/p14/ 14/p15/ 15/p16/ 16/p17/ 17/
p18/ 18/p19/ 19/p20/ 20/p21/ 21/p22/ 22/p23/ 23/p24/ 24/p25/ 25/p26/ 26/
p27/ 27/p28/ 28/p29/ 29/p30/ 30/p31/ 31/p32/ 32/p33/ 33/p34/ 34/p35/ 35/
p36/ 36/p37/ 37/p38/ 38/p39/ 39/p40/ 40/p41/ 41/p42/ 42/p43/ 43/p44/ 44/
p45/ 45/p46/ 46/p47/ 47/p48/ 48/p49/ 49/p50/ 50/p51/ 51/p52/ 52/p53/ 53/
p54/ 54/p55/ 55/p56/ 56/p57/ 57/p58/ 58/p59/ 59/p60/ 60/p61/ 61/p62/ 62/
p63/ 63/p64/ 64/p65/ 65/p66/ 66/p67/ 67/p68/ 68/p69/ 69/p70/ 70/p71/ 71/
p72/ 72/p73/ 73/p74/ 74/
-----#
      500      1      1 /pl=01:ss=60:pp= 1:lz=60:hz=60/type=chexc/ispb = 1/isel =      1
3000.00000 5000.00000
1.01E+14
2.30E+04
3.34E-16 1.09E-11 5.49E-11 6.25E-11 1.84E-09 6.89E-10 1.70E-10 8.21E-11
4.66E-11 9.19E-11 9.39E-11 6.39E-11 4.24E-11 4.20E-11 5.17E-14 8.91E-16
3.72E-11 2.31E-10 3.22E-11 8.11E-13 2.51E-10 9.27E-11 1.48E-11 1.31E-08
9.72E-09 2.35E-11 2.20E-10 5.33E-11 7.27E-10 5.55E-11 2.76E-09 6.45E-09
1.52E-09 2.58E-09 2.05E-08 6.14E-08 4.23E-10 2.00E-11 1.97E-10 2.71E-10
2.45E-10 3.99E-09 5.76E-10 1.43E-10 4.87E-11 1.30E-11 4.74E-11 3.67E-10
1.17E-09 1.03E-11 1.57E-10 4.38E-11 2.14E-11 2.13E-11 1.86E-11 3.36E-12
1.54E-10 1.86E-10 2.25E-11 2.16E-13 1.24E-10 9.15E-11 1.76E-11 6.11E-14
1.77E-11 1.92E-11 1.12E-10 1.08E-10 4.77E-10 3.42E-10 5.23E-11 6.09E-10
8.99E-11 4.25E-12 5.67E-10 7.06E-10 1.42E-10 1.39E-11 4.16E-10 1.57E-11
3.94E-10 9.35E-10 1.44E-09 4.24E-12 1.18E-10 4.42E-11 1.19E-10 8.11E-09
1.99E-08 9.44E-10 5.36E-12 2.24E-13 1.09E-09 4.20E-09 3.91E-10 3.22E-11
1.63E-10 1.14E-11 1.41E-10 7.89E-11 1.04E-10 3.49E-11 4.49E-11 8.12E-12
9.82E-11 2.34E-11 2.84E-11 8.50E-14 5.05E-12 2.44E-11 5.70E-10 6.74E-10
3.11E-10 3.02E-13 1.80E-17 1.47E-12 3.49E-10 5.23E-08 2.36E-08 8.37E-10
1.70E-10 2.11E-13 1.34E-11 1.87E-11 5.78E-14 9.79E-16 4.50E-12 1.66E-11
2.24E-13 6.27E-12 1.34E-10 1.87E-09 7.01E-10 1.90E-10 4.70E-11 1.30E-13
2.36E-11 2.76E-11 1.04E-10 5.75E-11 1.12E-09 1.90E-10 1.52E-12 2.73E-17
2.65E-13 9.39E-11 5.82E-09 5.11E-09 1.89E-11 1.59E-10 5.77E-11 4.21E-14
2.90E-11 6.17E-10 4.57E-10 1.31E-09 1.64E-08 1.22E-09 1.09E-13 9.64E-11
2.72E-10 3.52E-12 2.32E-12 1.26E-10 7.97E-10 1.60E-10 5.99E-12 3.38E-11
1.11E-10 5.69E-11 1.19E-10 4.87E-11 2.43E-10 8.16E-11 2.81E-11 3.89E-12
1.76E-11 2.42E-11 8.82E-12 6.16E-15 2.02E-13 5.83E-11 6.32E-10 1.37E-09
2.42E-11 6.26E-15 5.72E-17 3.71E-12 3.28E-10 1.04E-09 6.30E-11 3.37E-12
1.85E-11 1.13E-10 4.97E-12 2.34E-11 3.85E-10 1.45E-10 4.44E-10 2.51E-10
2.82E-11 2.13E-10 7.54E-10 2.65E-09 1.97E-10 3.04E-08 4.05E-08 3.34E-10
4.58E-09 2.20E-09 5.53E-11 6.27E-10 2.55E-10 1.36E-10 9.55E-12 1.88E-11
2.66E-13 2.49E-13 5.32E-11 5.49E-11 7.31E-13 1.84E-11 5.86E-12 5.29E-15
0.00E+00 4.35E-17 1.92E-11 6.73E-09 1.04E-08 1.60E-10 2.39E-11 1.92E-10
6.18E-11 1.97E-11 6.96E-11 7.76E-11 1.42E-09 3.27E-10 1.67E-11 7.69E-10
6.72E-10 1.59E-10 9.29E-12 5.06E-12 4.66E-10 3.67E-10 7.18E-11 8.91E-11
1.04E-10 1.94E-12 5.19E-17 2.95E-16 1.59E-12 2.05E-11 1.30E-10 1.04E-10
5.39E-11 4.85E-11 3.60E-13 1.13E-10 6.40E-10 2.14E-09 8.44E-10 1.59E-12
1.64E-13 3.37E-11 5.89E-11 6.79E-11 1.90E-11 1.12E-10 2.23E-10 5.92E-11
4.33E-10 4.88E-09 7.00E-10 1.94E-11 5.81E-11 5.12E-12 1.07E-13 1.26E-11
1.24E-11 9.81E-14 6.34E-16 3.79E-12 6.51E-11 5.76E-11 3.15E-10 4.13E-11
2.33E-10 1.87E-10 5.58E-12 9.91E-10 2.07E-09 1.14E-10 8.75E-13 5.56E-11
4.10E-11 9.70E-12 2.97E-10 2.81E-08 3.77E-08 6.03E-10 2.69E-09 1.21E-08
8.14E-10 1.45E-11 8.47E-13 3.73E-11 4.21E-11 3.25E-11 5.78E-10 2.47E-10
1.17E-10 3.75E-11 5.21E-11 2.41E-12 4.27E-16 0.00E+00 0.00E+00 0.00E+00
6.24E-14 1.72E-10 2.16E-09 4.94E-10 6.94E-12 3.26E-15 0.00E+00 0.00E+00
1.66E-14 1.71E-11 1.07E-10 1.12E-11 2.94E-11 3.02E-10 2.56E-10 8.63E-11
4.47E-11 6.14E-11 3.85E-11 3.37E-11 2.18E-09 3.63E-09 3.57E-10 2.91E-11
3.24E-12 3.07E-10 6.83E-10 4.50E-11 9.15E-11 1.15E-09 2.76E-10 3.86E-11
9.59E-11 3.69E-11 1.10E-11 1.23E-10 2.76E-11 5.13E-14 3.26E-19 0.00E+00
1.80E-14 3.68E-11 5.02E-10 1.71E-10 2.30E-12 4.55E-16 0.00E+00 0.00E+00
0.00E+00 0.00E+00 4.37E-18 1.92E-13 3.83E-11 1.23E-10 4.04E-11 5.52E-11
6.59E-11 2.95E-11 4.65E-11 2.03E-11 6.84E-11 2.67E-09 1.08E-08 1.06E-09
1.07E-10 1.65E-09 8.16E-10 1.17E-10 7.78E-11 8.18E-13 2.25E-13 8.30E-11
3.68E-10 6.08E-11 7.75E-11 9.06E-12 9.77E-15 3.58E-14 3.93E-10 2.75E-08
3.30E-08 1.06E-09 5.55E-10 5.83E-11 3.10E-11 4.37E-13 1.64E-16 2.88E-12
4.21E-10 9.32E-10 5.04E-10 3.79E-09 8.18E-10 3.48E-11 2.44E-11 1.63E-10
4.59E-10 1.28E-10 7.12E-11 2.06E-11 1.10E-13 1.11E-17 1.25E-13 1.56E-11
3.28E-11 1.66E-12 8.00E-16 1.45E-13 4.19E-11 1.73E-10 2.76E-11 1.92E-10
1.17E-10 5.35E-11 1.33E-10 4.22E-11 3.71E-12 6.30E-11 2.93E-11 2.47E-13
1.67E-17 1.29E-18 8.65E-14 4.37E-11 3.10E-10 1.81E-10 8.14E-11 3.67E-12
3.07E-11 4.61E-11 3.66E-10 1.72E-09 2.70E-10 5.60E-12 1.48E-14 2.08E-14
6.27E-12 3.08E-11 1.87E-11 4.46E-10 3.69E-10 1.08E-10 8.22E-11 2.77E-11
3.25E-09 8.79E-09 7.20E-10 8.21E-13 1.20E-14 2.65E-11 7.75E-10 9.47E-10

```

```

1.03E-10 1.51E-12 3.03E-11 2.31E-11 4.45E-13 6.72E-12 1.33E-10 7.92E-11
1.50E-12 4.06E-11 2.86E-10 2.72E-10 2.16E-09 2.27E-09 8.53E-11 4.72E-11
6.54E-11 1.47E-11 1.93E-13 1.03E-11 9.59E-11 6.20E-11 1.38E-12 6.86E-16
1.43E-12 1.21E-10 2.77E-10 2.22E-11
C-----
C Wavelength ranges:
C
C      wvmin(A)      wvmax(A)
C      -----      -----
C      3000.00      5000.00
C
C      emis_thres =   1.00D-12
C
C
C      Bundle-n population code parameters:
C
C      nip    = 0      intd   = 3      iprs   = 1      ilow   = 1
C      ionip  = 0      nionip= 2      ilprs  = 1      ivdisp= 0
C      cion   = 1.0    cpy    = 1.0
C
C      ts(K)    = 1.00D+08      w       = 0.00D+00      w1     = 1.00D+08
C
C      zimp(1) = 7.40D+01      amimp(1)= 1.35D+02      frimp(1)= 1.00D-05
C
C
C      adf25 file : /home/asg/adas_modules/module_6/demo_b/adf25_bn#74_w61_n1.dat
C      Code   : adas316
C      Producer : Alessandra Giunta
C      Date   : 18/06/13
C
C-----

```

3 Demo (c) Comparing active W emission to bremsstrahlung background

DEMO C: Comparing active W emission to bremsstrahlung background

PURPOSE: To generate active spectrum and continuum for W and compare the emission. This is a proper application of ADAS tools (use of ADAS316 to produce the feature photon emissivity coefficients (FPEC) in the adf40 format, in order to generate the spectrum).

The emissivity due to spectral lines is given by the FPEC times the fractional abundances at equilibrium, as calculated by ADAS405.

The continuum emission is calculated by the routine
/home/adas/adas/idl/adaslib/atomic/continuo.pro

EXAMPLE: This demo consists of three main points:

1. Set up the plasma environment: define temperature and density profiles, beam position and establish the relevant ionisation stages.
The data (distance along line of sight, electron temperature and electron density) come from an ITER scenario (H-mode).
For calculating which ionisation stage occurs in the region defined by the beam, ADAS405 is used. This calculate the ionisation balance at equilibrium for W. The input files are the adf11 specidief by year 50.
2. Make adf40 for W. The input file is in the adf25 format.
This is made using as input the adf01 generated for W51+ to W71+, as described in Demo a, and the adf25 template bn_cxs_template.dat.
ADAS316 is used to create the adf40 (See Demo b).
The directories created locally (adf01, adf25 and adf40) contain the data produced by this demo:
 - a) ./adf01/w/
w51_n1.dat w55_n1.dat w59_n1.dat w63_n1.dat w67_n1.dat w71_n1.dat
w52_n1.dat w56_n1.dat w60_n1.dat w64_n1.dat w68_n1.dat
w53_n1.dat w57_n1.dat w61_n1.dat w65_n1.dat w69_n1.dat
w54_n1.dat w58_n1.dat w62_n1.dat w66_n1.dat w70_n1.dat
 - b) ./adf25/a25_p316/bn#74/
bn#74_w51_n1.dat bn#74_w57_n1.dat bn#74_w63_n1.dat bn#74_w69_n1.dat
bn#74_w52_n1.dat bn#74_w58_n1.dat bn#74_w64_n1.dat bn#74_w70_n1.dat
bn#74_w53_n1.dat bn#74_w59_n1.dat bn#74_w65_n1.dat bn#74_w71_n1.dat
bn#74_w54_n1.dat bn#74_w60_n1.dat bn#74_w66_n1.dat
bn#74_w55_n1.dat bn#74_w61_n1.dat bn#74_w67_n1.dat
bn#74_w56_n1.dat bn#74_w62_n1.dat bn#74_w68_n1.dat
 - c) ./adf40/w/
fpec_w51_n1.dat fpec_w57_n1.dat fpec_w63_n1.dat fpec_w69_n1.dat
fpec_w52_n1.dat fpec_w58_n1.dat fpec_w64_n1.dat fpec_w70_n1.dat
fpec_w53_n1.dat fpec_w59_n1.dat fpec_w65_n1.dat fpec_w71_n1.dat
fpec_w54_n1.dat fpec_w60_n1.dat fpec_w66_n1.dat

```
fpec_w55_n1.dat  fpec_w61_n1.dat  fpec_w67_n1.dat  
fpec_w56_n1.dat  fpec_w62_n1.dat  fpec_w68_n1.dat
```

3. Generate the active emission using the adf40 produced in point 2 and the continuum emission. .The active emission is generated combining the adf40 FPEC with the frantional abundances at equilibrium computed by ADAS405.

The continuum emission is calculated by the routine continuo.pro

DEMO c1: Explore implications of plasma conditions on choice of tungsten stages

1. Specify distance alond line of sight, electron temperature and density.
2. Identify the temperature where the beam exists.
3. Use run_adas405.pro to establish the ionisation stages of W which occur in that region.

Program: demo_c_1.pro

Sample of output files:demo_c_1_temp_dens.ps, demo_c_1_frac.ps

DEMO c2: Generate adf40 W active emission with run_adas316

1. Use read_adf25.pro to read the adf25 template.
2. Set up the input value for the new adf25 and the adf01 to be used.
3. Use write_adf25.pro to write the adf25 to be used as input for the ADAS316 run.
4. Use run_adas316.pro to produce the adf40.

Program: demo_c_2.pro

Sample of output files: files contained in the adf01, adf25 and adf40 directories created locally.

DEMO c3: Construct active spectrum by combining adf40 with ionisation balance and generate continuum spectrum with ADAS routine continuo.pro

1. Define plasma condintions (temperature and density).
2. Set up the adf40 (W51+ to W71+).
3. Use run_adas405.pro for calculatin the fractgional abundances for W.
4. Use read-adf40.pro to read data from adf40
(W line emission, called active emission in the program).
5. Build up the active emission mutiplying FPEC from adf40 times the fractional abundances.
6. Integrate the emission over beam size.
7. Plot the integrated active emission as a function of wavelength.
8. Use continuo.pro to calculate the continuum emission and ingrate along the line of sight.
9. Plot the active integrated emission and continuum integrated emission as a function of wavelength.

Program: demo_c_3.pro

Sample of output files: demo_c_3_active.ps, demo_c_3_compare.ps

3.1 Demo (c) Figures

3.1.1 Demo (c-1) demo_c/demo_c_1.fraction.pdf

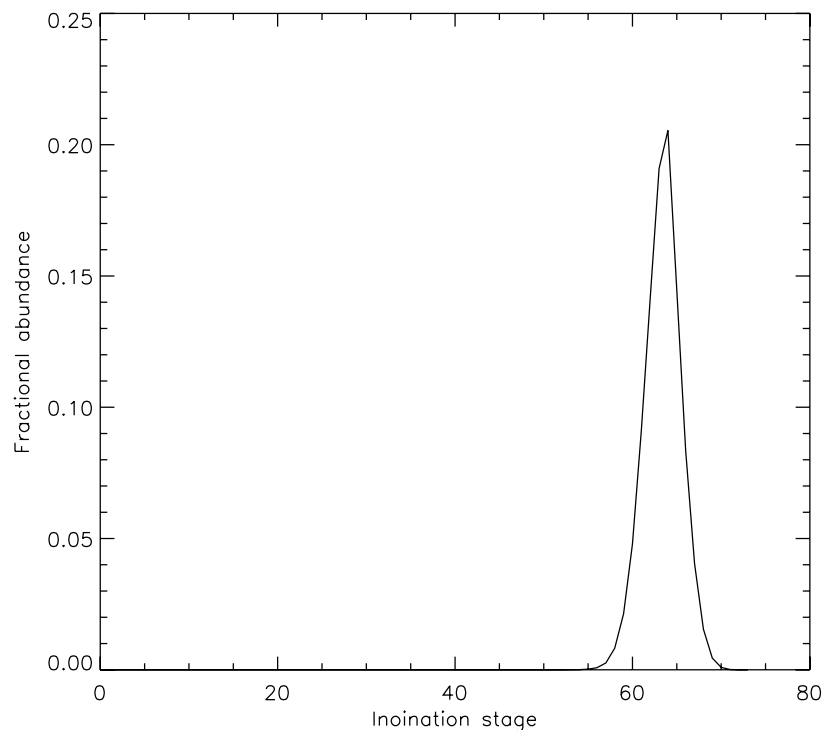


Figure 2:

3.1.2 Demo (c-1) demo_c/demo_c_1.temp.dens.pdf

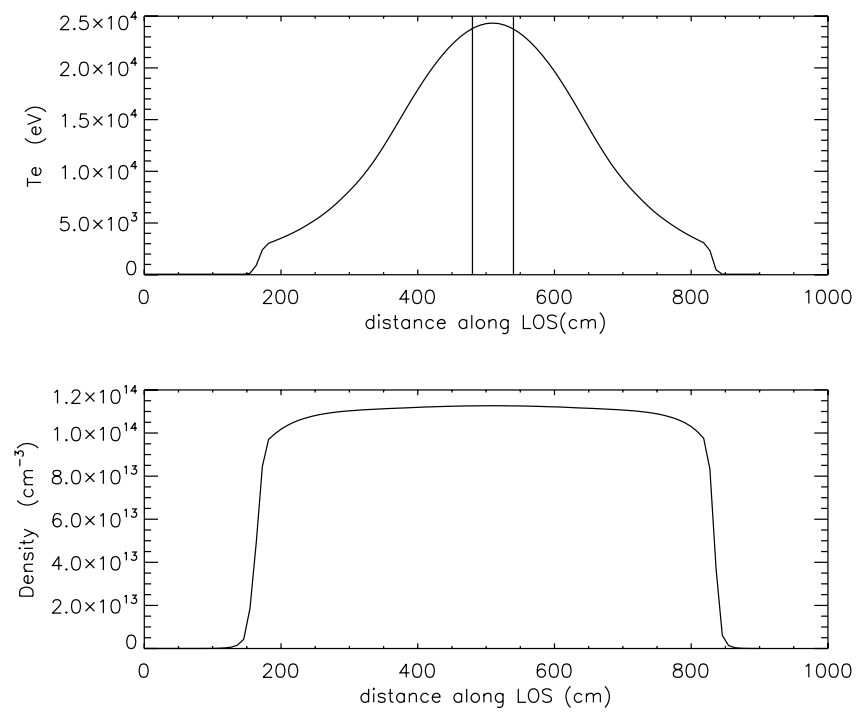


Figure 3:

3.1.3 Demo (c-3) demo_c/demo_c_3.active.pdf

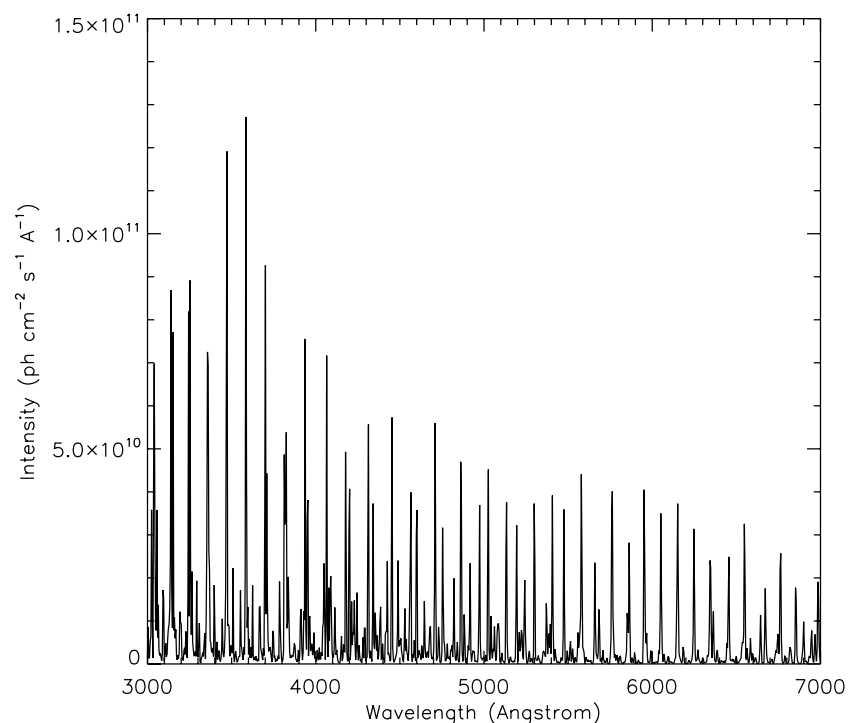


Figure 4:

3.1.4 Demo (c-3) demo_c/demo_c_3.compare.pdf

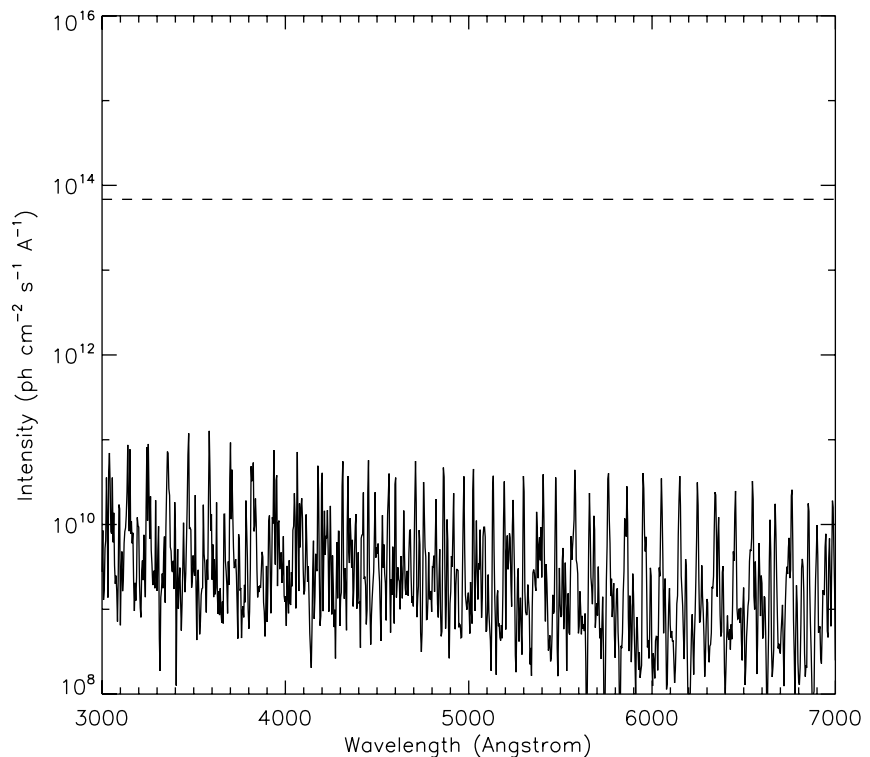


Figure 5:

3.2 Demo (c) IDL procedures

3.2.1 Demo (c-1) demo_c_1.pro

```

pro demo_c_1

; Data from ITER scenario 2 (H-mode)

d = [ 0.0000e+00, 9.0909e+00, 1.8182e+01, 2.7273e+01, 3.6364e+01, $
      4.5455e+01, 5.4545e+01, 6.3636e+01, 7.2727e+01, 8.1818e+01, $
      9.0909e+01, 1.0000e+02, 1.0909e+02, 1.1818e+02, 1.2727e+02, $
      1.3636e+02, 1.4545e+02, 1.5455e+02, 1.6364e+02, 1.7273e+02, $
      1.8182e+02, 1.9091e+02, 2.0000e+02, 2.0909e+02, 2.1818e+02, $
      2.2727e+02, 2.3636e+02, 2.4545e+02, 2.5455e+02, 2.6364e+02, $
      2.7273e+02, 2.8182e+02, 2.9091e+02, 3.0000e+02, 3.0909e+02, $
      3.1818e+02, 3.2727e+02, 3.3636e+02, 3.4545e+02, 3.5455e+02, $
      3.6364e+02, 3.7273e+02, 3.8182e+02, 3.9091e+02, 4.0000e+02, $
      4.0909e+02, 4.1818e+02, 4.2727e+02, 4.3636e+02, 4.4545e+02, $
      4.5455e+02, 4.6364e+02, 4.7273e+02, 4.8182e+02, 4.9091e+02, $
      5.0000e+02, 5.0909e+02, 5.1818e+02, 5.2727e+02, 5.3636e+02, $
      5.4545e+02, 5.5455e+02, 5.6364e+02, 5.7273e+02, 5.8182e+02, $
      5.9091e+02, 6.0000e+02, 6.0909e+02, 6.1818e+02, 6.2727e+02, $
      6.3636e+02, 6.4545e+02, 6.5455e+02, 6.6364e+02, 6.7273e+02, $
      6.8182e+02, 6.9091e+02, 7.0000e+02, 7.0909e+02, 7.1818e+02, $
      7.2727e+02, 7.3636e+02, 7.4545e+02, 7.5455e+02, 7.6364e+02, $
      7.7273e+02, 7.8182e+02, 7.9091e+02, 8.0000e+02, 8.0909e+02, $
      8.1818e+02, 8.2727e+02, 8.3636e+02, 8.4545e+02, 8.5455e+02, $
      8.6364e+02, 8.7273e+02, 8.8182e+02, 8.9091e+02, 9.0000e+02 ]]

te = [ 5.0000e+01, 5.0000e+01, 5.0000e+01, 5.0000e+01, 5.0000e+01, $
       5.0000e+01, 5.0000e+01, 5.0000e+01, 5.0000e+01, 5.0000e+01, $
       5.0000e+01, 5.0947e+01, 1.3802e+02, 8.9934e+02, 2.4124e+03, $
       3.0462e+03, 3.2800e+03, 3.5272e+03, 3.7913e+03, 4.0776e+03, $
       4.3872e+03, 4.7341e+03, 5.1028e+03, 5.4936e+03, 5.9293e+03, $
       6.4070e+03, 6.9345e+03, 7.5085e+03, 8.1055e+03, 8.7299e+03, $
       9.4337e+03, 1.0205e+04, 1.1033e+04, 1.1930e+04, 1.2889e+04, $
       1.3882e+04, 1.4895e+04, 1.5920e+04, 1.6921e+04, 1.7885e+04, $
       1.8818e+04, 1.9700e+04, 2.0513e+04, 2.1264e+04, 2.1951e+04, $
       2.2557e+04, 2.3085e+04, 2.3523e+04, 2.3869e+04, 2.4125e+04, $
       2.4280e+04, 2.4333e+04, 2.4284e+04, 2.4134e+04, 2.3878e+04, $
       2.3532e+04, 2.3092e+04, 2.2558e+04, 2.1946e+04, 2.1253e+04, $
       2.0491e+04, 1.9666e+04, 1.8767e+04, 1.7811e+04, 1.6826e+04, $
       1.5803e+04, 1.4753e+04, 1.3717e+04, 1.2713e+04, 1.1744e+04, $
       1.0820e+04, 9.9907e+03, 9.2201e+03, 8.5092e+03, 7.8700e+03, $
       7.2528e+03, 6.6671e+03, 6.1215e+03, 5.6368e+03, 5.1965e+03, $
       4.7808e+03, 4.3867e+03, 4.0308e+03, 3.6993e+03, 3.3895e+03, $
       3.0920e+03, 2.3507e+03, 4.7135e+02, 5.4887e+01, 5.0000e+01, $
       5.0000e+01, 5.0000e+01, 5.0000e+01, 5.0000e+01 ]

```

```

dens = [1.2644e+10,  1.0410e+10,  1.0000e+10,  1.0000e+10,  1.0000e+10,  $  

        1.0000e+10,  1.0920e+10,  1.3384e+10,  1.6654e+10,  2.5761e+10,  $  

        4.0784e+10,  7.1152e+10,  1.3571e+11,  2.7752e+11,  6.3022e+11,  $  

        1.5611e+12,  4.2606e+12,  1.8577e+13,  4.8794e+13,  8.4619e+13,  $  

        9.7046e+13,  9.9647e+13,  1.0178e+14,  1.0352e+14,  1.0492e+14,  $  

        1.0609e+14,  1.0699e+14,  1.0780e+14,  1.0845e+14,  1.0896e+14,  $  

        1.0940e+14,  1.0977e+14,  1.1006e+14,  1.1031e+14,  1.1052e+14,  $  

        1.1073e+14,  1.1090e+14,  1.1104e+14,  1.1118e+14,  1.1133e+14,  $  

        1.1145e+14,  1.1157e+14,  1.1167e+14,  1.1180e+14,  1.1194e+14,  $  

        1.1207e+14,  1.1215e+14,  1.1223e+14,  1.1232e+14,  1.1240e+14,  $  

        1.1248e+14,  1.1254e+14,  1.1258e+14,  1.1261e+14,  1.1264e+14,  $  

        1.1265e+14,  1.1266e+14,  1.1266e+14,  1.1264e+14,  1.1261e+14,  $  

        1.1258e+14,  1.1254e+14,  1.1248e+14,  1.1240e+14,  1.1232e+14,  $  

        1.1222e+14,  1.1215e+14,  1.1207e+14,  1.1193e+14,  1.1178e+14,  $  

        1.1166e+14,  1.1155e+14,  1.1144e+14,  1.1130e+14,  1.1115e+14,  $  

        1.1100e+14,  1.1086e+14,  1.1067e+14,  1.1045e+14,  1.1023e+14,  $  

        1.0994e+14,  1.0958e+14,  1.0916e+14,  1.0864e+14,  1.0795e+14,  $  

        1.0711e+14,  1.0608e+14,  1.0475e+14,  1.0302e+14,  1.0064e+14,  $  

        9.7578e+13,  8.3379e+13,  3.6986e+13,  6.0841e+12,  1.4363e+12,  $  

        3.9416e+11,  1.1876e+11,  3.7860e+10,  1.4183e+10,  1.0000e+10  ]  
  

set_plot,'ps'  

device, /isolatin1, font_index=8  

device, bits=8, filename='demo_c_1_temp_dens.ps',  $  

    font_size = 14, xsize=18.0, ysize=16.0, $  

    yoffset=7.0, /color;  

device, /helvetica  
  

!p.multi = [0,1,2]  
  

; Plot plasma temperature  

plot, d, te, xtitle='distance along LOS(cm)', ytitle='Te (eV)'  
  

; show location of beam volume  

oplot, [480, 480], [!y.crange[0], !y.crange[1]]  

oplot, [540, 540], [!y.crange[0], !y.crange[1]]  
  

; plot density  

plot, d, dens, xtitle='distance along LOS (cm)', ytitle='Density (cm^-3)'  

!p.multi = 0  
  

device, /close  

set_plot,'X'

```

```

!p.font=-1

; Find Te where beam exists
print, te[i4indf(d,480):i4indf(d,540)]

; Establish which ionisation stages of tungsten occur in this region
; Equilibrium ionisation balance for W with central ADAS year 50 set

te    = 24.0e3
dens = 1.01e14

run_adas405, uid='adas', year=50, elem='w', te=te, dens=dens, frac=frac

set_plot,'ps'
device, /isolatin1, font_index=8
device, bits=8, filename='demo_c_1_frac.ps', $
      font_size = 14, xsize=18.0, ysize=16.0, $
      yoffset=7.0, /color;
device, /helvetica

plot, indgen(74), frac.ion,xtitle='Ionination stage',  $
      ytitle='Fractional abundance'

device, /close
set_plot,'X'
!p.font=-1

end

```

3.2.2 Demo (c-2) demo_c_2.pro

```

pro demo_c_2

;generate the adf40 for W
spawn, 'pwd', res
root =res[0]

te    = 23.0e3
tp    = te
dens = 1.01e14

z_low = 51
z_high = 71

```

```

iz      = indgen(z_high-z_low+1) + z_low
n_z    = n_elements(iz)

npix  = [1000]
wvmin = [3000]
wvmax = [7000]

adf25 = 'bn_cxs_template.dat'

read_adf25, file=adf25, fulldata=all_25

for j = 0, n_z-1 do begin

  izr = iz[j]

  print, 'Processing stage ' + string(izr)

  all = all_25

  all.iz1 = izr
  all.cxfiile = root + '/adf01/w/w' + string(izr, format='(i2.2)') + '_n1.dat'
  all.densa = dens
  all.denpa = 0.0
  all.denimpa = 0.0
  all.denionia = dens

  all.tea   = te * 11605.0
  all.tpa   = tp * 11605.0
  all.timpa = te * 11605.0
  all.tiona = tp * 11605.0

  all.zimpa = 74.0
  all.amimpa = 135.0
  all.frimpa = 1.0e-5

  adf25 = root + '/adf25/a25_p316/bn#74/bn#74_w' + $
           string(izr, format='(i2)') + '_n1.dat'
  write_adf25, outfile=adf25, fulldata=all

  adf40 = root + '/adf40/w/fpec_w' + string(izr, format='(i2.2)') + '_n1.dat'

  run_adas316, adf25=adf25, adf40=adf40, $
               npix = npix, wvmin=wvmin, wvmax=wvmax

endfor

end

```

3.2.3 Demo (c-3) demo_c_3.pro

```
PRO demo_c_3

; Local plasma conditions of beam plasma intersection

te    = 20.0e3
dens = 1.01e14

; Set of CX adf40 emission

adf40 = file_search('adf40/w/fpec*.dat', count=nfiles)
z_low = 51
z_high = 71
iz     = indgen(z_high-z_low+1) + z_low
n_z    = n_elements(iz)

; Equilibrium ionisation balance for W with central ADAS year 50 set

run_adas405, uid='adas', year=50, elem='w', te=te, dens=dens, frac=frac

; Construct the spectrum from adf40 and multiply by fractional abundance
; Note that adas316 generated adf40 at the reference Te/Ne/Eb condition
; ie there is no ability to interpolated to different plasma conditions.

npix  = 1000
wmin  = 3000.0
wmax  = 7000.0
wave  = adas_vector(low=wmin, high=wmax, num=npix, /linear)
delta = wave[1] - wave[0]

emiss_active = fltarr(npix)                      ; Cumulative spectrum

k = 0
for iz = z_low, z_high do begin

    read_adf40, file=adf40[k], fulldata=all

    emiss_active = emiss_active + frac.ion[0,iz] * all.fpec / delta
        ; fPECs are /pixel, we need /Angstrom

    k += 1

endfor

; Integrate the emission over beam size - assume an ITER DNB of 2MW power,
```

```

; 50keV/amu energy and height of 45cm - assume a W concentration of 1e-5

conc = 1.0e-5
nbeam = 6.0e8
hbeam = 45.0

emiss_active_int = emiss_active * nbeam * (conc * dens) * hbeam

set_plot,'ps'
device, /isolatin1, font_index=8
device, bits=8, filename='demo_c_3_active.ps', $
    font_size = 14, xsize=18.0, ysize=16.0, $
    yoffset=7.0, /color;
device, /helvetica

plot, wave, emiss_active_int,$
    xtitle='Wavelength (Angstrom)', $
    ytitle = 'Intensity (ph cm^-2!n s!u-1!n A!u-1!n)', $
    xmargin=[12,3]

device, /close
set_plot,'X'
!p.font=-1

; Calculate the continuum emission from H only using ITER reference scenario 2
; and a vertical line of sight. The plasma profiles along the LOS are

d = [ 0.0000e+00, 9.0909e+00, 1.8182e+01, 2.7273e+01, 3.6364e+01, $
      4.5455e+01, 5.4545e+01, 6.3636e+01, 7.2727e+01, 8.1818e+01, $
      9.0909e+01, 1.0000e+02, 1.0909e+02, 1.1818e+02, 1.2727e+02, $
      1.3636e+02, 1.4545e+02, 1.5455e+02, 1.6364e+02, 1.7273e+02, $
      1.8182e+02, 1.9091e+02, 2.0000e+02, 2.0909e+02, 2.1818e+02, $
      2.2727e+02, 2.3636e+02, 2.4545e+02, 2.5455e+02, 2.6364e+02, $
      2.7273e+02, 2.8182e+02, 2.9091e+02, 3.0000e+02, 3.0909e+02, $
      3.1818e+02, 3.2727e+02, 3.3636e+02, 3.4545e+02, 3.5455e+02, $
      3.6364e+02, 3.7273e+02, 3.8182e+02, 3.9091e+02, 4.0000e+02, $
      4.0909e+02, 4.1818e+02, 4.2727e+02, 4.3636e+02, 4.4545e+02, $
      4.5455e+02, 4.6364e+02, 4.7273e+02, 4.8182e+02, 4.9091e+02, $
      5.0000e+02, 5.0909e+02, 5.1818e+02, 5.2727e+02, 5.3636e+02, $
      5.4545e+02, 5.5455e+02, 5.6364e+02, 5.7273e+02, 5.8182e+02, $
      5.9091e+02, 6.0000e+02, 6.0909e+02, 6.1818e+02, 6.2727e+02, $
      6.3636e+02, 6.4545e+02, 6.5455e+02, 6.6364e+02, 6.7273e+02, $
      6.8182e+02, 6.9091e+02, 7.0000e+02, 7.0909e+02, 7.1818e+02, $
      7.2727e+02, 7.3636e+02, 7.4545e+02, 7.5455e+02, 7.6364e+02, $
      7.7273e+02, 7.8182e+02, 7.9091e+02, 8.0000e+02, 8.0909e+02, $
      8.1818e+02, 8.2727e+02, 8.3636e+02, 8.4545e+02, 8.5455e+02, $
      8.6364e+02, 8.7273e+02, 8.8182e+02, 8.9091e+02, 9.0000e+02 ]]

te = [ 5.0000e+01, 5.0000e+01, 5.0000e+01, 5.0000e+01, 5.0000e+01, $
```

```

5.0000e+01, 5.0000e+01, 5.0000e+01, 5.0000e+01, 5.0000e+01, $
5.0000e+01, 5.0000e+01, 5.0000e+01, 5.0000e+01, 5.0000e+01, $
5.0000e+01, 5.0947e+01, 1.3802e+02, 8.9934e+02, 2.4124e+03, $
3.0462e+03, 3.2800e+03, 3.5272e+03, 3.7913e+03, 4.0776e+03, $
4.3872e+03, 4.7341e+03, 5.1028e+03, 5.4936e+03, 5.9293e+03, $
6.4070e+03, 6.9345e+03, 7.5085e+03, 8.1055e+03, 8.7299e+03, $
9.4337e+03, 1.0205e+04, 1.1033e+04, 1.1930e+04, 1.2889e+04, $
1.3882e+04, 1.4895e+04, 1.5920e+04, 1.6921e+04, 1.7885e+04, $
1.8818e+04, 1.9700e+04, 2.0513e+04, 2.1264e+04, 2.1951e+04, $
2.2557e+04, 2.3085e+04, 2.3523e+04, 2.3869e+04, 2.4125e+04, $
2.4280e+04, 2.4333e+04, 2.4284e+04, 2.4134e+04, 2.3878e+04, $
2.3532e+04, 2.3092e+04, 2.2558e+04, 2.1946e+04, 2.1253e+04, $
2.0491e+04, 1.9666e+04, 1.8767e+04, 1.7811e+04, 1.6826e+04, $
1.5803e+04, 1.4753e+04, 1.3717e+04, 1.2713e+04, 1.1744e+04, $
1.0820e+04, 9.9907e+03, 9.2201e+03, 8.5092e+03, 7.8700e+03, $
7.2528e+03, 6.6671e+03, 6.1215e+03, 5.6368e+03, 5.1965e+03, $
4.7808e+03, 4.3867e+03, 4.0308e+03, 3.6993e+03, 3.3895e+03, $
3.0920e+03, 2.3507e+03, 4.7135e+02, 5.4887e+01, 5.0000e+01, $
5.0000e+01, 5.0000e+01, 5.0000e+01, 5.0000e+01, 5.0000e+01, ]
]

dens = [1.2644e+10, 1.0410e+10, 1.0000e+10, 1.0000e+10, 1.0000e+10, $
1.0000e+10, 1.0920e+10, 1.3384e+10, 1.6654e+10, 2.5761e+10, $
4.0784e+10, 7.1152e+10, 1.3571e+11, 2.7752e+11, 6.3022e+11, $
1.5611e+12, 4.2606e+12, 1.8577e+13, 4.8794e+13, 8.4619e+13, $
9.7046e+13, 9.9647e+13, 1.0178e+14, 1.0352e+14, 1.0492e+14, $
1.0609e+14, 1.0699e+14, 1.0780e+14, 1.0845e+14, 1.0896e+14, $
1.0940e+14, 1.0977e+14, 1.1006e+14, 1.1031e+14, 1.1052e+14, $
1.1073e+14, 1.1090e+14, 1.1104e+14, 1.1118e+14, 1.1133e+14, $
1.1145e+14, 1.1157e+14, 1.1167e+14, 1.1180e+14, 1.1194e+14, $
1.1207e+14, 1.1215e+14, 1.1223e+14, 1.1232e+14, 1.1240e+14, $
1.1248e+14, 1.1254e+14, 1.1258e+14, 1.1261e+14, 1.1264e+14, $
1.1265e+14, 1.1266e+14, 1.1266e+14, 1.1264e+14, 1.1261e+14, $
1.1258e+14, 1.1254e+14, 1.1248e+14, 1.1240e+14, 1.1232e+14, $
1.1222e+14, 1.1215e+14, 1.1207e+14, 1.1193e+14, 1.1178e+14, $
1.1166e+14, 1.1155e+14, 1.1144e+14, 1.1130e+14, 1.1115e+14, $
1.1100e+14, 1.1086e+14, 1.1067e+14, 1.1045e+14, 1.1023e+14, $
1.0994e+14, 1.0958e+14, 1.0916e+14, 1.0864e+14, 1.0795e+14, $
1.0711e+14, 1.0608e+14, 1.0475e+14, 1.0302e+14, 1.0064e+14, $
9.7578e+13, 8.3379e+13, 3.6986e+13, 6.0841e+12, 1.4363e+12, $
3.9416e+11, 1.1876e+11, 3.7860e+10, 1.4183e+10, 1.0000e+10, ]
]

nd      = n_elements(d)

; call continuo with 100 pixels and integrate along LOS

nw      = 100
wave_c = adas_vector(low=wmin, high=wmax, num=nw)

continuo, wave_c, te, 1, 1, contff_d, contin_d

```

```

emiss_cont = contin_d * (rebin(reform(dens, 1, nd), nw, nd))^2.0
; nb this inflates dens along wavelength

emiss_cont_int = dblarr(nw)

for j = 0, nw-1 do emiss_cont_int[j] = int_tabulated(d, emiss_cont[j,*], /double)

; Compare the contributions by plotting the results on one graph

xmin = wmin
xmax = wmax
ymin = min([emiss_active_int, emiss_cont_int], max=ymax)
ymin = 1e8
ymax = 1e15

set_plot,'ps'
device, /isolatin1, font_index=8
device, bits=8, filename='demo_c_3_compare.ps', $
    font_size = 14, xsize=18.0, ysize=16.0, $
    yoffset=7.0, /color;
device, /helvetica

plot_io, [xmin, xmax], [ymin, ymax], /nodata, $
    xtitle = 'Wavelength (Angstrom)', $
    ytitle = 'Intensity (ph cm^-2!n s^-1!n A^-1!n)'

oplot, wave_c, emiss_cont_int, line=2, thick=5
oplot, wave, emiss_active_int

device, /close
set_plot,'X'
!p.font=-1

END

```

4 Demo (d) Looking at Stark multiplet emission for the H-beam

DEMO D: Looking at Stark multiplet emission for the H-beam

PURPOSE: Look at the hydrogen Stark feature as components and as a Doppler broadened feature.

EXAMPLE: For this demo a deuterium beam and a deuterium plasma are considered.

Beam details are the following:

H beam mass (deuterium): 2.0

Energy: 78.0e3e V/amu

Temperature: 10.0 eV

Density: 1.00e10 cm⁻³

Direction cosines for velocity components: x = 0.0, y = 0.0, z = 1.0

Plasma details are the following:

H plasma mass (deuterium): 2.0

Temperature: 4440.0 eV

Density: 2.49e13 cm⁻³

Effective charge: 2.0

Magnetic field details are the following:

Value: 3.3915 Tesla

Direction cosines for components: x = 0.788, y = 0.788, z = 0.0

Electric field details are the following:

Value: 0.0000 Volts

Direction cosines for components: x = 1.000, y = 1.000, z = 0.0

Viewing line of sight details are the following:

Direction cosines for components: x = 0.8701, y = -0.047, z = 0.4905

Specific sigma polarisation: 1.0

Specific pi polarisation: 1.0

H Balmer alpha line is chosen:

n_lower=2

n_upper=3

DEMO d1: Working offline with adas305_get_stark.pro

1. Define beam, plasma, magnetic, electric and observed line of sight details.

2. Use adas305_get_stark.pro to get Stark and Doppler-broadened features for D(n=3-2).

3. Plot Stark line emission and Doppler broadening.

Program: demo_d.pro

Output file: demo_d.ps

4.1 Demo (d) Figures

4.1.1 Demo (d-1) demo_d/demo_d.pdf

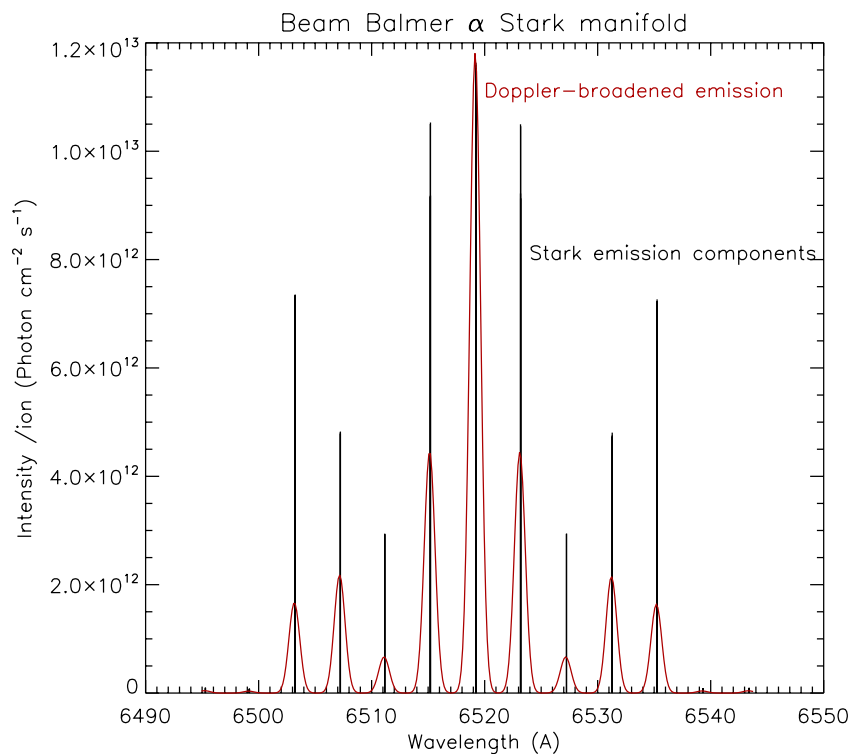


Figure 6:

4.2 Demo (d) IDL procedures

4.2.1 Demo (d-1) demo.d/demo_d.pro

```
pro demo_d
;Use adas305_get_stark.pro to calculate the D(n=3-2) Stark manifold.

;Set all parameters

;Beam details: H beam mass -> 2 for deuterium; energy in eV/amu, te in eV,
;density in cm-3, dc_X,dc_y,dc_z are velocity component directions
beam = {mass : 2.0, energy : 78.0e3, te : 10.0, density : 1.00e10, $
        dc_x : 0.0, dc_y : 0.0, dc_z : 1.0}

;Plasma details
plasma = {mass : 2.0, te : 4440.0, density : 2.49e13, zeff : 2.0}

;Magnetic field details
bfield = {value : 3.3915, dc_x : 0.788, dc_y : 0.788, dc_z : 0.0}

;Electric field details
efield = {value : 0.0000, dc_x : 1.000, dc_y : 1.0000, dc_z : 0.0000}

;Viewing line of sight details
obs = {dc_x : 0.8701, dc_y : -0.047, dc_z : 0.4905, sigma : 1.0, pi : 1.0}

;Number of pixels
npix = 360

;Use adas305_get_stark.pro to get the wavelength components of stark feature
;together with the associated emission and the emission Doppler-bradened on to
;the wavelength grid
adas305_get_stark, beam      = beam,      $
plasma       = plasma,      $
bfield       = bfield,      $
efield       = efield,      $
obs          = obs,          $
n_lower      = 2,          $
n_upper      = 3,          $
wave_comp    = wave_comp,   $
emiss_comp   = emiss_comp,  $
wave_min     = wave_min,   $
wave_max     = wave_max,   $
npix         = npix,         $
adf22        = adf22,        $
emiss_doppler = emiss_doppler, $
wave_doppler  = wave_doppler, $
/doppler,/auto_wave
```

```

;Plot Stark line emission and Doppler broadening for D(n=3-2)
loadct,3
set_plot,'ps'
device, /isolatin1, font_index=8
device, bits=8, filename='demo_d.ps',           $
      font_size = 14, xsize=18.0, ysize=16.0, $ 
      yoffset=7.0, /color
device, /helvetica

plot, wave_comp, emiss_comp,/nodata, $
      title='Beam Balmer !7a!3 Stark manifold',xmargin=[12,3],$ 
      xtitle='Wavelength (A)', $
      ytitle = 'Intensity /ion (Photon cm!u-2!n s!u-1!n)'
for i = 0, n_elements(wave_comp)-1 do oplot,[wave_comp[i],wave_comp[i]], $
      [0,emiss_comp[i]]
plots, wave_doppler, emiss_doppler,color=120

xyouts,6524.,8.e12,'Stark emission components'
xyouts,6520.,1.1e13,'Doppler-broadened emission',color=120

device, /close
set_plot,'X'
!p.font=-1

end

```

C.7 module_7

MODULE 7

Calculating fundamental atomic structure and electron impact cross-section data - Autostructure and R-Matrix.

Demonstration script

Hugh Summers, Nigel Badnell, Martin O'Mullane and Alessandra Giunta
September 29, 2013

Contents

| | |
|---|-----------|
| 1 Demo (a) Introducing the Cowan code | 3 |
| 1.1 Demo (a) Figures | 5 |
| 1.2 Demo (a) Procedures | 5 |
| 1.2.1 Demo (a-1) demo_d/fe22.dat | 5 |
| 1.2.2 Demo (a-2) demo_a/ic#fe22.dat | 5 |
| 1.2.3 Demo (a-3) demo_a/demo_a_3.sh | 7 |
| 1.2.4 Demo (a-3) demo_a/fe22.inst | 7 |
| 1.2.5 Demo (a-3) demo_a/fe22.pp | 7 |
| 1.2.6 Demo (a-3) demo_a/fe22_offline.dat | 8 |
| 2 Demo (b) Introducing the Autostructure code | 9 |
| 2.1 Demo (b) Figures | 10 |
| 2.2 Demo (b) Procedures | 10 |
| 2.2.1 Demo (b-1) demo_b/ic#fe22_adf27.dat | 10 |
| 2.2.2 Demo (b-1) demo_b/ls#fe22_adf27.dat | 11 |
| 2.2.3 Demo (b-2) demo_b/demo_b_2.sh | 11 |
| 2.2.4 Demo (b-2) demo_b/adf04ic.dat | 11 |
| 2.2.5 Demo (b-2) demo_b/adf04ls.dat | 13 |
| 2.2.6 Demo (b-3) demo_b/demo_b3.pro | 14 |
| 2.2.7 Demo (b-3) demo_b/ic#fe22_as.dat | 14 |
| 3 Demo (c) Compare the resulting adf04 files | 16 |
| 3.1 Demo (c) Figures | 17 |
| 3.1.1 Demo (c-1) demo_c/adas811_plot_example1.pdf | 17 |
| 3.1.2 Demo (c-1) demo_c/adas811_plot_example2.pdf | 18 |
| 3.2 Demo (c) Procedures | 19 |
| 3.2.1 Demo (c-1) demo_c/belike_nrb05#fe22.dat | 19 |

| | |
|---|-----------|
| 4 Demo (d) R-Matrix | 21 |
| 4.1 Demo (d) Figures | 22 |
| 4.2 Demo (d) Procedures | 22 |
| 4.2.1 Demo (d-1) demo.d/adas803.pl | 22 |
| 4.2.2 Demo (d-1) demo.d/Makefile | 23 |
| 4.2.3 Demo (d-1) demo.d/parallel_procfile | 25 |
| 4.2.4 Demo (d-1) demo.d/input.dat | 25 |

1 Demo (a) Introducing the Cowan code

DEMO A: Introducing the Cowan code

PURPOSE: To calculate excitation cross section using Plane Wave Born (PWB) approximation, as implemented within ADAS801 using the Cowan code.

The input file is in the adf34 format.

This gives the set of configurations according to the parity for each ionisation stage.

The format is fixed. It requires the element symbol, the atomic number, the ionisation stage charge +1 and the configurations to build up the appropriate atomic structure.

The output is a Type 1 or 3 adf04 data file (See Module 1 Demo c)... .

EXAMPLE: For this demo Be-like Fe (Fe22+) is considered.

The input file in the adf34 format for the ADAS801 run is fe22.dat.

For adas8#1 offline run, the executable is

/home/adas/offline_adas/adas8#1/scripts/run_adas8#1.

It requires the input file adf34, fe22.dat, together with two other files, fe22.inst and fe22.pp, which set up the type of transition (electric dipole, magnetic dipole etc.), the temperature range requested for calculating the cross sections, scale factors and the other parameter needed for the run.

Type 3 adf04 in ic resolution has been established as output for this demo:

- for the interactive run the output adf04 is ic#fe22.dat;
- for the offline run the output adf04 is fe22_offline.dat.

COMMENTS: Note that the configurations must be grouped according to their parity.

For example for F22+, 15 configurations are included in the adf34 fe22.dat as follows:

| | | |
|---------|-----|---------|
| 2s2 | 1s2 | 2s2 |
| 2s1 3s1 | 1s2 | 2s1 3s1 |
| 2s1 4s1 | 1s2 | 2s1 4s1 |
| 2s1 3d1 | 1s2 | 2s1 3d1 |
| 2s1 4d1 | 1s2 | 2s1 4d1 |
| 2p2 | 1s2 | 2p2 |
| 2p1 3p1 | 1s2 | 2p1 3p1 |
| 2p1 4p1 | 1s2 | 2p1 4p1 |
| 2s1 2p1 | 1s2 | 2s1 2p1 |
| 2s1 3p1 | 1s2 | 2s1 3p1 |
| 2s1 4p1 | 1s2 | 2s1 4p1 |
| 2s1 4f1 | 1s2 | 2s1 4f1 |
| 2p1 3s1 | 1s2 | 2p1 3s1 |
| 2p1 3d1 | 1s2 | 2p1 3d1 |
| 2p1 4d1 | 1s2 | 2p1 4d1 |

According to the Parity ($P=(-1)^{\sum(l_i)}$), the first group include only even configurations:

| | | |
|---------|-----|---------|
| 2s2 | 1s2 | 2s2 |
| 2s1 3s1 | 1s2 | 2s1 3s1 |
| 2s1 4s1 | 1s2 | 2s1 4s1 |
| 2s1 3d1 | 1s2 | 2s1 3d1 |
| 2s1 4d1 | 1s2 | 2s1 4d1 |
| 2p2 | 1s2 | 2p2 |
| 2p1 3p1 | 1s2 | 2p1 3p1 |
| 2p1 4p1 | 1s2 | 2p1 4p1 |

while the second group includes only odd configurations:

| | | |
|---------|-----|---------|
| 2s1 2p1 | 1s2 | 2s1 2p1 |
| 2s1 3p1 | 1s2 | 2s1 3p1 |
| 2s1 4p1 | 1s2 | 2s1 4p1 |
| 2s1 4f1 | 1s2 | 2s1 4f1 |
| 2p1 3s1 | 1s2 | 2p1 3s1 |
| 2p1 3d1 | 1s2 | 2p1 3d1 |
| 2p1 4d1 | 1s2 | 2p1 4d1 |

DEMO a1: Examine the adf34 driver file for Be-like Fe (Fe22+)

1. Open the adf34 file fe22.dat and explore it.

Sample of adf34 files: fe22.dat

DEMO a2: Use interactive ADAS801 to make Fe22+ adf04 file

1. Run ADAS801 interactively.

2. Set up Intermediate Coupling adf04 in the output window.

Output file: ic#fe22.dat

DEMO a3: Use offline_adas/adas8#1 for same Fe22+

1. Look at the input files fe22.inst and fe22.pp.

2. Type /home/adas/offline_adas/adas8#1/scripts/run_adas8#1 fe22.dat fe22.inst fe22.pp from the command line.

Sample of script: demo_a_3.sh

Input files: fe22.dat, fe22.inst, fe22.pp

Output file: fe22_offline.dat

1.1 Demo (a) Figures

1.2 Demo (a) Procedures

1.2.1 Demo (a-1) demo.d/fe22.dat

```
2 -5 2 10 1.0 5.d-09 5.d-11-2 0130 1.0 0.65 0.0 0.5
26 23 Fe 2s2 1s2 2s2
26 23 Fe 2s1 3s1 1s2 2s1 3s1
26 23 Fe 2s1 4s1 1s2 2s1 4s1
26 23 Fe 2s1 3d1 1s2 2s1 3d1
26 23 Fe 2s1 4d1 1s2 2s1 4d1
26 23 Fe 2p2 1s2 2p2
26 23 Fe 2p1 3p1 1s2 2p1 3p1
26 23 Fe 2p1 4p1 1s2 2p1 4p1
26 23 Fe 2s1 2p1 1s2 2s1 2p1
26 23 Fe 2s1 3p1 1s2 2s1 3p1
26 23 Fe 2s1 4p1 1s2 2s1 4p1
26 23 Fe 2s1 4f1 1s2 2s1 4f1
26 23 Fe 2p1 3s1 1s2 2p1 3s1
26 23 Fe 2p1 3d1 1s2 2p1 3d1
26 23 Fe 2p1 4d1 1s2 2p1 4d1
-1
```

1.2.2 Demo (a-2) demo.a/ic#fe22.dat

```
FE+22 26 23 15730300.0
1 1S2 2S2 (1)0( 0.0) 0.0
2 1S2 2S1 2P1 (3)1( 0.0) 354118.2
3 1S2 2S1 2P1 (3)1( 1.0) 382472.7
4 1S2 2S1 2P1 (3)1( 2.0) 467040.0
5 1S2 2S1 2P1 (1)1( 1.0) 696851.6
6 1S2 2P2 (3)1( 0.0) 960656.6
7 1S2 2P2 (3)1( 1.0) 1027340.8
.
81 1S2 2P1 4D1 (1)3( 3.0) 12617526.6
82 1S2 2P1 4D1 (1)1( 1.0) 12620938.0
-1 633.698 146.252 141.219 61.9155 60.3980 59.3358 34.3952 33.7317
23.0 3 2.65+05 5.29+05 1.06+06 1.59+06 2.65+06 5.29+06 7.94+06
3 1 7.04+07 9.66-03 1.01-02 1.09-02 1.15-02 1.24-02 1.37-02 1.46-02
5 1 1.62+10 3.34-01 3.42-01 3.58-01 3.72-01 3.95-01 4.36-01 4.63-01
.
82 79 1.27+00 2.11-02 2.55-02 2.88-02 3.02-02 3.14-02 3.24-02 3.27-02
82 81 9.20-07 1.43-02 1.90-02 2.38-02 2.66-02 3.02-02 3.51-02 3.80-02
-1
-1 -1
C-----
```

C Configuration
C Eissner == Standard R % Parentage

```

C   1  521522      ==  1S2 2S2          97  1 1S  1S/
C   2  521512513    ==  1S2 2S1 2P1     100  1 2S  2S/ 1 2P  3P/
C   3  521512513    ==  1S2 2S1 2P1      97  1 2S  2S/ 1 2P  3P/
C   4  521512513    ==  1S2 2S1 2P1     100  1 2S  2S/ 1 2P  3P/
C   5  521512513    ==  1S2 2S1 2P1      97  1 2S  2S/ 1 2P  1P/
C   6  521523       ==  1S2 2P2          92  1 3P  3P/
.
.
C   77 521513519    ==  1S2 2P1 4D1      58  1 2P  2P/ 1 2D  3D/
C   78 521513519    ==  1S2 2P1 4D1      71  1 2P  2P/ 1 2D  3P/
C   79 521513519    ==  1S2 2P1 4D1      51  1 2P  2P/ 1 2D  3P/
C   80 521513519    ==  1S2 2P1 4D1     100  1 2P  2P/ 1 2D  3P/
C   81 521513519    ==  1S2 2P1 4D1      73  1 2P  2P/ 1 2D  1F/
C   82 521513519    ==  1S2 2P1 4D1      74  1 2P  2P/ 1 2D  1P/
C
C (R) - Levels (or levels within a term) have been reassigned
C      from their principal component.
C
C (excl) - Levels included in structure but no A-value or
C           collision strength calculated.
C
C-----
C
C   Generated from Cowan Atomic Structure Program
C
C   From IFG file : /home/mog/adas/pass/ifg#fe22.dat
C
C   Options in effect
C
C   Coupling      Avalue      numtemps      Lweight      Isonuclear      Comment Level
C   IC            YES         14             NO            NO              2
C
C
C   Cowan code options
C -----
C
C   SCF method used : HR
C
C   Scale factors for Slater Parameters : 80 90 80 80 80
C
C   Optically allowed transitions : Yes
C
C   Optically forbidden transitions (M1) : Both Parities
C
C   Optically forbidden transitions (E2) : Both Parities
C
C   Born Collision-Strength - forbidden : 0 -> 2
C
C   Born Collision-Strength - allowed   : 1 -> 1
C

```

```

C   Parity 1      Parity 2      Allowed
C       550          753          1071      initially
C       550          753          1071      reduced
C
C   Note: The Born method does NOT calculate spin changing transitions
C   correctly. You should supplement for important transitions of this type.
C
C-----
C
C   Code      : ADAS801
C   Producer : Martin O'Mullane
C   Date     : 22/05/13
C
C-----

```

1.2.3 Demo (a-3) demo_a/demo_a_3.sh

```
/home/adas/offline_adas/adas8#1/scripts/run_adas8#1 fe22.dat fe22.inst fe22.pp
```

1.2.4 Demo (a-3) demo_a/fe22.inst

```

z0 26
zi 22
parity-1 8 : 8 1 2 3 4 5 6 7 8
parity-2 7 : 7 1 2 3 4 5 6 7
E2 3
M1 3
scale 80 90 80 80 80
temperature 25
1.00e+03 1.47e+03 2.15e+03 3.16e+03 4.64e+03 6.81e+03 1.00e+04 1.47e+04
2.15e+04 3.16e+04 4.64e+04 6.81e+04 1.00e+05 1.47e+05 2.15e+05 3.16e+05
4.64e+05 6.81e+05 1.00e+06 1.47e+06 2.15e+06 3.16e+06 4.64e+06 6.81e+06
1.00e+07

```

1.2.5 Demo (a-3) demo_a/fe22.pp

```

1
Martin O'Mullane
14-05-2014
5
C
C   Cowan plane wave Born method
C
C   Scale factors 80 90 80 80 80
C
&FILES ifgfile = 'ifg#fe22.dat' , outfile = 'fe22_offline.dat' &END
&OPTIONS ip = 15730300.0, coupling = 'IC' , aval = 'YES' , isonuclear =
'NO' , quantity = 'RATES' , lweight = 'NO' , comments = 2 , numtemp = 14 , &END
1 2 3 5 7 9 11 12 13 14 15 17 19 20
parity-1 8 : 8 1 2 3 4 5 6 7 8

```

parity-2 7 : 7 1 2 3 4 5 6 7

1.2.6 Demo (a-3) demo_a/fe22_offline.dat

```
FE+22      26      23      15730300.0
  1 1S2 2S2          (1)0( 0.0)          0.0
  2 1S2 2S1 2P1      (3)1( 0.0)      354118.2
  3 1S2 2S1 2P1      (3)1( 1.0)      382472.7
  4 1S2 2S1 2P1      (3)1( 2.0)      467040.0
  5 1S2 2S1 2P1      (1)1( 1.0)      696851.6
  .
  81 1S2 2P1 4D1      (1)3( 3.0)      12617526.6
  82 1S2 2P1 4D1      (1)1( 1.0)      12620938.0
 -1      633.698 146.252 141.219 61.9155 60.3980 59.3358 34.3952 33.7317
23.0      3      5.29+05 7.78+05 1.14+06 2.45+06 5.29+06 1.14+07 2.45+07
  3      1 7.04+07 1.01-02 1.05-02 1.10-02 1.22-02 1.37-02 1.54-02 1.73-02
  5      1 1.62+10 3.42-01 3.50-01 3.60-01 3.91-01 4.36-01 4.90-01 5.52-01

  82 79 1.27+00 2.55-02 2.75-02 2.91-02 3.13-02 3.24-02 3.30-02 3.32-02
  82 81 9.20-07 1.90-02 2.16-02 2.43-02 2.97-02 3.51-02 4.06-02 4.60-02
 -1
 -1 -1
C-----
C
C           Configuration
C           Eissner      == Standard      R % Parentage
C
C     1 521522      == 1S2 2S2      97 1 1S 1S/
C     2 521512513    == 1S2 2S1 2P1    100 1 2S 2S/ 1 2P 3P/
C
C     81 521513519    == 1S2 2P1 4D1      73 1 2P 2P/ 1 2D 1F/
C     82 521513519    == 1S2 2P1 4D1      74 1 2P 2P/ 1 2D 1P/
C
C (R) - Levels (or levels within a term) have been reassigned
C       from their principal component.
C
C (excl) - Levels included in structure but no A-value or
C           collision strength calculated.
C
C-----
```

C

C Generated from Cowan Atomic Structure Program

C

C From IFG file : ifg#fe22.dat

C

C Options in effect

C

| Coupling | Avalue | numtemp | Lweight | Isonuclear | Comment | Level |
|----------|--------|---------|---------|------------|---------|-------|
| IC | YES | 14 | NO | NO | | 2 |

```

C
C Cowan code options
C -----
C
C Cowan plane wave Born method
C
C Scale factors 80 90 80 80 80
C
C Parity 1    Parity 2    Allowed
C      550        753        1071    initially
C      550        753        1071    reduced
C
C Note: The Born method does NOT calculate spin changing transitions
C correctly. You should supplement for important transitions of this type.
C
C-----
C
C Code      : ADAS801
C Producer  : Martin O'Mullane
C Date      : 14-05-2014
C
C-----

```

2 Demo (b) Introducing the Autostructure code

DEMO B: Introducing the Autostructure code

PURPOSE: To calculate excitation cross section in the Distorted Wave (DW) approximation using the ADAS offline version adas7#1. The code is a full implementation of the program AUTOSTRUCTURE, which has been developed by N.R. Badnell.

The input file for the AUTOSTRUCTURE run is in the adf27 format. This format is different from the adf34 which drives the ADAS801 run. It contains a series of parameters which regulate the type of calculation (RUN=''), coupling scheme (CUP=''), free electron energy ranges (EMIN='', EMAX=''), the orbital specification (e.g. 2 0 2 1 3 0 3 1 3 2 4 0 4 1 4 2 4 3) and the occupation numbers (e.g. 1 0 0 0 1 0 0 0 means one electron in 2s orbital and one electron in 3d orbital). See the ADAS manual for further parameter specifications.

EXAMPLE: As for Demo a, Be-like Fe (Fe22+) is considered.
The input files in the adf27 format are the following:

- for ls resolution: ls#fe22_adf27.dat;
- for ic resolution: ic#fe22_adf27.dat

The executable is /home/adas/offline_adas/adas7#1/bin/as24.x.

The output are Type 5 adf04 (See Module 1 Demo c) data files in ls and ic

resolution.

They will be provided with Eissner configuration. In order to convert them from Eissner to Standard configuration the program /home/asg/adas_dev/idl/adaslib/proc_adf/trim_cophps_adf04.pro is used. This program reduces the number of levels (and transitions) of an adf04 file to those below 105% of the ionisation potential, changes the Eissner configuration to standard and re-orders the transition list.

COMMENTS: Note that for this demo a restricted number of transitions has been included in the cross section calculation. This has been done to constrain the running time.

DEMO b1: Examine adf27 driver file for Fe22+

1. Open the adf27 files ic#fe22_adf27.dat and ls#fe22_adf27.dat and explore them. Sample of adf27 files: ic#fe22_adf27.dat, ls#fe22_adf27

DEMO b2: Offline_adas/adas7#1 for Fe22+ distorted wave

1. Type /home/adas/offline_adas/adas7#1/bin/as24.x < ic#fe22_adf27.dat for producing a Type 5 adf04 in ic resolution.
(Note that this will take a few minutes.)
 2. Type /home/adas/offline_adas/adas7#1/bin/as24.x < ls#fe22_adf27.dat for producing a Type 5 adf04 in ic resolution.
(Note that this will take a few minutes.)
- Sample of script: demo_b_2.sh
Output files: adf04ic, adf04ls

DEMO b3: Use trim_cophps_adf04.pro to trim AS adf04 and
get Standard Configurations

1. Use trim_cophps_adf04.pro to remove the levels above the ionisation potential and convert the configuration from Eissner to Standard notation.
Program: demo_b_3.pro
Output file: ic#fe22_as.dat

2.1 Demo (b) Figures

2.2 Demo (b) Procedures

2.2.1 Demo (b-1) demo.b/ic#fe22.adf27.dat

```
A.S. Be-like fe22 structure - energies + radiative rates + dw adf04 type 5
&SALGEB RUN='DE' CUP='ICR' KCOR1=1 KCOR2=1 NMETA=2 MXCONF=9 MXVORB=9  &END
2 0 2 1 3 0 3 1 3 2 4 0 4 1 4 2 4 3
2   0   0   0   0   0   0   0   0   0
1   1   0   0   0   0   0   0   0   0
1   0   1   0   0   0   0   0   0   0
```

```

1   0   0   1   0   0   0   0   0
1   0   0   0   1   0   0   0   0
1   0   0   0   0   1   0   0   0
1   0   0   0   0   0   1   0   0
1   0   0   0   0   0   0   1   0
1   0   0   0   0   0   0   0   1
&SMINIM NZION=26 ORTHOG='NO' JPRINT=-33 MAXE=719 MSTEP=12 &END
&SRADCON MENG=-14 EMIN=0.719 EMAX=719 NDE=8 MENGI=-1 &END
 3.943264 6.866504 9.786447 10.75793 86.6706 89.10385 110.4799 122.3742

```

2.2.2 Demo (b-1) demo_b/ls#fe22_adf27.dat

```

A.S. Be-like fe22 structure - energies + radiative rates + dw adf04 type 5
&SALGEB RUN='DE' CUP='LSR' KCOR1=1 KCOR2=1 NMETA=2 MXCONF=9 MXVORB=9 &END
2 0 2 1 3 0 3 1 3 2 4 0 4 1 4 2 4 3
2   0   0   0   0   0   0   0   0   0   0
1   1   0   0   0   0   0   0   0   0
1   0   1   0   0   0   0   0   0   0
1   0   0   1   0   0   0   0   0   0
1   0   0   0   1   0   0   0   0   0
1   0   0   0   0   1   0   0   0   0
1   0   0   0   0   0   1   0   0   0
1   0   0   0   0   0   0   1   0   0
1   0   0   0   0   0   0   0   0   1
&SMINIM NZION=26 ORTHOG='NO' JPRINT=-33 MAXE=719 MSTEP=12 &END
&SRADCON MENG=-14 EMIN=0.719 EMAX=719 NDE=8 MENGI=-1 &END
3.943264 6.866504 9.786447 10.75793 86.6706 89.10385 110.4799 122.3742

```

2.2.3 Demo (b-2) demo_b/demo_b_2.sh

```
/home/adas/offline_adas/adas7#1/bin/as24.x < ic#fe22_adf27.dat  
/home/adas/offline_adas/adas7#1/bin/as24.x < ls#fe22_adf27.dat
```

2.2.4 Demo (b-2) demo_b/adf04ic.dat

| FE+22 | 26 | 23 | 15732424.0413 |
|-------|--------|------------|---------------|
| 1 | 522 | (1)0(0.0) | 0.0000 |
| 2 | 512513 | (3)1(0.0) | 294125.9172 |
| 3 | 512513 | (3)1(1.0) | 325899.9255 |
| 4 | 512513 | (3)1(2.0) | 415988.7673 |
| 5 | 512513 | (1)1(1.0) | 707772.8090 |
| 6 | 512514 | (3)0(1.0) | 8870629.5839 |
| 7 | 512514 | (1)0(0.0) | 8951832.3306 |
| 8 | 512515 | (3)1(0.0) | 9033381.3395 |
| 9 | 512515 | (3)1(1.0) | 9039155.3069 |
| 10 | 512515 | (3)1(2.0) | 9069060.1402 |
| 11 | 512515 | (1)1(1.0) | 9091505.2370 |
| 12 | 512516 | (3)2(1.0) | 9158129.9078 |
| 13 | 512516 | (3)2(2.0) | 9162034.5349 |
| 14 | 512516 | (3)2(3.0) | 9168854.9245 |

| | | | |
|-------|-----------|---|---------------|
| 15 | 512516 | (1)2(2.0) | 9234055.2919 |
| 16 | 512517 | (3)0(1.0) | 11914413.9492 |
| 17 | 512517 | (1)0(0.0) | 11938997.7345 |
| 18 | 512518 | (3)1(0.0) | 11978429.8706 |
| 19 | 512518 | (3)1(1.0) | 11980543.3733 |
| 20 | 512518 | (3)1(2.0) | 11993395.2560 |
| 21 | 512518 | (1)1(1.0) | 12000726.8394 |
| 22 | 512519 | (3)2(1.0) | 12030232.6316 |
| 23 | 512519 | (3)2(2.0) | 12031822.9851 |
| 24 | 512519 | (3)2(3.0) | 12034771.8869 |
| 25 | 512519 | (1)2(2.0) | 12053979.2430 |
| 26 | 51251A | (3)3(2.0) | 12056986.4039 |
| 27 | 51251A | (3)3(3.0) | 12057710.0117 |
| 28 | 51251A | (3)3(4.0) | 12059219.6822 |
| 29 | 51251A | (1)3(3.0) | 12063174.2569 |
| -1 | | 610.369 141.144 135.886 61.3953 59.9111 58.9282 34.1663 33.5524 | |
| 23.00 | 5 | 7.19-01 1.74+00 3.35+00 5.92+00 1.00+01 1.65+01 2.69+01 | |
| 2 | 1 1.00-30 | 1.26-03 1.25-03 1.23-03 1.20-03 1.16-03 1.09-03 9.94-04 | |
| 3 | 1 5.05+07 | 1.50-02 1.51-02 1.53-02 1.67-02 1.54-02 1.46-02 1.53-02 | |
| 4 | 1 1.00-30 | 6.27-03 6.21-03 6.12-03 5.98-03 5.76-03 5.43-03 4.95-03 | |
| 5 | 1 2.18+10 | 4.15-01 4.18-01 4.23-01 4.30-01 4.44-01 4.98-01 4.46-01 | |
| 6 | 1 1.00-30 | 1.25-03 1.23-03 1.20-03 1.16-03 1.09-03 1.00-03 8.76-04 | |
| 7 | 1 1.00-30 | 1.23-02 1.24-02 1.25-02 1.27-02 1.29-02 1.32-02 | |
| 8 | 1 1.00-30 | 2.92-04 2.87-04 2.82-04 2.73-04 2.61-04 2.42-04 2.15-04 | |
| 9 | 1 1.48+12 | 1.62-03 1.63-03 1.64-03 1.65-03 1.68-03 1.73-03 1.81-03 | |
| 10 | 1 1.00-30 | 1.45-03 1.43-03 1.40-03 1.36-03 1.30-03 1.21-03 1.07-03 | |
| 11 | 1 1.14+13 | 6.41-03 6.55-03 6.73-03 7.01-03 7.46-03 8.18-03 9.34-03 | |
| 12 | 1 1.00-30 | 1.81-03 1.78-03 1.75-03 1.69-03 1.60-03 1.47-03 1.29-03 | |
| 13 | 1 1.12+08 | 3.09-03 3.05-03 2.99-03 2.89-03 2.75-03 2.55-03 2.26-03 | |
| 14 | 1 1.00-30 | 4.22-03 4.16-03 4.07-03 3.93-03 3.73-03 3.43-03 3.02-03 | |
| 15 | 1 2.17+10 | 1.75-02 1.77-02 1.80-02 1.84-02 1.91-02 2.02-02 2.16-02 | |
| 16 | 1 1.00-30 | 4.23-04 4.16-04 4.07-04 3.92-04 3.70-04 3.39-04 2.96-04 | |
| 17 | 1 1.00-30 | 2.32-03 2.33-03 2.34-03 2.36-03 2.39-03 2.44-03 2.50-03 | |
| 18 | 1 1.00-30 | 1.09-04 1.08-04 1.06-04 1.03-04 9.80-05 9.11-05 8.08-05 | |
| 19 | 1 7.65+11 | 5.09-04 5.10-04 5.11-04 5.12-04 5.16-04 5.22-04 5.36-04 | |
| 20 | 1 1.00-30 | 5.46-04 5.39-04 5.29-04 5.13-04 4.90-04 4.55-04 4.04-04 | |
| 21 | 1 4.63+12 | 1.42-03 1.44-03 1.47-03 1.53-03 1.62-03 1.77-03 2.00-03 | |
| 22 | 1 1.00-30 | 5.18-04 5.12-04 5.02-04 4.86-04 4.63-04 4.29-04 3.81-04 | |
| 23 | 1 2.93+07 | 8.83-04 8.72-04 8.56-04 8.31-04 7.94-04 7.39-04 6.62-04 | |
| 24 | 1 1.00-30 | 1.21-03 1.19-03 1.17-03 1.13-03 1.08-03 1.00-03 8.89-04 | |
| 25 | 1 2.87+09 | 2.72-03 2.74-03 2.78-03 2.84-03 2.94-03 3.09-03 3.27-03 | |
| 26 | 1 1.00-30 | 4.38-04 4.30-04 4.19-04 4.01-04 3.75-04 3.38-04 2.88-04 | |
| 27 | 1 1.10+06 | 6.28-04 6.19-04 6.04-04 5.82-04 5.49-04 5.04-04 4.40-04 | |
| 28 | 1 1.00-30 | 7.88-04 7.75-04 7.54-04 7.22-04 6.75-04 6.09-04 5.19-04 | |
| 29 | 1 2.47+07 | 9.57-04 9.69-04 9.89-04 1.02-03 1.07-03 1.15-03 1.23-03 | |
| -1 | | | |
| -1 | -1 | | |

2.2.5 Demo (b-2) demo.b/adf04ls.dat

| | | | | | | | | |
|-------|-----------|------------|---------------|---------|---------|---------|---------|---------|
| FE+22 | 26 | 23 | 15732424.0413 | | | | | |
| 1 | 522 | (1)0(0.0) | 0.0000 | | | | | |
| 2 | 512513 | (3)1(4.0) | 375367.8485 | | | | | |
| 3 | 512513 | (1)1(1.0) | 698925.8983 | | | | | |
| 4 | 512514 | (3)0(1.0) | 8870629.5839 | | | | | |
| 5 | 512514 | (1)0(0.0) | 8951832.3306 | | | | | |
| 6 | 512515 | (3)1(4.0) | 9057167.1848 | | | | | |
| 7 | 512515 | (1)1(1.0) | 9085386.2500 | | | | | |
| 8 | 512516 | (3)2(7.0) | 9164564.9183 | | | | | |
| 9 | 512516 | (1)2(2.0) | 9233669.9138 | | | | | |
| 10 | 512517 | (3)0(1.0) | 11914413.9492 | | | | | |
| 11 | 512517 | (1)0(0.0) | 11938997.7345 | | | | | |
| 12 | 512518 | (3)1(4.0) | 11988406.7848 | | | | | |
| 13 | 512518 | (1)1(1.0) | 11997851.8701 | | | | | |
| 14 | 512519 | (3)2(7.0) | 12032956.1843 | | | | | |
| 15 | 512519 | (1)2(2.0) | 12053753.8930 | | | | | |
| 16 | 51251A | (3)3(10.0) | 12058262.5629 | | | | | |
| 17 | 51251A | (1)3(3.0) | 12062940.7455 | | | | | |
| -1 | 610.369 | 141.144 | 135.886 | 61.3953 | 59.9111 | 58.9282 | 34.1663 | 33.5524 |
| 23.00 | 5 | 7.19-01 | 1.74+00 | 3.35+00 | 5.92+00 | 1.00+01 | 1.65+01 | 2.69+01 |
| 2 | 1 1.00-30 | 1.13-02 | 1.12-02 | 1.10-02 | 1.08-02 | 1.04-02 | 9.78-03 | 8.92-03 |
| 3 | 1 2.15+10 | 4.26-01 | 4.29-01 | 4.34-01 | 4.41-01 | 4.56-01 | 5.10-01 | 4.56-01 |
| 3 | 2 1.00-30 | 3.37-02 | 3.33-02 | 3.26-02 | 3.15-02 | 2.99-02 | 2.76-02 | 2.44-02 |
| 4 | 1 1.00-30 | 1.25-03 | 1.23-03 | 1.20-03 | 1.16-03 | 1.09-03 | 1.00-03 | 8.76-04 |
| 4 | 2 2.28+12 | 3.83-03 | 3.82-03 | 3.81-03 | 3.80-03 | 3.81-03 | 3.81-03 | 3.85-03 |
| 5 | 1 1.00-30 | 1.23-02 | 1.23-02 | 1.24-02 | 1.25-02 | 1.27-02 | 1.29-02 | 1.32-02 |
| 5 | 2 1.00-30 | 1.03-03 | 1.02-03 | 1.00-03 | 9.74-04 | 9.35-04 | 8.77-04 | 7.94-04 |
| 6 | 1 1.00-30 | 2.62-03 | 2.58-03 | 2.53-03 | 2.45-03 | 2.34-03 | 2.17-03 | 1.93-03 |
| 6 | 2 4.21+09 | 8.07-02 | 8.07-02 | 8.07-02 | 8.05-02 | 8.03-02 | 8.03-02 | 8.01-02 |
| 7 | 1 1.29+13 | 7.16-03 | 7.32-03 | 7.52-03 | 7.84-03 | 8.36-03 | 9.18-03 | 1.05-02 |
| 7 | 2 1.00-30 | 7.42-03 | 7.32-03 | 7.17-03 | 6.92-03 | 6.56-03 | 6.05-03 | 5.34-03 |
| 8 | 1 1.00-30 | 9.04-03 | 8.92-03 | 8.73-03 | 8.43-03 | 7.99-03 | 7.35-03 | 6.47-03 |
| 8 | 2 2.04+13 | 2.37-01 | 2.38-01 | 2.40-01 | 2.42-01 | 2.47-01 | 2.55-01 | 2.68-01 |
| 9 | 1 2.18+10 | 1.76-02 | 1.78-02 | 1.81-02 | 1.85-02 | 1.92-02 | 2.03-02 | 2.17-02 |
| 9 | 2 1.00-30 | 1.82-02 | 1.79-02 | 1.74-02 | 1.68-02 | 1.58-02 | 1.44-02 | 1.24-02 |
| 10 | 1 1.00-30 | 4.23-04 | 4.16-04 | 4.07-04 | 3.92-04 | 3.70-04 | 3.39-04 | 2.96-04 |
| 10 | 2 7.08+11 | 1.16-03 | 1.15-03 | 1.14-03 | 1.13-03 | 1.11-03 | 1.08-03 | 1.05-03 |
| 11 | 1 1.00-30 | 2.32-03 | 2.33-03 | 2.34-03 | 2.36-03 | 2.39-03 | 2.44-03 | 2.50-03 |
| 11 | 2 1.00-30 | 3.91-04 | 3.87-04 | 3.80-04 | 3.71-04 | 3.56-04 | 3.34-04 | 3.03-04 |
| 12 | 1 1.00-30 | 9.83-04 | 9.71-04 | 9.52-04 | 9.24-04 | 8.82-04 | 8.19-04 | 7.27-04 |
| 12 | 2 1.19+09 | 1.78-02 | 1.77-02 | 1.76-02 | 1.75-02 | 1.74-02 | 1.72-02 | 1.69-02 |
| 13 | 1 5.39+12 | 1.60-03 | 1.62-03 | 1.67-03 | 1.73-03 | 1.84-03 | 2.02-03 | 2.29-03 |
| 13 | 2 1.00-30 | 2.67-03 | 2.63-03 | 2.58-03 | 2.49-03 | 2.36-03 | 2.18-03 | 1.93-03 |
| 14 | 1 1.00-30 | 2.59-03 | 2.56-03 | 2.51-03 | 2.43-03 | 2.31-03 | 2.15-03 | 1.91-03 |
| 14 | 2 6.34+12 | 4.71-02 | 4.72-02 | 4.73-02 | 4.76-02 | 4.79-02 | 4.87-02 | 4.99-02 |
| 15 | 1 2.90+09 | 2.74-03 | 2.76-03 | 2.80-03 | 2.86-03 | 2.96-03 | 3.11-03 | 3.30-03 |
| 15 | 2 1.00-30 | 6.50-03 | 6.40-03 | 6.25-03 | 6.02-03 | 5.67-03 | 5.18-03 | 4.51-03 |
| 16 | 1 1.00-30 | 1.84-03 | 1.81-03 | 1.76-03 | 1.68-03 | 1.57-03 | 1.42-03 | 1.21-03 |

```

16    2 1.02+10 9.84-03 9.80-03 9.73-03 9.63-03 9.51-03 9.40-03 9.34-03
17    1 2.58+07 9.72-04 9.86-04 1.01-03 1.04-03 1.09-03 1.18-03 1.27-03
17    2 1.00-30 2.54-03 2.49-03 2.42-03 2.30-03 2.14-03 1.90-03 1.60-03
-1
-1    -1

```

2.2.6 Demo (b-3) demo.b/demo_b3.pro

```

pro demo_b_3

trim_cophps_adf04, infile='adf04ic', outfile='ic#fe22_as.dat'
end

```

2.2.7 Demo (b-3) demo.b/ic#fe22_as.dat

| FE+22 | 26 | 23 15732424.0(1s) | | | |
|-------|---|---|---------------|-----|--|
| 1 | 1S2 2S2 | (1)0(0.0) | 0.0000 | {X} | |
| 2 | 1S2 2S1 2P1 | (3)1(0.0) | 294125.9172 | {X} | |
| 3 | 1S2 2S1 2P1 | (3)1(1.0) | 325899.9255 | {X} | |
| 4 | 1S2 2S1 2P1 | (3)1(2.0) | 415988.7673 | {X} | |
| 5 | 1S2 2S1 2P1 | (1)1(1.0) | 707772.8090 | {X} | |
| 6 | 1S2 2S1 3S1 | (3)0(1.0) | 8870629.5839 | {X} | |
| 7 | 1S2 2S1 3S1 | (1)0(0.0) | 8951832.3306 | {X} | |
| 8 | 1S2 2S1 3P1 | (3)1(0.0) | 9033381.3395 | {X} | |
| 9 | 1S2 2S1 3P1 | (3)1(1.0) | 9039155.3069 | {X} | |
| 10 | 1S2 2S1 3P1 | (3)1(2.0) | 9069060.1402 | {X} | |
| 11 | 1S2 2S1 3P1 | (1)1(1.0) | 9091505.2370 | {X} | |
| 12 | 1S2 2S1 3D1 | (3)2(1.0) | 9158129.9078 | {X} | |
| 13 | 1S2 2S1 3D1 | (3)2(2.0) | 9162034.5349 | {X} | |
| 14 | 1S2 2S1 3D1 | (3)2(3.0) | 9168854.9245 | {X} | |
| 15 | 1S2 2S1 3D1 | (1)2(2.0) | 9234055.2919 | {X} | |
| 16 | 1S2 2S1 4S1 | (3)0(1.0) | 11914413.9492 | {X} | |
| 17 | 1S2 2S1 4S1 | (1)0(0.0) | 11938997.7345 | {X} | |
| 18 | 1S2 2S1 4P1 | (3)1(0.0) | 11978429.8706 | {X} | |
| 19 | 1S2 2S1 4P1 | (3)1(1.0) | 11980543.3733 | {X} | |
| 20 | 1S2 2S1 4P1 | (3)1(2.0) | 11993395.2560 | {X} | |
| 21 | 1S2 2S1 4P1 | (1)1(1.0) | 12000726.8394 | {X} | |
| 22 | 1S2 2S1 4D1 | (3)2(1.0) | 12030232.6316 | {X} | |
| 23 | 1S2 2S1 4D1 | (3)2(2.0) | 12031822.9851 | {X} | |
| 24 | 1S2 2S1 4D1 | (3)2(3.0) | 12034771.8869 | {X} | |
| 25 | 1S2 2S1 4D1 | (1)2(2.0) | 12053979.2430 | {X} | |
| 26 | 1S2 2S1 4F1 | (3)3(2.0) | 12056986.4039 | {X} | |
| 27 | 1S2 2S1 4F1 | (3)3(3.0) | 12057710.0117 | {X} | |
| 28 | 1S2 2S1 4F1 | (3)3(4.0) | 12059219.6822 | {X} | |
| 29 | 1S2 2S1 4F1 | (1)3(3.0) | 12063174.2569 | {X} | |
| -1 | | | | | |
| 23.0 | 3 | 7.19-01 1.74+00 3.35+00 5.92+00 1.00+01 1.65+01 2.69+01 | | | |
| 2 | 1 1.00-30 1.26-03 1.25-03 1.23-03 1.20-03 1.16-03 1.09-03 9.94-04 | | | | |
| 3 | 1 5.05+07 1.50-02 1.51-02 1.53-02 1.67-02 1.54-02 1.46-02 1.53-02 | | | | |

| | | | | | | | | | |
|----|----|---------|---------|---------|---------|---------|---------|---------|---------|
| 4 | 1 | 1.00-30 | 6.27-03 | 6.21-03 | 6.12-03 | 5.98-03 | 5.76-03 | 5.43-03 | 4.95-03 |
| 5 | 1 | 2.18+10 | 4.15-01 | 4.18-01 | 4.23-01 | 4.30-01 | 4.44-01 | 4.98-01 | 4.46-01 |
| 6 | 1 | 1.00-30 | 1.25-03 | 1.23-03 | 1.20-03 | 1.16-03 | 1.09-03 | 1.00-03 | 8.76-04 |
| 7 | 1 | 1.00-30 | 1.23-02 | 1.24-02 | 1.24-02 | 1.25-02 | 1.27-02 | 1.29-02 | 1.32-02 |
| 8 | 1 | 1.00-30 | 2.92-04 | 2.87-04 | 2.82-04 | 2.73-04 | 2.61-04 | 2.42-04 | 2.15-04 |
| 9 | 1 | 1.48+12 | 1.62-03 | 1.63-03 | 1.64-03 | 1.65-03 | 1.68-03 | 1.73-03 | 1.81-03 |
| 10 | 1 | 1.00-30 | 1.45-03 | 1.43-03 | 1.40-03 | 1.36-03 | 1.30-03 | 1.21-03 | 1.07-03 |
| 11 | 1 | 1.14+13 | 6.41-03 | 6.55-03 | 6.73-03 | 7.01-03 | 7.46-03 | 8.18-03 | 9.34-03 |
| 12 | 1 | 1.00-30 | 1.81-03 | 1.78-03 | 1.75-03 | 1.69-03 | 1.60-03 | 1.47-03 | 1.29-03 |
| 13 | 1 | 1.12+08 | 3.09-03 | 3.05-03 | 2.99-03 | 2.89-03 | 2.75-03 | 2.55-03 | 2.26-03 |
| 14 | 1 | 1.00-30 | 4.22-03 | 4.16-03 | 4.07-03 | 3.93-03 | 3.73-03 | 3.43-03 | 3.02-03 |
| 15 | 1 | 2.17+10 | 1.75-02 | 1.77-02 | 1.80-02 | 1.84-02 | 1.91-02 | 2.02-02 | 2.16-02 |
| 16 | 1 | 1.00-30 | 4.23-04 | 4.16-04 | 4.07-04 | 3.92-04 | 3.70-04 | 3.39-04 | 2.96-04 |
| 17 | 1 | 1.00-30 | 2.32-03 | 2.33-03 | 2.34-03 | 2.36-03 | 2.39-03 | 2.44-03 | 2.50-03 |
| 18 | 1 | 1.00-30 | 1.09-04 | 1.08-04 | 1.06-04 | 1.03-04 | 9.80-05 | 9.11-05 | 8.08-05 |
| 19 | 1 | 7.65+11 | 5.09-04 | 5.10-04 | 5.11-04 | 5.12-04 | 5.16-04 | 5.22-04 | 5.36-04 |
| 20 | 1 | 1.00-30 | 5.46-04 | 5.39-04 | 5.29-04 | 5.13-04 | 4.90-04 | 4.55-04 | 4.04-04 |
| 21 | 1 | 4.63+12 | 1.42-03 | 1.44-03 | 1.47-03 | 1.53-03 | 1.62-03 | 1.77-03 | 2.00-03 |
| 22 | 1 | 1.00-30 | 5.18-04 | 5.12-04 | 5.02-04 | 4.86-04 | 4.63-04 | 4.29-04 | 3.81-04 |
| 23 | 1 | 2.93+07 | 8.83-04 | 8.72-04 | 8.56-04 | 8.31-04 | 7.94-04 | 7.39-04 | 6.62-04 |
| 24 | 1 | 1.00-30 | 1.21-03 | 1.19-03 | 1.17-03 | 1.13-03 | 1.08-03 | 1.00-03 | 8.89-04 |
| 25 | 1 | 2.87+09 | 2.72-03 | 2.74-03 | 2.78-03 | 2.84-03 | 2.94-03 | 3.09-03 | 3.27-03 |
| 26 | 1 | 1.00-30 | 4.38-04 | 4.30-04 | 4.19-04 | 4.01-04 | 3.75-04 | 3.38-04 | 2.88-04 |
| 27 | 1 | 1.10+06 | 6.28-04 | 6.19-04 | 6.04-04 | 5.82-04 | 5.49-04 | 5.04-04 | 4.40-04 |
| 28 | 1 | 1.00-30 | 7.88-04 | 7.75-04 | 7.54-04 | 7.22-04 | 6.75-04 | 6.09-04 | 5.19-04 |
| 29 | 1 | 2.47+07 | 9.57-04 | 9.69-04 | 9.89-04 | 1.02-03 | 1.07-03 | 1.15-03 | 1.23-03 |
| -1 | | | | | | | | | |
| -1 | -1 | | | | | | | | |

3 Demo (c) Compare the resulting adf04 files

DEMO C: Compare the resulting adf04 files

PURPOSE: To compare different adf04 data files using ADAS811 interactively.

EXAMPLE: For this demo adf04 files generated using R-Matrix (from central ADAS), Distorted Wave (DW), produced by AUTOSTRUCTURE (ADAS7#1 - Demo B), and Plane Wave Born (PWB), produced by Cowan (ADAS801 - Demo A)) are compared. The program used is ADAS811.

COMMENTS: Note that the adf04 data files which have to be compared, must have same configuration strings. For this demo, the three adf04 file used have been edited in order to have the same configuration strings:

- R-Matrix: copied locally from central ADAS and edited (belike_nrb05#fe22.dat)
Example:

```
SOURCE      EDITED
2s2          1s2 2s2
2s1 2p1      1s2 2s1 2p1
```

.....

- DW: copied locally from Module 7 Demo B and edited (ic#fe22_as.dat)
Example:

```
SOURCE      EDITED
522          1s2 2s2
512513      1s2 2s1 2p1
```

.....

- Cowan: taken from Module 7 Demo A, not edited.

DEMO c1: Examine common transitions between above datasets
with interactive ADAS811

1. Edit the adf04 files to be compared in order to have same configuration strings.
2. Use ADAS811 interactively to compare the collision strengths for different transitions.

Input files: belike_nrb05#fe22.dat, ic#fe22_as.dat, ../demo_a/ic#fe22.dat
Sample of output files: adas811_plot_example1.ps, adas811_plot_example2.ps

3.1 Demo (c) Figures

3.1.1 Demo (c-1) demo_c/adas811_plot_example1.pdf

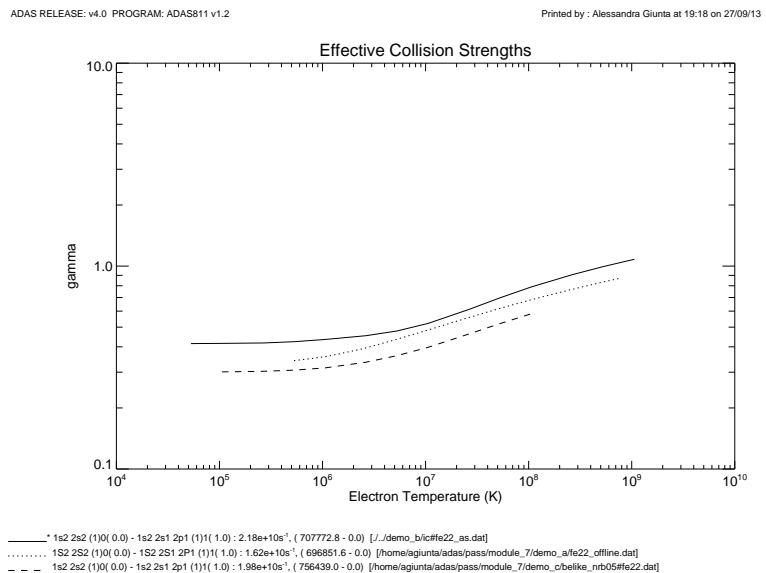


Figure 1:

3.1.2 Demo (c-1) demo_c/adas811_plot_example2.pdf

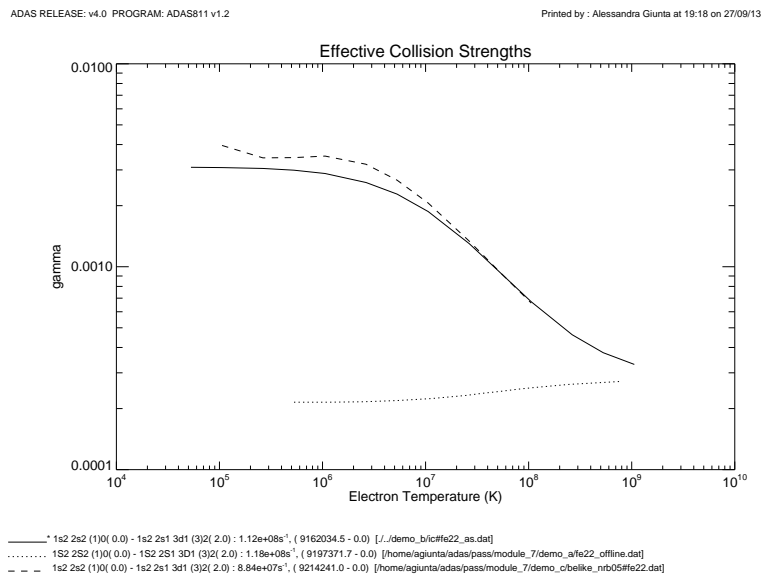


Figure 2:

3.2 Demo (c) Procedures

3.2.1 Demo (c-1) demo_c/belike_nrb05#fe22.dat

```
Fe+22      26      23      15730000.0
  1 1s2 2s2      (1)0( 0.0)          0.
  2 1s2 2s1 2p1      (3)1( 0.0)      345707.
  3 1s2 2s1 2p1      (3)1( 1.0)      377694.
  4 1s2 2s1 2p1      (3)1( 2.0)      469122.
  5 1s2 2s1 2p1      (1)1( 1.0)      756439.

  .
  96 1s2 2p1 4f1      (3)2( 1.0)      12638336.
  97 1s2 2p1 4d1      (1)1( 1.0)      12641921.
  98 1s2 2p1 4f1      (1)2( 2.0)      12642691.

  -1
23.00      3      1.06+05 2.64+05 5.29+05 1.06+06 2.64+06 5.29+06 1.06+07
  2      1 0.00+00 4.75-03 3.77-03 3.05-03 2.61-03 2.66-03 2.57-03 2.11-03
  3      1 4.72+07 2.35-02 1.96-02 1.70-02 1.54-02 1.57-02 1.61-02 1.58-02

  .
  .
  97 96 8.34+01 3.06-02 3.19-02 3.35-02 3.55-02 3.85-02 4.10-02 4.37-02
  98 96 8.68-01 7.00-02 6.82-02 6.55-02 6.15-02 5.45-02 4.87-02 4.34-02
  98 97 1.32+02 6.55+00 7.44+00 8.45+00 9.63+00 1.13+01 1.24+01 1.36+01
  -1
  -1 -1
C-----
C
C
C Details of the calculations are in
C
C Chidichimo,M. C., Del Zanna, G., Mason, H.E.,
C Badnell,N. R., Tully, J.A., Berrington, K.A., 2005,
C Atomic Data from the IRON Project LVI. Electron excitation of Be-like Fe
C     XXIII, A\&A, 430, 331
C
C Complete OMEGA file from GDZ processed thru adasexj by NRB.
C
C A-values calculated with AUTOSTRUCTURE including all n=4 levels
C (RAD='ALL' CUP='ICM' KUTSO=-17 KCUT=0).
C All A-values of the Ek and M1 transitions have been summed up and
C combined with M2, see next.
C
C M2 data have been calculated with SUPERSTRUCTURE for lower levels 1 thru 10
C and upper levels 2 thru 45 by GDZ.
C NAME: N R Badnell
C DATE: 05/05/05
C
C UPDATES
C
C Allan Whiteford, 09/05/05
```

```
C
C Fixed formatting
C Added element symbol
C
C Nigel Badnell and Allan Whiteford, 10/05/05
C
C Supplemented with more complete M2 data, also note that the previous M2
C data were incorrectly indexed.
C
C The M2 A-values are obtained from a 45-configuration SUPERSTRUCTURE run
C with term energy corrections and observed energies (whenever available),
C see Del Zanna, Chidichimo and Mason 2005 A&A 432, 1137 - produced by GDZ
C
C-----
```

4 Demo (d) R-Matrix

DEMO D: R-Matrix

PURPOSE: To examine the driver files and instructions for an R-Matrix run.

EXAMPLE: The offline program dedicated to R-Matrix within ADAS is ADAS#3. For this demo the set of scripts and input files needed for an R-Matrix run is shown.

DEMO d1: Examine driver file and computer configuration
instructions to calculate R-Matrix cross sections
for Fe22+.

Samples of scripts and input files: adas803.pl, Makefile, currentsite,
parallel_procfile, input.dat

4.1 Demo (d) Figures

4.2 Demo (d) Procedures

4.2.1 Demo (d-1) demo_d/adas803.pl

```
#!/usr/bin/perl
use List::Util qw[min max];
#-----
#
# adas8#3      : ADAS8#3 - Automated R-matrix calculations
#
# AUTHOR       : Allan Whiteford, Mike Witthoeft, Stuart Loch and Connor Ballance
# DATE         : 26-09-2005
#
# MODIFIED:
#
#          1.1      Allan Whiteford
# 26-09-2005
#          First Release
#          1.2      Allan Whiteford
#          Fixed bug where the month was wrong by one.
#          1.3      Allan Whiteford
#          Allowed --outer=N for specification of chunk.
# Only re-run structure if necessary.
#          1.4      Allan Whiteford
#          Fixed bug in maximum allowed occupation
# Added --example output
#          1.5      Allan Whiteford
#          Added --root option
# Made --archive option more sensible
#
#          2011 :
#
#          1.6      Mike Witthoeft, Stuart Loch and Connor Ballance
#          Added --dip option for calculation D- and B- matrices
#          for the general case
#          Added OMEGA filtering for numerical failures
#          Replaced omgmerge with arrange
#
#          2012
#
#          1.7      Connor Ballance and Stuart Loch
#          Now an 'accelerated' parallel approach in which
#          every partial wave and diagonalisation is carried
#          out concurrently.
#
#          Added utility codes : hfilter,dfilter (no input required)
#
#
# VERSION:
```

```

#      1.1    26-09-2005
#      1.2    22-01-2007
# 1.3    09-07-2007
# 1.4    11-08-2008
# 1.5    20-08-2008
#      1.6    19-09-2011
#-----

sub auto_maxc
{
mkdir ("maxc", 0755);
chdir ("maxc");
symlink("../str/radout","radial");

# return;
. .
if ($actionadf)
{
make_adf_file();
}

if ($actionarc)
{
        archive_output();
}

```

4.2.2 Demo (d-1) demo.d/Makefile

```

#####
#
#                               ADAS8#3 Makefile
#
#
# This makefile:
# * Compiles necessary R-matrix codes
# * Produces "proc" file for adas8#3 script
# * Downloads codes from the web
#
# Necessary modifications:
# * Define where your binary files should go
# * Specify if you want parallel or just serial
#   binaries.
# * Include (or write) an appropriate .def file.
# * Define a wget username/password (in def file)
#
# Usage:
# * "make" will build all codes
#

```

```

#
#          * "make directories"
#          * "make update_serial"
#          * "make update_utility"
#          * "make update_parallel"
#          * "make clean"
#
# Updates:
# V1.0 Allan Whiteford, 26/09/05
#     First Release
#
#                         V1.1 MCW, SDL, CPB      1/6/10
#
#                         V1.2      Martin O'Mullane, Mike Witthoeft,
#                               Stuart Loch, Connor Ballance (14/10/11)
#                               - Introduce REPOScode and REPOSpParam
#                               which can be set to CB or NRB repositories
#                               for finer control over retrieving the code
#                               and parameter files.
#                               - radiation damping for the general case
#
#####
#
# Codes to make by default, options are any combination of
# serial, parallel and utility. This can be overridden at the
# command line by, e.g., "make parallel"
#
CODETYPE = serial utility parallel
#
# Include here machine dependent definitions and choose which repository
# from which to draw the code and dimensions.
#
include currentsite
#
BIN = $(BASE)/bin
#
# Where you want the automatically generated procfiles to go.
# Note that the main adas8#3 script expects the procfile to be
# in ~/.adas8#3proc unless you specify otherwise with --proc=
# you can specify /dev/null if you don't want a procfile
#
SPROCFILE = $(BIN)/serial_procfile
PPROCFILE = $(BIN)/parallel_procfile
. . .
$(p_stgfdamp): $(p_stgfdamp_src) $(p_stgfdamp_header)
@$(ECHO) 'Compiling outer region stage Fdamp...'
@$(CP) $(p_stgfdamp_header) $(p_stgfdamp_param)
@$(PFF) $(PFFLAGS) $(p_stgfdamp_src) -o $(p_stgfdamp) $(PLFLAGS)

```

```

@$(RM) $(p_stgfdamp_param) *.mod

$(p_stgicfdamp): $(p_stgicfdamp_src) $(p_stgicfdamp_header)
@$(ECHO) 'Compiling outer region stage ICFdamp...'
@$(CP) $(p_stgicfdamp_header) $(p_stgicfdamp_param)
@$(PFF) $(PFFLAGS) $(p_stgicfdamp_src) -o $(p_stgicfdamp) $(PLFLAGS)
@$(RM) $(p_stgicfdamp_param) *.mod

```

4.2.3 Demo (d-1) demo.d/parallel.profile

```

GENERAL
chunk_size = 1000
internal_split = 10
adf00_path = /home/adas/adas/adf00
matrix_type = K

EXECUTABLE INFORMATION
auto          1 /home/mog/rmx_test/bin/autos.x
stg1_ex       4 /usr/lib64/openmpi/bin/mpirun -np 4 /home/mog/rmx_test/bin/pstg1r.x
stg2_ex       4 /usr/lib64/openmpi/bin/mpirun -np 4 /home/mog/rmx_test/bin/pstg2r.x
stg3_ex       50 /usr/lib64/openmpi/bin/mpirun -np 50 /home/mog/rmx_test/bin/pstg3r.x
stg1_dip      4 /usr/lib64/openmpi/bin/mpirun -np 4 /home/mog/rmx_test/bin/pstg1r.x
stg2_dip      12 /usr/lib64/openmpi/bin/mpirun -np 12 /home/mog/rmx_test/bin/pstg2r_dip.x
stg3_dip      4 /usr/lib64/openmpi/bin/mpirun -np 4 /home/mog/rmx_test/bin/pstg3r_dip.x
stgd_dip     4 /usr/lib64/openmpi/bin/mpirun -np 4 /home/mog/rmx_test/bin/pstgd_dip.x
stg1_tcc      1 /home/mog/rmx_test/bin/stg1r.x
stg2_tcc      1 /home/mog/rmx_test/bin/stg2r.x
stgjk_tcc    1 /home/mog/rmx_test/bin/stgjk.x
stgf_ex       4 /usr/lib64/openmpi/bin/mpirun -np 4 /home/mog/rmx_test/bin/pstgf.x
stgicf_ex    4 /usr/lib64/openmpi/bin/mpirun -np 4 /home/mog/rmx_test/bin/pstgicf.x
stgfdamp_ex  4 /usr/lib64/openmpi/bin/mpirun -np 4 /home/mog/rmx_test/bin/pstgfdamp.x
stgicfdamp_ex 4 /usr/lib64/openmpi/bin/mpirun -np 4 /home/mog/rmx_test/bin/pstgicfdamp.x
stgb          1 /home/mog/rmx_test/bin/stgb.x
stg1_nx       1 /home/mog/rmx_test/bin/stg1r.x
stg2_nx       4 /usr/lib64/openmpi/bin/mpirun -np 4 /home/mog/rmx_test/bin/pstg2r.x
stg3_nx       4 /usr/lib64/openmpi/bin/mpirun -np 4 /home/mog/rmx_test/bin/pstg3r.x
stgf_nx       4 /usr/lib64/openmpi/bin/mpirun -np 4 /home/mog/rmx_test/bin/pstgf.x
stgicf_nx    4 /usr/lib64/openmpi/bin/mpirun -np 4 /home/mog/rmx_test/bin/pstgicf.x
omadd         1 /home/mog/rmx_test/bin/omadd.x
om2omu        1 /home/mog/rmx_test/bin/om2omu.x
omr2omc        1 /home/mog/rmx_test/bin/omr2omc.x
adasexj      1 /home/mog/rmx_test/bin/adasexj.x
arrange       1 /home/mog/rmx_test/bin/arrange.x
dfilter       1 /home/mog/rmx_test/bin/dfilter.x

```

4.2.4 Demo (d-1) demo.d/input.dat

```

GENERAL
2Jmax_ex = 21
2Jmax_nx = 55

```

```
maxc = 42
mesh_fine = 0.0000015
mesh_coarse = 0.001
maxe/ionpot = 3
rdamp = 1
adamp = 0
accel = 0
```

```
CONFIGURATION LIST
1s1
2s1
2p1
3s1
3p1
3d1
4s1
4p1
4d1
4f1
5s1
5p1
5d1
5f1
5g1
```

```
SCALING PARAMETERS
1s = 1.0
2s = 1.0
2p = 1.0
3s = 1.0
3p = 1.0
3d = 1.0
4s = 1.0
4p = 1.0
4d = 1.0
4f = 1.0
```

C.8 module_8

MODULE 8

Observing, modelling and analysing solar spectra

Demonstration script

Hugh Summers, Martin O'Mullane and Alessandra Giunta

September 29, 2013

Contents

| | |
|---|-----------|
| 1 Demo (a) Exploiting line ratios | 3 |
| 1.1 Demo (a) Figures | 5 |
| 1.1.1 Demo (a-1) demo_a/demo_a_1_graph205.pdf | 5 |
| 1.1.2 Demo (a-1) demo_a/demo_a_1_graph207.pdf | 6 |
| 1.1.3 Demo (a-2) demo_a/demo_a_2.pdf | 7 |
| 1.2 Demo (a) IDL procedures | 8 |
| 1.2.1 Demo (a-2) demo_a_2.pro | 8 |
| 1.3 Demo (a) Tables and datasets | 10 |
| 1.3.1 Demo (a-1) adf04/copch#26/chv6_ic#fe11.dat | 10 |
| 1.3.2 Demo (a-1) demo_a/demo_a_1_paper205.txt | 10 |
| 1.3.3 Demo (a-1) demo_a/demo_a_1_paper207.txt | 12 |
| 1.3.4 Demo (a-2) demo_a/demo_a_2_pecfile.dat | 13 |
| 2 Demo (b) Building up contribution functions and the kernel | 15 |
| 2.1 Demo (b) Figures | 17 |
| 2.1.1 Demo (b-2) demo_b/demo_b_2_graph412.pdf | 17 |
| 2.1.2 Demo (b-3) demo_b/demo_b_3_adas205.pdf | 19 |
| 2.2 Demo (b) IDL procedures | 20 |
| 2.2.1 Demo (b-2) demo_b_2.pro | 20 |
| 2.3 Demo (b) Tables and datasets | 23 |
| 2.3.1 Demo (b-1) arch601/intensity/sumer_cds_eis_qs.dat | 23 |
| 2.3.2 Demo (b-1) arch601/abundance/abund.coronal_phillips08 | 23 |
| 2.3.3 Demo (b-1) arch601/kernel/kernel_n1e10.dat | 23 |
| 2.3.4 Demo (b-2) demo_b/demo_b_2_paper412.txt | 24 |
| 3 Demo (c) Differential Emission Measure (DEM) analysis | 26 |
| 3.1 Demo (c) Figures | 29 |
| 3.1.1 demo_c/demo_c_gft.pdf | 29 |
| 3.1.2 demo_c/demo_c_dem.pdf | 30 |
| 3.2 Demo (c) datasets | 31 |
| 3.2.1 demap_output.dat | 31 |

| | |
|---|-----------|
| 4 Demo (d) Evaluating escape factors | 33 |
| 4.1 Demo (d-1) Figures | 35 |
| 4.2 Demo (d-1) IDL procedure | 35 |
| 4.3 Demo (d-2) Figures | 38 |
| 4.4 Demo (d-2) Tables | 41 |
| 4.4.1 demo_d-2/adas214.pass | 41 |
| 4.4.2 demo_d-2/demo_d_pec_adas214.dat | 47 |
| 5 Demo (e) Working with Non-Maxwellians | 50 |
| 5.1 Demo (e) Figures | 52 |
| 5.1.1 Demo (e-1) demo_e/nonmax_c2.pdf | 52 |
| 5.2 Demo (e) IDL procedures | 53 |
| 5.2.1 Demo (e-1) demo_e/demo_e.pro | 53 |
| 5.3 Demo (e-1) Tables and drivers | 56 |
| 5.3.1 demo_e-1/instruction.kappa | 56 |
| 5.3.2 demo_e-1/instruction.dru | 56 |
| 5.3.3 demo_e-1/adf37.DT_1.dat | 56 |
| 5.3.4 demo_e-1/c2_max.dat | 57 |
| 5.3.5 demo_e-1/c2_kappa.dat | 57 |
| 5.3.6 demo_e-1/c2_dru.dat | 58 |
| 5.3.7 demo_e-1/c2_num.dat | 59 |

1 Demo (a) Exploiting line ratios

DEMO a: Exploiting line ratios

PURPOSE: The contour of line ratio as a function of Te and Ne show when the ratio depend on Te or Ne (e.g. for a certain value of Ne the ratio has Ne constant in a wide range o Te or vice-versa). It helps to find line ratios which give Te or Ne diagnostic.

EXAMPLE: In the solar case a line ratio used as electron diagnostic is: Fe+11 193.51 Ang. / (186.86 Ang. + 186.88 Ang.). This ratio is observed by Hinode/EIS.

The transitions are the following:

193.51 Ang. 3s2 3p3 4S3/2 - 3p2 3d 4P3/2
186.86 Ang. 3s2 3p3 2D3/2 - 3p2 3d 2F5/2
186.88 Ang. 3s2 3p3 2D5/2 - 3p2 3d 2F7/2

Therefore, IC resolution is required.

The adf04 for Fe+11 in IC resolution within ADAS are the following:

1. /home/adas/adas/adf04/copmm#26/ic#fe11.dat
2. /home/adas/adas/adf04/cophps/dw/ic#fe11.dat
3. /home/adas/adas/adf04/plike/plike_al97#fe11.dat
4. /home/adas/adas/adf04/copch#26/chv6_ic#fe11.dat

The preferred adf04 for the demo is 4., because it contains the most recent calculation for Fe+11 (R-matrix from Storey et al. 2005).

COMMENTS: If the preferred adf04 is 2. (new DW from AUTOSTRUCTURE), then before using the adf04, in most cases and especially using the IC resolution, it is necessary to cut the file to remove the transitions arising from the levels above the ionisation potential. This is done using trim_cophps_adf04.pro (in /home/adas/idl/adaslib/proc_adf/).

DEMO a-1: Using ADAS205 and ADAS207 from interactive ADAS windows.

1. Use ADAS205 to create a contour.pass file
(input files : adf04/copch#26/chv6_ic#fe11.dat
output files: pass/demo_a_1_graph205.ps
: pass/demo_a_1_paper205.txt
: pass/contour.pass).
2. Use the contour.pass as input for ADA207
(input files : contour.pass
output files: pass/demo_a_1_graph207.ps
: pass/demo_a_1_paper207.txt).

DEMO a-2: Displaying line ratios using the command line.

1. Use `read_adf15.pro` to read an `adf15` dataset of the PEC for the line considered.
- OR
1. If the PEC is not available, use `run_adas208.pro` to produce the PEC and then use `read_adf15.pro` to read it.
 2. Plot the PEC ratio as a function of T_e and N_e in a contour plot.
 3. Compare the plots obtained in DEMO a-1 and DEMO a-2.
(idl procedure: `demo_a/demo_a_2.pro`
input files : `adf04/copch#26/chv6_ic#fe11.dat`
output files : `pass/demo_a_2.txt`
 : `pass/demo_a_2_pecfile.dat`
 : `pass/demo_a_2.ps`

1.1 Demo (a) Figures

1.1.1 Demo (a-1) demo.a/demo.a.1_graph205.pdf

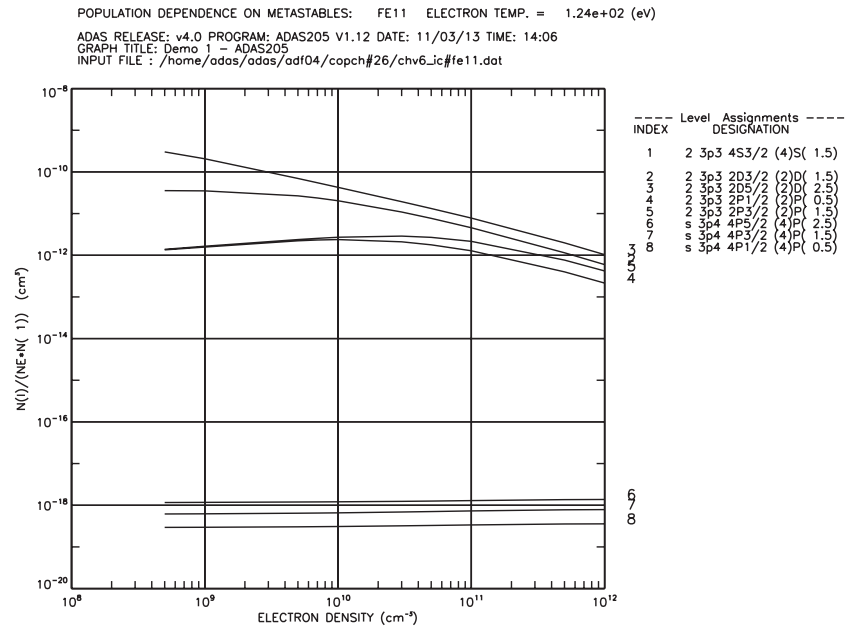


Figure 1: Population ratios $N_i/(N_e N_1)$ vs N_e at fixed T_e . Note the traces for $i = 2, 3, 4, 5$ at low density have not become flat. They have not reached the coronal limit at these densities and are large ($N_i \sim N_1$) - properly they should be treated as metastables

1.1.2 Demo (a-1) demo_a/demo_a_1_graph207.pdf

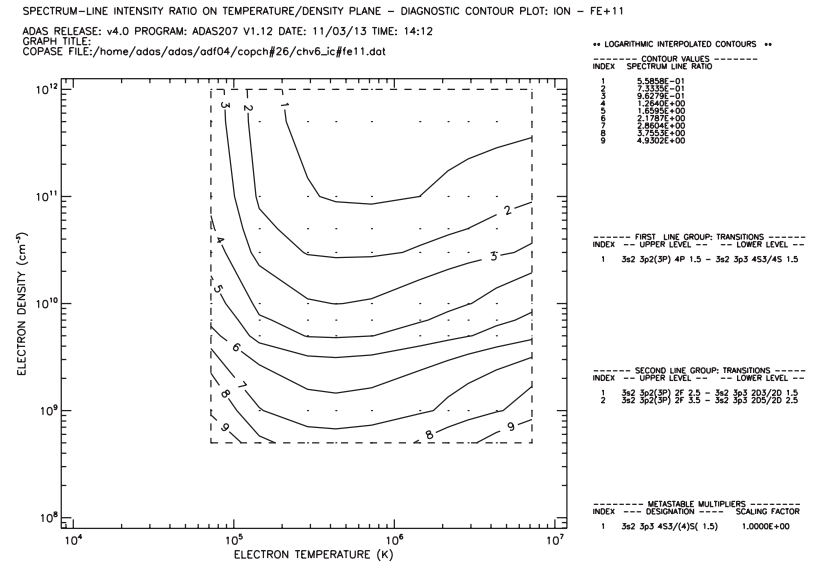


Figure 2: Contour plot of emissivity ratio in the T_e/N_e plane. ADAS207 graphical output.

1.1.3 Demo (a-2) demo_a/demo_a_2.pdf

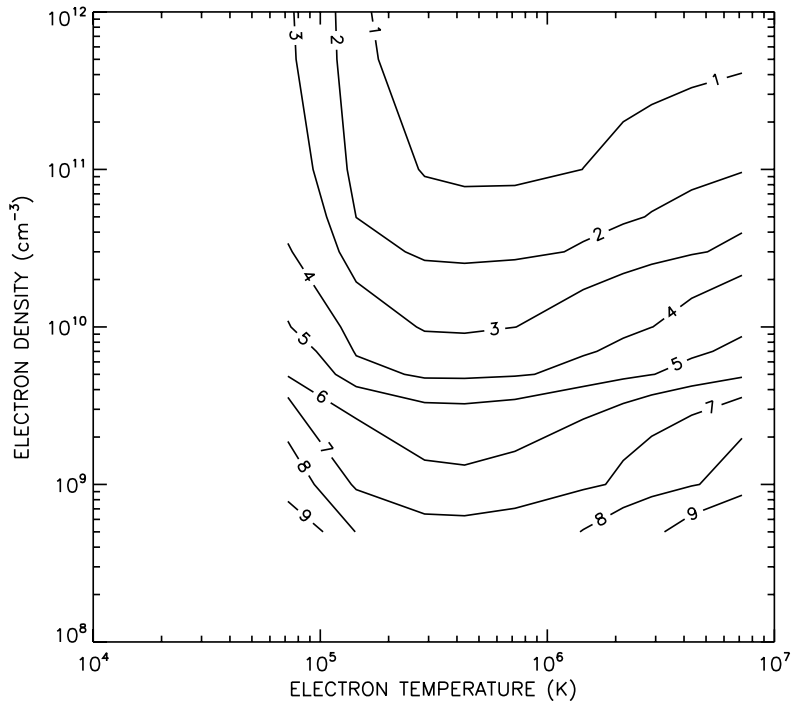


Figure 3: Contour plot of emissivity ratio in the T_e/N_e plane. Calculated in IDL at the command lines with script *demo_a_2.pro* and main procedures *run_adas208* and *read_adf15.pro*

1.2 Demo (a) IDL procedures

1.2.1 Demo (a-2) demo_a_2.pro

Demonstration IDL procedure using *run_adas208.pro* and *read_adf15*.

```
pro demo_a_2
;Use run_adas208 to produce a PEC
;for Fe+11 193.51 A/(186.86 A+186.88 A): density diagnostic in
;the solar case

;define electron temperature (eV) and electron density array (cm-3)
te=[6.204E+00,1.241E+01,2.482E+01,3.722E+01,6.204E+01,1.241E+02,1.861E+02,$
    2.482E+02,3.722E+02,6.204E+02]
dens=[5.000E+08,1.000E+09,5.000E+09,7.000E+09,1.000E+10,3.000E+10,5.000E+10,$
    1.000E+11,5.000E+11,1.000E+12]

nte=n_elements(te)
ndens=n_elements(dens)

;define input values for run_adas208
unit_te = 'eV'
unit_dens = 'cm-3'

wmin      = 100.
wmax      = 300.
amin      = 1.0e-3

adf04='home/hps/adas_central/adas/adf04/copch#26/chv6_ic#fe11.dat'

meta_list=[1]

;Use run_adas208.pro to produce a PEC file of the type adf15
run_adas208, adf04=adf04,
              te=te,dens=dens, unit_te=unit_te,unit_dens=unit_dens,      $
              meta=meta_list,                                     $
              wmin=100.0, wmax=300.0, amin=1e6,                  $
              log='demo_a_2.txt', /pec, pass_dir='.',pop=pop      $

cmd = 'mv pec.pass demo_a_2_pecfile.dat'
spawn, cmd, /sh

;Use read_adf15.pro to read the PEC file produced by run_adas208.pro
file='demo_a_2_pecfile.dat'
block=[2,3,5]
nblock=n_elements(block)

data=fltarr(nblock,nte,ndens)
```

```

for i=0,nblock-1 do begin
    read_adf15,file=file,block=block[i],te=te,dens=dens,    $
        data=idata,wlngh=wlngh,/all
    data[i,*,*]=idata
endfor

;plot the line ratio
set_plot,'ps'
device, /isolatin1, font_index=8
device, bits=8, filename='demo_a_2.ps',   $
    font_size = 14, xsize=18.0, ysize=16.0, $
    yoffset=7.0, /color
device, /helvetica

;contour plot
contour,data[0,*,*]/(data[1,*,*]+data[2,*,*]),te*11604.,dens, $
    xtit='ELECTRON TEMPERATURE (K)',                      $
    ytit='ELECTRON DENSITY (cm!u-3!n)',                  $
    c_annotation=['1','2','3','4','5','6','7','8','9'],   $
    /xlog,/ylog,
    lev=[5.6931e-1,7.4804e-1,9.8289e-1,1.2915e0,1.6969e0, $
        2.2296e0,2.9296e0,3.8494e0,5.0579e0]

;intesity ratio versus electron density at a fixed electron temperature
plot_oo,dens,data[0,5,*]/(data[1,5,*]+data[2,5,*]),      $
    xtit='ELECTRON DENSITY (cm!u-3!n)',                  $
    ytit='SPECTRUM LINE RATIO (PH)'

;intesity ratio versus electron temperature at a fixed electron density
plot_oo,te*11604.,data[0,*,4]/(data[1,*,4]+data[2,*,4]),   $
    xtit='ELECTRON TEMPERATURE (K)',                      $
    ytit='SPECTRUM LINE RATIO (PH)'

device, /close
set_plot,'X'
!p.font=-1

end

```

1.3 Demo (a) Tables and datasets

1.3.1 Demo (a-1) adf04/copch#26/chv6_ic#fe11.dat

Input adf04 dataset for interactive execution of ADAS205.

```

FE+11      26      12      2668150.5
  1 3s2 3p3 4S3/2      (4)0( 1.5)      0.
  2 3s2 3p3 2D3/2      (2)2( 1.5)      44491.0
  3 3s2 3p3 2D5/2      (2)2( 2.5)      48820.0
  4 3s2 3p3 2P1/2      (2)1( 0.5)      76629.0

141 3s2 3p 3d 4P3/2      (4)2( 1.5)      1014582.0
142 3s2 3p3 3d 2S1/2      (2)0( 0.5)      1014750.0
143 3s2 3p 3d 4D1/2      (4)2( 0.5)      1015458.0
-1

12.0      3      4.00+03 8.00+03 1.20+04 2.00+04 4.00+04 8.00+04 1.20+05 2.00+05 4.00+05 8.00+05 1.20+06 2.00+06 4.00+06
2      1 5.64+01 7.63+01 7.64+01 7.64+01 7.65+01 7.66+01 7.65+01 7.61+01 7.35+01 6.07+01 4.24+01 3.26+01 2.26+01 1.32+01
3      1 2.34+00 1.02+00 1.02+00 1.02+00 1.02+00 1.01+00 1.00+00 9.58+01 7.87+01 5.53+01 4.27+01 3.00+01 1.80+01
4      1 1.93+02 2.70+01 2.70+01 2.69+01 2.68+01 2.65+01 2.61+01 2.47+01 1.96+01 1.33+01 9.93+02 6.65+02 3.69+02
5      1 3.47+02 4.73+01 4.75+01 4.77+01 4.80+01 4.89+01 5.02+01 5.09+01 4.98+01 4.03+01 2.73+01 2.04+01 1.36+01 7.53+02

141 25 1.00+30 2.47+04 2.47+04 2.46+04 2.45+04 2.41+04 2.34+04 2.28+04 2.17+04 1.98+04 1.74+04 1.57+04 1.34+04 1.03+04
142 25 1.00+30 4.07+04 4.06+04 4.06+04 4.04+04 3.99+04 3.91+04 3.82+04 3.66+04 3.32+04 2.81+04 2.46+04 1.98+04 1.38+04
143 25 1.00+30 1.14+04 1.14+04 1.14+04 1.13+04 1.12+04 1.09+04 1.07+04 1.02+04 9.17+05 7.78+05 6.85+05 5.53+05 3.87+05
-1
-1 -1

C-----
C
C Data generated from CHIANTI version 6.0
C
C     http://www.chianti.rl.ac.uk/
C
C CHIANTI references
C -----
C
C-----
C
C Filtered adf04 file to
C - sort energy levels
C - remove non physical A values from
C energy level reversals
C - remove energies above ionisation potential
C - remove duplicate transitions
C
C Code      : ADAS utility program, filter04
C Date      : 04-08-2009
C Producer  : Martin O'Mullane
C
C-----

```

1.3.2 Demo (a-1) demo_a/demo_a_1.paper205.txt

Output summary text data set from interactive execution of ADAS205.

```

ADAS RELEASE: v4.0 PROGRAM: ADAS205 V1.12 DATE: 21/03/13 TIME: 09:11
***** TABULAR OUTPUT FROM METASTABLE POPULATION PROGRAM: ADAS205 - DATE: 21/03/13 *****
INPUT COPASE FILE NAME: /home/hps/adas_central/adas/adf04/copch#26/chv6_ic#fe11.dat

ION      NUCLEAR      RECOMBINING      ----- IONIZATION POTENTIAL -----
CHARGE (Z0)    ION CHARGE (Z1)    (wave number <cm-1>)      (rydbergs)
-----      2668150.      24.3140284

FE+11      26      12      2668150.      24.3140284

-----      ENERGY LEVELS      -----
INDEX      CONFIGURATION      (2S+1)L(1)      ----- ENERGY RELATIVE TO LEVEL 1 -----      ENERGY RELATIVE TO IONISATION POTENTIAL -----
(wave number <cm-1>)      (rydbergs)      (wave number <cm-1>)      (rydbergs)
-----      -----
  1 3s2 3p3 4S3/2      (4)0( 1.5)      0.      0.0000000      2668150.      24.3140284
  2 3s2 3p3 2D3/2      (2)2( 1.5)      44491.      0.4046125      2623750.      23.9994158
  3 3s2 3p3 2D5/2      (2)2( 2.5)      48820.      0.4448815      2619330.      23.8691469
  4 3s2 3p3 2P1/2      (2)1( 0.5)      76629.      0.6982963      2591522.      23.6157321
  5 3s2 3p3 2P3/2      (2)1( 1.5)      82567.      0.7524075      2585584.      23.5616269
  6 3s 3p4 4P5/2      (4)1( 2.5)      273532.      2.4926123      2394618.      21.8214161

139 3s2 3p 3d 4D7/2      (4)2( 3.5)      1012175.      9.2236370      1655976.      15.0993914
140 3s2 3p 3d 4D5/2      (4)2( 2.5)      1013361.      9.2344447      1654790.      15.0795837
141 3s2 3p 3d 4D3/2      (4)2( 1.5)      1014582.      9.2448422      1653648.      15.0691861
142 3s 3p3 3d 2S1/2      (2)0( 0.5)      1014750.      9.2471022      1653400.      15.0669262
143 3s2 3p 3d 4D1/2      (4)2( 0.5)      1015458.      9.2535540      1652692.      15.0604744

-- INPUT COPASE FILE TEMPERATURES: (TE=TP=TH) --
INDEX      (kelvin)      (eV)      (reduced)
-----      -----
  1      4.00E+03      3.45E+01      2.78E+01
  2      8.00E+03      6.89E+01      5.56E+01
  3      1.20E+04      1.03E+00      8.33E+01
  4      2.00E+04      1.72E+00      1.39E+02
  5      4.00E+04      3.45E+00      2.78E+02

```

6 8.00E+04 6.89E+00 5.56E+02
 7 1.20E+05 1.03E+01 8.33E+02
 8 2.00E+05 1.72E+01 1.39E+03
 9 4.00E+05 3.45E+01 2.78E+03
 10 8.00E+05 6.89E+01 5.56E+03
 11 1.20E+06 1.03E+02 8.33E+03
 12 2.00E+06 1.72E+02 1.39E+04
 13 4.00E+06 3.45E+02 2.78E+04

INPUT COPASE FILE INFORMATION:

 NUMBER OF ELECTRON IMPACT TRANSITIONS = 1638
 NUMBER OF PROTON IMPACT TRANSITIONS = 0
 NUMBER OF CHARGE EXCHANGE RECOMBINATIONS = 0
 NUMBER OF FREE ELECTRON RECOMBINATIONS = 0

METASTABLE INFORMATION:

 NUMBER OF ORDINARY LEVELS = 142
 NUMBER OF METASTABLES = 1

METASTABLE DETAILS

| METASTABLE INDEX | ENERGY LEVEL INDEX | DESIGNATION |
|------------------|--------------------|------------------------|
| 1 | 1 | 2 3p3 4s3/2 (4)S(1.5) |

OUTPUT PLASMA PARAMETERS:

 NUMBER OF TEMPERATURES = 10
 NUMBER OF DENSITIES/RATIOS = 10

| INDEX | TEMPERATURES (UNITS: eV) | | | INDEX | DENSITIES (UNITS: cm ⁻³) | | | RATIOS | |
|-------|--------------------------|-------------|-----------------------|-------|--------------------------------------|-------------|-------------|-------------|--|
| | ELECTRON <TE> | PROTON <TP> | NEUTRAL HYDROGEN <NH> | | ELECTRON <NE> | PROTON <NP> | NH/NE | N(Z+1)/N(Z) | |
| 1 | 6.294E+00 | 1.000E+00 # | 1.000E+00 # | 1 | 5.000E+08 | 0.000E+00 # | 0.000E+00 # | 0.000E+00 # | |
| 2 | 1.241E+01 | 1.000E+00 # | 1.000E+00 # | 2 | 1.000E+09 | 0.000E+00 # | 0.000E+00 # | 0.000E+00 # | |
| 3 | 2.482E+01 | 1.000E+00 # | 1.000E+00 # | 3 | 5.000E+09 | 0.000E+00 # | 0.000E+00 # | 0.000E+00 # | |
| 4 | 3.722E+01 | 1.000E+00 # | 1.000E+00 # | 4 | 7.000E+09 | 0.000E+00 # | 0.000E+00 # | 0.000E+00 # | |
| 5 | 6.294E+01 | 1.000E+00 # | 1.000E+00 # | 5 | 1.000E+10 | 0.000E+00 # | 0.000E+00 # | 0.000E+00 # | |
| 6 | 1.241E+02 | 1.000E+00 # | 1.000E+00 # | 6 | 3.000E+10 | 0.000E+00 # | 0.000E+00 # | 0.000E+00 # | |
| 7 | 1.861E+02 | 1.000E+00 # | 1.000E+00 # | 7 | 5.000E+10 | 0.000E+00 # | 0.000E+00 # | 0.000E+00 # | |
| 8 | 2.482E+02 | 1.000E+00 # | 1.000E+00 # | 8 | 1.000E+11 | 0.000E+00 # | 0.000E+00 # | 0.000E+00 # | |
| 9 | 3.722E+02 * | 1.000E+00 # | 1.000E+00 # | 9 | 5.000E+11 | 0.000E+00 # | 0.000E+00 # | 0.000E+00 # | |
| 10 | 6.294E+02 * | 1.000E+00 # | 1.000E+00 # | 10 | 1.000E+12 | 0.000E+00 # | 0.000E+00 # | 0.000E+00 # | |

KEY: * = WARNING - TEMPERATURE OUT OF RANGE
 - EXTRAPOLATION REQUIRED
 # = PARAMETER NOT USED IN CALCULATIONS

NOTE: NH/NE = NEUTRAL HYDROGEN DENSITY / ELECTRON DENSITY
 N(Z+1)/N(Z) = STAGE ABUNDANCES

 PROTON IMPACT COLLISIONS - NOT INCLUDED
 IONIZATION RATES - NOT INCLUDED
 NEUTRAL HYDROGEN CHARGE EXCHANGE - NOT INCLUDED
 FREE ELECTRON RECOMBINATION - NOT INCLUDED

TABLE KEY:
 NE = ELECTRON DENSITY
 TE = ELECTRON TEMPERATURE
 I = ENERGY LEVEL INDEX
 IMET = METASTABLE INDEX
 IORD = ORDINARY LEVEL INDEX

NUMBER OF PROTON IMPACT COLLISIONS INCLUDED = 0
 NUMBER OF FREE ELECTRON RECOMBINATIONS INCLUDED = 0
 NUMBER OF CHARGE EXCHANGE RECOMBINATIONS INCLUDED = 0

NE(CM-3)= 5.0000E+08 1.0000E+09 5.0000E+09 7.0000E+09 1.0000E+10 3.0000E+10 5.0000E+10 1.0000E+11 5.0000E+11 1.0000E+12

EQUILIBRIUM METASTABLE POPULATION DEPENDENCE ON DENSITY AT TE = 6.20E+00 EV = 7.20E+04 KELVIN

| IMET I | 1 | 1 | 1.0000E+00 |
|--------|---|---|------------|------------|------------|------------|------------|------------|------------|------------|
| 1 | | | | | | | | | | |

POPULATION DEPENDENCE ON DENSITY AND METASTABLE 1

| IORD I | 1 | 2 | 3 | 4 | 5 | 6 | 7 | 8 | 9 | 10 | 11 | 12 | 13 | 14 | 15 | 16 | 17 | 18 | 19 | 20 | 21 | 22 | 23 | 24 | 25 | 26 | 27 | 28 | 29 | 30 | 31 | 32 | 33 | 34 | 35 | 36 | 37 | 38 | 39 | 40 | 41 | 42 | 43 | 44 | 45 | 46 | 47 | 48 | 49 | 50 | 51 | 52 | 53 | 54 | 55 | 56 | 57 | 58 | 59 | 60 | 61 | 62 | 63 | 64 | 65 | 66 | 67 | 68 | 69 | 70 | 71 | 72 | 73 | 74 | 75 | 76 | 77 | 78 | 79 | 80 | 81 | 82 | 83 | 84 | 85 | 86 | 87 | 88 | 89 | 90 | 91 | 92 | 93 | 94 | 95 | 96 | 97 | 98 | 99 | 100 | 101 | 102 | 103 | 104 | 105 | 106 | 107 | 108 | 109 | 110 | 111 | 112 | 113 | 114 | 115 | 116 | 117 | 118 | 119 | 120 | 121 | 122 | 123 | 124 | 125 | 126 | 127 | 128 | 129 | 130 | 131 | 132 | 133 | 134 | 135 | 136 | 137 | 138 | 139 | 140 | 141 | 142 | 143 | 144 | 145 | 146 | 147 | 148 | 149 | 150 | 151 | 152 | 153 | 154 | 155 | 156 | 157 | 158 | 159 | 160 | 161 | 162 | 163 | 164 | 165 | 166 | 167 | 168 | 169 | 170 | 171 | 172 | 173 | 174 | 175 | 176 | 177 | 178 | 179 | 180 | 181 | 182 | 183 | 184 | 185 | 186 | 187 | 188 | 189 | 190 | 191 | 192 | 193 | 194 | 195 | 196 | 197 | 198 | 199 | 200 | 201 | 202 | 203 | 204 | 205 | 206 | 207 | 208 | 209 | 210 | 211 | 212 | 213 | 214 | 215 | 216 | 217 | 218 | 219 | 220 | 221 | 222 | 223 | 224 | 225 | 226 | 227 | 228 | 229 | 230 | 231 | 232 | 233 | 234 | 235 | 236 | 237 | 238 | 239 | 240 | 241 | 242 | 243 | 244 | 245 | 246 | 247 | 248 | 249 | 250 | 251 | 252 | 253 | 254 | 255 | 256 | 257 | 258 | 259 | 260 | 261 | 262 | 263 | 264 | 265 | 266 | 267 | 268 | 269 | 270 | 271 | 272 | 273 | 274 | 275 | 276 | 277 | 278 | 279 | 280 | 281 | 282 | 283 | 284 | 285 | 286 | 287 | 288 | 289 | 290 | 291 | 292 | 293 | 294 | 295 | 296 | 297 | 298 | 299 | 300 | 301 | 302 | 303 | 304 | 305 | 306 | 307 | 308 | 309 | 310 | 311 | 312 | 313 | 314 | 315 | 316 | 317 | 318 | 319 | 320 | 321 | 322 | 323 | 324 | 325 | 326 | 327 | 328 | 329 | 330 | 331 | 332 | 333 | 334 | 335 | 336 | 337 | 338 | 339 | 340 | 341 | 342 | 343 | 344 | 345 | 346 | 347 | 348 | 349 | 350 | 351 | 352 | 353 | 354 | 355 | 356 | 357 | 358 | 359 | 360 | 361 | 362 | 363 | 364 | 365 | 366 | 367 | 368 | 369 | 370 | 371 | 372 | 373 | 374 | 375 | 376 | 377 | 378 | 379 | 380 | 381 | 382 | 383 | 384 | 385 | 386 | 387 | 388 | 389 | 390 | 391 | 392 | 393 | 394 | 395 | 396 | 397 | 398 | 399 | 400 | 401 | 402 | 403 | 404 | 405 | 406 | 407 | 408 | 409 | 410 | 411 | 412 | 413 | 414 | 415 | 416 | 417 | 418 | 419 | 420 | 421 | 422 | 423 | 424 | 425 | 426 | 427 | 428 | 429 | 430 | 431 | 432 | 433 | 434 | 435 | 436 | 437 | 438 | 439 | 440 | 441 | 442 | 443 | 444 | 445 | 446 | 447 | 448 | 449 | 450 | 451 | 452 | 453 | 454 | 455 | 456 | 457 | 458 | 459 | 460 | 461 | 462 | 463 | 464 | 465 | 466 | 467 | 468 | 469 | 470 | 471 | 472 | 473 | 474 | 475 | 476 | 477 | 478 | 479 | 480 | 481 | 482 | 483 | 484 | 485 | 486 | 487 | 488 | 489 | 490 | 491 | 492 | 493 | 494 | 495 | 496 | 497 | 498 | 499 | 500 | 501 | 502 | 503 | 504 | 505 | 506 | 507 | 508 | 509 | 510 | 511 | 512 | 513 | 514 | 515 | 516 | 517 | 518 | 519 | 520 | 521 | 522 | 523 | 524 | 525 | 526 | 527 | 528 | 529 | 530 | 531 | 532 | 533 | 534 | 535 | 536 | 537 | 538 | 539 | 540 | 541 | 542 | 543 | 544 | 545 | 546 | 547 | 548 | 549 | 550 | 551 | 552 | 553 | 554 | 555 | 556 | 557 | 558 | 559 | 560 | 561 | 562 | 563 | 564 | 565 | 566 | 567 | 568 | 569 | 570 | 571 | 572 | 573 | 574 | 575 | 576 | 577 | 578 | 579 | 580 | 581 | 582 | 583 | 584 | 585 | 586 | 587 | 588 | 589 | 590 | 591 | 592 | 593 | 594 | 595 | 596 | 597 | 598 | 599 | 600 | 601 | 602 | 603 | 604 | 605 | 606 | 607 | 608 | 609 | 610 | 611 | 612 | 613 | 614 | 615 | 616 | 617 | 618 | 619 | 620 | 621 | 622 | 623 | 624 | 625 | 626 | 627 | 628 | 629 | 630 | 631 | 632 | 633 | 634 | 635 | 636 | 637 | 638 | 639 | 640 | 641 | 642 | 643 | 644 | 645 | 646 | 647 | 648 | 649 | 650 | 651 | 652 | 653 | 654 | 655 | 656 | 657 | 658 | 659 | 660 | 661 | 662 | 663 | 664 | 665 | 666 | 667 | 668 | 669 | 670 | 671 | 672 | 673 | 674 | 675 | 676 | 677 | 678 | 679 | 680 | 681 | 682 | 683 | 684 | 685 | 686 | 687 | 688 | 689 | 690 | 691 | 692 | 693 | 694 | 695 | 696 | 697 | 698 | 699 | 700 | 701 | 702 | 703 | 704 | 705 | 706 | 707 | 708 | 709 | 710 | 711 | 712 | 713 | 714 | 715 | 716 | 717 | 718 | 719 | 720 | 721 | 722 | 723 | 724 | 725 | 726 | 727 | 728 | 729 | 730 | 731 | 732 | 733 | 734 | 735 | 736 | 737 | 738 | 739 | 740 | 741 | 742 | 743 | 744 | 745 | 746 | 747 | 748 | 749 | 750 | 751 | 752 | 753 | 754 | 755 | 756 | 757 | 758 | 759 | 760 | 761 | 762 | 763 | 764 | 765 | 766 | 767 | 768 | 769 | 770 | 771 | 772 | 773 | 774 | 775 | 776 | 777 | 778 | 779 | 780 | 781 | 782 | 783 | 784 | 785 | 786 | 787 | 788 | 789 | 790 | 791 | 792 | 793 | 794 | 795 | 796 | 797 | 798 | 799 | 800 | 801 | 802 | 803 | 804 | 805 | 806 | 807 | 808 | 809 | 810 | 811 | 812 | 813 | 814 | 815 | 816 | 817 | 818 | 819 | 820 | 821 | 822 | 823 | 824 | 825 | 826 | 827 | 828 | 829 | 830 | 831 | 832 | 833 | 834 | 835 | 836 | 837 | 838 | 839 | 840 | 841 | 842 | 843 | 844 | 845 | 846 | 847 | 848 | 849 | 850 | 851 | 852 | 853 | 854 | 855 | 856 | 857 | 858 | 859 | 860 | 861 | 862 | 863 | 864 | 865 | 866 | 867 | 868 | 869 | 870 | 871 | 872 | 873 | 874 | 875 | 876 | 877 | 878 | 879 | 880 | 881 | 882 | 883 | 884 | 885 | 886 | 887 | 888 | 889 | 890 | 891 | 892 | 893 | 894 | 895 | 896 | 897 | 898 | 899 | 900 | 901 | 902 | 903 | 904 | 905 | 906 | 907 | 908 | 909 | 910 | 911 | 912 | 913 | 914 | 915 | 916 | 917 | 918 | 919 | 920 | 921 | 922 | 923 | 924 | 925 | 926 | 927 | 928 | 929 | 930 | 931 | 932 | 933 | 934 | 935 | 936 | 937 | 938 | 939 | 940 | 941 | 942 | 943 | 944 | 945 | 946 | 947 | 948 | 949 | 950 | 951 | 952 | 953 | 954 | 955 | 956 | 957 | 958 | 959 | 960 | 961 | 962 | 963 | 964 | 965 | 966 | 967 | 968 | 969 | 970 | 971 | 972 | 973 | 974 | 975 | 976 | 977 | 978 | 979 | 980 | 981 | 982 | 983 | 984 | 985 | 986 | 987 | 988 | 989 | 990 | 991 | 992 | 993 | 994 | 995 | 996 | 997 | 998 | 999 | 1000 | 1001 | 1002 | 1003 | 1004 | 1005 | 1006 | 1007 | 1008 | 1009 | 1010 | 1011 | 1012 | 1013 | 1014 | 1015 | 1016 | 1017 | 1018 | 1019 | 1020 | 1021 | 1022 | 1023 | 1024 | 1025 | 1026 | 1027 | 1028 | 1029 | 1030 | 1031 | 1032 | 1033 | 1034 | 1035 | 1036 | 1037 | 1038 | 1039 | 1040 | 1041 | 1042 | 1043 | 1044 | 1045 | 1046 | 1047 | 1048 | 1049 | 1050 | 1051 | 1052 | 1053 | 1054 | 1055 | 1056 | 1057 | 1058 | 1059 | 1060 | 1061 | 1062 | 1063 | 1064 | 1065 | 1066 | 1067 | 1068 | 1069 | 1070 | 1071 | 1072 | 107 |
|--------|---|---|---|---|---|---|---|---|---|----|----|----|----|----|----|----|----|----|----|----|----|----|----|----|----|----|----|----|----|----|----|----|----|----|----|----|----|----|----|----|----|----|----|----|----|----|----|----|----|----|----|----|----|----|----|----|----|----|----|----|----|----|----|----|----|----|----|----|----|----|----|----|----|----|----|----|----|----|----|----|----|----|----|----|----|----|----|----|----|----|----|----|----|----|----|----|----|----|----|-----|-----|-----|-----|-----|-----|-----|-----|-----|-----|-----|-----|-----|-----|-----|-----|-----|-----|-----|-----|-----|-----|-----|-----|-----|-----|-----|-----|-----|-----|-----|-----|-----|-----|-----|-----|-----|-----|-----|-----|-----|-----|-----|-----|-----|-----|-----|-----|-----|-----|-----|-----|-----|-----|-----|-----|-----|-----|-----|-----|-----|-----|-----|-----|-----|-----|-----|-----|-----|-----|-----|-----|-----|-----|-----|-----|-----|-----|-----|-----|-----|-----|-----|-----|-----|-----|-----|-----|-----|-----|-----|-----|-----|-----|-----|-----|-----|-----|-----|-----|-----|-----|-----|-----|-----|-----|-----|-----|-----|-----|-----|-----|-----|-----|-----|-----|-----|-----|-----|-----|-----|-----|-----|-----|-----|-----|-----|-----|-----|-----|-----|-----|-----|-----|-----|-----|-----|-----|-----|-----|-----|-----|-----|-----|-----|-----|-----|-----|-----|-----|-----|-----|-----|-----|-----|-----|-----|-----|-----|-----|-----|-----|-----|-----|-----|-----|-----|-----|-----|-----|-----|-----|-----|-----|-----|-----|-----|-----|-----|-----|-----|-----|-----|-----|-----|-----|-----|-----|-----|-----|-----|-----|-----|-----|-----|-----|-----|-----|-----|-----|-----|-----|-----|-----|-----|-----|-----|-----|-----|-----|-----|-----|-----|-----|-----|-----|-----|-----|-----|-----|-----|-----|-----|-----|-----|-----|-----|-----|-----|-----|-----|-----|-----|-----|-----|-----|-----|-----|-----|-----|-----|-----|-----|-----|-----|-----|-----|-----|-----|-----|-----|-----|-----|-----|-----|-----|-----|-----|-----|-----|-----|-----|-----|-----|-----|-----|-----|-----|-----|-----|-----|-----|-----|-----|-----|-----|-----|-----|-----|-----|-----|-----|-----|-----|-----|-----|-----|-----|-----|-----|-----|-----|-----|-----|-----|-----|-----|-----|-----|-----|-----|-----|-----|-----|-----|-----|-----|-----|-----|-----|-----|-----|-----|-----|-----|-----|-----|-----|-----|-----|-----|-----|-----|-----|-----|-----|-----|-----|-----|-----|-----|-----|-----|-----|-----|-----|-----|-----|-----|-----|-----|-----|-----|-----|-----|-----|-----|-----|-----|-----|-----|-----|-----|-----|-----|-----|-----|-----|-----|-----|-----|-----|-----|-----|-----|-----|-----|-----|-----|-----|-----|-----|-----|-----|-----|-----|-----|-----|-----|-----|-----|-----|-----|-----|-----|-----|-----|-----|-----|-----|-----|-----|-----|-----|-----|-----|-----|-----|-----|-----|-----|-----|-----|-----|-----|-----|-----|-----|-----|-----|-----|-----|-----|-----|-----|-----|-----|-----|-----|-----|-----|-----|-----|-----|-----|-----|-----|-----|-----|-----|-----|-----|-----|-----|-----|-----|-----|-----|-----|-----|-----|-----|-----|-----|-----|-----|-----|-----|-----|-----|-----|-----|-----|-----|-----|-----|-----|-----|-----|-----|-----|-----|-----|-----|-----|-----|-----|-----|-----|-----|-----|-----|-----|-----|-----|-----|-----|-----|-----|-----|-----|-----|-----|-----|-----|-----|-----|-----|-----|-----|-----|-----|-----|-----|-----|-----|-----|-----|-----|-----|-----|-----|-----|-----|-----|-----|-----|-----|-----|-----|-----|-----|-----|-----|-----|-----|-----|-----|-----|-----|-----|-----|-----|-----|-----|-----|-----|-----|-----|-----|-----|-----|-----|-----|-----|-----|-----|-----|-----|-----|-----|-----|-----|-----|-----|-----|-----|-----|-----|-----|-----|-----|-----|-----|-----|-----|-----|-----|-----|-----|-----|-----|-----|-----|-----|-----|-----|-----|-----|-----|-----|-----|-----|-----|-----|-----|-----|-----|-----|-----|-----|-----|-----|-----|-----|-----|-----|-----|-----|-----|-----|-----|-----|-----|-----|-----|-----|-----|-----|-----|-----|-----|-----|-----|-----|-----|-----|-----|-----|-----|-----|-----|-----|-----|-----|-----|-----|-----|-----|-----|-----|-----|-----|-----|-----|-----|-----|-----|-----|-----|-----|-----|-----|-----|-----|-----|-----|-----|-----|-----|-----|-----|-----|-----|-----|-----|-----|-----|-----|-----|-----|-----|-----|-----|-----|-----|-----|-----|-----|-----|-----|-----|-----|-----|-----|-----|-----|-----|-----|-----|-----|-----|-----|-----|-----|-----|-----|-----|-----|-----|-----|-----|-----|-----|-----|-----|-----|-----|-----|-----|-----|-----|-----|-----|-----|-----|-----|-----|-----|-----|-----|-----|-----|-----|-----|-----|-----|-----|-----|-----|-----|-----|-----|-----|-----|-----|-----|-----|-----|-----|-----|-----|-----|-----|-----|-----|-----|-----|-----|-----|-----|-----|-----|-----|-----|-----|-----|-----|-----|-----|-----|-----|-----|-----|-----|-----|-----|-----|-----|-----|-----|-----|-----|-----|-----|-----|-----|-----|-----|-----|-----|-----|-----|-----|-----|-----|-----|-----|-----|-----|-----|-----|-----|-----|-----|-----|-----|-----|-----|-----|-----|-----|-----|-----|-----|-----|-----|-----|-----|-----|-----|-----|-----|-----|-----|-----|-----|-----|-----|-----|-----|-----|-----|-----|-----|-----|-----|-----|-----|-----|-----|-----|-----|-----|-----|-----|-----|-----|-----|-----|-----|-----|-----|-----|-----|-----|-----|-----|-----|-----|-----|-----|-----|-----|-----|-----|-----|-----|-----|-----|-----|-----|-----|-----|-----|-----|-----|-----|-----|-----|-----|-----|-----|-----|-----|-----|-----|-----|-----|-----|-----|-----|-----|-----|-----|-----|-----|-----|-----|-----|-----|-----|-----|-----|-----|-----|-----|-----|-----|-----|-----|-----|-----|-----|-----|-----|-----|-----|-----|-----|-----|-----|-----|-----|-----|-----|-----|-----|-----|-----|------|------|------|------|------|------|------|------|------|------|------|------|------|------|------|------|------|------|------|------|------|------|------|------|------|------|------|------|------|------|------|------|------|------|------|------|------|------|------|------|------|------|------|------|------|------|------|------|------|------|------|------|------|------|------|------|------|------|------|------|------|------|------|------|------|------|------|------|------|------|------|------|------|-----|
|--------|---|---|---|---|---|---|---|---|---|----|----|----|----|----|----|----|----|----|----|----|----|----|----|----|----|----|----|----|----|----|----|----|----|----|----|----|----|----|----|----|----|----|----|----|----|----|----|----|----|----|----|----|----|----|----|----|----|----|----|----|----|----|----|----|----|----|----|----|----|----|----|----|----|----|----|----|----|----|----|----|----|----|----|----|----|----|----|----|----|----|----|----|----|----|----|----|----|----|----|-----|-----|-----|-----|-----|-----|-----|-----|-----|-----|-----|-----|-----|-----|-----|-----|-----|-----|-----|-----|-----|-----|-----|-----|-----|-----|-----|-----|-----|-----|-----|-----|-----|-----|-----|-----|-----|-----|-----|-----|-----|-----|-----|-----|-----|-----|-----|-----|-----|-----|-----|-----|-----|-----|-----|-----|-----|-----|-----|-----|-----|-----|-----|-----|-----|-----|-----|-----|-----|-----|-----|-----|-----|-----|-----|-----|-----|-----|-----|-----|-----|-----|-----|-----|-----|-----|-----|-----|-----|-----|-----|-----|-----|-----|-----|-----|-----|-----|-----|-----|-----|-----|-----|-----|-----|-----|-----|-----|-----|-----|-----|-----|-----|-----|-----|-----|-----|-----|-----|-----|-----|-----|-----|-----|-----|-----|-----|-----|-----|-----|-----|-----|-----|-----|-----|-----|-----|-----|-----|-----|-----|-----|-----|-----|-----|-----|-----|-----|-----|-----|-----|-----|-----|-----|-----|-----|-----|-----|-----|-----|-----|-----|-----|-----|-----|-----|-----|-----|-----|-----|-----|-----|-----|-----|-----|-----|-----|-----|-----|-----|-----|-----|-----|-----|-----|-----|-----|-----|-----|-----|-----|-----|-----|-----|-----|-----|-----|-----|-----|-----|-----|-----|-----|-----|-----|-----|-----|-----|-----|-----|-----|-----|-----|-----|-----|-----|-----|-----|-----|-----|-----|-----|-----|-----|-----|-----|-----|-----|-----|-----|-----|-----|-----|-----|-----|-----|-----|-----|-----|-----|-----|-----|-----|-----|-----|-----|-----|-----|-----|-----|-----|-----|-----|-----|-----|-----|-----|-----|-----|-----|-----|-----|-----|-----|-----|-----|-----|-----|-----|-----|-----|-----|-----|-----|-----|-----|-----|-----|-----|-----|-----|-----|-----|-----|-----|-----|-----|-----|-----|-----|-----|-----|-----|-----|-----|-----|-----|-----|-----|-----|-----|-----|-----|-----|-----|-----|-----|-----|-----|-----|-----|-----|-----|-----|-----|-----|-----|-----|-----|-----|-----|-----|-----|-----|-----|-----|-----|-----|-----|-----|-----|-----|-----|-----|-----|-----|-----|-----|-----|-----|-----|-----|-----|-----|-----|-----|-----|-----|-----|-----|-----|-----|-----|-----|-----|-----|-----|-----|-----|-----|-----|-----|-----|-----|-----|-----|-----|-----|-----|-----|-----|-----|-----|-----|-----|-----|-----|-----|-----|-----|-----|-----|-----|-----|-----|-----|-----|-----|-----|-----|-----|-----|-----|-----|-----|-----|-----|-----|-----|-----|-----|-----|-----|-----|-----|-----|-----|-----|-----|-----|-----|-----|-----|-----|-----|-----|-----|-----|-----|-----|-----|-----|-----|-----|-----|-----|-----|-----|-----|-----|-----|-----|-----|-----|-----|-----|-----|-----|-----|-----|-----|-----|-----|-----|-----|-----|-----|-----|-----|-----|-----|-----|-----|-----|-----|-----|-----|-----|-----|-----|-----|-----|-----|-----|-----|-----|-----|-----|-----|-----|-----|-----|-----|-----|-----|-----|-----|-----|-----|-----|-----|-----|-----|-----|-----|-----|-----|-----|-----|-----|-----|-----|-----|-----|-----|-----|-----|-----|-----|-----|-----|-----|-----|-----|-----|-----|-----|-----|-----|-----|-----|-----|-----|-----|-----|-----|-----|-----|-----|-----|-----|-----|-----|-----|-----|-----|-----|-----|-----|-----|-----|-----|-----|-----|-----|-----|-----|-----|-----|-----|-----|-----|-----|-----|-----|-----|-----|-----|-----|-----|-----|-----|-----|-----|-----|-----|-----|-----|-----|-----|-----|-----|-----|-----|-----|-----|-----|-----|-----|-----|-----|-----|-----|-----|-----|-----|-----|-----|-----|-----|-----|-----|-----|-----|-----|-----|-----|-----|-----|-----|-----|-----|-----|-----|-----|-----|-----|-----|-----|-----|-----|-----|-----|-----|-----|-----|-----|-----|-----|-----|-----|-----|-----|-----|-----|-----|-----|-----|-----|-----|-----|-----|-----|-----|-----|-----|-----|-----|-----|-----|-----|-----|-----|-----|-----|-----|-----|-----|-----|-----|-----|-----|-----|-----|-----|-----|-----|-----|-----|-----|-----|-----|-----|-----|-----|-----|-----|-----|-----|-----|-----|-----|-----|-----|-----|-----|-----|-----|-----|-----|-----|-----|-----|-----|-----|-----|-----|-----|-----|-----|-----|-----|-----|-----|-----|-----|-----|-----|-----|-----|-----|-----|-----|-----|-----|-----|-----|-----|-----|-----|-----|-----|-----|-----|-----|-----|-----|-----|-----|-----|-----|-----|-----|-----|-----|-----|-----|-----|-----|-----|-----|-----|-----|-----|-----|-----|-----|-----|-----|-----|-----|-----|-----|-----|-----|-----|-----|-----|-----|-----|-----|-----|-----|-----|-----|-----|-----|-----|-----|-----|-----|-----|-----|-----|-----|-----|-----|-----|-----|-----|-----|-----|-----|-----|-----|-----|-----|-----|-----|-----|-----|-----|-----|-----|-----|-----|-----|-----|-----|-----|-----|-----|-----|-----|-----|-----|-----|-----|-----|-----|-----|-----|-----|-----|-----|-----|-----|-----|-----|-----|-----|-----|-----|-----|-----|-----|-----|-----|-----|-----|-----|-----|-----|-----|-----|-----|-----|-----|-----|-----|-----|-----|-----|-----|-----|-----|-----|-----|-----|-----|-----|-----|-----|-----|-----|-----|-----|-----|-----|-----|-----|-----|-----|-----|-----|-----|-----|-----|-----|-----|-----|-----|-----|-----|-----|-----|-----|-----|-----|-----|-----|-----|-----|-----|-----|-----|-----|-----|-----|-----|-----|-----|-----|-----|-----|-----|-----|-----|-----|-----|-----|-----|-----|-----|-----|-----|-----|-----|-----|-----|-----|-----|-----|-----|-----|-----|-----|-----|-----|-----|------|------|------|------|------|------|------|------|------|------|------|------|------|------|------|------|------|------|------|------|------|------|------|------|------|------|------|------|------|------|------|------|------|------|------|------|------|------|------|------|------|------|------|------|------|------|------|------|------|------|------|------|------|------|------|------|------|------|------|------|------|------|------|------|------|------|------|------|------|------|------|------|------|-----|

```

TE (EV) -----
6.20E+00 | 1.00E+00 1.00E+00
1.24E+01 | 1.00E+00 1.00E+00
2.48E+01 | 1.00E+00 1.00E+00
3.72E+01 | 1.00E+00 1.00E+00
6.20E+01 | 1.00E+00 1.00E+00
1.24E+02 | 1.00E+00 1.00E+00
1.86E+02 | 1.00E+00 1.00E+00
2.48E+02 | 1.00E+00 1.00E+00
3.72E+02 | 1.00E+00 1.00E+00
6.20E+02 | 1.00E+00 1.00E+00

LEVEL = 143 - EQUILIBRIUM POPULATION
-----
NE (CM-3) 5.00E+00 1.00E+00 5.00E+00 7.00E+00 1.00E+10 3.00E+10 5.00E+10 1.00E+11 5.00E+11 1.00E+12
TE (EV) -----
6.20E+00 | 3.84E-16 7.90E-16 4.39E-15 6.38E-15 9.24E-15 3.00E-14 5.16E-13 5.52E-13 1.11E-12
1.24E+01 | 6.75E-12 1.38E-11 7.53E-11 1.08E-10 1.50E-10 5.00E-10 8.76E-10 1.81E-09 9.47E-09 1.91E-08
2.48E+01 | 7.35E-10 1.50E-09 8.06E-09 1.15E-08 1.68E-08 5.38E-08 9.24E-08 1.91E-07 1.00E-06 2.02E-06
3.72E+01 | 3.17E-09 6.45E-09 3.45E-08 4.91E-08 7.16E-08 2.29E-07 3.93E-07 8.15E-07 4.27E-06 8.61E-06
6.20E+01 | 9.08E-09 1.85E-08 9.82E-08 1.40E-07 2.04E-07 6.50E-07 1.11E-06 2.31E-06 1.22E-05 2.46E-05
1.24E+02 | 1.62E-08 3.29E-08 1.74E-07 2.47E-07 3.60E-07 1.15E-06 4.97E-06 4.09E-05 2.18E-05 4.41E-05
1.86E+02 | 1.70E-08 3.46E-08 1.83E-07 2.60E-07 3.78E-07 1.21E-06 2.07E-06 4.32E-06 2.31E-05 4.70E-05
2.48E+02 | 1.63E-08 3.31E-08 1.75E-07 2.48E-07 3.61E-07 1.15E-06 4.98E-06 4.13E-06 2.23E-05 4.53E-05
3.72E+02 | 1.41E-08 2.88E-08 1.52E-07 2.16E-07 3.14E-07 1.00E-06 1.73E-06 3.61E-06 1.96E-05 4.00E-05
6.20E+02 | 1.09E-08 2.22E-08 1.17E-07 1.67E-07 2.43E-07 7.77E-07 1.34E-06 2.81E-06 1.54E-05 3.16E-05

```

1.3.3 Demo (a-1) demo.a/demo_a_1_paper207.txt

Output summary text data set from interactive execution of ADAS207.

```

ADAS RELEASE: v4.0 PROGRAM: ADAS207 V1.12 DATE: 21/03/13 TIME: 09:20
***** TABULAR OUTPUT FROM SPECTRUM LINE DIAGNOSTIC PROGRAM: ADAS207 - DATE: 21/03/13 ****
INPUT CONTOUR-PASSING FILE DSN: /home/hps/adas_central/adas/pass/contour.pass
ASSOCIATED COPASE FILE DSN: /home/hps/adas_central/adas/adif04/copch26/chv6_ic#felli.dat

ION NUCLEAR RECOMBINING ----- IONIZATION POTENTIAL -----
CHARGE (Z0) ION CHARGE (Z1) (wave number <cm-1>) (rydbergs)
-----
FE+11 26 12 2668150. 24.3140284

INDEX CONFIGURATION (2S+1)L(C) ----- ENERGY LEVELS -----
(wave number <cm-1>) (rydbergs) ENERGY RELATIVE TO LEVEL 1 ----- ENERGY RELATIVE TO IONISATION POTENTIAL -----
(wave number <cm-1>) (rydbergs)
-----
1 3s2 3p3 4S3/2 (4)0( 1.5) . 9.0000000 2668150. 24.3140284
2 3s2 3p3 2D3/2 (2)2( 1.5) 44401. 0.4046125 2623750. 23.9994158
3 3s2 3p3 2D5/2 (2)2( 2.5) 48820. 0.4448815 2619330. 23.8691469
4 3s2 3p3 2P1/2 (2)1( 0.5) 76629. 0.6982963 2591522. 23.6157321
5 3s2 3p3 2P3/2 (2)1( 1.5) 82567. 0.7524075 2585584. 23.5616269
6 3s 3p4 4P5/2 (4)1( 2.5) 273532. 2.4926123 2394618. 21.8214161
.
141 3s2 3p 3d2 4D3/2 (4)2( 1.5) 1014502. 9.2448422 1653648. 15.0691861
142 3s 3p3 3d 2S1/2 (2)0( 0.5) 1014750. 9.2471022 1653400. 15.0669262
143 3s2 3p 3d2 4D1/2 (4)2( 0.5) 1015458. 9.2535540 1652692. 15.0604744

METASTABLE INFORMATION:
NUMBER OF ORDINARY LEVELS = 142
NUMBER OF METASTABLES = 1
----- METASTABLE DETAILS -----
METASTABLE ENERGY LEVEL ----- DESIGNATION -----
INDEX INDEX
1 1 3s2 3p3 4S3/(4)S( 1.5)

***** NEUTRAL HYDROGEN CHARGE EXCHANGE NOT INCLUDED *****
***** FREE ELECTRON RECOMBINATION NOT INCLUDED *****

INPUT PLASMA PARAMETERS:
----- NUMBER OF ELECTRON TEMPERATURES = 10
----- NUMBER OF ELECTRON DENSITIES = 10
INDEX ----- TE: ELECTRON TEMPERATURES ----- INDEX -- NE: ELECTRON DENSITIES --
(kelvin) (eV) (reduced) (cm-3) (reduced)
-----
1 7.200E+04 6.204E+00 5.000E+02 1 5.000E+08 1.395E+01
2 1.440E+05 1.241E+01 1.000E+03 2 1.000E+09 2.791E+01
3 2.880E+05 2.482E+01 2.000E+03 3 5.000E+09 1.395E+02
4 4.320E+05 3.722E+01 3.000E+03 4 7.000E+09 1.954E+02
5 7.200E+05 6.204E+01 5.000E+03 5 1.000E+10 2.791E+02
6 1.440E+06 1.241E+02 1.000E+04 6 3.000E+10 8.372E+02
7 2.160E+06 1.861E+02 1.500E+04 7 5.000E+10 1.395E+03
8 2.880E+06 2.482E+02 2.000E+04 8 1.000E+11 2.791E+03
9 4.320E+06 3.722E+02 3.000E+04 9 5.000E+11 1.395E+04
10 7.200E+06 6.204E+02 5.000E+04 10 1.000E+12 2.791E+04

```

TABLE KEY:

NE = ELECTRON DENSITY
 TE = ELECTRON TEMPERATURE
 ***** SPECTRUM LINE INTENSITIES & RATIOS: CONTROL DATA *****
 TRANSIENT CONDITIONS: EQUILIBRIUM

----- METASTABLE LEVEL SCALING FACTORS -----
 INDEX LEVEL DESIGNATION SCALING FACTOR
 1 1 3s2 3p3 4S/(4)S(1.5) 1.0000E+00

----- FIRST COMPOSITE LINE GROUP ASSEMBLY -----
 TRANSTN -- UPPER LEVEL -- TRANSITION
 INDEX INDEX INDEX TYPE UPPER LEVEL LOWER LEVEL A-VALUE (SEC-1)
 1 29 30 ORD <3s2 3p2(3P) (4)P(0.5)> - <3s2 3p3 4S/(4)S(1.5)> 8.66E+10

----- SECOND COMPOSITE LINE GROUP ASSEMBLY -----
 TRANSTN -- UPPER LEVEL -- TRANSITION
 INDEX INDEX INDEX TYPE UPPER LEVEL LOWER LEVEL A-VALUE (SEC-1)
 1 177 37 ORD <3s2 3p2(3P) (2)F(2.5)> - <3s2 3p3 2D3/(2)D(1.5)> 9.94E+10
 2 319 39 ORD <3s2 3p2(3P) (2)F(3.5)> - <3s2 3p3 2D5/(2)D(2.5)> 1.06E+11

***** SPECTRUM LINE INTENSITIES & RATIOS: RESULTS *****

FIRST COMPOSITE LINE GROUP ASSEMBLY - SPECTRUM LINE INTENSITIES
 NE (CM-3) 5.00E+08 1.00E+09 5.00E+09 7.00E+09 1.00E+10 3.00E+10 5.00E+10 1.00E+11 5.00E+11 1.00E+12
 TE (kelvin)
 7.20E+04 | 1.64E-04 3.29E-04 1.69E-03 2.38E-03 3.43E-03 1.06E+00 1.78E-02 3.60E-02 1.82E-01 3.66E-01
 1.44E+05 | 2.28E-02 4.58E-02 2.32E-01 3.28E-01 4.71E-01 1.44E+00 2.43E+00 4.91E+00 2.49E+01 4.99E+01
 2.88E+05 | 2.28E-01 4.58E-01 2.32E+00 3.26E+00 4.68E+00 1.43E+01 2.39E+01 4.83E+01 2.44E+02 4.89E+02
 4.32E+05 | 4.59E-01 9.21E-01 4.65E+00 6.53E+00 9.37E+00 2.85E+01 4.77E+01 9.62E+01 4.86E+02 9.74E+02
 7.20E+05 | 7.49E-01 1.59E+00 7.57E-01 1.06E+01 1.52E+01 4.61E+01 7.73E+01 1.56E+02 7.86E+02 1.57E+03
 1.44E+06 | 9.69E-01 1.94E+00 9.76E+00 1.37E+01 1.96E+01 5.93E+01 9.93E+01 2.00E+02 1.01E+03 2.02E+03
 2.16E+06 | 1.01E+00 2.92E+00 1.01E+01 1.42E+01 2.03E+01 6.14E+01 1.03E+02 2.07E+02 1.04E+03 2.09E+03
 2.88E+06 | 1.00E+00 2.91E+00 1.01E+01 1.41E+01 2.02E+01 6.11E+01 1.02E+02 2.06E+02 1.04E+03 2.08E+03
 4.32E+06 | 9.66E-01 1.93E+00 9.70E+00 1.36E+01 1.95E+01 5.88E+01 9.83E+01 1.98E+02 9.97E+02 2.00E+03
 7.20E+06 | 8.86E-01 1.77E+00 8.89E+00 1.25E+01 1.78E+01 5.38E+01 8.99E+01 1.81E+02 9.12E+02 1.83E+03

SECOND COMPOSITE LINE GROUP ASSEMBLY - SPECTRUM LINE INTENSITIES
 NE (CM-3) 5.00E+08 1.00E+09 5.00E+09 7.00E+09 1.00E+10 3.00E+10 5.00E+10 1.00E+11 5.00E+11 1.00E+12
 TE (kelvin)
 7.20E+04 | 5.62E-05 1.56E-04 1.59E-03 2.51E-03 4.03E-03 1.61E-02 2.95E-02 6.46E-02 3.55E-01 7.20E-01
 1.44E+05 | 1.24E-02 3.48E-02 3.38E-01 5.35E-01 6.62E-01 3.32E+00 6.57E+00 1.47E+01 0.33E+01 1.76E+02
 2.88E+05 | 1.51E-01 4.18E-01 3.07E-00 6.20E+00 1.01E+01 4.18E+01 8.84E+01 1.76E+02 1.03E+03 2.16E+03
 4.32E+05 | 3.15E-01 8.56E-01 8.21E+00 1.30E+01 2.10E+01 8.69E+01 1.64E+02 3.74E+02 3.19E+03 4.49E+03
 7.20E+05 | 5.12E-01 1.46E+00 1.32E+01 2.11E+01 3.42E+01 1.42E+02 2.71E+02 6.25E+02 3.75E+03 7.73E+03
 1.44E+06 | 6.16E-01 1.73E+00 1.65E+01 2.62E+01 4.25E+01 1.81E+02 3.45E+02 8.09E+02 5.05E+03 1.05E+04
 2.16E+06 | 5.92E-01 1.69E+00 1.64E+01 2.60E+01 4.22E+01 1.81E+02 3.48E+02 8.23E+02 5.25E+03 1.10E+04
 2.88E+06 | 5.52E-01 1.60E+00 1.57E+01 2.49E+01 4.05E+01 1.75E+02 3.37E+02 8.02E+02 5.22E+03 1.10E+04
 4.32E+06 | 4.79E-01 1.42E+00 1.42E+01 2.26E+01 3.68E+01 1.60E+02 3.11E+02 7.46E+02 4.97E+03 1.06E+04
 7.20E+06 | 3.80E-01 1.16E+00 1.19E+01 1.91E+01 3.12E+01 1.38E+02 2.68E+02 6.50E+02 4.45E+03 9.57E+03

SPECTRUM LINE INTENSITY RATIO
 NE (CM-3) 5.00E+08 1.00E+09 5.00E+09 7.00E+09 1.00E+10 3.00E+10 5.00E+10 1.00E+11 5.00E+11 1.00E+12
 TE (kelvin)
 7.20E+04 | 2.91E+00 2.10E+00 1.06E+00 9.47E-01 8.50E-01 6.03E+01 5.57E-01 5.14E-01 5.08E-01
 1.44E+05 | 1.83E+00 1.34E+00 6.90E-01 6.13E-01 5.47E-01 4.09E-01 3.70E-01 3.34E-01 2.99E-01 2.94E-01
 2.88E+05 | 1.51E+00 1.12E+00 5.84E-01 5.19E-01 4.62E-01 3.41E-01 3.05E-01 2.72E-01 2.38E-01 2.33E-01
 4.32E+05 | 1.46E+00 1.08E+00 5.67E-01 5.03E-01 4.47E-01 3.27E-01 2.92E-01 2.57E-01 2.22E-01 2.17E-01
 7.20E+05 | 1.46E+00 5.68E-01 5.03E-01 4.45E-01 3.23E-01 2.85E-01 2.49E-01 2.09E-01 2.04E-01
 1.44E+06 | 1.57E+00 1.12E+00 5.91E-01 5.23E-01 4.61E-01 3.29E-01 2.88E-01 2.47E-01 2.00E-01 1.92E-01
 2.16E+06 | 1.70E+00 1.19E+00 6.19E-01 5.46E-01 4.81E-01 3.39E-01 2.95E-01 2.51E-01 1.99E-01 1.90E-01
 2.88E+06 | 1.82E+00 1.25E+00 6.44E-01 5.68E-01 4.99E-01 3.49E-01 3.03E-01 2.56E-01 1.99E-01 1.89E-01
 4.32E+06 | 2.02E+00 1.36E+00 6.84E-01 6.03E-01 5.29E-01 3.66E-01 3.16E-01 2.65E-01 2.01E-01 1.89E-01
 7.20E+06 | 2.33E+00 1.53E+00 7.45E-01 6.54E-01 5.72E-01 3.91E-01 3.35E-01 2.78E-01 2.05E-01 1.91E-01

1.3.4 Demo (a-2) demo_a/demo_a_2.pecfile.dat

Output pec data set from command line use of demo_a_2.pro.

```

50 /FE+11 EMISSIVITY COEFFTS./
191.7 4 10 /FILENM = _ic#fe11/TYPE = EXCIT /INDM = T/ISEL = 1
5.00E+08 1.00E+09 5.00E+09 7.00E+09 1.00E+10 3.00E+10 5.00E+10 1.00E+11
5.00E+11 1.00E+12
6.20E+00 1.24E+01 2.48E+01 3.72E+01 6.20E+01 1.24E+02 1.86E+02 2.48E+02
3.72E+02 6.20E+02
1.02E-12 1.27E-10 1.22E-09 2.43E-09 3.97E-09 5.29E-09 5.56E-09 5.59E-09
5.48E-09 5.17E-09
9.67E-13 1.19E-10 1.14E-09 2.27E-09 3.72E-09 4.97E-09 5.25E-09 5.29E-09
5.20E-09 4.93E-09
8.17E-13 9.61E-11 9.12E-10 1.82E-09 3.01E-09 4.11E-09 4.39E-09 4.46E-09
4.43E-09 4.25E-09
7.85E-13 9.11E-11 8.61E-10 1.72E-09 2.85E-09 3.90E-09 4.18E-09 4.25E-09
4.24E-09 4.08E-09
7.52E-13 8.59E-11 8.08E-10 1.61E-09 2.67E-09 3.67E-09 3.95E-09 4.03E-09
4.03E-09 3.89E-09
6.65E-13 7.18E-11 6.60E-10 1.31E-09 2.17E-09 3.00E-09 3.25E-09 3.33E-09
3.35E-09 3.27E-09
6.35E-13 6.67E-11 6.05E-10 1.20E-09 1.98E-09 2.72E-09 2.94E-09 3.02E-09

```

```

3.05E-09 2.98E-09
6.06E-13 6.17E-11 5.49E-10 1.08E-09 1.76E-09 2.40E-09 2.58E-09 2.65E-09
2.67E-09 2.61E-09
5.78E-13 5.65E-11 4.89E-10 9.44E-10 1.50E-09 1.98E-09 2.08E-09 2.10E-09
2.08E-09 2.00E-09
5.75E-13 5.58E-11 4.80E-10 9.24E-10 1.46E-09 1.90E-09 1.99E-09 2.00E-09
1.97E-09 1.87E-09
190.3 10 10 /FILMEN = _ic#fe11/TYPE = EXCIT /INDM = T/ISEL = 2
5.00E+08 1.00E+09 5.00E+09 7.00E+09 1.00E+10 3.00E+10 5.00E+10 1.00E+11
5.00E+11 1.00E+12
6.20E+00 1.24E+01 2.88E+01 3.72E+01 6.20E+01 1.24E+02 1.86E+02 2.48E+02
3.72E+02 6.20E+02

3.42E-11 3.04E-11
3.71E-15 8.32E-13 9.65E-12 1.96E-11 3.15E-11 3.94E-11 4.00E-11 3.92E-11
3.71E-11 3.37E-11
C-----
C
C PHOTON EMISSIVITY COEFFICIENTS:
C
C -----
C INFORMATION
C -----
C NUCLEAR CHARGE = 26
C ION CHARGE +1 = 12
C
C SPECIFIC ION FILE : /home/adas/adas/adf04/copch#26/chv6_ic#fe11.dat
C EXPANSION FILE : No projection data was used in this case.
C
C No ionisation data has been included
C
C OPTIONS : LNORM=T LPSEL=F LZSEL=F LIOSEL=F
C             LHSEL=F LRSEL=F LISEL=F LNSEL=F
C
C
C Configuration      (2s+1)l(w-1/2)          Energy (cm**-1)
C   1   3s2 3p3 4S3/2      (4)0( 1.5)          0.0
C   2   3s2 3p3 2D3/2      (2)2( 1.5)        44401.0
C   3   3s2 3p3 2D5/2      (2)2( 2.5)        48820.0
C   4   3s2 3p3 2P1/2      (2)1( 0.5)        76629.0
C   5   3s2 3p3 2P3/2      (2)1( 1.5)        82567.0
C
C   140 3s2 3p 3d2 4D5/2      (4)2( 2.5)    1013361.0
C   141 3s2 3p 3d2 4D3/2      (4)2( 1.5)    1014592.0
C   142 3s 3p3 3d 2S1/2      (2)0( 0.5)    1014750.0
C   143 3s2 3p 3d2 4D1/2      (4)2( 0.5)    1015458.0
C
C
C ISEL  WAVELENGTH      TRANSITION      TYPE  METASTABLE  IMET NMET IP
C -----
C   1.    191.68   27(4)1( 2.5)- 1(4)0( 1.5) EXCIT   T   1
C   2.    190.25   29(4)1( 1.5)- 1(4)0( 1.5) EXCIT   T   1
C   3.    183.55   39(2)3( 3.5)- 3(2)2( 2.5) EXCIT   T   1
C   4.    189.35   30(4)1( 0.5)- 1(4)0( 1.5) EXCIT   T   1
C   5.    183.54   37(2)3( 2.5)- 2(2)2( 1.5) EXCIT   T   1
C   6.    187.32   40(2)2( 2.5)- 5(2)1( 1.5) EXCIT   T   1
C   7.    216.74   26(2)1( 1.5)- 3(2)2( 2.5) EXCIT   T   1
C
C CODE : ADAS208
C PRODUCER : Hugo Summers
C DATE : 22/03/13
C
C-----
```

2 Demo (b) Building up contribution functions and the kernel

DEMO b: Building up contribution functions and the kernel.

PURPOSE: Build up the contribution functions $G(Te(Ne))$ using a model with constant electron density or constant electron pressure (Pe^*Ne^*Te). The final scope is to create a collection file, called kernel, which contains the G -functions for all the lines observed by a spectrometer, e.g. SUMER and CDS onboard SoHO and EIS onboard Hinode.

The observed lines with their intensities are collected within the directory /home/adas/adas/arch601/intensity/. An intensity file is created by hand by the user. It contains the line specifications: elements, ionisation stages, wavelengths, transitions, indices to detect the blends, indices to relate each line to the respective contribution function (G-index), observed intensities and observed errors. In the intensity files, the link between observations and theory is given by the G-index. These indices specify the transition as it appears in the adf20 and it is kept in the kernel file. The kernel is a collection file (in /home/adas/adas/arch601/kernel/), which contains the G -functions for all the selected transitions. Finally in /home/adas/adas/arch601/abundance/ there is a collection of elemental abundances, which are needed for the Differential Emission Measure (DEM) analysis (DEMO c).

EXAMPLE: In the solar case the intensity file /home/adas/adas/arch601/intensity/sumer_cds_eis_qs.dat contains intensities observed by SoHO/SUMER, SoHO/CDS and Hinode/EIS. The G -functions are built up for the lines present in that intensity file. A model with constant electron density $Ne=1.e10$ cm $^{-3}$ and a model with constant pressure $Pe=1.e14$ K cm $^{-3}$ are used.

The lines included in the demo are the following:

| INSTRUMENT | ION | WAVEL.(Ang.) | TRANSITION | LOG(Te(K)) |
|------------|-------|--------------|------------------------------|------------|
| from CDS | O+4 | 629.732 | 2s2 1S0 - 2s 2p 1P1 | 5.35 |
| from CDS | Ne+3 | 542.070 | 2s2 2p3 4S3/2 - 2s 2p4 4P3/2 | 5.20 |
| from CDS | Ne+3 | 543.886 | 2s2 2p3 4S3/2 - 2s 2p4 4P5/2 | 5.20 |
| from SUMER | Si+1 | 1304.370 | 3s2 3p 2P1/2 - 3s 3p2 2S1/2 | 4.45 |
| from SUMER | Si+1 | 1309.276 | 3s2 3p 2P3/2 - 3s 3p2 2S1/2 | 4.45 |
| from EIS | Si+6 | 275.353 | 2s2 2p4 3P2 - 2s 2p5 3P2 | 5.80 |
| from EIS | Si+6 | 275.667 | 2s2 2p4 3P1 - 2s 2p5 3P1 | 5.80 |
| from CDS | Si+11 | 520.662 | 2s 2S1/2 - 2p 2P1/2 | 6.30 |

The adf04 used for the demo are the following:

/home/adas/adas/adf04/adas#8/cop98#8_ls#o4.dat
/home/adas/adas/adf04/adas#10/cop98#10_ic#ne3.dat
/home/adas/adas/adf04/copch#14/chv6_ic#si1.dat

/home/adas/adas/adf04/copch#14/chv6_ic#si6.dat
/home/adas/adas/adf04/copch#14/chv6_ic#si11.dat

The adf11 are specified by 96.

The ration NH/Ne is taken from the tabulated value of McWhirter et al.1975,A&A,40,63.

COMMENTS: The line have been chosen to cover a large temperature range. The output files of ADAS412 are a set of files .pass in the adf20 format and a set of files .ps. All of them are needed to build up the kernel (DEMO 5).

DEMO b-1: Exploiting arch601: abundance, intensity and kernel.
Look at the files collected in /home/adas/adas/arch601/abundance/,
/home/adas/adas/arch601/intensity/,/home/adas/adas/arch601/kernel/.

DEMO b-2: Using ADAS412 and looking at adf20.

1. Use ADAS412 with the interactive ADAS windows.

(sample of output files: goft_o4_n1e10.pass and goft_o4_n1e10.ps)

2a. Use run_adas412.pro to produce the G(T).

2b. Use read_adf20.pro to read the file produced by point 2a.

2c. Plot the G(T) as a function of Te.

Program: demo_b_4.pro

Sample of output files: goft_idl_o4_n1e10.pass and goft_idl_o4_n1e10.ps

3. Produce a set of adf20 using methods 1. and 2. at Ne=1.e10 cm⁻³
and at Pe=1.e14 K cm⁻³

DEMO b-3: Using ADAS506 to produce the kernel.

1. Using ADAS506 with the interactive ADAS windows to produce a kernel.

The input files are the adf20 produced by DEMO 4.

The output files are: kernel_n1e10.dat and kernel_p1e14.dat.

(sample of output plots: plot_adas506_o4_n1e10.ps)

2.1 Demo (b) Figures

2.1.1 Demo (b-2) demo.b/demo.b_2_graph412.pdf

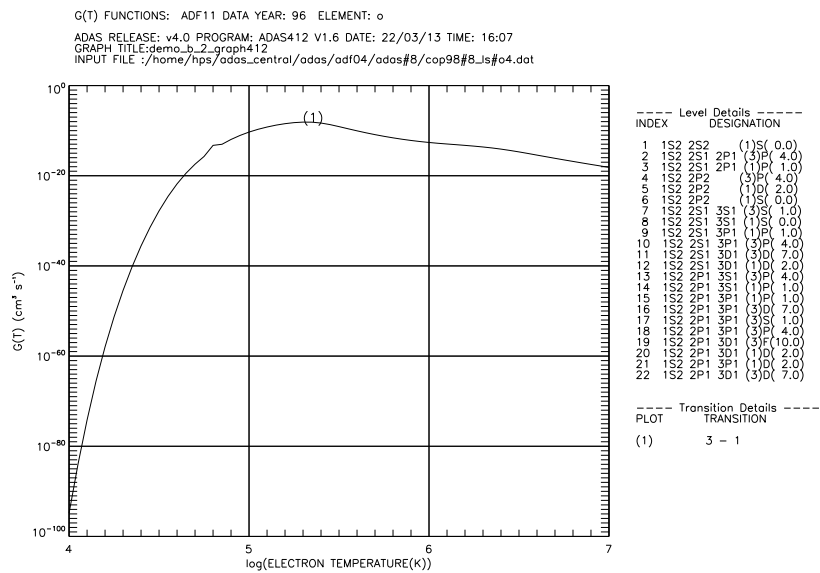


Figure 4: GTe-function plot vs Te for and O⁺⁴ transition

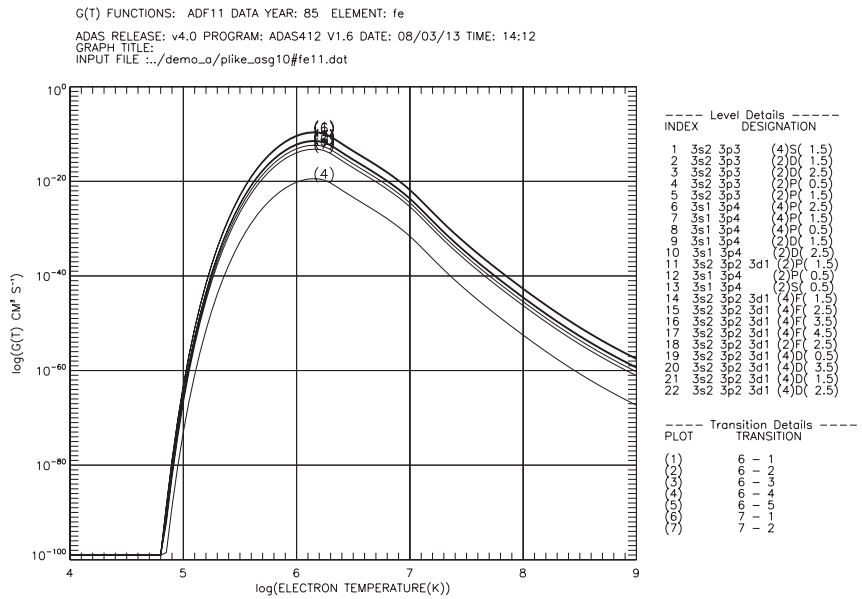


Figure 5: demo_b/goft.pdf

2.1.2 Demo (b-3) demo_b/demo_b_3_adas205.pdf

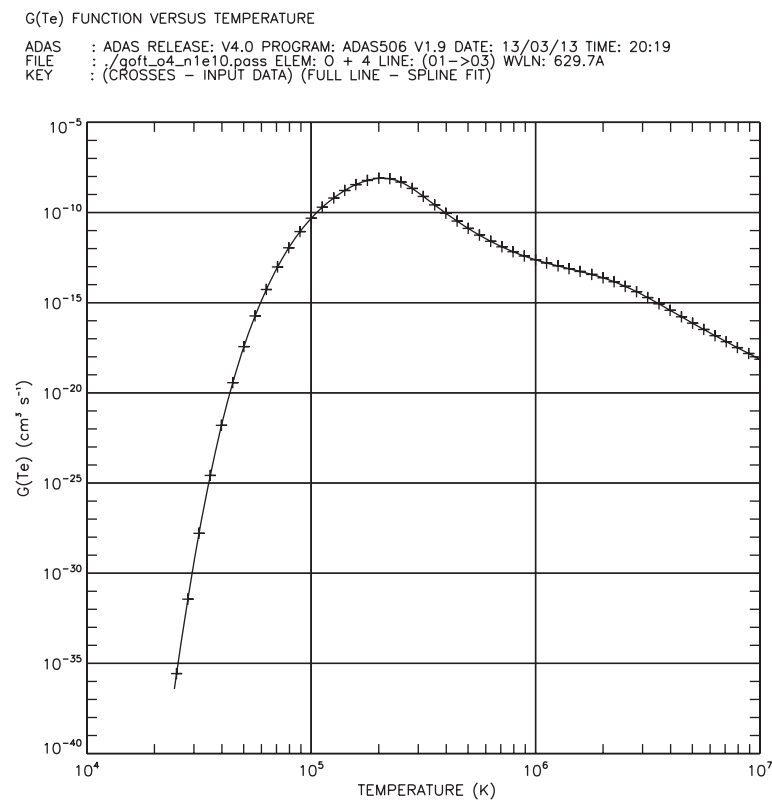


Figure 6: demo_b/plot_adas506_o4_n1e10.pdf

2.2 Demo (b) IDL procedures

2.2.1 Demo (b-2) demo.b_2.pro

```
pro demo_b_4
;using run_adas412.pro to build up the contribution functions

;define electron temperature array (Kelvin)
te=adas_vector(low=1.e4,high=1.e7,num=61)

;model with constant electron density at 1.e10 cm-3
dens=adas_vector(low=1.e10,high=1.e10,num=61)

;model with constant electron pressure (K cm-3)
pressure=adas_vector(low=1.e14,high=1.e14,num=61)

;build an array of files which include the adf04 required
adf04=['/home/adas/adas/adf04/adas#8/cop98#8_ls#o4.dat',      $
       '/home/adas/adas/adf04/adas#10/cop98#10_ic#ne3.dat',    $
       '/home/adas/adas/adf04/copch#14/chv6_ic#si1.dat',      $
       '/home/adas/adas/adf04/copch#14/chv6_ic#si6.dat',      $
       '/home/adas/adas/adf04/copch#14/chv6_ic#si11.dat'  ]

nadf04=n_elements(adf04)

year=96
elem=['o','ne','si']
ionstage=[4,3,1,3,11]
uid='ADAS'
;nnumber of line for each adf04 file
nline=[1,2,2,2,1]

;indices of upper states
upper=[3,6,7,9,9,6,7,2]

;indices of lower states
lower=[1,1,1,1,2,1,2,1]

;spectroscopic wavelengths
assigned=[629.732,543.886,542.070,1304.370,1309.276,275.353,275.667,520.662]

;use run_adas412.pro to produce the adf20
;model with constant density
;oxygen line O+4 629.732
run_adas412,adf04=adf04[0],year=year,elem=elem[0],uid=uid,          $
              te=te,dens=dens,                                     $
              upper=upper[0],lower=lower[0],                         $
```

```

        assigned=assigned[0],                                     $
adf20='goft_idl_'+strtrim(elem[0],2)+strtrim(string(ionstage[0]),2)+'_n1e10.pass'

;neon lines Ne+3 543.886,542.070
run_adas412,adf04=adf04[1],year=year,elem=elem[1],uid=uid,          $
te=te,dens=dens,                                              $
upper=upper[1:2],lower=lower[1:2],                                $
assigned=assigned[1:2],                                         $
adf20='goft_idl_'+strtrim(elem[1],2) $                         $
+strtrim(string(ionstage[1]),2)+'_n1e10.pass'

;silicon lines Si+1 1304.370,1309.276
run_adas412,adf04=adf04[2],year=year,elem=elem[2],uid=uid,          $
te=te,dens=dens,                                              $
upper=upper[3:4],lower=lower[3:4],                                $
assigned=assigned[3:4],                                         $
adf20='goft_idl_'+strtrim(elem[2],2) $                         $
+strtrim(string(ionstage[2]),2)+'_n1e10.pass'

;silicon lines Si+3 275.353,275.667
run_adas412,adf04=adf04[3],year=year,elem=elem[2],uid=uid,          $
te=te,dens=dens,                                              $
upper=upper[5:6],lower=lower[5:6],                                $
assigned=assigned[5:6],                                         $
adf20='goft_idl_'+strtrim(elem[2],2) $                         $
+strtrim(string(ionstage[3]),2)+'_n1e10.pass'

;silicon line Si+11 520.662
run_adas412,adf04=adf04[4],year=year,elem=elem[2],uid=uid,          $
te=te,dens=dens,                                              $
upper=upper[7:7],lower=lower[7:7],                                $
assigned=assigned[7:7],                                         $
adf20='goft_idl_'+strtrim(elem[2],2) $                         $
+strtrim(string(ionstage[4]),2)+'_n1e10.pass'

;model with constant pressure
;oxygen line O+4 629.732
run_adas412,adf04=adf04[0],year=year,elem=elem[0],uid=uid,          $
te=te,pressure=pressure,                                         $
upper=upper[0],lower=lower[0],                                    $
assigned=assigned[0],                                         $
adf20='goft_idl_'+strtrim(elem[0],2) $                         $
+strtrim(string(ionstage[0]),2)+'_p1e14.pass'

;neon lines Ne+3 543.886,542.070
run_adas412,adf04=adf04[1],year=year,elem=elem[1],uid=uid,          $

```

```

        te=te,pressure=pressure,                      $
        upper=upper[1:2],lower=lower[1:2],           $
        assigned=assigned[1:2],                      $
        adf20='goft_idl_'+strtrim(elem[1],2) $      $
            +strtrim(string(ionstage[1]),2)+'_p1e14.pass'

;silicon lines Si+1 1304.370,1309.276
run_adas412,adf04=adf04[2],year=year,elem=elem[2],uid=uid,          $
    te=te,pressure=pressure,                      $
    upper=upper[3:4],lower=lower[3:4],           $
    assigned=assigned[3:4],                      $
    adf20='goft_idl_'+strtrim(elem[2],2) $      $
        +strtrim(string(ionstage[2]),2)+'_p1e14.pass'

;silicon lines Si+3 275.353,275.667
run_adas412,adf04=adf04[3],year=year,elem=elem[2],uid=uid,          $
    te=te,pressure=pressure,                      $
    upper=upper[5:6],lower=lower[5:6],           $
    assigned=assigned[5:6],                      $
    adf20='goft_idl_'+strtrim(elem[2],2) $      $
        +strtrim(string(ionstage[3]),2)+'_p1e14.pass'

;silicon line Si+11 520.662
run_adas412,adf04=adf04[4],year=year,elem=elem[2],uid=uid,          $
    te=te,pressure=pressure,                      $
    upper=upper[7:7],lower=lower[7:7],           $
    assigned=assigned[7:7],                      $
    adf20='goft_idl_'+strtrim(elem[2],2) $      $
        +strtrim(string(ionstage[4]),2)+'_p1e14.pass'

;use read_adf20.pro to read adf20 for O+4 629.732 at n1e10 and plot it
file='goft_idl_o4_n1e10.pass'
block=1
read_adf20,file=file, block=block,te=te,data=gft,dens=dens,/kelvin

set_plot,'ps'
device, /isolatin1, font_index=8
device, bits=8, filename='goft_idl_o4_n1e10.ps',   $
    font_size = 14, xsize=18.0, ysize=16.0, $      $
    yoffset=7.0, /color
device, /helvetica
plot_io,alog10(te),gft,tit='G(T) FUNCTION FOR O!u+4!n 629.732 Ang.',$      $
    xtit='log(TEMPERATURE(K))',                 $
    ytit='G(T) CM!u3!n S!u-1!n'

plot_io,alog10(te),gft,tit='G(T) FUNCTION FOR O!u+4!n 629.732 Ang.',$      $
    xtit='log(TEMPERATURE(K))',                 $
    ytit='G(T) CM!u3!n S!u-1!n',                 $

```

```
xs=1, xr=[4., 7.], ys=1, yr=[1.e-20, 1.e-5]
```

```
device, /close
set_plot,'X'
!p.font=-1
```

```
end
```

2.3 Demo (b) Tables and datasets

2.3.1 Demo (b-1) arch601/intensity/sumer_cds_eis_qs.dat

| | | spectr. | configuration | configuration | G-in | blnd | observed | observed | uncert. |
|-----------------------------------|---|------------|---|---------------|------|------|------------|------------|------------|
| | | wavelength | | | | | wavelength | intensity | |
| \UNITS=PHOTONS/SEC/STER/CM2 | | | | | | | | | |
| -Lines for the integral inversion | | | | | | | | | |
| Si+1 | N | 1309.276 | 3s^2 3p ^2P_{3/2}-3s 3p^2 ^2S_{1/2} | | 2 | 0 | 1309.181 | 8.6928e+12 | 1.7812e+11 |
| Ne+3 | E | 543.886 | \$2s^2 2p^3 ^4S_{3/2}-2s^2 2p^4 ^4P_{5/2} | | 1 | 0 | 544.028 | 2.2161e+11 | 7.2878e+09 |
| O +4 | N | 629.732 | 2s^2 ^2P_{0}-2s 2p ^1P_{1} | | 1 | 0 | 629.750 | 1.4535e+13 | 4.5605e+11 |
| Si+6 | N | 275.667 | 2s^2 2p^4 ^3P_1-2s 2p^5 ^3P_1 | | 2 | 0 | 275.708 | 3.8530e+10 | 4.6620e+09 |
| Si+11 | E | 520.662 | \$2s^2 2S_{1/2}-2p ^2P_{1/2} | | 1 | 0 | 520.805 | 9.5996e+10 | 5.5300e+09 |
| - | | | | | | | | | |
| -Lines to be reconstructed | | | | | | | | | |
| *from SoHO/SUMER | | | | | | | | | |
| Si+1 | N | 1304.370 | 3s^2 3p ^2P_{1/2}-3s 3p^2 ^2S_{1/2} | | -1 | 0 | 1304.315 | 4.4333e+12 | 2.4451e+11 |
| *from SoHO/CDS | | | | | | | | | |
| Ne+3 | E | 542.070 | \$2s^2 2p^3 ^4S_{3/2}-2s 2p^4 ^4P_{3/2} | | -2 | 0 | 542.211 | 1.4489e+11 | 6.0760e+09 |
| *from Hinode/EIS | | | | | | | | | |
| Si+6 | N | 275.353 | 2s^2 2p ^4 ^3P_2-2s 2p^5 ^3P_2 | | -1 | 0 | 275.394 | 2.2509e+11 | 8.4046e+09 |

2.3.2 Demo (b-1) arch601/abundance/abund.coronal_phillips08

| | | | |
|----|-------|-------|-------|
| H | 12.00 | 12.00 | 12.00 |
| HE | 10.90 | 10.90 | 10.90 |
| C | 8.58 | 8.58 | 8.58 |
| N | 8.02 | 8.02 | 8.02 |
| O | 8.90 | 8.87 | 8.93 |
| NE | 8.10 | 8.10 | 8.10 |
| NA | 7.10 | 7.10 | 7.10 |
| MG | 8.15 | 8.15 | 8.15 |
| AL | 7.26 | 7.26 | 7.26 |
| SI | 8.14 | 8.12 | 8.16 |
| S | 7.34 | 7.34 | 7.34 |
| AR | 6.45 | 6.45 | 6.45 |
| CA | 7.14 | 7.14 | 7.14 |
| FE | 8.07 | 8.07 | 8.07 |
| NI | 7.02 | 7.02 | 7.02 |

2.3.3 Demo (b-1) arch601/kernel/kernel_n1e10.dat

```
NE+ 3 /ITRANS= 1/NTEMP= 94/APPWAV= 543.900/SPWAV= 0.000/
./goft_ne3_n1e10.pass
4.35 4.40 4.45 4.50 4.55 4.60 4.65 4.70 4.75 4.80 4.85 4.90 4.95 5.00 5.05 5.10
5.15 5.20 5.25 5.30 5.35 5.40 5.45 5.50 5.55 5.60 5.65 5.70 5.75 5.80 5.85 5.90
5.95 6.00 6.05 6.10 6.15 6.20 6.25 6.30 6.35 6.40 6.45 6.50 6.55 6.60 6.65 6.70
6.75 6.80 6.85 6.90 6.95 7.00 7.05 7.10 7.15 7.20 7.25 7.30 7.35 7.40 7.45 7.50
7.55 7.60 7.65 7.70 7.75 7.80 7.85 7.90 7.95 8.00 8.05 8.10 8.15 8.20 8.25 8.30
8.35 8.40 8.45 8.50 8.55 8.60 8.65 8.70 8.75 8.80 8.85 8.90 8.95 9.00
4.9910E-31 1.7790E-27 1.9190E-24 8.5530E-22 1.7940E-19 1.8440E-17 8.6820E-16
1.8260E-14 2.0420E-13 1.5190E-12 8.3470E-12 3.5090E-11 1.0980E-10 2.3890E-10
3.7510E-10 4.7370E-10 5.1760E-10 4.8990E-10 4.0140E-10 2.8650E-10 1.8160E-10
1.0310E-10 5.2620E-11 2.4370E-11 1.0380E-11 3.9770E-12 1.2320E-12 2.6970E-13
4.2010E-14 5.2300E-15 6.1350E-16 7.7100E-17 1.2020E-17 2.3330E-18 5.2620E-19
1.2870E-19 3.3400E-20 9.2650E-21 2.7600E-21 8.8040E-22 2.9520E-22 1.0190E-22
```

```

3.5530E-23 1.2270E-23 4.1290E-24 1.3260E-24 3.9890E-25 1.1240E-25 2.9920E-26
7.5930E-27 1.8930E-27 4.8190E-28 1.3020E-28 4.0680E-29 0.0000E+00 0.0000E+00
0.0000E+00 0.0000E+00 0.0000E+00 0.0000E+00 0.0000E+00 0.0000E+00 0.0000E+00
NE+ 3 /ITRANS= 2/NTEMP= 94/APPWAV= 542.100/SPWAV= 0.000/
./gofit_ne3_nle10.pass
4.35 4.40 4.45 4.50 4.55 4.60 4.65 4.70 4.75 4.80 4.85 4.90 4.95 5.00 5.05 5.10
5.15 5.20 5.25 5.30 5.35 5.40 5.45 5.50 5.55 5.60 5.65 5.70 5.75 5.80 5.85 5.90
5.95 6.00 6.05 6.10 6.15 6.20 6.25 6.30 6.35 6.40 6.45 6.50 6.55 6.60 6.65 6.70
6.75 6.80 6.85 6.90 6.95 7.00 7.05 7.10 7.15 7.20 7.25 7.30 7.35 7.40 7.45 7.50
7.55 7.60 7.65 7.70 7.75 7.80 7.85 7.90 7.95 8.00 8.05 8.10 8.15 8.20 8.25 8.30
8.35 8.40 8.45 8.50 8.55 8.60 8.65 8.70 8.75 8.80 8.85 8.90 8.95 9.00
3.2110E-31 1.1500E-27 1.2450E-24 5.5720E-22 1.1720E-19 1.2080E-17 5.6990E-16
1.2010E-14 1.3450E-13 1.0020E-12 5.5100E-12 2.3200E-11 7.2710E-11 1.5840E-10
2.4900E-10 3.1480E-10 3.4440E-10 3.2620E-10 2.6740E-10 1.9090E-10 1.2100E-10
6.8660E-11 3.5020E-11 1.6210E-11 6.9000E-12 2.6570E-12 8.4390E-13 1.8770E-13
2.9230E-14 3.6070E-15 4.0850E-16 5.0910E-17 7.9300E-18 1.5360E-18 3.4610E-19
8.4530E-20 2.1910E-20 6.0680E-21 1.8050E-21 5.7500E-22 1.9250E-22 6.6410E-23
2.3110E-23 7.9770E-24 2.6800E-24 8.6000E-25 2.5850E-25 7.2760E-26 1.9360E-26
4.9080E-27 1.2220E-27 3.1090E-28 8.3950E-29 2.6190E-29 0.0000E+00 0.0000E+00
0.0000E+00 0.0000E+00 0.0000E+00 0.0000E+00 0.0000E+00 0.0000E+00 0.0000E+00
0 + 4 /ITRANS= 1/NTEMP= 94/APPWAV= 629.700/SPWAV= 0.000/
./gofit_o4_nle10.pass
4.35 4.40 4.45 4.50 4.55 4.60 4.65 4.70 4.75 4.80 4.85 4.90 4.95 5.00 5.05
6.1740E-41 2.7220E-36 3.6220E-32 1.6310E-28 2.6360E-25 1.5850E-22 3.6730E-2
SI+11 /ITRANS= 1/NTEMP= 94/APPWAV= 520.700/SPWAV= 520.600/
./gofit_s11_nle10_ch6.pass
4.35 4.40 4.45 4.50 4.55 4.60 4.65 4.70 4.75 4.80 4.85 4.90 4.95 5.00 5.05
0.0000E+00 0.0000E+00 0.0000E+00 0.0000E+00 0.0000E+00 0.0000E+00 0.0000E+00
SI+ 1 /ITRANS= 1/NTEMP= 94/APPWAV= 1248.300/SPWAV= 1304.300/
./gofit_s11_nle10_ch6.pass
4.35 4.40 4.45 4.50 4.55 4.60 4.65 4.70 4.75 4.80 4.85 4.90 4.95 5.00 5.05
8.5320E-12 5.1400E-12 3.5220E-12 2.7170E-12 2.1620E-12 1.5920E-12 9.1820E-1
SI+ 1 /ITRANS= 2/NTEMP= 94/APPWAV= 1253.600/SPWAV= 1309.200/
./gofit_s11_nle10_ch6.pass
4.35 4.40 4.45 4.50 4.55 4.60 4.65 4.70 4.75 4.80 4.85 4.90 4.95 5.00 5.05
1.6960E-11 1.0220E-11 7.0010E-12 5.4000E-12 4.2980E-12 3.1650E-12 1.8250E-1
SI+ 6 /ITRANS= 1/NTEMP= 94/APPWAV= 267.600/SPWAV= 275.300/
./gofit_s16_nle10_ch6.pass
4.35 4.40 4.45 4.50 4.55 4.60 4.65 4.70 4.75 4.80 4.85 4.90 4.95 5.00 5.05
1.0000E-99 2.1680E-97 1.3740E-86 1.2000E-76 1.2170E-67 1.1740E-59 8.8490E-5
SI+ 6 /ITRANS= 2/NTEMP= 94/APPWAV= 268.000/SPWAV= 275.600/
./gofit_s16_nle10_ch6.pass
4.35 4.40 4.45 4.50 4.55 4.60 4.65 4.70 4.75 4.80 4.85 4.90 4.95 5.00 5.05
1.0000E-99 3.4010E-98 2.2000E-87 1.9590E-77 2.0180E-68 1.9740E-60 1.5070E-5
XX

```

2.3.4 Demo (b-2) demo.b/demo.b_2_paper412.txt

```

0 + 4 /NLEVELS= 44/NKNOTS= 61/NLINES= 1/
-----  

SOURCE FILES:  

-----  

IONISATION BALANCE DATA - /home/hps/adas_central/adas/adf11.<>cd96#0.dat  

SPECIFIC ION FILE DATA - /home/hps/adas_central/adas/adf04/adas#8/cop98#8_ls#o4.dat  

-----  

PROCESSING CODE DATE USER IDENTIFIER  

-----  

ADAS 412 22/03/13 Hugh Summers  

-----  

ENERGY LEVEL INDEXING  

-----  

INDX CODE S L IJ  

-----  

1 1S2 2S2 1(0) 0.0  

2 1S2 2S1 2P1 3(1) 4.0  

3 1S2 2S1 2P1 1(1) 1.0  

4 1S2 2P2 3(1) 4.0

```

```

5    IS2 2P2      1(2) 2.0
6    IS2 2P2      1(0) 0.0
7    IS2 2S1 3S1  3(0) 1.0

40   IS2 2S1 5D1  1(2) 2.0
41   IS2 2S1 5G1  3(4)13.0
42   IS2 2S1 5G1  1(4) 4.0
43   IS2 2S1 5F1  3(3)19.0
44   IS2 2S1 5F1  1(3) 3.0

PLASMA MODEL (FINITE DENSITY IONISATION BALANCE =YES)
-----
TE(K)    NE(CM-3)  P(KCM-3)  NH/NE    TIME(S)  LOG(TE)  LOG(NE)  LOG(P)
-----+-----+-----+-----+-----+-----+-----+-----+
1.00E+04 1.00E+10 1.00E+14 1.61E+00 4.00     10.00    14.00
1.12E+04 1.00E+10 1.12E+14 1.43E+00 4.05     10.00    14.05
1.26E+04 1.00E+10 1.26E+14 1.33E+00 4.10     10.00    14.10
1.41E+04 1.00E+10 1.41E+14 1.24E+00 4.15     10.00    14.15
1.58E+04 1.00E+10 1.58E+14 1.17E+00 4.20     10.00    14.20

6.31E+06 1.00E+10 6.31E+16 8.29E-01 6.89     10.00    16.89
7.08E+06 1.00E+10 7.08E+16 8.29E-01 6.85     10.00    16.85
7.94E+06 1.00E+10 7.94E+16 8.29E-01 6.90     10.00    16.90
8.91E+06 1.00E+10 8.91E+16 8.29E-01 6.95     10.00    16.95
1.00E+07 1.00E+10 1.00E+17 8.29E-01 7.00     10.00    17.00

TABLE OF G(T) VALUES (CM3 S-1) FOR O V
-----
TRANS INDEX 1       2       3       4       5       6       7       8       9       10
APPROX WLENGTH 629.7 0.0     0.0     0.0     0.0     0.0     0.0     0.0     0.0
SPECTR WLENGTH 629.700 0.000 0.000 0.000 0.000 0.000 0.000 0.000 0.000 0.000
TRANSITION 1- 3    0- 0    0- 0    0- 0    0- 0    0- 0    0- 0    0- 0    0- 0
LOG(TE(K))          .          .          .          .          .          .          .          .          .
-----+-----+-----+-----+-----+-----+-----+-----+-----+-----+
4.00    1.481E-95 0.000E+00 0.000E+00 0.000E+00 0.000E+00 0.000E+00 0.000E+00 0.000E+00 0.000E+00
4.05    1.218E-84 0.000E+00 0.000E+00 0.000E+00 0.000E+00 0.000E+00 0.000E+00 0.000E+00 0.000E+00
4.10    6.776E-75 0.000E+00 0.000E+00 0.000E+00 0.000E+00 0.000E+00 0.000E+00 0.000E+00 0.000E+00
4.15    2.972E-66 0.000E+00 0.000E+00 0.000E+00 0.000E+00 0.000E+00 0.000E+00 0.000E+00 0.000E+00
4.20    1.101E-58 0.000E+00 0.000E+00 0.000E+00 0.000E+00 0.000E+00 0.000E+00 0.000E+00 0.000E+00

6.80    1.490E-17 0.000E+00 0.000E+00 0.000E+00 0.000E+00 0.000E+00 0.000E+00 0.000E+00 0.000E+00
6.85    6.876E-18 0.000E+00 0.000E+00 0.000E+00 0.000E+00 0.000E+00 0.000E+00 0.000E+00 0.000E+00
6.90    3.219E-18 0.000E+00 0.000E+00 0.000E+00 0.000E+00 0.000E+00 0.000E+00 0.000E+00 0.000E+00
6.95    1.526E-18 0.000E+00 0.000E+00 0.000E+00 0.000E+00 0.000E+00 0.000E+00 0.000E+00 0.000E+00
7.00    7.322E-19 0.000E+00 0.000E+00 0.000E+00 0.000E+00 0.000E+00 0.000E+00 0.000E+00 0.000E+00

C-----
C
C TRANSITION LIST FOR O V
C-----
C IND  TRANSITION APP. WVL.(A)  EXACT WVL.(A)  LOWER ST.  UPPER ST.
C-----+-----+-----+-----+-----+-----+-----+
C 1    1 - 3    629.7      629.7      1(0) 0.0    1(1) 1.0
C
C CODE : ADAS412
C PRODUCER : Hugh Summers
C DATE : 22/03/13
C
C-----
```

3 Demo (c) Differential Emission Measure (DEM) analysis

DEMO C: Differential Emission Measure (DEM) analysis.

PURPOSE: Evaluate the DEM as a function of electron temperature, once a set of observed spectral line intensities (archived in /home/adas/adas/arch601/intensity/), G(Te) functions (produced by DEMO b and archived in /home/adas/adas/arch601/kernel/) and elemental abundances (archived in /home/adas/adas/arch601/abundance/) are given. See Lanzafame et al. 2002, A&A, 384, 242 for details on the technique.

Furthermore, once a first estimate of DEM is evaluated, it is possible to perform the elemental abundance analysis.

The method is described by Lanzafame et al. 2005, A&A, 432, 1063.

The directory arch601 is exploited in DEMO b. This provide the input files for the DEM analysis:

1. ELEMENTAL ABUNDANCES: /home/adas/adas/arch601/abundance/
The file can appear in a logarithmic scale A(E) or linear scale N(E), with the hydrogen abundance N(H)=1.

The logarithmic scale is given by the following:

$$A(H) = \log N(H) - 12.$$
$$A(E) = \log [N(E)/N(H)] + 12.$$

2. OBSERVED INTENSITIES: /home/adas/adas/arch601/intensity/
The line intensities come from observations (see DEMO b). They are divided into two sets:

- a. lines used for the inversion
- b. lines used in the forward sense (i.e. to compare the reconstructed intensities to the observed intensities).

The main criteria for the selection of suitable lines for point a. are the following: a) free from blends; b) optically thin; c) density insensitive; d) corresponding accurate atomic data; e) large temperature coverage.

3. SET OF CONTRIBUTION FUNCTIONS: /home/adas/adas/arch601/kernel/
This is done in DEMO b.

EXAMPLE: The observed lines used for this demo are already listed in the EXAMPLE of DEMO b.

They are collected in the intensity file:
/home/adas/adas/arch601/intensity/sumer_cds_eis_qs.dat

LINES SELECTED FOR THE INVERSION (using the criteria of point 2.):

```

ION    WAVELENGTH(Ang.)    LOG(Te(K))
Si+1   1309.276          4.45
Ne+3   543.886          5.20
O+4    629.732          5.35
Si+6   275.667          5.80
Si+11  520.662          6.30
S
LINES USED IN THE FORWARD SENSE
ION    WAVELENGTH(Ang.)    LOG(Te(K))
Si+1   1304.370          4.45
Ne+3   542.070          5.20
Si+6   275.353          5.80

```

Note that at the lines which arise from Si+1 are slightly affected by opacity. However, using an escape factor approach (see also DEMO D), the observed intensities have been corrected to be consistent with the optically thin study.

Regarding the elemental abundances, there are three test files:

1. Abundances from Phillips et al. 2008, that is the most recent collection of coronal abundances:
`/home/adas/adas/arch601/abundance/abund.coronal_phillips08`

2. Abundances from Meyer et al. 1985, that is an example of high-FIP depletion (i.e. elements with their First Ionisation Potential, FIP, greater than 10 eV are depleted compared to their photospheric values):
`/home/adas/adas/arch601/abundance/abundance.coronal_meyer85`

3. Abundances from Fludra & Schmelz 1999, that is an example of hybrid abundances:
`/home/adas/adas/arch601/abundance/abund.hybrid_fludra99`

COMMENTS: The DEM technique is one of the most widely used methods available for the interpretation of astronomical spectral lines. However, although this method is less familiar in spectroscopic studies of fusion plasma, it can be applied to determine impurity concentration, impurity variation in time and impurity influx in fusion.

DEMO c-1: Choice of the lines for the integral inversion

The choice of the line used for integral inversion is done in the intensity file (`/home/adas/adas/arch601/intensity/sumer_cds_eis_qs.dat`) by removing the minus in front of the G-index.

e.g.: LINE USED FOR INTEGRAL INVERSION

G-ind

Si+1...N...1309.276 ... 2 0 1309.181 8.6928e+12 1.7812e+11

LINE USED IN THE FORWARD SENSE

G-ind

```
Si+1...N...1304.370 .. -1      0      1309.181    8.6928e+12   1.7812e+11
```

The G-index (2 or the first line and 1 for the second line of the previous example) connect the intensity file to the kernel (kernel_n1e10.dat or kernel_p1e14.dat) produced in DEMO b.

DEMO c-2: Using ADAS601: DEM inversion and abundance analysis

1. Run ADAS601 from the interactive windows.
2. Select the input files:
(e.g. abundance: /home/adas/adas/arch601/abundance/abund.coronal_phillips08
intensity: /home/adas/adas/arch601/intensity/sumer_cds_eis_qs.dat
kernel: /home/adas/adas/arch601/kernel/kernel_n1e10.dat)
3. Select Run --> execute integral inversion
(output files: demap_output.dat, demo_c_dem.ps, demo_c_gft.ps)
If values for elemental abundance are sought, then:
4. Select Run --> abundance analysis
(output files: demap_abund.dat, demap_abund.log)
The output demap_abund.dat can be used as input for abundance. It provides the new values of elemental abundances and the error bar (max and min values).

```
\end{document}
```

3.1 Demo (c) Figures

3.1.1 demo_c/demo_c_gft.pdf

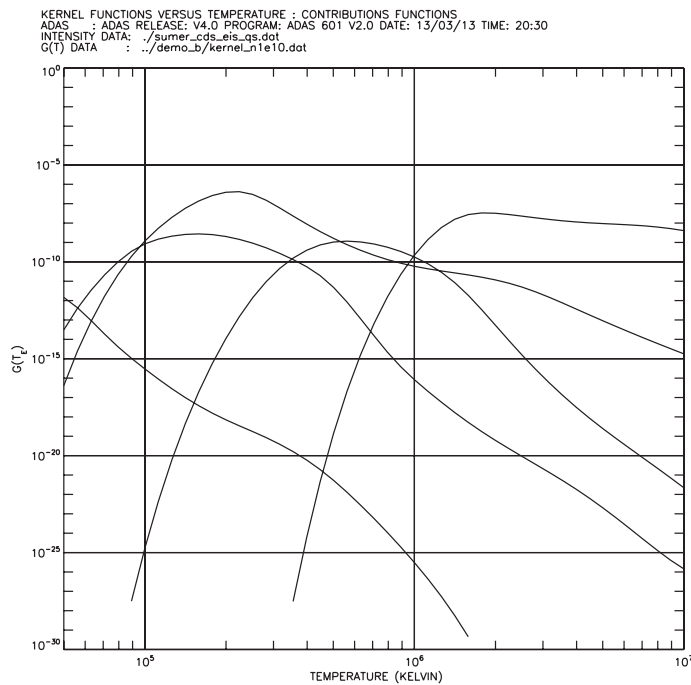


Figure 7: demo_c/demo_c_gft.pdf

3.1.2 demo_c/demo_c_dem.pdf

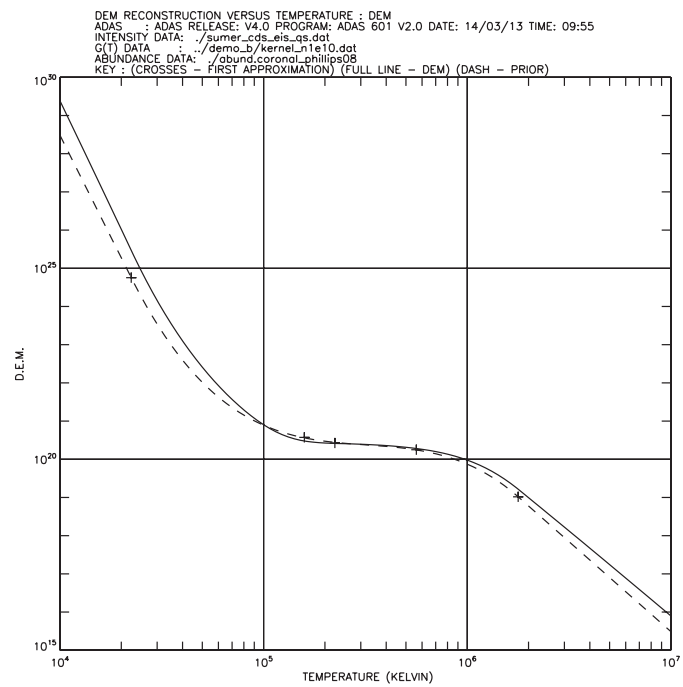


Figure 8: demo_c/demo_c_dem.pdf

3.2 Demo (c) datasets

3.2.1 demap_output.dat

```

ADAS RELEASE: v4.0 PROGRAM: ADAS 601 V2.0 DATE: 14/03/13 TIME: 09:59
***** TABULAR OUTPUT FROM INTEGRAL INVERSION - PROGRAM: ADAS 601 V2.0 - DATE: 14/03/13 ****
INTENSITY DATA FILE NAME: ./sumer_cds_eis_qs.dat
KERNEL DATA FILE NAME: ./demo_b/kernel_nie10.dat
ABUNDANCE DATA FILE NAME: ./abund.coronal_phillips08

CONSTANT VARIANCE = 0.0023993561
SMOOTHING PARAMETER = 0.17788084

----- SINGLE LINES -----
ION SPECTROSCOP. PEAK RECONSTR. OBSERVED RECONSTR. OBSERVED
WAVELENGTH TEMP INTENSITY INTENSITY QFR INTENSITY INTENSITY EPS SIG DEV
log(T) erg/cm2/s erg/cm2/s ph/cm2/s ph/cm2/s
-----
Si+ 1 1309.276 4.35 131.889 131.889 1.000 8.693e+12 8.693e+12 4.028e+11 8.725e+09 8.966e-08
Ne+ 3 543.886 5.20 8.094 8.094 1.000 2.216e+11 2.216e+11 5.368e+10 3.570e+08 4.873e-07
O + 4 629.732 5.35 458.492 458.502 1.000 1.453e+13 1.453e+13 3.470e+12 2.234e+10 4.443e-07
Si+ 6 275.667 5.75 2.777 2.776 1.000 3.853e+10 3.853e+10 7.671e+09 2.284e+08 2.403e-07
Si+11 520.662 6.25 3.662 3.663 1.000 9.600e+10 9.600e+10 1.366e+10 2.709e+08 6.514e-09
-----

----- BLENDS -----
ION SPECTROSCOP. PEAK RECONSTR. OBSERVED RECONSTR. OBSERVED
WAVELENGTH TEMP Iblnd INTENSITY INTENSITY QFR INTENSITY INTENSITY EPS SIG DEV
log(T) erg/cm2/s erg/cm2/s ph/cm2/s ph/cm2/s
-----
CHISQUARE = 0.000528555
NUMBER OF TRANSITION USED FOR THE INTEGRAL INVERSION = 5
-----

----- PREDICTED INTENSITIES -----
ION SPECTROSCOP. PEAK RECONSTR. OBSERVED RECONSTR. OBSERVED
WAVELENGTH TEMP INTENSITY INTENSITY QFR INTENSITY INTENSITY DEV
log(T) erg/cm2/s erg/cm2/s ph/cm2/s ph/cm2/s
-----
Si+ 1 1304.370 4.35 66.592 67.516 0.986 4.373e+12 4.433e+12 6.162e-02
Ne+ 3 542.070 5.15 5.399 5.310 1.017 1.473e+11 1.449e+11 1.610e-01
Si+ 6 275.353 5.70 15.073 16.239 0.928 2.089e+11 2.251e+11 3.695e+00
-----

----- DIFFERENTIAL EMISSION MEASURE -----
N TEMP DEM N TEMP DEM N TEMP DEM N TEMP DEM
1 1.0e+04 2.4e+29 11 2.0e+04 1.0e+26 21 4.0e+04 1.2e+23 31 8.1e+04 1.8e+21 41 1.6e+05 2.9e+20
2 1.1e+04 1.1e+29 12 2.2e+04 4.5e+25 22 4.3e+04 7.0e+22 32 8.7e+04 1.4e+21 42 1.7e+05 2.8e+20
3 1.1e+04 5.1e+28 13 2.3e+04 2.1e+25 23 4.6e+04 4.3e+22 33 9.3e+04 1.0e+21 43 1.9e+05 2.7e+20
4 1.2e+04 2.4e+28 14 2.5e+04 9.7e+24 24 5.0e+04 2.7e+22 34 1.0e+05 8.0e+20 44 2.0e+05 2.7e+20
5 1.3e+04 1.1e+28 15 2.7e+04 4.7e+24 25 5.3e+04 1.7e+22 35 1.1e+05 6.4e+20 45 2.2e+05 2.6e+20
6 1.4e+04 5.0e+27 16 2.8e+04 2.4e+24 26 5.7e+04 1.1e+22 36 1.1e+05 5.2e+20 46 2.3e+05 2.6e+20
7 1.5e+04 2.3e+27 17 3.1e+04 1.2e+24 27 6.1e+04 7.5e+21 37 1.2e+05 4.4e+20 47 2.5e+05 2.6e+20
8 1.6e+04 1.0e+27 18 3.3e+04 6.5e+23 28 6.6e+04 5.1e+21 38 1.3e+05 3.8e+20 48 2.7e+05 2.5e+20
9 1.7e+04 4.8e+26 19 3.5e+04 3.6e+23 29 7.1e+04 3.6e+21 39 1.4e+05 3.4e+20 49 2.8e+05 2.5e+20
10 1.9e+04 2.2e+26 20 3.8e+04 2.0e+23 30 7.6e+04 2.5e+21 40 1.5e+05 3.1e+20 50 3.1e+05 2.5e+20
51 3.3e+05 2.4e+20 61 6.6e+05 1.7e+20 71 1.3e+06 4.8e+19 81 2.7e+06 2.9e+18 91 5.3e+06 1.3e+17
52 3.5e+05 2.4e+20 62 7.1e+05 1.6e+20 72 1.4e+06 3.9e+19 82 2.8e+06 2.1e+18 92 5.7e+06 9.6e+16

```

| | | | | | | | | | | | | | | |
|----|---------|---------|----|---------|---------|----|---------|---------|----|---------|---------|-----|---------|---------|
| 53 | 3.8e+05 | 2.3e+20 | 63 | 7.6e+05 | 1.5e+20 | 73 | 1.5e+06 | 3.1e+19 | 83 | 3.1e+06 | 1.5e+18 | 93 | 6.1e+06 | 7.0e+16 |
| 54 | 4.0e+05 | 2.3e+20 | 64 | 8.1e+05 | 1.3e+20 | 74 | 1.6e+06 | 2.4e+19 | 84 | 3.3e+06 | 1.1e+18 | 94 | 6.6e+06 | 5.2e+16 |
| 55 | 4.3e+05 | 2.2e+20 | 65 | 8.7e+05 | 1.2e+20 | 75 | 1.7e+06 | 1.8e+19 | 85 | 3.5e+06 | 8.4e+17 | 95 | 7.1e+06 | 3.8e+16 |
| 56 | 4.6e+05 | 2.1e+20 | 66 | 9.3e+05 | 1.1e+20 | 76 | 1.9e+06 | 1.3e+19 | 86 | 3.8e+06 | 6.1e+17 | 96 | 7.6e+06 | 2.8e+16 |
| 57 | 5.0e+05 | 2.1e+20 | 67 | 1.0e+06 | 9.5e+19 | 77 | 2.0e+06 | 9.7e+18 | 87 | 4.0e+06 | 4.5e+17 | 97 | 8.1e+06 | 2.0e+16 |
| 58 | 5.3e+05 | 2.0e+20 | 68 | 1.1e+06 | 8.2e+19 | 78 | 2.2e+06 | 7.1e+18 | 88 | 4.3e+06 | 3.3e+17 | 98 | 8.7e+06 | 1.5e+16 |
| 59 | 5.7e+05 | 1.9e+20 | 69 | 1.1e+06 | 7.0e+19 | 79 | 2.3e+06 | 5.3e+18 | 89 | 4.6e+06 | 2.4e+17 | 99 | 9.3e+06 | 1.1e+16 |
| 60 | 6.1e+05 | 1.8e+20 | 70 | 1.2e+06 | 5.9e+19 | 80 | 2.5e+06 | 3.9e+18 | 90 | 5.0e+06 | 1.8e+17 | 100 | 1.0e+07 | 7.9e+15 |

4 Demo (d) Evaluating escape factors

DEMO D: Evaluating escape factors for spectral line emission and for
collisional-radiative population calculations of excited states

PURPOSE: To treat line affected by moderate optically thickness (e.g. C II, CIII or Si II lines in the solar case). The opacity alters the emergent flux, because of the loss of photons out of the line of sight due to scattering and absorption. Additionally, it affects the population distribution within the absorbing atoms (leading to modification to the population structure caused by photo-absorptions) and may cause partial frequency redistribution, which can modify the emission profiles. Two type of escape factor are calculated by the program:

1. line escape fasctor, which describes the emitted radiance along the line of sight;
2. population escape factor, which modifies in practice the A-values (i.e.the radiative transition probabilities in the adf04 are reduced with respect to the values they assume when the plasma is optically thin).

The input of the program is an adf04 data file.

The outputs are the following:

1. a modified adf04, where the A-value take into account the effects of the opacity.
2. three plots (normalised escape factor as a function of optical depth, line profile with modified profiles for a range of optical depths, the emergent flux ratio between specific transitions as a function of column density when selected0

EXAMPLE: In the solar case, the escape factor approach is used for the nalysis of lines which arise from ions such as C+1, C+2, Si+1 (See Fischbacher et al.2000,A&A, 357,767 and Brooks et al.2000,A&A,357,697).

The lines include in the demo are the following:

| ION | WAVEL.(Ang.) | TRANSITION | INTENSITY |
|-----|--------------|---------------------|-----------|
| C+2 | 1174.93 | 2s 2p 3P1 - 2p2 3P2 | I(1-2) |
| C+2 | 1175.26 | 2s 2p 3P0 - 2p2 3P1 | I(0-1) |
| C+2 | 1175.71 | 2s 2p 3P2 - 2p2 3P2 | I(2-2) |
| C+2 | 1176.37 | 2s 2p 3P1 - 2p2 3P2 | I(1-2) |

These lines are observed by SoHO/SUMER and provide a good example of opacity sentitive and insensitive line ratios.

The input adf04 is /home/adas/adas/adf04/copjl#be/copjl#be_jl#c2j.dat.
The output adf04 is adas214.pass.

Assuming a plane parallel atmosphere, the input parameters for the demo are the following:

LINE PROFILE: Doppler

DENSITY DISTRIBUTION: Homogeneous (through the layer)

PLASMA GEOMETRY: Disk (large slab,similar to plane parallel geometry of the solar

```

atmosphere)
DENSITY: 5.e10 cm-3
DIMENSION(b): 1000. cm
ION TEMPERATURE: 80000. K
ELECTRON TEMPERATURE: 80000. K
ASPECT RATIO (a/b - where a is the radius of the disk and 2b the thickness):
10000.
SCAN: if selected YES --> NO.SPEPS:10; MIN FACTOR: 0.10; MAX FACTOR: 100.
OBSERVED SPECTRUM LINES:    UPPER LEVEL    LOWER LEVEL    WAVELENGTH (Ang.)
                           8                  3                1174.93
                           7                  2                1175.26
                           8                  4                1175.71
                           7                  4                1176.37

```

In the case of C+2 the line ratio $I(2-2)/I(1-2)$ is opacity sensitive while $I(0-1)/I(2-1)$ is opacity insensitive. The plot `demo_d.ps` can be compared with the observed intensity ratios of Fig.1 in the paper of Brooks et al. 2000, A&A, 357, 697. The ratio $I(2-2)/I(1-2)$ close to the limb approaches the value 0.9, while it is 2.0-2.5 going to the disk centre. On the disk, the emitting layer is only moderately thick and so the value is close to the optically thin value, which is ~3.

COMMENTS: This approach works for moderate opacity only, otherwise, if the optical depth is too big, the A-values are set equal to zero.

DEMO 8: Using ADAS214

1. Use ADAS214 with the interactive ADAS windows. Select all the parameters as above. (output files: `adas214.pass`, `adas214_escape.ps`, `adas214_profile.ps`, `adas214_ratio.ps`)

DEMO 9: Looking at the modified line ratios

1. Use `run_adas208.pro` to produce the PEC from
 - optically thin `adf04`: `/home/adas/adas/adf04/copjl#be/copjl#be_jl#c2j.dat`
 - optically thick `adf04` produced by DEMO 8: `adas214.pass`
 2. Read the PEC file using `read_adf15.pro`
 3. Plot the opacity sensitive and insensitive line ratios and compare them.
- Program: `demo_d.pro`
Output files: `demo_d.ps`, `demo_d_pec.dat`, `demo_d_pec_adas214.dat`

4.1 Demo (d-1) Figures

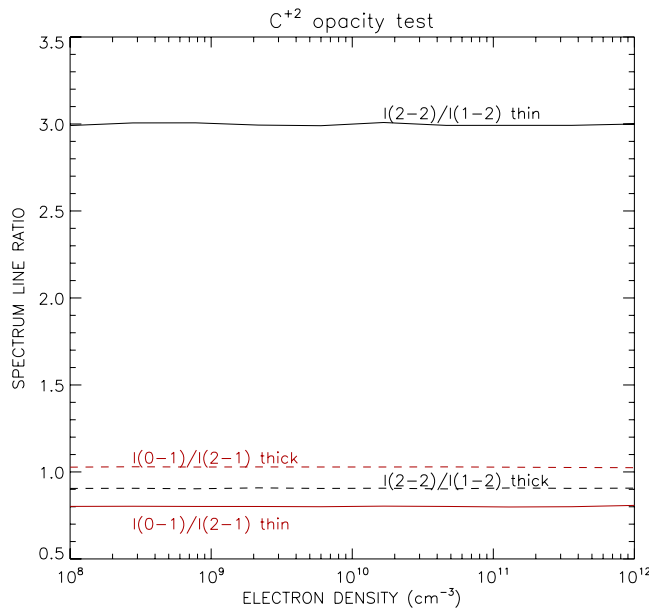


Figure 9: demo_d/demo_d_line_ratios.pdf

4.2 Demo (d-1) IDL procedure

```

pro demo_d
;To compare line ratios affected by opacity to the respective optically thin ratios.

;define electron temperature (K) and electron density array (cm-3)
tek=[1.e4,4.e4,8.e4,1.e5,4.e5,8.e5,1.e6,4.e6,8.e6,1.e7]
;Te in eV
te=tek/11604.
dens=adas_vector(low=1.e8,high=1.e12,num=10)

nte=n_elements(te)
ndens=n_elements(dens)

;Define input parameters for run_adas208.pro
unit_te = 'eV'
unit_dens = 'cm-3'

```

```

wmin      = 1170.
wmax      = 1180.
amin      = 1.0e3

;optically thin adf04
adf04='/home/adas/adas/adf04/copjl#be/copjl#be_jl#c2j.dat'
;optically thick adf04 produced by ADAS214
adf04_adas214='adas214.pass'

;define the metastables
meta_list=[1]

;run_adas208.pro for the population structure using
;the optically thin and thick adf04 files
run_adas208, adf04=adf04,
              te=te,dens=dens, unit_te=unit_te,unit_dens=unit_dens,
              meta=meta_list,
              wmin=wmin, wmax=wmax, amin=amin,
              /pec, pass_dir='.',pop=pop

$          $          $

file_move,'pec.pass','demo_d_pec.dat',/overwrite

run_adas208, adf04=adf04_adas214,
              te=te,dens=dens, unit_te=unit_te,unit_dens=unit_dens,
              meta=meta_list,
              wmin=wmin, wmax=wmax, amin=amin,
              /pec, pass_dir='.',pop=pop

$          $          $

file_move,'pec.pass','demo_d_pec_adas214.dat',/overwrite

;define output PEC files in the format of adf15
file='demo_d_pec.dat'
fileop='demo_d_pec_adas214.dat'

;define input parameters for read_adf15.pro
block=[3,1,4,2]
blockop=[1,2,5,6]
nblock=n_elements(block)

data=fltarr(nblock,nte,ndens)
dataop=fltarr(nblock,nte,ndens)

;use read_adf15.pro to read the PEC files
for i=0,nblock-1 do begin
    read_adf15,file=file,block=block[i],te=te,dens=dens,   $
                  data=idata,wlngh=wlngh,/all
    data[i,*,*]=idata
    read_adf15,file=fileop,block=blockop[i],te=te,dens=dens,   $
                  data=idataop,wlngh=wlngh,/all
    dataop[i,*,*]=idataop

```

```

endfor

;plot the line ratios as a function of electron density
loadct,3
set_plot,'ps'
device, /isolatin1, font_index=8
device, bits=8, filename='demo_d.ps',  $
    font_size = 14, xsize=18.0, ysize=16.0, $
    yoffset=7.0, /color
device, /helvetica

plot_oi,dens,data[1,2,*]/data[0,2,*],ys=1,yr=[0.5,3.5],      $
    tit='C!u+2!n opacity test',      $
    xtit='ELECTRON DENSITY (cm!u-3!n)',           $
    ytit='SPECTRUM LINE RATIO'
oplot,dens,dataop[1,2,*]/dataop[0,2,*],line=2

oplot,dens,data[2,2,*]/data[3,2,*],color=120
oplot,dens,dataop[2,2,*]/dataop[3,2,*],line=2,color=120

xyouts,dens[5],3.03,'I(2-2)/I(1-2) thin'
xyouts,dens[5],0.92,'I(2-2)/I(1-2) thick'

xyouts,dens[1],0.67,'I(0-1)/I(2-1) thin',color=120
xyouts,dens[1],1.05,'I(0-1)/I(2-1) thick',color=120

device, /close
set_plot,'X'
!p.font=-1

end

```

4.3 Demo (d-2) Figures

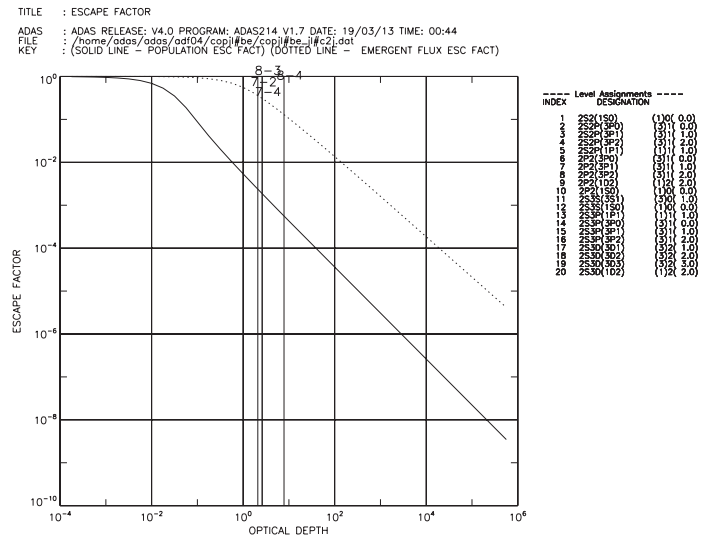


Figure 10: demo_d/demo_d_adas214_escape.pdf

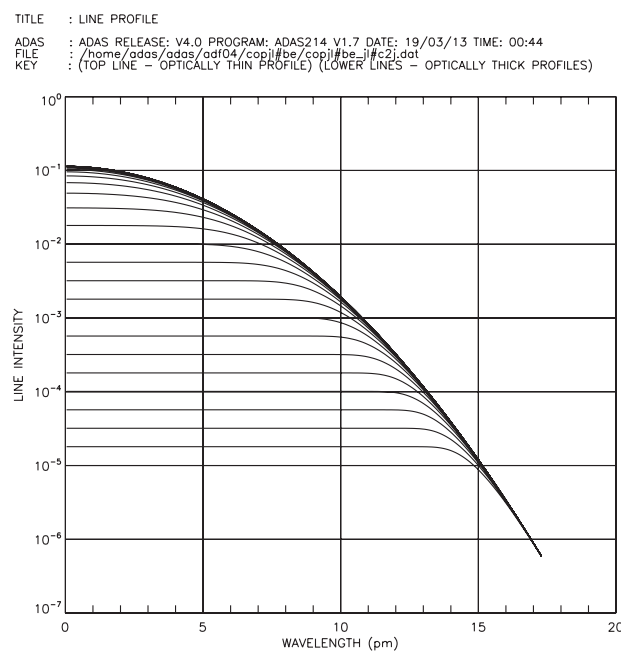


Figure 11: demo_d/demo_d_adas214_profile.pdf

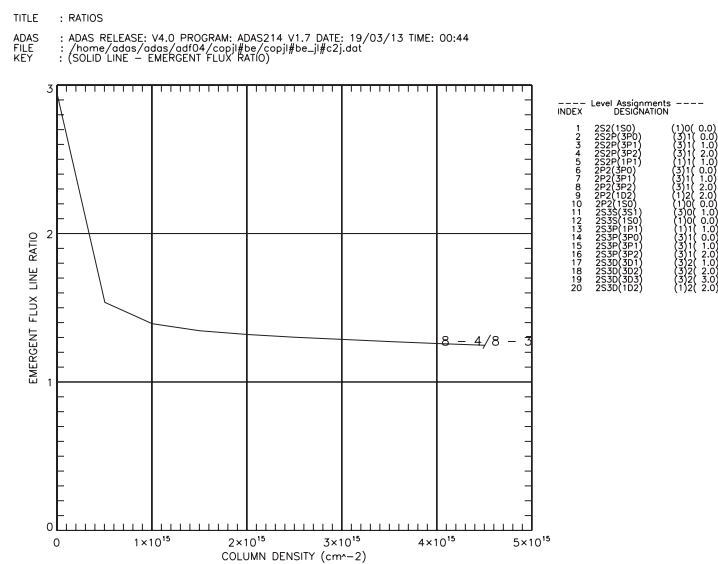


Figure 12: demo_d/demo_d_adas214_ratio.pdf

4.4 Demo (d-2) Tables

4.4.1 demo_d-2/adas214.pass

```

C + 2          6          3          386241.
1  2S2(1S0)    (1)0( 0.0)      0.0
2  2S2P(3P0)   (3)1( 0.0)    52367.1
3  2S2P(3P1)   (3)1( 1.0)    52390.8
4  2S2P(3P2)   (3)1( 2.0)    52447.1
5  2S2P(1P1)   (1)1( 1.0)   102352.0
6  2P2(3P0)    (3)1( 0.0)   137425.7
7  2P2(3P1)    (3)1( 1.0)   137454.4
8  2P2(3P2)    (3)1( 2.0)   137502.0
9  2P2(1D2)    (1)2( 2.0)   145876.1
10 2P2(1S0)    (1)0( 0.0)   182519.9
11 2S3S(3S1)   (3)0( 1.0)   238213.0
12 2S3S(1S0)   (1)0( 0.0)   247170.3
13 2S3P(1P1)   (1)1( 1.0)   258931.3
14 2S3P(3P0)   (3)1( 0.0)   259705.6
15 2S3P(3P1)   (3)1( 1.0)   259711.2
16 2S3P(3P2)   (3)1( 2.0)   259724.3
17 2S3D(3D1)   (3)2( 1.0)   270010.8
18 2S3D(3D2)   (3)2( 2.0)   270011.9
19 2S3D(3D3)   (3)2( 3.0)   270014.7
20 2S3D(1D2)   (1)2( 2.0)   276482.9
-1
3.00   3  9.00+03 1.80+04 4.50+04 9.00+04 1.80+05 4.50+05 9.00+05 1.80+06
2  1 1.00-30 1.19-01 1.13-01 1.08-01 9.51-02 7.81-02 5.44-02 3.84-02 2.44-02
3  1 1.04+02 3.58-01 3.40-01 3.23-01 2.85-01 2.34-01 1.63-01 1.15-01 7.32-02
4  1 5.22-03 5.96-01 5.67-01 5.39-01 4.75-01 3.91-01 2.72-01 1.92-01 1.22-01
5  1 5.23+04 3.75+00 3.88+00 4.10+00 4.48+00 5.15+00 6.64+00 8.07+00 9.93+00
6  1 1.00-30 1.30-03 1.75-03 2.47-03 2.53-03 2.17-03 1.46-03 9.75-04 7.55-04
7  1 9.23-04 3.89-03 5.25-03 7.41-03 7.60-03 6.50-03 4.38-03 2.93-03 2.27-03
8  1 3.83-02 6.48-03 8.75-03 1.24-02 1.27-02 1.08-02 7.31-03 4.88-03 3.78-03
9  1 2.37+03 3.85-01 3.89-01 3.94-01 3.84-01 3.63-01 3.38-01 3.15-01 3.02-01
10 1 1.00-30 7.12-02 7.71-02 8.29-02 8.01-02 7.70-02 7.89-02 7.70-02 7.64-02
11 1 1.00-30 2.67-01 2.28-01 1.55-01 1.06-01 7.12-02 4.20-02 2.89-02 1.60-02
12 1 1.00-30 3.24-01 3.03-01 2.68-01 2.52-01 2.60-01 3.04-01 3.40-01 3.44-01
13 1 9.88+05 1.66-01 1.51-01 1.13-01 9.47-02 9.71-02 1.40-01 2.15-01 2.50-01
14 1 1.00-30 1.81-02 1.54-02 1.08-02 8.29-03 6.85-03 5.34-03 3.99-03 2.44-03
15 1 4.72+05 5.43-02 4.63-02 3.25-02 2.49-02 2.05-02 1.60-02 1.20-02 7.33-03
16 1 1.00-30 9.05-02 7.72-02 5.42-02 4.14-02 3.42-02 2.67-02 2.00-02 1.22-02
17 1 1.00-30 4.51-02 4.13-02 3.66-02 3.39-02 2.99-02 2.23-02 1.61-02 1.05-02
18 1 1.00-30 7.52-02 6.89-02 6.10-02 5.64-02 4.99-02 3.72-02 2.69-02 1.74-02
19 1 1.00-30 2.05-01 9.64-02 8.53-02 7.90-02 6.98-02 5.21-02 3.76-02 2.44-02
20 1 1.00-30 1.68-01 1.61-01 1.68-01 1.95-01 2.53-01 3.75-01 4.79-01 4.93-01
3  2 6.28-07 9.62-01 1.02+00 1.11+00 1.03+00 8.41-01 5.67-01 5.41-01 5.41-01
4  2 1.00-30 7.18-01 8.31-01 1.09+00 1.06+00 8.70-01 6.10-01 5.88-01 5.88-01
5  2 1.45-03 3.29-01 3.49-01 3.21-01 2.72-01 2.11-01 1.33-01 8.63-02 5.25-02
6  2 1.00-30 3.17-02 3.02-02 3.20-02 3.51-02 3.99-02 5.05-02 6.02-02 7.26-02
7  2 1.07+06 2.12+00 2.02+00 2.14+00 2.34+00 2.67+00 3.37+00 4.03+00 4.85+00
8  2 1.00-30 6.94-02 6.60-02 6.99-02 7.67-02 8.72-02 1.10-01 1.32-01 1.59-01
9  2 1.00-30 1.42-01 1.40-01 1.40-01 1.42-01 1.36-01 1.06-01 7.76-02 5.52-02
10 2 1.00-30 2.44-02 2.34-02 2.24-02 2.02-02 1.66-02 1.13-02 7.79-03 4.93-03
11 2 1.63+07 4.23-01 3.32-01 2.09-01 1.42-01 1.08-01 1.04-01 1.27-01 1.32-01
12 2 1.00-30 8.85-02 7.73-02 5.28-02 3.86-02 2.98-02 2.05-02 1.37-02 7.94-03
13 2 1.00-30 1.06-01 9.34-02 6.77-02 5.13-02 3.87-02 2.56-02 1.74-02 1.02-02
14 2 1.00-30 3.30-01 2.93-01 2.37-01 2.09-01 1.97-01 1.99-01 2.04-01 2.04-01
15 2 1.00-30 9.91-02 8.80-02 7.10-02 6.27-02 5.90-02 5.95-02 6.11-02 6.12-02
16 2 1.00-30 1.04-01 9.23-02 7.45-02 6.58-02 6.18-02 6.24-02 6.40-02 6.42-02
17 2 1.83+07 4.39-01 4.21-01 4.25-01 4.68-01 5.57-01 7.77-01 1.03+00 1.31+00
18 2 1.00-30 5.36-02 5.14-02 5.19-02 5.71-02 6.80-02 9.49-02 1.25-01 1.60-01
19 2 1.00-30 4.63-02 4.45-02 4.49-02 4.94-02 5.88-02 8.21-02 1.08-01 1.39-01
20 2 1.00-30 8.33-02 7.55-02 6.41-02 5.52-02 4.48-02 3.02-02 2.01-02 1.22-02
4  3 3.72-06 2.78+00 3.10+00 3.79+00 3.62+00 2.97+00 2.05+00 1.97+00 1.97+00
5  3 1.09-03 9.88-01 1.02+00 9.63-01 8.14-01 6.32-01 4.00-01 2.59-01 1.58-01
6  3 3.19+06 2.12+00 2.02+00 2.14+00 2.34+00 2.67+00 3.37+00 4.03+00 4.85+00
7  3 1.10+06 1.75+00 1.66+00 1.76+00 1.93+00 2.19+00 2.78+00 3.31+00 3.99+00
8  3 6.26+05 2.78+00 2.64+00 2.80+00 3.07+00 3.49+00 4.42+00 5.27+00 6.35+00
9  3 4.85+03 4.27-01 4.20-01 4.19-01 4.26-01 4.07-01 3.18-01 2.33-01 1.66-01
10 3 1.85+03 7.31-02 7.03-02 6.72-02 6.07-02 4.98-02 3.39-02 2.34-02 1.48-02
11 3 1.31+07 1.27+00 9.96-01 6.27-01 4.26-01 3.25-01 3.11-01 3.82-01 3.95-01
12 3 1.00-30 2.66-01 2.32-01 1.58-01 1.16-01 8.95-02 6.16-02 4.11-02 2.38-02
13 3 1.00-30 3.17-01 2.80-01 2.03-01 1.54-01 1.16-01 7.67-02 5.23-02 3.06-02

```

| | | | | | | | | | | |
|----|---|---------|---------|---------|---------|---------|---------|---------|---------|---------|
| 14 | 3 | 1.00-30 | 9.91-02 | 8.80-02 | 7.10-02 | 6.27-02 | 5.90-02 | 5.95-02 | 6.11-02 | 6.12-02 |
| 15 | 3 | 1.00-30 | 1.14+00 | 1.02+00 | 8.20-01 | 7.25-01 | 6.81-01 | 6.88-01 | 7.05-01 | 7.07-01 |
| 16 | 3 | 1.00-30 | 3.54-01 | 3.15-01 | 2.54-01 | 2.24-01 | 2.11-01 | 2.13-01 | 2.18-01 | 2.19-01 |
| 17 | 3 | 1.89+07 | 4.01-01 | 3.85-01 | 3.88-01 | 4.27-01 | 5.09-01 | 7.09-01 | 9.36-01 | 1.20+00 |
| 18 | 3 | 1.01+07 | 1.04+00 | 9.97-01 | 1.00+00 | 1.11-00 | 1.32+00 | 1.84+00 | 2.42+00 | 3.11+00 |
| 19 | 3 | 1.00-30 | 1.68-01 | 1.61-01 | 1.63-01 | 1.79-01 | 2.13-01 | 2.97-01 | 3.93-01 | 5.03-01 |
| 20 | 3 | 1.00-30 | 2.50-01 | 2.27-01 | 1.92-01 | 1.66-01 | 1.35-01 | 9.06-02 | 6.04-02 | 3.65-02 |
| 5 | 4 | 1.81-03 | 1.65+00 | 1.70+00 | 1.61+00 | 1.36+00 | 1.05+00 | 6.67-01 | 4.31-01 | 2.63-01 |
| 6 | 4 | 1.00-30 | 6.94-02 | 6.60-02 | 6.99-02 | 7.67-02 | 8.72-02 | 1.10-01 | 1.32-01 | 1.59-01 |
| 7 | 4 | 1.04+06 | 2.82+00 | 2.68+00 | 2.84+00 | 3.11+00 | 3.54+00 | 4.48+00 | 5.34+00 | 6.44+00 |
| 8 | 4 | 5.67+05 | 8.09+00 | 7.69+00 | 8.15+00 | 8.94+00 | 1.02+01 | 1.29+01 | 1.54+01 | 1.85+01 |
| 9 | 4 | 2.97+04 | 7.11-01 | 7.01-01 | 6.98-01 | 7.10-01 | 6.79-01 | 5.31-01 | 3.88-01 | 2.76-01 |
| 10 | 4 | 1.00-30 | 1.22-01 | 1.17-01 | 1.12-01 | 1.01-01 | 8.30-02 | 5.65-02 | 3.90-02 | 2.47-02 |
| 11 | 4 | 1.22+07 | 2.12+00 | 1.66+00 | 1.05+00 | 7.09-01 | 5.41-01 | 5.18-01 | 6.37-01 | 6.58-01 |
| 12 | 4 | 1.00-30 | 4.43-01 | 3.87-01 | 2.64-01 | 1.93-01 | 1.49-01 | 1.03-01 | 6.86-02 | 3.97-02 |
| 13 | 4 | 1.00-30 | 5.29-01 | 4.67-01 | 3.38-01 | 2.56-01 | 1.94-01 | 1.28-01 | 8.72-02 | 5.10-02 |
| 14 | 4 | 1.00-30 | 1.05-01 | 9.35-02 | 7.55-02 | 6.67-02 | 6.27-02 | 6.33-02 | 6.49-02 | 6.50-02 |
| 15 | 4 | 1.00-30 | 3.57-01 | 3.17-01 | 2.56-01 | 2.26-01 | 2.12-01 | 2.14-01 | 2.20-01 | 2.20-01 |
| 16 | 4 | 1.00-30 | 2.22+00 | 1.97+00 | 1.59+00 | 1.40+00 | 1.32+00 | 1.33+00 | 1.37+00 | 1.37+00 |
| 17 | 4 | 3.43+07 | 1.32-01 | 1.27-01 | 1.28-01 | 1.41-01 | 1.67-01 | 2.33-01 | 3.08-01 | 3.95-01 |
| 18 | 4 | 1.14+07 | 5.26-01 | 5.05-01 | 5.09-01 | 5.61-01 | 6.68-01 | 9.32-01 | 1.23+00 | 1.58+00 |
| 19 | 4 | 6.85+06 | 2.03+00 | 1.95+00 | 1.96+00 | 2.16+00 | 2.57+00 | 3.59+00 | 4.74+00 | 6.07+00 |
| 20 | 4 | 1.00-30 | 4.17-01 | 3.78-01 | 3.21-01 | 2.76-01 | 2.24-01 | 1.51-01 | 1.01-01 | 6.09-02 |
| 6 | 5 | 2.10+02 | 9.74-02 | 9.71-02 | 9.62-02 | 9.00-02 | 7.81-02 | 5.70-02 | 4.10-02 | 2.74-02 |
| 7 | 5 | 1.47+01 | 2.92-01 | 2.91-01 | 2.89-01 | 2.70-01 | 2.34-01 | 1.71-01 | 1.23-01 | 8.23-02 |
| 8 | 5 | 1.37+03 | 4.87-01 | 4.85-01 | 4.81-01 | 4.50-01 | 3.91-01 | 2.85-01 | 2.05-01 | 1.37-01 |
| 9 | 5 | 2.01+05 | 1.10+01 | 1.14+01 | 1.23+01 | 1.35+01 | 1.52+01 | 1.89+01 | 2.18+01 | 2.59+01 |
| 10 | 5 | 6.76+06 | 3.39+00 | 3.51+00 | 3.82+00 | 4.20+00 | 4.83+00 | 6.31+00 | 7.73+00 | 9.49+00 |
| 11 | 5 | 1.00-30 | 1.28+00 | 1.02+00 | 6.40-01 | 4.08-01 | 2.51-01 | 1.30-01 | 7.77-02 | 4.24-02 |
| 12 | 5 | 6.80+07 | 6.60-01 | 5.75-01 | 3.88-01 | 2.74-01 | 2.10-01 | 1.89-01 | 2.20-01 | 2.26-01 |
| 13 | 5 | 1.00-30 | 1.25+00 | 1.12+00 | 8.41-01 | 7.02-01 | 6.48-01 | 6.61-01 | 6.95-01 | 6.99-01 |
| 14 | 5 | 1.00-30 | 1.12-01 | 1.01-01 | 7.62-02 | 5.84-02 | 4.43-02 | 2.89-02 | 1.93-02 | 1.13-02 |
| 15 | 5 | 1.00-30 | 3.36-01 | 3.04-01 | 2.29-01 | 1.75-01 | 1.33-01 | 8.68-02 | 5.79-02 | 3.38-02 |
| 16 | 5 | 1.00-30 | 5.60-01 | 5.06-01 | 3.81-01 | 2.92-01 | 2.22-01 | 1.45-01 | 9.65-02 | 5.63-02 |
| 17 | 5 | 1.00-30 | 2.52-01 | 2.16-01 | 1.73-01 | 1.45-01 | 1.16-01 | 7.78-02 | 5.21-02 | 3.10-02 |
| 18 | 5 | 1.00-30 | 4.19-01 | 3.60-01 | 2.88-01 | 2.41-01 | 1.93-01 | 1.30-01 | 8.68-02 | 5.16-02 |
| 19 | 5 | 1.00-30 | 5.87-01 | 5.04-01 | 4.04-01 | 3.38-01 | 2.70-01 | 1.82-01 | 1.22-01 | 7.22-02 |
| 20 | 5 | 1.32+07 | 1.60+00 | 1.65+00 | 1.91+00 | 2.35+00 | 3.05+00 | 4.49+00 | 5.92+00 | 7.78+00 |
| 7 | 6 | 1.00-30 | 8.44-01 | 8.16-01 | 7.38-01 | 6.65-01 | 5.75-01 | 4.31-01 | 4.16-01 | 4.16-01 |
| 8 | 6 | 1.00-30 | 4.97-01 | 4.80-01 | 4.39-01 | 4.10-01 | 3.82-01 | 3.48-01 | 3.45-01 | 3.45-01 |
| 9 | 6 | 1.00-30 | 3.82-01 | 3.75-01 | 3.59-01 | 3.51-01 | 3.30-01 | 2.55-01 | 1.81-01 | 1.24-01 |
| 10 | 6 | 1.00-30 | 3.08-02 | 3.92-02 | 3.73-02 | 3.62-02 | 3.25-02 | 2.41-02 | 1.69-02 | 1.12-02 |
| 11 | 6 | 1.00-30 | 7.48-02 | 6.93-02 | 4.94-02 | 3.27-02 | 2.00-02 | 9.76-03 | 5.72-03 | 5.28-03 |
| 12 | 6 | 1.00-30 | 1.11-02 | 1.00-02 | 6.73-03 | 4.45-03 | 2.82-03 | 1.52-03 | 1.11-03 | 6.35-04 |
| 13 | 6 | 1.00-30 | 3.19-01 | 1.01-01 | 6.59-02 | 4.25-02 | 2.60-02 | 1.28-02 | 7.22-03 | 3.90-03 |
| 14 | 6 | 1.00-30 | 4.12-02 | 3.33-02 | 2.10-02 | 1.36-02 | 8.74-03 | 4.93-03 | 2.94-03 | 2.90-03 |
| 15 | 6 | 7.75+05 | 3.24-01 | 2.62-01 | 1.65-01 | 1.07-01 | 6.87-02 | 3.88-02 | 2.31-02 | 2.28-02 |
| 16 | 6 | 1.00-30 | 1.53-01 | 1.24-01 | 7.80-02 | 5.08-02 | 3.25-02 | 1.83-02 | 1.09-02 | 1.08-02 |
| 17 | 6 | 1.00-30 | 1.07-01 | 9.11-02 | 6.09-02 | 4.15-02 | 2.72-02 | 1.52-02 | 9.61-03 | 8.96-03 |
| 18 | 6 | 1.00-30 | 2.38-01 | 2.03-01 | 1.35-01 | 9.21-02 | 6.03-02 | 3.37-02 | 2.14-02 | 1.99-02 |
| 19 | 6 | 1.00-30 | 9.13-02 | 7.76-02 | 5.19-02 | 3.53-02 | 2.31-02 | 1.29-02 | 8.19-03 | 7.64-03 |
| 20 | 6 | 1.00-30 | 1.47-01 | 1.18-01 | 7.50-02 | 5.11-02 | 3.38-02 | 1.85-02 | 1.12-02 | 6.22-03 |
| 8 | 7 | 1.00-30 | 2.16+00 | 2.09+00 | 1.91+00 | 1.76+00 | 1.57+00 | 1.31+00 | 1.28+00 | 1.28+00 |
| 9 | 7 | 1.00-30 | 1.15+00 | 1.12+00 | 1.08+00 | 1.05+00 | 9.89-01 | 7.64-01 | 5.44-01 | 3.72-01 |
| 10 | 7 | 1.00-30 | 1.22-01 | 1.18-01 | 1.12-01 | 1.09-01 | 9.76-02 | 7.22-02 | 5.08-02 | 3.37-02 |
| 11 | 7 | 1.00-30 | 2.24-01 | 2.08-01 | 1.48-01 | 9.82-02 | 5.99-02 | 2.93-02 | 1.72-02 | 1.58-02 |
| 12 | 7 | 1.00-30 | 3.34-02 | 3.01-02 | 2.04-02 | 1.34-02 | 8.47-03 | 4.57-03 | 3.32-03 | 1.90-03 |
| 13 | 7 | 1.00-30 | 3.56-01 | 3.02-01 | 1.98-01 | 1.28-01 | 7.79-02 | 3.84-02 | 2.16-02 | 1.17-02 |
| 14 | 7 | 2.33+06 | 3.24-01 | 2.62-01 | 1.65-01 | 1.07-01 | 6.87-02 | 3.88-02 | 2.31-02 | 2.28-02 |
| 15 | 7 | 5.82+05 | 4.79-01 | 3.87-01 | 2.44-01 | 1.59-01 | 1.02-01 | 5.73-02 | 3.41-02 | 3.37-02 |
| 16 | 7 | 5.70+05 | 7.47-01 | 6.04-01 | 3.80-01 | 2.47-01 | 1.58-01 | 8.95-02 | 5.33-02 | 5.26-02 |
| 17 | 7 | 1.00-30 | 3.97-01 | 3.38-01 | 2.26-01 | 1.54-01 | 1.01-01 | 5.61-02 | 3.56-02 | 3.32-02 |
| 18 | 7 | 1.00-30 | 3.93-01 | 3.34-01 | 2.23-01 | 1.52-01 | 1.96-02 | 5.56-02 | 3.53-02 | 3.29-02 |
| 19 | 7 | 1.00-30 | 5.16-01 | 4.39-01 | 2.93-01 | 2.00-01 | 1.31-01 | 7.30-02 | 4.63-02 | 4.32-02 |
| 20 | 7 | 1.00-30 | 4.40-01 | 3.52-01 | 2.25-01 | 1.53-01 | 1.01-01 | 6.17-02 | 3.37-02 | 1.87-02 |
| 9 | 8 | 1.00-30 | 1.91+00 | 1.87+00 | 1.79+00 | 1.75+00 | 1.65+00 | 1.27+00 | 9.06-01 | 6.20-01 |
| 10 | 8 | 1.00-30 | 2.04-01 | 1.96-01 | 1.87-01 | 1.81-01 | 1.63-01 | 1.20-01 | 8.46-02 | 5.61-02 |
| 11 | 8 | 1.00-03 | 3.74-01 | 3.46-01 | 2.47-01 | 1.64-01 | 9.98-02 | 4.88-02 | 2.86-02 | 2.64-02 |
| 12 | 8 | 1.00-30 | 5.56-02 | 5.01-02 | 3.40-02 | 2.23-02 | 1.41-02 | 7.62-03 | 5.53-03 | 3.17-03 |
| 13 | 8 | 1.00-30 | 5.94-01 | 5.04-01 | 3.29-01 | 2.13-01 | 1.30-01 | 6.49-02 | 3.61-02 | 1.95-02 |
| 14 | 8 | 1.00-30 | 1.53-01 | 1.24-01 | 7.80-02 | 5.08-02 | 3.25-02 | 1.83-02 | 1.09-02 | 1.08-02 |
| 15 | 8 | 9.51+05 | 8.24-01 | 6.66-01 | 4.19-01 | 2.73-01 | 1.75-01 | 9.86-02 | 5.87-02 | 5.80-02 |
| 16 | 8 | 1.66+06 | 1.74+00 | 1.41+00 | 8.85-01 | 5.76-01 | 3.69-01 | 2.08-01 | 1.24-01 | 1.22-01 |
| 17 | 8 | 1.00-30 | 3.06-01 | 2.60-01 | 1.74-01 | 1.18-01 | 7.74-02 | 4.32-02 | 2.74-02 | 2.56-02 |

```

18 8 1.00-30 6.75-01 5.74-01 3.83-01 2.61-01 1.71-01 9.54-02 6.05-02 5.64-02
19 8 1.00-30 1.23+00 1.05+00 6.99-01 4.76-01 3.12-01 1.74-01 1.10-01 1.03-01
20 8 1.00-30 7.33-01 5.87-01 3.75-01 2.55-01 1.69-01 1.03-01 5.62-02 3.11-02
10 9 4.34+01 6.31-01 6.40-01 6.79-01 7.18-01 7.51-01 8.09-01 8.39-01 8.41-01
11 9 1.00-30 1.54+00 1.16+00 7.05-01 4.35-01 2.50-01 1.13-01 6.06-02 3.18-02
12 9 1.00-30 6.22-01 5.32-01 3.49-01 2.27-01 1.61-01 1.28-01 1.25-01 1.25-01
13 9 1.96+07 1.66+00 1.53+00 1.16+00 9.69-01 9.31-01 1.09+00 1.32+00 1.44+00
14 9 1.00-30 2.25-01 2.08-01 1.43-01 9.16-02 5.45-02 2.60-02 1.44-02 7.78-03
15 9 1.00-30 6.75-01 6.23-01 4.28-01 2.75-01 1.63-01 7.81-02 4.32-02 2.33-02
16 9 1.00-30 1.13+00 1.04+00 7.13-01 4.58-01 2.72-01 1.30-01 7.19-02 3.89-02
17 9 1.00-30 4.93-01 4.02-01 2.52-01 1.61-01 9.89-02 5.06-02 2.94-02 1.60-02
18 9 1.00-30 8.21-01 6.70-01 4.20-01 2.69-01 1.65-01 8.43-02 4.91-02 2.61-02
19 9 1.00-30 1.15+00 9.38-01 5.88-01 3.76-01 2.31-01 1.18-01 6.87-02 3.73-02
20 9 1.00-30 1.39+00 1.20+00 9.28-01 7.92-01 6.99-01 6.32-01 5.99-01 5.94-01
10 10 1.00-30 5.32-01 4.48-01 2.86-01 1.79-01 1.05-01 5.09-02 2.84-02 1.51-02
12 10 1.00-30 4.71-01 4.12-01 2.81-01 1.98-01 1.41-01 1.00-01 8.91-02 8.82-02
13 10 1.64+07 2.19-01 2.21-01 1.90-01 1.66-01 1.61-01 1.90-01 2.48-01 2.71-01
14 10 1.00-30 2.96-02 2.72-02 1.89-02 1.28-02 8.28-03 4.45-03 2.63-03 1.43-03
15 10 1.00-30 8.80-02 8.16-02 5.67-02 3.84-02 2.49-02 1.33-02 7.88-03 4.30-03
16 10 1.00-30 1.48-01 1.36-01 9.46-02 6.40-02 4.14-02 2.22-02 1.31-02 7.17-03
17 10 1.00-30 5.50-02 4.99-02 3.81-02 2.84-02 2.00-02 1.16-02 7.18-03 4.05-03
18 10 1.00-30 9.17-02 8.31-02 6.35-02 4.74-02 3.34-02 1.93-02 1.20-02 6.75-03
19 10 1.00-30 1.28-01 1.16-01 8.89-02 6.63-02 4.67-02 2.70-02 1.68-02 9.45-03
20 10 1.00-30 4.38-01 3.86-01 3.11-01 2.82-01 2.78-01 2.91-01 2.96-01 2.96-01
12 11 1.00-30 3.56+00 2.70+00 1.58+00 9.87-01 6.16-01 3.29-01 1.97-01 1.05-01
13 11 1.00-30 2.47+00 1.81+00 1.05+00 6.94-01 4.62-01 2.60-01 1.59-01 8.59-02
14 11 1.99+06 6.90+00 7.31+00 7.04+00 8.19+00 1.04+01 1.42+01 1.72+01 2.03+01
15 11 5.50+05 2.07+01 2.19+01 2.11+01 2.46+01 3.12+01 4.27+01 5.15+01 6.10+01
16 11 3.10+01 3.45+01 3.65+01 3.52+01 4.09+01 5.20+01 7.12+01 8.59+01 1.02+02
17 11 1.00-30 1.96+00 2.04+00 2.19+00 2.35+00 2.56+00 2.78+00 2.84+00 2.84+00
18 11 1.00-30 3.27+00 3.39+00 3.65+00 3.92+00 4.27+00 4.64+00 4.73+00 4.73+00
19 11 1.00-30 4.58+00 4.75+00 5.10+00 5.49+00 5.98+00 6.50+00 6.63+00 6.63+00
20 11 1.00-30 7.99-01 7.34-01 6.27-01 5.33-01 4.20-01 2.66-01 1.67-01 9.88-02
13 12 1.11+05 1.32+01 1.41+01 1.78+01 2.44+01 3.33+01 4.64+01 5.52+01 6.51+01
14 12 1.00-30 2.41-01 1.84-01 1.12-01 7.41-02 4.91-02 2.72-02 1.64-02 8.85-03
15 12 1.00-30 7.23-01 5.53-01 3.36-01 2.22-01 1.47-01 8.17-02 4.92-02 2.66-02
16 12 1.00-30 1.20+00 9.22-01 5.60-01 3.70-01 2.45-01 1.36-01 8.21-02 4.42-02
17 12 1.00-30 3.29-01 2.62-01 1.79-01 1.30-01 9.14-02 5.23-02 3.15-02 1.73-02
18 12 1.00-30 5.49-01 4.36-01 2.98-01 2.17-01 1.52-01 8.71-02 5.25-02 2.89-02
19 12 1.00-30 7.68-01 6.10-01 4.17-01 3.03-01 2.13-01 1.22-01 7.36-02 4.04-02
20 12 1.00-30 3.03+00 3.10+00 3.44+00 3.83+00 4.22+00 4.58+00 4.63+00 4.63+00
14 13 1.00-30 1.08+00 8.55-01 5.36-01 3.59-01 2.40-01 1.36-01 8.30-02 4.50-02
15 13 1.00-30 3.25+00 2.57+00 1.61+00 1.08+00 7.21-01 4.07-01 2.49-01 1.35-01
16 13 1.00-30 5.42+00 4.28+00 2.68+00 1.80+00 1.20+00 6.79-01 4.15-01 2.25-01
17 13 1.00-30 8.07-01 6.58-01 4.82-01 3.78-01 2.83-01 1.68-01 1.03-01 5.75-02
18 13 1.00-30 1.35+00 1.10+00 8.03-01 6.30-01 4.72-01 2.80-01 1.71-01 9.58-02
19 13 1.00-30 1.88+00 1.54+00 1.12+00 8.81-01 6.60-01 3.92-01 2.39-01 1.34-01
20 13 2.54+05 3.20+01 3.38+01 4.09+01 5.03+01 6.28+01 8.31+01 1.01+02 1.20+02
17 14 1.05+05 9.58+00 1.06+01 1.40+01 1.84+01 2.36+01 3.13+01 3.79+01 4.45+01
18 14 1.00-30 1.82-01 2.01-01 2.66-01 3.49-01 4.48-01 5.94-01 7.20-01 8.46-01
19 14 1.00-30 2.30-01 2.54-01 3.36-01 4.40-01 5.56-01 7.50-01 9.10-01 1.07+00
20 14 1.00-30 3.10-01 2.88-01 2.53-01 2.15-01 1.66-01 9.92-02 6.02-02 3.50-02
17 15 1.12+05 7.19+00 7.95+00 1.05+01 1.38+01 1.77+01 2.34+01 2.84+01 3.34+01
18 15 5.48+04 2.44+01 2.70+01 3.57+01 4.68+01 6.01+01 7.97+01 9.66+01 1.14+02
19 15 1.00-30 7.09-01 7.84-01 1.04+00 1.36+00 1.74+00 2.31+00 2.80+00 3.30+00
20 15 1.00-30 9.30-01 8.64-01 7.58-01 6.44-01 4.98-01 2.98-01 1.81-01 1.05-01
17 16 1.34+05 9.58-01 1.06+00 1.40+00 1.84+00 2.36+00 3.13+00 3.79+00 4.45+00
18 16 6.67+04 8.91+00 9.86+00 1.30+01 1.71+01 2.19+01 2.91+01 3.52+01 4.14+01
19 16 3.60+04 4.36+01 4.82+01 6.36+01 8.35+01 1.07+02 1.42+02 1.72+02 2.03+02
20 16 1.00-30 1.55+00 1.44+00 1.26+00 1.07+00 8.30-01 4.96-01 3.01-01 1.75-01
20 17 1.00-30 1.83+00 1.69+00 1.46+00 1.22+00 9.35-01 5.63-01 3.49-01 2.03-01
20 18 1.00-30 3.04+00 2.82+00 2.43+00 2.04+00 1.56+00 9.38-01 5.81-01 3.39-01
20 19 1.00-30 4.26+00 3.94+00 3.40+00 2.85+00 2.18+00 1.31+00 8.13-01 4.74-01
-1
-1 -1
C-----
C
C Energy Levels
C The results from NSRDS NBS3 SECT 3 were used. These were the same
C as the results of Edlen (Phys. Scr 32, 86, 1985 and 28, 51, 1983)
C who only considered n=2 levels. The NSRDS values are also those of
C Moore and Gallacher "Tables of Spectra of hydrogen, carbon, nitrogen
C and oxygen atoms and ions" CRC press 1993.
C

```

```

C Ionisation Potential
C As energy levels.
C
C A Values
C For transitions between n = 2 levels the results of the compilation
C by Allard et al (Astron Astrophys Suppl Ser 84, 563, 1990) were used
C and for values not given by them the results of Nussbaumer and Storey
C (Astron Astrophys 74, 244, 1979) were used. The Nussbaumer and Storey
C results were adopted for forbidden transitions by Allard et al.
C For the 2-3 and 3-4 transitions the results of Idrees and Das (J Phys B
C 22, 3609, 1989) were used.
C For transitions involving n = 3 levels again the results of Allard et al
C were adopted.
C For the important 2s2 1S - 2s2p 3P1 transition Allard et al recommend a
C value of 93.98 s-1. Recently Kwong et al (Ap J 411, 431, 1993) have
C published a measured value of 121 +/- 7 s-1. There have been two recent
C calculation of this rate, Fleming et al (Phys. Scr 49, 316, 1994) giving
C 104 +/- 4 s-1 and Fischer (Phys Scr 49, 323, 1994) giving 103 +/- 3 s-1.
C Here we adopt 104 s-1.
C
C Collision Data
C The data recommended in a review by Berrington (ADNDT 57, 71, 1994) are
C adopted.
C The results of Berrington (J Phys B, 18, L395, 1985) and Berrington et al
C (J Phys B 22, 665, 1989 and JET Report JT7/11345) were adopted for
C transitions between n=2 levels and for transitions involving levels 3
C respectively. These results were obtained from a 12 eigenstate R-matrix
C calculation. The 12 states correspond to the 20 lowest fine structure
C levels. For transitions between n = 2 levels the partial wave expansion
C was for total angular momentum L <= 9. For some transitions the partial
C wave expansion is slowly convergent and care was taken to allow for this.
C For transitions involving n=3 levels it appears that partial waves up to
C L <= 11 were included. However, the slow convergence of the partial
C wave expansion was a problem which was dealt with by writing a new no-
C exchange R-matrix package. In addition for dipole allowed transitions a
C top-up procedure was adopted, care being taken that the Coulomb-Bethe
C approximation was valid when it was applied.
C These calculations gave effective collision strengths between LS terms.
C Berrington (ADNDT 57, 71, 1994) in a review recommends the work of
C Berrington et al (ADNDT 33, 195, 1985) for fine structure transitions
C involving 2s2p 3P or 2p2 3P. These recommendations were adopted.
C For the former Keenan et al (Ap J 389, 443, 1992) give the unpublished
C rates from Berrington's 1985 calculation. However they are at most 7%
C different (2-4, lowest temperature value) and the Keenan et al results
C are only at three low close temperature.
C To obtain the fine structure collision rates statistical weight factors
C were used except for the transitions given in the tables below.
C
C The tables give the percentages of the total collision strength going into
C each of the fine structure transitions at a reduced temperature of 1e4.
C
C 2s2p 3Pj - 2p2 3Pj'
C
C   j  j'    NIV      OV      OV     NeVII   NeVII   AQ      Use
C   (CC)     (CC)    (DW)    (CC)    (DW)
C   0  0    0.16    0.115   0.09    0.08    0.07      0.16
C   0  1   10.67   10.8    11.23   10.79   11.07   11.1    10.7
C   0  2    0.35    0.214   0.11    0.12    0.09      0.35
C
C   1  0    10.72   10.76   11.23   10.79   10.88   11.1    10.7
C   1  1     8.82    8.65    7.71    8.56    8.57    8.33    8.8
C   1  2   13.99   13.93   12.56   14.19   14.02   12.89   14.0
C
C   2  0    0.35    0.21    0.11    0.12    0.08      0.35
C   2  1   14.15   13.99   14.26   14.19   14.02   13.89   14.2
C   2  2   40.81   41.38   42.72   41.16   41.22   41.67   40.8
C
C The values adopted are close to that of N IV. The N IV calculation is
C by Ramsbottom et al (see adf04 file), the O V CC data are from Kato, Lang
C and Berrington (see adf04 file). The DW calculations are Sampson (see
C copsm#be). The Ne VII data are from ADF04 file (JL95).
C

```

```

C 2s2p 3Pj - 2s3d 3Dj'
C
C   j j'    NIV      OV      OV      AQ
C           (CC)     (CC)    (CC1)   NeVII
C   0 1    9.09    9.04    9.74   11.11
C   0 2    1.11    1.13    0.78
C   0 3    0.96    1.01    0.77
C
C   1 1    8.30    8.26    8.37    8.33
C   1 2   21.48   21.32   22.88   25.00
C   1 3    3.48    3.61    2.62
C
C   2 1    2.73    2.75    2.22    0.56
C   2 2   10.91   10.72   10.23    8.33
C   2 3   41.95   42.17   42.39   46.67
C
C   The values adopted are those of N IV. The N IV calculation is by
C   Ramsbottom et al (see adf04 file), the O V CC data are from Kato, Lang
C   and Berrington (see adf04 file) and CC1 is adf04 from 89 (or 90).
C
C
C 2s2p 3Pj - 2s3p 3Pj'
C
C   j j'    NIV      OV      OV      NeVII
C           (CC)     (CC)    (CC1)   (DW)
C   0 0    6.87    7.00    8.24    5.51
C   0 1    2.06    1.89    1.05    0.54
C   0 2    2.16    2.36    1.78    1.12
C
C   1 0    2.06    1.92    1.04    0.51
C   1 1   23.77   24.52   26.88   17.46
C   1 2    7.37    7.36    5.33    39.96
C
C   2 0    2.19    2.45    1.79    1.11
C   2 1    7.42    7.66    5.31    2.44
C   2 2   46.09   44.86   48.58   31.39
C
C   The values adopted are those of N IV. The N IV calculation is by
C   Ramsbottom et al (see adf04 file), the O V CC data are from Kato, Lang
C   and Berrington (see adf04 file) and CC1 is adf04 from 89 (or90). The DW
C   calculation for Ne VII is from Sampson et al (1984) from JL95.
C
C
C 2p2 3Pj - 2s3p 3Pj'
C
C   j j'    NIV      OV      NeVII  AQ
C           (CC)     (CC)   (DW)
C   0 0    0.86    0.14    0.24
C   0 1    6.75    0.84   10.19   11.1
C   0 2    3.23    0.77    0.72
C
C   1 0    6.76    0.85   10.11   11.11
C   1 1   10.00    1.76    8.87    8.33
C   1 2   15.64    3.08   14.67   12.89
C
C   2 0    3.22    0.72    0.68
C   2 1   17.23    2.80   13.92   13.89
C   2 2   36.31   89.04   40.61   41.67
C
C   The values adopted are those of N IV. The N IV calculation is by
C   Ramsbottom et al (see adf04 file), the O V CC data are from Kato, Lang
C   and Berrington (see adf04 file). The DW calculation for Ne VII is from
C   Sampson et al (1984) from JL95.
C
C
C 2p2 3Pj - 2s3d 3Dj'
C
C   j j'    NIV      OV      NeVII
C           (CC)     (CC)   (DW)
C   0 1    2.73    3.61    2.94
C   0 2    5.98    4.33    6.36
C   0 3    2.28    3.09    2.02
C
C   1 1   10.19    8.49   10.80

```

```

C   1 2    9.87  12.32  10.00
C   1 3    12.89  12.32  12.74
C
C   2 1    7.69  7.79  7.18
C   2 2    17.27  16.50  17.46
C   2 3    31.11  31.56  30.51
C
C   The values adopted are essentially that of N V. The N IV calculation
C   is by Ramsbottom et al (see adf04 file), the O V CC data are from Kato,
C   Lang and Berrington (see adf04 file). The DW data for Ne VII are from
C   Sampson et al (1984) from JL95.
C
C   2s3p 3Pj - 2s3d 3Dj'
C
C   j j'    OV      AQ
C   (CC)
C   0 1    9.98  11.11
C   0 2    0.19
C   0 3    0.24
C
C   1 1    7.54  8.33
C   1 2    25.52  25.00
C   1 3    0.74
C
C   2 1    1.02  0.56
C   2 2    9.29  8.33
C   2 3    45.48  46.17
C
C   The values adopted are for O V. The O V CC data are from Kato, Lang
C   and Berrington (see adf04 file).
C
C   In processing the 2p2 3P - 2s3p 3P data, it was noted that this is given
C   as a forbidden transition. However, it has a fairly large A value.
C   So allowed behaviour was forced on it when running ADAS 102. At the
C   highest temperature given here this gives a 1% increase in the effective
C   collision strength between the LS terms.
C
C   J LANG    June 1995.
C
C   Update: 03/06/02 A D Whiteford - amended ion charge from 3 to 2.
C
C-----
```

C-----
C ADAS ADF04 DATA - SCDS info: @(#)\$Header:
C /home/adascvs/adas/adf04/copjl#be/copjl#be_jl#c2j.dat,v 2.2 2004/07/06 21:27:01
C whitefor Exp \$ D
C-----
C-----
C 18/03/13
C produced with ADAS214 and the following data:
C input data file: /home/adas/adas/adf04/copjl#be/copjl#be_jl#c2j.dat
C dens distn: Homogeneous
C geometry: Disk
C profile: Doppler
C m = 6., Te = 80000.0K, Tg = 80000.0K, l = 1.00E+03cm,
C na or nion = 2.50E+12cm^-3
C-----

4.4.2 demo_d-2/demo_d_pec_adas214.dat

```

6 /C + 2 EMISSIVITY COEFFTS./
1174.9 A 10 10 /FILMEM = 214.pass/TYPE = EXCIT /INDM = T/ISEL = 1
1.00E+08 2.78E+08 7.74E+08 2.15E+09 5.99E+09 1.67E+10 4.64E+10 1.29E+11
3.59E+11 1.00E+12
8.62E-01 3.45E+00 6.89E+00 8.62E+00 3.45E+01 6.89E+01 8.62E+01 3.45E+02
6.89E+02 8.62E+02
1.84E-16 1.47E-10 8.97E-10 1.21E-09 1.96E-09 1.48E-09 1.29E-09 4.19E-10
2.34E-10 1.95E-10
2.30E-16 1.70E-10 1.00E-09 1.34E-09 2.11E-09 1.59E-09 1.38E-09 4.45E-10
2.47E-10 2.06E-10
3.41E-16 2.25E-10 1.24E-09 1.63E-09 2.48E-09 1.87E-09 1.63E-09 5.16E-10
2.82E-10 2.33E-10
5.51E-16 3.23E-10 1.64E-09 2.14E-09 3.23E-09 2.51E-09 2.20E-09 7.04E-10
3.77E-10 3.10E-10
8.24E-16 4.41E-10 2.11E-09 2.73E-09 4.35E-09 3.64E-09 3.27E-09 1.17E-09
6.32E-10 5.19E-10
1.04E-15 5.32E-10 2.46E-09 3.18E-09 5.43E-09 4.95E-09 4.63E-09 2.15E-09
1.27E-09 1.06E-09
1.16E-15 5.85E-10 2.67E-09 3.45E-09 6.17E-09 5.99E-09 5.78E-09 3.64E-09
2.56E-09 2.26E-09
1.21E-15 6.20E-10 2.82E-09 3.65E-09 6.68E-09 6.70E-09 6.57E-09 5.09E-09
4.21E-09 3.92E-09
1.20E-15 6.51E-10 2.97E-09 3.84E-09 7.02E-09 7.14E-09 7.06E-09 5.98E-09
5.27E-09 5.04E-09
1.10E-15 6.59E-10 3.01E-09 3.88E-09 6.98E-09 7.14E-09 7.08E-09 6.22E-09
5.59E-09 5.37E-09
1175.7 A 10 10 /FILMEM = 214.pass/TYPE = EXCIT /INDM = T/ISEL = 2
1.00E+08 2.78E+08 7.74E+08 2.15E+09 5.99E+09 1.67E+10 4.64E+10 1.29E+11
3.59E+11 1.00E+12
8.62E-01 3.45E+00 6.89E+00 8.62E+00 3.45E+01 6.89E+01 8.62E+01 3.45E+02
6.89E+02 8.62E+02
1.66E-16 1.33E-10 8.12E-10 1.09E-09 1.78E-09 1.34E-09 1.16E-09 3.79E-10
2.12E-10 1.77E-10
2.09E-16 1.54E-10 9.06E-10 1.21E-09 1.91E-09 1.44E-09 1.25E-09 4.03E-10
2.24E-10 1.86E-10
3.09E-16 2.03E-10 1.12E-09 1.47E-09 2.24E-09 1.70E-09 1.47E-09 4.67E-10
2.55E-10 2.11E-10
4.99E-16 2.92E-10 1.49E-09 1.94E-09 2.93E-09 2.28E-09 2.00E-09 6.38E-10
3.42E-10 2.81E-10
7.47E-16 3.99E-10 1.91E-09 2.47E-09 3.94E-09 3.29E-09 2.96E-09 1.06E-09
5.73E-10 4.70E-10
9.46E-16 4.82E-10 2.23E-09 2.88E-09 4.92E-09 4.49E-09 4.19E-09 1.95E-09
1.15E-09 9.63E-10
1.05E-15 5.30E-10 2.41E-09 3.12E-09 5.59E-09 5.43E-09 5.23E-09 3.30E-09
2.32E-09 2.05E-09
1.09E-15 5.61E-10 2.56E-09 3.31E-09 6.05E-09 6.07E-09 5.95E-09 4.61E-09
3.81E-09 3.55E-09
1.08E-15 5.89E-10 2.69E-09 3.48E-09 6.36E-09 6.47E-09 6.39E-09 5.42E-09
4.77E-09 4.56E-09
9.97E-16 5.97E-10 2.73E-09 3.51E-09 6.32E-09 6.46E-09 6.41E-09 5.64E-09
5.06E-09 4.87E-09
1176.0 A 10 10 /FILMEM = 214.pass/TYPE = EXCIT /INDM = T/ISEL = 3
1.00E+08 2.78E+08 7.74E+08 2.15E+09 5.99E+09 1.67E+10 4.64E+10 1.29E+11
3.59E+11 1.00E+12
8.62E-01 3.45E+00 6.89E+00 8.62E+00 3.45E+01 6.89E+01 8.62E+01 3.45E+02
6.89E+02 8.62E+02
1.62E-17 1.09E-11 6.55E-11 8.85E-11 1.42E-10 1.04E-10 8.86E-11 2.43E-11
1.23E-11 9.90E-12
3.69E-17 2.27E-11 1.28E-10 1.70E-10 2.47E-10 1.76E-10 1.49E-10 3.87E-11
1.90E-11 1.51E-11
8.59E-17 4.99E-11 2.69E-10 3.54E-10 5.06E-10 3.61E-10 3.06E-10 7.80E-11
3.74E-11 2.97E-11
1.79E-16 9.92E-11 5.16E-10 6.78E-10 1.04E-09 7.80E-10 6.72E-10 1.83E-10
8.81E-11 6.98E-11
3.01E-16 1.59E-10 7.98E-10 1.05E-09 1.83E-09 1.52E-09 1.35E-09 4.42E-10
2.24E-10 1.89E-10
4.00E-16 2.04E-10 1.00E-09 1.33E-09 2.59E-09 2.37E-09 2.21E-09 9.86E-10
5.65E-10 4.68E-10
4.55E-16 2.31E-10 1.12E-09 1.50E-09 3.09E-09 3.03E-09 2.92E-09 1.81E-09
1.26E-09 1.11E-09
4.81E-16 2.48E-10 1.21E-09 1.61E-09 3.40E-09 3.46E-09 3.39E-09 2.62E-09
2.15E-09 2.00E-09

```

```

4.92E-16 2.66E-10 1.29E-09 1.71E-09 3.60E-09 3.72E-09 3.68E-09 3.12E-09
2.74E-09 2.62E-09
4.90E-16 2.81E-10 1.35E-09 1.78E-09 3.63E-09 3.75E-09 3.73E-09 3.28E-09
2.94E-09 2.82E-09
1175.6 A 10 10 /FILMEM = 214.pass/TYPE = EXCIT /INDM = T/ISEL = 4
1.00E+08 2.78E+08 7.74E+08 2.15E+09 5.99E+09 1.67E+10 4.64E+10 1.29E+11
3.59E+11 1.00E+12
8.62E-01 3.45E+00 6.89E+00 8.62E+00 3.45E+01 6.89E+01 8.62E+01 3.45E+02
6.89E+02 8.62E+02
6.81E-17 5.57E-11 3.47E-10 4.71E-10 7.87E-10 5.87E-10 5.07E-10 1.58E-10
8.57E-11 7.08E-11
8.71E-17 6.53E-11 3.90E-10 5.25E-10 8.51E-10 6.34E-10 5.48E-10 1.69E-10
9.11E-11 7.51E-11
1.32E-16 8.76E-11 4.89E-10 6.48E-10 1.01E-09 7.55E-10 6.53E-10 1.98E-10
1.05E-10 8.65E-11
2.18E-16 1.28E-10 6.60E-10 8.63E-10 1.33E-09 1.03E-09 8.98E-10 2.77E-10
1.45E-10 1.18E-10
3.30E-16 1.76E-10 8.57E-10 1.11E-09 1.82E-09 1.51E-09 1.35E-09 4.72E-10
2.51E-10 2.04E-10
4.21E-16 2.14E-10 1.00E-09 1.30E-09 2.28E-09 2.07E-09 1.93E-09 8.80E-10
5.15E-10 4.30E-10
4.71E-16 2.36E-10 1.09E-09 1.42E-09 2.60E-09 2.51E-09 2.41E-09 1.50E-09
1.05E-09 9.26E-10
4.96E-16 2.52E-10 1.16E-09 1.51E-09 2.81E-09 2.81E-09 2.75E-09 2.11E-09
1.74E-09 1.62E-09
5.08E-16 2.69E-10 1.24E-09 1.60E-09 2.98E-09 3.01E-09 2.97E-09 2.49E-09
2.19E-09 2.09E-09
5.08E-16 2.86E-10 1.30E-09 1.67E-09 3.01E-09 3.05E-09 3.02E-09 2.62E-09
2.34E-09 2.25E-09
1175.3 A 10 10 /FILMEM = 214.pass/TYPE = EXCIT /INDM = T/ISEL = 5
1.00E+08 2.78E+08 7.74E+08 2.15E+09 5.99E+09 1.67E+10 4.64E+10 1.29E+11
3.59E+11 1.00E+12
8.62E-01 3.45E+00 6.89E+00 8.62E+00 3.45E+01 6.89E+01 8.62E+01 3.45E+02
6.89E+02 8.62E+02
6.63E-17 5.42E-11 3.37E-10 4.58E-10 7.66E-10 5.71E-10 4.93E-10 1.53E-10
8.34E-11 6.89E-11
8.47E-17 6.36E-11 3.80E-10 5.11E-10 8.28E-10 6.17E-10 5.33E-10 1.64E-10
8.86E-11 7.30E-11
1.29E-16 8.52E-11 4.75E-10 6.30E-10 9.81E-10 7.34E-10 6.35E-10 1.93E-10
1.03E-10 8.42E-11
2.12E-16 1.24E-10 6.42E-10 8.40E-10 1.30E-09 1.00E-09 8.73E-10 2.69E-10
1.41E-10 1.15E-10
3.21E-16 1.72E-10 8.33E-10 1.08E-09 1.77E-09 1.47E-09 1.32E-09 4.59E-10
2.44E-10 1.99E-10
4.09E-16 2.08E-10 9.75E-10 1.27E-09 2.22E-09 2.01E-09 1.88E-09 8.56E-10
5.01E-10 4.18E-10
4.59E-16 2.30E-10 1.06E-09 1.38E-09 2.53E-09 2.44E-09 2.35E-09 1.46E-09
1.02E-09 9.01E-10
4.82E-16 2.45E-10 1.13E-09 1.47E-09 2.74E-09 2.73E-09 2.68E-09 2.06E-09
1.69E-09 1.57E-09
4.94E-16 2.62E-10 1.20E-09 1.56E-09 2.89E-09 2.93E-09 2.89E-09 2.43E-09
2.13E-09 2.03E-09
4.94E-16 2.78E-10 1.26E-09 1.63E-09 2.93E-09 2.97E-09 2.94E-09 2.55E-09
2.28E-09 2.19E-09
1176.4 A 10 10 /FILMEM = 214.pass/TYPE = EXCIT /INDM = T/ISEL = 6
1.00E+08 2.78E+08 7.74E+08 2.15E+09 5.99E+09 1.67E+10 4.64E+10 1.29E+11
3.59E+11 1.00E+12
8.62E-01 3.45E+00 6.89E+00 8.62E+00 3.45E+01 6.89E+01 8.62E+01 3.45E+02
6.89E+02 8.62E+02
6.44E-17 5.27E-11 3.28E-10 4.45E-10 7.44E-10 5.55E-10 4.79E-10 1.49E-10
8.10E-11 6.70E-11
8.24E-17 6.18E-11 3.69E-10 4.96E-10 8.05E-10 6.00E-10 5.18E-10 1.59E-10
8.61E-11 7.10E-11
1.25E-16 8.28E-11 4.62E-10 6.12E-10 9.54E-10 7.14E-10 6.17E-10 1.87E-10
9.97E-11 8.18E-11
2.06E-16 1.21E-10 6.24E-10 8.16E-10 1.26E-09 9.72E-10 8.49E-10 2.62E-10
1.37E-10 1.12E-10
3.12E-16 1.67E-10 8.10E-10 1.05E-09 1.72E-09 1.43E-09 1.28E-09 4.46E-10
2.37E-10 1.93E-10
3.98E-16 2.02E-10 9.48E-10 1.23E-09 2.16E-09 1.96E-09 1.82E-09 8.32E-10
4.87E-10 4.06E-10
4.46E-16 2.23E-10 1.03E-09 1.34E-09 2.45E-09 2.37E-09 2.28E-09 1.42E-09
9.95E-10 8.76E-10
4.69E-16 2.38E-10 1.10E-09 1.43E-09 2.66E-09 2.66E-09 2.60E-09 2.00E-09

```

```

1.64E-09 1.53E-09
4.80E-16 2.55E-10 1.17E-09 1.52E-09 2.81E-09 2.85E-09 2.81E-09 2.36E-09
2.07E-09 1.98E-09
4.80E-16 2.70E-10 1.23E-09 1.58E-09 2.85E-09 2.89E-09 2.85E-09 2.48E-09
2.21E-09 2.13E-09
C-----
C
C PHOTON EMISSIVITY COEFFICIENTS:
C
C
C INFORMATION
C -----
C
C NUCLEAR CHARGE = 6
C ION CHARGE +1 = 3
C
C SPECIFIC ION FILE : adas214.pass
C EXPANSION FILE : No projection data was used in this case.
C
C No ionisation data has been included
C
C OPTIONS : LNORM=T LPSEL=F LZSEL=F LIOSEL=F
C             LHSEL=F LRSEL=F LISEL=F LNSEL =F
C
C
C Configuration          (2s+1)l(w-1/2)      Energy (cm**-1)
C   1  2S2(1S0)           (1)0( 0.0)        0.0
C   2  2S2P(3P0)          (3)1( 0.0)        52367.1
C   3  2S2P(3P1)          (3)1( 1.0)        52390.8
C   4  2S2P(3P2)          (3)1( 2.0)        52447.1
C   5  2S2P(1P1)          (1)1( 1.0)        102352.0
C   6  2P2(3P0)           (3)1( 0.0)        137425.7
C   7  2P2(3P1)           (3)1( 1.0)        137454.4
C   8  2P2(3P2)           (3)1( 2.0)        137502.0
C   9  2P2(1D2)           (1)2( 2.0)        145876.1
C  10  2P2(1S0)           (1)0( 0.0)        182519.9
C  11  2S3S(3S1)          (3)0( 1.0)        238213.0
C  12  2S3S(1S0)          (1)0( 0.0)        247170.3
C  13  2S3P(1P1)          (1)1( 1.0)        258931.3
C  14  2S3P(3P0)          (3)1( 0.0)        259705.6
C  15  2S3P(3P1)          (3)1( 1.0)        259711.2
C  16  2S3P(3P2)          (3)1( 2.0)        259724.3
C  17  2S3D(3D1)          (3)2( 1.0)        270010.8
C  18  2S3D(3D2)          (3)2( 2.0)        270011.9
C  19  2S3D(3D3)          (3)2( 3.0)        270014.7
C  20  2S3D(1D2)          (1)2( 2.0)        276482.9
C
C
C ISEL  WAVELENGTH      TRANSITION      TYPE    METASTABLE   IMET   NMET   IP
C -----
C   1.   1174.93   8(3)1( 2.0)- 3(3)1( 1.0)  EXCIT      T   1
C   2.   1175.71   8(3)1( 2.0)- 4(3)1( 2.0)  EXCIT      T   1
C   3.   1175.99   6(3)1( 0.0)- 3(3)1( 1.0)  EXCIT      T   1
C   4.   1175.59   7(3)1( 1.0)- 3(3)1( 1.0)  EXCIT      T   1
C   5.   1175.26   7(3)1( 1.0)- 2(3)1( 0.0)  EXCIT      T   1
C   6.   1176.37   7(3)1( 1.0)- 4(3)1( 2.0)  EXCIT      T   1
C
C CODE : ADAS208
C PRODUCER : Alessandra Giunta
C DATE : 19/03/13
C
C-----

```

5 Demo (e) Working with Non-Maxwellians

DEMO E: Non-Maxwellian rates

PURPOSE: To generate adf04 data files type 4 (Non-Maxwellian averaged) and calculate the population of excited state using run_adas218.pro population code.

The ADAS format which delivers fundamental electron-ion collision data and atomic structure calculations is adf04. As discussed in Module 1 Demo c, there are five types of adf04. The most common is the type 3, which provides the Maxwellian averaged Upsilon (effective collision strength) as a function of electron temperature. Cross sections unaveraged over a distributions are collected in adf04 type 1 and adf04 type 5. Type 1 gives the collision strengths as a function of the threshold parameter X (see Module 1 Demo c for more details), while type 5 contains the collision strengths as a function of the final state energy.

For Non-Maxwellian case, type 4 adf04 is introduced.
This adf04 provides the effective collision strengths convolved with a defined Non-Maxwellian distribution as a function of the effective temperature. Non_Maxwellian distributions (analytic distributions, such as Kappa and Druyvestyn, or numerical distributions) are collected in the adf37 ADAS data format.

Type 1 and type 5 adf04 data files are used together with adf37 to produce adf04 type 4.

While the population calculation for a Maxwellian type 3 adf04 is performed by ADAS208 (or run_adas208.pro from the command line), the code to compute the population of excited states for Non-Maxwellian type 4 adf04 is run_adas218.pro

EXAMPLE: For this demo C2+ is considered. The input file is the following
adf04 type 5:
`/home/adas/adas/adf04/cophps#be/dw/ls#c2_t5.dat`
The free electron distributions included in the demo are:
- Maxwellian distribution
- Kappa distribution, with the parameter kappa=5
- Druyvestyn istribution, with the parameter x=2.5
- a numerical distribution EEDF (for JET discharge #74380 -
block 1 : 0.033m from outer divertor, Te(maxw) ~ 4eV)

To generate the adf04 convolved with Maxwellian (type 3) and Non-Maxwellian (type 4) distributions, /home/adas/offline_adas/adas7#3/bin/adf04_om2ups.x is used. The input and output files for this run are the following:

- for Maxwellian distribution:
output file=c2_max.dat (type 3 adf04)

```

- for Kappa distribution:
  input file=instruction.kappa
  output file=c2_kappa.dat
- for Druyvestyn istribution:
  input file=instruction.dru
  output file=c2_dru.dat
- for numerical distribution:
  input file=adf37_DT_1.dat
  output file=c2_num.dat

```

To calculate the populations of excited level run_adas208.pro is used for the Maxwellian case and run_adas218.pro for the three Non-Maxwellian cases.

COMMENTS: Note that for the numerical distribution a single temperature is used.

DEMO e1: Converting adf04 type 5 to adf04 type 4 using ADAS7#3
and run ADAS218 for non-Maxwellian populations.

1. Specify the type 5 adf04.
2. Convolve the four adf04 with the defined free electron distributions.
3. Use run_adas208.pro to calculate the population for the Maxwellian case.
4. Use run_adas218.pro to calculate the population for the Non-Maxwellian case.
5. Plot the populations as a function of excited states for the four cases.

Program: demo_e.pro

Input files: instruction.kappa, instruction.dru, adf37_DT_1.dat

Output file: c2_max.dat, c2_kappa.dat, c2_dru.dat, c2_num.dat, demo_e.ps

5.1 Demo (e) Figures

5.1.1 Demo (e-1) demo_e/nonmax_c2.pdf

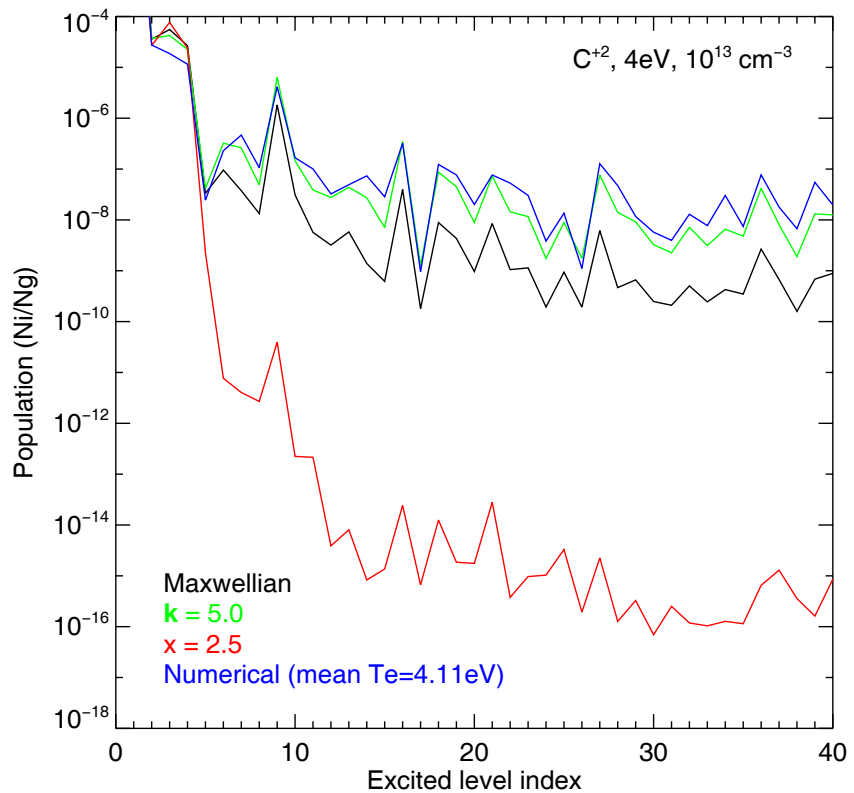


Figure 13: Comparison of populations with different distribution functions .

5.2 Demo (e) IDL procedures

5.2.1 Demo (e-1) demo_e/demo_e.pro

```
pro demo_e
;Compare the excited populations of C+2 at 4eV (max abundance for Maxwellian)
;against kappa, Druyvesteyn and numerical EEDFs

;Specify the adf04 type 5 file for C2+
adf04_in = '/home/adas/adas/adf04/cophps#be/dw/ls#c2_t5.dat'

;-----
; Run adas7#3 adf04_om2ups to generate an adf04 with
; (a) Maxwellian
; (b) kappa=5.0
; (c) Druyvesteyn, x=2.5
; (d) numerical adf37
;-----

exe = '/home/adas/offline_adas/adas7#3/bin/adf04_om2ups.x'

cmd_a = exe + ' ' + adf04_in + ' c2_max.dat'
spawn, cmd_a

all = [' &instruction',
       '   adf04_in = '' + adf04_in + ''',',
       '   adf04_out = ''c2_kappa.dat'',',
       '   numte=5, te= 1e4, 2e4, 5e4, 7e4, 1e5, ittype=1,',',
       '   kappa=5.0',
       ' &end'                                $ ; fortran namelist
                                                 $ ; input adf04 file name
                                                 $ ; output adf04 file name
                                                 $ ; temperatures in K
                                                 $ ; kappa value
                                                 ]
]

adas_writefile, file='instruction.kappa', all=all

cmd_b = exe + ' -finstruction.kappa'
spawn, cmd_b

all = [' &instruction',
       '   adf04_in = '' + adf04_in + ''',',
       '   adf04_out = ''c2_dru.dat'',',
       '   numte=5, te= 1e4, 2e4, 5e4, 7e4, 1e5, ittype=1,',',
       '   x=2.5',
       ' &end'                                $ ; fortran namelist
                                                 $ ; input adf04 file name
                                                 $ ; output adf04 file name
                                                 $ ; temperatures in K
                                                 $ ; Druyvesteyn x value
                                                 ]
]

adas_writefile, file='instruction.dru', all=all

cmd_c = exe + ' -finstruction.dru'
spawn, cmd_c
```

```

cmd_d = exe + ' ' + adf04_in + ' c2_num.dat adf37_DT_1.dat 4'
; spawn, cmd_d

;-----
; Run population code at 4eV, 1e13 cm-3
;   (a) adas208
;   (b), (c), (d) adas218
;-----

te      = 4.0
dens    = 1e13
unit_te = 'ev'
unid_dens = 'cm-3'
meta_list = [1]

;Use run-adas208.pro to calculate the population
;from the type 3 Maxwellian adf04
run_adas208, adf04='c2_max.dat',
              te=te,dens=dens, unit_te=unit_te,unit_dens=unit_dens,
              meta=meta_list,
              log='paper-208.txt', pass_dir='.', pop=pop_max           $

;Use run-adas218.pro to calculate the population
;from the type 4 Non-Maxwellian adf04
;for a Kappa distribution
run_adas218, adf04='c2_kappa.dat',
              te=te,dens=dens, unit_te=unit_te,unit_dens=unit_dens,
              meta=meta_list,
              log='paper-208.txt', pass_dir='.', pop=pop_kappa           $

;Use run-adas218.pro to calculate the population
;from the type 4 Non-Maxwellian adf04
;for a Druyvesteyn distribution
run_adas218, adf04='c2_dru.dat',
              te=te,dens=dens, unit_te=unit_te,unit_dens=unit_dens,
              meta=meta_list,
              log='paper-208.txt', pass_dir='.', pop=pop_dru           $

;Use run-adas218.pro to calculate the population
;from the type 4 Non-Maxwellian adf04
;for a numerical distribution
te = 4.118 ; EEDF mean Te
run_adas218, adf04='c2_num.dat',
              te=te,dens=dens, unit_te=unit_te,unit_dens=unit_dens,
              meta=meta_list,
              log='paper-208.txt', pass_dir='.', pop=pop_num           $

```

```

;-----
; Plot populations
;-----

index      = indgen(pop_max.numlev) + 1
dep_max    = pop_max.dependence
dep_kappa   = pop_kappa.dependence
dep_dru     = pop_dru.dependence
dep_num     = pop_num.dependence

xmin = 1
xmax = 40
ymin = 1e-18
ymax = 1e-4

set_plot,'ps'
device, /isolatin1, font_index=8
device, bits=8, filename='demo_e.ps', $
        font_size = 14, xsize=18.0, ysize=16.0, $
        yoffset=7.0, /color
device, /helvetica

plot_io, [xmin, xmax], [ymin, ymax], /nodata, ystyle=1,$
        xtitle = 'Excited level index', $
        ytitle = 'Population (Ni/Ng)'

oplot, index, dep_max, thick=3
oplot, index, dep_kappa, line=1
oplot, index, dep_dru, line=2
oplot, index, dep_num, line=3

device, /close
set_plot,'X'
!p.font=-1

end

```

5.3 Demo (e-1) Tables and drivers

5.3.1 demo_e-1/instruction.kappa

```
&instruction
  adf04_in = '/home/adas/adas/adf04/cophps#be/dw/ls#c2_t5.dat',
  adf04_out = 'c2_kappa.dat',
  numte=5, te= 1e4, 2e4, 5e4, 7e4, 1e5, itttype=1,
  kappa=5.0
&end
```

5.3.2 demo_e-1/instruction.dru

```
&instruction
  adf04_in = '/home/adas/adas/adf04/cophps#be/dw/ls#c2_t5.dat',
  adf04_out = 'c2_dru.dat',
  numte=5, te= 1e4, 2e4, 5e4, 7e4, 1e5, itttype=1,
  x=2.5
&end
```

5.3.3 demo_e-1/adf37_DT_1.dat

```
ADF37 - Non-Maxwellian distribution FE_1
      2           ; format of file 1 => superposition; 2 => numerical
      2           ; energy units 1 => K; 2 => eV
     116          ; number of tabulated values
       1          ; number of tabulated temperatures
       1          ; cutoff threshold
      3 1.00e+00 ; high energy behaviour
1.00e-01 1.00e+01 2.01e+01 3.01e+01 4.01e+01 5.01e+01 6.02e+01
7.02e+01 8.02e+01 9.02e+01 1.00e+02 1.10e+02 1.20e+02 1.30e+02
1.40e+02 1.50e+02 1.60e+02 1.70e+02 1.80e+02 1.90e+02 2.01e+02
2.11e+02 2.21e+02 2.31e+02 2.41e+02 2.51e+02 2.61e+02 2.71e+02
2.81e+02 2.91e+02 3.01e+02 3.11e+02 3.21e+02 3.31e+02 3.41e+02
3.51e+02 3.61e+02 3.71e+02 3.81e+02 3.91e+02 4.01e+02 4.11e+02
4.21e+02 4.31e+02 4.41e+02 4.51e+02 4.61e+02 4.71e+02 4.81e+02
4.91e+02 5.01e+02 5.11e+02 5.21e+02 5.31e+02 5.41e+02 5.51e+02
5.61e+02 5.71e+02 5.81e+02 5.91e+02 6.02e+02 6.12e+02 6.22e+02
6.32e+02 6.42e+02 6.52e+02 6.62e+02 6.72e+02 6.82e+02 6.92e+02
7.02e+02 7.12e+02 7.22e+02 7.32e+02 7.42e+02 7.52e+02 7.62e+02
7.72e+02 7.82e+02 7.92e+02 8.02e+02 8.12e+02 8.22e+02 8.32e+02
8.42e+02 8.52e+02 8.62e+02 8.72e+02 8.82e+02 8.92e+02 9.02e+02
9.12e+02 9.22e+02 9.32e+02 9.42e+02 9.52e+02 9.62e+02 9.72e+02
9.82e+02 9.92e+02 1.00e+03 1.01e+03 1.02e+03 1.03e+03 1.04e+03
1.05e+03 1.06e+03 1.07e+03 1.08e+03 1.09e+03 1.10e+03 1.11e+03
1.12e+03 1.13e+03 1.14e+03 1.15e+03
2.00e-01 2.34e-02 2.04e-03 3.78e-04 2.10e-04 1.73e-04 1.55e-04
1.44e-04 1.34e-04 1.23e-04 1.12e-04 1.03e-04 9.22e-05 8.45e-05
7.77e-05 7.19e-05 6.42e-05 6.00e-05 5.50e-05 5.02e-05 4.61e-05
4.18e-05 3.75e-05 3.50e-05 3.23e-05 2.92e-05 2.62e-05 2.49e-05
2.22e-05 2.11e-05 1.88e-05 1.72e-05 1.55e-05 1.40e-05 1.31e-05
1.14e-05 1.04e-05 9.00e-06 8.32e-06 7.98e-06 7.10e-06 6.56e-06
5.83e-06 5.24e-06 4.51e-06 4.30e-06 4.08e-06 3.71e-06 3.13e-06
2.79e-06 2.71e-06 2.45e-06 2.41e-06 2.24e-06 1.81e-06 1.63e-06
1.51e-06 1.34e-06 1.36e-06 1.13e-06 1.02e-06 8.61e-07 8.93e-07
9.20e-07 7.19e-07 6.44e-07 5.61e-07 5.05e-07 3.99e-07 3.98e-07
3.27e-07 2.85e-07 2.99e-07 2.80e-07 1.93e-07 2.25e-07 2.10e-07
2.48e-07 1.67e-07 1.24e-07 1.55e-07 9.10e-08 7.78e-08 8.18e-08
1.06e-07 9.46e-08 8.88e-08 8.37e-08 9.00e-08 4.28e-08 5.39e-08
3.16e-08 3.71e-08 2.35e-08 2.57e-08 2.27e-08 1.38e-08 2.03e-08
2.62e-08 1.31e-08 1.56e-08 2.52e-08 9.63e-09 6.93e-09 2.29e-09
1.08e-08 1.33e-08 1.53e-08 1.74e-08 8.72e-09 1.82e-08 1.23e-08
1.06e-08 2.00e-08 2.82e-09 2.42e-09
C-----
C
C Description: Example EEDF from David Tskhakaya.
C           For JET discharge #74380
C           block 1 : 0.033m from outer divertor, Te(maxw) ~ 4eV
C
C Author : Martin O'Mullane
C Date   : 26-09-2010
C
C-----
```

5.3.4 demo_e-1/c2_max.dat

```
C + 2      6      3   386267.9284(1s)
  1 522          (1)0( 0.0)    0.0000 {X}
  2 512513        (3)1( 4.0)   53491.3156 {X}
  3 512513        (1)1( 1.0)   110439.0290 {X}
  4 523          (3)1( 4.0)   139893.6726 {X}
  5 523          (1)2( 2.0)   152571.3874 {X}
  6 523          (1)0( 0.0)   193818.1952 {X}

  44 513515          (1)0( 0.0)   361672.4582 {X}
-1  21.5297 3.13997 2.53196 1.23495 1.08165 1.00320 0.65687 0.59645 0.56432
3.00 3         9.00+02 1.80+03 4.50+03 9.00+03 1.80+04 4.50+04 9.00+04 1.80+05
  2  1 1.00-30 1.11+00 1.11+00 1.10+00 1.08+00 1.04+00 9.52-01 8.46-01 7.08-01
  3  1 2.23+09 3.76+00 3.77+00 3.79+00 3.85+00 3.97+00 4.29+00 4.74+00 5.48+00
  3  2 1.00-30 2.57+00 2.57+00 2.55+00 2.51+00 2.43+00 2.22+00 1.96+00 1.60+00
  4  1 1.00-30 5.39-02 5.38-02 5.35-02 5.28-02 5.14-02 4.76-02 4.23-02 3.48-02
  4  2 1.56+09 2.17+01 2.17+01 2.19+01 2.21+01 2.27+01 2.42+01 2.63+01 2.98+01
  4  3 1.00-30 9.84-01 9.82-01 9.75-01 9.59-01 9.27-01 8.48-01 7.53-01 6.30-01
  5  1 2.75+03 7.93-02 7.94-02 7.97-02 8.04-02 8.19-02 8.64-02 9.37-02 1.06-01
  5  2 1.00-30 1.72+00 1.72+00 1.70+00 1.68+00 1.63+00 1.49+00 1.33+00 1.12+00

  44 43 6.93-16 8.13-01 8.09-01 7.84-01 7.33-01 6.42-01 4.92-01 4.02-01 3.53-01
-1
-1 -1
C-----
c comments from original adf04 file
C-----
c Autostructure distorted wave production of adf04 datasets
c
c
c Script : /home/adas/offline_adas/adas7#3/scripts/
c           process_ion_dw_adf27_to_adf04.pl
c
c Codes   : /home/adas/offline_adas/adas7#1/bin/as25.x
c           /home/adas/offline_adas/adas7#3/bin/adf04_om2ups.x
c Driver   : /home/adas/adas/adf27/dw/belike/copphs#be/dw/ls#c2.dat
c Outputs  : /home/adas/adas/adf04/copphs#be/dw/ls#c2.dat.
c           /home/adas/adas/adf04/copphs#be/dw/ls#c2_t5.dat.
c
c Producer: Alessandra Giunta
c Date     : 11-09-2012
c
c-----
c-----c
c Conversion of an adf04 dataset from type 5 to type 3
c
c Parameter: Cowan ion threshold shift = F
c
c
c Producer : Alessandra Giunta
c Date     : 19-07-2013
c
c-----c
```

5.3.5 demo_e-1/c2_kappa.dat

```
C + 2      6      3   386267.9284(1s)
  1 522          (1)0( 0.0)    0.0000 {X}
  2 512513        (3)1( 4.0)   53491.3156 {X}
  3 512513        (1)1( 1.0)   110439.0290 {X}
  4 523          (3)1( 4.0)   139893.6726 {X}
  5 523          (1)2( 2.0)   152571.3874 {X}
  6 523          (1)0( 0.0)   193818.1952 {X}

  44 513515          (1)0( 0.0)   361672.4582 {X}
-1  21.5297 3.13997 2.53196 1.23495 1.08165 1.00320 0.65687 0.59645 0.56432
3.00 4         1.00+04 2.00+04 5.00+04 7.00+04 1.00+05
  2  1 1.00-30 7.32+00 1.25+00 7.60-01 7.42-01 7.31-01 0.00+00
  1  2 0.00+00 1.19+00 1.16+00 1.06+00 1.01+00 9.53-01-3.27+00
  3  1 2.23+09 7.25+03 3.66+01 4.87+00 4.21+00 4.17+00 0.00+00
  1  3 0.00+00 4.24+00 4.36+00 4.70+00 4.90+00 5.17+00 0.00+00
```

```

3 2 1.00-30 2.25+01 3.14+00 1.77+00 1.71+00 1.67+00-1.43+01
2 3 0.00+00 2.77+00 2.69+00 2.48+00 2.36+00 2.21+00 0.00+00
4 1 1.00-30 2.00+03 1.34+00 5.71-02 3.99-02 3.31-02 2.31-01

43 44 0.00+00 8.14-01 7.26-01 5.73-01 5.20-01 4.71-01 0.00+00
-1
-1 -1
c-----
c comments from original adf04 file
c-----
c Autostructure distorted wave production of adf04 datasets
c
c
c Script : /home/adas/offline_adas/adas7#3/scripts/
c           process_ion_dw_adf27_to_adf04.pl
c
c Codes : /home/adas/offline_adas/adas7#1/bin/as25.x
c           /home/adas/offline_adas/adas7#3/bin/adf04_om2ups.x
c Driver : /home/adas/adas/adf27/dw/belike/copbps#be/ls#c2.dat
c Outputs : /home/adas/adas/adf04/copbps#be/dw/ls#c2.dat.
c           /home/adas/adas/adf04/copbps#be/dw/ls#c2_t5.dat.
c
c Producer: Alessandra Giunta
c Date : 11-09-2012
c
c-----
c-----c
c Conversion of an adf04 dataset from type 5 to type 4
c
c Parameter: Cowan ion threshold shift = F
c kappa distribution : 5.0000E+00
c
c Producer : Alessandra Giunta
c Date : 19-07-2013
c
c-----
c-----c

```

5.3.6 demo_e-1/c2_dru.dat

```

C + 2      6      3   386267.9284(1s)
1 522          (1)0( 0.0)    0.0000 {X}
2 512513        (3)1( 4.0)    53491.3156 {X}
3 512513        (1)1( 1.0)    110439.0290 {X}
4 523          (3)1( 4.0)    139893.6726 {X}
5 523          (1)2( 2.0)    152571.3874 {X}
6 523          (1)0( 0.0)    193818.1952 {X}

44 513515        (1)0( 0.0)    361672.4582 {X}
-1 21.5297 3.13997 2.53196 1.23495 1.08165 1.00320 0.65687 0.59645
3.00 4 1.00+04 2.00+04 5.00+04 7.00+04 1.00+05
2 1 1.00-30 4.00-08 1.63-01 1.22+00 1.14+00 9.82-01 0.00+00
1 2 0.00+00 9.44-01 9.00-01 7.97-01 7.45-01 6.82-01-3.27+00
3 1 2.23+09 1.00-30 2.69-08 1.68+00 4.05+00 5.58+00 0.00+00
1 3 0.00+00 3.43+00 3.57+00 3.94+00 4.15+00 4.45+00 0.00+00
3 2 1.00-30 3.33-09 2.31-01 2.82+00 2.70+00 2.32+00-1.43+01
2 3 0.00+00 2.19+00 2.10+00 1.86+00 1.73+00 1.57+00 0.00+00
4 1 1.00-30 1.00-30 1.01-17 5.48-03 2.96-02 5.03-02 2.31-01
1 4 0.00+00 4.63-02 4.47-02 4.02-02 3.76-02 3.42-02 0.00+00
2 1.56+09 3.05-27 2.21-03 1.93+01 2.86+01 3.25+01-6.38+00
2 4 0.00+00 1.97+01 2.03+01 2.21+01 2.31+01 2.45+01 0.00+00
4 3 1.00-30 6.59-02 9.94-01 1.02+00 8.91-01 7.63-01 9.65-03
3 4 0.00+00 8.38-01 8.00-01 7.11-01 6.65-01 6.08-01 0.00+00
5 1 2.75+03 1.00-30 9.64-22 3.84-03 3.71-02 8.83-02-3.18+00
1 5 0.00+00 7.14-02 7.31-02 7.83-02 8.18-02 8.69-02 0.00+00

43 44 0.00+00 6.19-01 5.07-01 3.60-01 3.25-01 3.02-01 0.00+00
-1
-1 -1
c-----
c comments from original adf04 file
c-----
c Autostructure distorted wave production of adf04 datasets
c

```

```

c
c Script  : /home/adas/offline_adas/adas7#3/scripts/
c           process_ion_dw.adf27_to_adf04.pl
c
c Codes   : /home/adas/offline_adas/adas7#1/bin/as25.x
c           /home/adas/offline_adas/adas7#3/bin/adf04_om2ups.x
c Driver  : /home/adas/adas/adf27/dw/belike/copphs#be/ls#c2.dat
c Outputs : /home/adas/adas/adf04/copphs#be/dw/ls#c2.dat.
c           /home/adas/adas/adf04/copphs#be/dw/ls#c2_t5.dat.
c
c Producer: Alessandra Giunta
c Date    : 11-09-2012
c
c-----
c-----
```

c Conversion of an adf04 dataset from type 5 to type 4

c Parameter: Cowan ion threshold shift = F

c Druyvesteyn distribution : 2.5000E+00

c Producer : Alessandra Giunta

c Date : 19-07-2013

c

5.3.7 demo_e-1/c2_num.dat

```

C + 2       6      3 386267.9284(1s)
  1 522      (1)0( 0.0) 0.0000 {X}
  2 512513   (3)1( -4.0) 53491.3156 {X}
  3 512513   (1)1( 1.0) 110439.0290 {X}
  4 523       (3)1( -4.0) 139893.6726 {X}
  5 523       (1)2( 2.0) 152571.3874 {X}
  6 523       (1)0( 0.0) 193818.1952 {X}

  44 513515   (1)0( 0.0) 361672.4582 {X}
-1 21.5297 3.13997 2.53196 1.23495 1.08165 1.00320 0.65687 0.59645
3.00 4       4.78+04
  2 1 1.00-30 9.24-01 0.00+00
  1 2 0.00+00 2.62+00-3.27+00
  3 1 2.23+09 3.48+00 0.00+00
  1 3 0.00+00 1.04+01 0.00+00
  2 1 1.00-30 2.00+00-1.43+01
  2 3 0.00+00 6.07+00 0.00+00
  4 1 1.00-30 2.89-02 2.31-01
  1 4 0.00+00 1.28-01 0.00+00
  4 2 1.56+09 1.60+01-6.38+00
  2 4 0.00+00 5.92+01 0.00+00
  4 3 1.00-30 1.32+00 9.65-03
  3 4 0.00+00 2.33+00 0.00+00
  5 1 2.75+03 1.16-01-3.18+00
  1 5 0.00+00 2.14-01 0.00+00

  43 44 0.00+00 1.79+00 0.00+00
-1
-1 -1
c-----
```

c comments from original adf04 file

c-----

c Autostructure distorted wave production of adf04 datasets

c

c Script : /home/adas/offline_adas/adas7#3/scripts/
c process_ion_dw.adf27_to_adf04.pl
c

c Codes : /home/adas/offline_adas/adas7#1/bin/as25.x
c /home/adas/offline_adas/adas7#3/bin/adf04_om2ups.x
c Driver : /home/adas/adas/adf27/dw/belike/copphs#be/ls#c2.dat
c Outputs : /home/adas/adas/adf04/copphs#be/dw/ls#c2.dat.
c /home/adas/adas/adf04/copphs#be/dw/ls#c2_t5.dat.
c

c Producer: Alessandra Giunta

c Date : 11-09-2012

```
c
c-----
c-----  
c  
c Conversion of an adf04 dataset from type 5 to type 4  
c  
c Parameter: Cowan ion threshold shift = F  
c adf37 distribution : adf37_DT_1.dat  
c  
c Producer : Martin O'Mullane  
c Date     : 28-05-2013  
c  
c-----
```

Appendix D

ADAS-EU WATC: Other talks

D.1 Modelling Lyman and Fulcher band spectra - Prof. Kurt Behringer

Modelling of Lyman and Fulcher Band Spectra



purpose:

interpretation of Lyman and Fulcher spectra
from fusion and technical plasmas,
for H_2 , D_2 , T_2 , HD , DT

program:

- calculation of wavelengths (Λ -doubling)
- and line strengths (Hönl-London, intensity alternation, A-values),
- coupled to a collisional-radiative model for vibrational population,
- projection up of ground state rotational population with T_{rot}

sources of molecular data, Lyman bands

General philosophy:

use detailed experimental data, if available,
but complement with polynomial fits (**only** good for low J- or v-levels)

H_2
 1X : R. J. Spindler JQSRT, 9, 597-626 (1969), page 606, table 3
 1B : R. J. Spindler, page 609, table 4
(calculated, but experimentally verified)

$\rightarrow E(v), B_v, D_v, H_v$
 $\rightarrow E(v), B_v, D_{vp}, H_v$

D_2

R.S. Freund and J.A.Schiavone, J. Phys. Chem. Ref. Data, 14, 235 (1985) $\rightarrow E(v)$
 1X : Samir Kassi et al., 2012 (internet) $\rightarrow B_v, D_v, H_v$,
 1B : NIST $\rightarrow B, D, \alpha, \beta$
 1B : Arno de Lange et al., arXiv:1204.3024v1 [physics.atom-ph] 13 Apr 2012 (internet)
individual levels of B-state
(all data experimental)

other isotopomers to be implemented

sources of molecular data, Fulcher bands

H₂

fit data G.H. Dieke and R.W. Blue, Phys. Rev. 47, 261 (1935) → B, D, α , error in NIST D'
vibrational and rotational energies: G. H. Dieke, J. Molec. Spectroscopy, 1958 (Λ -doubling)
remark: Dieke's and NIST's formulas : Dieke: $F(J)=B^*[J^*(J+1)-\Lambda^2] - \dots$, shift in v_{00}

D₂

fit data G.H. Dieke and R.W. Blue, Phys. Rev. 47, 261 (1935) → B, D, α
detailed level energies: R.S. Freund and J.A. Schiafone, J. Phys. Chem. Ref. Data, 14, 235 (1985)

T₂

fit data G.H. Dieke, F.S. Tomkins, Phys. Rev. 76, 283 (1949) → B, D, α , error in NIST data

HD

fit data G.H. Dieke, R.W. Blue, Phys. Rev. 47, 261 (1935) → B, D, α

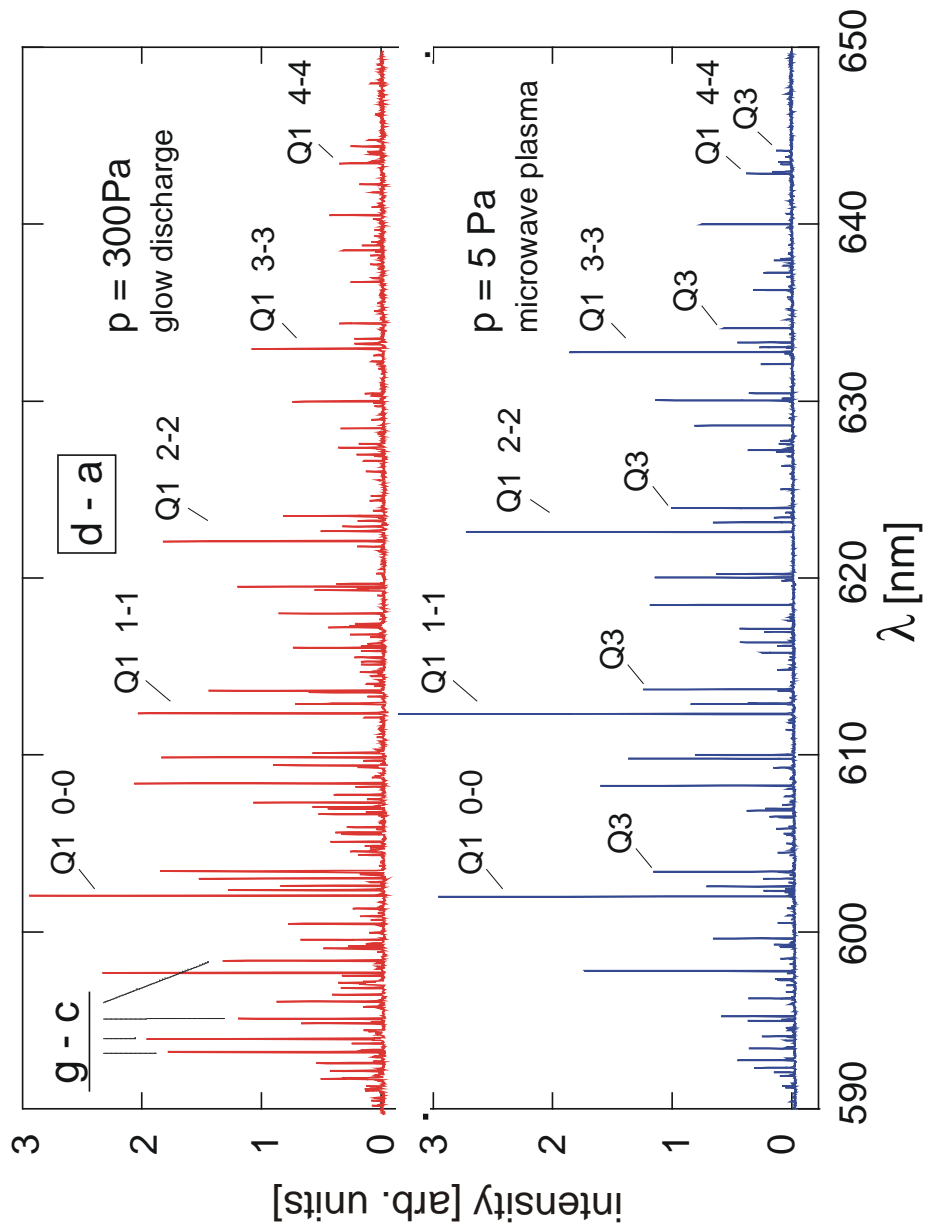
(all experimental, only low J-values)

DT

coefficients scaled from D2 and T2 using reduced masses from Fantz et al. ([Excel sheet](#))
average taken of the two calculations. Checked with Fantz's eV data. v_{00} adjusted

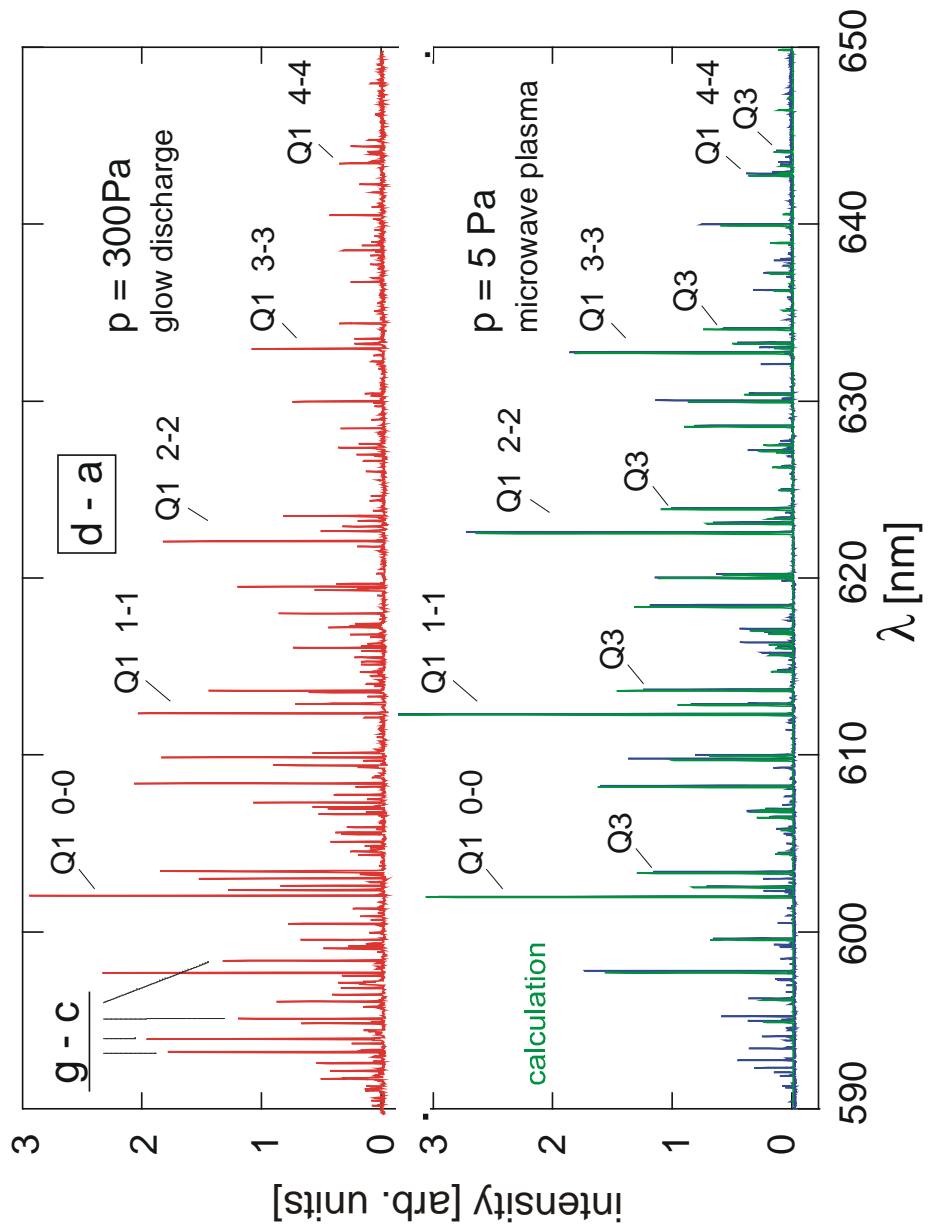


experimental H₂ Fulcher spectra

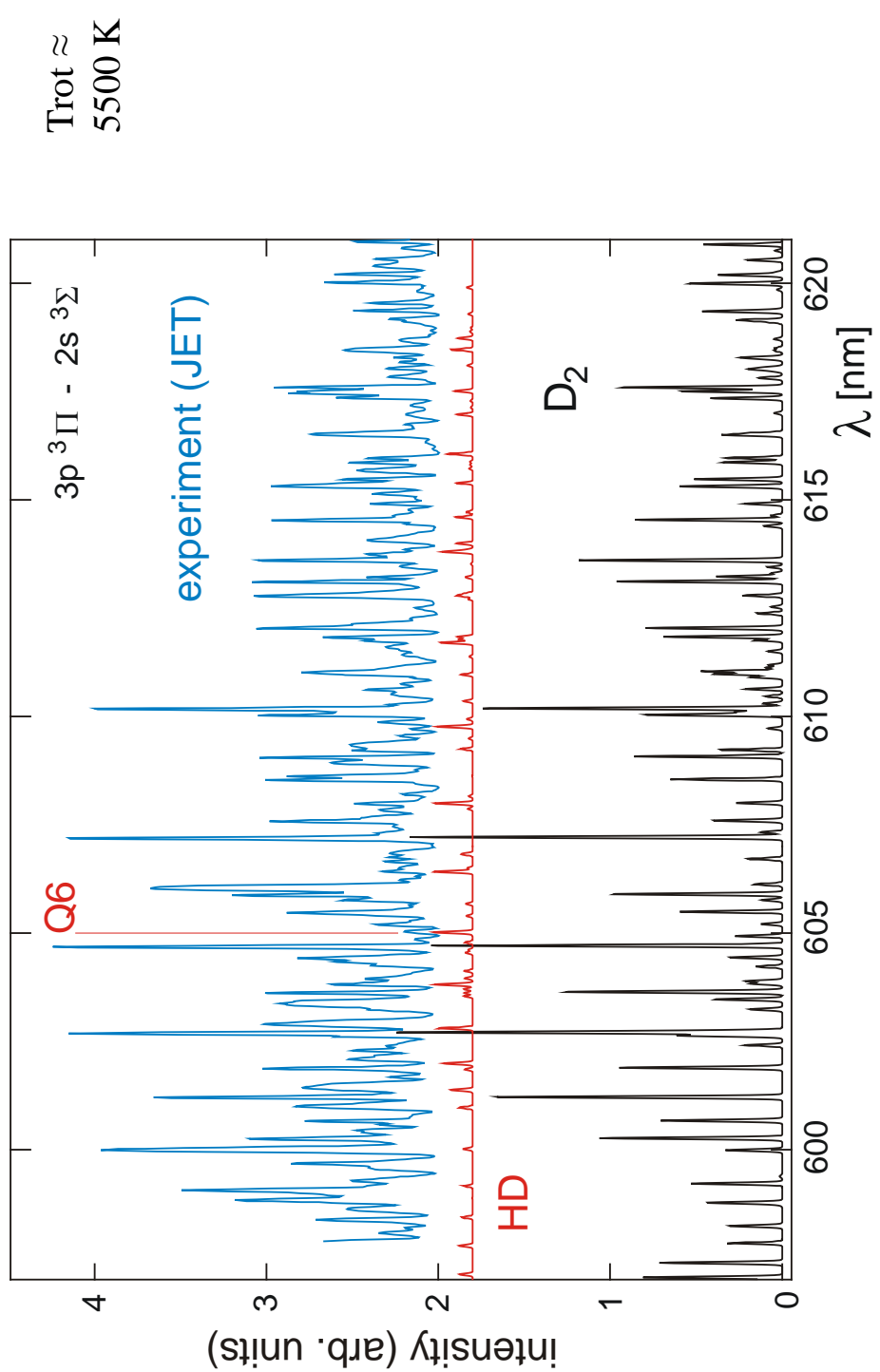




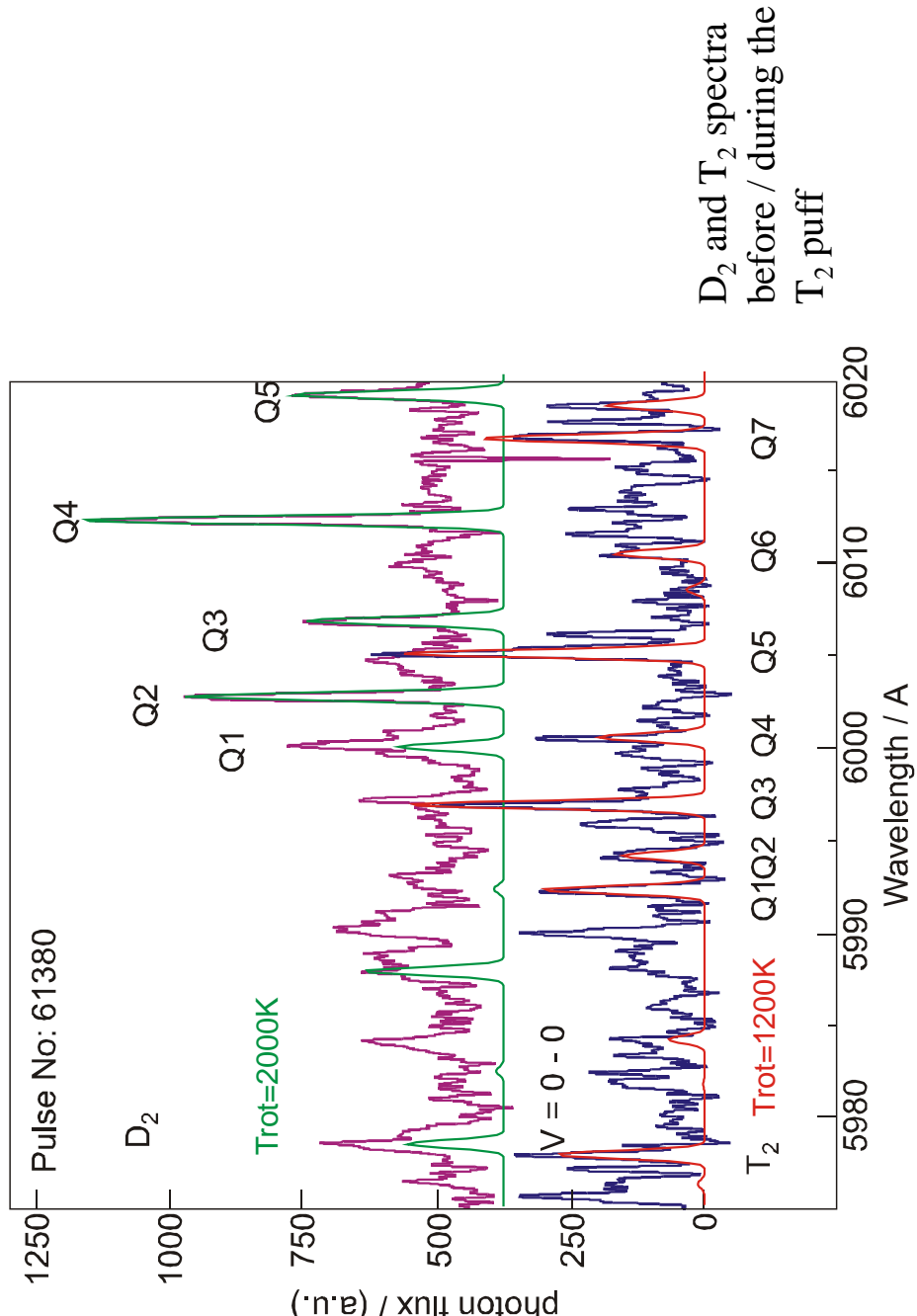
experimental H₂ Fulcher spectra + calculation



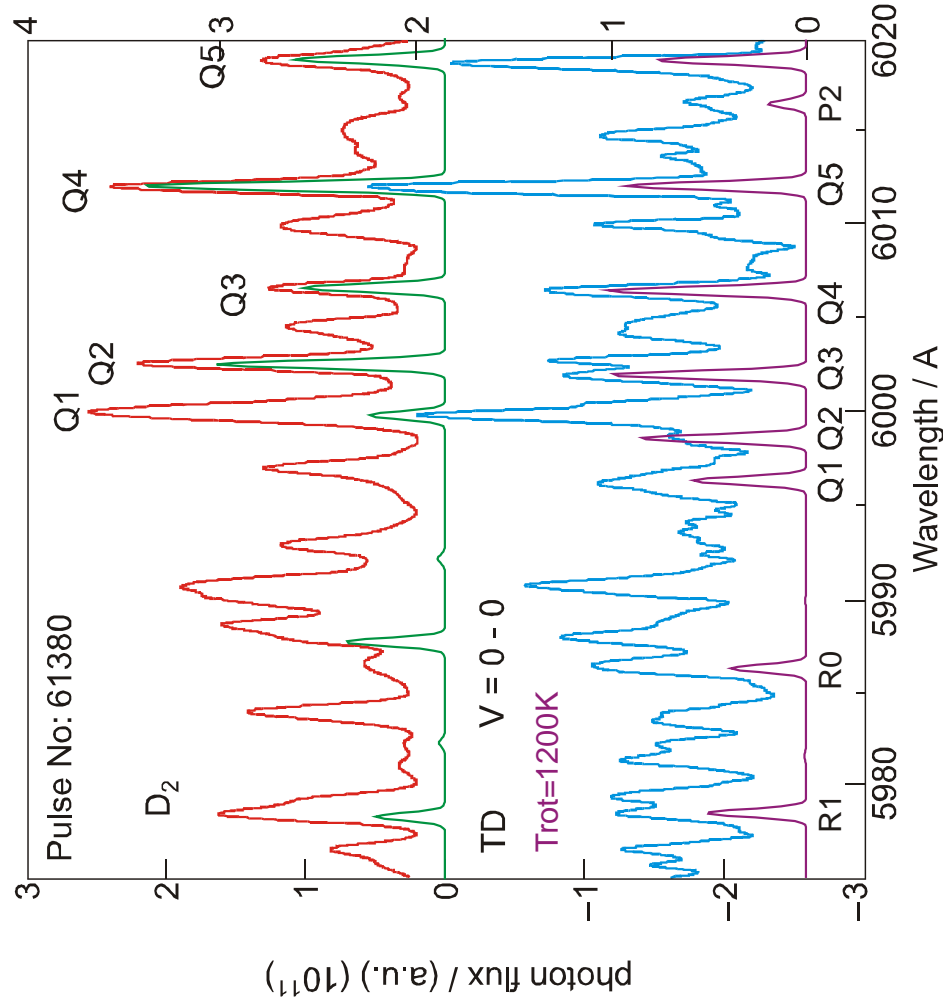
D₂ spectra (G. Sergienko et al., EFDA-JET-CP(12)02/12)

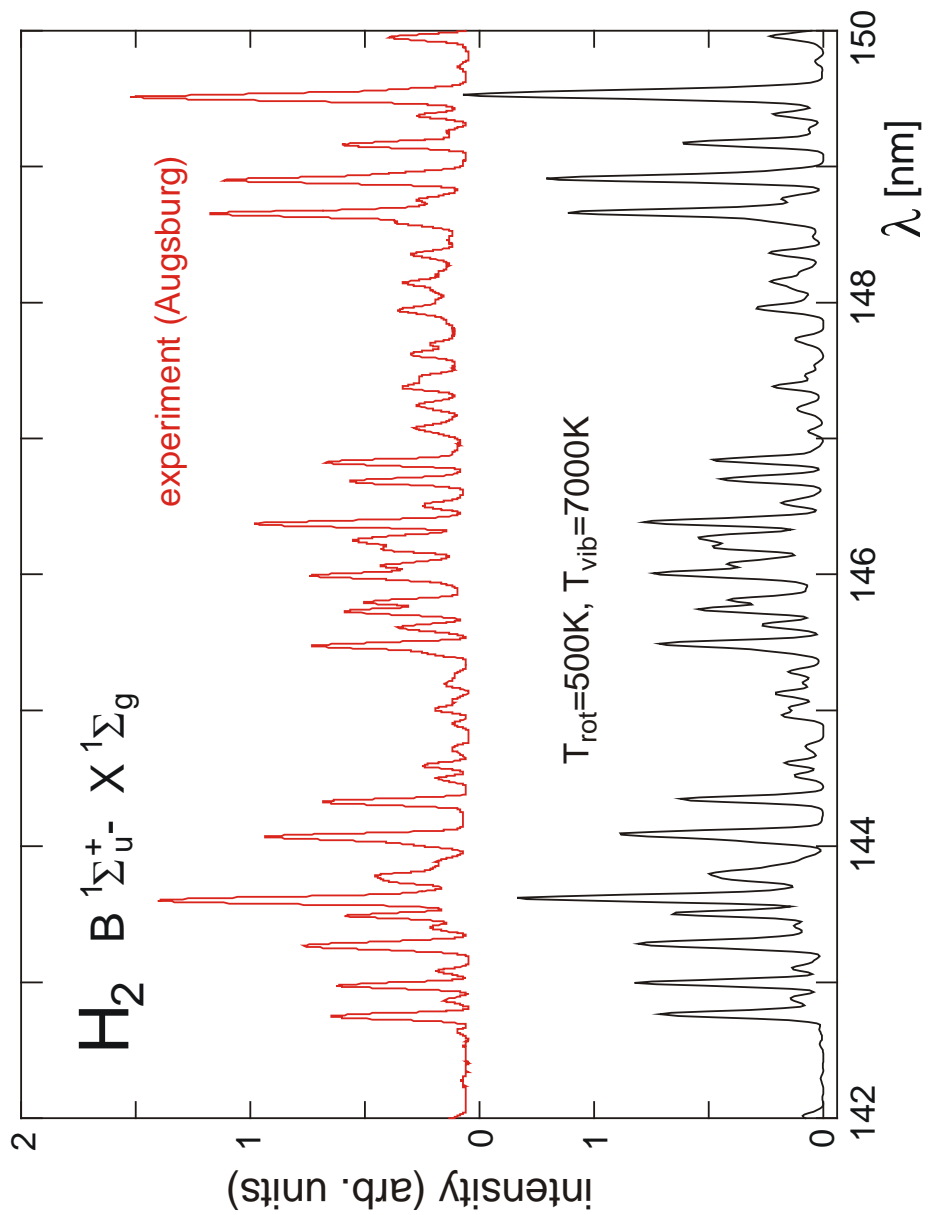


D₂/T₂ spectra (A. Pospieszczynski et al., EFDA-JET-CP(05)02-18)



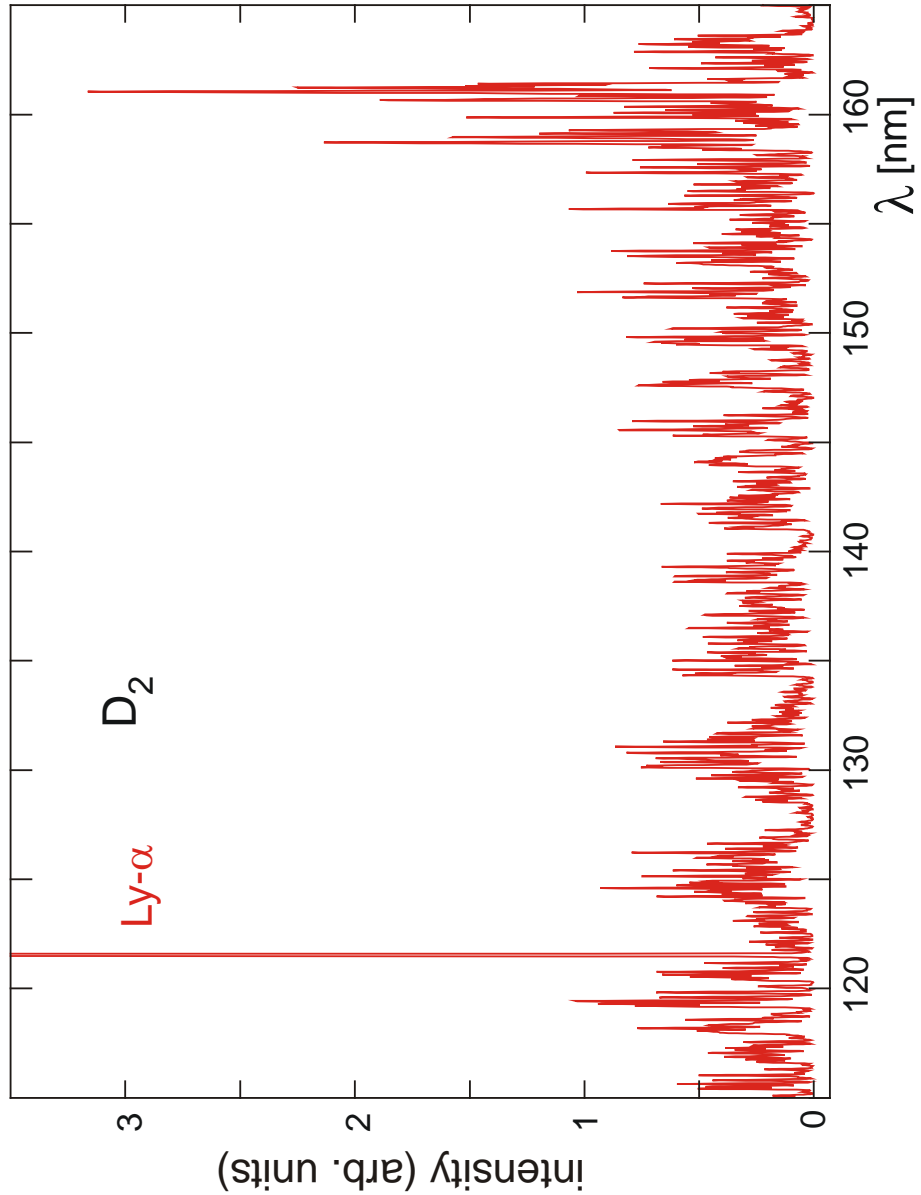
D₂/TD spectra (A. Pospieszczynski et al., EFDA-JET-CP(05)02-18)



details of H_2 Lyman bands

IPP

D₂ Lyman bands



concluding statements

precise calculated spectra are available for H₂ and isotopomers

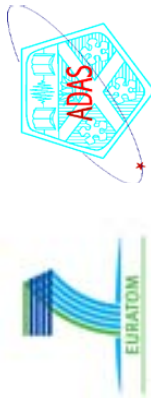
detailed level energy information is being used where available, otherwise the usual fit formulas are applied

spectra of other bands can be added if required

very good agreement with JET spectra



D.2 H₂ collisional-radiative modelling - Dr. Francisco Guzman



H₂ collisional-radiative modelling

work in progress and further thoughts

Francisco Guzman* and Hugh Summers

*Aix-Marseille Université, CNRS, PIIM, Marseille

Contents

1. The complete set of generalised collisional-radiative coefficients.
2. Photon emissivities and photon efficiencies.
3. Linking into plasma modelling.
4. Conclusions.

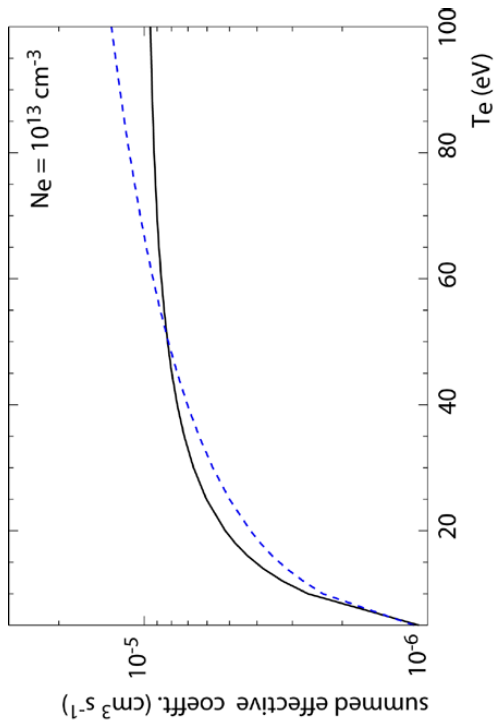
1.1 The complete H₂ generalised collisional-radiative coefficients

| MDF11 Subclass | Character | CR | GCR |
|---|---|-----|-----|
| $\mathcal{M}\mathcal{R}\mathcal{E}\mathcal{D}$ | eff. metastable cross-coupling coefft. | x | x |
| $\mathcal{M}\mathcal{A}\mathcal{R}\mathcal{E}\mathcal{D}$ | eff. recombination coefft. | x | x |
| $\mathcal{M}\mathcal{X}\mathcal{E}\mathcal{D}$ | eff. cross-coupling coefft. via recom. | x | x |
| $\mathcal{M}\mathcal{I}\mathcal{E}\mathcal{D}$ | eff. ionisation coefft. | x | x |
| $\mathcal{M}\mathcal{C}\mathcal{R}\mathcal{X}\mathcal{A}\mathcal{C}\mathcal{D}$ | eff. recom. coefft. via parent CX | x | x |
| $\mathcal{M}\mathcal{C}\mathcal{R}\mathcal{C}\mathcal{D}$ | eff. ionisation coefft. via CX | x | x |
| $\mathcal{P}\mathcal{D}\mathcal{E}\mathcal{D}$ | partial eff. dissoc. coefft. | x | x |
| $\mathcal{P}\mathcal{A}\mathcal{D}\mathcal{E}\mathcal{D}$ | partial eff. dissoc. coefft. via recom. | x | x |
| $\mathcal{P}\mathcal{D}\mathcal{Y}\mathcal{E}\mathcal{D}$ | partial eff. dissoc. coefft. via atom.ionis. | x | x |
| $\mathcal{P}\mathcal{A}\mathcal{D}\mathcal{Y}\mathcal{C}\mathcal{D}$ | partial eff. dissoc. coefft. via recom. and atomic ionisation | x | x |
| MDF15 Subclass | Character | | |
| $\mathcal{M}\mathcal{P}\mathcal{E}\mathcal{C}$ | photon emiss. coefft. | x | x |
| $\mathcal{M}\mathcal{F}\mathcal{P}\mathcal{E}\mathcal{C}$ | feature photon emiss. coefft. | (x) | (x) |

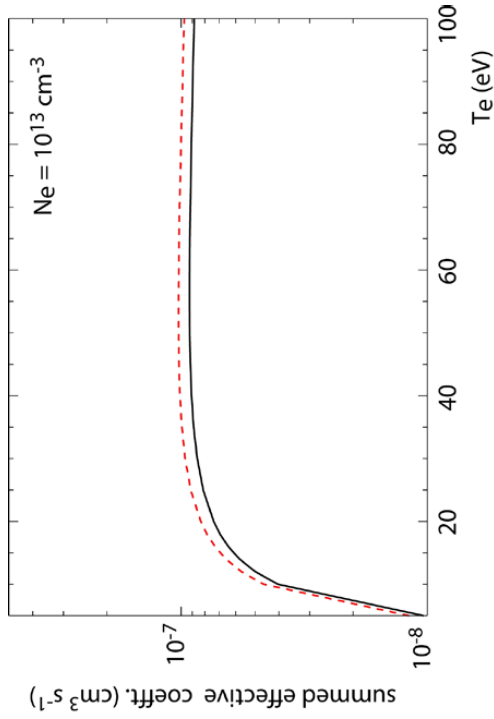
The generalised collisional matrix reductions follow broadly the same path as for atoms and ions. But there are some new coefficients.
The full set currently being calculated by ADAS905 is shown on the right.
GCR denotes the molecular metastable resolved set, while the **CR** set are averaged over equilibrium metastable populations.

1.2 Effective H_2 generalised collisional-radiative coefficients

The full validation of the collisional-radiative model and its organisation for ADAS is a substantial task, which is still underway at this time. It is hoped that the complete system will be ready for the next release of ADAS. Some illustrations follow:



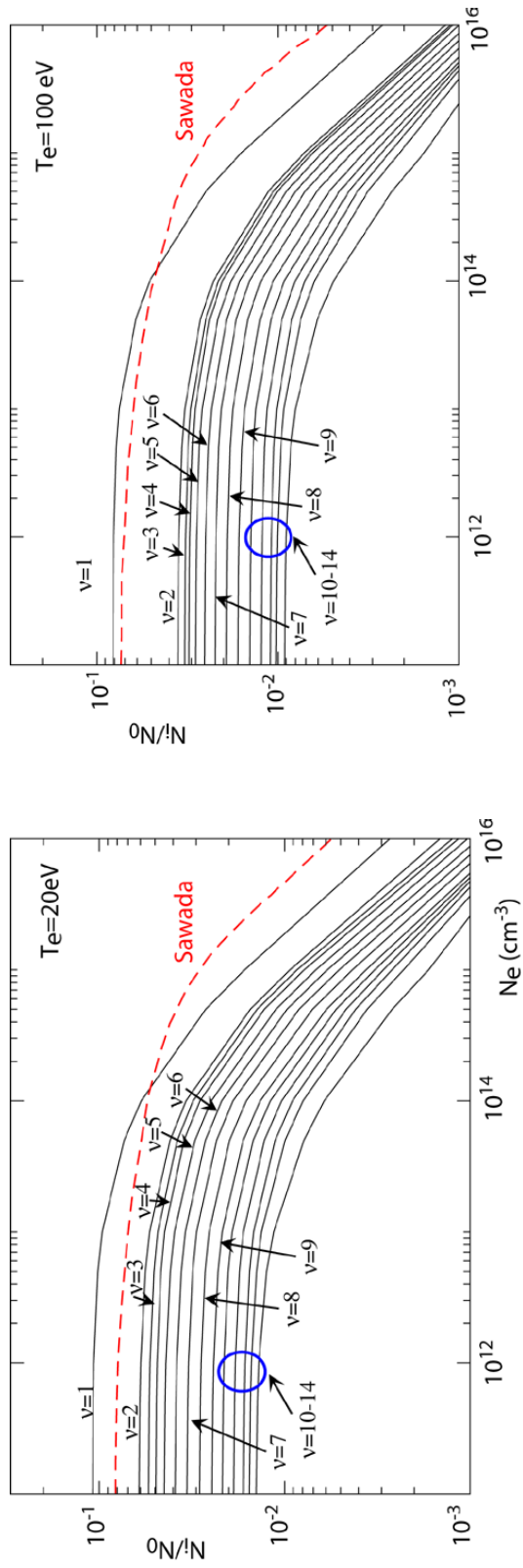
Comparative check sum over vibrational substates of effective dissociation and ionization coefficients:
 $H_2(X^1\Sigma_g^+; v = 0 - 14) + e \rightarrow H + H + e$
 $H_2(X^1\Sigma_g^+; v = 0 - 14) + e \rightarrow H_2^+(X^2\Sigma_g^+) + e \rightarrow e + e$



Comparative check sum over vibrational substates of effective cross-coupling coefficients:
 $H_2(X^1\Sigma_g^+; v = 0 - 14) + e \rightarrow H_2(c^3\Pi_u; v = 0 - 19) + e$
 electronic resolution of upper state
 full vibrational resolution

1.3 Ground electronic state vibrational populations

Ground state vibrational populations. For comparison the single representative excited vibrational population of Sawada & Fujimoto [J. Appl. Phys. 78, 2913 (1995)] is shown.

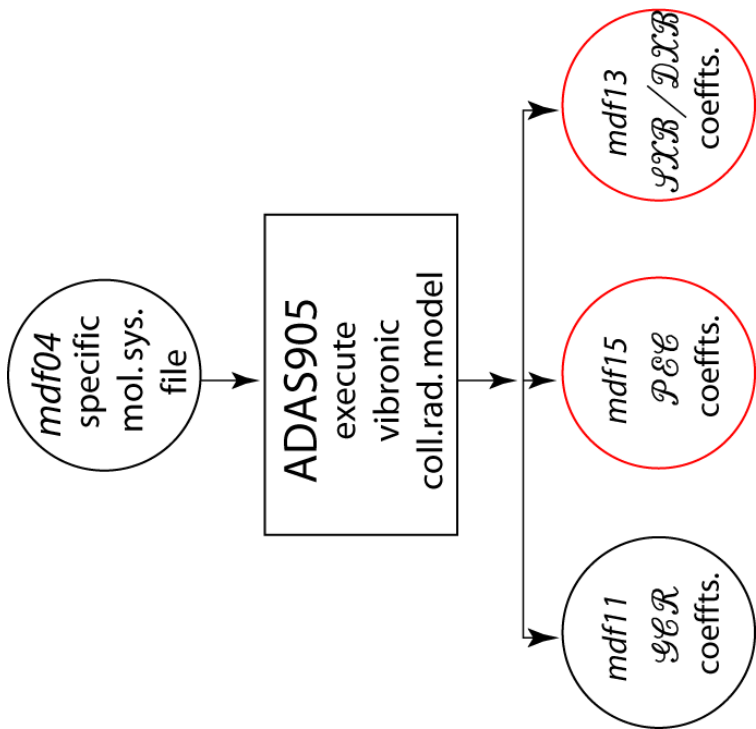


Although broad consistency is indicated, exact values and high density behaviour remain unclear.
More detailed comparisons are being pursued.

2.1 Schematic of ADAS905 output data

The various molecular data output formats from ADAS905 are shown in the schematic.

The principal GCR coefficients in format *mdf11*, have been described in the module 3 lecture.



Here, attention is focussed on format *mdf13* and *mdf15* which correspond to the ionisation per photon and emissivity formats *adf13* and *adf15* of atomic collisional-radiative modelling.

There are more independent contributions to the emissivities in the molecular case. Also **dissociations per photon** must be evaluated as well as the familiar **ionisations per photon**.

2.2 The categories of mdf15 data format

Molecular PECs should be obtained for vibrational resolved spectral bands. A subroutine which finds the required molecular band inside an spectral range is being checked.

- Excitation:
$$\mathcal{PEC}_{\sigma, (j, \nu) \rightarrow (j', \nu')}^{(exc)} = A_{(j, \nu) \rightarrow (j', \nu')} \mathcal{F}_{(j, \nu), \sigma}^{(exc)}$$
- Direct charge exchange:
$$\mathcal{PEC}_{\sigma, (j^+, \nu^+) \rightarrow (j'^+, \nu'^+)}^{(CX)} = A_{(j^+, \nu^+) \rightarrow (j'^+, \nu'^+)} \mathcal{F}_{(j^+, \nu^+), \sigma}^{(exc)}$$
- Inverse charge exchange:
$$\mathcal{PEC}_{\rho, (j, \nu) \rightarrow (j', \nu')}^{(ICX)} = A_{(j, \nu) \rightarrow (j', \nu')} \mathcal{F}_{(j, \nu), \rho}^{(ICX)}$$
- Ionisation:
$$\mathcal{PEC}_{\sigma, (j^+, \nu^+) \rightarrow (j'^+, \nu'^+)}^{(ion)} = A_{(j^+, \nu^+) \rightarrow (j'^+, \nu'^+)} \mathcal{F}_{(j^+, \nu^+), \sigma}^{(ion)}$$
- Recombination:
$$\mathcal{PEC}_{\rho, (j, \nu) \rightarrow (j', \nu')}^{(rec)} = A_{(j, \nu) \rightarrow (j', \nu')} \mathcal{F}_{(j, \nu), \rho}^{(rec)}$$

Furthermore, the molecular metastables contribution to atomic lines should can also be obtained by summing the different dissociation paths.

- Contribution to atom PECs:
$$\mathcal{PEC}_{\sigma, j^{(A)} \rightarrow j'^{(A)}} = A_{j^{(A)} \rightarrow j'^{(A)}} \sum_p^{diss. process} \mathcal{F}_{j^{(A)}, \sigma}^{(P)}$$

2.2 The categories of the mdf13 data format

SXB and DXB coefficient can be obtained from GCR molecular effective coefficient for ionization and dissociation processes:

$$\bullet \text{ Ionisation per photon: } SXB_{\sigma,(j,\nu) \rightarrow (j',\nu')} = \sum_{\rho}^{M'} \frac{\mathcal{MS}\mathcal{C}\mathcal{D}_{\rho\sigma}}{A_{(j,\nu) \rightarrow (j',\nu')}\mathcal{F}_{(j,\nu),\sigma}^{(exc)}}$$
$$\bullet \text{ Dissociation per photon: } DXB_{\sigma,(j,\nu) \rightarrow (j',\nu')} = \sum_{\mu}^{M''} \frac{\sum_{diss.\,paths} [\text{diss. coeffs.}]_{\mu\sigma}}{A_{(j,\nu) \rightarrow (j',\nu')}\mathcal{F}_{(j,\nu),\sigma}^{(exc)}}$$

DXB need to consider all possible dissociation paths from a molecular metastable.
These derived data will be stored in *mdf13* formats

3.1 Linking into plasma modelling

The collisional-radiative coefficients described earlier are appropriate as the source terms in **fluid equations** such as EDGE2D.

Use in **Monte Carlo** modelling in codes such as EIRENE is somewhat different in that probabilities for reaction paths and differential cross-sections are required. It is useful to speculate on accommodating ADAS molecular CR modelling for such usage.

The metastable state (molecular, atomic or ionic) may be viewed as a quasi-particle carrying its set of instantaneously created and annihilated states with it. It is like a **dressed particle**. We can give and effective reaction cross-section simply dividing by an appropriate ion speed. Such xsects. (and partial xsects.) can be prepared from ADAS as required for modelling codes.

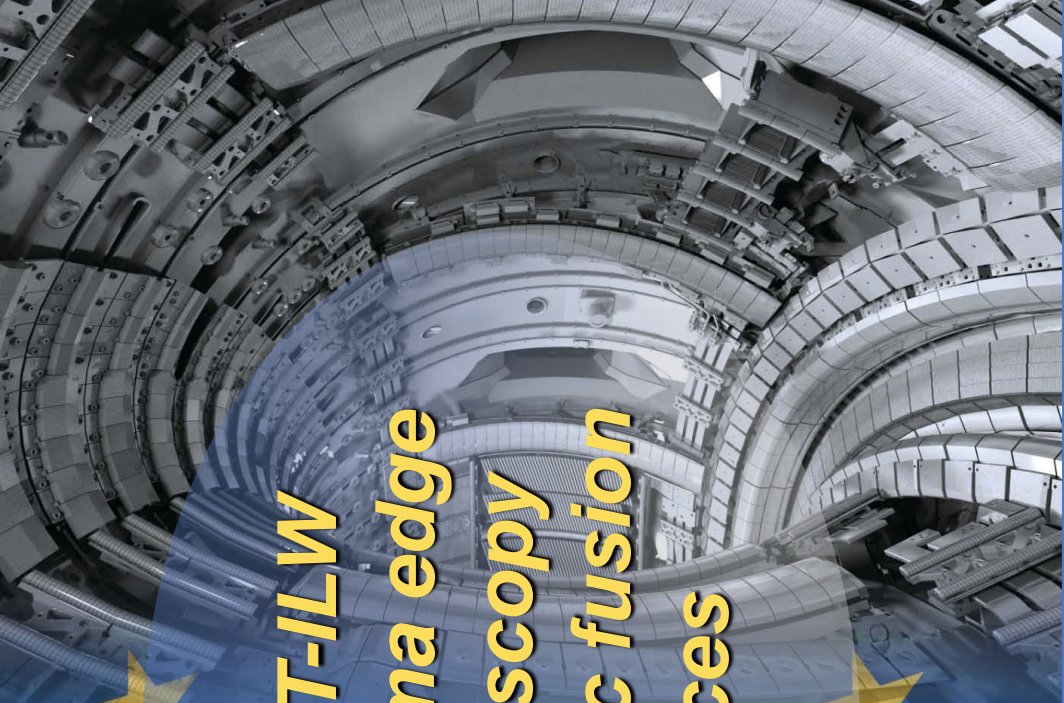
For dominant (metastable) states, simpler differential forms may be ‘planted’ on the effective total dressed reaction cross-section.

The metastable set for the H₂ molecular system is quite large and a potential bottleneck in calculations. The technique of representative metastable vibrational states is being examined as an intermediary between full GCR and CR.

4.1 Conclusions

- Extension of the ADAS molecular reaction database is continuing with additional ion impact reactions currently being integrated.
- The generalised collisional-radiative coefficients of ADAS format *mdf11* are somewhat more elaborate than the familiar *adf11* classes for atoms. As for the atom case, we expect to position both CR and GCR forms, the former (averaged over vibrational sub-structure) being easier for basic usage.
- The emissivity and photon efficiency quantities for molecules for formats *mdf15* and *mdf13* are again somewhat more extensive than their atomic counterparts. The codes for their production are being tested at this time.
- It is suggested that the GCR coefficients can be manipulated into somewhat more convenient forms as **dressed particle reactions** for Monte Carlo modelling. The implementation is being discussed with integrated tokamak modellers.
- Aspirations for double or triply differential cross-sections for all processes are unrealistic. On the other hand, accurate total cross-sections may be used to prepare multipliers for simpler differential cross-section forms.
- Extension is planned to the other hydrogen molecule isotopomers, which will include exploitation of isotopic scaling, in the future.

D.3 The JET-ILW and plasma edge spectroscopy in metallic fusion devices
- Dr. Sebasijan Brezinsek



The JET-ILW and plasma edge spectroscopy in metallic fusion devices

S. Brezinsek

G. v. Rooij

J.W. Coenen

A.G. Meigs

M. Stamp

A. Pospieszczyk

G. Sergienko, T. Pütterich

M. O'Mullane, M. Laengner

and JET-FEDA contributors

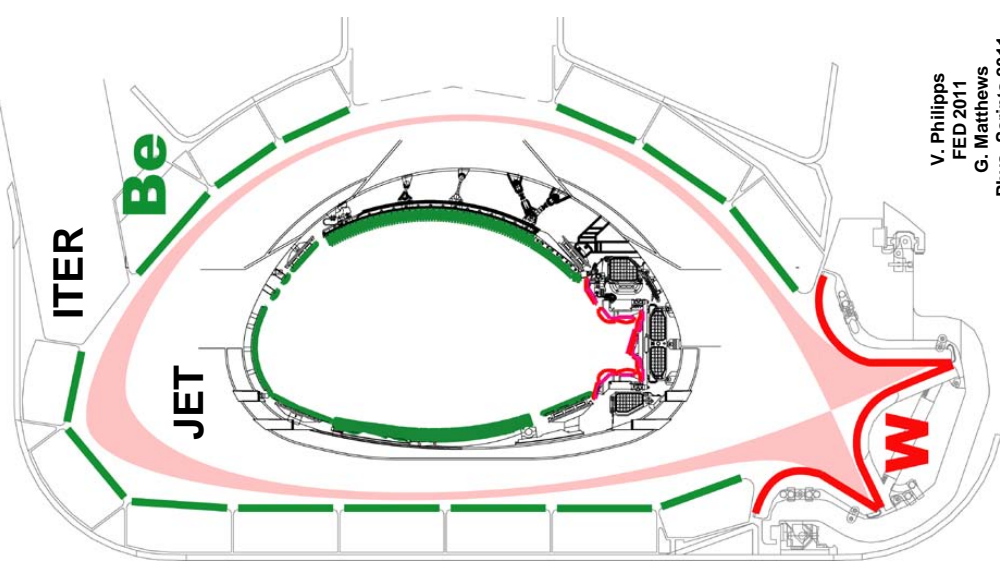
APIP Conference, Auburn, 9.9.2013

Outline

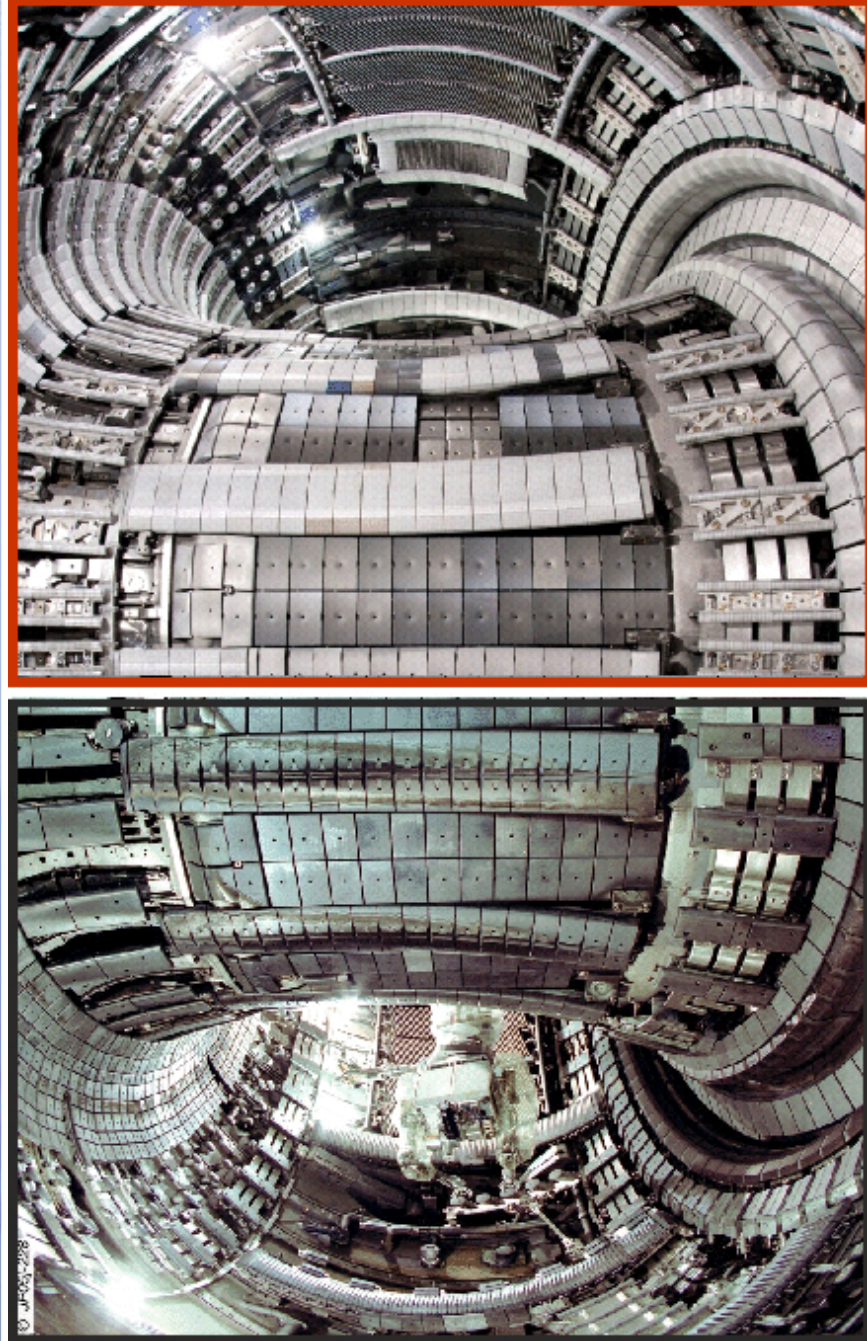
- ITER-Like Wall at JET: Installation, Key Results and Issues related to W components
- W sputtering and W edge spectroscopy
 - Line identification of WI and WII
 - Photon efficiency determination: experiment and modelling
 - W sputtering yields and prompt redeposition
 - Summary

Metallic Walls: ITER-Like Wall at JET

- ITER-material mix used for the first in a tokamak
 - “Carbon-free” environment
 - Reduced tritium retention
 - Loss of carbon as main radiator
 - Change in operational space
 - Need for better plasma control
 - Need for heat load mitigation schemes
- Main goals of the ILW experiment
 - I. Demonstrate low fuel retention, migration and possible fuel recovery*
 - II. Demonstrate plasma compatibility with metallic walls*
- Input to the decision about the first ITER divertor
 - “Be”
 - W



JET-C vs. JET-ILW



- ITER wall material combination, but only inertial cooled plasma-facing components
- Installation of 2t of W and 2t of Be (~82 000 components) by remote handling

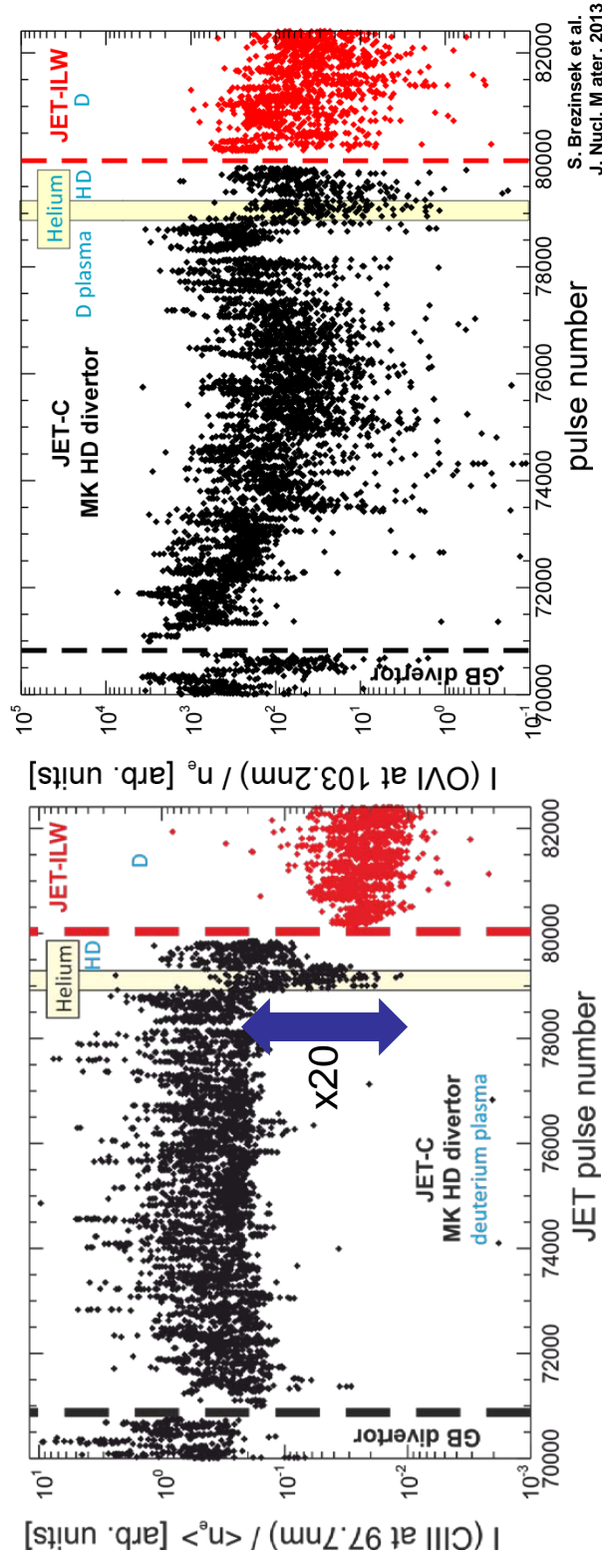


EEJET

Residual Carbon and Oxygen

Main chamber CIII and outer divertor CII edge fluxes:

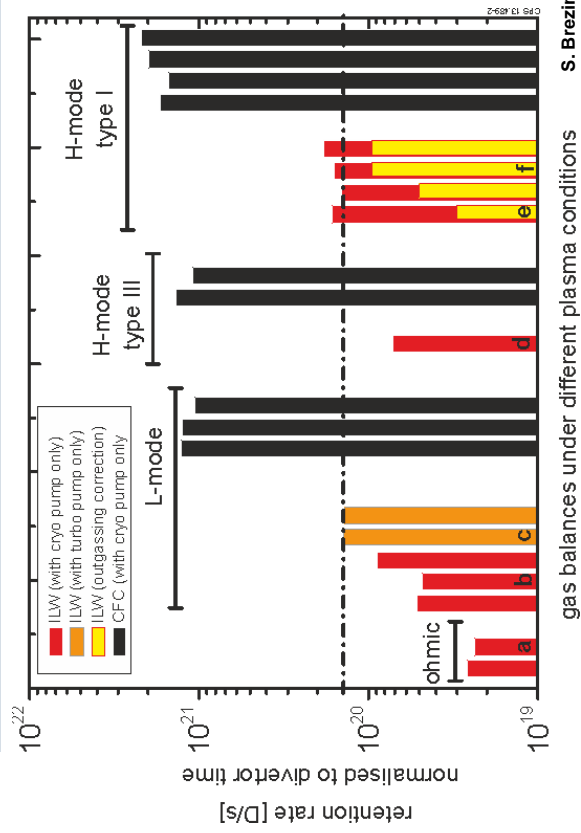
- Residual **C dropped** with ILW installation **by one order of magnitude**
- **Dedicated comparison** pulses show a **drop** of about a **factor 20** in divertor
- **Oxygen gettered by Be**, but still present at very low levels in the plasma



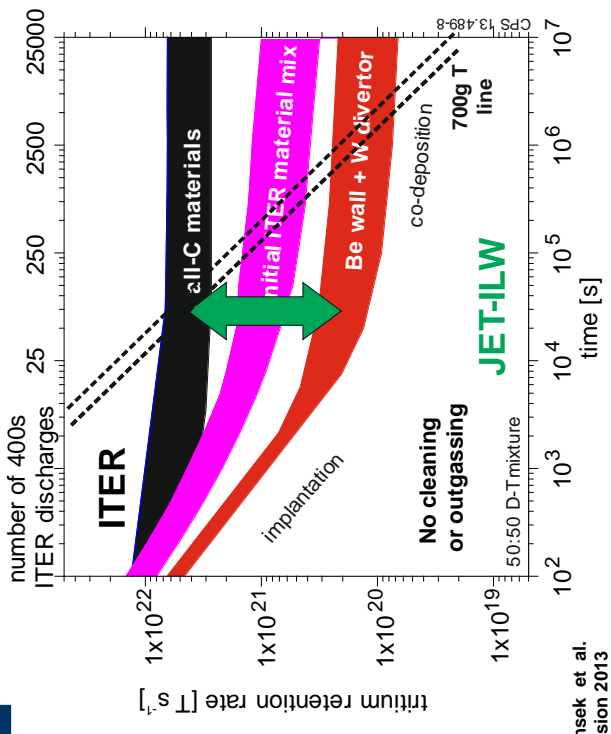
- Comparable C reduction also observed in core and edge concentrations by CXRS
- Averaged Z_{eff} dropped from 1.9 (JET-C) to 1.2 (JET-ILW)
- Primary erosion source of Be in JET-ILW is smaller than C in JET-C

Key Result: Long Term Fuel Retention

Global gas balance: injected-pumped D₂
= retained D atoms



ITER predictions confirmed

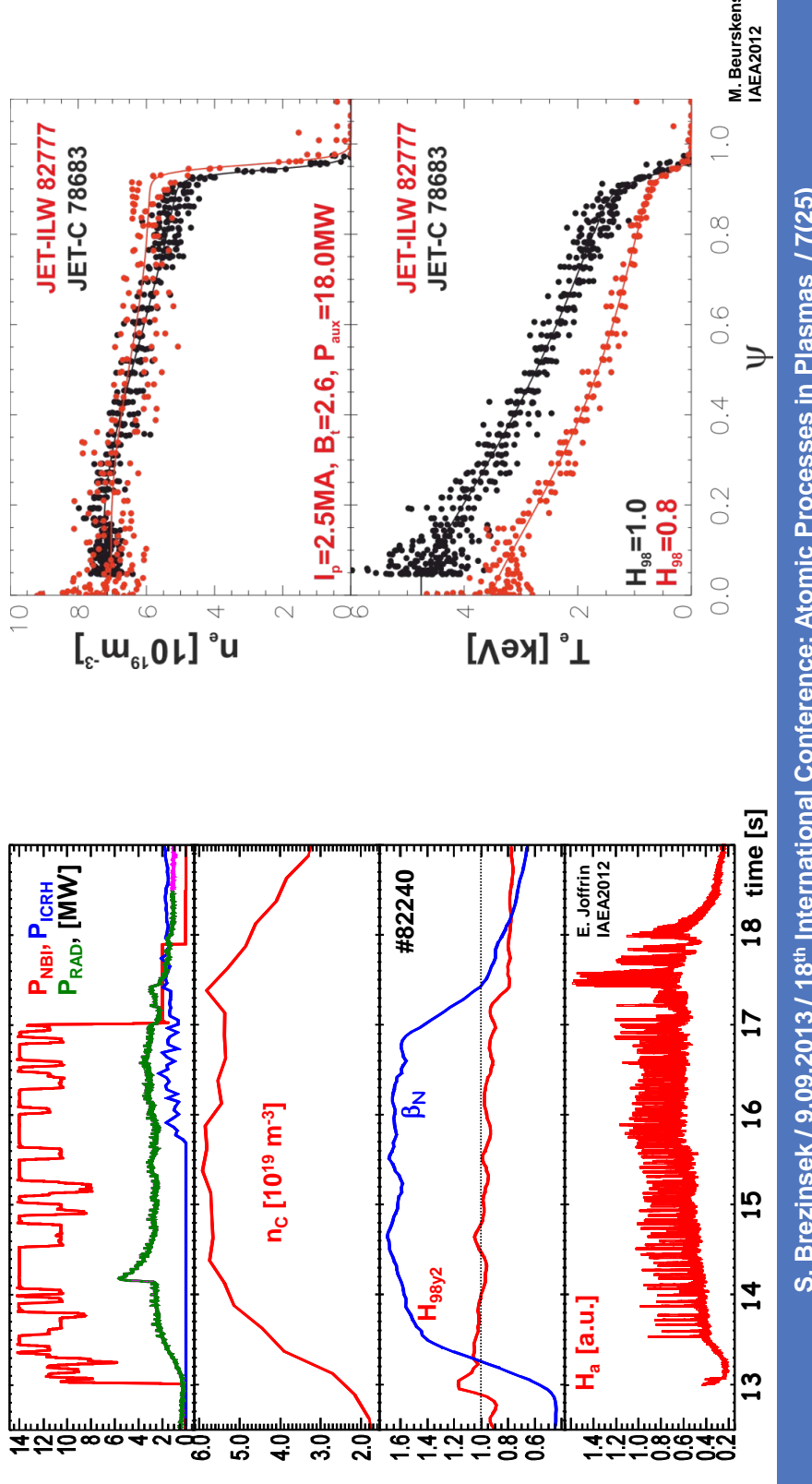


- Reduction of fuel retention rate by more than one order magnitude
- Long-term retention mechanism: implantation and co-deposition (dominant)
- Reasons for the reduction from JET-C to JET-ILW:

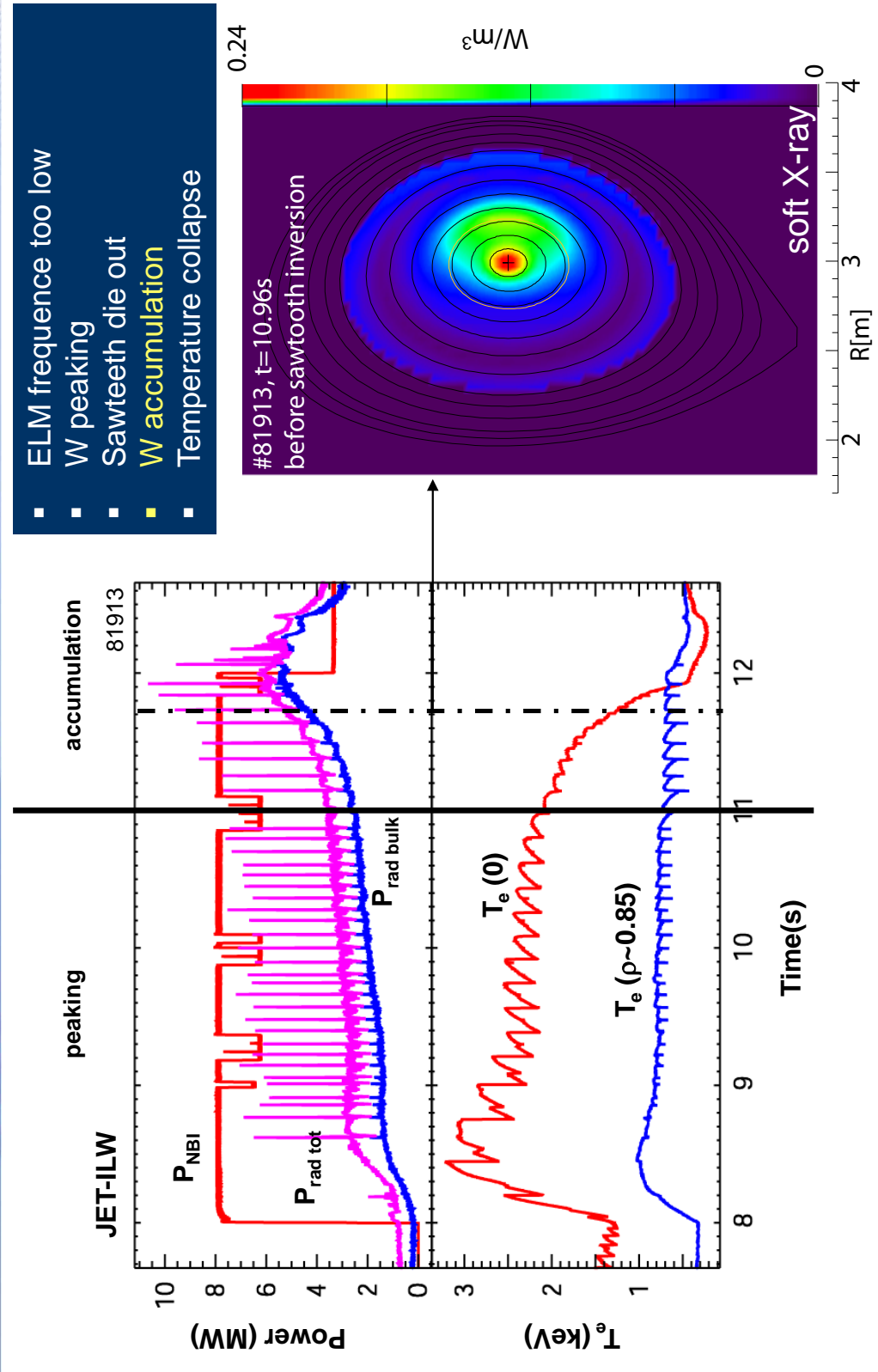
- Be primary source and Be transport to divertor smaller than C in JET-C
- Lower fuel content in Be co-deposits in comparison with C co-deposits

Key Result: Stable H-mode Operation

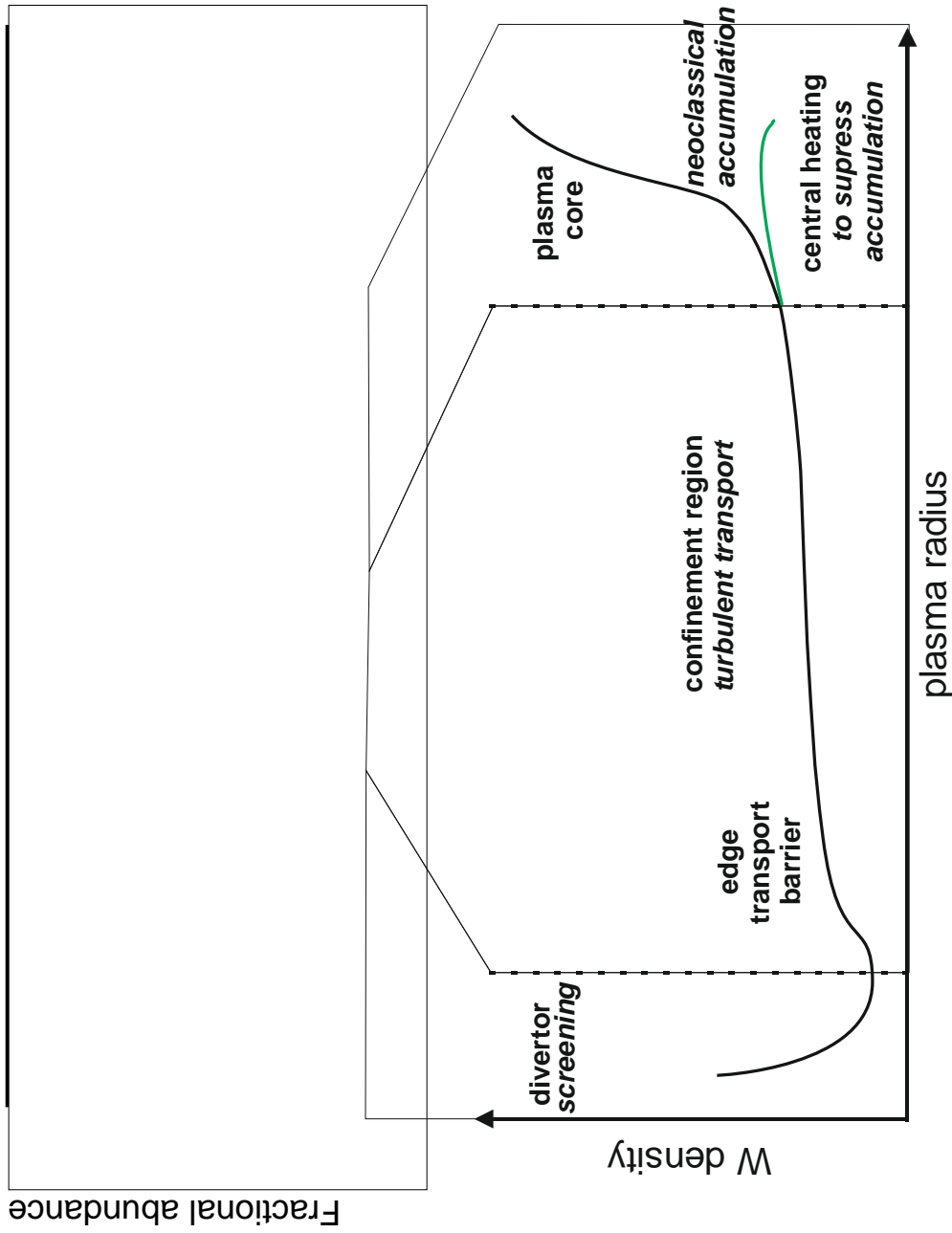
- **Type I ELMy H-modes achieved** in low and high triangular plasma with NBI
- Operational window is smaller and requires W control techniques to avoid accumulation
- Confinement lower due higher fuelling and lower pedestal temperature



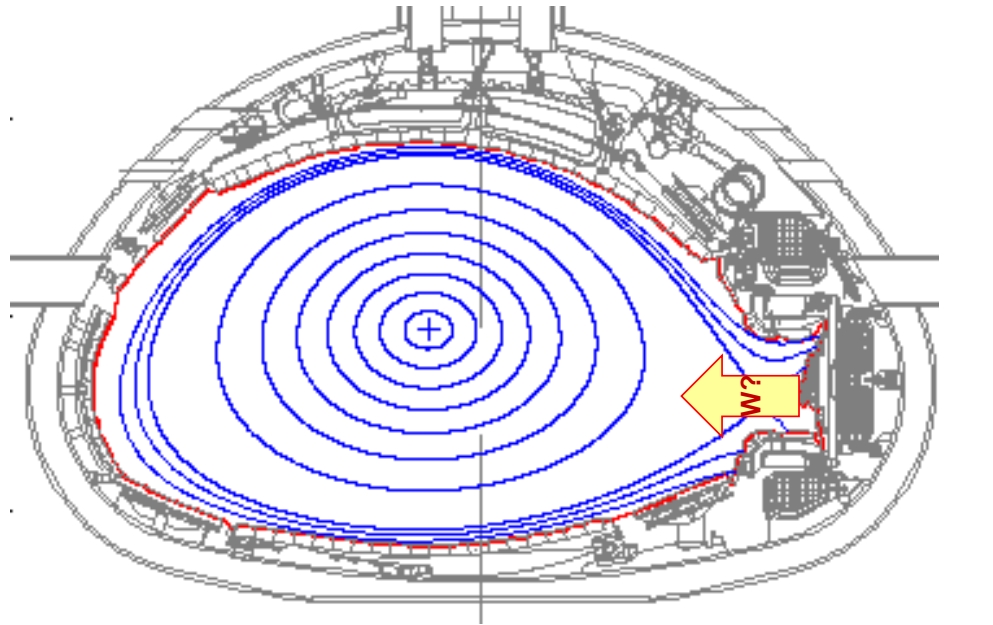
Issue: W Transport and Accumulation



Key diagnostic: W spectroscopy in JET

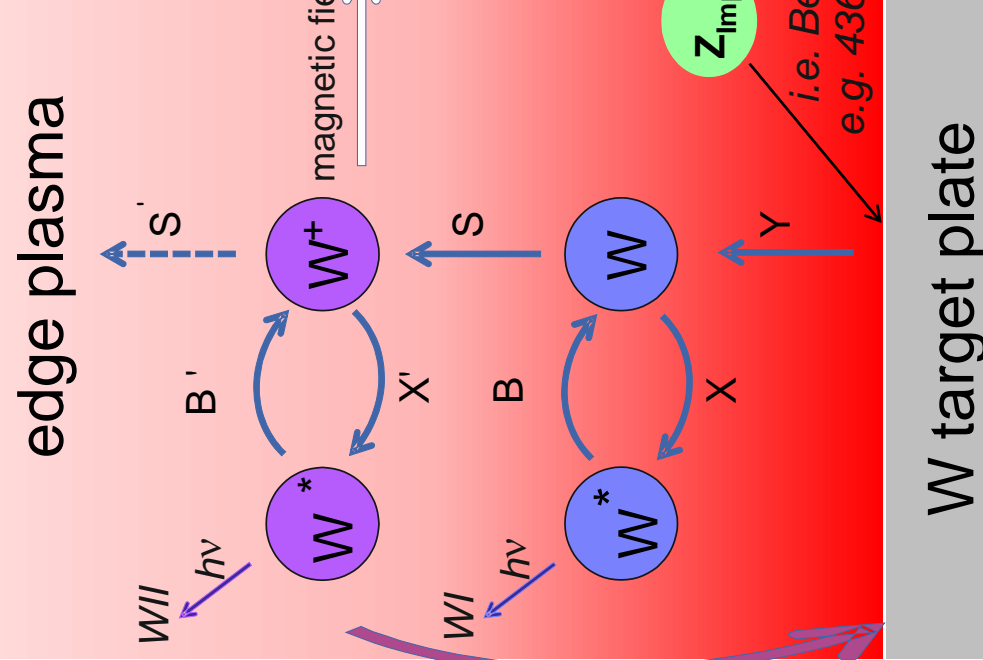


W Sources in JET



- Critical issue: strong W source (outer divertor)
- Best plasma performance in JET-CFC obtained in
 - plasmas with low density in the divertor
 - plasmas with large ELMs
- ⇒ Not possible with W divertor
 - Low density means high T_e and energy of impinging ions => strong W sputtering
 - Large ELMs carry high energy ions => melting and sputtering of W possible
- Needs best compromise:
 - Low W sputtering (gas fuelling)
 - High W divertor screening (geometry)
 - Small ELMs to flush confined W (ELM pacing)
 - Central heating to avoid accumulation
- W divertor spectroscopy
 - Impurity flux and Balmer spectroscopy

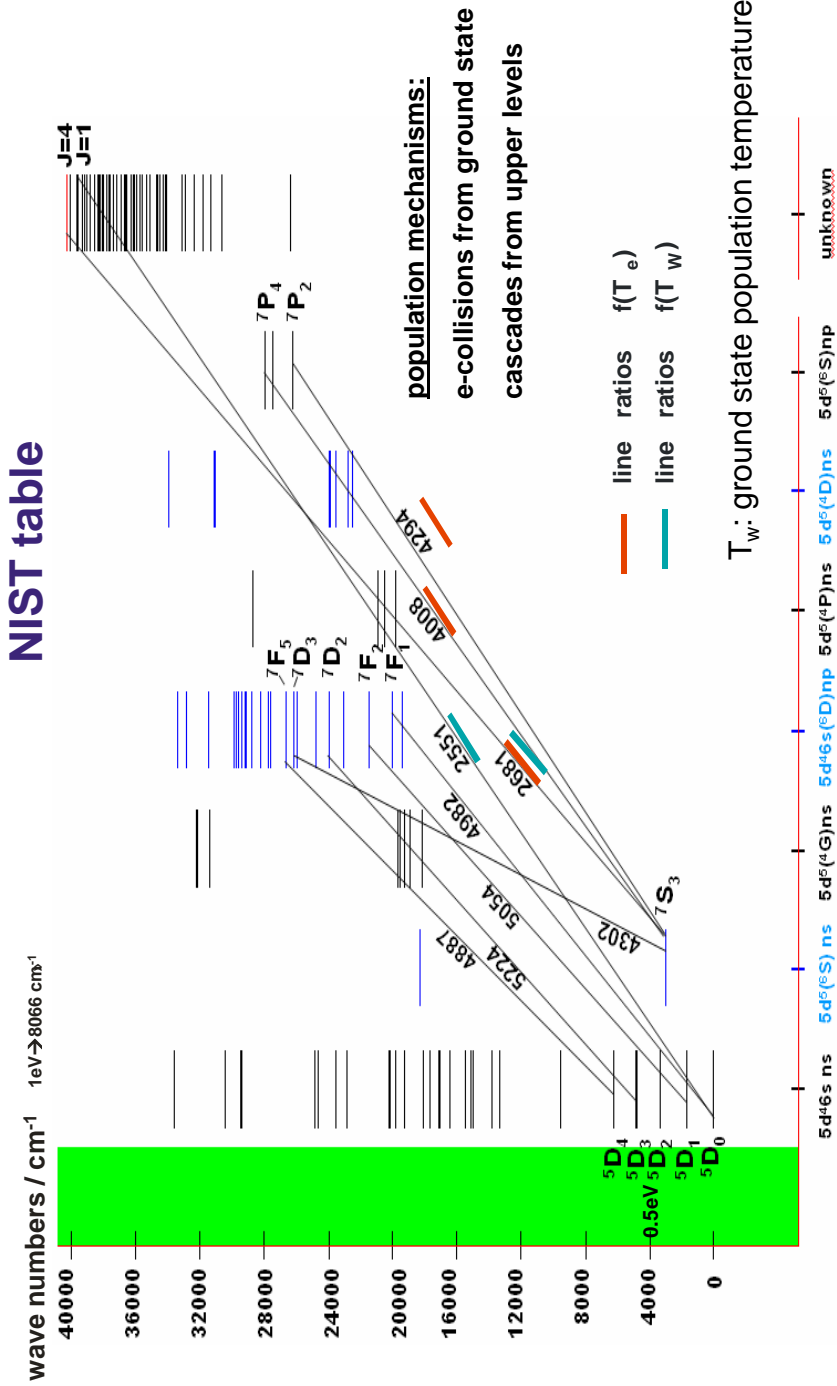
W source spectroscopy



- W sputtering only by impurities above energetic threshold of $\sim 10\text{eV}$
 \Rightarrow at JET: Be ions + residual O and C
 - W released and can be observed as Bell
- $$\Gamma_W = \frac{4\pi}{h\nu} \cdot I_W \frac{S}{XB}$$
- Larmor radius of W^+ is so large that W can be promptly re-deposited at the target plate before emitting a WII photon
 - Essential for quantification:
 - Identification of suitable WI, WII lines
 - S/XB values for these transition
 - Experimental determination of effective S/XB values at different devices
 - Benchmarking theoretical calculations

Grotian Diagram for Neutral W

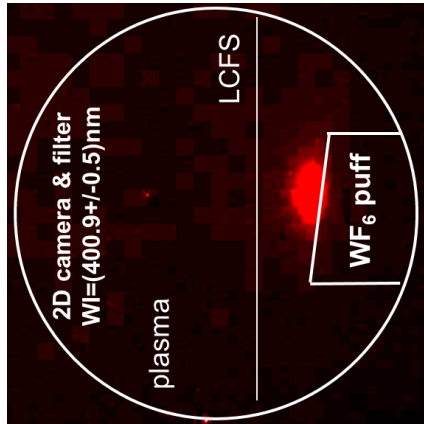
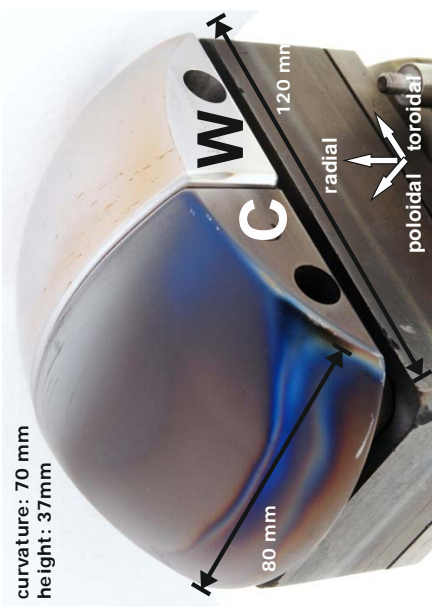
- Complex level diagramm and ground state structure



- Selection of most prominent transitions with equal lower or upper state

TEXTOR Experiments: W Sputtering and WF₆ Injection

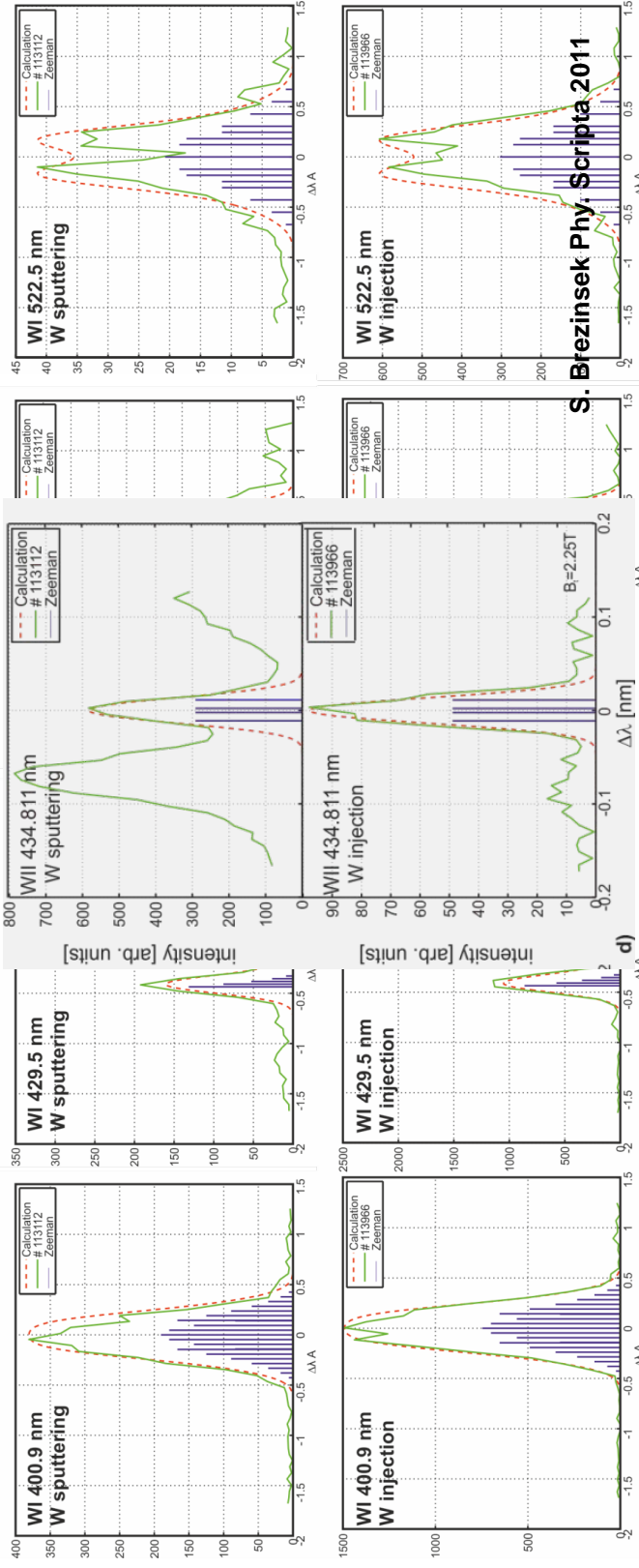
- Twin Limiter experiment with variation of impact energies of impinging impurities
- Determination of the W sputtering yield and the impurity composition
- S/XB values from corresponding WF₆ injection experiments (comparable plasmas)



- WF₆ injection experiment with gas inlet and negligible limiter surface
 - Well-known amount of W injected / direct dissociation at about T_e~0.1eV
 - Prompt re-deposition minimised / no impact from local deposition of W
- Multiple injections with variation of local plasma conditions

Comparison of W atoms from Sputtering and Injection

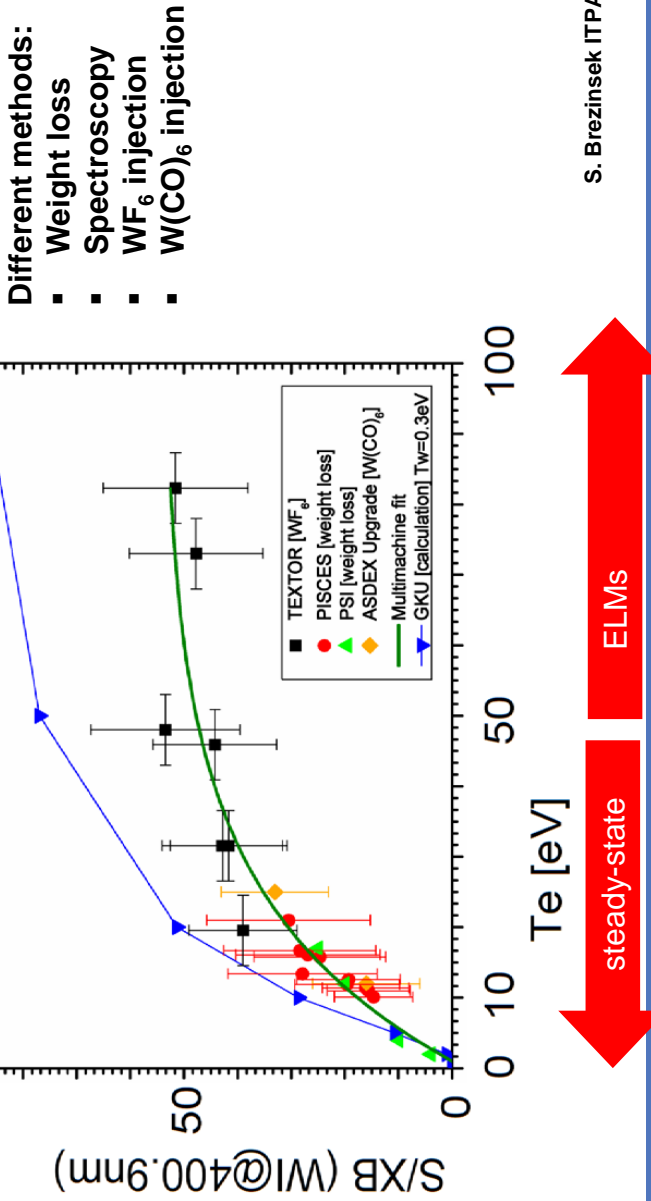
- Is W from WF_6 dissociation representative for W from sputtering?
 - **No difference in line shape** of different WI and WIll lines
 - Line ratios of WI lines with same lower level comparable in sputtered and injected W
 - **WIll lines measured** and quantified in WF_6 injections



- Full coverage of all emission lines between 363 and 715 nm
- Main favourite lines: WI at 400.875 nm and UV lines identified
- Alternative lines to weak or blended by impurities from Be, C, Ar, N etc.

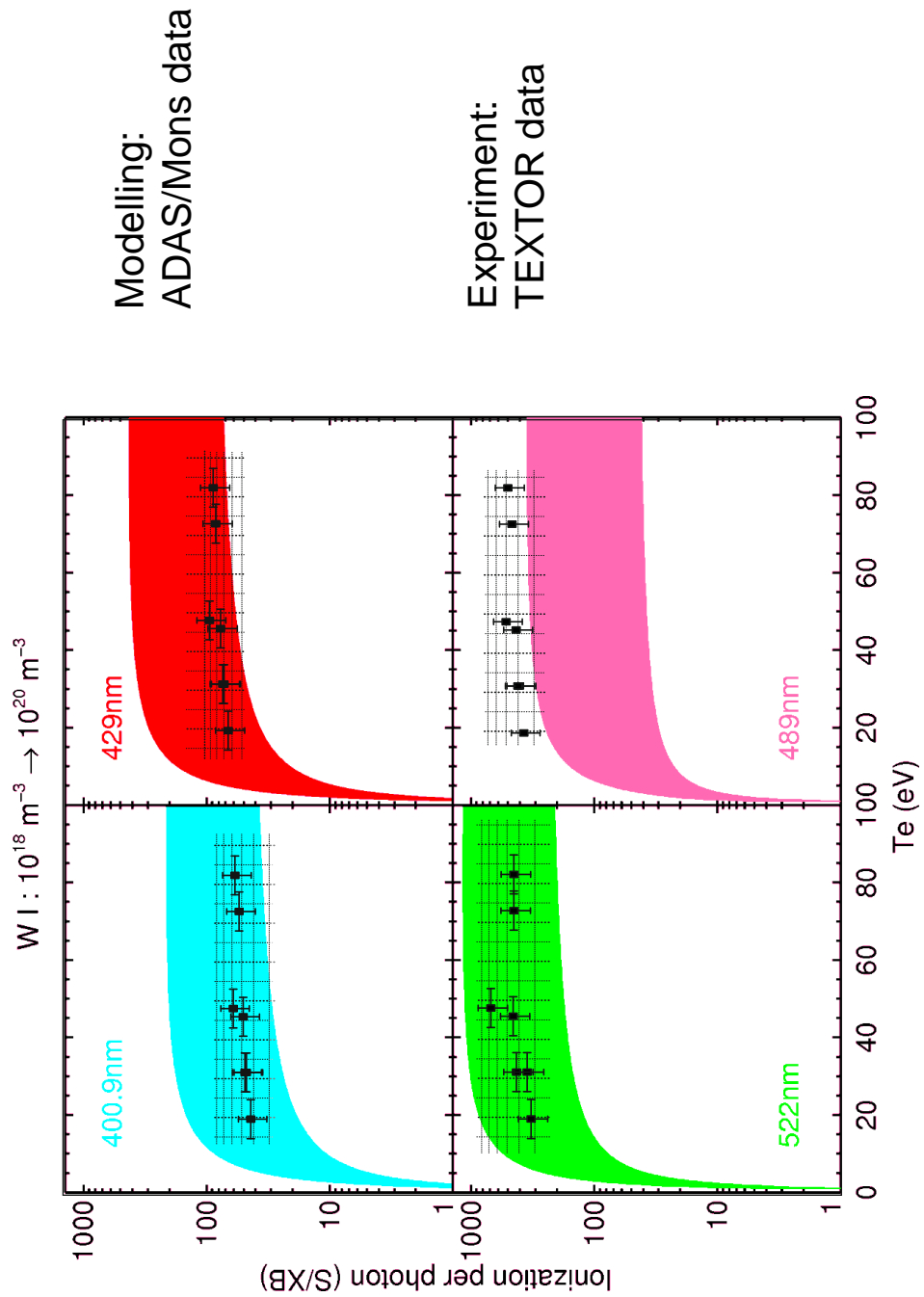
Photon Efficiencies for WI

- WI at 400.9nm best documented line
- Multimachine fit of effective S/XB values applied for quantification of W fluxes
- Contrast to AUG data which uses constant 20 (but works only in the range od 5-15 eV)
- JET outer divertor hotter and has larger ELM energy drops (higher T_e)



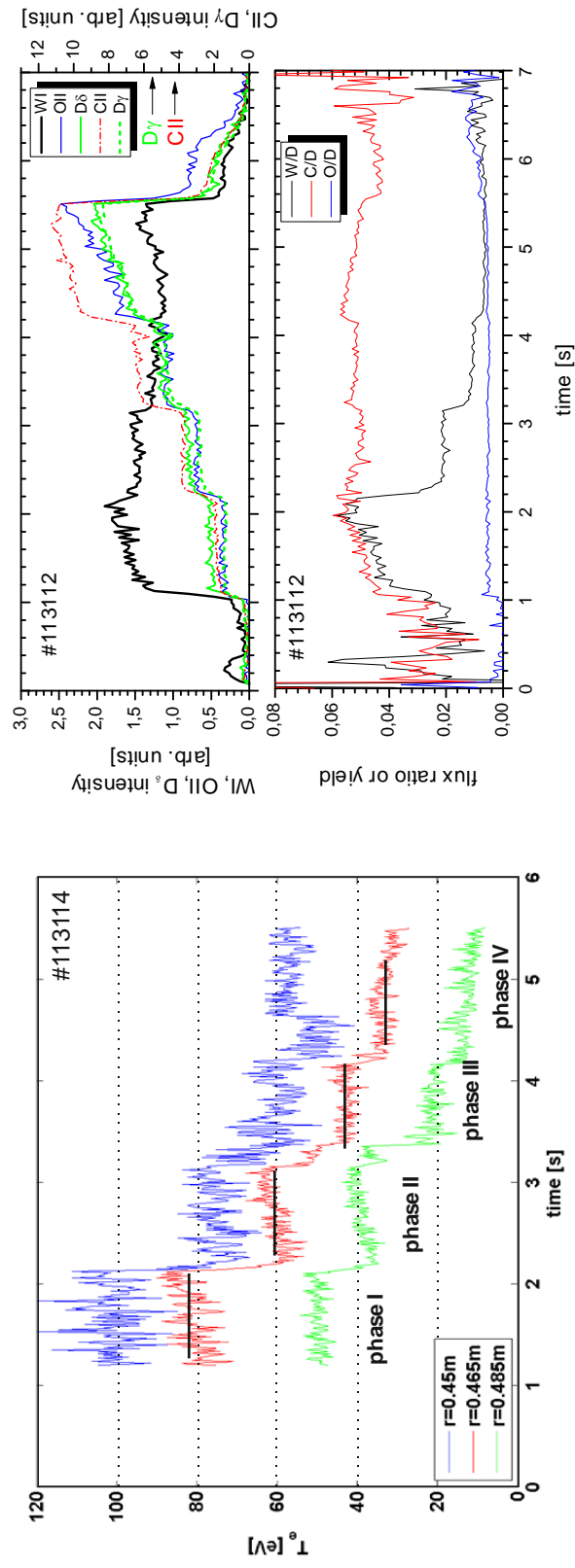
S. Brezinsek ITPA 2012

Effectice S/XB for different W lines



W sputtering in TEXTOR

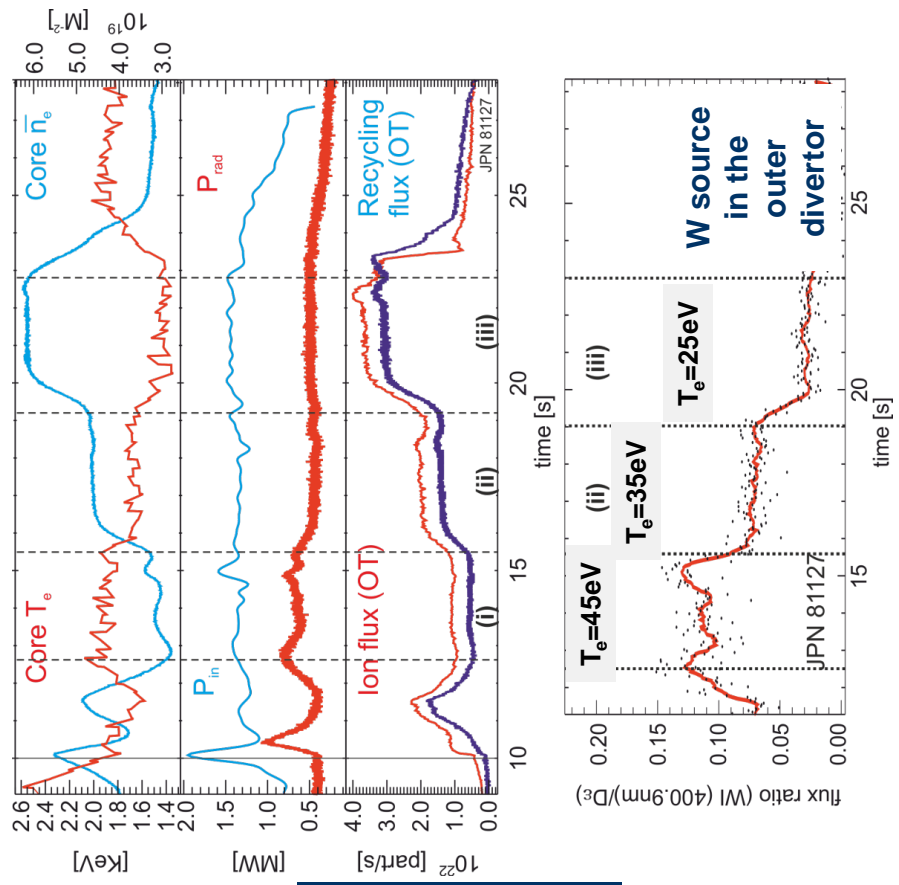
- Twin Limiter experiment with 4 density / temperature steps
- S/XB values from corresponding WF_6 injection experiments
- Effective sputtering yield drops with electron temperature / ion energy reduction
- Sputtering by O (0.7%) and C (5.0%) from background flux (C^{4+})





EEJET

W Sputtering in JET: L-mode



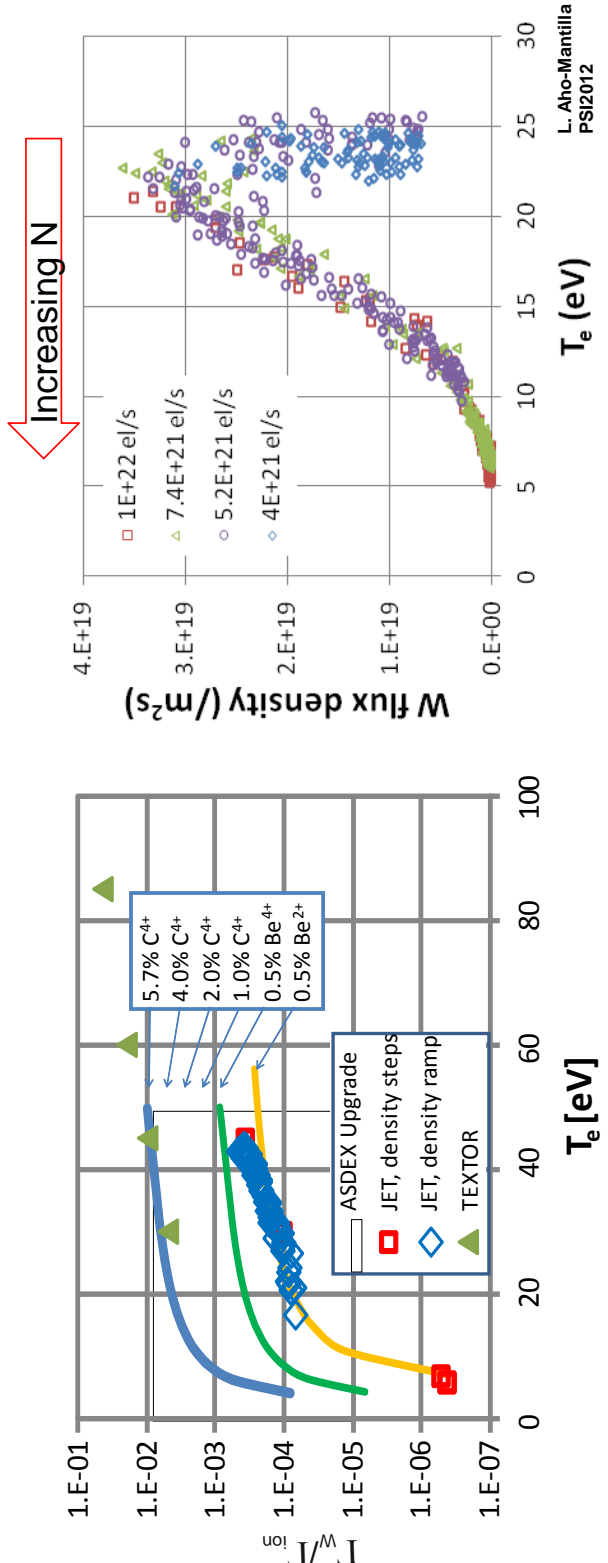
Low recycling regime (steady-state):

- **W sputtering** decreases with density increase and temperature decrease
- Impact of flux increase to the target compensated by drop in temperature
- Sputtering **caused by impurity ions (here: Be ions)**

W Sputtering Yields

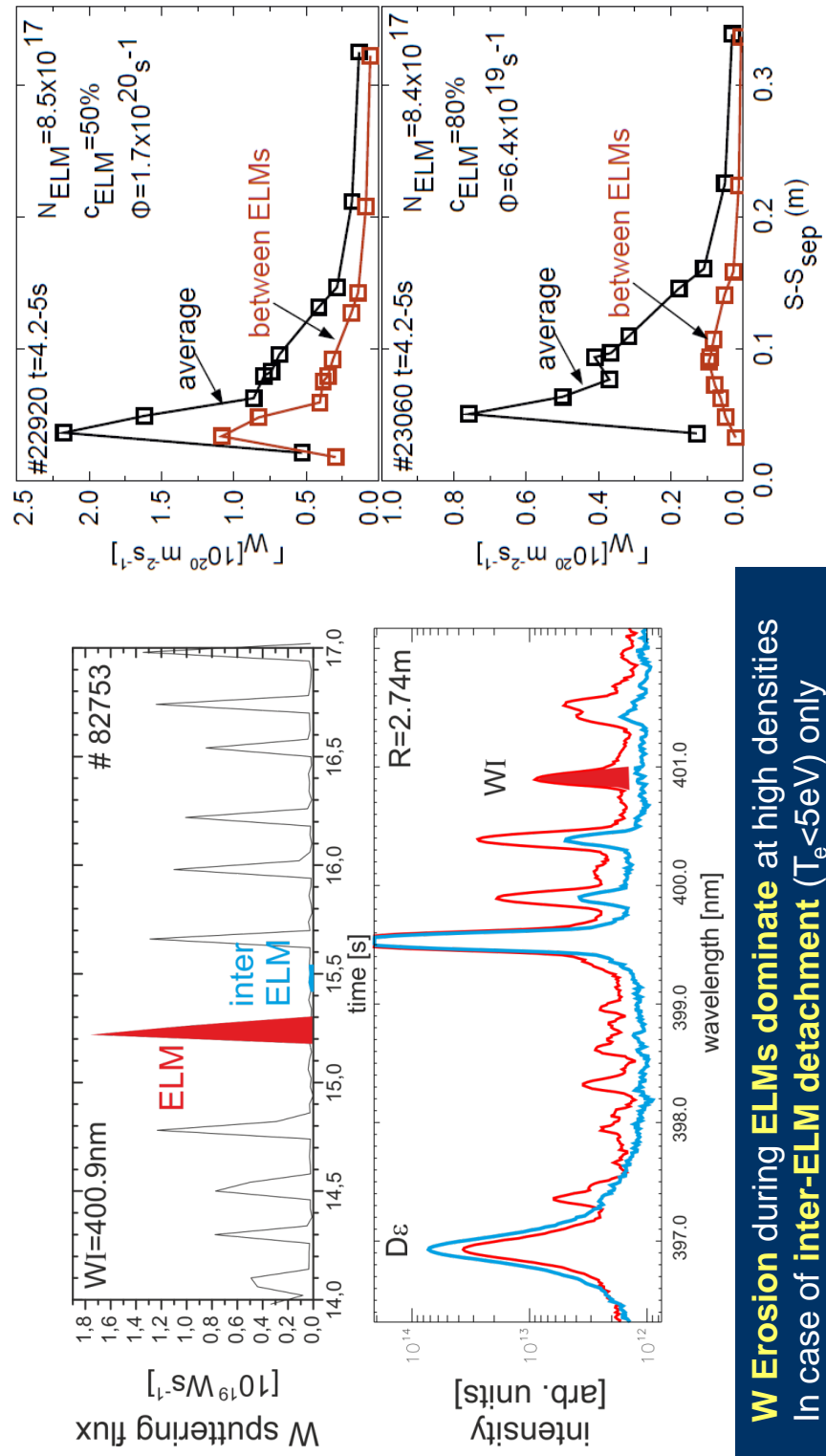
Inter-ELM and steady-state regimes with low T_e and low W sputtering achieved

Competition between higher impurity flux and local cooling in seeded discharges



Divertor **plasma cooling** by deuterium fuelling or by deuterium+nitrogen seeding leads to **reduction of W source** => below phys. sputtering threshold

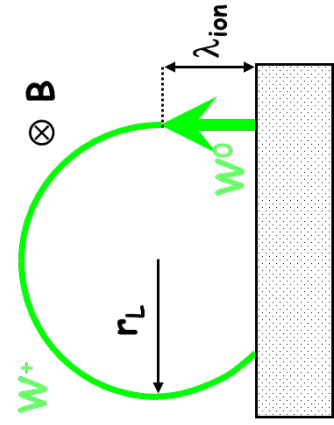
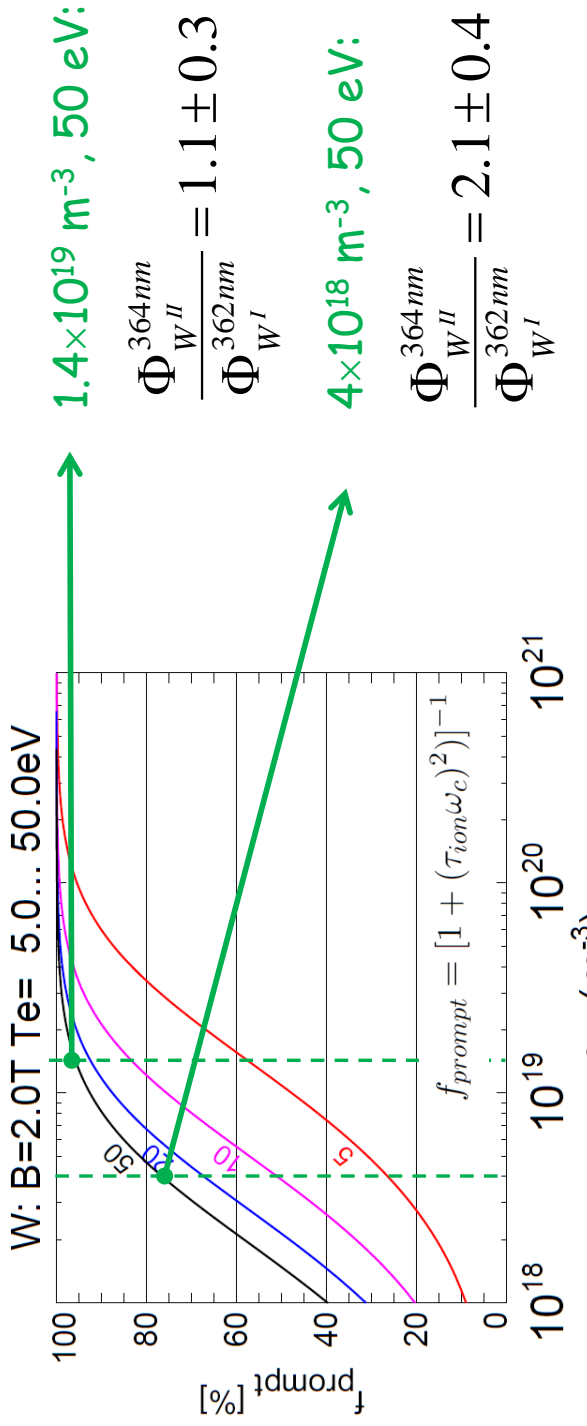
W Sputtering in JET: H-mode



- **W Erosion** during **ELMs** dominate at high densities
- In case of **inter-ELM detachment** ($T_e < 5 \text{ eV}$) only **residual W source** (even with N_2 seeding) by **ELMs**
- **Total W screening in divertor is about factor 100**

ASDEX: Dux et al., J Nucl Mat 390–391 (2009) 858

Prompt redeposition: Ratio of WII / WI

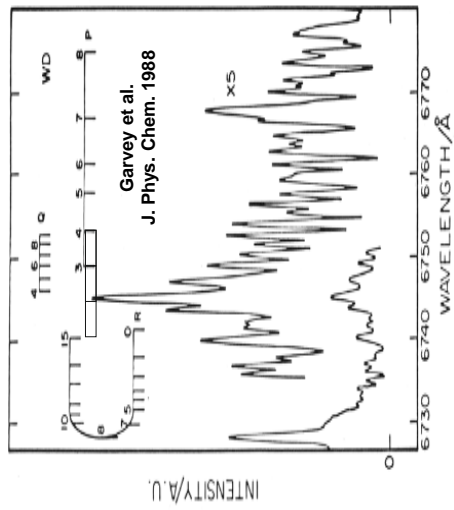


$$\Gamma_{W'} = \frac{S' + R_{redep}}{XB'}(T_e)\Gamma_{h\nu}$$

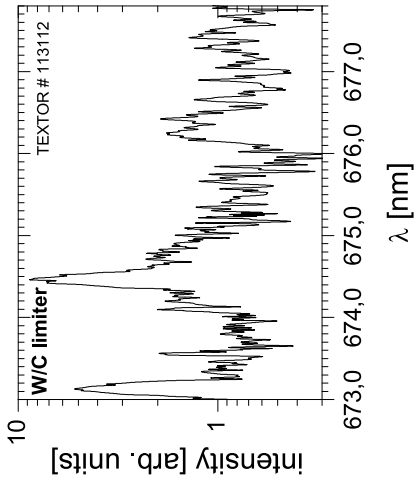
- **Prompt redeposition** amounts to more than **50%**
- Comparable to TEXTOR results at 50eV

Molecular Species in the Plasma Edge

WD molecule



Garvey et al.
J. Phys. Chem. 1988



- Molecular species are present in the JET-ILW
 - **D₂ d-a transition**: Recycling flux
=> understood and good set of data (EIRENE)
 - **BeD A-X band** : Swift chemical sputtering
=> empiric set of S/XB values
=> more work required
 - **WD A-X band** : Swift chemical sputtering
=> just identified => no S/XBs
=> more work required
 - **ND A-X band** : Volume or surface reaction
=> just identified => no S/XBs
=> more work required
 - **N₂, CD** in minor quantities
 - Limited atomic and molecular data available

Summary

- JET-ILW successful in operation and main goals achieved
- W accumulation observed in cases of low density observation

- W influx spectroscopy established on basis of WI emission
- WI photon efficiency calibration by WF₆ injection
- W sputtering measured in T-TEXTOR, JET
 - Sputtering determined by impurities (C, O, Be...)
 - Strong dependence on impact energy
 - Energetic threshold observed in detached conditions
 - Residual W sputtering determined by ELMs
 - Prompt redeposition determined to at least 50% at 50eV
 - Formation of WD observed
 - Impurity seeding can promote detachment in W divertor
- W_{III}, W_{IV} transitions ?

D.4 ADAS forward discussion - Dr. William Morris

What should the ADAS profile be through to ITER and how should it be staffed and resourced?

(Discussion)

- Programme needs (where not covered by Sebastijan)
- ADAS needs
- How might ADAS fit in EU Consortium, direct ITER work
- Collect ideas to help all three
- ADAS-EU has made a huge difference – we must build on it

William Morris

ADAS-EU: Final meeting and special workshop

Culham

30 Sep 2013 - 3 Oct 2013

Programme needs: plasma exhaust (experiments and modelling)

Divertor radiation

- location and magnitude, tools to design, e.g. multiple species
- accuracy

Detachment processes

- diagnostics, e.g. T from molecular spectroscopy
- how do we transport a recipe in one machine and gas mix to another?

PWI issues

- ionisation of sputtered tungsten, beryllium – high accuracy needed?

Confidence that results are OK in regimes where there are

- non-thermal (anisotropic?) effects (high electron heat flux)
- non-local effects (long mean free path)
- transients (can we aspire to model small ELMs, filaments and blobs?)
- Should we always convert original data to T_e ?

[These just to trigger any ideas for gaps/R&D not in the plan]

Programme needs: plasma exhaust (experiments and modelling) - ideas

Divertor radiation

Detachment processes

PWI issues

Confidence that results are OK in regimes where there are

[These just to trigger any ideas for gaps/R&D not in the plan]

Programme needs: pedestal and core (experiments and modelling)

Some scenarios require very high radiation fractions (>90%?)

- very high accuracy needed in the models (80% and divertor melts?) – any issues in atomic physics or is it all in transport and n_e , n_z T_e uncertainties??
- nature of the radiative losses (e.g. photons vs particles, what wavelengths, where poloidally)

Pedestal

- very high spatial gradients
- ions can explore range of n_e and T_e in a single orbit?

Core

- very high temperatures
- small deviations from Maxwellian electrons, e.g. high local ECRH or ICRH power density

Other

- pellet fuelling processes (very high local gradients?)
- dust (SOL too) – low ionisation states in unexpected places
- Supersonic or cluster fuelling?
- Synthetic diagnostics (bolometers?)

Programme needs: pedestal and core experiments and modelling) - ideas

Some scenarios require very high radiation fractions (>90%?)

Pedestal

Core

- Raw data goes to relativistic energies, but kinematic calcs non-rel? Can be fixed, just time.

Other

- Common tools and approaches core-SOL
- E.g. large gas feed close to diagnostics – in divertor as well.
- MGI – radiative efficiency? Huge densities. Start a combined plasma+A&M project?
- Non-thermal electrons in sheath – is there a gap? “Easy” to calculate, but what is the edf? How big an effect?
- Modellers need to propagate ADAS errors.
- Opacity – pellets, divertor, MGI. ADAS can do up to opt depth ~0.2.
- Need some parameterisation (can't handle first principles all the time)
- Need opaque experiments. Where? [KB says done on ASDEX]

ADAS needs - I

Original data

- species
- accuracy

Validation of ADAS rate coefficients etc

- What gaps?
- What approaches?
- What mix of devices (tokamaks, linear, ECR etc)
- Can programmes and diagnostics be adapted to help? (e.g. MAST Upgrade...)

ADAS needs - II

People

- what attracts the type of people needed (even if they pass through)?
- raw science? fusion relevance?
- can programmes be adapted to help?
- A: raw science, fusion relevance, and stability
- How to get theoretical atomic physicists into any given lab? (critical size of activity)
- Need university link – at least two. EU only – why not outside (as well). Try to get new input from non-EU.
- Modellers are key ingredient (interface between tok/stell and A&M). Identify where the advances are needed that make a difference.
- A&M savvy people in mainline

ADAS in EU Consortium

Links to main Consortium programme to implement Roadmap

- Organised via headlines (like JET) and projects (especially for DEMO development), with leaders from the community (names announced after 8th Oct)
- ITM being restructured:
 - code management, verification and standards under CD: “Code development for integrated modelling”
 - code validation and new codes (plasma) in the other parts, e.g. MST1, MST2

In addition a “Basic Research” line – ADAS role?

- Call imminent, reply mid Nov (tbc)
 - Criteria: excellence of principle investigator and the project
 - Projects need a fusion focus (e.g. an exhaust challenge)
 - Stand-alone proposals? Contributions to other proposals as well
- ADAS needed all over the place, but how managed/championed? Subset of ADAS steering committee? Champion(s) among the new leadership team?**

ADAS for ITER

Diagnostic design

- EU – via the consortia on F4E contracts
- International – how? [DAs often ADAS members and using in design]

ITER scenarios

- Specific EU and IO contracts (needs legal entity)
- Members or 3rd parties to F4E contracts for scenario modelling (these may be assisted by the EU Consortium in future)

So – ADAS in several places, but how managed/championed?

May need subset of ADAS steering committee to look at EU activities? (and others for JA, CN, KO, US, IN, RF...). Champion(s) in the DAs?

Appendix E

ADAS-EU WATC: ADAS codes and data formats

E.1 ADAS manual: version 4.0: contents pages

University of Strathclyde

Atomic Data and Analysis Structure

User manual
Version for UNIX/IDL

H. P. Summers

4th Edition - Version 4.0

2013

Table of Contents

Introduction

- General principles
- General organisation
- ADAS on a Unix workstation
- ADAS documentation
- The ADAS library
- Atomic data entry and verification

Atomic data entry and verification

- ADAS101: Electron impact cross-section - graphing and rate evaluation
- ADAS102: Electron impact excitation rate - graphing and interpolation
- ADAS103: Dielectronic recombination - graphing and interpolation
- ADAS105: Electron impact ionisation cross-section - graphing and rate evaluation
- ADAS106: Electron impact ionisation rate - graphing and interpolation
- ADAS108: Electron impact excitation of neutral atoms and molecules

Population processing

- ADAS201: Specific z excitation - graph and fit coefficient
- ADAS202: General z recom/ionis - extraction from general z file
- ADAS203: General z excitation - extraction from general z file
- ADAS204: Specific z recom/ionis - process collisional radiative coefficients and populations
- ADAS205: Specific z excitation - process metastable and excited state populations
- ADAS206: Specific z excitation - process total and specific line power
- ADAS207: Metastable and excited population - process line emissivities
- ADAS208: Specific z excitation - advanced population processing
- ADAS209: General level bundling
- ADAS210: General level unbundling
- ADAS211: Radiative recombination - process for specific ion file
- ADAS212: Dielectronic recombination - process for specific ion file
- ADAS213: Collisional ionisation - process for specific ion file
- ADAS214: Escape Factors for Line Emission and Population Calculations
- ADAS215: Specific ion file - temperature regrid

ADAS216: Population and emissivity error analysis

ADAS217: Create hydrogen series limit feature file - **in development space**

ADAS218: Non-Maxwellian population structure - **command line code**

Charge exchange processing

ADAS301: State selective charge exchange data - graph and fit cross-section

ADAS302: Ion/atom data - graph and fit cross-section

ADAS303: Effective charge exchange spectroscopy emission data - graph and fit coefficient

ADAS304: Effective beam emission spectroscopy stopping data - graph and fit coefficient

ADAS305: Hydrogen beam Stark feature model - **command line code**

ADAS306: Charge exchange spectroscopy - process effective coefficients: j-resolved

ADAS307: Charge exchange spectroscopy - process effective coefficients: j-resolved/scan

ADAS308: Charge exchange spectroscopy - process effective coefficients: l-resolved

ADAS309: Charge exchange spectroscopy - process effective coefficients: l-resolved/scan

ADAS310: Beam emission spectroscopy - process beam stopping and emission : H-beam

ADAS311: Beam emission spectroscopy - process beam stopping and emission : He-beam

ADAS312: Post-process population data for hydrogen beam stopping and emission

ADAS313: Post-process population data for helium beam stopping and emission

ADAS314: Convert QCX to effective cross-sections

ADAS315: Preparation and extraction of universal adf49/adf01 CX cross-section data

ADAS316: medium/heavy element CXS – eff. coeffts. in bundle-n model

ADAS317: medium/heavy element CXS – eff. coeffts. in bundle-nl(j) model - **in development space**

ADAS319: Advanced H beam model with mixed fields and field ionisation - **in development space**

Recombination and ionisation processing

ADAS401: Isoelectronic sequence data - graph and fit coefficient

ADAS402: Isonuclear sequence data - graph and fit coefficient

ADAS403: Merge iso-electronic master files

ADAS404: Isonuclear master data - extract from isoelectronic master data

ADAS405: Equilibrium ionisation - process metastable populations and emission functions

ADAS406: Transient ionisation - process metastable populations and emission functions

ADAS407: Iso-nuclear parameter sets - prepare optimised power parameters

ADAS408: Iso-nuclear master data - prepare from iso-nuclear parameter sets

ADAS409: Equilibrium ionisation – prepare G(Te,Ne) function tables

ADAS410: Dielectronic recombination – graph and fit data

ADAS411: Radiative recombination – graph and fit data
ADAS412: Equilibrium ionisation - prepare G(Te) function tables
ADAS413: Collisional ionisation – graph and fit data
ADAS414: Prepare soft X-ray filter file
ADAS415: Display spectral filter file
ADAS416: Superstages – repartition adf11 and emissivity datasets
ADAS417: Apply filter to F_PEC coefficients and F_G(Te,Ne) functions - **not implemented**

General interrogation programs

ADAS501: SXB - graph and fit ionisation per photon coefficients
ADAS502: SZD - graph and fit zero-density ionisation rate coefficients
ADAS503: PEC - graph and fit photon emissivity coefficients
ADAS504: PZD - graph and fit radiated power coefficients
ADAS505: QTX - graph and fit thermal charge exchange coefficients
ADAS506: GFT - graph and fit G(Te) functions
ADAS507: GCF - graph and fit generalised contribution functions
ADAS508: GTN - graph and fit G(Te,Ne) functions
ADAS509: SCX - graph and fit charge exchange cross-sections
ADAS510: F-PEC - graph envelope feature photon emissivity coefficients

Data analysis and spectral fitting

ADAS601: Differential emission measure analysis
ADAS602: Spectral line profile fitting
ADAS603: Zeeman multiplet line fitting
ADAS605: General ADAS feature inspection

Creating and using dielectronic data

ADAS701: Autostructure
ADAS702: Postprocessor - Autostructure > adf09 file
ADAS703: Postprocessor - Autostructure > adf04 file
ADAS704: Postprocessor - Autostructure > adf18 file
ADAS705: Merge and bundle partial files > adf04 file- **command line code**
ADAS706: Calculate doubly excited state populations and satellite line feature file- **in development space**
ADAS708: Calculate l-redistribution for Rydberg DR resonance populations- **in development space**

Creating and manipulating adf04 files

ADAS801: Calculate Cowan atomic structure
ADAS802: Calculate distorted wave cross-sections
ADAS803: Postprocess distorted wave cross-sections > adf04 file- **not implemented**
ADAS804: Calculate cross-sections and rate coefficients
ADAS805: Calculate radiative Gaunt factors- **not implemented**
ADAS806: Merge, clean and check adf04 files
ADAS807: Prepare cross-referencing files
ADAS808: Create composite iso-nuclear adf34, adf40 and adf41 driver files
ADAS809: Non-Maxwellian modelling - change adf04 file type
ADAS810: Generate envelope feature photon emissivity coefficient
ADAS811: Compare rate coefficients from adf04 files
ADAS812: Compare adf04 files (scatter plot)

General molecular processing

ADAS901: Interrogate fundamental data (mdf02)
ADAS902: Interrogate rates and lifetimes (mdf04 & mdf33) - **in development space**
ADAS903: Generate rate data - **in development space**
ADAS904: Assemble data collections for population models (mdf04) - **in development space**
ADAS905: H₂ molecular vibronic population calculation - **in development space**
ADAS906: Interrogate molecular collisional-radiative coefficients - **in development space**
ADAS907: Interrogate molecular collisional-radiative coefficients - **in development space**
ADAS908: Generate and compare diatomic rovibration band structure - **in development space**

Offline ADAS

ADAS3#1: AUTOSTRUCTURE iso-seq. mass production for bnl(j) models- **in development space**
ADAS7#1: AUTOSTRUCTURE base calculation (struct./RR/DR/DW/PWB/PI/PE operational modes)
ADAS7#3: AUTOSTRUCTURE PWB & DW iso-seq. mass production for adf04 datasets
ADAS8#1: COWAN base calculation (struct./PWB operational modes)
ADAS8#2: COWAN CADW iso-nuc. ionisation cross-section mass production for adf23
ADAS8#3: RMTRX base calculation for adf04
ADAS8#4: COWAN PWB heavy species iso-nuc. mass production with optimised power for adf11

Appendix A

ADAS data formats

ADF00: ground configurations and ionisation potentials

ADF01: bundle-n and bundle-nl charge exchange cross-sections

ADF02: ion impact cross-sections with named participant

ADF03: recombination, ionisation and power parameter sets

ADF04: resolved specific ion data collections

ADF05: general z excitation data collections

ADF06: general z recombination/ionisation data collections

ADF07: direct resolved electron impact ionisation data collections

ADF08: direct resolved radiative recombination coefficients

ADF09: direct resolved dielectronic recombination coefficients

ADF10: iso-electronic master files

ADF11: iso-nuclear master files

ADF12: charge exchange effective emission coefficients

ADF13: ionisation per photon coefficients

ADF14: thermal charge exchange coefficients

ADF15: photon emissivity coefficients

ADF16: generalised contribution functions

ADF17: condensed projection matrices

ADF18: cross-referencing data

ADF19: zero density radiative power

ADF20: G(Te) functions

ADF21: effective beam stopping coefficients

ADF22: effective beam emission coefficients

ADF23: state selective electron impact ionisation coefficients

ADF24: state selective charge transfer cross-sections

ADF25: driver data-set for special population calculations: \a25_p204,\ a25_p316,\ a25_p317.

ADF26: bundle-n and bundle-nl populations of excited states in beams

ADF27: driver data-sets for ADAS701 calculations

ADF28: driver data-sets for ADAS702 calculations

ADF29: driver data-sets for ADAS707 calculations

ADF30: driver data-sets for ADAS708 postprocessing

ADF31: feature files for satellite line spectral simulation

ADF32: driver data-sets for ADAS802 calculations
ADF33: driver data-sets for ADAS803 postprocessing
ADF34: driver data-sets for ADAS801 calculations
ADF35: spectral filter data
ADF36: feature files for series limit spectral simulation
ADF37: non-Maxwellian distribution function files
ADF38: Seaton - opacity photo-excitation
ADF39: Seaton - opacity - photo-ionisation
ADF40: Envelope feature photon emissivity coefficients
ADF41: driver data-sets for offline ADAS#1 calculations
ADF42: driver data-sets for ADAS810 calculations
ADF43: GTN photon emissivity functions
ADF44: F_GTN envelope feature emissivity functions
ADF45: feature files for continuum emission
ADF46: Driver data sets for AUTOSTRUCTURE bbgp and bnl(j) base data generation
ADF47: Assigned to fundamental diatomic structure data – unused (assign to MDF00)
ADF48: State selective radiative recombination coefficients
ADF49 : Universal z-scaled bundle-n and bundle-nl charge exchange cross-sections
ADF50: Exact motional Stark perturbed H atom data
ADF53: Ion reaction dressing matrices
ADF54: General promotional rule sets
ADF55: General dielectronic recombination promotional rule sets
ADF56: General ionisation promotional rule sets

MDF00: Fundamental diatomic data
MDF01: Driver parameter sets for *nist*, *behr* and *pickett* rovibrational spectra
MDF02: Molecular system collisional reaction data collections
MDF04: Vibronic specific molecular system data collections
MDF11: Molecular system generalised collisional-radiative coefficients
MDF13: Molecular vibronic ionisation and dissociation per photon coefficients
MDF15: Molecular vibronic photon emissivity coefficients
MDF33: Molecular system collisional reaction rate coefficient data collections

Appendix B

ADAS FORTRAN and IDL subroutine libraries
FORTRAN subroutine and code access from IDL
ADAS offline codes for support calculations
Library index - FORTRAN
Library index - IDL

Appendix C

ADAS-EXCEL spreadsheets